

SITE-SELECTIVE UNACTIVATED ALIPHATIC C–H FUNCTIONALIZATION AS A  
STRATEGY FOR MOLECULAR DIVERSIFICATION

William Lawrence Czaplyski

A dissertation submitted to the faculty of The University of North Carolina at Chapel Hill in  
partial fulfillment of the requirements for the degree of Doctor of Philosophy in the  
Department of Chemistry.

Chapel Hill  
2018

Approved by:

Erik Alexanian

David Nicewicz

Marcey Waters

Jillian Dempsey

Frank Leibfarth

© 2018  
William Lawrence Czaplyski  
ALL RIGHTS RESERVED

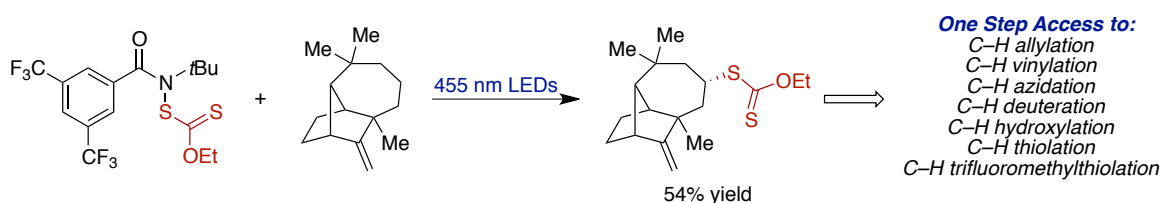
## ABSTRACT

William Lawrence Czaplyski: Site-Selective Unactivated Aliphatic C–H Functionalization as a Strategy for Molecular Diversification  
(Under the direction of Erik J. Alexanian)

### I. Strategies for Intermolecular Functionalization of Unactivated Aliphatic C–H Bonds

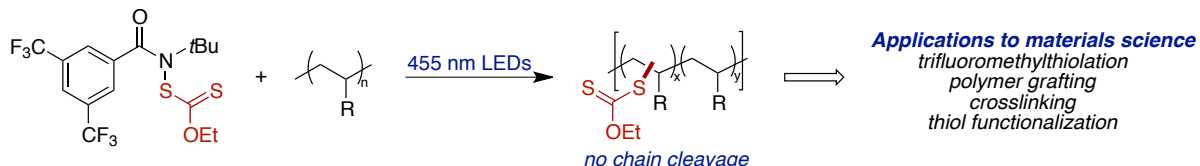
Aliphatic carbon–hydrogen (C–H) bonds are omnipresent in organic compounds, and strategies for their selective functionalization offer unique abilities in organic synthesis. Recent developments in the field of unactivated aliphatic C–H functionalization are described, and the advantages and limitations associated with them are discussed.

### II. Intermolecular Aliphatic C–H Xanthylation as a Strategy for Small Molecule Diversification



The development of a site-selective aliphatic C–H xanthylation using an *N*-xanthylamide reagent is detailed. The alkyl xanthate products are converted into a wide array of functionality, highlighting the utility as a strategy for two-step C–H diversification.

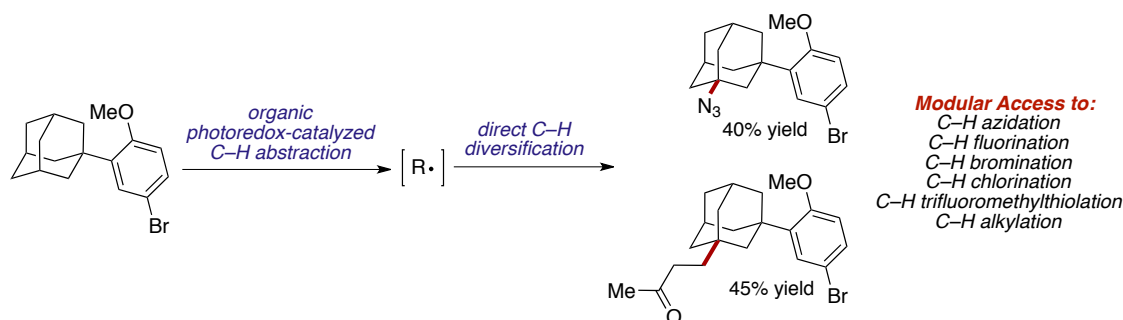
### III. C–H Xanthylation as a Strategy for Polyolefin Functionalization and Diversification



The application of the previously described aliphatic C–H xanthylation to polyolefins is shown. High levels of polymer functionalization are observed without the need for excess

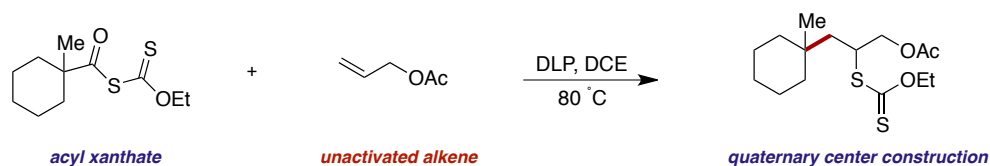
*N*-xanthylamide reagent, and problematic chain scission does not occur. The strategy is also amenable to the functionalization of high molecular weight commodity polyolefins.

#### IV. Development of an Organic Photoredox-Catalyzed Strategy for Modular Aliphatic C–H Functionalization



A modular unactivated aliphatic C–H functionalization strategy using photoredox catalysis is presented. The one-step conversion of C–H to C–N, C–F, C–Br, C–Cl, C–S, and C–C bonds is shown, and mechanistic studies suggest the intermediacy of an oxygen-centered radical. Preliminary results toward polyolefin functionalization are also discussed.

#### V. Quaternary Center Construction via Coupling of Acyl Xanthates with Unactivated Alkenes



The construction of quaternary centers from the addition of tertiary acyl xanthates to unactivated olefins is described. A wide variety of functionality is compatible with the transformation, and the subsequent reactivity of alkyl xanthate products allows for the products of net carbodifunctionalization reactions to be accessed.



To my parents, for their love and support.

## ACKNOWLEDGEMENTS

First, I would like to thank my advisor, Erik Alexanian, for his support during the last five years. With his mentorship, I learned more than I thought I could about chemistry, working as part of a team, and always striving to improve myself. Even though the next step of my journey takes me out of chemistry, I know that the skills I learned working with Erik will serve me well going forward. I also want to thank Frank Leibfarth and Dave Nicewicz for their support during our collaborative projects and willingness to allow the chemistry to go in unexpected directions. Additionally, I am grateful to Marcey Waters and Jillian Dempsey for their contributions to my time at UNC and for serving on my committee.

I am grateful to the members of the Alexanian group with whom I spent my graduate career. Your support and presence made graduate school an unforgettable experience, especially those who were part of the radicals subgroup: Benjamin Giglio, Ryan Quinn, Anthony Carestia, Nicholas Jenkins, Carla Morton, Christina Na, Tim Fazekas, and Matthew Tierney. I especially want to thank the members of the Alexanian, Leibfarth, and Nicewicz groups with whom I collaborated on projects: Christina Na, Nicholas Jenkins, Jill Williamson, and Kaila Margrey. I was fortunate enough to work with each of you at different points during my graduate school career, and I learned a tremendous amount from each of our collaborations. Additionally, I am grateful to the Crimmins and Nicewicz groups for their use of instrumentation and chemicals and to Kyle Brennaman for his assistance with

spectroscopic studies. I also want to thank Brandie Ehrmann for her assistance with mass spectrometry and for always being willing to talk about anything.

I would not be where I am today without the influence of those who taught me chemistry in my earlier years, including Hadan Kauffman and Brian Kennedy during my time in high school. I was extremely fortunate to work with Elizabeth Harbron during my undergraduate and masters work at William & Mary, and she helped me grow tremendously as a scientist, thinker, and person.

My parents, Doris and Lawrence Czaplyski, have been a critical part of my success. I am truly grateful for their unwavering love and support throughout my entire life, and I would not be where I am today without them. My friends have provided constant support throughout graduate school and have given me the perspective to get to the finish line, whether or not we are actually in the same state. I especially want to thank Addie Merians, Kelsey Miller, Katelyn Power and Valerie Ressler for their support throughout this time in my life. I'm especially thankful to Kaila Margrey for her support throughout the daily ups and downs of graduate school, and I'm so excited that we've finally done it!

## TABLE OF CONTENTS

LIST OF FIGURES.....	xii
LIST OF TABLES.....	xvii
LIST OF ABBREVIATIONS AND SYMBOLS.....	xviii
CHAPTER 1: Strategies for the Intermolecular Functionalization of Unactivated Aliphatic C–H Bonds.....	1
1.1 Introduction.....	1
1.2 Intramolecular Aliphatic C–H Functionalization.....	2
1.3 Intermolecular Aliphatic C–H Functionalization.....	4
1.3.1 Unactivated Aliphatic C–H Oxidation.....	4
1.3.2 Unactivated Aliphatic C–H Amination.....	7
1.3.3 Unactivated Aliphatic C–H Trifluoromethylthiolation.....	9
1.3.4 Unactivated Aliphatic C–H Halogenation.....	10
1.3.5 Unactivated Aliphatic C–H Alkylation.....	13
1.4 Outlook.....	14
References.....	16
CHAPTER 2: Intermolecular Aliphatic C–H Xanthylation as a Strategy for Molecular Diversification.....	19
2.1 Introduction.....	19

2.2	Background.....	20
2.2.1	Properties and Synthesis of Alkyl Xanthates.....	20
2.2.2	Advantages and Reactivity of Alkyl Xanthates.....	21
2.3	Reaction Development.....	25
2.3.1	Initial Studies.....	27
2.3.2	Reaction Scope.....	31
2.3.3	Mechanistic Studies.....	35
2.3.4	Post-Reactions.....	37
2.3.5	Amine Nucleophilicity.....	40
2.4	Conclusions.....	42
	References.....	43
CHAPTER 3: C–H Xanthylation as a Strategy for Polyolefin Functionalization and Diversification.....		45
3.1	Background.....	45
3.1.1	Strategies for Polyolefin Functionalization.....	46
3.1.2	Recent Approaches to Polyolefin Post-Polymerization Modifications.....	49
3.2	Reaction Design.....	54
3.2.1	Xanthylation of Poly(ethylethylene).....	55
3.2.2	Regioselectivity Studies via Small Molecule Model Substrate .....	60
3.2.3	Polyolefin Diversification.....	63
3.2.4	Application to Commodity Polyolefins.....	65
3.3	Conclusions.....	68
	References.....	69

CHAPTER 4: Development of an Organic Photoredox-Catalyzed Strategy for Modular Aliphatic C–H Functionalization.....	71
4.1 Introduction.....	71
4.2 Photoredox-Catalyzed C–H Bond Functionalization.....	72
4.3 Reaction Development.....	73
4.3.1 Reaction Optimization.....	73
4.3.2 C–H Azidation Substrate Scope.....	76
4.3.3 Development of Modular C–H Transformations.....	78
4.3.4 C–H Functionalization of Complex Targets.....	80
4.3.5 Mechanistic Experiments.....	81
4.3.6 Proposed Mechanism.....	84
4.4 Application Toward Polyolefin Azidation.....	85
4.5 Conclusions.....	87
References.....	89
CHAPTER 5: Quaternary Center Construction via Coupling of Acyl Xanthates with Unactivated Alkenes.....	91
5.1 Introduction.....	91
5.2 Background.....	93
5.3 Reaction Development.....	94
5.3.1 Optimization.....	94
5.3.2 Substrate Scope.....	96
5.3.3 Mechanistic Studies and Hypothesis.....	100
5.3.4 Diversification of Xanthate Products .....	101
5.4 Conclusions.....	102

References.....	103
APPENDIX A: Supporting Information for Chapter 2.....	105
APPENDIX B: Supporting Information for Chapter 3.....	203
APPENDIX C: Supporting Information for Chapter 4.....	246
APPENDIX D: Supporting Information for Chapter 5.....	290

## LIST OF FIGURES

Figure 1.1	Bioactive compounds containing unactivated aliphatic C–H bonds.....	1
Figure 1.2	Enzyme-catalyzed aliphatic C–H functionalizations.....	2
Figure 1.3	Hoffmann-Löffler-Freytag reaction.....	3
Figure 1.4	Amide-directed unactivated aliphatic C–H alkylation.....	3
Figure 1.5	Bond dissociation energies of representative organic compounds.....	4
Figure 1.6	Unactivated aliphatic C–H oxidation via strained electrophilic heterocycles...	5
Figure 1.7	Iron-catalyzed unactivated aliphatic C–H bond oxidation.....	6
Figure 1.8	Polyoxometalate-catalyzed unactivated alkane C–H oxidation.....	6
Figure 1.9	Electrochemical aliphatic C–H oxidation.....	7
Figure 1.10	Unactivated aliphatic C–H amination.....	7
Figure 1.11	Aliphatic C–H azidation.....	8
Figure 1.12	Silver-catalyzed unactivated aliphatic C–H trifluoromethylthiolation.....	9
Figure 1.13	Photoredox-catalyzed unactivated aliphatic C–H trifluoromethylthiolation.....	9
Figure 1.14	Methods of aliphatic C–H fluorination.....	10
Figure 1.15	Unactivated aliphatic C–H halogenation using manganese porphyrin catalysts.....	11
Figure 1.16	Unactivated aliphatic C–H bromination using <i>N</i> -bromoamides.....	12
Figure 1.17	Proposed mechanism for C–H bromination using <i>N</i> -bromoamides.....	12
Figure 1.18	Unactivated aliphatic C–H chlorination using <i>N</i> -chloroamides.....	13
Figure 1.19	Unactivated aliphatic C–H alkylation using polyoxotungstate catalysis.....	14
Figure 1.20	C–H alkylation using a photoexcited aryl ketone.....	14
Figure 2.1	Thiocarbonyl compounds.....	20
Figure 2.2	Alkyl xanthate synthesis via nucleophilic substitution.....	21



Figure 2.3	Polar aminolysis of xanthate functionality.....	21
Figure 2.4	Tin-based radical addition to an unactivated olefin.....	22
Figure 2.5	Radical xanthate addition to unactivated olefins.....	23
Figure 2.6	Carbon-carbon bond-forming group transfer reactions of alkyl xanthates.....	24
Figure 2.7	Carbon-heteroatom bond-forming group transfer reactions of alkyl xanthates.....	24
Figure 2.8	C–H xanthylation of hydrocarbon solvents.....	25
Figure 2.9	Reagent design for C–H xanthylation.....	25
Figure 2.10	Previous synthesis and application of <i>N</i> -xanthylamides.....	26
Figure 2.11	Unsuccessful synthesis of <i>N</i> -xanthylamide <b>2.8</b> .....	26
Figure 2.12	Preparation of <i>N</i> -xanthylamide <b>2.8</b> .....	27
Figure 2.13	UV-Vis absorbance spectrum of xanthylamide <b>2.8</b> .....	29
Figure 2.14	Substrate scope for aliphatic C–H xanthylation.....	32
Figure 2.15	C–H xanthylation of complex molecules.....	34
Figure 2.16	Mechanistic experiments.....	36
Figure 2.17	Proposed mechanism for C–H xanthylation.....	36
Figure 2.18	C–H transformations of complex substrates via alkyl xanthate intermediates.....	37
Figure 2.19	Two-step C–H diversification of (+)-sclareolide.....	40
Figure 2.20	Acidic additives to mitigate amine nucleophilicity.....	41
Figure 2.21	Resistance of dithiocarbamates to polar aminolysis.....	42
Figure 3.1	Structures of widely used commodity polyolefins.....	45
Figure 3.2	Ziegler-Natta chain-growth polymerization of ethylene.....	46
Figure 3.3	Copolymerization of ethylene with functionalized monomers.....	47

Figure 3.4	Copolymerization of ethylene with a monomer containing borane functionality.....	48
Figure 3.5	Post-polymerization modification of polyethylene with maleic anhydride.....	49
Figure 3.6	Copper catalyzed C–H insertion of poly(1-butene).....	49
Figure 3.7	Polyolefin dehydrogenation via an iridium pincer complex.....	50
Figure 3.8	C–H oxidation of polyethylene- <i>alt</i> -propylene using a manganese porphyrin catalyst.....	51
Figure 3.9	Polyolefin C–H borylation/hydroxylation via rhodium catalysis.....	51
Figure 3.10	Nickel-catalyzed polyethylene functionalization.....	53
Figure 3.11	NHPI-catalyzed amination of polyethylene.....	53
Figure 3.12	C–H azidation of isotactic polypropylene.....	54
Figure 3.13	Representative $^1\text{H}$ NMR spectrum of xanthylated PEE.....	57
Figure 3.14	$^1\text{H}$ – $^{13}\text{C}$ HSQC of xanthylated PEE.....	58
Figure 3.15	GPC chromatograms of xanthylated PEE.....	59
Figure 3.16	FT-IR spectra of xanthylated PEE.....	59
Figure 3.17	Thermal Chugaev elimination of PEE.....	60
Figure 3.18	Differential scanning calorimetry curves used to determine $T_g$ of xanthylated PEE.....	60
Figure 3.19	DEPT NMR experiment on 15 mol % xanthylated PEE.....	61
Figure 3.20	Synthesis of model substrate <b>3.2</b> .....	61
Figure 3.21	Synthesis of tertiary xanthate <b>3.3</b> .....	62
Figure 3.22	Gas chromatograms of model substrate alkyl xanthates.....	62
Figure 3.23	Diversification of xanthylated PEE.....	63
Figure 3.24	Reaction of HBPE with maleic anhydride.....	67

Figure 4.1	Photoredox-based activated C–H bond alkylation and arylation.....	72
Figure 4.2	Substrate scope for C–H azidation.....	77
Figure 4.3	C–H Diversification via reagent selection.....	78
Figure 4.4	Modular C–H diversification of bioactive complex molecules.....	81
Figure 4.5	Stern-Volmer quenching of acridinium catalyst.....	82
Figure 4.6	Addition of <b>4.29</b> to acridinium catalyst <b>4.1</b> <sup>1</sup> H NMR. ....	83
Figure 4.7	Reactions with dibasic phosphate <b>4.29</b> .....	84
Figure 4.8	Proposed mechanism for C–H azidation.....	84
Figure 4.9	Initial azidation attempt with PEE.....	86
Figure 4.10	Productive C–H azidation and CuAAC of PEE.....	86
Figure 4.11	Infrared spectrum of <b>4.33</b> .....	86
Figure 4.12	Gel permeation chromatogram of <b>4.34</b> .....	87
Figure 4.13	C–H azidation and CuAAC of HBPE.....	88
Figure 5.1	Quaternary center formation via Barton esters.....	91
Figure 5.2	Reductive coupling of unactivated alkenes with electron-poor alkenes.....	92
Figure 5.3	Generation of quaternary centers via coupling of tertiary alcohols or carboxylic acid derivatives with activated alkenes.....	92
Figure 5.4	Strategies for the synthesis of tertiary alkyl xanthates .....	93
Figure 5.5	Acyl xanthate synthesis and decomposition pathway.....	94
Figure 5.6	Two-step decarbonylative addition of a cyclopropyl acyl xanthate to allyl acetate.....	94
Figure 5.7	Lack of reactivity with secondary acyl xanthates in the alkene addition .....	96
Figure 5.8	Mechanistic experiments.....	100

Figure 5.9	Proposed mechanism for quaternary construction via acyl xanthates .....	101
Figure 5.10	Diversification of xanthate coupling products.....	102

## LIST OF TABLES

Table 2.1	Optimization of C–H xanthylation via radical initiation.....	28
Table 2.2	Optimization of light-mediated C–H xanthylation.....	30
Table 2.3	Optimization of C–H xanthylation with (+)-sclareolide.....	31
Table 3.1	C–H xanthylation of poly(ethylethylene).....	56
Table 3.2	Xanthylation of commodity polyolefins.....	66
Table 4.1	Optimization of C–H azidation with cyclooctane.....	74
Table 4.2	Optimization of C–H azidation with methyl 6-methylheptanoate.....	75
Table 4.3	Optimization of C–H alkylation with cyclooctane.....	80
Table 5.1	Optimization for quaternary center construction.....	95
Table 5.2	Unactivated olefin scope for intermolecular quaternary center construction .....	97
Table 5.3	Acyl xanthate scope for intermolecular quaternary center construction.....	98
Table 5.4	Intramolecular quaternary center construction via cyclizations of unsaturated tertiary acyl xanthates.....	99

## LIST OF ABBREVIATIONS AND SYMBOLS

$^{13}\text{C}$ NMR	Carbon-13 nuclear magnetic resonance
$^1\text{H}$ NMR	Proton magnetic resonance
Å	Angstrom
Ac	Acetyl
acac	acetylacetone
AIBN	Azobisisobutyronitrile
BDE	Bond dissociation enthalpy
BLED	Blue light emitting diode
Boc	<i>tert</i> -butyloxycarbonyl
bpy	2,2'-bipyridyl
BPO	Benzoyl peroxide
Bz	Benzoate
CFL	Compact Fluorescent Light
CuAAC	Copper (I)-catalyzed azide alkyne cycloaddition
CV	Cyclic voltammetry
Đ	Dispersity
DCB	1,2-Dichlorobenzene
DCE	1,2-Dichloroethane
DCM	Dichloromethane
DEPT	Distortionless Enhancement by Polarization Transfer
Dfs	2,6-Difluorophenylsulfonate
DLP	Dilauroyl peroxide

DMF	<i>N,N</i> -Dimethylformamide
DSC	Differential Scan Calorimetry
DTBP	Di- <i>tert</i> -butyl peroxide
$e^-$	Electron
$E^*$	Excited state redox potential
$E_{1/2}$	Half-wave potential
$E_{p/2}$	Half-peak potential
EDA	Ethylene Diamine
ESI	Electrospray ionization
ET	Electron Transfer
Et <sub>2</sub> O	Diethyl ether
EtOH	Ethanol
EtOAc	Ethyl Acetate
eV	Electronvolt
GC	Gas Chromatography
GPC	Gel permeation chromatography
HBPE	Hyperbranched polyethylene
Hex	Hexyl
HFIP	1,1,1,3,3,3-Hexafluoroisopropanol
HRMS	High resolution mass spectrometry
$h\nu$	Photon or energy of a photon
<i>i</i> -PP	Isotactic polypropylene
IR	Infrared

$k$	General symbol for rate constant
LED	Light emitting diode
M	Molar or mol L <sup>-1</sup>
$M_N$	Number average molar mass
m/z	Mass per charge
MeCN	Acetonitrile
Mes	Mesityl
MS	Mass spectrometry
MVK	Methyl vinyl ketone
NCS	<i>N</i> -chlorosuccinimide
NFSI	<i>N</i> -fluorobenzenesulfonimide
NHPI	<i>N</i> -hydroxyphthalimide
NMR	Nuclear magnetic resonance
nm	Nanometer
ns	Nanosecond
PDA	Photodiode array
PDI	Polydispersity index
PE	Polyethylene
PP	Polypropylene
PEE	Poly(ethylene)
PEP	Polyethylene- <i>alt</i> -propylene
PhCl	Chlorobenzene
PhH	Benzene



PhCF <sub>3</sub>	Trifluorotoluene
PhMe	Toluene
Piv	Pivalate
PB	Polyisobutylene
PMP	<i>Para</i> -methoxy phenyl
PPM	Post-polymerization Modification
RAFT	Reversible Addition Fragmentation Transfer
SCE	Saturated calomel electrode
SET	Single electron transfer
T	Temperature
TBA	Tetra <i>n</i> -butylammonium
TMS	Trimethylsilyl
<i>t</i> -Bu	<i>tert</i> -Butyl
TCSPC	Time correlated single photon counting
TEMPO or TEMPO•	(2,2,6,6-Tetramethylpiperdin-1-yl)oxyl
TFA	Trifluoroacetic acid
TFE	2,2,2-Trifluoroethanol
<i>T<sub>g</sub></i>	Glass Transition Temperature
TGA	Thermal Gravimetric Analysis
THF	Tetrahydrofuran
Ts	<i>p</i> -Toluenesulfonyl
UV-Vis	Ultraviolet-visible absorption spectroscopy
V	Volt

$W$	Watts
$\tau_F$	Lifetime of fluorescence
$\lambda$	Wavelength

## CHAPTER ONE: STRATEGIES FOR INTERMOLECULAR FUNCTIONALIZATION OF UNACTIVATED ALIPHATIC C–H BONDS

### 1.1 Introduction

The field of organic synthesis has long relied on functional group manipulations and interconversions to access desired compounds. Despite the clear success of this traditional strategy, there exist limitations in the ability to access novel bond-forming reactions distal from existing molecular functionality. Within organic compounds, aliphatic C–H bonds are ubiquitous but have been underutilized as a potential functional group handle due to their inertness compared to traditionally manipulated moieties. Additionally, the abundance and chemical similarity of these bonds renders them challenging to differentiate, making site-selectivity of any potential C–H functionalization reaction a significant obstacle. For instance, each bioactive compound shown in **Figure 1.1** possesses over 18 aliphatic C–H bonds, and a reaction involving these bonds could, in principle, occur at any site.

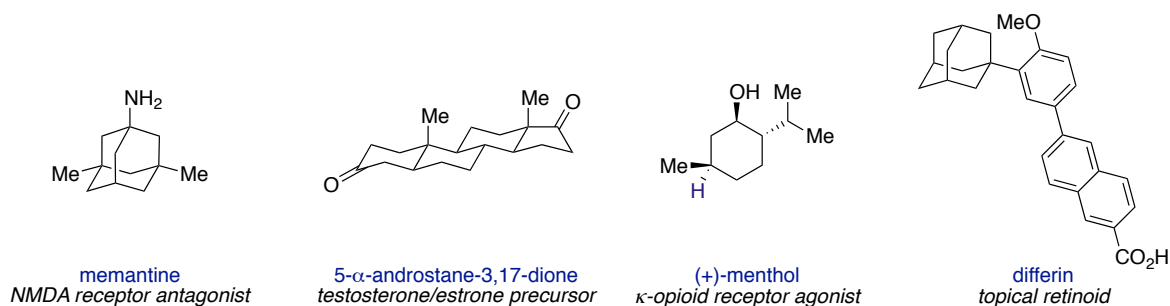


**Figure 1.1** Bioactive compounds containing unactivated aliphatic C–H bonds.

In nature, enzymes have evolved the ability to catalyze several types of C–H functionalizations, including oxidation and halogenation reactions (**Figure 1.2**).<sup>1,2</sup> These

reactions tend to proceed with exquisite levels of site- and stereoselectivity, but are often limited in scope due to the necessity that the substrate engage with the enzyme's complex active site. The ability to access similarly selective transformations with chemical reagents would significantly broaden the substrate scope for such reactions and make them accessible to synthetic chemists.<sup>3–6</sup> This would enable diverse aliphatic C–H bonds to be used as functional handles, allowing for different and useful retrosynthetic disconnections and novel strategies for constructing and derivatizing complex molecules.<sup>7</sup>

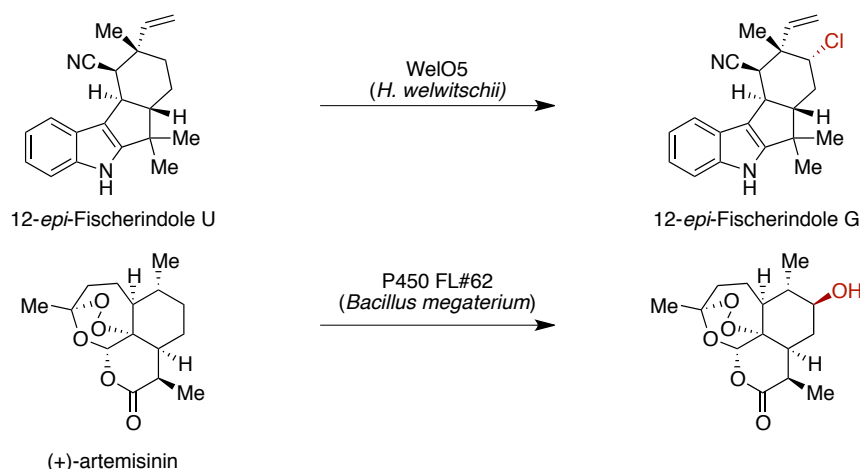


**Figure 1.2** Enzyme-catalyzed aliphatic C–H functionalizations.

## 1.2 Intramolecular Aliphatic C–H Functionalization

One existing strategy to achieve high levels of site-selectivity for C–H functionalizations is to use a preexisting functional group or a derivative thereof as a directing group for intramolecular reactivity. Such a strategy exploits inherent conformational biases to afford products with high levels of selectivity for a particular site. For instance, the Hofmann-Löffler-Freytag reaction involves the use of *N*-haloamines to generate amine cation radicals capable of performing a kinetically favorable 1,5-hydrogen atom abstraction (**Figure 1.3**).<sup>8,9</sup> The resultant carbon-centered radical can abstract a halogen atom to propagate the radical chain, and subsequent basic workup leads to pyrrolidines via a

net intramolecular C–H amination. Several improvements on this reactivity have been reported with the aim of increasing functional group tolerance and synthetic utility,<sup>10,11</sup> and they display the same site selectivity due to the intramolecular nature of the reaction.

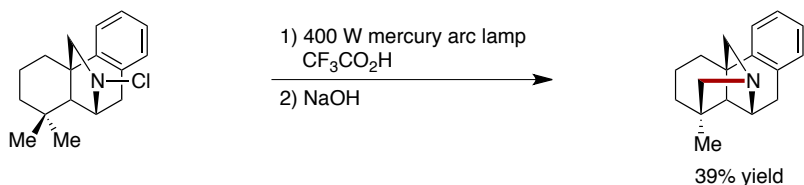


**Figure 1.3** Hoffmann-Löffler-Freytag reaction.

More recently, several examples of substrate directed C–H alkylation proceeding through a similar strategy have been reported. Knowles and Rovis independently disclosed the use of photoredox catalysis to generate amidyl radicals poised to undergo 1,5-hydrogen atom abstraction with a pendant alkane (**Figure 1.4**).<sup>12,13,14</sup> The resultant carbon-centered radical underwent conjugate addition to activated olefin acceptors, producing net substrate-directed C–H alkylation products. Although Knowles reported initial results toward intermolecular C–H alkylation in the same work, they necessitated the use of 10 equivalents of alkane substrate, restricting synthetic utility.

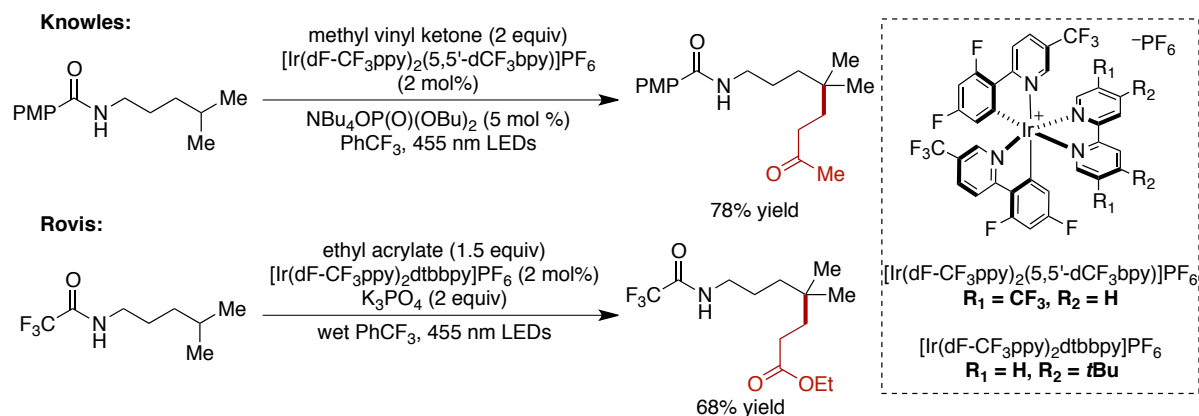


**Figure 1.4** Amide-directed unactivated aliphatic C–H alkylation.

### 1.3 Intermolecular Aliphatic C–H Functionalization

In contrast to intramolecular strategies that use inherent molecular functionality to direct reactivity, intermolecular reactions do not possess such advantages with respect to site selectivity. Additionally, increased kinetic favorability due to increased effective concentration of the reactive components is absent for intermolecular reactions. While selective intermolecular C–H functionalizations would offer great benefits to chemical synthesis, there are several factors that have hindered the development of these reactions. In many cases, excess hydrocarbon substrate is required to achieve synthetically useful yields; however, this limits the application to the late-stage derivatization of more complex and valuable substrates. Additionally, few reagents are capable of both efficient and regioselective C–H functionalizations due to the inherent high reactivity associated with such species and the comparable bond strengths of many aliphatic C–H bonds (**Figure 1.5**).<sup>15</sup> Despite these challenges, however, significant advances have been made in this arena.

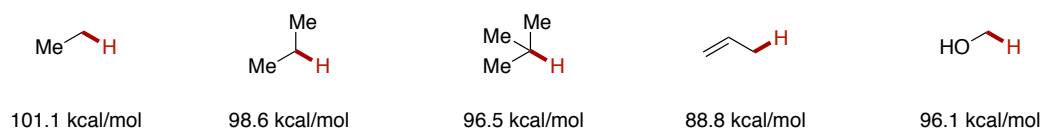


**Figure 1.5** Bond dissociation energies of representative organic compounds.

#### 1.3.1 Unactivated Aliphatic C–H Oxidation

Since the 1980's, C–H bond oxidations have been studied in the context of strained oxygen-containing heterocycles. Curci developed an oxidation system using dioxirane reagents derived from acetone or trifluoroacetone (**Figure 1.6**).<sup>16,17,18</sup> A variety of alkanes were oxidized in high yields and short reaction times, with site selectivity generally for hydroxylation at the most electron-rich tertiary site. Mechanistic studies suggest that a concerted, asynchronous C–H insertion occurs to provide the oxidized products.<sup>19</sup> However, the dioxirane reagents exhibit limited utility due to instability at temperatures above –20 °C

and to visible light. To mitigate these operational issues, Du Bois developed a catalytic method to access oxaziridines *in situ* using a benzoxathiazine catalyst, aqueous hydrogen peroxide, and acetic acid.<sup>20</sup> Similar site selectivity for electron-rich tertiary sites is observed with this system.

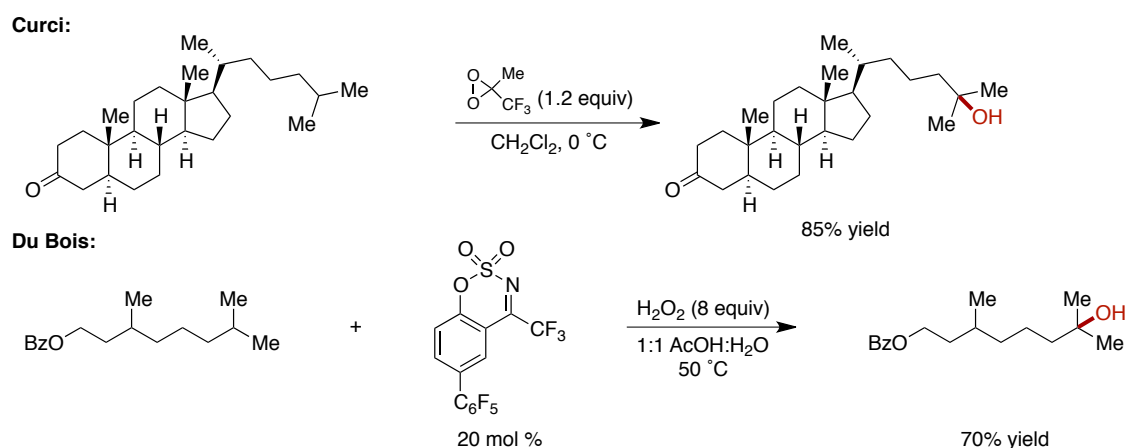


**Figure 1.6** Unactivated aliphatic C–H oxidation via strained electrophilic heterocycles.

Transition metal-catalyzed biomimetic oxidation systems constitute an additional class of aliphatic C–H oxidation reactions. In 2007, White first reported a selective aliphatic oxidation reaction that favored tertiary C–H bonds using an iron (II) catalyst, hydrogen peroxide, and acetic acid (**Figure 1.7**).<sup>21</sup> This system could functionalize tertiary C–H bonds distal to electron-withdrawing groups, though isolation and recycling of unreacted starting material was often necessary to achieve synthetically useful yields. Changing the ligand set on the catalyst allowed for selectivity to be controlled by nonbonding interactions between the substrate and catalyst,<sup>22,23</sup> whereas the prior work had utilized the substrate's inherent stereoelectronic biases. More recently, strategies to expand the substrate scope to nitrogenous heterocycles, which are problematic for metal-oxo catalysts, have also been developed.<sup>24</sup>

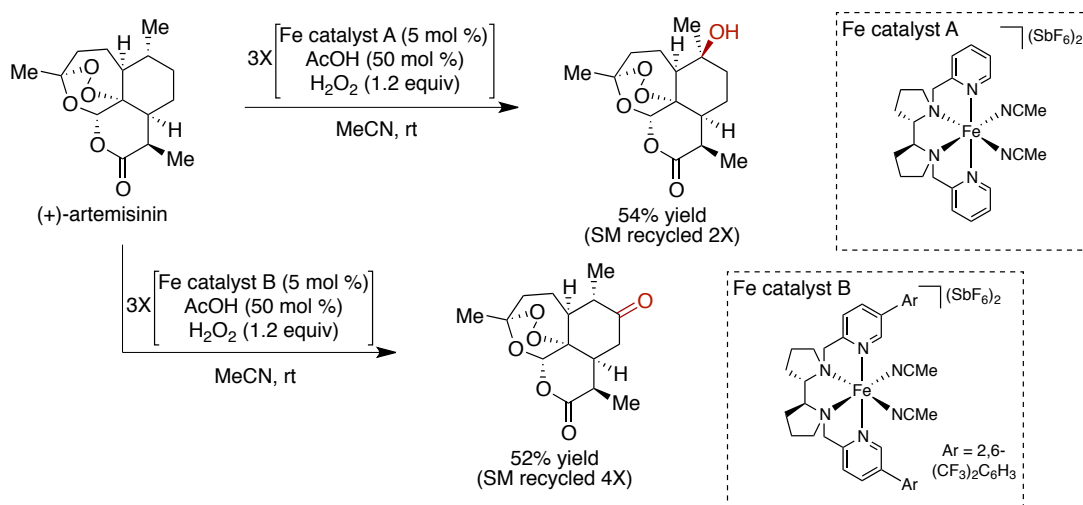


**Figure 1.7** Iron-catalyzed unactivated aliphatic C–H bond oxidation.

Mizuno disclosed a secondary-selective hydroxylation of alkanes using a polyoxometalate catalyst and hydrogen peroxide (**Figure 1.8**).<sup>25</sup> Steric bulk around the divanadium-substituted phosphotungstate catalyst suppresses tertiary functionalization, and accordingly, oxidation is favored at methylene sites. Moreover, this methodology demonstrates the synthesis of alcohols, with no observed overoxidation to the corresponding ketone. Despite these advantages, the substrate scope is limited to simple alkanes with no additional functionality.

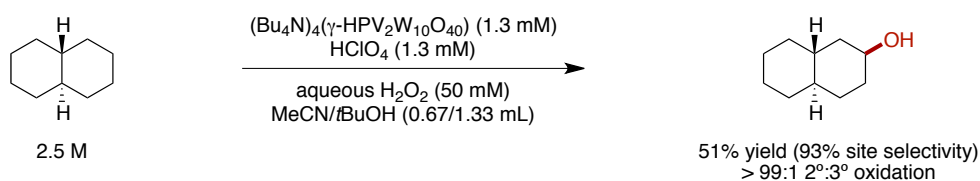


**Figure 1.8** Polyoxometalate-catalyzed unactivated alkane C–H oxidation.

Recently, Baran reported the electrochemical oxidation of alkanes to form ketones or alcohols (**Figure 1.9**).<sup>26</sup> Under these conditions, quinuclidine can be oxidized to the cation radical and abstract electron-rich C–H bonds, forming carbon-centered radicals that can be trapped with molecular oxygen. Selectivity is observed for electron-rich secondary C–H bonds or tertiary sites in molecules in which they are present. The utility of this strategy was



highlighted with an oxidation of (+)-sclareolide on 50 g scale to complete a synthesis of 2-oxo-yahazunone.

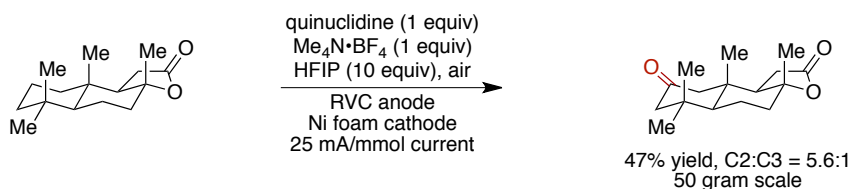


**Figure 1.9** Electrochemical aliphatic C–H oxidation.

### 1.3.2 Unactivated Aliphatic C–H Amination

Due to the abundance of nitrogen functionality in complex bioactive molecules, several groups have pursued methods to enable C–H amination of unactivated alkanes. Baran disclosed a Ritter-type amination of unactivated aliphatic C–H bonds using a copper catalyst and NFSI with acetonitrile as the nitrogen source to deliver amides following basic hydrolysis (**Figure 1.10**).<sup>27</sup> Substrates with alcohol or ketone functionality underwent directed amination, and alkane substrates without any functionality generally favored methylene functionalization. Du Bois also reported a method for C–H amination through the controlled generation of rhodium nitrenoids capable of C–H insertion.<sup>28</sup> Selectivity is generally observed for the most electron-rich tertiary site, but benzylic functionalization can also occur. This work was later extended in a collaboration with Sigman to develop a model for describing the site selectivity of the amination.<sup>29</sup>

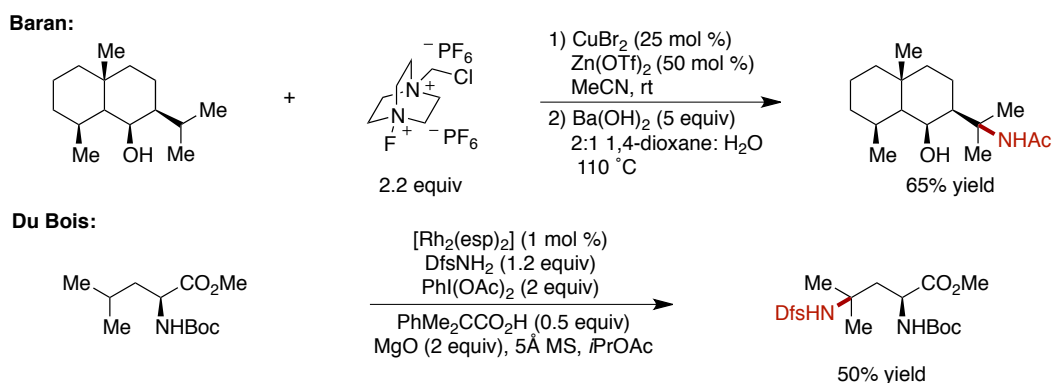


**Figure 1.10** Unactivated aliphatic C–H amination.

In 2015, Hartwig reported an intermolecular azidation of tertiary C–H bonds using an iron (II) catalyst, tridentate bis(oxazoline) ligand, and an azidoiodinane as the azide source (**Figure 1.11**).<sup>30,31</sup> Functionalization occurred at tertiary sites distal from electron-withdrawing moieties, but yields were generally modest. Tang has also reported a C–H azidation using potassium persulfate as the abstracting agent.<sup>32</sup> Excess substrate was needed to achieve synthetically useful yields in several examples, and either secondary or tertiary azidation could be observed, dependent on the specific substrate. Groves has also developed a methodology for C–H azidation using a manganese porphyrin catalyst.<sup>33,34</sup> Reactivity occurred generally at benzylic or tertiary sites if present in the substrate, and mechanistic studies suggested the intermediacy of a manganese (V) oxo species capable of C–H abstraction. A recent expansion of this work used trimethylsilyl isocyanate to access aliphatic isocyanates and substituted ureas.<sup>35</sup>

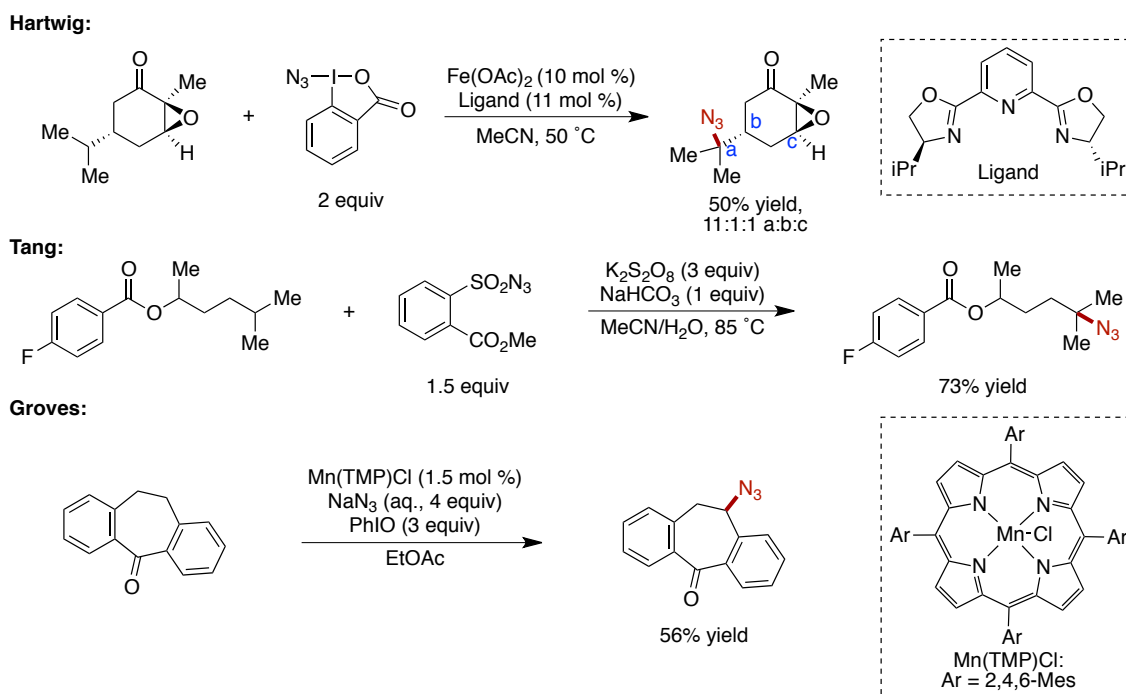


**Figure 1.11** Aliphatic C–H azidation.

### 1.3.3 Unactivated Aliphatic C–H Trifluoromethylthiolation

Due to the high electronegativity and lipophilicity of the trifluoromethylthiol group, its installation into drug molecules has been of interest to medicinal chemists.<sup>36</sup> Tang<sup>37</sup> and Liu and Chen<sup>38</sup> independently reported the C–H trifluoromethylthiolation of unactivated alkanes using stoichiometric silver (I) trifluoromethanethiolate and a persulfate oxidant (**Figure 1.12**). Selectivity for functionalization of the most electron-rich C–H bond was generally observed, affording tertiary trifluoromethanethiolates in cases where tertiary C–H bonds are present; otherwise, mixtures of secondary isomers are generally observed.

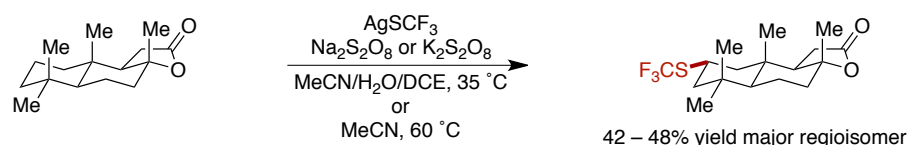


**Figure 1.12** Silver-catalyzed unactivated aliphatic C–H trifluoromethylthiolation.

Glorius has developed a strategy for aliphatic C–H trifluoromethylthiolation using photoredox catalysis (**Figure 1.13**).<sup>39</sup> The excited state iridium catalyst can undergo single electron transfer (SET) from a benzoate anion, generating an oxygen-centered radical capable of abstracting C–H bonds. The resultant carbon-centered radical can react with a *N*-(trifluoromethylthiol)phthalimide trap to form the C–S bond. Tertiary C–H bonds preferentially undergo functionalization, with high levels of site selectivity for positions distal from electron-withdrawing groups.

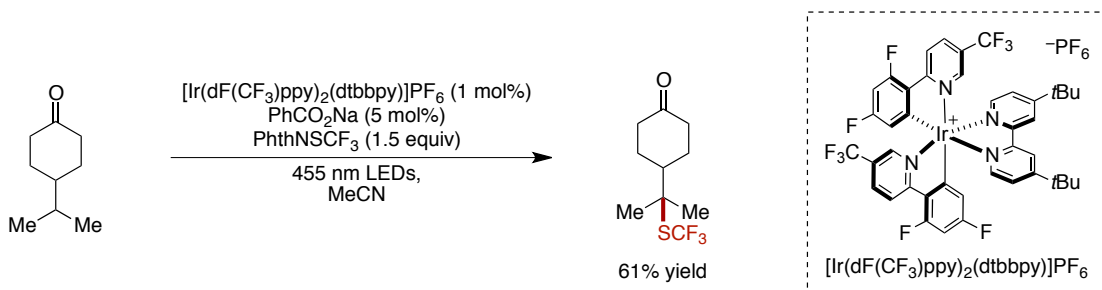


**Figure 1.13** Photoredox-catalyzed unactivated aliphatic C–H trifluoromethylthiolation.

### 1.3.4 Unactivated Aliphatic C–H Halogenation

There has been widespread interest in the C–H halogenation of unactivated alkanes due to the synthetic utility of alkyl halides and the generally beneficial effects of fluorination on the properties of medicinal chemistry compounds. Lectka has worked extensively in this field, disclosing several methods for C–H fluorination including a system cocatalytic in copper and NHPI with Selectfluor as the fluorine atom source (**Figure 1.14**).<sup>40</sup> Selectivity for benzylic positions is generally observed, and yields tend to be modest. Later work showed the ability of 1,2,4,5-tetracyanobenzene to form secondary alkyl radicals that could be trapped with Selectfluor.<sup>41</sup> Britton disclosed a method of unactivated aliphatic C–H fluorination using a tungsten photocatalyst.<sup>42</sup> Selectivity was generally for the most electron-rich C–H bond, either tertiary or secondary depending on substrate. Several other methods have been disclosed, often necessitating UV irradiation or transition metal catalysts.<sup>43</sup>

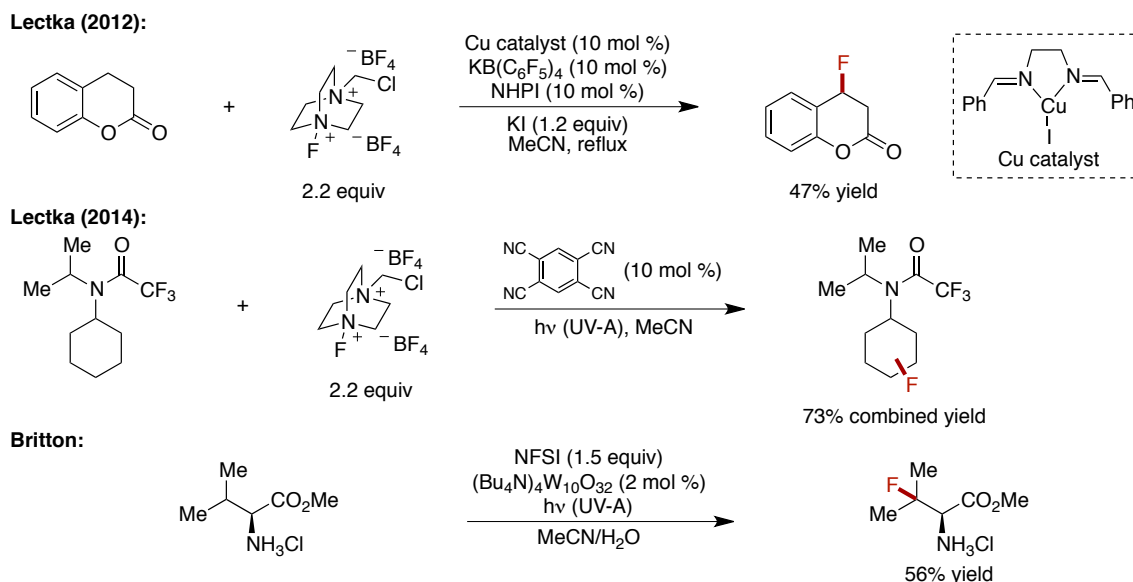


**Figure 1.14** Methods of aliphatic C–H fluorination.

Through the use of manganese porphyrin catalysis, Groves accomplished both the chlorination and fluorination of unactivated aliphatic C–H bonds (**Figure 1.15**).<sup>44,45</sup> Both

reactions are believed to proceed via a manganese (V) oxo species capable of abstracting C–H bonds, and chlorination could be achieved using sodium hypochlorite to form a putative manganese (IV) hypochlorite. Most substrates are used in excess to achieve synthetically useful yields, and little functional group tolerance is demonstrated. For fluorination, a manganese (IV) fluoride is generated *in situ*, and the bulky mesityl substituents on the porphyrin are believed to provide significant steric hindrance to the catalyst, enabling C–H abstraction at the most electron-rich and sterically accessible methylene sites.

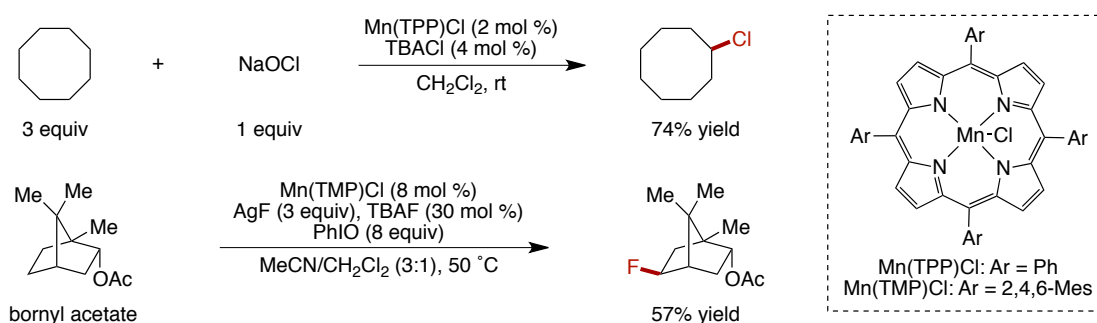


**Figure 1.15** Unactivated aliphatic C–H halogenation using manganese porphyrin catalysts.

In 2014, prior work in the Alexanian group detailed a site-selective C–H bromination that used *N*-bromoamides with visible light initiation to generate amidyl radicals capable of C–H bond abstraction (**Figure 1.16**).<sup>46</sup> While a number of bromoamides were surveyed, the most efficient reagent **1.1** possessed an electron-deficient bis(trifluoromethyl)-substituted arene and a *tert*-butyl substituent on nitrogen. A high degree of selectivity was observed for secondary bromination compared to tertiary sites in the same molecule, such as for methylcyclohexane, despite the lower BDEs associated with the tertiary C–H bonds. This is due to the significant steric bulk surrounding the amidyl radical, which cannot effectively abstract C–H bonds from the hindered tertiary sites, complementary to many other C–H functionalization reactions. For more complex hydrocarbon substrates, such as decalin,

adamantane and 1,2-dimethylcyclohexane, high levels of site selectivity were observed, and good yields were observed with the substrate as limiting reagent in all examples.

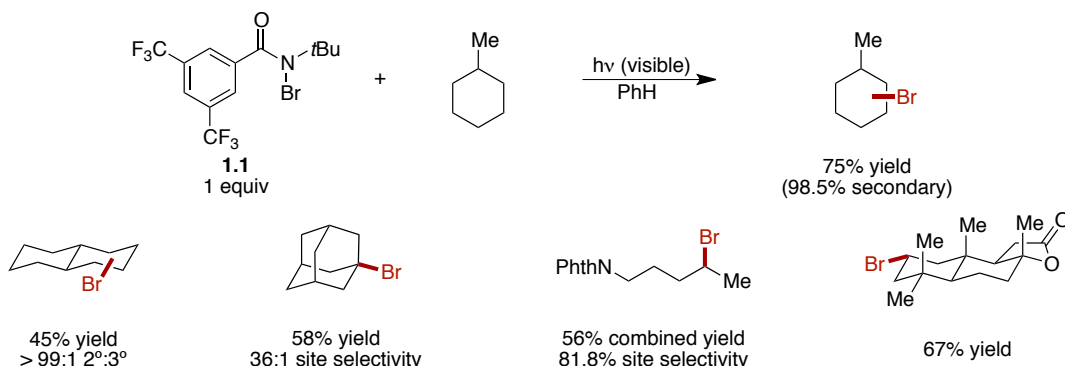


**Figure 1.16** Unactivated aliphatic C–H bromination using *N*-bromoamides.

In addition to steric selectivity, *N*-bromoamide **1.1** exhibits a high degree of electronic selectivity for the most distal methylene relative to an electron-withdrawing substituent. For example, *N*-pentylphthalimide was brominated in 81.8% selectivity for the most distal methylene site with a combined yield of 56%. The stereoelectronic selectivity was illustrated with the terpenoid natural product (+)-sclareolide, which underwent bromination at the most sterically accessible and electron-rich methylene site to produce a single brominated diastereomer.

Upon exposure to visible light, N–Br bond homolysis occurs, forming a putative amidyl radical **1.2** (Figure 1.17). This highly electrophilic nitrogen-centered radical can abstract a C–H bond from an alkane substrate, forming a carbon-centered radical.

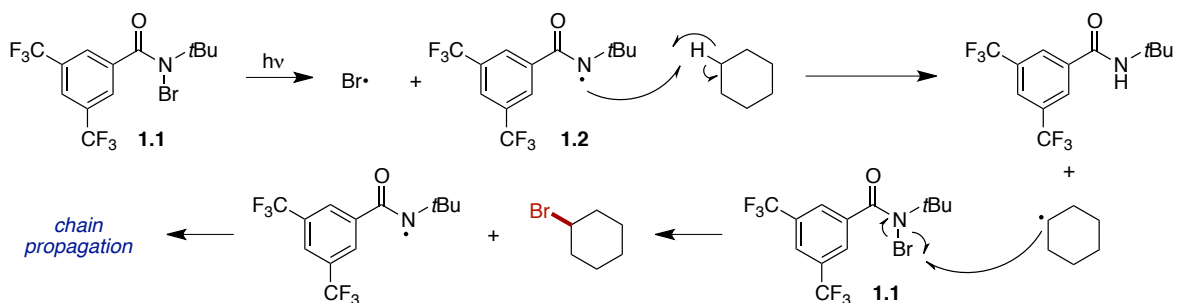


**Figure 1.17** Proposed mechanism for C–H bromination using *N*-bromoamides.

This species can abstract a bromine atom from another molecule of **1.1**, forming the alkyl bromide product in a chain-propagating step. From a competition experiment between cyclohexane and  $d_{12}$ -cyclohexane, a kinetic isotope effect of  $k_H/k_D = 5.8$  was measured, consistent with the occurrence of irreversible C–H bond abstraction.

A similar reagent, *N*-chloroamide **1.3**, was developed to allow for the visible light-mediated C–H chlorination of unactivated alkanes (**Figure 1.18**).<sup>47</sup> Stoichiometric cesium carbonate was added to prevent trace acid from reacting with **1.3** to produce molecular chlorine, which could undergo nonselective background chlorination. Similar site selectivities were observed as with the C–H bromination, including reactivity generally occurring at the most electron-rich methylene site. In collaboration with the Vanderwal group, (+)-sclareolide was chlorinated in 82% yield on gram scale to provide the starting material for a total synthesis of chlorolissoclimide, an antiproliferative diterpenoid.

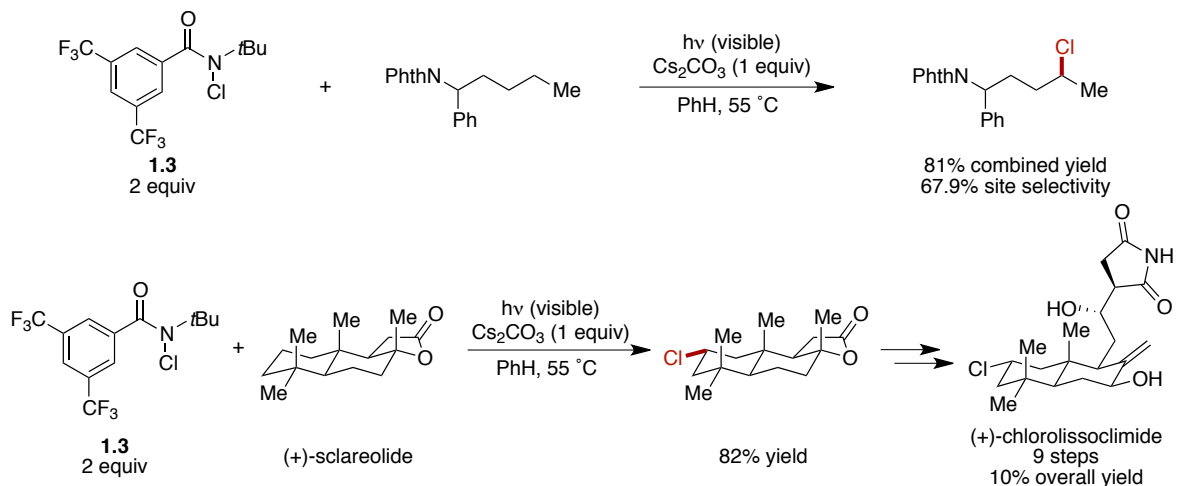


**Figure 1.18** Unactivated aliphatic C–H chlorination using *N*-chloroamides.

### 1.3.5 Unactivated Aliphatic C–H Alkylation

Compared to other C–H transformations of unactivated alkanes, perhaps the most useful disconnection that has been significantly underdeveloped is alkylation with olefinic traps to form new C–C bonds. While work has been accomplished using polyoxotungstate

catalysts as hydrogen atom-abstracting species with UV irradiation,<sup>48,49</sup> the substrate undergoing functionalization is often used in significant excess. Nonetheless, site selectivity for the most electron-rich C–H bond can be accomplished with such systems (**Figure 1.19**).<sup>50</sup>

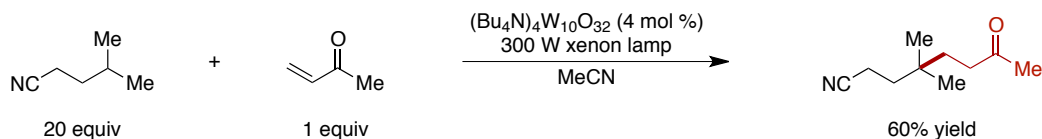


**Figure 1.19** Unactivated aliphatic C–H alkylation using polyoxotungstate catalysis.

Recent work by Murafuji used 2-chloroanthraquinone under UV irradiation to form C–H alkylation products with 1,1-bis(phenylsulfonyl)ethylene as the olefin trap (**Figure 1.20**).<sup>51</sup> Cyclohexane and several adamantane derivatives could be alkylated in good yields, but the substrate was generally the limiting reagent. For olefin, ether, or amine-containing substrates, reactivity occurred adjacent to these activating groups.

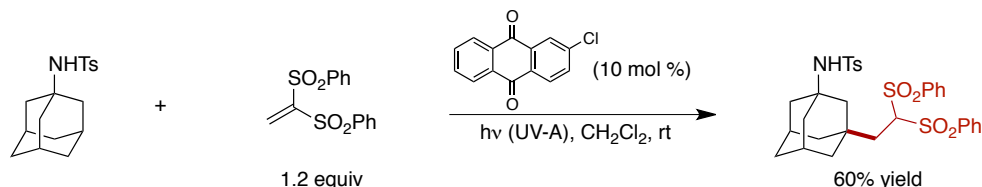


**Figure 1.20** C–H alkylation using a photoexcited aryl ketone.

## 1.4 Outlook

Despite the challenges associated with functionalizing unactivated aliphatic C–H bonds, great advances have been made in this field in recent years. A variety of C–H transformations are now accessible to synthetic chemists, and many groups continue to cultivate these methodologies further. Nonetheless, several significant problems plague the existing approaches. Many transformations are relatively inefficient and can only be used to access synthetically useful yields of functionalized products when the substrate is used in excess, limiting the applicability toward late-stage purposes. Additionally, a relatively small number of C–H transformations have been developed to date compared to the amount that



might be envisioned, offering fairly narrow utility in the context of late-stage diversification. Finally, new reagents or catalysts are generally required to develop novel transformations with consistent site selectivity, rendering the diversification of substrates through C–H functionalization impractical.

## REFERENCES

- (1) Hillwig, M. L.; Liu, X. *Nat. Chem. Biol.* **2014**, *10*, 921–923.
- (2) Zhang, K.; Shafer, B. M.; Demars, M. D.; Stern, H. A.; Fasan, R. *J. Am. Chem. Soc.* **2012**, *134*, 18695–18704.
- (3) Newhouse, T.; Baran, P. S. *Angew. Chem. Int. Ed.* **2011**, *50*, 3362–3374.
- (4) Yamaguchi, J.; Yamaguchi, A. D.; Itami, K. *Angew. Chem. Int. Ed.* **2012**, *51*, 8960–9009.
- (5) White, M. C. *Science* **2012**, *335*, 807–809.
- (6) Qin, Y.; Zhu, L.; Luo, S. *Chem. Rev.* **2017**, *117*, 9433–9520.
- (7) Cernak, T.; Dykstra, K. D.; Tyagarajan, S.; Vachal, P.; Krska, S. W. *Chem Soc Rev* **2016**, *45*, 546–576.
- (8) Shibnuma, Y.; Okamoto, T. *Chem. Pharm. Bull. (Tokyo)* **1985**, *33*, 3187–3194.
- (9) Majetich, G.; Wheless, K. *Tetrahedron* **1995**, *51*, 7095–7129.
- (10) In *Comprehensive Organic Name Reactions and Reagents*; John Wiley & Sons, Inc.: Hoboken, NJ, USA, 2010.
- (11) Wappes, E. A.; Fosu, S. C.; Chopko, T. C.; Nagib, D. A. *Angew. Chem. Int. Ed.* **2016**, *55*, 9974–9978.
- (12) Choi, G. J.; Zhu, Q.; Miller, D. C.; Gu, C. J.; Knowles, R. R. *Nature* **2016**, *539*, 268–271.
- (13) Chu, J. C. K.; Rovis, T. *Nature* **2016**, *539*, 272–275.
- (14) Chen, D.-F.; Chu, J. C. K.; Rovis, T. *J. Am. Chem. Soc.* **2017**, *139*, 14897–14900.
- (15) Blanksby, S. J.; Ellison, G. B. *Acc. Chem. Res.* **2003**, *36*, 255–263.
- (16) Mello, R.; Fiorentino, M.; Fusco, C.; Curci, R. *J. Am. Chem. Soc.* **1989**, *111*, 6749–6757.
- (17) Bovicelli, P.; Lupattelli, P.; Mincione, E.; Prencipe, T.; Curci, R. *J. Org. Chem.* **1992**, *57*, 2182–2184.
- (18) Bovicelli, P.; Lupattelli, P.; Mincione, E.; Prencipe, T.; Curci, R. *J. Org. Chem.* **1992**, *57*, 5052–5054.

- (19) Curci, R.; D'Accolti, L.; Fusco, C. *Acc. Chem. Res.* **2006**, *39*, 1–9.
- (20) Brodsky, B. H.; Du Bois, J. *J. Am. Chem. Soc.* **2005**, *127*, 15391–15393.
- (21) Chen, M. S.; White, M. C. *Science* **2007**, *318*, 783–787.
- (22) Chen, M. S.; White, M. C. *Science* **2010**, *327*, 566–571.
- (23) Gormisky, P. E.; White, M. C. *J. Am. Chem. Soc.* **2013**, *135*, 14052–14055.
- (24) Howell, J. M.; Feng, K.; Clark, J. R.; Trzepakowski, L. J.; White, M. C. *J. Am. Chem. Soc.* **2015**, *137*, 14590–14593.
- (25) Kamata, K.; Yonehara, K.; Nakagawa, Y.; Uehara, K.; Mizuno, N. *Nat. Chem.* **2010**, *2*, 478–483.
- (26) Kawamata, Y.; Yan, M.; Liu, Z.; Bao, D.-H.; Chen, J.; Starr, J. T.; Baran, P. S. *J. Am. Chem. Soc.* **2017**, *139*, 7448–7451.
- (27) Michaudel, Q.; Thevenet, D.; Baran, P. S. *J. Am. Chem. Soc.* **2012**, *134*, 2547–2550.
- (28) Roizen, J. L.; Zalatan, D. N.; Du Bois, J. *Angew. Chem. Int. Ed.* **2013**, *52*, 11343–11346.
- (29) Bess, E. N.; DeLuca, R. J.; Tindall, D. J.; Oderinde, M. S.; Roizen, J. L.; Du Bois, J.; Sigman, M. S. *J. Am. Chem. Soc.* **2014**, *136*, 5783–5789.
- (30) Sharma, A.; Hartwig, J. F. *Nature* **2015**, *517*, 600–604.
- (31) Karimov, R. R.; Sharma, A.; Hartwig, J. F. *ACS Cent. Sci.* **2016**, *2*, 715–724.
- (32) Zhang, X.; Yang, H.; Tang, P. *Org. Lett.* **2015**, *17*, 5828–5831.
- (33) Huang, X.; Bergsten, T. M.; Groves, J. T. *J. Am. Chem. Soc.* **2015**, *137*, 5300–5303.
- (34) Huang, X.; Groves, J. T. *ACS Catal.* **2016**, *6*, 751–759.
- (35) Huang, X.; Zhuang, T.; Kates, P. A.; Gao, H.; Chen, X.; Groves, J. T. *J. Am. Chem. Soc.* **2017**, *139*, 15407–15413.
- (36) Landelle, G.; Panossian, A.; R Leroux, F. *Curr. Top. Med. Chem.* **2014**, *14*, 941–951.
- (37) Guo, S.; Zhang, X.; Tang, P. *Angew. Chem. Int. Ed.* **2015**, *54*, 4065–4069.
- (38) Wu, H.; Xiao, Z.; Wu, J.; Guo, Y.; Xiao, J.-C.; Liu, C.; Chen, Q.-Y. *Angew. Chem. Int. Ed.* **2015**, *54*, 4070–4074.

- (39) Mukherjee, S.; Maji, B.; Tlahuext-Aca, A.; Glorius, F. *J. Am. Chem. Soc.* **2016**, *138*, 16200–16203.
- (40) Bloom, S.; Pitts, C. R.; Miller, D. C.; Haselton, N.; Holl, M. G.; Urheim, E.; Lectka, T. *Angew. Chem. Int. Ed.* **2012**, *51*, 10580–10583.
- (41) Bloom, S.; Knippel, J. L.; Lectka, T. *Chem Sci* **2014**, *5*, 1175–1178.
- (42) Halperin, S. D.; Fan, H.; Chang, S.; Martin, R. E.; Britton, R. *Angew. Chem. Int. Ed.* **2014**, *53*, 4690–4693.
- (43) Lin, A.; Huehls, C. B.; Yang, J. *Org Chem Front* **2014**, *1*, 434–438.
- (44) Liu, W.; Groves, J. T. *J. Am. Chem. Soc.* **2010**, *132*, 12847–12849.
- (45) Liu, W.; Huang, X.; Cheng, M.-J.; Nielsen, R. J.; Goddard, W. A.; Groves, J. T. *Science* **2012**, *337*, 1322–1325.
- (46) Schmidt, V. A.; Quinn, R. K.; Brusoe, A. T.; Alexanian, E. J. *J. Am. Chem. Soc.* **2014**, *136*, 14389–14392.
- (47) Quinn, R. K.; Könst, Z. A.; Michalak, S. E.; Schmidt, Y.; Szklarski, A. R.; Flores, A. R.; Nam, S.; Horne, D. A.; Vanderwal, C. D.; Alexanian, E. J. *J. Am. Chem. Soc.* **2016**, *138*, 696–702.
- (48) Dondi, D.; Fagnoni, M.; Molinari, A.; Maldotti, A.; Albini, A. *Chem. - Eur. J.* **2004**, *10*, 142–148.
- (49) Okada, M.; Fukuyama, T.; Yamada, K.; Ryu, I.; Ravelli, D.; Fagnoni, M. *Chem Sci* **2014**, *5*, 2893–2898.
- (50) Yamada, K.; Okada, M.; Fukuyama, T.; Ravelli, D.; Fagnoni, M.; Ryu, I. *Org. Lett.* **2015**, *17*, 1292–1295.
- (51) Kamijo, S.; Takao, G.; Kamijo, K.; Tsuno, T.; Ishiguro, K.; Murafuji, T. *Org. Lett.* **2016**, *18*, 4912–4915.

## CHAPTER TWO: INTERMOLECULAR ALIPHATIC C–H XANTHYLATION AS A STRATEGY FOR SMALL MOLECULE DIVERSIFICATION

Adapted from: Czaplyski, W. L.; Na, C. G.; Alexanian, E. J. *J. Am. Chem. Soc.* **2016**, *138*, 13854. Copyright 2017 American Chemical Society.

### 2.1 Introduction

The development of methods for the site-selective conversion of ubiquitous aliphatic C–H bonds into C–heteroatom or C–C bonds provides powerful opportunities in the synthesis of natural products, agrochemicals, and pharmaceuticals.<sup>1–4</sup> Strategies that use a directing group to dictate regioselectivity have been used in a variety of applications due to the improved kinetics associated with intramolecular reactivity. However, since this method requires certain functionality to be present in a compound, it does not lend itself to a broad approach for C–H functionalization. The development of site-selective intermolecular C–H functionalization strategies, however, would allow for more generalizable applications to complex molecule construction and diversification.

While significant progress has been made in this field (see **Chapter 1**), there are still several challenges that restrict broad utility of current methods. To avoid problems with reaction efficiency and unnecessary waste production, the substrate undergoing functionalization must be the limiting reagent. However, many modern strategies use the substrate in excess to obtain synthetically useful quantities of functionalized product. Furthermore, the types of transformations currently accessible through alkane functionalization are limited, with oxidation, azidation, and halogenation being among the

most explored and few examples of C–C bond forming reactions. Expansion of the scope of C–H transformations available would broaden the utility of alkane functionalization as a strategy for chemical synthesis. Additionally, current methods rely on reagents or catalysts that possess individual selectivity profiles, rendering it difficult to modulate C–H transformations at a given site on a molecule. A strategy for C–H functionalization that can provide a number of different transformations with common site selectivity would allow for advances in diversification of complex molecules.<sup>5</sup>

## 2.2 Background

### 2.2.1 Properties and Synthesis of Alkyl Xanthates

In targeting a diversification strategy for aliphatic C–H functionalization, we were drawn to the well-precedented reactivity of the xanthate, or dithiocarbonate, group (**Figure 2.1**),<sup>6–8</sup> thiocarbonyl compounds related to dithiocarbamates, trithiocarbonates, and several others. Due to the disparity in atomic size between the carbon and sulfur atoms in the thiocarbonyl, there is relatively poor overlap between the p orbitals of the two atoms compared to that between carbon and oxygen in an analogous carbonyl compound. This results in a weaker  $\pi$  bond in the thiocarbonyl, causing it to be both longer than a carbonyl (1.6 Å vs. 1.25 Å) and weaker in bond strength by 40–50 kcal/mol. These factors increase the radicophilicity of the xanthate functional group, making it susceptible to nucleophilic radical addition on sulfur and attractive for use in chain processes.

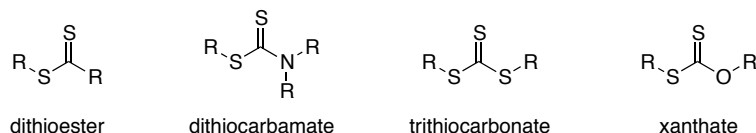


**Figure 2.1** Thiocarbonyl compounds.

Primary or secondary aliphatic xanthates are generally accessed via the substitution reaction of the corresponding alkyl halide or tosylate with commercially available potassium ethyl xanthate,<sup>9</sup> costing as little as \$0.45/gram (**Figure 2.2**). These primary or secondary alkyl xanthates are usually stable under ambient conditions without special handling.

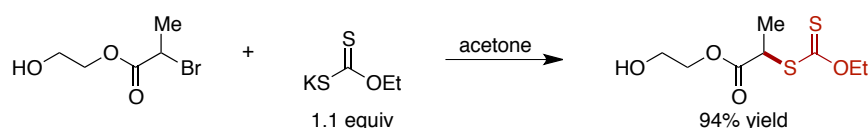


**Figure 2.2** Alkyl xanthate synthesis via nucleophilic substitution.

However, there are few strategies to access tertiary alkyl xanthates, and they are generally substrate-specific and limited in scope (see **Chapter 5.2**). The xanthate group is generally compatible with a wide range of other common moieties, with basic nitrogen functionality as a notable exception. In the presence of such functionality, xanthates undergo rapid polar aminolysis (**Figure 2.3**), delivering the corresponding thiocarbamate and thiol.<sup>10</sup> Other thiocarbonyl derivatives, such as dithiocarbamates, are more resistant to such degradative pathways, owing to lowered electrophilicity at the thiocarbonyl.

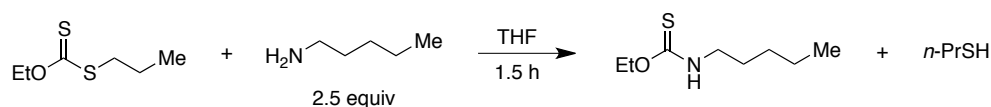


**Figure 2.3** Polar aminolysis of xanthate functionality.

### 2.2.2 Advantages and Reactivity of Alkyl Xanthates

A conventional tin-mediated radical addition of a carbon-centered radical derived from an alkyl halide to an activated alkene is shown in **Figure 2.4**.<sup>11</sup> In the desired pathway, thermal decomposition of a radical initiator, generally either an azo compound or peroxide, leads to a carbon-centered radical that abstracts a hydrogen atom from tributyl tin hydride,  $\text{Bu}_3\text{SnH}$ , forming  $\text{Bu}_3\text{Sn}\cdot$ . Due to the relatively high tin–halogen bond strength ( $\text{Sn–Br} = 80$  kcal/mol), this stannyl radical can abstract a halogen atom from the alkyl halide, forming

carbon-centered radical **2.1**. This species can add to the activated olefin, irreversibly forming a new carbon-carbon bond and new radical **2.2**. Abstraction of a hydrogen atom from tributyltin hydride affords the addition product and facilitates chain propagation.

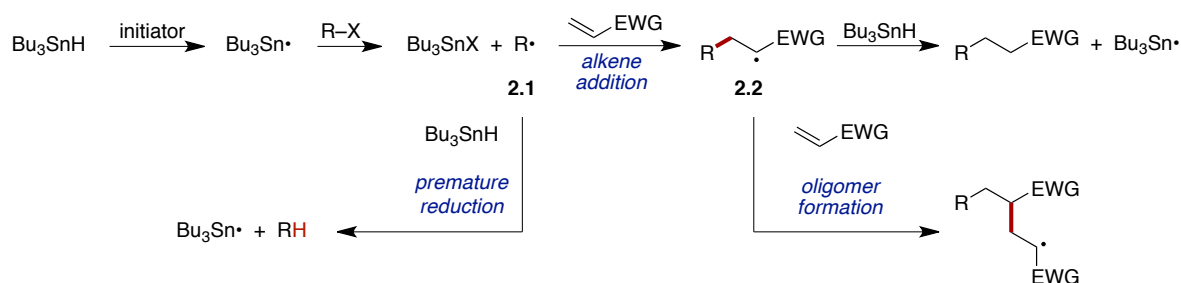


**Figure 2.4** Tin-based radical addition to an activated olefin.

Several steps of this tin-based strategy are problematic, however. If the concentration of tributyltin hydride is too high, premature reduction of **2.1** can occur, leading to an alkane byproduct. If, however, the concentration of alkene is too high, oligomerization processes of **2.2** can siphon olefin away and diminish yields. The use of an activated alkene in tandem with slow stannane addition has proven fruitful for intermolecular radical reaction development, but these tin-based processes are not compatible with unactivated olefins.

In comparison to tin-mediated reactions, radical pathways incorporating xanthates, such as net olefin carboxanthylation (**Figure 2.5**), possess several advantages.<sup>12</sup> In this manifold, thermal radical initiation generates carbon-centered radical **2.3** derived from the alkyl xanthate. If **2.3** reacts with another molecule of alkyl xanthate, it generates the tertiary captodatively stabilized radical **2.4**. Decomposition via  $\beta$ -scission could occur via cleavage of the C–O bond of the ethoxy group, but this pathway is thermodynamically unfavorable due to the formation of the unstable ethyl radical. Alternately,  $\beta$ -scission of either C–S bond leads to reformation of the alkyl xanthate and carbon-centered radical **2.3** in a degenerate process. Tertiary radical **2.4** has been termed a “reservoir species” in xanthate transfer



reactions, as it is a comparatively stable radical that provides a source of radical **2.3**, increasing its effective lifetime in solution.

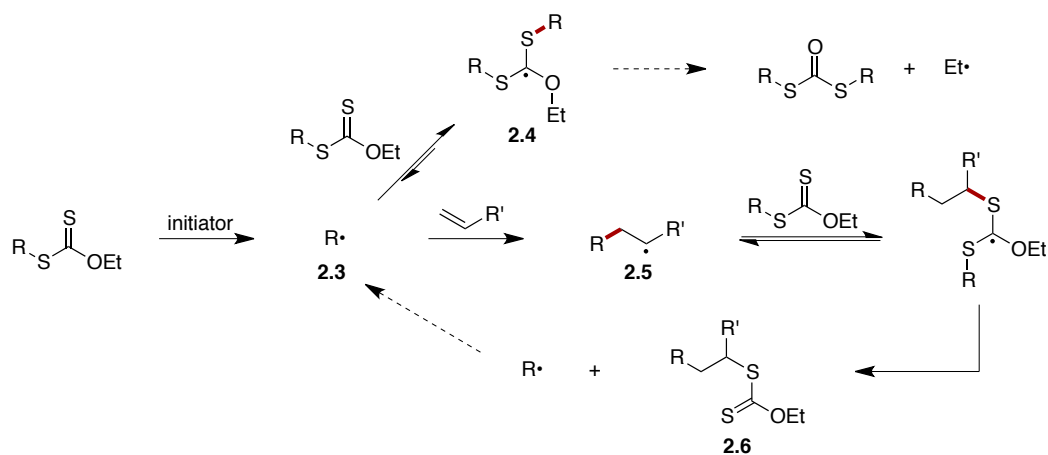


**Figure 2.5** Radical xanthate addition to unactivated olefins.

Due to the increased effective lifetime of **2.3** in solution, addition to unactivated olefins can occur without significant concern of premature reduction, affording new carbon-centered radical **2.5** in an irreversible addition. This species can undergo addition into another molecule of alkyl xanthate, which can in turn experience  $\beta$ -scission of a C–S bond, either returning the prior olefin adduct **2.5** or forming the carboxanthylation product **2.6** along with propagating radical **2.3**. The radical chain mechanism is driven forward by the relative stabilities of the two radical species. For the xanthate transfer reaction to function efficiently, the alkyl radical **2.3** must be more stable than **2.5**, leading to formation of the xanthate transfer product based on thermodynamic stability.

Besides coupling with unactivated olefins, a variety of other synthetically valuable transformations of alkyl xanthates exist. In 1998, Zard first reported the group transfer reaction of alkyl xanthates with allyl ethyl sulfone,<sup>13</sup> delivering allylated products in good yields (**Figure 2.6**). Other C–C bond forming reactions were also developed, including vinylation<sup>14</sup> and acylation<sup>15</sup> methods developed by Zard and Kim, respectively.

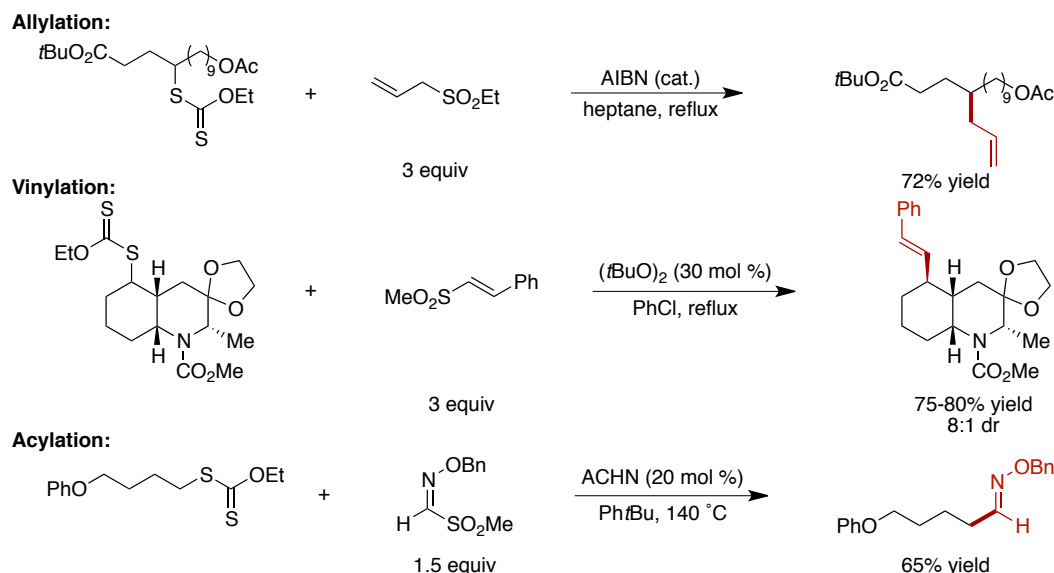


**Figure 2.6** Carbon-carbon bond-forming group transfer reactions of alkyl xanthates.

This radical group transfer strategy was extended to C–N bond formation through an azidation developed by Renaud using thermal initiation and ethanesulfonyl azide as the radical trap (**Figure 2.7**).<sup>16</sup> Reduction of an alkyl xanthate to the corresponding alkane or deuterated alkane is also possible using a strategy developed by Boivin,<sup>17</sup> which can be used to effect the net reductive coupling of an alkyl xanthate with an unactivated olefin.

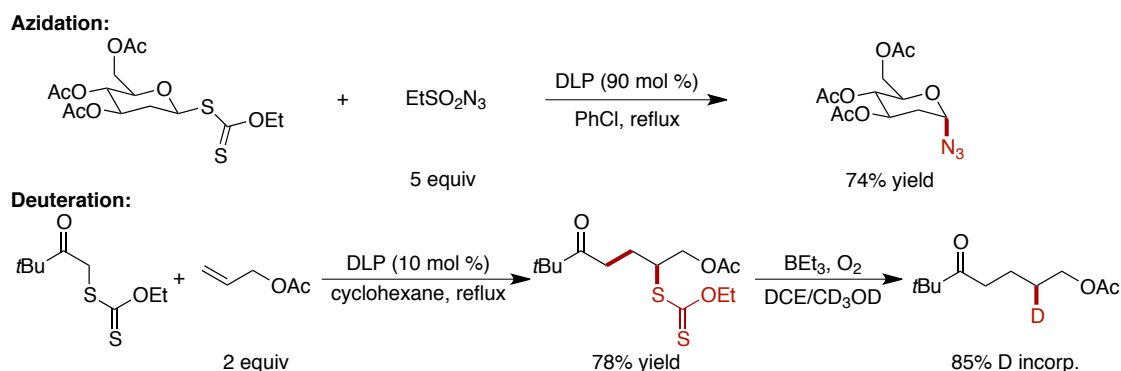


**Figure 2.7** Carbon-heteroatom bond-forming group transfer reactions of alkyl xanthates.

As a result of the broad utility of alkyl xanthates, we hypothesized that a site-selective, intermolecular aliphatic C–H xanthylation would enable access to a wide variety of net C–H

functionalization products currently inaccessible, providing new opportunities in chemical synthesis and the late-stage derivatization of complex natural products and pharmaceuticals.

One report exists in the literature of a direct C–H xanthylation reaction (**Figure 2.8**).<sup>18</sup> Liquid hydrocarbons, such as cyclohexane and cyclooctane, and ethereal solvents, such as 1,4-dioxane and tetrahydrofuran, were xanthylated by Oshima using transfer agent **2.7** and DLP as the initiator. However, the reported yields are based on **2.7** as limiting reagent, and, in fact, the functionalization required the use of the substrate as the reaction solvent to obtain these yields, corresponding to 250 – 300 equivalents.

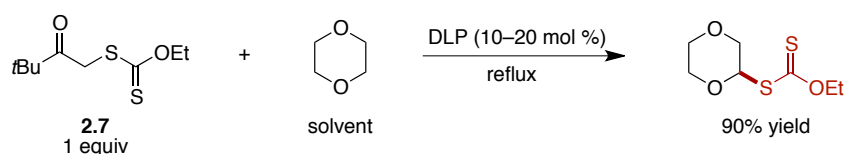


**Figure 2.8** C–H xanthylation of hydrocarbon solvents.

### 2.3 Reaction Development

Due to the potential power of C–H xanthylation as a platform for accessing a diverse range of net C–H functionalization products, we sought to develop a strategy to introduce this functionality into organic compounds. Owing to the precedent in our group in using *N*-bromoamides<sup>19</sup> and *N*-chloroamides<sup>20</sup> to enable C–H bromination and chlorination, respectively, we aimed to synthesize *N*-xanthylamide **2.8** as a reagent for intermolecular C–H xanthylation (**Figure 2.9**). We anticipated similar site-selectivity and functional group compatibility due to the intermediacy of the same putative amidyl radical.

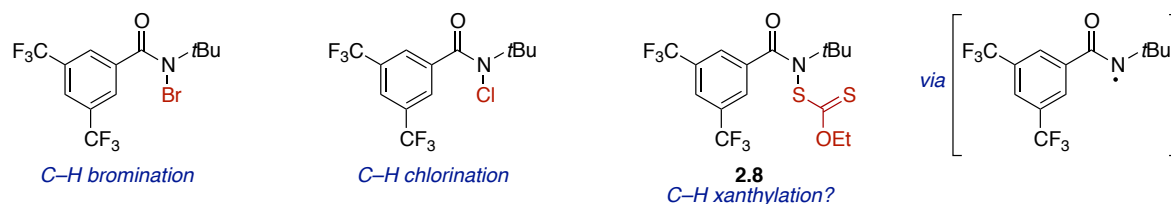


**Figure 2.9** Reagent design for C–H xanthylation.

In 2002, Zard reported the first synthesis of *N*-xanthylamides from the corresponding amides via deprotonation and trapping with a bisxanthate electrophile (**Figure 2.10**).<sup>21</sup> These xanthylamides possessed tethered alkenes such that thermal radical initiation enabled the synthesis of pyrrolidinone products via an amidyl radical cyclization in moderate yields. Although this work demonstrated the formation of amidyl radicals from *N*-xanthylamides, all examples were for intramolecular reactivity, with no intermolecular alkene additions disclosed and no examples of C–H abstraction with the amidyl radical noted.

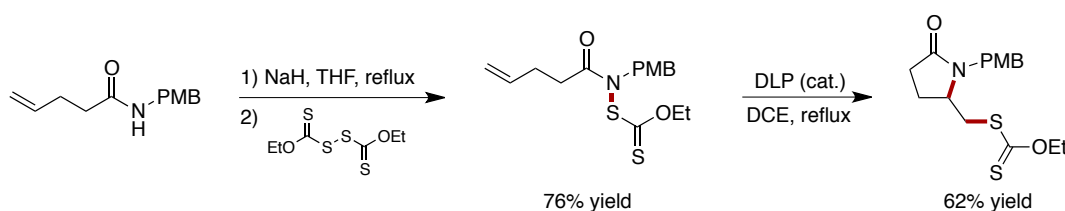


**Figure 2.10** Previous synthesis and application of *N*-xanthylamides.

In preparing **2.8**, we first followed Zard's approach, deprotonating the parent amide with sodium hydride and quenching with bisxanthate **2.9** (**Figure 2.11**). Under these conditions, only the parent amide and **2.9** were recovered, with no conversion to the desired *N*-xanthylamide. The use of other strong bases (KH, *n*-Buli) and modified reaction conditions (refluxing THF) was similarly unproductive. In the Zard work, the synthesized xanthylamides were derived from electron rich, non-hindered amides. In the context of accessing reagent **2.8**, the amidate generated via deprotonation is likely not sufficiently nucleophilic to react with the bisxanthate due to the steric hindrance around nitrogen as well as the electron-deficient nature of the bis(trifluoromethyl)arene.

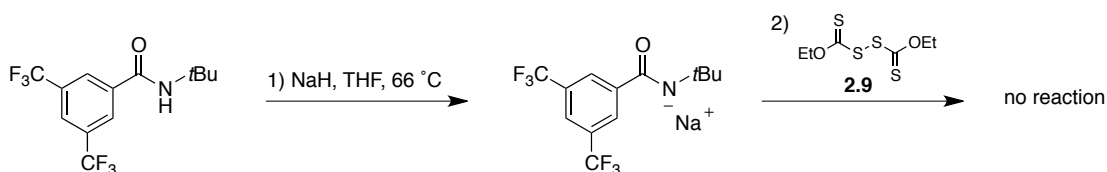


**Figure 2.11** Unsuccessful synthesis of *N*-xanthylamide **2.8**.

To circumvent the ineffectiveness of the prior method for synthesizing **2.8**, we adopted a two-step protocol from amide **2.10** (**Figure 2.12**). Chlorination under conditions previously developed by our lab enabled access to *N*-chloroamide **2.11** in excellent yield without the need for purification.<sup>20</sup> Adapting a procedure developed in the literature for *N*-chlorosuccinimide and *N*-chlorophthalimide as substrates,<sup>22</sup> we synthesized **2.8** in moderate yield on decagram scale by treatment of the chloroamide with commercially available potassium ethyl xanthate in dilute acetonitrile solution.

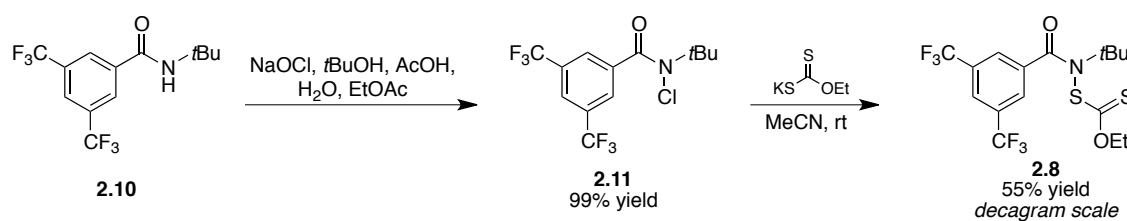


**Figure 2.12** Preparation of *N*-xanthylamide **2.8**.

Xanthylamide **2.8** is stable when stored at 0 °C in a benchtop freezer for at least four months, with no degradation to the parent amide observed. Additionally, upon storage in CDCl<sub>3</sub> at room temperature exposed to ambient laboratory lighting for two months, less than 5% decomposition to the parent amide is observed. Thermogravimetric analysis (TGA) by Jill Williamson in Frank Leibfarth's group revealed that **2.8** is stable at temperatures up to 135 °C, at which point 10% mass loss occurs. Xanthylamide **2.8** is now commercially available through a licensing agreement with Sigma-Aldrich (product number 901415).

### 2.3.1 Initial Studies

With reagent **2.8** readily accessible, we sought to explore its utility toward achieving substrate-limited C–H xanthylation. We began our studies using cyclooctane as a model alkane substrate due to its high boiling point (151 °C/740 mmHg) and 16 equivalent secondary C–H bonds (**Table 2.1**). Inspired by the work of Zard with radical reactions using

alkyl xanthates, we first screened several initiators at elevated temperatures using solvents that do not possess aliphatic C–H bonds susceptible to abstraction.

**Table 2.1** Optimization of C–H xanthylation via radical initiation.

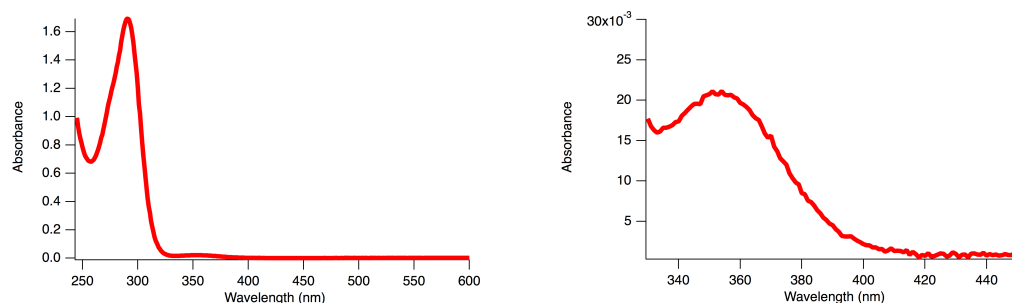
Entry	Initiation	Temperature	Solvent	N–S Cleaved	Yield <sup>a</sup> (Based on Cleaved N–S)
1	AIBN (10 mol %)	80 °C	PhH	24%	22% (92%)
2	DLP (10 mol %)	80 °C	PhH	36%	25% (69%)
3	BPO (10 mol %)	80 °C	PhH	26%	17% (65%)
4	AIBN (50 mol %)	80 °C	PhH	49%	43% (89%)
5	AIBN (2 x 10 mol %)	80 °C	PhH	65%	56% (87%)
6	BPO (10 mol %)	100 °C	PhCl	63%	39% (62%)
7	( <i>t</i> BuO) <sub>2</sub> (10 mol %)	130 °C	PhCl	37%	23% (62%)

<sup>a</sup>NMR yield with hexamethyldisiloxane (HMDS) as internal standard.

In benzene at 80 °C, 10 mol % AIBN, DLP, or BPO provided low yield of the desired cyclooctyl xanthate product by <sup>1</sup>H NMR analysis of the crude reaction mixture (**Table 2.1, entries 1 – 3**). The amount of N–S bond cleavage could be quantified in these reactions, providing an additional metric for determining reaction efficiency. Since the highest yield based on N–S cleavage occurred with AIBN, these conditions were further modified. Increasing the amount of AIBN led to 43% yield of the xanthate product (**Table 2.1, entry 4**), and portionwise addition of AIBN gave a maximum of 56% yield (**Table 2.1, entry 5**). However, further optimization with AIBN proved futile, with no additional increases in yield for cyclooctane. Additionally, these conditions proved non-generalizable to other substrates with stereoelectronically non-equivalent C–H bonds. We speculated that in order to increase the yield further, higher temperatures might be necessary. Using chlorobenzene as the solvent

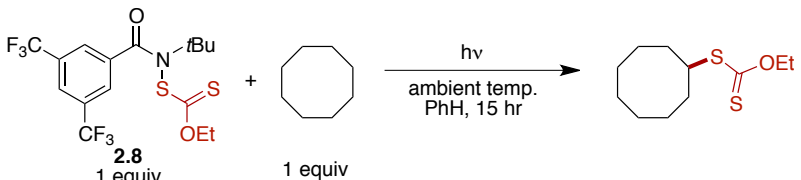
at 100 °C with BPO as the initiator produced several unidentified byproducts (**Table 2.1**, **entry 6**), and using DTBP at 130 °C also did not improve the yield (**Table 2.1**, **entry 7**).

Due to the lack of success using radical initiators to achieve C–H xanthylation, we explored additional methods of reaction initiation. Xanthylamide **2.8** possesses two distinct absorbance peaks in the UV-Vis spectrum (**Figure 2.13**), a large peak with  $\lambda_{\text{max}} = 291$  nm and a significantly smaller peak at  $\lambda_{\text{max}} = 354$  nm, with absorbance tailing into the visible region, ending at about 430 nm. Accordingly, we investigated photochemical initiation of the C–H xanthylation via several different light sources, including UV-A lamps, visible compact fluorescent lights (CFLs), and 455 nm blue LEDs (BLEDs).



**Figure 2.13** UV-Vis absorbance spectrum of xanthylamide **2.8** in CH<sub>2</sub>Cl<sub>2</sub>. Right: Expansion of UV-A region.

At the concentration used for our prior halogenation work (0.15 M), UV-A irradiation proved superior, delivering xanthylated cyclooctane in 73% yield with full N–S bond cleavage (**Table 2.2**, **entry 1**). Visible CFL irradiation produced only trace amounts of product (**Table 2.2**, **entry 2**), and BLEDs gave 51% yield with full xanthylamide conversion (**Table 2.2**, **entry 3**). Increasing the concentration slightly decreased the yield for UV-A irradiation and slightly increased that for the CFL (**Table 2.2**, **entries 4 – 5**). The most striking increase was observed using BLEDs, through which we obtained 81% yield of the xanthylation product with full N–S bond cleavage (**Table 2.2**, **entry 6**). Owing to success with both UV-A and BLED irradiation, they were applied to other substrates.

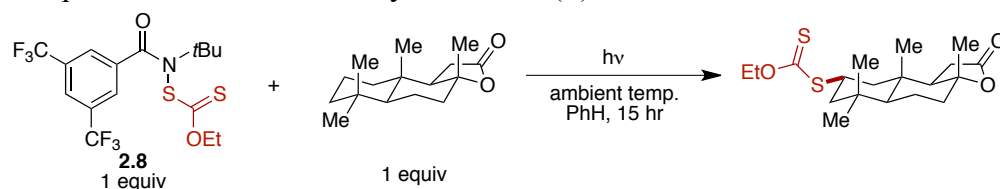
**Table 2.2** Optimization of light-mediated C–H xanthylation.


Entry	Light Source	Concentration	N–S Cleaved	Yield (Based on Cleaved N–S)
1	UV-A	0.15 M	100%	73% (73%)
2	Visible floodlamp	0.15 M	39%	5% (13%)
3	450 nm LED	0.15 M	100%	51% (51%)
4	UV-A	1 M	87%	64% (73%)
5	Visible floodlamp	1 M	22%	13% (59%)
6	450 nm LED	1 M	100%	81% (81%)

<sup>a</sup>NMR yield with hexamethyldisiloxane (HMDS) as internal standard.

We elected to continue optimization using the complex molecule (+)-sclareolide, owing to its partial electronic deactivation and challenges in site-selectivity (**Table 2.3**). Using UV-A irradiation with one equivalent of **2.8** and sclareolide at 0.15 M or 1 M in benzene led to only trace functionalization (**Table 2.3**, **entries 1 – 2**). Due to the stronger absorbance in the UV region of the spectrum, we believe that **2.8** undergoes more facile N–S cleavage under UV irradiation, reducing the opportunity for a successful radical chain reaction to propagate. When using BLED irradiation, however, at 0.15 M, 17% yield of the xanthylation product was observed (**Table 2.3**, **entry 3**). Increasing the concentration to 1 M further increased the yield to 45%, and switching the solvent to trifluorotoluene or hexafluorobenzene led to further increased yields of 60% and 65%, respectively (**Table 2.3**, **entries 4 – 7**). Trifluorotoluene with a concentration of 1 M proved to be the most general reaction conditions, and they were accordingly used going forward.



**Table 2.3** Optimization of C–H xanthylation with (+)-sclareolide.

Entry	Light Source	Concentration	N–S Cleaved	Yield <sup>a</sup> (Based on Cleaved N–S)
1	UV-A	0.15 M	100%	3% (3%)
2	UV-A	1 M	24%	5% (21%)
3	450 nm LED	0.15 M	91%	17% (19%)
4	450 nm LED	0.50 M	88%	27% (31%)
5	450 nm LED	1 M	91%	45% (49%)
6	450 nm LED	1 M (PhCF <sub>3</sub> )	93%	60% (65%)
7	450 nm LED	1 M (C <sub>6</sub> F <sub>6</sub> )	95%	65% (68%)

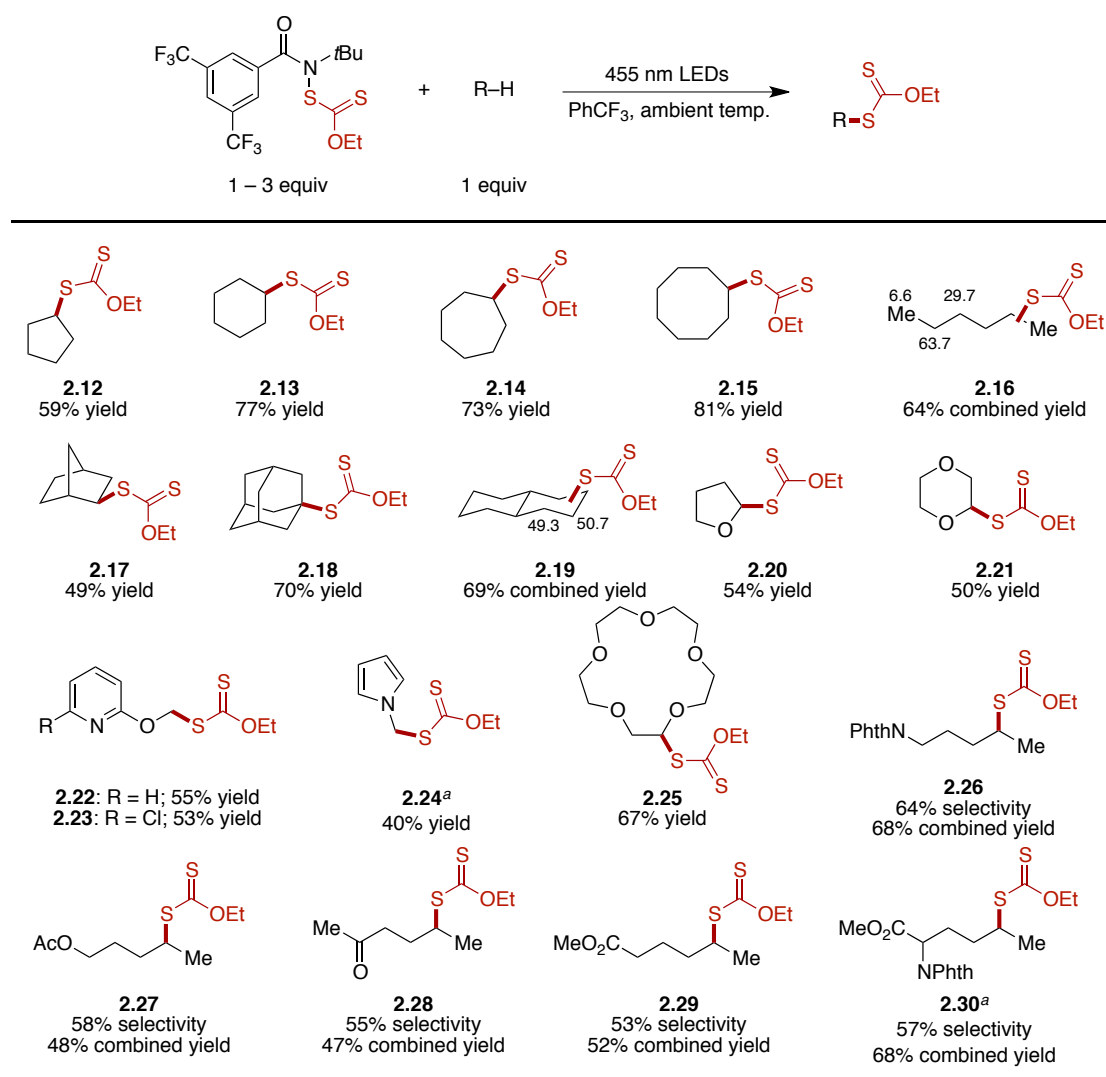
<sup>a</sup>NMR yield with hexamethyldisiloxane (HMDS) as internal standard.

### 2.3.2 Reaction Scope

With Christina Na, we evaluated the reactivity of **2.8** with a variety of hydrocarbon substrates (**Figure 2.14**). Cycloalkanes including cyclopentane, cyclohexane, cycloheptane, and cyclooctane all underwent xanthylation in good yield (59 – 85%). Xanthylation of *n*-hexane led to products **2.16** at the 1, 2, and 3 positions, with reactivity favoring functionalization at the secondary sites ( $k_{\text{secondary}}/k_{\text{primary}} \approx 11$ ), particularly the secondary position. Norbornane underwent xanthylation at the 2-position to produce the *exo* diastereomer **2.17** exclusively due to steric constraints. Consistent with precedent for our bromination and chlorination reactions, adamantane underwent functionalization at the sterically most accessible tertiary position to give **2.18** in 70% yield. Additionally, the reaction of *trans*-decalin led to exclusive xanthylation at the secondary positions, with no tertiary product as determined by GC analysis of the crude reaction mixture.

Having evaluated the reaction scope for simple hydrocarbons, we moved to evaluate the site selectivity and functional group compatibility of the transformation. Xanthylation

occurred at C–H bonds adjacent to heteroatoms, with site selectivity likely due to activation of these sites by hyperconjugation. Accordingly, tetrahydrofuran and 1,4-dioxane underwent xanthylation in modest yield to deliver **2.20** and **2.21**. Functionalization of substrates containing nitrogenous heterocycles was also efficient, such as for 2-methoxypyridine and 2-chloro-6-methoxypyridine, both of which underwent xanthylation on the methoxy substituent to afford **2.22** and **2.23**. Additionally, *N*-methylpyrrole underwent functionalization on the methyl group in modest yield to give **2.24**.



Yields refer to NMR yield with hexamethyldisiloxane (HMDS) as internal standard. <sup>a</sup>Isolated yield.

**Figure 2.14** Substrate scope for aliphatic C–H xanthylation.

Importantly, these substrates highlight that the reaction tolerates heterocyclic nitrogen functionality that is often problematic for metal-oxo catalysts. The use of 15-crown-5 as a substrate produced **2.25** in good yield, providing a new strategy for accessing derivatives of such compounds.

We also examined a series of linear substrates with an electron-withdrawing group as means of further studying the site selectivity. Electron-poor *N*-pentylphthalimide underwent functionalization favoring the distal methylene site (68% yield, 64% selectivity), owing to its status as the site bearing the most electron-rich secondary C–H bond. Several analogous ester and ketone substrates behaved similarly, giving mixtures of regioisomers with functionalization favored at the most distal methylene site. Additionally, *N*-phthalimide protected norleucine methyl ester underwent xanthylation in good yield to deliver **2.30** as a mixture of diastereomers. The electronic site selectivity exhibited with these substrates is consistent with that the previous halogenation work.

Because of the potential power associated with transformations of the xanthate functional group, we sought to study its application to the functionalization and diversification of complex bioactive molecules (**Figure 2.15**). The terpenoid (+)-sclareolide underwent xanthylation at the C2 position in 55% yield to produce **2.31**, distal from the electron-withdrawing lactone and at the most sterically accessible secondary C–H bond. To highlight the ability of the xanthylation reaction to be scaled-up, this reaction was performed as a batch on gram scale in 54% yield. The related compound (–)-ambroxide underwent xanthylation in 80% yield adjacent to oxygen at the most sterically accessible, electron-rich methylene site activated by hyperconjugation.

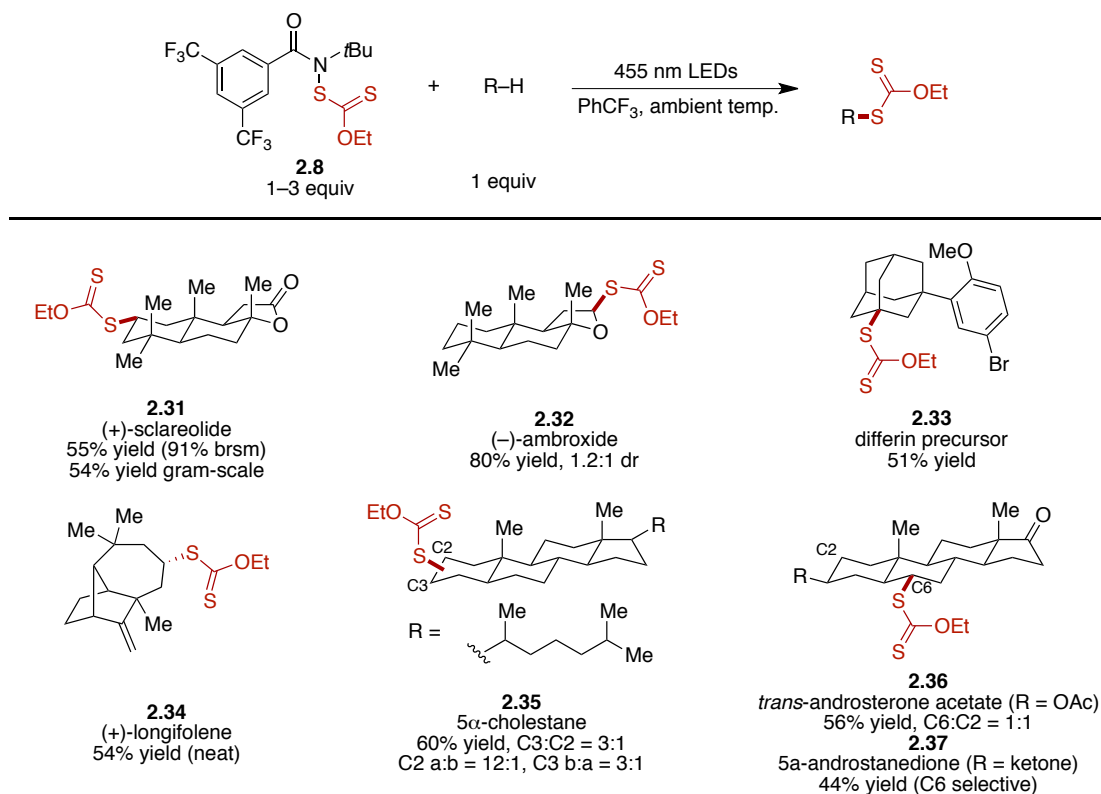


**Figure 2.15** C–H xanthylation of complex molecules.

A precursor to the topical retinoid differin produced derivative **2.33** in 51% yield, the result of xanthylation at the sterically most accessible tertiary C–H bond. A minor regioisomer resulting from functionalization on the methoxy group was also detected by <sup>1</sup>H NMR. The electron-rich arene present in this substrate would likely be problematic for metal oxo catalyzed reactions that occur under strongly oxidizing conditions. Similarly, the terpenoid (+)-longifolene, a classic molecule for endeavors in total synthesis, readily undergoes olefin oxidation with subsequent skeletal rearrangement under oxidizing conditions,<sup>23</sup> rendering other C–H functionalization strategies problematic. Under neat conditions (i.e. 1 equivalent **2.8** in 1 equivalent liquid (+)-longifolene), we could obtain xanthate **2.34** in 54% yield as a single diastereomer. Importantly, the olefin does not undergo any undesired reactivity under these conditions. The site selectivity results from C–H abstraction on the less hindered ring

system at the position not adjacent to a quaternary center, with xanthate transfer subsequently occurring away from the polycyclic system.

Due to their biological importance, we also examined the reaction with steroid frameworks. The reaction of 5 $\alpha$ -cholestane occurred on the steroidal A-ring in 60% combined yield, with 3:1 site selectivity of the C3:C2 positions. Despite the presence of seven tertiary C–H bonds and 13 methylene sites with no inherent substrate electronic factors dictating site selectivity, functionalization is restricted to the most sterically accessible secondary C–H bonds. More complex *trans*-androsterone acetate underwent xanthylation to give a 1:1 mixture of products at the C2 and C6 positions in 56% combined yield, each as a single diastereomer. Having observed this result, we wondered whether we could further deactivate the A-ring of the steroid to facilitate selective B-ring functionalization. Indeed, 5 $\alpha$ -androstanedione underwent xanthylation exclusively at the C6 position on the B-ring in 44% yield. For comparison, strategies for C–H oxidation using this substrate and iron oxo catalysts generally give poor site selectivity across several methylene and methine sites,<sup>24,25</sup> highlighting the utility of the present system for achieving intermolecular C–H functionalization.

### 2.3.3 Mechanistic Studies

To probe the mechanism of the C–H xanthylation, we performed a competition experiment between cyclohexane and cyclohexane-*d*<sub>12</sub>, which indicated a kinetic isotope effect of 6.3 (**Figure 2.16**). This value is comparable to that obtained for reactions using *N*-haloamides and is consistent with irreversible hydrogen atom abstraction by an amidyl radical in the rate determining step. Furthermore, addition of 1 equivalent of the persistent nitroxyl radical TEMPO completely inhibited the reaction of **2.8** with cyclooctane, with no

cyclooctyl xanthate produced but no TEMPO adduct detected by GC-MS analysis of the crude reaction mixture.

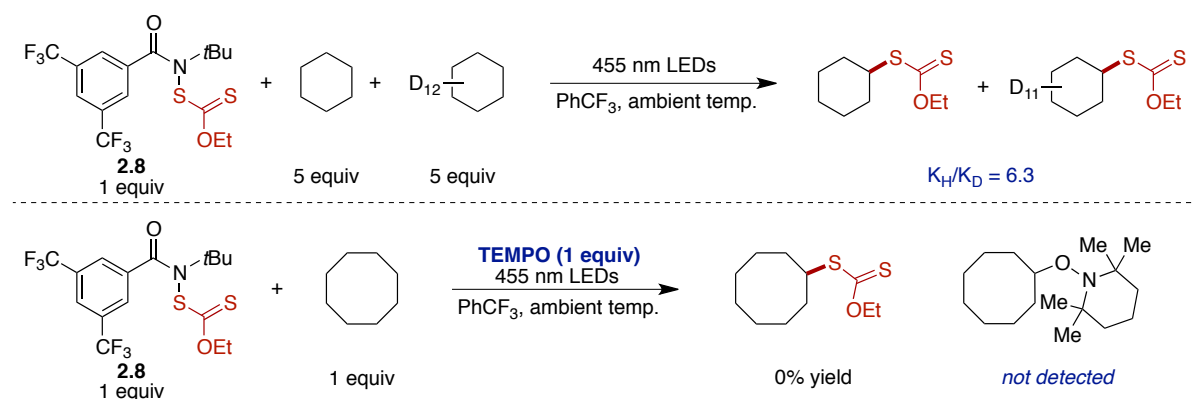


**Figure 2.16** Mechanistic experiments.

We believe that xanthylamide **2.8** can undergo photoexcitation followed by N–S bond homolysis, generating the reactive nitrogen-centered radical (**Figure 2.17**). Due to the disparity in bond dissociation free energies of the N–H bond and the C–H bond in the substrates, the amidyl radical can abstract a hydrogen atom to generate a carbon-centered radical. This species can add into the thiocarbonyl moiety of another molecule of **2.8**, generating a tertiary captodatively stabilized radical.

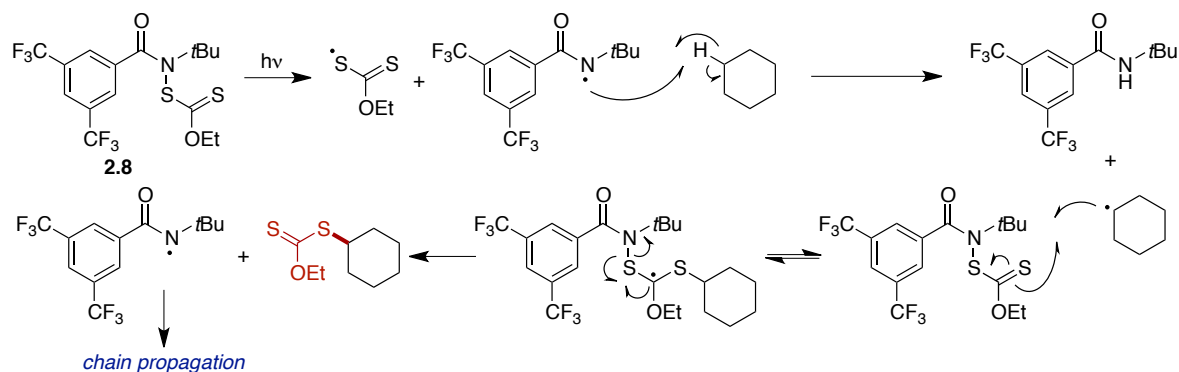


**Figure 2.17** Proposed mechanism for C–H xanthylation.

This intermediate can undergo  $\beta$ -scission to form the alkyl xanthate product and another molecule of amidyl radical, facilitating a chain process for xanthate transfer. Using blue light irradiation as the method of initiation limits the amount of N–S bond homolysis that can

occur due to the poor spectral overlap between the BLED sources and the absorbance of **2.8**, maximizing the amount of productive chain transfer that can occur.

### 2.3.4 Post-Reactions

Due to the wide number of potential transformations of the alkyl xanthate group, we view this aliphatic C–H xanthylation as a unique strategy to access a wide range of net C–H functionalization processes, including several with no synthetic precedent. This is due to the unique reactivity of the xanthate group in both radical and polar contexts. For instance, differin precursor xanthate **2.33** can be coupled with ethyl styryl sulfone<sup>14</sup> under radical-mediated conditions, affording **2.38**, the net product of C–H vinylation, in 55% yield (**Figure 2.18**). Polar reactivity of the xanthate group can also be exploited. The Lewis acid-mediated addition of bis(trimethylsilyl)thymine to (–)-ambroxide xanthate **2.32** via the oxocarbenium occurs to provide *N*-alkyl thymine derivative **2.39** in 87% yield.<sup>26</sup>

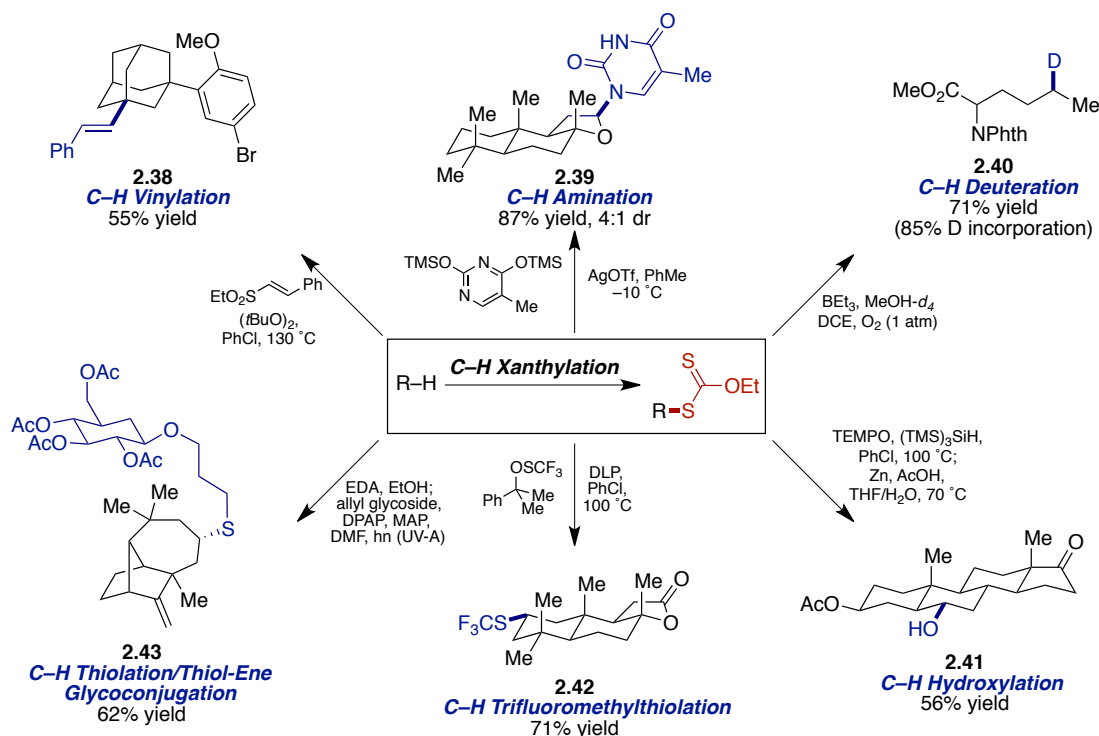


**Figure 2.18** C–H transformations of complex substrates via alkyl xanthate intermediates.

A selective deuteration of aliphatic C–H bonds would facilitate the preparation of isotopically enriched analogues, which may be expected to possess enhanced pharmacokinetic properties. Such compounds could be used for mechanistic and metabolic studies, and could eventually find use in pharmaceuticals.<sup>27</sup> Following publication of this work, a collaboration between the Macmillan group and Merck produced a photoredox-catalyzed strategy for the incorporation of deuterium or tritium atoms into activated C–H bond sites adjacent to nitrogen.<sup>28</sup> By treating norleucine xanthate **2.30** with CD<sub>3</sub>OD and Et<sub>3</sub>B/O<sub>2</sub> initiation, we were able to obtain reduced product **2.40** in good yield (71%, 85% deuterium incorporation).<sup>17</sup> By our two-step method, we are able to achieve net C–H deuteration of unactivated aliphatic sites, for which there is no other current strategy.

The oxidation of unactivated aliphatic C–H bonds is perhaps the most precedented alkane C–H functionalization, but there are still challenges associated with it, such as lack of control of oxidation state of the final product. In most cases, over-oxidation to the ketone occurs when secondary C–H bonds undergo functionalization, even when the alcohol is desirable. By the intermediacy of an alkyl xanthate, a functional group interconversion could be used to modulate the final product's oxidation state, especially due to the xanthylation's mild conditions. While working on this project, Christina Na developed conditions that allowed for the conversion of an alkyl xanthate to a hydroxyl group, reflecting a net hydroxylation of secondary C–H bonds. Adapting conditions previously developed for alkyl iodides<sup>29,30</sup> and related work with a dithiocarbamate,<sup>31</sup> she found that treating alkyl xanthate **2.36** with TEMPO and tris(trimethylsilyl)silane at elevated temperatures followed by Zn/AcOH reduction of the intermediate alkoxyamine delivered alcohol **2.41** in 56% yield as a single diastereomer. Alternatively, oxidation of the alkoxyamine with *m*CPBA could afford



the ketone analogue in comparable efficiency (59% yield). Due to the complete reliance on specific reagent selectivity, this method offers a unique strategy for controlling the oxidation state of products in C–H oxidation reactions.

The incorporation of the trifluoromethylthiol moiety into organic molecules has become desirable in recent years due to its ability to modulate the lipophilicity of bioactive compounds as well as its high electronegativity.<sup>32</sup> Christina Na developed conditions for the synthesis of trifluoromethylthiolates from alkyl xanthates by use of an SCF<sub>3</sub> transfer reagent developed by Shen,<sup>33</sup> highlighted in the synthesis of sclareolide derivative **2.42** in 71% yield. This strategy allows for net C–H trifluoromethylthiolation of unactivated secondary C–H bonds, which is complementary to the existing methods in the literature and is suitable for late-stage complex molecule functionalization.

Aliphatic thiols can participate in the thiol-ene click reaction, a strategy for bioconjugation that is a bioorthogonal alternative to azide-alkyne cycloadditions.<sup>34</sup> Additional applications of this strategy lie in polymer synthesis and materials science.<sup>35</sup> Thus an aliphatic C–H thiolation would facilitate access to a wide array of thiol-ene adducts from alkanes. Alkyl xanthates readily undergo aminolysis to reveal the corresponding thiol in generally high yields, allowing further access to thiol-ene adducts from the products of C–H xanthylation. To demonstrate this strategy, (+)-longifolene xanthate **2.34** was converted to the thiol in quantitative yield and then subjected to photochemical thiol-ene conditions, allowing for glycoconjugation to an allyl glycoside to form **2.43** in 62% yield.

To illustrate how C–H xanthylation can provide access to a wide range of derivatives of a single compound, we performed seven different transformations on sclareolide xanthate **2.31**. Through this net C–H diversification approach, we were able to access the products of

allylation, vinylation, azidation, deuteration, hydroxylation, thiolation, and trifluoromethylthiolation (**Figure 2.19**). Importantly, due to the nature of the transformations, all products maintained functionalization at the same position, highlighting the utility of our amidyl radical-mediated strategy in delivering complex molecule derivatives with consistent site selectivity. By simply switching the reagent set after the initial xanthylation, a diverse array of products can be accessed without the need for new C–H functionalization methodologies.

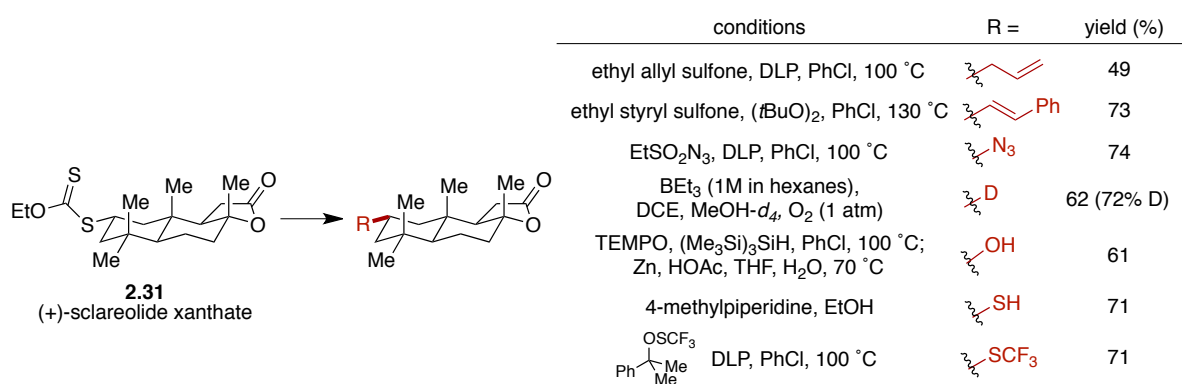


**Figure 2.19** Two-step C–H diversification of (+)-sclareolide.

### 2.3.5 Amine Nucleophilicity

Despite the utility of the transformation, there exists one major drawback, that nitrogen atoms are not well-tolerated overall. Although 2-methoxypyridine was an adequate substrate, if the methoxy substituent is moved to the 3- or 4- position, decomposition of the xanthate group occurs through a polar pathway. It is likely that the 2-methoxy substituent is able to sterically mitigate the nucleophilicity of the pyridine nitrogen, allowing for successful functionalization. Additionally, although phthalimide-protected primary amines were competent substrates in this chemistry, acetate, trifluoroacetate, or carbamate protected secondary amines were not, with reactions resulting in decomposition of the xanthate group via a polar pathway. It appears that these protecting groups, unlike phthalimide, are

insufficiently electron-withdrawing to render the amine lone pairs non-nucleophilic toward the thiocarbonyl. Tertiary amines possessed similar properties; when *N*-methylpiperidine was used as a substrate, decomposition of the xanthate group was observed.

To mitigate this problem of aminolysis, we attempted to use Lewis acid coordination to render the nitrogen non-nucleophilic (**Figure 2.20**). Screening a wide range of stoichiometric Lewis acids in the reaction of **2.8** with cyclooctane with a stoichiometric *N*-methylpiperidine additive led to no xanthylation product in any case. However, the use of (1*S*)-(+)-10-camphorsulfonic acid as a stoichiometric acidic additive in DCE led to 59% yield of the desired cyclooctyl xanthate, indicating that this strategy can, in fact, render amines non-nucleophilic under the reaction conditions.

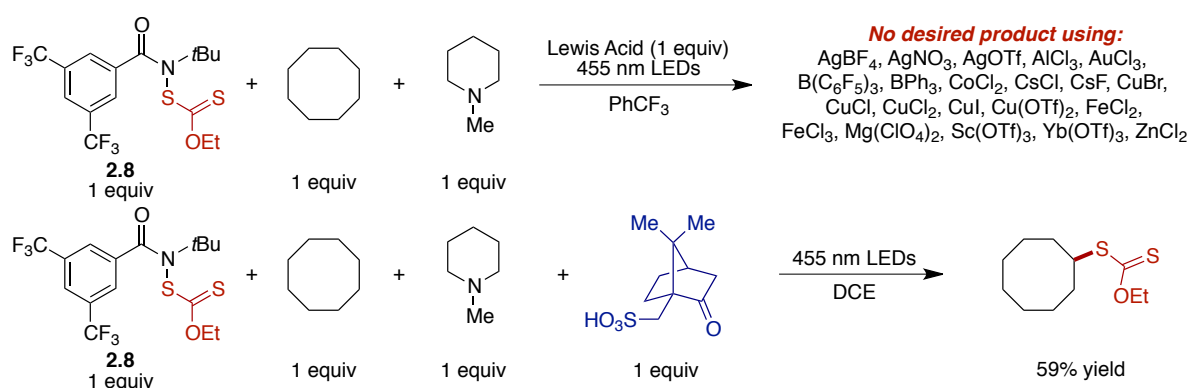


**Figure 2.20** Acidic additives to mitigate amine nucleophilicity.

If this strategy were used for C–H xanthylation of compounds containing nucleophilic nitrogen atoms, however, upon basic workup, the neutral amine would be able to react with the xanthate, causing product degradation. For successful functionalization of molecules containing basic nitrogen functionality, instead, a more promising strategy would be to design new functionalized amide reagents that are poised to transfer groups more resistant to aminolysis, such as dithiocarbamates (**Figure 2.21**).<sup>10</sup>

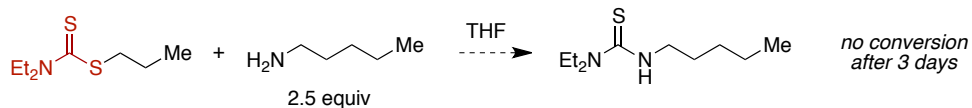


**Figure 2.21** Resistance of dithiocarbamates to polar aminolysis.

## 2.4 Conclusions

Through this work, we have developed a strategy for the direct xanthylation of unactivated aliphatic C–H bonds. The alkane substrate serves as the limiting reagent in all cases, selectivity in general favors the most electron-rich secondary C–H site, and the reaction occurs under extremely mild, visible light-mediated conditions. Due to the utility of alkyl xanthates in synthesis, the C–H xanthylation serves as a two-step strategy to achieve the net diversification of alkane substrates, accessing a wide variety of late-stage functionalization products with common site selectivity. We anticipate that these beneficial characteristics will give rise to applications in molecular diversification for the synthesis and late-stage derivatization of functionalized molecules in a variety of contexts.

## REFERENCES

- (1) Newhouse, T.; Baran, P. S. *Angew. Chem. Int. Ed.* **2011**, *50*, 3362–3374.
- (2) Yamaguchi, J.; Yamaguchi, A. D.; Itami, K. *Angew. Chem. Int. Ed.* **2012**, *51*, 8960–9009.
- (3) White, M. C. *Science* **2012**, *335*, 807–809.
- (4) Qin, Y.; Zhu, L.; Luo, S. *Chem. Rev.* **2017**, *117*, 9433–9520.
- (5) Cernak, T.; Dykstra, K. D.; Tyagarajan, S.; Vachal, P.; Krska, S. W. *Chem Soc Rev* **2016**, *45*, 546–576.
- (6) Quiclet-Sire, B.; Zard, S. Z. *Chem. - Eur. J.* **2006**, *12*, 6002–6016.
- (7) Quiclet-Sire, B.; Zard, S. Z. *Pure Appl. Chem.* **2010**, *83*.
- (8) Quiclet-Sire, B.; Zard, S. Z. *Beilstein J. Org. Chem.* **2013**, *9*, 557–576.
- (9) Nicolaÿ, R.; Kwak, Y.; Matyjaszewski, K. *Chem. Commun.* **2008**, 5336.
- (10) Le Neindre, M.; Magny, B.; Nicolaÿ, R. *Polym. Chem.* **2013**, *4*, 5577.
- (11) Giese, B.; González-Gómez, J. A.; Witzel, T. *Angew. Chem. Int. Ed. Engl.* **1984**, *23*, 69–70.
- (12) Zard, S. Z. *J. Phys. Org. Chem.* **2012**, *25*, 953–964.
- (13) Quiclet-Sire, B.; Seguin, S.; Zard, S. Z. *Angew. Chem. Int. Ed.* **1998**, *37*, 2864–2866.
- (14) Bertrand, F.; Quiclet-Sire, B.; Zard, S. Z. *Angew. Chem. Int. Ed.* **1999**, *38*, 1943–1946.
- (15) Kim, S.; Song, H.-J.; Choi, T.-L.; Yoon, J.-Y. *Angew. Chem. Int. Ed.* **2001**, *40*, 2524–2526.
- (16) Ollivier, C.; Renaud, P. *J. Am. Chem. Soc.* **2001**, *123*, 4717–4727.
- (17) Allais, F.; Boivin, J.; Nguyen, V. T. *Beilstein J. Org. Chem.* **2007**, *3*, 46.
- (18) Sato, A.; Yorimitsu, H.; Oshima, K. *Chem. – Asian J.* **2007**, *2*, 1568–1573.
- (19) Schmidt, V. A.; Quinn, R. K.; Brusoe, A. T.; Alexanian, E. J. *J. Am. Chem. Soc.* **2014**, *136*, 14389–14392.

- (20) Quinn, R. K.; Könst, Z. A.; Michalak, S. E.; Schmidt, Y.; Szklarski, A. R.; Flores, A. R.; Nam, S.; Horne, D. A.; Vanderwal, C. D.; Alexanian, E. J. *J. Am. Chem. Soc.* **2016**, *138*, 696–702.
- (21) Gagosz, F.; Moutrille, C.; Zard, S. Z. *Org. Lett.* **2002**, *4*, 2707–2709.
- (22) Kato, S.; Miyagawa, K.; Hattori, R.; Mizuta, M.; Ishida, M. *Synthesis* **1981**, *1981*, 746–748.
- (23) Dev, S. *Acc. Chem. Res.* **1981**, *14*, 82–88.
- (24) Canta, M.; Font, D.; Gómez, L.; Ribas, X.; Costas, M. *Adv. Synth. Catal.* **2014**, *356*, 818–830.
- (25) Font, D.; Canta, M.; Milan, M.; Cussó, O.; Ribas, X.; Klein Gebbink, R. J. M.; Costas, M. *Angew. Chem. Int. Ed.* **2016**, *55*, 5776–5779.
- (26) Jean-Baptiste, L.; Yemets, S.; Legay, R.; Lequeux, T. *J. Org. Chem.* **2006**, *71*, 2352–2359.
- (27) Harbeson, S. L.; Tung, R. D. In *Annual Reports in Medicinal Chemistry*; Elsevier, 2011; Vol. 46, pp. 403–417.
- (28) Loh, Y. Y.; Nagao, K.; Hoover, A. J.; Hesk, D.; Rivera, N. R.; Colletti, S. L.; Davies, I. W.; MacMillan, D. W. C. *Science* **2017**, *358*, 1182–1187.
- (29) Molawi, K.; Schulte, T.; Siegenthaler, K. O.; Wetter, C.; Studer, A. *Chem. - Eur. J.* **2005**, *11*, 2335–2350.
- (30) Sasaki, Y.; Kato, D.; Boger, D. L. *J. Am. Chem. Soc.* **2010**, *132*, 13533–13544.
- (31) Grainger, R. S.; Welsh, E. J. *Angew. Chem. Int. Ed.* **2007**, *46*, 5377–5380.
- (32) Landelle, G.; Panossian, A.; R Leroux, F. *Curr. Top. Med. Chem.* **2014**, *14*, 941–951.
- (33) Shao, X.; Xu, C.; Lu, L.; Shen, Q. *Acc. Chem. Res.* **2015**, *48*, 1227–1236.
- (34) Hoyle, C. E.; Bowman, C. N. *Angew. Chem. Int. Ed.* **2010**, *49*, 1540–1573.
- (35) Azagarsamy, M. A.; Anseth, K. S. *ACS Macro Lett.* **2013**, *2*, 5–9.

## CHAPTER THREE: C–H XANTHYLATION AS A STRATEGY FOR POLYOLEFIN FUNCTIONALIZATION AND DIVERSIFICATION

### 3.1 Background

Polyolefins are pervasive materials, with a variety of uses in different types of plastics, including packaging for food products, agriculture, and automobile parts.<sup>1</sup> The widespread use of polyolefins in such consumer contexts is in large part due to their desirable physical properties, including high tensile strength, low density, resistance to chemical degradation, and processibility. Several types of polyolefins, including polyethylene (PE) and polypropylene (PP), are semicrystalline materials (**Figure 3.1**), indicating an ability to become pliable above their melting temperature ( $T_m$ ) and solidify upon cooling to a temperature below this point. This property allows molding into a wide variety of sturdy shapes. In fact, polyolefins account for almost two-thirds of commodity thermoplastics used worldwide.<sup>1</sup> Other polyolefins, including polyisobutylene (PIB), are amorphous materials that can be crosslinked to form elastomers, indicating a high degree of elasticity.

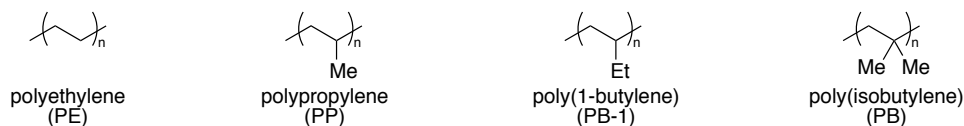


**Figure 3.1** Structures of widely used commodity polyolefins.

In the polymerization of  $\alpha$ -olefins, control over the molecular weight and stereochemistry of the resultant polymer is crucial due to the impact these factors have on physical and thermal properties of the material.<sup>1</sup> Among the most widely used strategies for polyolefin synthesis are a variant of transition metal-catalyzed chain-growth polymerizations,

pioneered by Ziegler and Natta (**Figure 3.2**), in which consecutive monomer units can be coupled in the absence of termination.<sup>2</sup> Efforts synthesizing new transition metal complexes capable of catalyzing  $\alpha$ -olefin polymerization have led to advances in the formation of polyolefins with good control of the resultant properties, especially with regard to stereochemistry.

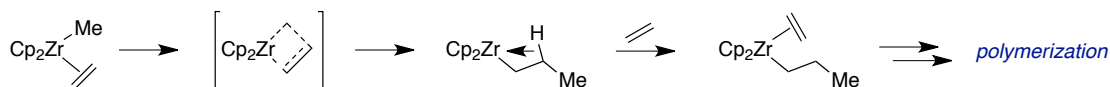


**Figure 3.2** Ziegler-Natta chain-growth polymerization of ethylene.

Despite the advantages associated with polyolefins as materials, there are several drawbacks as well.<sup>3</sup> These polymers often do not interface well with other materials due to their inherent lack of molecular functionality. This restricts applications in which combinations of polymers or materials are needed, including adhesives, composites, coatings, or other high-performance materials. Moreover, polyolefins have some degree of instability under weathering conditions, partially due to challenges in combining them with a protective agent.<sup>4</sup> The development of strategies to incorporate molecular functionality and chemical diversity into commodity polyolefins would enable access to improved and potentially new applications. In this context, a significant challenge is the incorporation of functionality without significantly altering the underlying properties of the polyolefin.

### 3.1.1 Strategies for Polyolefin Functionalization

Several strategies exist for the incorporation of functional groups into polyolefin compounds, one of which is the direct copolymerization of the  $\alpha$ -olefin with a monomer containing the desired polar functionality.<sup>5</sup> This approach allows for the direct incorporation of the desired functionality into the polymer while starting from simple, often commercially available monomers. However, this approach can only work ideally if the copolymerization



process is comparable in efficiency and material property control to that of the analogous homopolymerization. There are several factors that conspire against this idealized scenario. Much desirable heteroatomic functionality contained in the monomers is Lewis basic, forming complexes with the Lewis acidic polymerization catalysts instead of the requisite coordination to the olefin. These complexes inhibit polymerization and facilitate undesired side reactions, significantly reducing the efficiency of the process. Additionally, incorporation of the polar comonomer is nonrandom, creating materials that have the polar functionality unevenly distributed. Work to overcome these challenges pioneered by Brookhart with DuPont has focused in large part on the use of less oxophilic transition metal catalysts to minimize Lewis acid/base complex formation and reaction inhibition (**Figure 3.3**).<sup>6,7,8</sup>

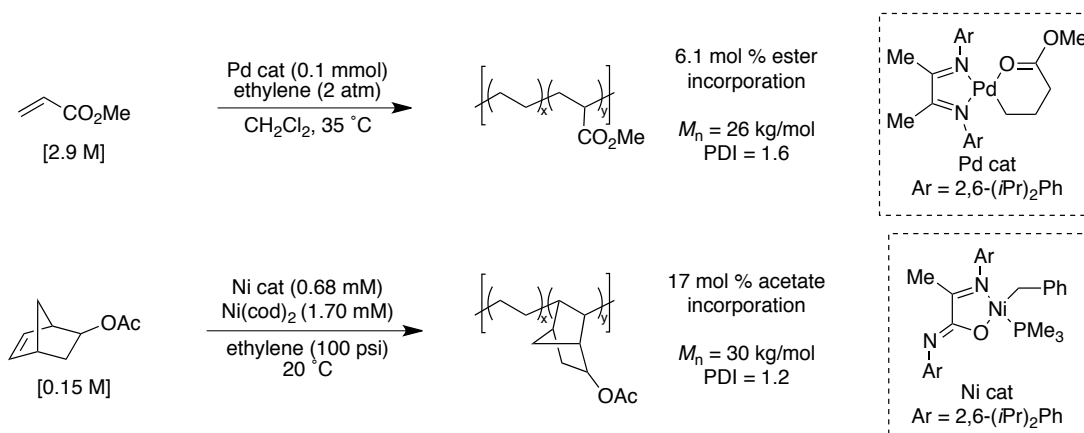


**Figure 3.3** Copolymerization of ethylene with functionalized monomers.

Additionally, a strategy has been developed that involves copolymerization of the  $\alpha$ -olefin with a monomer containing masked functionality to afford a copolymer that can be manipulated to install the desired functionality in a two-step process (**Figure 3.4**).<sup>9</sup> Judicious choice of monomer – including those containing boranes, *p*-methylstyrene, and divinylbenzene – allows for the copolymerization reaction to proceed without the possibility

of catalyst deactivation that hampers the direct copolymerization approach. However, this necessarily limits the functional groups that can be selected for incorporation into the polymer. Furthermore, the functional groups installed in the reactive copolymer must actually be able to undergo interconversion to the desired final functional group.

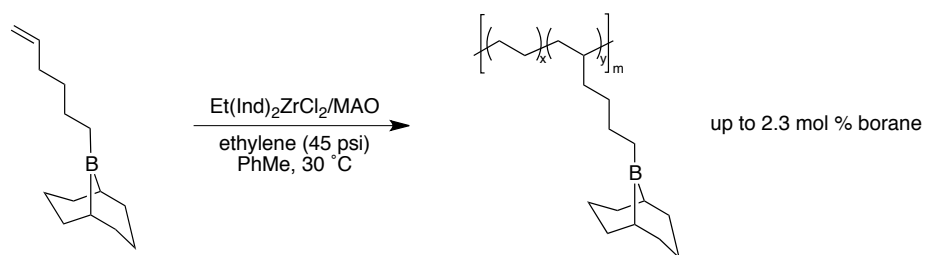


**Figure 3.4** Copolymerization of ethylene with a 9-BBN-containing monomer.

An alternate strategy to the above options averts the need for copolymerization and instead relies on C–H functionalization of a polyolefin to install desirable functional groups.<sup>3</sup> This strategy of post-polymerization modification (PPM) allows the use of preformed commodity polymers as substrates for reactivity, eliminating the need for new polymerization strategies and streamlining the preparation of functionalized materials suitable for a variety of applications. Ideal applications of PPM would also enable the modulation of functional group density in the polymer, which can be challenging with existing copolymerization strategies.

PPM is practiced commercially using radical-mediated processes initiated with thermal radical initiators, photooxidation, or mechanically. Reactive extrusion, a process in which reactivity occurs in the melt phase at high temperatures in an extruder, is generally used to access grafted polyolefins in commercial settings.<sup>10</sup> In this context, a radical initiator decomposes at high temperatures in the presence of maleic anhydride or a similar acceptor and abstracts the weakest polymeric C–H bond, generating a carbon-centered tertiary radical that can add into the radical trap (**Figure 3.5**). Since addition to another olefin is kinetically

unfavorable, subsequent C–H abstraction occurs from another polymer backbone, propagating the chain. However, due to the high temperatures required for initiation and polymer melting or solubility in organic solvents, deleterious processes including  $\beta$ -chain scission can occur.<sup>11</sup> This degrades the properties of the resultant material, making it less useful for potential applications.

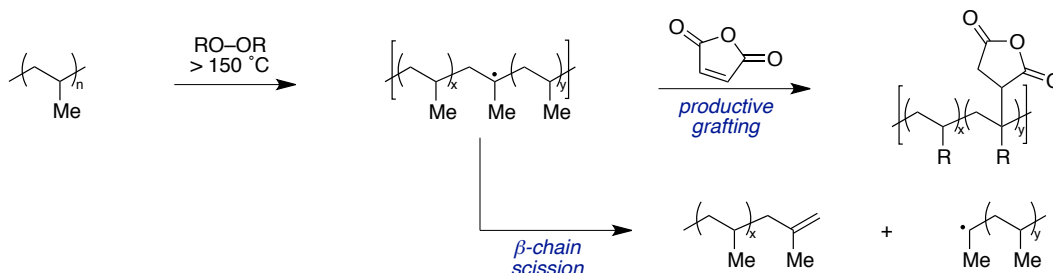


**Figure 3.5** Post-polymerization modification of polypropylene with maleic anhydride.

### 3.1.2 Recent Approaches to Polyolefin Post-Polymerization Modification

Several recent approaches to post-polymerization C–H functionalization have centered on the incorporation of additional functional groups, often through transition metal catalysis, to impart further functionality and opportunities for molecular diversification on the resultant materials. Brookhart and Pérez reported the functionalization of poly(1-butene) via copper-catalyzed insertion of the carbenoid derived from ethyl diazoacetate, present in significant excess relative to the monomer repeat unit (**Figure 3.6**).<sup>12</sup>

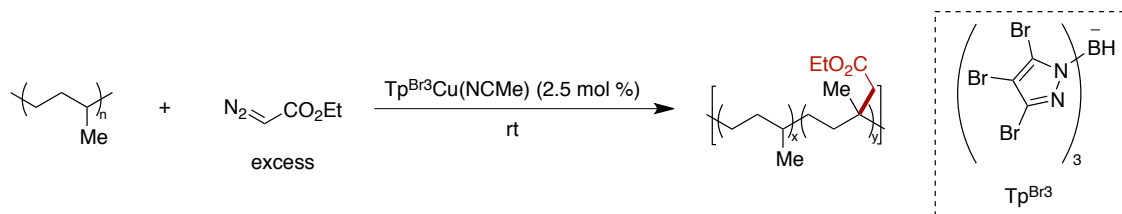


**Figure 3.6** Copper catalyzed C–H insertion of poly(1-butene).

C–H insertion occurred exclusively at the tertiary sites in up to 4 mol % functionalization, and chain scission was not observed. When a copolymer of ethylene and 1-octene was

subjected to the reaction conditions, however, functionalization favoring secondary sites occurred, likely due to the diminished amount of tertiary sites present.

The dehydrogenation of polyolefins has also been reported by Coates and Goldman as a strategy for controlling the functionality present (**Figure 3.7**).<sup>13</sup> Via catalysis by an iridium pincer complex, poly(1-hexene) could be dehydrogenated to 14 mol % of the hexene units present in the polymer, producing a mixture of olefin isomers that favored the terminal position. A more active iridium complex increased the amount of dehydrogenation to 18 mol %, but more olefin isomerization occurred. In both cases, the  $M_n$  and dispersity ( $\mathcal{D}$ ) of the resultant material were unchanged, indicating a lack of chain scission and polymer degradation.

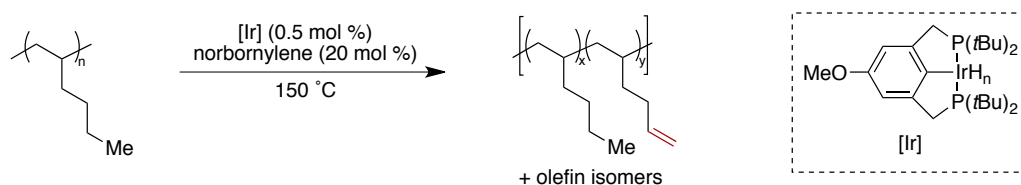


**Figure 3.7** Polyolefin dehydrogenation via an iridium pincer complex.

Boaen and Hillmyer reported the C–H oxidation of polyethylene-*alt*-propylene (PEP) using a manganese porphyrin catalyst with aqueous Oxone as the terminal oxidant and benzyldimethyltetradecylammonium chloride (BDTAC) as a phase transfer agent (**Figure 3.8**).<sup>14</sup> By IR and  $^1\text{H}$  NMR analysis, the products of oxidation were tertiary alcohols, resulting from functionalization at a site of branching, and ketones, arising from oxidation at methylene sites. Up to 1.4 mol % hydroxylation was observed by  $^1\text{H}$  NMR analysis after acetylation using a 5 kg/mol PEP, and the amount of functionalization could be controlled by the amount of Oxone included as well as the temperature of reaction. The reaction was also effective on larger PEP (50 kg/mol), with up to 1.6 mol % hydroxylation. In general, only small amounts of chain coupling were detected by GPC.

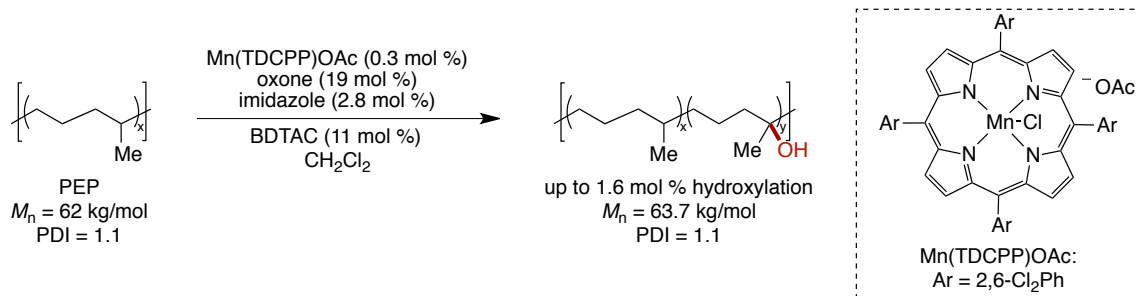


**Figure 3.8** C–H oxidation of polyethylene-*alt*-propylene using a manganese porphyrin catalyst.

Hartwig and Hillmyer collaborated to study the rhodium-catalyzed primary-selective borylation of poly(ethylene) (PEE) (**Figure 3.9**);<sup>15</sup> the resultant alkylboronate esters can be oxidized to afford primary alcohol substituents on the polyolefin after basic hydrogen peroxide workup. The C–H borylation reactions occur at elevated temperatures (150 – 200 °C), and the amount of pinacoldiborane included in the reaction is able to control the amount of borylation and subsequent hydroxylation, up to 19 mol % functionalization on a 37 kg/mol PEE with  $\text{Đ} = 1.06$ .

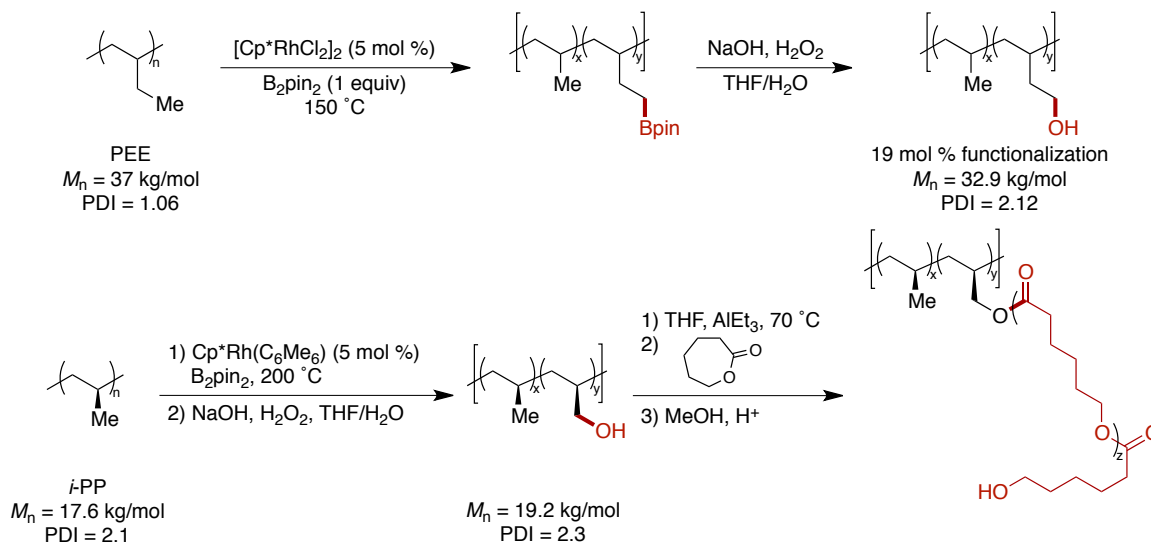


**Figure 3.9** Polyolefin C–H borylation/hydroxylation via rhodium catalysis.

On this polymer, increasing amounts of borylation/hydroxylation led to an increase in  $\text{Đ}$  (up to 2.12), indicating that chain coupling occurred under the reaction conditions. An increase of

$T_g$  of almost 55 °C occurred for the polymers containing the greatest amounts of hydroxylation, likely due to increased hydrogen bonding and other intermolecular interactions among the alcohol functionality.

This work was later extended to the oxidation of several different types of polypropylene (PP) under similar reaction conditions.<sup>16</sup> Commercial atactic PP ( $M_n = 16.1$  kg/mol,  $\bar{D} = 2.3$ ) underwent borylation/hydroxylation to give up to 1.3 mol % hydroxylation without a change in molecular weight distribution. The functionalization was also applied to stereoregular, semicrystalline PPs that are important industrially but potentially more challenging due to their high melting points and viscosities of the corresponding melts. For *i*-PP ( $M_n = 17.6$  kg/mol,  $\bar{D} = 2.1$ ), up to 1.5 mol % hydroxylation could be achieved, and for syndiotactic PP ( $M_n = 40.3$  kg/mol,  $\bar{D} = 2.4$ ) 0.35 mol % functionalization was possible. For these polyolefins, only minor changes in the polymer MWD occurred as a result of functionalization. Additionally, hydroxylated *i*-PP was used in the ring-opening polymerization (ROP) with  $\epsilon$ -caprolactone to access *i*-polypropylene-*graft*-polycaprolactone (PP-*g*-PCL) materials.

More recently, Lee and Hartwig reported the nickel-catalyzed C–H oxidation of polyethylenes with *m*CPBA as the oxidant (**Figure 3.10**).<sup>17</sup> Mixtures of hydroxyl, ketone, and chloride functionality were installed with up to 88% selectivity for hydroxylation. The functionalization of several types of PE was studied, including low-density polyethylene (LDPE,  $M_n = 10.2$  kg/mol,  $\bar{D} = 8.65$ ), high-density polyethylene (HDPE,  $M_n = 10.3$  kg/mol,  $\bar{D} = 11.2$ ), and linear low-density polyethylene (LLDPE,  $M_n = 23.6$  kg/mol,  $\bar{D} = 5.2$ ). Up to 5.5 functional groups per 100 monomer units were incorporated in the functionalization

reactions, and the resultant hydroxylated materials were used for ROP with  $\epsilon$ -caprolactone to synthesize polyethylene-*graft*-polycaprolactone (PE-*g*-PCL).

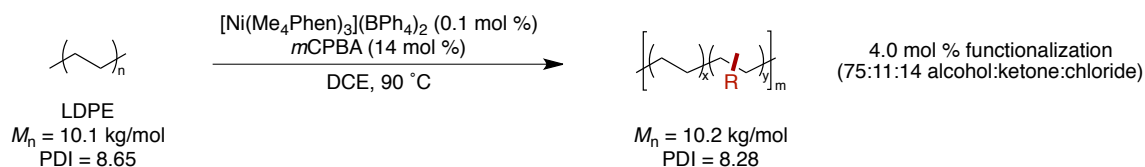


**Figure 3.10** Nickel-catalyzed polyethylene functionalization.

Compared to transition metal-catalyzed strategies for polyolefin functionalization, very few solely organic variants have been reported. The amination of polyethylene ( $M_n = 7.9 \text{ kg/mol}$ ,  $\text{Đ} = 1.83$ ) using NHPI as a C–H abstracting reagent and dialkyl azodicarboxylates as the radical trap has been reported by Sun and Chen (**Figure 3.11**).<sup>18</sup> Up to 15 mol % amination was observed using di-*tert*-butyl azodicarboxylate as the radical trap with no evidence of chain scission or coupling occurring under the reaction conditions. Blends of the functionalized PE with poly(methyl methacrylate) (PMMA) could be obtained, whereas they could not be with the unfunctionalized PE, highlighting potential applications of the system. Additionally, the Boc groups in the product could be deprotected to reveal hydrazine-functionalized material poised for further reactivity.

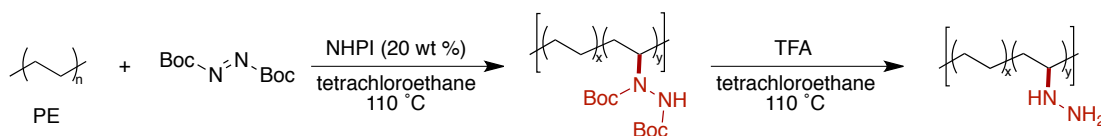


**Figure 3.11** NHPI-catalyzed amination of polyethylene.

Liu and Bielawski have reported the azidation of isotactic polypropylene (*i*-PP) using a readily accessible azidoiodindane in the absence of exogenous radical initiator (**Figure 3.12**),<sup>19</sup> with C–H abstraction likely occurring via the iodanyl radical. Up to 3.5% azidation could be achieved, occurring only at tertiary C–H bonds as determined by  $^1\text{H}$  and  $^{13}\text{C}$  NMR spectroscopy. The resultant azidated *i*-PP in all cases possessed a significant decrease in  $M_n$ ,

indicative of chain cleavage under the reaction conditions, as well as a decrease in  $\bar{D}$ . The degree of polymer azidation was determined via elemental analysis, and azidation was also verified by FT-IR. Thermal azide-alkyne cycloadditions were performed with ethyl propiolate and diethyl acetylenedicarboxylate, accessing tetrazoles bearing ester functionality. Additionally, an alkyne-terminated poly(ethylene glycol) (PEG) was coupled to the azidated PP via copper-catalyzed azide-alkyne cycloaddition (CuAAC), facilitating the synthesis of a PP-*graft*-PEG copolymer.

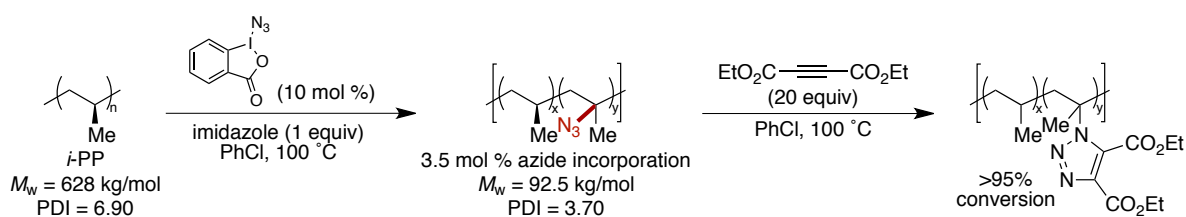


**Figure 3.12** C–H azidation of isotactic polypropylene.

In the majority of recent methods for polyolefin C–H functionalization, transition metal catalysts are used to enable the desired transformations. However, one of the major polyolefin degradation pathways, auto-oxidation via hydroperoxide formation and decomposition, can be catalyzed by transition metals or Lewis acidic metal compounds.<sup>20</sup> Because of the challenges associated with fully eliminating these compounds from a polymeric product, there exists the possibility that the final material can remain contaminated with these substances, potentially impacting their downstream stability. Consequently, strategies for post-polymerization modification that avoid the use of transition metals or Lewis acidic compounds are underutilized but desirable.

### 3.2 Reaction Design

In collaboration with the Leibfarth group, we saw an opportunity to apply the C–H xanthylation reaction we had previously developed for small molecule synthesis (see



**Chapter 2)** to the context of polymer functionalization. Due to the selectivity of the xanthylation for secondary sites, we anticipated that we could develop a strategy for polyolefin functionalization that would avoid chain scission and subsequent degradation of the polymer properties. We also hoped to modulate the amount of polymer functionalization based on the reaction stoichiometry, which would grant control over the functionalized material produced. Additionally, xanthylated polyolefins would possess a valuable functional handle that would enable access to a diverse range of polymer products with applications in a variety of contexts.

### 3.2.1 Xanthylation of Poly(ethylethylene)

We previously reported the site-selective, intermolecular C–H xanthylation of small molecules using a bench-stable, commercially available *N*-xanthylamide **3.1** initiated by exposure to blue light.<sup>21</sup> In collaboration with Jill Williamson in the Leibfarth group, we undertook initial studies into the reactivity of **3.1** with polyolefins. As a well-defined model branched polyolefin substrate, we used poly(ethylethylene) (PEE) with an average molecular weight ( $M_n$ ) of 3.6 kg/mol,  $\bar{D}$  of 1.26, and approximately 40 ethyl branches per 100 carbons.<sup>15</sup> The primary advantage of using PEE in these initial studies was its solubility in a range of organic solvents at the ambient temperature provided by the blue LEDs. In contrast, commodity polyolefins such as polyethylene and polypropylene require heating above 100 °C for dissolution in organic solvents.

After subjecting a mixture of xanthylamide **3.1** and PEE in trifluorotoluene to blue LED irradiation for 19 h, we observed C–H xanthylation of PEE. By changing the relative stoichiometry of **3.1** to the repeat unit of the polymer, we were able to modulate the amount of resultant xanthylation as determined by <sup>1</sup>H NMR analysis (**Table 3.1**). Increasing the

amount of **3.1** led to a concomitant increase in xanthate incorporation into the polymer (Table 3.1, entries 2–6), up to 18 mol % xanthate (Table 3.1, entry 6). Beyond this point, addition of more **3.1** did not result in further polymer xanthylation. Importantly, the repeat unit of the polymer was always in excess or equimolar with respect to **3.1**. This diverges from much of the PPM literature discussed previously, in which the functionalizing reagent is often present in great excess, and possesses significant implications for the commercial applications of the C–H xanthylation.

**Table 3.1** C–H xanthylation of poly(ethylethylene).

entry	equiv X: repeat unit	percent xanthylation <sup>a</sup>	regioselectivity <sup>a</sup> 2°:1°	<i>M<sub>n</sub></i> (kg/mol) <sup>b</sup>	PDI
1	0	0	–	3.6	1.26
2	1:20	3	2.3:1	4.2	1.28
3	1:10	5	1.8:1	3.6	1.31
4	1:5	10	1.8:1	4.5	1.30
5	1:2	15	2.3:1	3.6	1.30
6	1:1	18	2.2:1	4.8	1.32
7 <sup>c</sup>	1:10	6	1.8:1	4.3	1.33

<sup>a</sup>Percent xanthylation and regioselectivity determined via <sup>1</sup>H NMR analysis. <sup>b</sup>*M<sub>n</sub>* values obtained from GPC based on polystyrene standards. <sup>c</sup>Reaction performed in the absence of solvent at 60 °C.

The reaction also proceeded when **3.1** was dissolved neat in PEE without trifluorotoluene (Table 3.1, entry 7), offering potential advantages for industrial applications. Similarly to the small molecule xanthylation, the major byproduct of the xanthylation is a bisxanthate dimer. Whereas xanthylated small molecules required chromatographic separation for purification, xanthylated PEE can be purified by polymer precipitation in methanol.

To study the polyolefin xanthylation reactions quantitatively, we relied on  $^1\text{H}$  NMR analysis. Following reaction of **3.1** and PEE under standard conditions, we observed new resonances at  $\delta$  3.1 ppm, 3.7 – 4.0 ppm, and 4.6 ppm in the  $^1\text{H}$  NMR spectra (**Figure 3.13**).

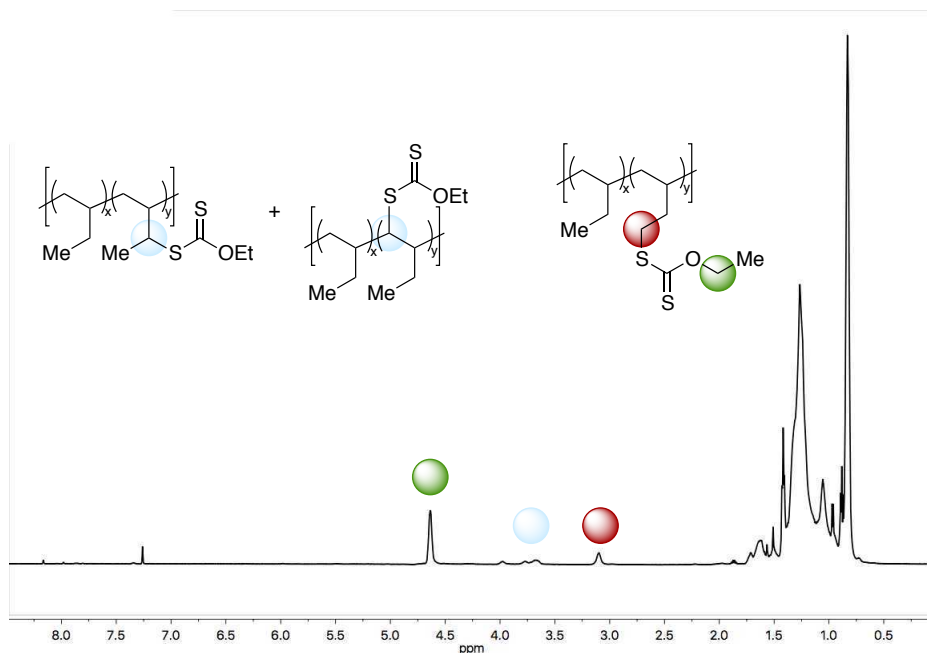


**Figure 3.13** Representative  $^1\text{H}$  NMR spectrum of xanthylated PEE.

In accordance with our previous work and verified by  $^1\text{H}$ – $^{13}\text{C}$  heteronuclear single quantum coherence (HSQC) NMR experiments (**Figure 3.14**), the peaks were assigned as those corresponding to primary xanthylation (3.1 ppm), secondary xanthylation (3.7 – 4.0 ppm), and the ethoxy of the xanthate group (4.6 ppm). Integration of these peaks allowed for determination of the amount of PEE functionalization that occurred in each reaction. In all cases, we observed a roughly 2:1 preference for functionalization of secondary C–H bonds over that of primary sites. For comparison, the xanthylation of *n*-hexane favors secondary functionalization over primary by a ratio of 14:1 (see **Chapter 2.3.2**). The secondary sites in PEE are more sterically encumbered than those of *n*-hexane, both on the polymer backbone and on the side chains. Since the amidyl radical responsible for C–H abstraction is sterically hindered due to the presence of the *t*-butyl substituent, it is likely unable to abstract hydrogen

atoms from the secondary sites of PEE as effectively as with *n*-hexane. Secondary polymer xanthylation could occur on either the backbone or side chain methylene positions, but the relative amounts of xanthylation at each site are currently not known.

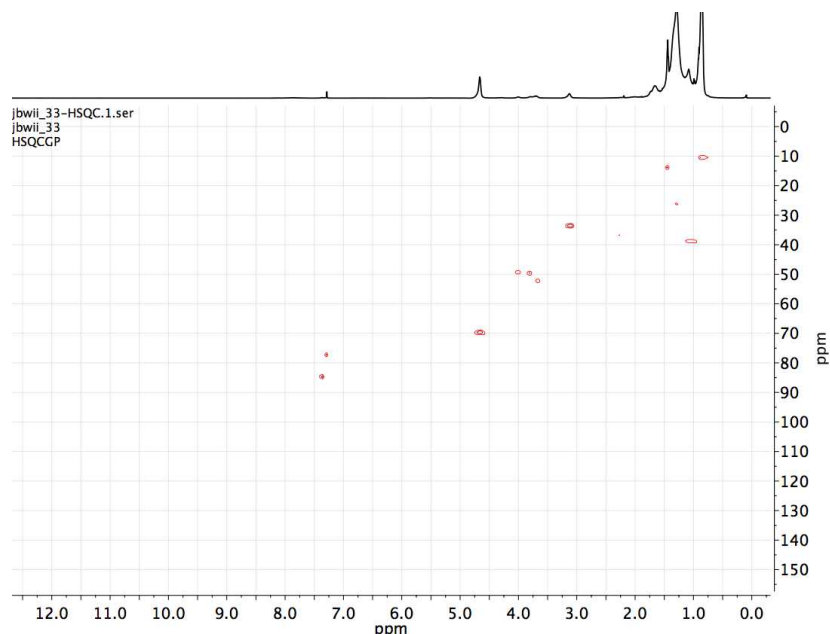


**Figure 3.14**  $^1\text{H}$ – $^{13}\text{C}$  HSQC of xanthylated PEE.

Analysis of the resultant xanthylated PEE provided additional insights into the effectiveness of the functionalization. After xanthylation, gel permeation chromatography (GPC) traces shifted slightly to indicate higher  $M_n$  (**Figure 3.15**), consistent with incorporation of the xanthate into the polymer. The GPC traces also revealed that  $\bar{D}$  did not change significantly following polymer xanthylation, indicating a lack of the cross-linking that can occur with traditional polyolefin functionalization strategies.<sup>22</sup> Only at high amounts of **3.1** relative to repeat unit was small shouldering observed in the GPC trace, suggestive of a small amount of radical-based cross-linking. Monitoring of the GPC photodiode array spectrum at a 33 minute retention time, the point at which the functionalized polymer elutes, showed an absorption peak with  $\lambda_{\text{max}} = 283$  nm, which is consistent with the absorption spectra of other aliphatic xanthates containing no other functionality.<sup>23</sup>

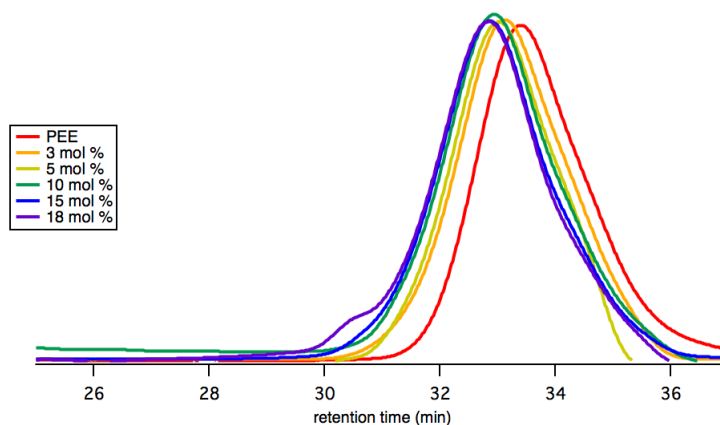


**Figure 3.15** GPC chromatograms of xanthylated PEE.

Fourier-transform infrared spectroscopy (FT-IR) showed absorbances at 1209 and 1050  $\text{cm}^{-1}$  (**Figure 3.16**), indicative of a thiocarbonyl. As the amount of polymer xanthylation increased as determined by  $^1\text{H}$  NMR, the intensity of the corresponding xanthate IR stretches also rose.

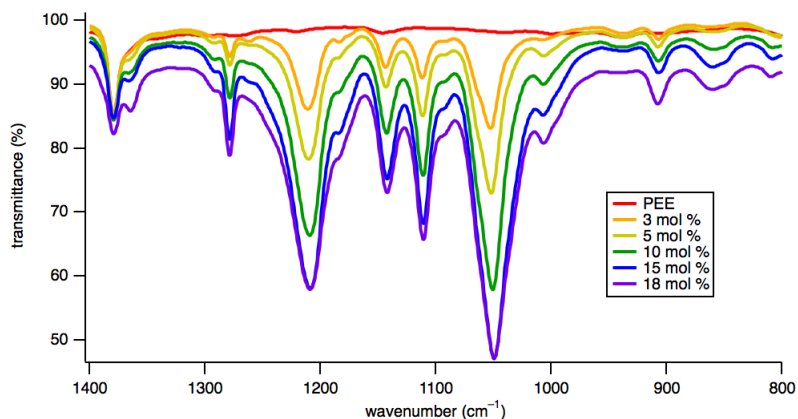


**Figure 3.16** FT-IR spectra of xanthylated PEE.

The thermal properties of the resulting xanthylated PEE samples were also examined to better understand how xanthylation impacts polyolefins. Thermal gravimetric analysis (TGA) of unfunctionalized PEE revealed a decomposition temperature ( $T_D$ ) at 412  $^{\circ}\text{C}$ , when the polymer lost 10% of its initial mass. For all xanthylated polymers, TGA showed a partial mass loss beginning at approximately 250  $^{\circ}\text{C}$ , and as the amount of xanthylation increased, the magnitude of mass lost at this temperature also rose. This is likely due to thermally

driven Chugaev elimination (**Figure 3.17**), which expels carbonyl sulfide, or homolytic C–S bond cleavage with subsequent loss of carbon disulfide.<sup>24</sup>

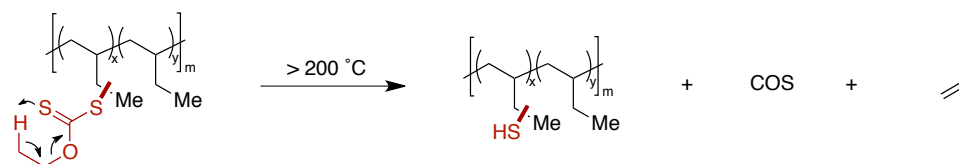


**Figure 3.17** Thermal Chugaev elimination of PEE.

The glass transition temperature ( $T_g$ ) values of the amorphous polyolefin materials were measured via differential scanning calorimetry (DSC). When data were taken from the second heating cycle with a ramp rate of 10 °C/min, unfunctionalized PEE was found to have  $T_g = -53$  °C (**Figure 3.18**). Following xanthylation, an increase of up to 30 °C in  $T_g$  was observed, with the greatest value observed at the highest amount of xanthate incorporation. This trend in  $T_g$  is likely due to the xanthate group increasing the rigidity of the polymer.

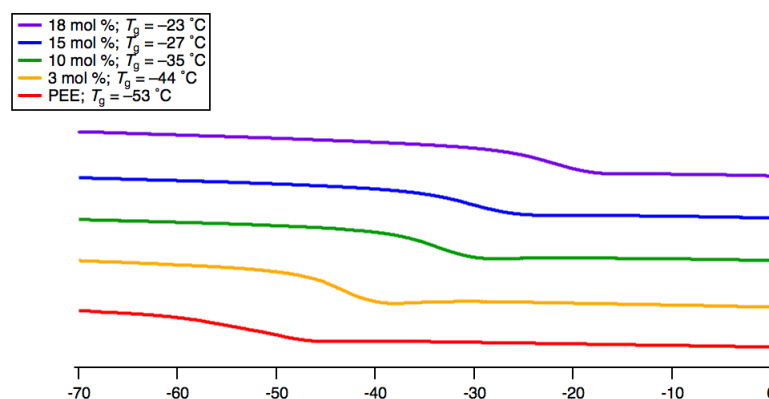


**Figure 3.18** Differential scanning calorimetry curves used to determine the  $T_g$  of xanthylated PEE. All data taken from the 2<sup>nd</sup> heating cycle at a rate of 10 °C/min.

### 3.2.2 Regioselectivity Studies via Small Molecule Model Substrate

Based on  $^1\text{H}$  NMR chemical shifts, both primary and secondary xanthylation occurred when PEE was the substrate. To further support this conclusion, we performed a series of Distortionless Enhancement by Polarization Transfer (DEPT) NMR experiments on 15 mol % functionalized PEE (**Figure 3.19**). In the  $^{13}\text{C}$  NMR spectrum, the resonance at  $\delta$  70 ppm

corresponds to the carbon to which the xanthate is attached. In the DEPT 45 experiment, which does not display signals from quaternary carbons, this peak is still visible. However, this does not definitively rule out tertiary functionalization, as the quaternary carbon associated with a tertiary alkyl xanthate could overlap with other signals.

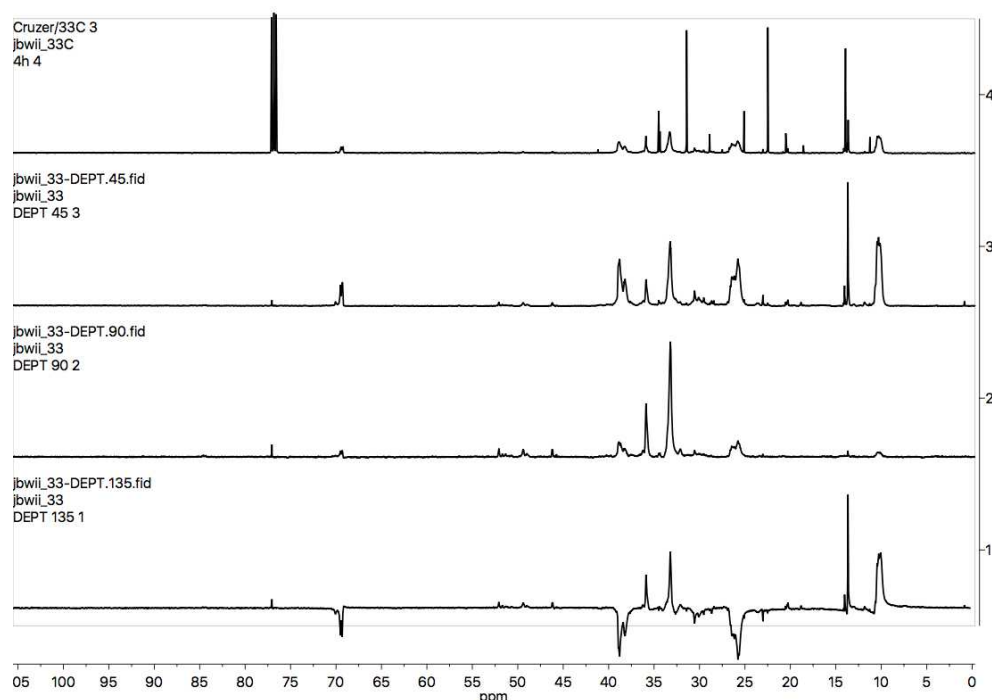


**Figure 3.19** DEPT NMR experiments on 15 mol % xanthylated PEE.

To determine whether tertiary polymer functionalization occurs by analogy, we synthesized the small molecule 4-ethyl-2,6-dimethylheptane **3.2** from 2,6-dimethylheptan-4-one via Wittig reaction and hydrogenation (**Figure 3.20**). This substrate has a similar steric environment to the backbone of PEE, as it possesses a tertiary carbon with an ethyl substituent flanked by two *iso*-butyl groups.

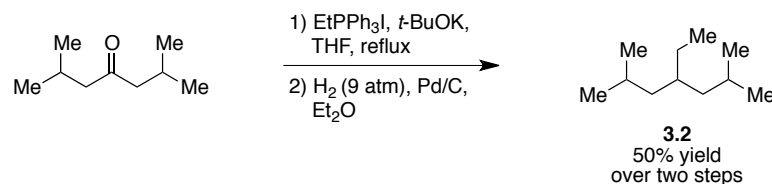


**Figure 3.20** Synthesis of model substrate **3.2**.

We subjected **3.2** to xanthylation with **3.1** and analyzed the results by gas chromatography (GC). Independently, we synthesized the product **3.3** that would arise from tertiary xanthylation via decarbonylation of the analogous tertiary acyl xanthate (**Figure 3.21**).

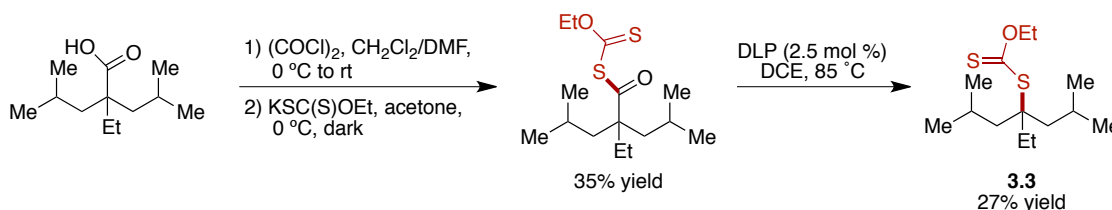


**Figure 3.21** Synthesis of tertiary xanthate **3.3**.

By comparison of the tertiary standard GC trace with that of the reaction of **3.2** (**Figure 3.22**), we concluded that no tertiary C–H functionalization occurred in the small molecule system and that it would be unlikely for it to occur with PEE. Despite the unlikelihood of tertiary C–H abstraction occurring in the polyolefin reactions, it is nonetheless possible for the extended polymeric system to form tertiary radicals via radical isomerization reactions. However, the rate of xanthate group transfer is about four orders of magnitude greater than such an isomerization,<sup>25,26</sup> suggesting that the carbon-centered radicals present do not have a sufficient lifetime for this pathway to occur.

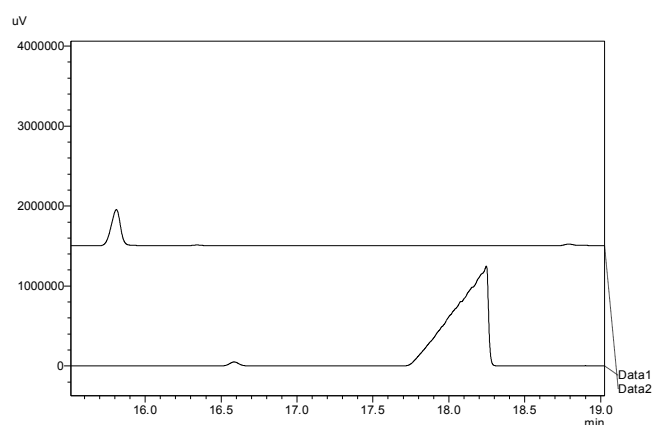


**Figure 3.22** Gas chromatograms of model substrate alkyl xanthates. Top: tertiary xanthate **3.3** standard. Bottom: products of reaction of **3.1** with **3.2**.



### 3.2.3 Polyolefin Diversification

Following polyolefin functionalization with xanthate groups, several new net C–H transformations of polyolefins are accessible, through both radical and polar-mediated processes. Accordingly, a wide assortment of functional materials with currently unknown physical and chemical properties will become available. By comparison, most traditional methods of PPM can only install a single functional group. While these moieties, such as alcohols and azides, can be used to access further derivatization products, the scope of such materials is inherently limited to common reactions of those functional groups, such as oxidation or copper (I)-catalyzed azide-alkyne cycloaddition (CuAAC), respectively.

As a survey of the utility of xanthylated polyolefins for generating materials with further molecular diversity, we applied several types of radical-based transformations to xanthylated PEE (**Figure 3.23**).

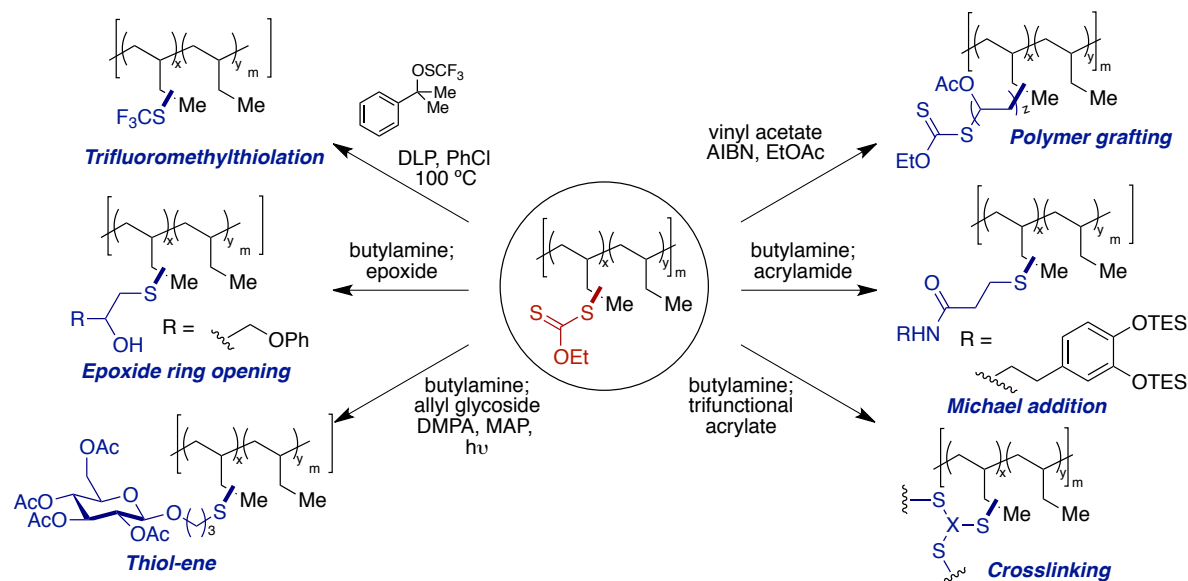


**Figure 3.23** Diversification of xanthylated PEE.

Using a reagent developed by Shen and coworkers<sup>27</sup> in a transformation we developed in the context of small molecule derivatization (see **Chapter 2.3.4**),<sup>21</sup> we were able to effect the

conversion of the xanthate group to the trifluoromethylthiol moiety. This functional group has been explored in the context of medicinal chemistry due to its combination of high electronegativity and lipophilicity,<sup>28</sup> and related studies in the context of polymeric material have been underreported to date.

We were able to use the xanthate handle as a macromolecular chain-transfer agent for reversible addition-fragmentation chain-transfer (RAFT) polymerization with vinyl acetate.<sup>29</sup> Using the xanthylated polymer as the chain-transfer agent with vinyl acetate and AIBN initiation, we could access a PEE-*graft*-poly(vinyl acetate) copolymer. Analysis via DSC revealed two  $T_g$  values at  $-50.6\text{ }^{\circ}\text{C}$  and  $26.4\text{ }^{\circ}\text{C}$ , consistent with the formation of a graft copolymer, and GPC revealed that  $M_n = 17\text{ kg/mol}$  and  $\text{Đ} = 2.00$ , both higher than the xanthylated PEE. As a point of comparison, polymerization of vinyl acetate under similar conditions without the chain-transfer agent afforded a material with a far higher  $M_n$  and  $\text{Đ}$  ( $52\text{ kg/mol}$  and  $3.07$ , respectively). These data indicate the importance of the xanthylated PEE in bestowing control on the vinyl acetate copolymerization. Nonetheless, aliphatic xanthates are not ideal chain-transfer agents for RAFT polymerization. The transfer of different thiocarbonyl compounds, such as dithiocarbamates and trithiocarbonates, would enable the polymerization of a wider range of monomers to access a variety of grafted copolymers.

In addition to radical-based xanthate transformations, we also explored the chemistry of the corresponding thiol derivatives, accessible via simple aminolysis of the xanthylated PEE. From a diversity-oriented viewpoint, the deprotected thiol group enables a wide range of further derivatization due to its applicability toward thiol-Michael additions to acrylamides or acrylates, photochemical thiol-ene reactions with unactivated olefins, and epoxide

openings.<sup>30</sup> To showcase the utility of thiolated PEE, we prepared a catechol-containing compound from conjugate addition into the corresponding acrylamide. The catechol group present in the final product possesses utility in adhesive applications,<sup>31,32</sup> making it an attractive option for improving this property in polyolefins.

Through thiol-Michael addition to a trifunctional acrylate, a crosslinked polyolefin elastomer was accessed. This reactivity possesses implications as a strategy to accomplish branched polyolefin crosslinking from commodity materials. Additionally, photochemical thiol-ene reactions were possible, as shown by the reaction of the thiolated polymer with an allylglycoside to afford glycosylated PEE. Due to the polarity imparted by the saccharide group, potential applicability lies in the mixing of cellulose and polyolefin blends,<sup>33</sup> which can be challenging due to the lack of other functionality in polyolefins. Finally, use of the thiol for epoxide ring-opening was accomplished with glycidyl phenyl ether, affording a polymer product containing a free hydroxyl group.

#### **3.2.4 Application to Commodity Polyolefins**

To extend this work further to commercial polyolefins, a few additional factors needed to be taken into consideration. Unlike PEE, which exists as an amorphous solid, most commodity polyolefins are semicrystalline thermoplastics that do not readily dissolve in organic solvents at room temperature. Rather, elevated temperatures and solvents amenable to such conditions are generally required. Subjecting PEE to blue light-initiated xanthylation with 10 mol % **3.1** at 120 °C in 1,2-dichlorobenzene (DCB) afforded PEE functionalized with 3 mol % xanthate. This is similar to the analogous reaction run at ambient temperature, in which 5 mol % polymer xanthylation is observed. Having successfully translated the reaction

at ambient conditions to elevated temperature, we hypothesized that we would be able to further extend it to conditions suitable for functionalizing commodity polyolefins.

Consequently, we performed the xanthylation reaction on several additional polyolefins. Low molecular weight semicrystalline polyethylene (PE) with  $T_m = 92\text{ }^{\circ}\text{C}$  underwent xanthylation at  $120\text{ }^{\circ}\text{C}$  in DCB, providing a material that had a slight increase in  $M_n$  but without any significant change in  $\bar{D}$  (**Table 3.2**); these data indicate that no chain degradation processes occurred. Commercial high-density polyethylene (HDPE, ExxonMobil<sup>TM</sup> HD6719;  $T_m = 131\text{ }^{\circ}\text{C}$ ) also underwent efficient xanthylation, with 5 mol % functionalization being observed with 10 mol % **3.1** used.

**Table 3.2** Xanthylation of commodity polyolefins.

substrate	equiv X: repeat unit	percent xanthylation <sup>a</sup>	before reaction		before reaction	
			$M_n$ (kg/mol) <sup>b</sup>	$M_w$ (kg/mol) <sup>b</sup>	$M_n$ (kg/mol) <sup>b</sup>	$M_w$ (kg/mol) <sup>b</sup>
PE	1:10	8	4.5	9.6	4.7	10
HDPE	1:10	5	15	1.42	15	62
hyperbranched PE	1:20	3	29	47	35	57
	1:10	7	29	47	36	65
	1:2	13	29	47	36	67
LLDPE	1:10	4	8.1	31	13	46
EP copolymer	1:10	3	463	490	521	605

<sup>a</sup>Percent xanthylation determined via  $^1\text{H}$  NMR analysis. <sup>b</sup> $M_n$  values obtained from GPC based on polyethylene standards for HDPE and LLDPE, and based on polystyrene standards for all other polymers.

We also studied the xanthylation of hyperbranched polyethylene (HBPE) with  $M_n = 29$  kg/mol and containing 13% branch sites, as prepared by Brookhart,<sup>34</sup> as a higher molecular weight material. Under the xanthylation conditions, an increase in  $M_n$  is observed with minimal change in  $\bar{D}$ , consistent with incorporation of the xanthate moiety and a lack of chain cleavage. At relatively high amounts of **3.1** (50 mol %), a slight increase in  $\bar{D}$  is observed, which corresponds to a tailing to higher molecular weight polymers. Although this cannot currently be controlled under the xanthylation conditions, there is precedent to suggest that this change could offer improvements to the melt strength of branched polyolefins.<sup>35</sup> As a point of comparison, the reaction of HBPE with maleic anhydride at elevated temperatures showed significant decreases in  $M_n$  (**Figure 3.24**), consistent with degradation via chain scission.

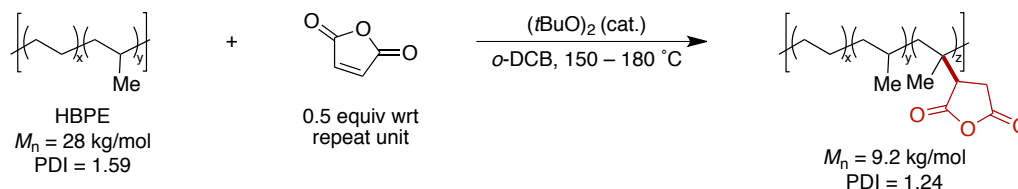


**Figure 3.24** Reaction of HBPE with maleic anhydride.

Having observed promising results in the functionalization of other polyolefins, we sought to expand the xanthylation to commercially available materials containing branching; C–H functionalization of such substrates without concomitant chain scission in a metal-free system is currently without precedent. Accordingly, we subjected a commercial copolymer of ethylene and 1-hexene designated as linear low-density polyethylene (LLDPE, Dow<sup>TM</sup> DNDA-1081;  $T_m = 113$  °C) to the reaction conditions at 120 °C and observed 4 mol % xanthylation. Critically, no chain scission was observed for this material. Finally, we wanted to extend our methodology to the functionalization of high molecular weight commercial polyolefins. To this end, a multi-arm polyolefin elastomer was derived from the

hydrogenation of polyisoprene (PI) star polymer (Kraton G1750). The resultant material can be thought of as a perfectly alternating copolymer of ethylene and propylene, containing 25 methyl branches per 100 carbons. Upon reaction with 10 mol % **3.1** at 60 °C, 3 mol % xanthylation occurred, a similar amount of functionalization as with PEE under the high temperature conditions. No chain scission was observed, highlighting the utility of our system in the functionalization of commercial high molecular weight polyolefins.

### **3.3 Conclusions**

We have developed a new strategy for the post-polymerization modification of polyolefins through an extension of our small molecule C–H xanthylation methodology. The present approach offers several benefits compared to existing strategies for PPM, including no coincident chain scission. Our system requires no transition metal catalysts, mitigating the corresponding concern of oxidative degradation of the final material. By adjusting the amount of xanthylamide present in the system relative to repeat unit of the polymer, we could tune the amount of xanthylation that occurred. Owing to the versatility of the alkyl xanthate group and its thiol derivative, we were able to leverage our approach toward accessing polyolefins containing useful functionalities. Such materials could be used as compatibilizers toward next-generation thermoplastic engineering materials. Additionally, due to the initial results in the functionalization of commodity polyolefins, we anticipate that this method will find use in industrial applications and will provide a novel strategy for accessing functionalized materials.

## REFERENCES

- (1) Liu, P.; Liu, W.; Wang, W.-J.; Li, B.-G.; Zhu, S. *Macromol. React. Eng.* **2016**, *10*, 156–179.
- (2) Domski, G. J.; Rose, J. M.; Coates, G. W.; Bolig, A. D.; Brookhart, M. *Prog. Polym. Sci.* **2007**, *32*, 30–92.
- (3) Boen, N. K.; Hillmyer, M. A. *Chem. Soc. Rev.* **2005**, *34*, 267.
- (4) Melchore, J. A. *Ind. Eng. Chem. Prod. Res. Dev.* **1962**, *1*, 232–235.
- (5) Diamanti, S. J.; Ghosh, P.; Shimizu, F.; Bazan, G. C. *Macromolecules* **2003**, *36*, 9731–9735.
- (6) Johnson, L. K.; Mecking, S.; Brookhart, M. *J. Am. Chem. Soc.* **1996**, *118*, 267–268.
- (7) Ittel, S. D.; Johnson, L. K.; Brookhart, M. *Chem. Rev.* **2000**, *100*, 1169–1204.
- (8) Nakamura, A.; Ito, S.; Nozaki, K. *Chem. Rev.* **2009**, *109*, 5215–5244.
- (9) Chung, T. C.; Lu, H. L.; Li, C. L. *Polym. Int.* **1995**, *37*, 197–205.
- (10) Moad, G. *Prog. Polym. Sci.* **1999**, *24*, 81–142.
- (11) Gloor, P. .; Tang, Y.; Kostanska, A. .; Hamielec, A. . *Polymer* **1994**, *35*, 1012–1030.
- (12) Díaz-Requejo, M. M.; Wehrmann, P.; Leatherman, M. D.; Trofimenko, S.; Mecking, S.; Brookhart, M.; Pérez, P. J. *Macromolecules* **2005**, *38*, 4966–4969.
- (13) Ray, A.; Zhu, K.; Kissin, Y. V.; Cherian, A. E.; Coates, G. W.; Goldman, A. S. *Chem. Commun.* **2005**, 3388.
- (14) Boen, N. K.; Hillmyer, M. A. *Macromolecules* **2003**, *36*, 7027–7034.
- (15) Kondo, Y.; García-Cuadrado, D.; Hartwig, J. F.; Boen, N. K.; Wagner, N. L.; Hillmyer, M. A. *J. Am. Chem. Soc.* **2002**, *124*, 1164–1165.
- (16) Bae, C.; Hartwig, J. F.; Boen Harris, N. K.; Long, R. O.; Anderson, K. S.; Hillmyer, M. A. *J. Am. Chem. Soc.* **2005**, *127*, 767–776.
- (17) Bunesco, A.; Lee, S.; Li, Q.; Hartwig, J. F. *ACS Cent. Sci.* **2017**, *3*, 895–903.
- (18) Zhou, H.; Wang, S.; Huang, H.; Li, Z.; Plummer, C. M.; Wang, S.; Sun, W.-H.; Chen, Y. *Macromolecules* **2017**, *50*, 3510–3515.

- (19) Liu, D.; Bielawski, C. W. *Polym. Int.* **2017**, *66*, 70–76.
- (20) Foster, G. N.; Wasserman, S. H.; Yacka, D. J. *Macromol. Mater. Eng.* **1997**, *252*, 11–32.
- (21) Czaplyski, W. L.; Na, C. G.; Alexanian, E. J. *J. Am. Chem. Soc.* **2016**, *138*, 13854–13857.
- (22) Rätzsch, M.; Bucka, H.; Hesse, A.; Reichelt, N.; Borsig, E. *Macromol. Symp.* **1998**, *129*, 53–77.
- (23) Pomianowski, A.; Leja, J. *Can. J. Chem.* **1963**, *41*, 2219–2230.
- (24) Tschugaeff, L. *Berichte Dtsch. Chem. Ges.* **1899**, *32*, 3332–3335.
- (25) Wang, K.; Villano, S. M.; Dean, A. M. *J. Phys. Chem. A* **2015**, *119*, 7205–7221.
- (26) Coote, M. L.; Radom, L. *Macromolecules* **2004**, *37*, 590–596.
- (27) Shao, X.; Xu, C.; Lu, L.; Shen, Q. *Acc. Chem. Res.* **2015**, *48*, 1227–1236.
- (28) Landelle, G.; Panossian, A.; R Leroux, F. *Curr. Top. Med. Chem.* **2014**, *14*, 941–951.
- (29) Stenzel, M. H.; Cummins, L.; Roberts, G. E.; Davis, T. P.; Vana, P.; Barner-Kowollik, C. *Macromol. Chem. Phys.* **2003**, *204*, 1160–1168.
- (30) Le Neindre, M.; Nicolaÿ, R. *Polym. Int.* **2014**, *63*, 887–893.
- (31) Wang, C. X.; Braendle, A.; Menyo, M. S.; Pester, C. W.; Perl, E. E.; Arias, I.; Hawker, C. J.; Klinger, D. *Soft Matter* **2015**, *11*, 6173–6178.
- (32) Kord Forooshani, P.; Lee, B. P. *J. Polym. Sci. Part Polym. Chem.* **2017**, *55*, 9–33.
- (33) Kim, H.-S.; Lee, B.-H.; Choi, S.-W.; Kim, S.; Kim, H.-J. *Compos. Part Appl. Sci. Manuf.* **2007**, *38*, 1473–1482.
- (34) Tempel, D. J.; Johnson, L. K.; Huff, R. L.; White, P. S.; Brookhart, M. *J. Am. Chem. Soc.* **2000**, *122*, 6686–6700.
- (35) Yoshii, F.; Makuuchi, K.; Kikukawa, S.; Tanaka, T.; Saitoh, J.; Koyama, K. *J. Appl. Polym. Sci.* **1996**, *60*, 617–623.



## CHAPTER FOUR: DEVELOPMENT OF AN ORGANIC PHOTOREDOX-CATALYZED STRATEGY FOR MODULAR ALIPHATIC C–H FUNCTIONALIZATION

Adapted from: Margrey, K. A.; Czaplyski, W. L.; Nicewicz, D. A.; Alexanian, E. J. *J. Am. Chem. Soc.* **2018**, *140*, 4213. Copyright 2017 American Chemical Society.

### 4.1 Introduction

The strategic functionalization of unactivated aliphatic C–H bonds offers novel approaches to challenging problems in chemical synthesis.<sup>1–4</sup> However, the abundance and low reactivity of such bonds has long precluded the development of methods to functionalize them with high levels of site selectivity and access a variety of products from their functionalization. In recent years, several strategies have been developed to achieve intermolecular aliphatic C–H functionalization in a variety of contexts (see **Chapter 1**). Nonetheless, these methods are inherently limited because a single catalyst or reagent generally can only access a single C–H transformation and possesses immutable site selectivity; to achieve novel reactivity, entirely new reagents or systems must be discovered.

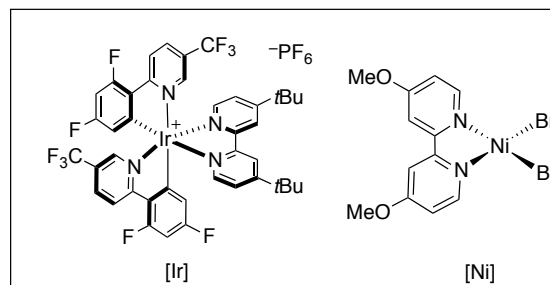
The ability to access a variety of products from a single alkane substrate with common site selectivity would provide the opportunity for the diversification of unactivated aliphatic C–H bonds. While prior work in the Alexanian group accomplished a diversification strategy in two synthetic steps using C–H xanthylation as the linchpin (see **Chapter 2**),<sup>5</sup> a more ideal approach would consist of a direct, one-step conversion of aliphatic C–H bonds into a range of functional groups. Such a strategy would decouple the

C–H abstraction event from the radical trapping step, allowing for different products to be accessed with common site selectivity by simple substitution of the radical trap.

## 4.2 Photoredox-Catalyzed C–H Bond Functionalization

Photoredox catalysis has been developed extensively in recent years as a strategy to generate reactive open shell species that enable unique chemical reactivity.<sup>6–8</sup> In this manifold, excited state metal complexes or organic dyes can act as single electron photooxidants or reductants toward a wide range of functionality. Photoredox methods have been harnessed to functionalize aliphatic C–H bonds that are activated by hyperconjugation<sup>9</sup> of heteroatoms or  $\pi$  systems. Such bonds have lower BDEs compared to those that are unactivated, enhancing their proclivity for radical abstraction. For instance, MacMillan has extensively demonstrated the use of photoredox catalysis for functionalizing these types of bonds to achieve C–H alkylation and arylation adjacent to heteroatoms (**Figure 4.1**).<sup>10–16</sup>

### Alkylation:



### Arylation:

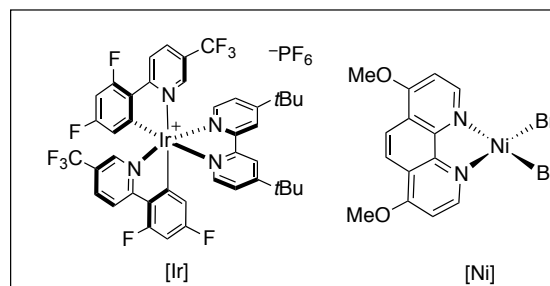
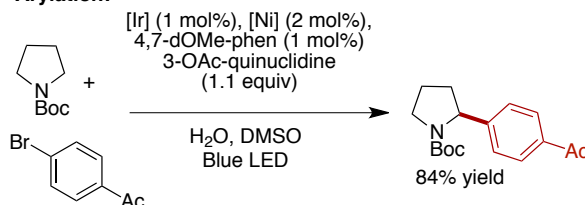


**Figure 4.1** Photoredox-based activated C–H bond alkylation and arylation.

The Nicewicz lab has previously disclosed the means to generate several reactive intermediates including arene,<sup>17,18</sup> alkene,<sup>19</sup> and amine cation radicals<sup>20</sup> that can serve as

electrophilic coupling partners in bond-forming reactions. The generation of these intermediates hinges on the ability of the corresponding arene, alkene, or amine to undergo direct single electron transfer (SET) with a highly oxidizing excited state acridinium photoredox catalyst. Unlike these compounds, however, unactivated alkanes cannot undergo such electron transfer processes with most excited state photooxidants.

### 4.3 Reaction Development

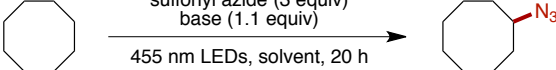
In collaboration with Kaila Margrey in the Nicewicz group, we sought to develop a photoredox-catalyzed method for unactivated aliphatic C–H bond functionalization. Inspired by the ability of iridium photoredox catalysts to generate benzoyloxy radicals for C–H abstraction (see **Chapter 1.3.3**),<sup>21</sup> we wondered whether an acridinium catalyst could generate a reactive intermediate capable of performing aliphatic C–H abstraction. This would decouple the abstraction and radical trapping steps, allowing for the possibility of a modular C–H functionalization system.

#### 4.3.1 Reaction Optimization

We believed that a highly oxidizing acridinium photoredox catalyst **4.1** ( $E_{1/2}(\text{cat}^*/\text{cat}^\bullet) = +2.08\text{V vs SCE}$ )<sup>22</sup> would be capable of oxidatively generating heteroatom-centered radicals that could abstract C–H bonds from unactivated alkanes. We initially found that blue LED irradiation of cyclooctane in the presence of catalyst **4.1** and sulfonyl azide **4.2** in a DCE/pH 8 aqueous phosphate buffer solvent system produced azidocyclooctane in 32% yield (**Table 4.1, entry 1**). The use of tribasic potassium phosphate ( $\text{K}_3\text{PO}_4$ ) instead of the phosphate buffer lead to 30% yield of the azidation product, but the addition of more  $\text{K}_3\text{PO}_4$  led to decreases in the yield (**Table 4.1, entries 2 – 3**). Modification of the solvent from DCE to a 1:1 mixture of DCE/TFE lead to product in a 40% yield (**Table 4.1, entry 4**) and using

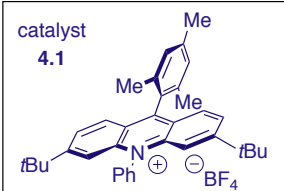
TFE as the only solvent increased the yield more to 50% (**Table 4.1, entry 5**). Replacing TFE with HFIP provided an even higher yield of 70% of the azide product (**Table 4.1, entry 6**), with an optimal concentration of 0.1 M (**Table 4.1, entries 7 – 8**). The pH 8 buffer did provide the desired product in 60% yield; however, it was less effective than K<sub>3</sub>PO<sub>4</sub> (**Table 4.1, entry 9**). The same yield was observed when sulfonyl azide **4.2** was replaced with a more electron-deficient compound **4.3** (**Table 4.1, entry 10**). Since **4.3** was more consistently effective for other substrates, we elected to study the substrate scope with **4.3**.

**Table 4.1** Optimization of C–H azidation with cyclooctane.



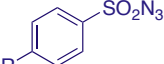
catalyst **4.1** (5 mol %)  
sulfonyl azide (3 equiv)  
base (1.1 equiv)

455 nm LEDs, solvent, 20 h



catalyst **4.1**

sulfonyl azide



**4.2**; R = NHAc  
**4.3**; R = CF<sub>3</sub>

Entry	Sulfonyl Azide	Solvent (concentration)	Base	<sup>1</sup> H NMR Yield
1	<b>4.2</b>	DCE/pH 8 phosphate buffer (4:1, 0.1 M)	–	32%
2	<b>4.2</b>	DCE (0.1 M)	K <sub>3</sub> PO <sub>4</sub>	30%
3	<b>4.2</b>	DCE (0.1 M)	K <sub>3</sub> PO <sub>4</sub> (3 equiv)	23%
4	<b>4.2</b>	DCE/TFE (1:1, 0.1 M)	K <sub>3</sub> PO <sub>4</sub>	40%
5	<b>4.2</b>	TFE (0.1 M)	K <sub>3</sub> PO <sub>4</sub>	50%
6	<b>4.2</b>	HFIP (0.1 M)	K <sub>3</sub> PO <sub>4</sub>	70%
7	<b>4.2</b>	HFIP (0.05 M)	K <sub>3</sub> PO <sub>4</sub>	53%
8	<b>4.2</b>	HFIP (0.2 M)	K <sub>3</sub> PO <sub>4</sub>	65%
9	<b>4.2</b>	HFIP/pH 8 phosphate buffer (4:1, 0.1 M)	–	60%
10	<b>4.3</b>	HFIP (0.1 M)	K <sub>3</sub> PO <sub>4</sub>	71%

To probe the site selectivity for the C–H azidation, we subjected methyl 6-methylheptanoate to the previously optimized conditions and found functionalization exclusively at the tertiary position in 71% yield with good mass balance (**Table 4.2, entry 1**). We wanted to further explore how critical the base identity was for reactivity by varying this component of the reaction. Dibasic potassium phosphate provided the azide in 52% yield

(**Table 4.2, entry 2**) and monobasic potassium phosphate only provided 9% yield of the desired product (**Table 4.2, entry 3**). Based on Glorius' work, we explored the ability of benzoate salts to undergo single electron oxidation in our azidation method. Both the potassium and tetrabutylammonium benzoate salts afforded the tertiary product, albeit in low yield (**Table 4.2, entries 4 – 5**). Similarly, low yields were observed for sodium bicarbonate (**Table 4.2, entry 6**). Sodium carbonate provided the tertiary azide in 61% yield; however, mass recovery was poor compared to other bases, possibly due to deleterious polar processes (**Table 4.2, entry 7**). Switching to cesium carbonate resulted in an inferior yield and similarly poor mass balance (**Table 4.2, entry 8**). Hünig's base only provided trace product (**Table 4.2, entry 9**), suggesting a necessity of anionic character in the base for reactivity to occur. For all bases explored, functionalization occurred exclusively at the tertiary site, with no secondary products detected by  $^1\text{H}$  NMR analysis, consistent with a common role of the bases in the mechanism.

**Table 4.2** Optimization of C–H azidation with methyl 6-methylheptanoate.

Entry	Base	$^1\text{H}$ NMR Yield	Remaining Substrate
1	$\text{K}_3\text{PO}_4$	71%	28%
2	$\text{K}_2\text{HPO}_4$	52%	48%
3	$\text{KH}_2\text{PO}_4$	9%	71%
4	KOBz	39%	60%
5	(NBu <sub>4</sub> )OBz	32%	68%
6	$\text{NaHCO}_3$	36%	56%
7	$\text{Na}_2\text{CO}_3$	61%	15%
8	$\text{Cs}_2\text{CO}_3$	33%	16%
9	<i>i</i> Pr <sub>2</sub> NEt	3%	95%

### 4.3.2 C–H Azidation Substrate Scope

Using the optimized conditions, we explored the substrate scope for the direct C–H azidation. Cyclic hydrocarbons provided azides **4.4** – **4.6** in good yields (**Figure 4.2**). *Trans*-decalin afforded **4.7** as a combined 57% combined yield of only secondary products, and adamantane could be functionalized exclusively at the tertiary C–H site to give **4.8** in 75 % yield. Benzylic sites could be functionalized as demonstrated with *n*-propyl benzene producing **4.9** in modest yield. *Tert*-butylcyclohexane reacted at the tertiary position, forming azide **4.10**, and *cis*-4-methylcyclohexyl pivalate produced **4.12** in 52% yield. Azidation of isobutylbenzene could be accomplished, favoring functionalization at the tertiary position to give **4.11** in modest yield, which serves as a precursor to the psychostimulant pharmaceutical phentermine.

Based on our observations, in that preferential functionalization occurred at tertiary sites instead of secondary and primary positions, we wanted to further probe the site selectivity of the C–H azidation. As previously shown, methyl-6-methylheptanoate produced tertiary azide **4.13** in 71% yield as a single regioisomer. Methyl hexanoate, which contains several electronically deactivated secondary C–H bonds and no tertiary sites, did not undergo functionalization with this system, highlighting strong sensitivity the substrate electronics. In order to examine the electronic site selectivity of the C–H azidation in more detail, several dihydrocitronellol derivatives were examined, each possessing two electronically differentiated tertiary C–H bonds. In all substrates, azidation was favored at the tertiary site distal to other functionality present. Acetate and benzoate esters formed **4.14** and **4.15** in 73% and 91% yield, respectively, with good levels of regioselectivity. Protected primary amines and halide functionalities were also tolerated, affording **4.16** and **4.17** in good yield.

Dihydrocitronellol itself was a competent substrate to access **4.18** in 63% yield with no observed oxidation of the free alcohol, highlighting the mild nature of the system. A phenyl ether-containing substrate afforded **4.19** in low yield and regioselectivity, even though oxidation of the arene is also possible using the acridinium catalyst. Nitrogen-containing heterocycles that are commonly problematic for metal-oxo catalyzed reactions but are important in the context of late stage functionalization of pharmaceuticals, could be tolerated in the system, such as with the azidation of a pyridyl ketone substrate to form **4.20**.

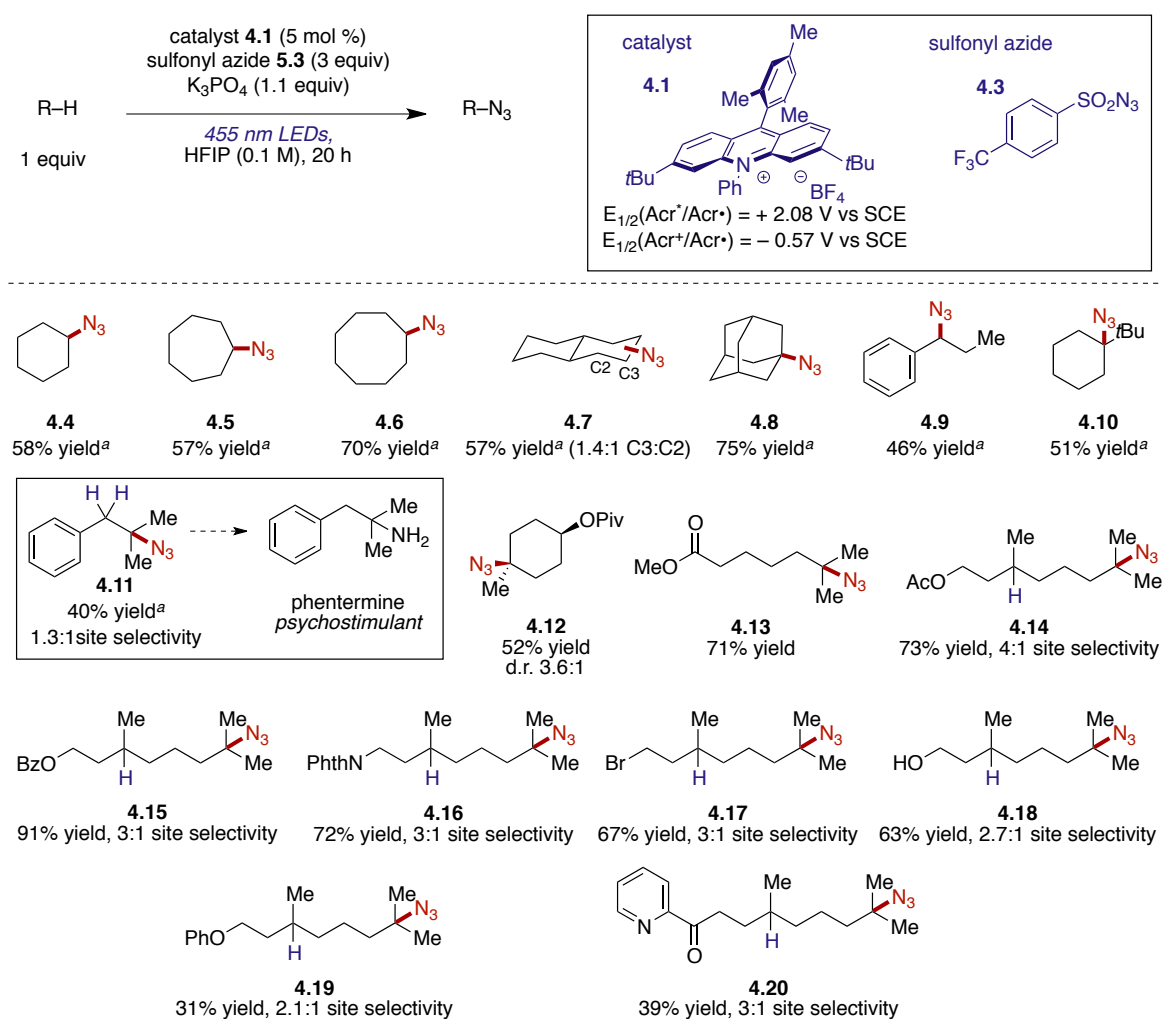


**Figure 4.2** Substrate scope for C–H azidation.

### 4.3.3 Development of Modular C–H Transformations

Having demonstrated the substrate scope of our azidation methodology, we wanted to expand our studies toward the development of a strategy for modular aliphatic C–H functionalization. Using cyclooctane as the substrate and limiting reagent, we investigated a variety of radical traps in place of the sulfonyl azide reagent (**Figure 4.3**). To solubilize all components fully, we chose to use DCE as the solvent with a pH 8 aqueous phosphate buffer instead of exogenous  $K_3PO_4$  as the base. Changing the sulfonyl azide trap for *N*-fluorobenzenesulfonimide (NFSI) delivered fluorocyclooctane in moderate yield.

#### C–H Diversification via Reagent Selection

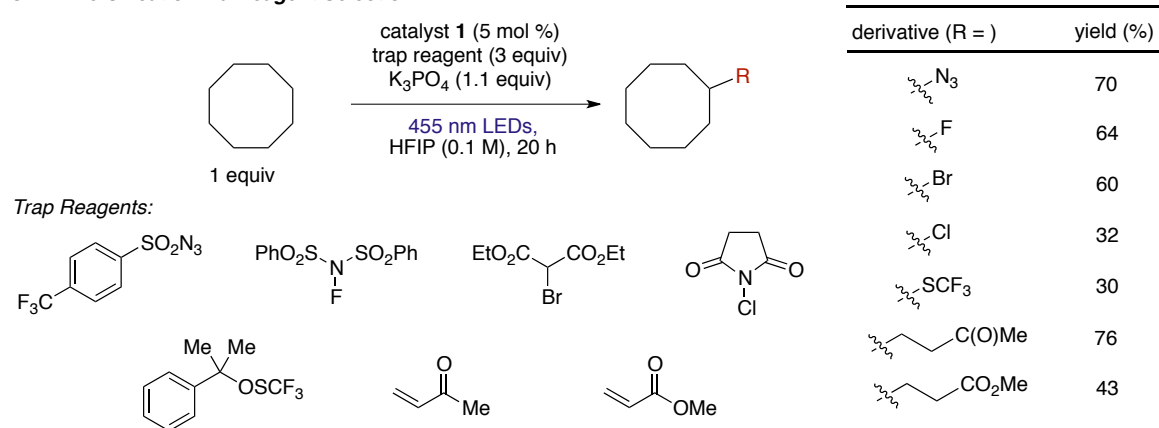


**Figure 4.3** C–H Diversification via reagent selection.

Other halogens could be installed using this strategy, enabling access to bromocyclooctane and chlorocyclooctane by using diethyl bromomalonate and *N*-chlorosuccinimide as the radical traps, respectively. Using a radical trifluoromethylthiol source developed by Shen,<sup>23</sup> we accessed trifluoromethylthiocyclooctane, albeit in low yields possibly arising from product instability over extended reaction times. No additional parameters were optimized for these reactions, so further effort could be exerted to improve each individual transformation's efficiency for synthetic applications. Nevertheless, we have demonstrated



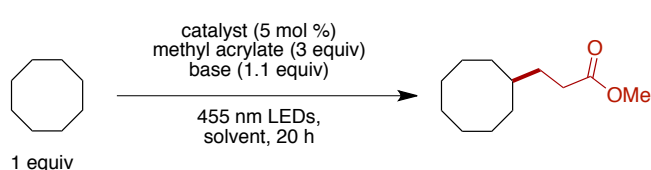
that a simple substitution of a single reaction component can produce a variety of C–H functionalization products in a single step.

We next pursued the development of a C–H alkylation reaction due to the relative lack of methods to accomplish this transformation as well as its potential power in late-stage derivatization (see **Chapter 1.3.5**). Recent studies by Knowles<sup>24</sup> and Rovis<sup>25,26</sup> have capitalized on photoredox catalysis to perform substrate-directed C–H alkylation using amidyl radicals, and we sought to accomplish a similar transformation without the kinetic advantage associated with intramolecularity.

We began our studies by examining the methyl acrylate as a trap in our system. A mixture of DCE and 2,2,2-trifluoroethanol (TFE) as the solvent with 4M pH 8 phosphate buffer as the base provided 10% of the desired alkylation product (**Table 4.3, entry 1**). Due to the relatively negative reduction potential of the radical produced after addition to the acrylate,<sup>27</sup> we used a more reducing acridinium catalyst **4.21** and found that the yield increased to 23% yield (**Table 4.3, entry 2**). TFE was essential for the desired reactivity (**Table 4.3, entry 3**), but TFE alone as the solvent proved inferior (**Table 4.3, entry 4**). Considering the importance of the base in our reaction, we explored whether a more basic buffer solution could increase the yield; however, pH 9 and 10 buffers were not as effective as the pH 8 buffer (**Table 4.3, entries 5 – 6**). A less concentrated 2M pH 8 buffer provided the adduct in the same yield as the 4M buffer (**Table 4.3, entry 7**). Increasing the amount of 4M pH 8 buffer while keeping the amount of organic solvent constant led to 43% yield of the desired adduct (**Table 4.3, entry 8**), but further increases proved deleterious (**Table 4.3, entry 9**). Similar conditions to those optimized for methyl acrylate enabled the use of methyl vinyl ketone (MVK) as the radical trap, affording the ketone adduct in 76% yield. To our

knowledge, this is the first report of a visible light-mediated unactivated aliphatic C–H bond alkylation using the substrate as the limiting reagent.

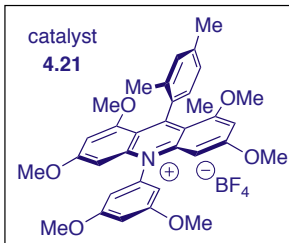
**Table 4.3** Optimization of C–H alkylation with cyclooctane.



1 equiv

catalyst (5 mol %)  
methyl acrylate (3 equiv)  
base (1.1 equiv)

455 nm LEDs,  
solvent, 20 h



catalyst  
**4.21**

Entry	Catalyst	Solvent (concentration)	<sup>1</sup> H NMR Yield
1	<b>4.1</b>	DCE/TFE/4M pH 8 phosphate buffer (7:1:2, 0.1 M)	10%
2	<b>4.21</b>	DCE/TFE/4M pH 8 phosphate buffer (7:1:2, 0.1 M)	23%
3	<b>4.21</b>	DCE/4M pH 8 phosphate buffer (4:1, 0.1 M)	0%
4	<b>4.21</b>	TFE/4M pH 8 phosphate buffer (4:1, 0.1 M)	5%
5	<b>4.21</b>	DCE/TFE/4M pH 9 phosphate buffer (7:1:2, 0.1 M)	12%
6	<b>4.21</b>	DCE/TFE/4M pH 10 phosphate buffer (7:1:2, 0.1 M)	2%
7	<b>4.21</b>	DCE/TFE/2M pH 8 phosphate buffer (7:1:2, 0.1 M)	23%
8	<b>4.21</b>	DCE/TFE/4M pH 8 phosphate buffer (7:1:4, 0.08 M)	<b>43%</b>
9	<b>4.21</b>	DCE/TFE/4M pH 8 phosphate buffer (7:1:8, 0.06 M)	23%

#### 4.3.4 C–H Functionalization of Complex Targets

We sought to highlight the applicability of our modular C–H functionalization system to bioactive molecules processing multiple potential sites of reactivity (**Figure 4.4**). Benzoate protected (–)-menthol afforded azide **4.22** in 54% yield, favoring functionalization at the most electron-rich tertiary position. Since adamantyl systems are present in several pharmaceutical compounds, we wanted to subject some of these compounds to our C–H transformations. The azidation of *N*-phthalimide protected memantine, an NMDA receptor antagonist used in the treatment of Alzheimer’s disease, exclusively produced the tertiary product **4.23** in 55% yield. The same substrate could be fluorinated using NFSI, providing **4.24** in 86% yield with functionalization again occurring at the tertiary position. A precursor

to differin, a topical retinoid, afforded tertiary azide **4.25** in modest yield, even in the presence of an oxidizable aromatic ring, highlighting the mild nature of our system. This substrate also could be alkylated using methyl vinyl ketone, forming **4.26** in 45% yield. Ibuprofen methyl ester, which contains both tertiary and benzylic sites, underwent azidation to afford a mixture of the tertiary and benzylic products **4.27** with a combined 57% yield. Previous reports of azidation of this substrate only provided benzylic functionalization, demonstrating that our system allows access to complimentary products of C–H functionalization. Steroid 5 $\alpha$ -cholestan-3-one, possessing 46 aliphatic C–H bonds, could be functionalized at the C17 and C25 positions in a combined 39% yield to produce **4.28**, similar to the selectivity observed in Curci's hydroxylation using dioxiranes.<sup>28</sup>

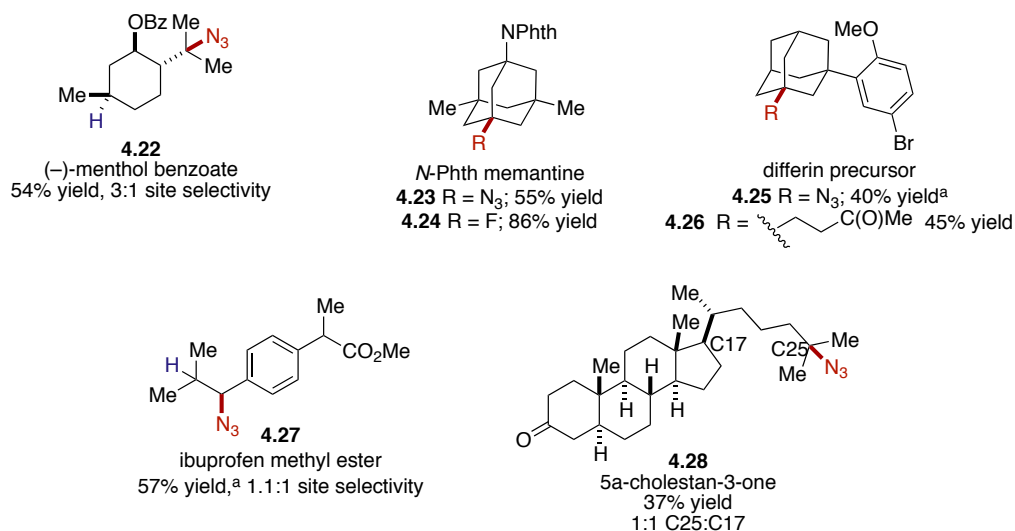


**Figure 4.4** Modular C–H diversification of bioactive complex molecules.

### 4.3.5 Mechanistic Experiments

While we had success in developing a modular C–H functionalization methodology for a range of substrates, the active C–H bond abstracting species remained unclear. To this end, we sought to clarify the role of each component of the reaction, focusing on the azidation in particular. Stern-Volmer analysis determined that the sulfonyl azide **4.3** did not

quench the fluorescence of the excited state acridinium. Based on the presence of  $\text{K}_3\text{PO}_4$  ( $\text{pK}_a = 7.21$  in  $\text{H}_2\text{O}$  for the conjugate base  $\text{K}_2\text{HPO}_4$ ) and HFIP ( $\text{pK}_a = 9.3$  in  $\text{H}_2\text{O}$ ) in the optimized reaction conditions, reversible deprotonation of HFIP is thermodynamically favorable. We wondered if the resultant alkoxide could be oxidized by the acridinium catalyst to produce an oxygen-centered radical capable of hydrogen atom abstraction. Stern-Volmer analysis with sodium 1,1,1,3,3,3-hexafluoroisopropoxide in HFIP indicated no quenching of the acridinium excited state fluorescence, however, suggesting this oxidation does not occur.

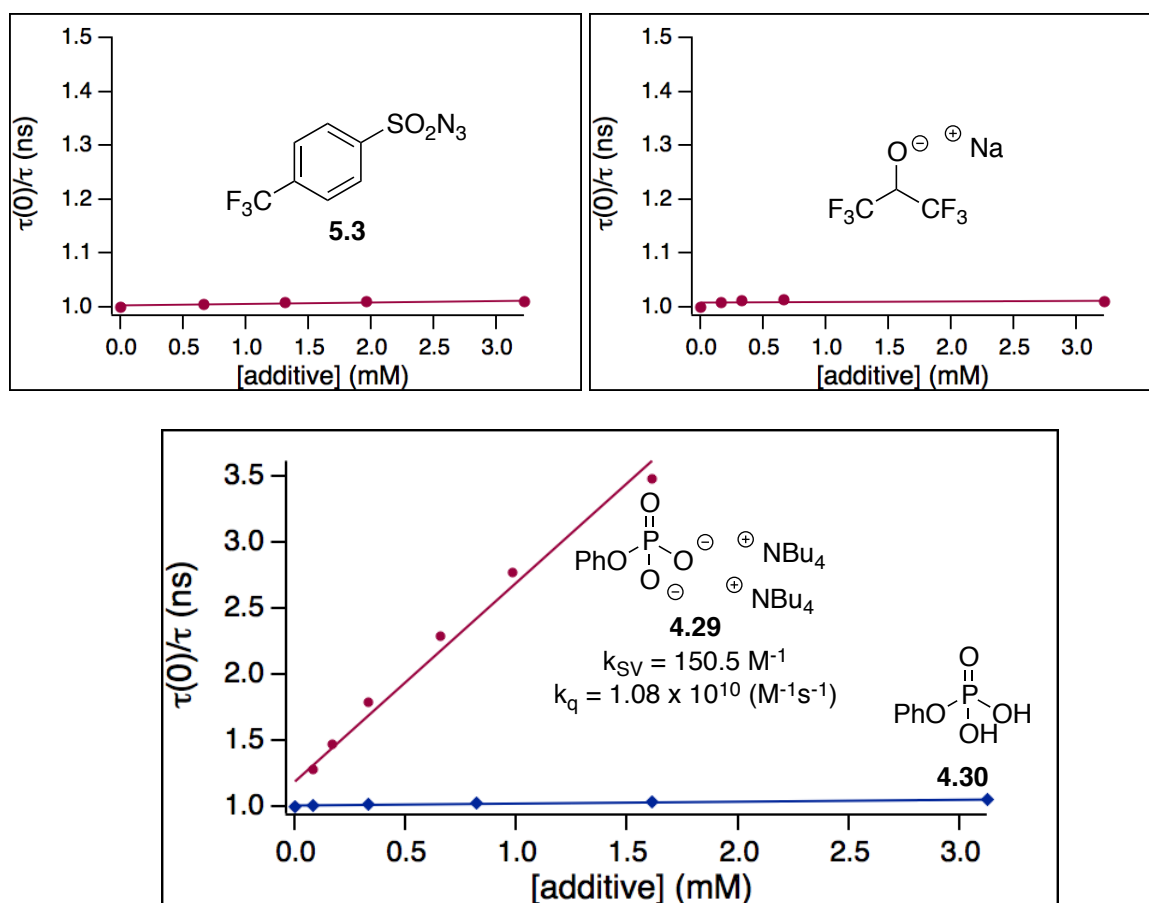


**Figure 4.5** Stern-Volmer quenching of acridinium catalyst.

We next examined the role of the base in the reaction. While  $\text{K}_3\text{PO}_4$  or the pH 8 phosphate buffer could be used in the reactions, we could not obtain reliable Stern-Volmer

quenching with them due to insolubility or immiscibility, regardless of the solvent used. To circumvent this issue, we synthesized a soluble dibasic phosphate salt **4.29** from the corresponding phosphoric acid **4.30**. We found that **4.29** could quench the excited state of the catalyst; however, the protonated derivative did not (**Figure 4.5**). This highlights the necessity for the anionic phosphate and not the phenoxy group for productive quenching. Addition of **4.29** also led to shifts in the  $^1\text{H}$  NMR spectra of the catalyst **4.1** in  $\text{CDCl}_3$  (**Figure 4.6**), suggesting a possible complex between the catalyst and salt in solution.

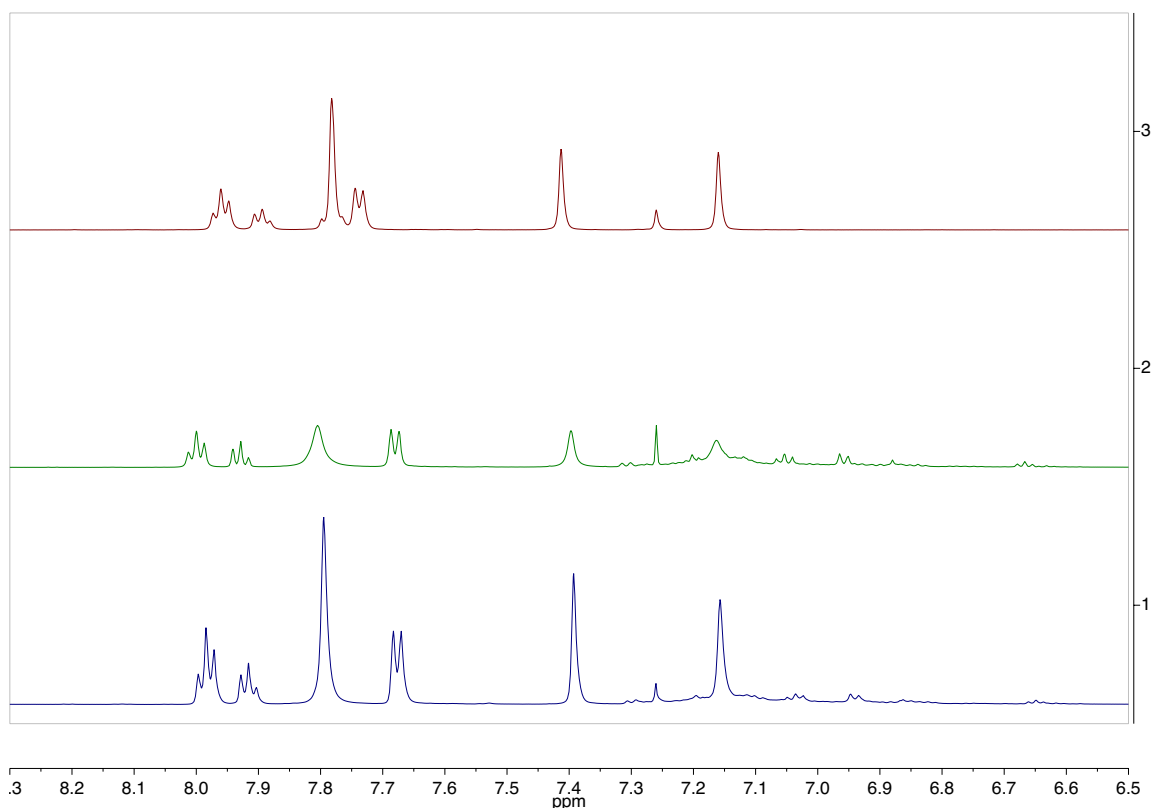


**Figure 4.6** Addition of **4.29** to acridinium catalyst **4.1**  $^1\text{H}$  NMR. Top: only catalyst **4.1**, Middle: 1 equiv of catalyst **4.1** and 1 equiv of **4.29**, Bottom: 2 equiv of catalyst **4.1** and 1 equiv of **4.29**.

We wanted to determine if dibasic phosphate **4.29** could be used in the C–H azidation. The use of substoichiometric **4.29** (5 or 20 mol %) produced up to 48% yield of azide **4.6**, consistent with a catalytic activity of the base (**Figure 4.7**). However, using

stoichiometric **4.29** led to a decrease in yield to 17%. With methyl 6-methylheptanoate as the substrate and 20 mol % **4.29**, azide **4.13** was formed in 20% yield. Importantly, tertiary functionalization occurred, suggesting that **4.29** and  $\text{K}_3\text{PO}_4$  serve the same role in the transformation.

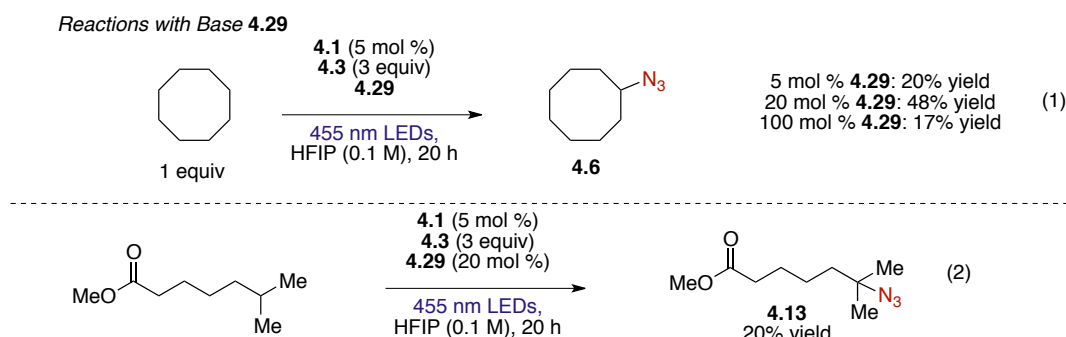


**Figure 4.7** Reactions with dibasic phosphate **4.29**.

### 4.3.6 Proposed Mechanism

We propose a mechanism consistent with these experiments (**Figure 4.8**). Using 455 nm LEDs, the acridinium photoredox catalyst can be excited and undergo SET with the phosphate salt, generating oxygen-centered radical **4.31**.

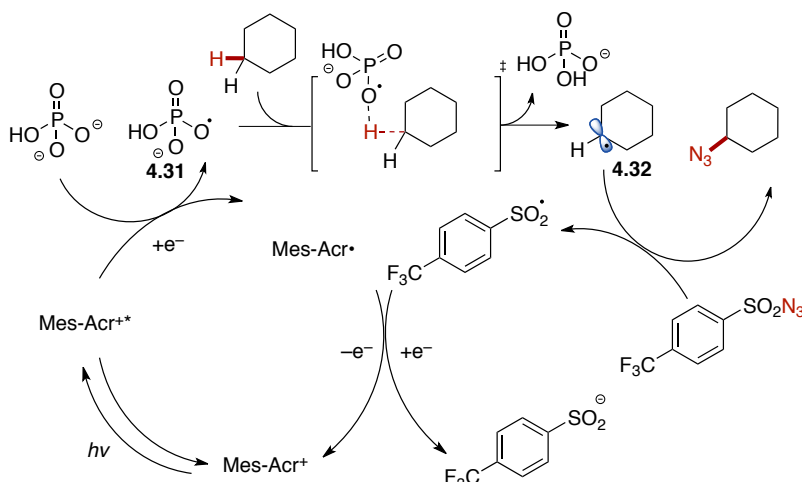


**Figure 4.8** Proposed mechanism for C–H azidation.

Abstraction of the most electron-rich C–H bond generates carbon-centered radical **4.32**, which is subsequently trapped by sulfonyl azide **4.3** to afford the desired product and a sulfonyl radical. Based on previous work in the Nicewicz lab,<sup>29</sup> we believe that this species is capable of oxidizing the acridine radical to regenerate the acridinium catalyst.

#### 4.4 Application Toward Polyolefin Azidation

We next sought to apply our photoredox-catalyzed C–H functionalization strategy toward the azidation of polyolefins, due to their widespread use as thermoplastics<sup>30</sup> but limited methods for obtaining materials containing additional functionality (see **Chapter 3.1**). Current methods of post-polymerization modification (PPM) that functionalize tertiary sites of polyolefins are plagued by chain scission processes that degrade the properties of the material, including recent examples of polyolefin azidation.<sup>31</sup> We wondered whether our system could achieve similar polyolefin azidation and minimize the deleterious processes.

In collaboration with Kaila Margrey in the Nicewicz group and Jill Williamson in the Leibfarth group, we studied the C–H azidation of poly(ethylethylene) (PEE). Under our previously optimized conditions, lack of azidation was verified by FT-IR spectroscopy and the lack of triazole formation after subjecting the crude polymer to copper-catalyzed azide-alkyne cycloaddition (CuAAC) conditions (**Figure 4.9**). Considering immiscibility of PEE with HFIP, we switched the solvent to DCE and observed no primary or secondary azidation by <sup>1</sup>H NMR analysis (**Figure 4.10**). However, the resultant polymer displayed a characteristic azide peak at 2098 cm<sup>-1</sup> after purification (**Figure 4.11**), indicating that azidation had occurred at exclusively tertiary positions. CuAAC of the azidated polymer formed a material with up to 4 mol % triazole incorporation, and GPC analysis indicated a slight decrease in *M*<sub>n</sub> and a similar value of *Đ* with respect to the unfunctionalized PEE

(**Figure 4.12**). A new absorbance peak was detected at 252 nm by PDA detection, indicating that aromatic functionality had been grafted to the polyolefin.

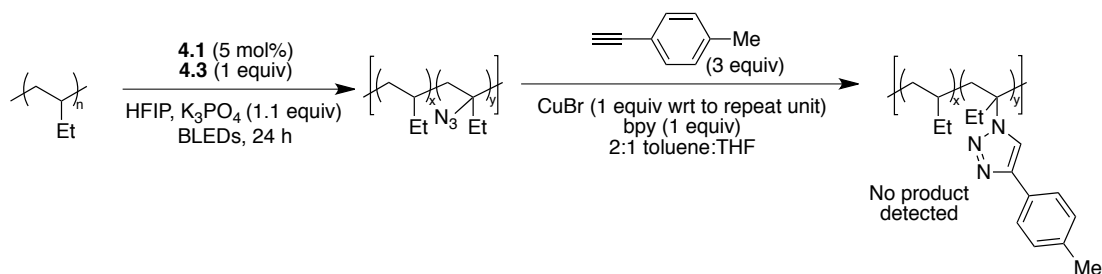


**Figure 4.9** Initial azidation attempt with PEE.

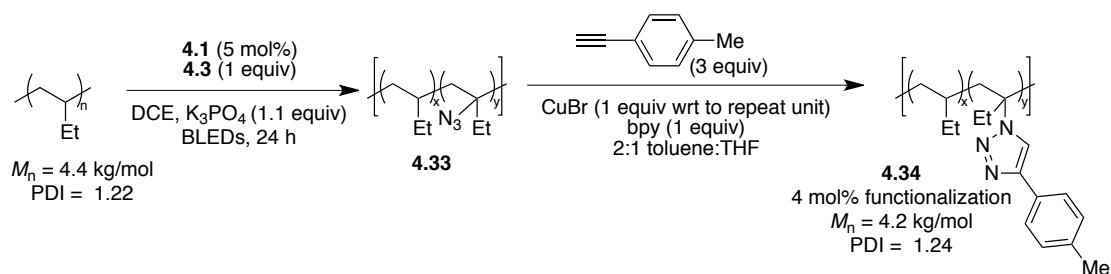


**Figure 4.10** Productive C-H azidation and CuAAC of PEE.

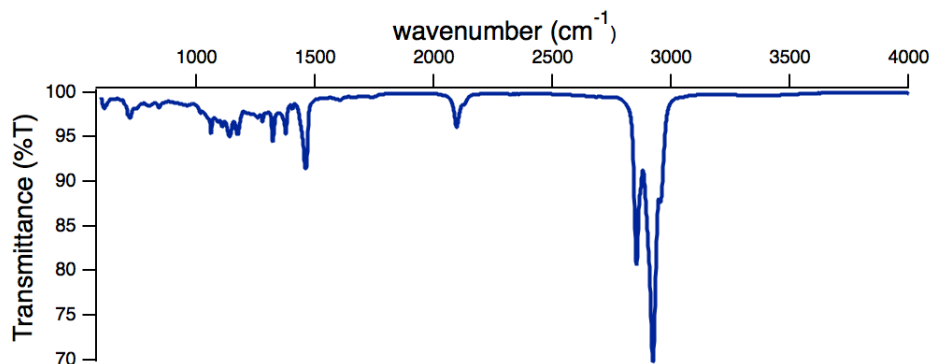


**Figure 4.11** Infrared spectrum of **4.33**, with azide stretch at 2100  $cm^{-1}$ .



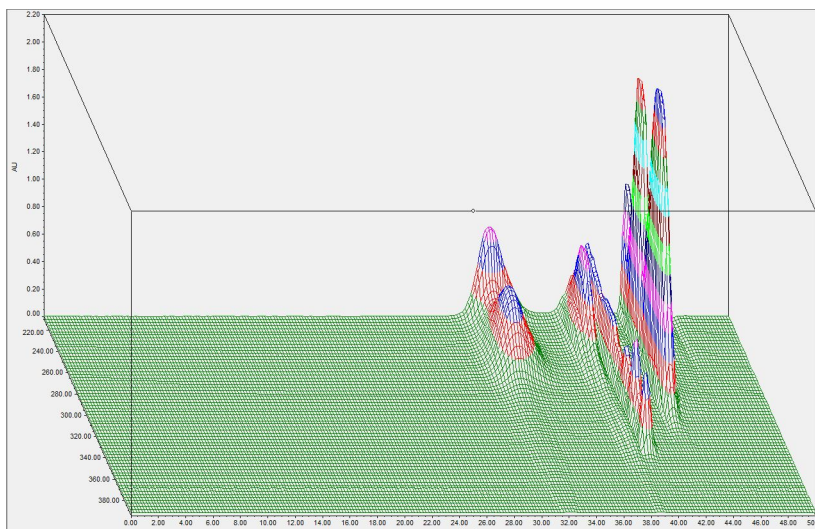


**Figure 4.12** Gel permeation chromatogram of **4.34**.

We further extended our studies to the functionalization of hyperbranched polyethylene (HBPE) as a higher molecular weight material with 13 mol % branching.<sup>32</sup> Azidation in DCE was unsuccessful, likely due to polymer immiscibility, but a mixture of chlorobenzene and DCE allowed for azidation to occur (**Figure 4.13**), as determined by FT-IR spectroscopy. Analysis by <sup>1</sup>H NMR again indicated that no primary or secondary azidation had occurred, and instead only tertiary functionalization was observed. GPC analysis showed no significant change in polymer properties, and CuAAC formed 0.5 mol % triazoles with respect to repeat unit. Accounting for the 13 mol % branching, 0.5 mol % triazole formation corresponds to functionalization at 3.8 mol % of the branch sites, similarly to PEE functionalization. Further work to optimize this transformation could allow for control over the amount of azidation, and the scope of both the polyolefin and the radical trap could be expanded.

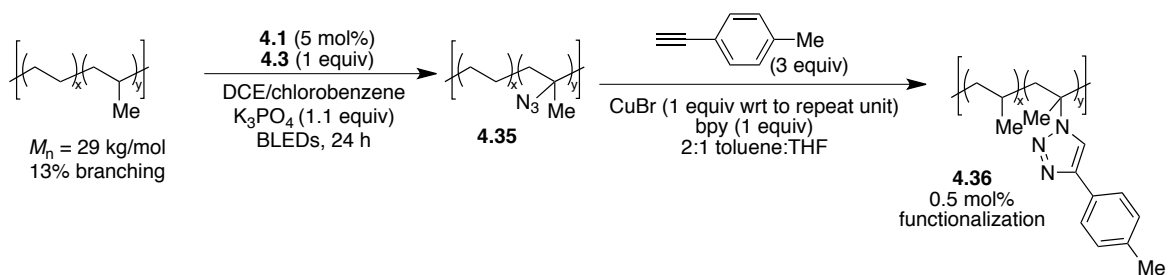


**Figure 4.13** C–H azidation and CuAAC of HBPE.

## 4.5 Conclusions

Through this work, we have developed a modular C–H functionalization strategy using mild conditions associated with organic photoredox catalysis. A number of small molecule substrates underwent efficient C–H azidation, and different transformations could be accessed simply by substituting the radical trap. Mechanistic studies suggest the intermediacy of an oxygen-centered radical responsible for the C–H abstraction. Preliminary results toward polyolefin azidation suggest the utility of the method in the field of post-polymerization modification.

## REFERENCES

- (1) Newhouse, T.; Baran, P. S. *Angew. Chem. Int. Ed.* **2011**, *50*, 3362–3374.
- (2) Yamaguchi, J.; Yamaguchi, A. D.; Itami, K. *Angew. Chem. Int. Ed.* **2012**, *51*, 8960–9009.
- (3) White, M. C. *Science* **2012**, *335*, 807–809.
- (4) Qin, Y.; Zhu, L.; Luo, S. *Chem. Rev.* **2017**, *117*, 9433–9520.
- (5) Czaplyski, W. L.; Na, C. G.; Alexanian, E. J. *J. Am. Chem. Soc.* **2016**, *138*, 13854–13857.
- (6) Prier, C. K.; Rankic, D. A.; MacMillan, D. W. C. *Chem. Rev.* **2013**, *113*, 5322–5363.
- (7) Shaw, M. H.; Twilton, J.; MacMillan, D. W. C. *J. Org. Chem.* **2016**, *81*, 6898–6926.
- (8) Romero, N. A.; Nicewicz, D. A. *Chem. Rev.* **2016**, *116*, 10075–10166.
- (9) Mendes, J.; Zhou, C.-W.; Curran, H. J. *J. Phys. Chem. A* **2014**, *118*, 1300–1308.
- (10) Hager, D.; MacMillan, D. W. C. *J. Am. Chem. Soc.* **2014**, *136*, 16986–16989.
- (11) Jeffrey, J. L.; Terrett, J. A.; MacMillan, D. W. C. *Science* **2015**, *349*, 1532–1536.
- (12) Le, C.; Liang, Y.; Evans, R. W.; Li, X.; MacMillan, D. W. C. *Nature* **2017**, *547*, 79–83.
- (13) Qvortrup, K.; Rankic, D. A.; MacMillan, D. W. C. *J. Am. Chem. Soc.* **2014**, *136*, 626–629.
- (14) Cuthbertson, J. D.; MacMillan, D. W. C. *Nature* **2015**, *519*, 74–77.
- (15) Jin, J.; MacMillan, D. W. C. *Angew. Chem. Int. Ed.* **2015**, *54*, 1565–1569.
- (16) Shaw, M. H.; Shurtleff, V. W.; Terrett, J. A.; Cuthbertson, J. D.; MacMillan, D. W. C. *Science* **2016**, *352*, 1304–1308.
- (17) Romero, N. A.; Margrey, K. A.; Tay, N. E.; Nicewicz, D. A. *Science* **2015**, *349*, 1326–1330.
- (18) Margrey, K. A.; McManus, J. B.; Bonazzi, S.; Zecri, F.; Nicewicz, D. A. *J. Am. Chem. Soc.* **2017**, *139*, 11288–11299.
- (19) Margrey, K. A.; Nicewicz, D. A. *Acc. Chem. Res.* **2016**, *49*, 1997–2006.

- (20) Margrey, K. A.; Levens, A.; Nicewicz, D. A. *Angew. Chem. Int. Ed.* **2017**, *56*, 15644–15648.
- (21) Mukherjee, S.; Maji, B.; Tlahuext-Aca, A.; Glorius, F. *J. Am. Chem. Soc.* **2016**, *138*, 16200–16203.
- (22) Joshi-Pangu, A.; Lévesque, F.; Roth, H. G.; Oliver, S. F.; Campeau, L.-C.; Nicewicz, D.; DiRocco, D. A. *J. Org. Chem.* **2016**, *81*, 7244–7249.
- (23) Shao, X.; Xu, C.; Lu, L.; Shen, Q. *Acc. Chem. Res.* **2015**, *48*, 1227–1236.
- (24) Choi, G. J.; Zhu, Q.; Miller, D. C.; Gu, C. J.; Knowles, R. R. *Nature* **2016**, *539*, 268–271.
- (25) Chu, J. C. K.; Rovis, T. *Nature* **2016**, *539*, 272–275.
- (26) Chen, D.-F.; Chu, J. C. K.; Rovis, T. *J. Am. Chem. Soc.* **2017**, *139*, 14897–14900.
- (27) Bortolamei, N.; Isse, A. A.; Gennaro, A. *Electrochimica Acta* **2010**, *55*, 8312–8318.
- (28) Bovicelli, P.; Lupattelli, P.; Mincione, E.; Prencipe, T.; Curci, R. *J. Org. Chem.* **1992**, *57*, 5052–5054.
- (29) Perkowski, A. J.; Nicewicz, D. A. *J. Am. Chem. Soc.* **2013**, *135*, 10334–10337.
- (30) Liu, P.; Liu, W.; Wang, W.-J.; Li, B.-G.; Zhu, S. *Macromol. React. Eng.* **2016**, *10*, 156–179.
- (31) Liu, D.; Bielawski, C. W. *Polym. Int.* **2017**, *66*, 70–76.
- (32) Bézier, D.; Daugulis, O.; Brookhart, M. *Organometallics* **2017**, *36*, 443–447.

## CHAPTER FIVE: QUATERNARY CENTER CONSTRUCTION VIA COUPLING OF ACYL XANTHATES WITH UNACTIVATED ALKENES

Adapted from: Jenkins, E. N.; Czaplyski, W. L.; Alexanian, E. J. *Org. Lett.* **2017**, *19*, 2350. Copyright 2017 American Chemical Society.

### 5.1 Introduction

When synthesizing compounds containing all-carbon quaternary centers, the construction of this component is often a significant challenge. Several strategies have been developed to overcome this obstacle, but few are general for intermolecular reactivity.<sup>1,2</sup> Radical-based methods are especially well-suited for this purpose, since they have early transition states and are less sensitive to steric constraints than are ionic processes,<sup>3</sup> allowing for the assembly of congested quaternary centers. An early example of this approach was in Barton's namesake esters (**Figure 5.1**), which serve as light-initiated progenitors of tertiary carbon-centered radicals that can undergo addition to activated olefins.<sup>4,5,6</sup> However, the generality of this strategy is limited due to the thermal and photochemical instability of the Barton ester-functionalized materials.

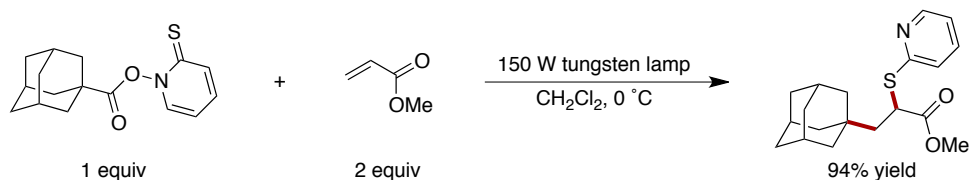


**Figure 5.1** Quaternary center formation via Barton esters.

Recent strategies have sought to generate nucleophilic tertiary carbon-centered radicals for similar addition processes to forge quaternary centers.<sup>7</sup> Baran and coworkers used an iron catalyst to activate trisubstituted or 1,1-disubstituted olefins and form tertiary

radicals, allowing for intermolecular coupling with electron-poor alkenes (**Figure 5.2**).<sup>8</sup> More recent extensions of this work have significantly expanded the substrate scope and provided mechanistic insight that allowed development of second-generation conditions.<sup>9</sup>

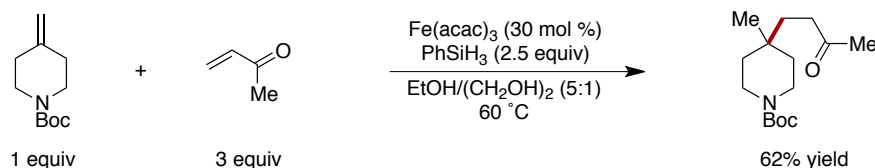


**Figure 5.2** Reductive coupling of unactivated alkenes with electron-poor alkenes.

Photoredox catalysis has also been used, most notably by Macmillan and Overman, to activate tertiary alcohol<sup>10–13</sup> and carboxylic acid<sup>14–17</sup> derivatives to generate nucleophilic tertiary radicals, which can similarly undergo intermolecular addition to activated olefins (**Figure 5.3**). Related strategies have been developed to use activated alkynes as electrophilic coupling partners to form quaternary centers,<sup>18,19</sup> and methods involving electrophilic tertiary radicals have also been disclosed.<sup>20</sup> Despite these advances, there is not a general method for the intermolecular coupling of a nucleophilic tertiary radical derived from a carboxylic acid with unactivated alkenes due to the electronic unsuitability of these coupling partners.<sup>21,22</sup>

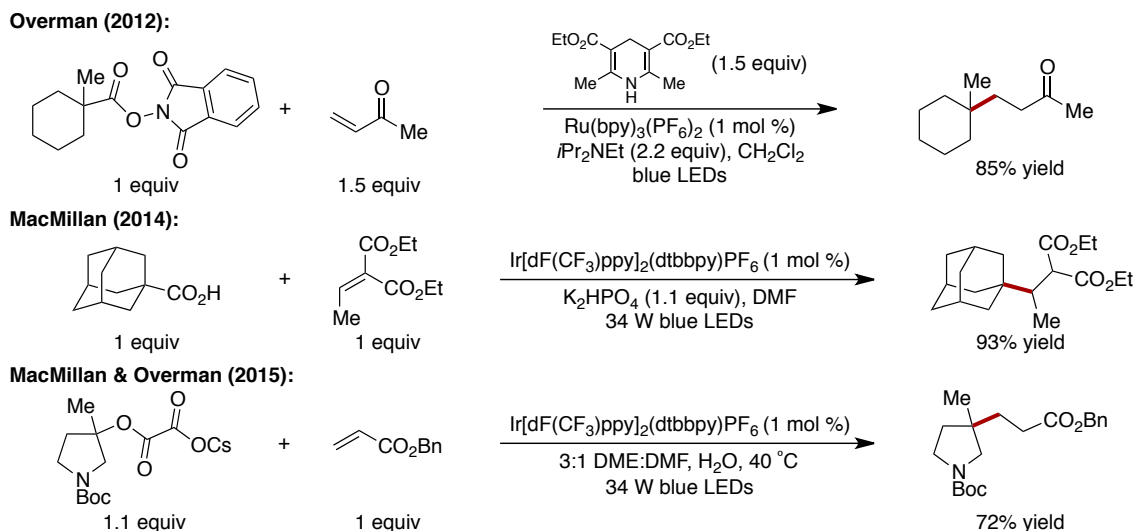


**Figure 5.3** Generation of quaternary centers via coupling of tertiary alcohol or carboxylic acid derivatives with activated alkenes.

## 5.2 Background

Although alkyl xanthates have been used for additions to unactivated alkenes in a variety of contexts (see **Chapter 2.2.2**), there are comparatively few examples of the formation of quaternary centers through this strategy. This is likely due to the dearth of approaches for accessing the requisite tertiary alkyl xanthate precursors that would enable quaternary center formation. Zard has reported the synthesis of such compounds through the thermal decomposition of symmetric diazo compounds and trapping with bisxanthate **5.1** (**Figure 5.4**),<sup>23</sup> though this method is limited in scope by the need to prepare the diazo starting materials. The most synthetically useful strategy to prepare tertiary alkyl xanthates is via reversible conjugate addition of potassium ethyl xanthate to  $\beta$ -disubstituted enones.<sup>24,25</sup> Superstoichiometric acetic or trifluoroacetic acid is needed to favor formation of the desired  $\beta$ -xanthyl ketone, restricting the additional functionality that can be present in the compound.

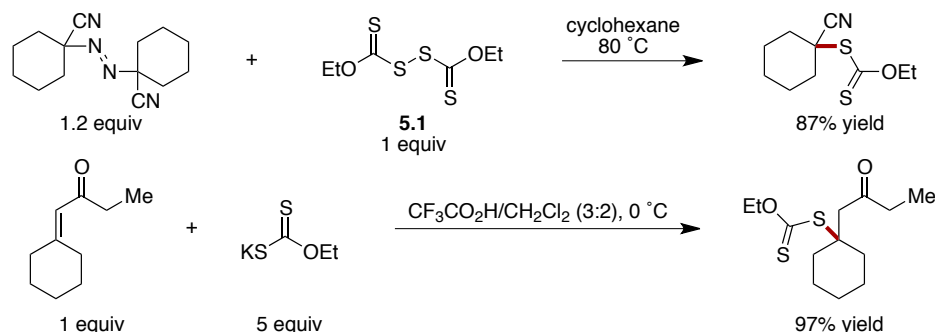


**Figure 5.4** Strategies for the synthesis of tertiary alkyl xanthates.

With these limitations in mind, we sought to use acyl xanthates as precursors to tertiary carbon-centered radicals that would possess the same benefits as tertiary alkyl xanthates without the corresponding challenges in preparation. Acyl xanthates are readily prepared by treating an acyl chloride with commercially available potassium ethyl xanthate (**Figure 5.5**), and they have been studied in a variety of contexts. Critical to the successful synthesis of acyl xanthates is the stoichiometry of the reaction, in that the acyl chloride

substrate must be used in slight excess with respect to the anionic xanthate. If excess xanthate salt is present, it can trigger an ionic chain decomposition pathway.<sup>26</sup>

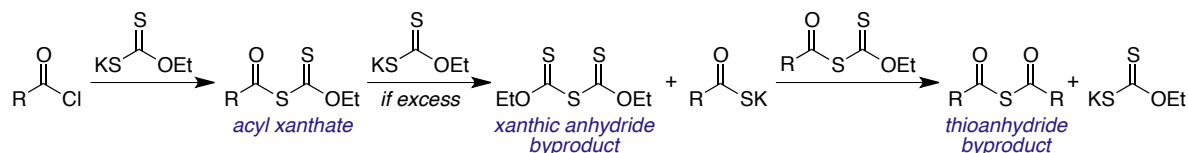


**Figure 5.5** Acyl xanthate synthesis and decomposition pathway.

The use of acyl xanthates in direct olefin additions to form quaternary centers is limited. Zard used a phenyl-substituted cyclopropyl acyl xanthate **5.2** to generate tertiary xanthate **5.3** in a decarbonylative reaction (**Figure 5.6**).<sup>27</sup> This intermediate was used in a second step for radical coupling with allyl acetate to produce **5.4** in very low overall yield, and the reaction was not generalizable to any additional substrates.

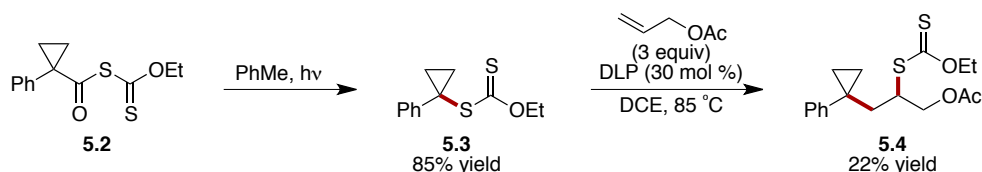


**Figure 5.6** Two-step decarbonylative addition of a cyclopropyl acyl xanthate to allyl acetate.

We hypothesized that using tertiary acyl xanthates as carbon-centered radical precursors would allow for decarbonylative coupling with unactivated alkenes to form quaternary centers in a general manner. We believed that this process would be kinetically favorable, owing to the relatively high rate of unimolecular decarbonylation to generate tertiary radicals (on the order of  $10^5 \text{ s}^{-1}$ ).<sup>28</sup>

## 5.3 Reaction Development

### 5.3.1 Optimization

This project was completed alongside another member of the Alexanian group, Nicholas Jenkins. Our studies began by optimizing the coupling of a 1-methylcyclohexanecarboxylic acid-derived acyl xanthate with allyl acetate (**Table 5.1**).



Dilauroyl peroxide (DLP) was a more efficient radical initiator than BPO or AIBN in benzene, giving 40% yield of the addition product with 5 equivalents of allyl acetate (**Table 5.1, entries 1 – 3**); accordingly, DLP was chosen as the initiator for further optimization.

**Table 5.1** Optimization for quaternary center construction.

1 equiv

entry	initiator	olefin equiv	solvent (concentration)	yield (%) <sup>a</sup>
1	BPO	5	PhH (0.3 M)	6
2	AIBN	5	PhH (0.3 M)	4
3	DLP	5	PhH (0.3 M)	40
4	DLP	2	PhH (0.3 M)	76
5	DLP	1.5	PhH (0.3 M)	45
6	DLP	2	PhMe (0.3 M)	35
7	DLP	2	PhCF <sub>3</sub> (0.3 M)	21
8	DLP	2	PhCl (0.3 M)	67
9	DLP	2	MeCN (0.3 M)	63
10	DLP	2	DCE (0.3 M)	70
11	DLP	2	DCE (1 M)	74

<sup>a</sup>NMR yield with hexamethyldisiloxane (HMDS) as internal standard.

Under these conditions, oligomerization of allyl acetate was observed as a byproduct pathway; lowering the amount of allyl acetate in the reaction to 2 equivalents gave 70% yield of the desired addition product (**Table 5.1, entry 4**), but further lessening the amount to 1.5 equivalents led to a marked decrease in yield (**Table 5.1, entry 5**). Several other solvents were screened in the reaction, with benzene and DCE performing the best (**Table 5.1, entries 6 – 10**). Although the reaction proceeded most efficiently in benzene, we later discovered that DCE at higher concentration was the most general solvent for the transformation when using 2 equivalents of the alkene trap and 10 mol % DLP (**Table 5.1, entry 11**). Under these

optimized reaction conditions, the acyl xanthate derived from cyclohexanecarboxylic acid did not undergo decarbonylation and subsequent addition (**Figure 5.7**), indicating that the reaction is uniquely effective for quaternary center construction.

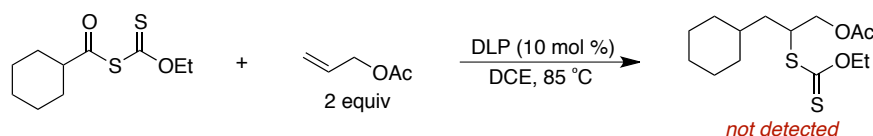


**Figure 5.7** Lack of reactivity with secondary acyl xanthates in the alkene addition.

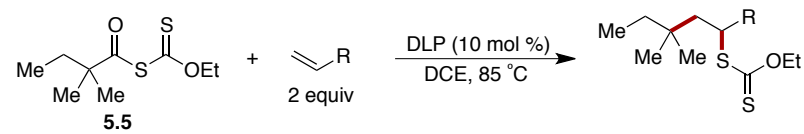
### 5.3.2 Substrate Scope

With the optimized conditions, we set out to explore the substrate scope of the transformation by varying the olefin component in the reaction with acyl xanthate **5.5** (**Table 5.2**). A variety of functional groups were tolerated in the reaction, including esters, protected amines, free alcohols, carbonyl compounds, epoxides, and phosphonates (**Table 5.2, entries 1 – 6**). Varying the number of carbons between the olefin and tethered functionality did not change the yield of the reaction (**Table 5.2, entries 1, 7, 8**), suggesting a lack of dependence on the electronic nature of the alkene; this is further supported by the efficient reaction of **XX** with the completely unactivated 1-octene (**Table 5.2, entry 9**).

The reaction yields were generally quite consistent across the different olefin partners, but tended to be moderate in all cases. This is partially due to formation of a primary alkyl xanthate byproduct resulting from the DLP initiation process, which prevents up to 20 mol % xanthate functionality from reacting with the tertiary carbon-centered radical formed after decarbonylation. Additionally, the secondary xanthate products formed are susceptible to minor degradation under the reaction conditions.

We next sought to study the scope of the transformation with respect to the acyl xanthate using allyl acetate as the coupling partner (**Table 5.3**). For recalcitrant substrates,

**Table 5.2** Unactivated olefin scope for intermolecular quaternary center construction.

			
entry	alkene	product	yield (%) <sup>b</sup>
1			62
2			61
3			62
4			61
5			61 1.1:1 dr
6			43
7			69
8			65
9			80 <sup>c</sup>

<sup>a</sup>Reactions were performed with [substrate]<sub>0</sub> = 1.0 M and 1 addition of 10 mol % DLP.<sup>b</sup>Isolated yields. <sup>c</sup>NMR yield with hexamethyldisiloxane (HMDS) as internal standard.

two additions of 10 mol % DLP were necessary to achieve synthetically useful yields. Cyclic quaternary centers could be formed in moderate yield by using cyclohexyl and *N*-tosylpiperidinyl substrates **5.15** and **5.17** to form **5.16** and **5.18**, respectively (Table 5.3, entries 1 – 2). Acyl xanthate **5.19** with β-acetate disubstitution provided triacetate **5.20** in good yield (Table 5.3, entry 3). Decalin acyl xanthate **5.21**, a mix of both *cis* and *trans* isomers, formed adduct **5.22** slightly favoring the *cis* isomer, showing applicability to the formation of quaternary centers at ring fusion sites (Table 5.3, entry 4). Acyl xanthate **5.23**,

**Table 5.3** Acyl xanthate scope for intermolecular quaternary center construction.

entry	acyl xanthate	product	yield (%) <sup>b</sup>
1	 5.15	 5.16	62
2	 5.17	 5.18	61
3	 5.19	 5.20	68
4	 5.21	 5.22	50 2.7:1 <i>cis:trans</i>
5	 5.23	 5.24	68
6	 5.25	 5.26	67 1.1:1 dr

<sup>a</sup>Reactions were performed with [substrate]<sub>0</sub> = 1.0 M and 1 – 2 additions of 10 mol % DLP. <sup>b</sup>Isolated yields.

derived from the cholesterol-lowering pharmaceutical gemfibrozil, provided the coupling adduct **5.24** in 68% yield (**Table 5.3, entry 5**). The acyl xanthate **5.25**, accessed from the bioactive natural product isosteviol,<sup>29</sup> provided **5.26** in 67% yield as a mixture of diastereomers at the new secondary xanthate position (**Table 5.3, entry 6**). Reaction with allyl acetate occurred exclusively on the less-hindered face of the ring system, resulting in the equatorial coupling product. The same stereochemical outcome was observed by Overman in syntheses of the *trans*-clerodanes, which possess a similar fused ring system.<sup>30,31</sup>

**Table 5.4** Intramolecular quaternary center construction via cyclizations of unsaturated tertiary acyl xanthates.

entry	alkene	product	yield (%)
1	 <b>5.27</b>	 <b>5.28</b>	82 <sup>c</sup>
2	 <b>5.29</b>	 <b>5.30</b>	71
3	 <b>5.31</b>	 <b>5.32</b>	74
4	 <b>5.33</b>	 <b>5.34</b>	65
5	 <b>5.35</b>	 <b>5.36</b>	70
		 <b>5.37</b>	5.36:5.37 = 5.7:1

<sup>a</sup>Reactions were performed with [substrate]<sub>0</sub> = 1.0 M and 1 – 2 additions of 10 mol % DLP. <sup>b</sup>Isolated yields.

<sup>c</sup>NMR yield with hexamethyldisiloxane (HMDS) as internal standard.

Having demonstrated the ability of this strategy to form quaternary centers for intermolecular couplings, we sought to expand the scope further to access quaternary center-forming ring-closing reactions, which have applications in complex molecule synthesis. Acyclic precursors **5.27** and **5.29** underwent decarbonylative 5-exo cyclization to form **5.28** and **5.30** in good yield (**Table 5.4**, entries 1 – 2). Although 6-exo ring closure by the intermediate acyl radical is possible, no cyclohexanone or dihydropyranone products are observed, indicating that decarbonylation is kinetically favorable under the reaction conditions. We also extended this methodology to the formation of spirocyclic compounds **5.32** and **5.34** derived from tetrahydropyranyl acyl xanthate **5.31** and *N*-tosylpiperidiny acyl xanthate **5.33**, respectively

(Table 5.4, entries 3 – 4). Such compounds are often challenging to access due to the steric congestion of the quaternary center. Additionally, other ring sizes could be accessed using this strategy; acyl xanthate **5.35** underwent decarbonylative 6-exo cyclization to form cyclohexane **5.36** in good yield, although cycloheptane **5.37**, resulting from 7-endo cyclization, was also formed in the reaction (Table 5.4, entry 5).

### 5.3.3 Mechanistic Studies

To investigate the reaction mechanism, we performed several additional experiments. At short reaction times (10 min instead of 2 h), piperidiny acyl xanthate **5.17** underwent decarbonylation to form tertiary xanthate **5.38** in 70% yield, and only 20% yield of addition product **5.18** was observed (Figure 5.8). In the absence of an olefin coupling partner, acyl xanthates have been shown to undergo decarbonylation to afford the corresponding alkyl xanthate.<sup>32</sup> Isolation of the tertiary alkyl xanthate and resubmission under normal reaction conditions led to the formation of adduct **5.18** in comparable yield to the standard reaction.

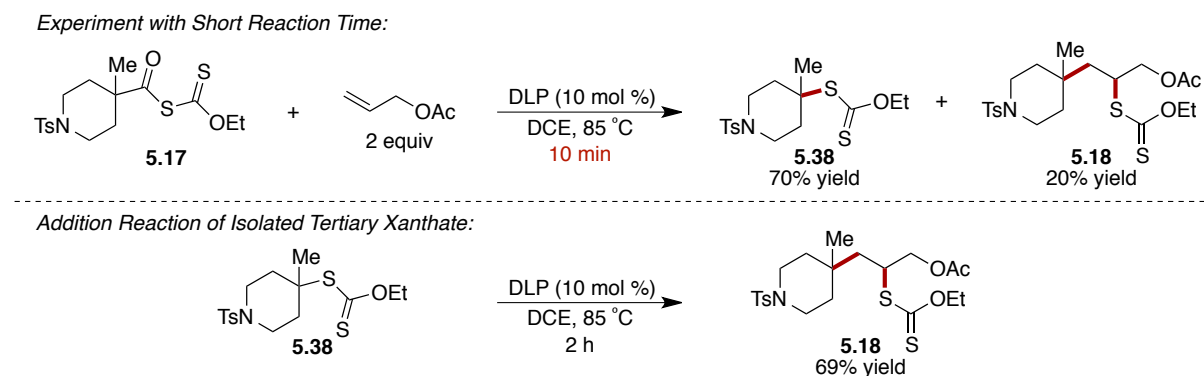


**Figure 5.8** Mechanistic experiments.

Based on these data, we believe that initiation with DLP leads to the formation of a tertiary acyl radical (Figure 5.9). At elevated temperatures, decarbonylation occurs to afford the tertiary carbon-centered radical, which can undergo addition/elimination with another molecule of starting material in a chain-propagating step that generates the tertiary alkyl

xanthate. Loss of xanthate via the addition/elimination of another primary or secondary carbon-centered radical can produce the tertiary radical, which undergoes addition to the olefin and generates a new secondary radical. Reversible addition to another xanthate-containing molecule and  $\beta$ -scission leads to the formation of the new quaternary center-containing product and further chain propagation.

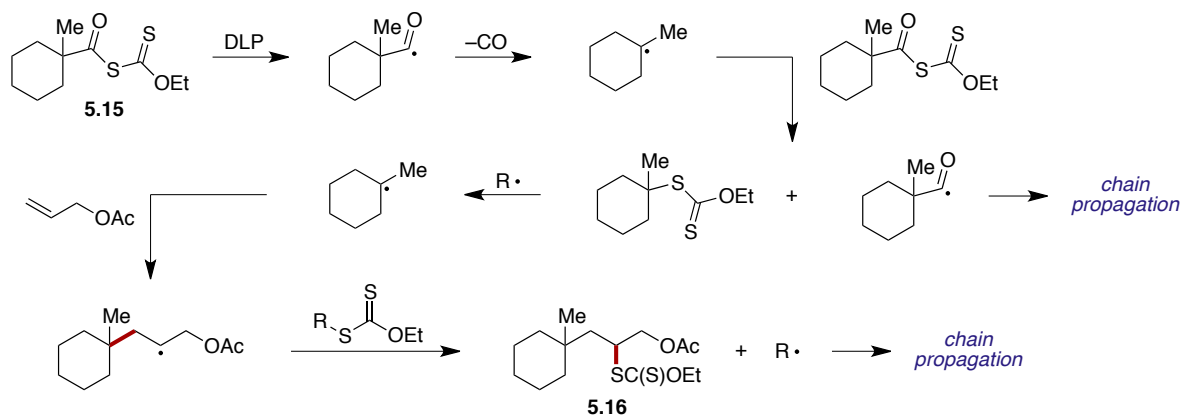


**Figure 5.9** Proposed mechanism for quaternary center construction via acyl xanthates.

### 5.3.4 Diversification of Xanthate Products

In alternative approaches using electron-poor olefins, the carbon-centered radical formed after alkene addition is trapped with an H atom source or reduced to the enolate for subsequent protonation. The present methodology instead installs a xanthate group, which serves as a handle for molecular diversification. Consequently, net alkene carbodifunctionalization transformations can be accessed in one step following the decarbonylative coupling. As a demonstration of this strategy, we coupled gemfibrozil-derived acyl xanthate **5.23** with *N*-Boc-allylamine in 61% yield and performed several divergent transformations on the resultant adduct (**Figure 5.10**). Aminolysis affords, in 85% yield, the thiol, which can be used in the bioorthogonal thiol-ene click reaction with a suitable alkene.<sup>33</sup> Using conditions we developed previously,<sup>34</sup> conversion of the xanthate to the ketone occurs in 65% yield, representing the net coupling of a tertiary radical with one

located at the  $\alpha$ -position of a carbonyl. Alkylation can occur via a radical group transfer strategy developed by Zard,<sup>35</sup> affording a net olefin dialkylation product in 61% yield. Finally, we showed the formation of the deuterated product from the alkyl xanthate,<sup>36</sup> due to deuterium's capacity for enhancing pharmacokinetic properties of compounds and the applications of deuterated compounds in metabolic studies.<sup>37</sup>

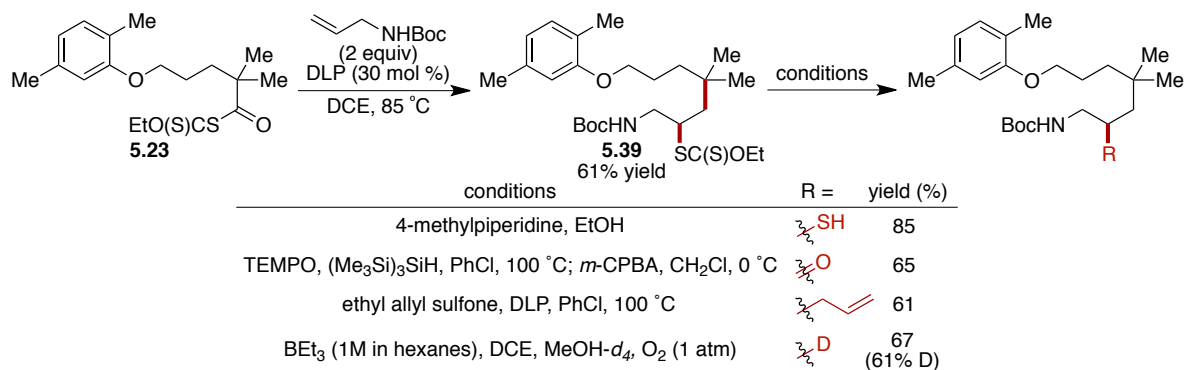


**Figure 5.10** Diversification of xanthate coupling products.

## 5.4 Conclusions

Through this work, we developed a strategy to accomplish the synthesis of quaternary centers through the decarbonylative coupling of tertiary acyl xanthates with unactivated terminal alkenes. The reaction proceeds under fairly mild conditions and is tolerant of a wide variety of functionality. This strategy allows for both inter- and intramolecular coupling reactions, with potential applications in complex molecule synthesis. Furthermore, the alkyl xanthate present in the products acts as a new functional handle, allowing for access to net carbodifunctionalization products.



## REFERENCES

- (1) Christoffers, J.; Baro, A.; John Wiley & Sons. Wiley-VCH: Weinheim, 2005.
- (2) Quasdorf, K. W.; Overman, L. E. *Nature* **2014**, *516*, 181–191.
- (3) Damm, W.; Giese, B.; Hartung, J.; Hasskerl, T.; Houk, K. N.; Hueter, O.; Zipse, H. *J. Am. Chem. Soc.* **1992**, *114*, 4067–4079.
- (4) Barton, D. H. R.; Crich, D.; Kretzschmar, G. *J. Chem. Soc. Perkin Trans. I* **1986**, 39–53.
- (5) Barton, D. H. R.; Chern, C.-Y.; Jaszberenyi, J. C. *Tetrahedron* **1995**, *51*, 1867–1886.
- (6) Barton, D. H. R.; Liu, W. *Tetrahedron Lett.* **1997**, *38*, 2431–2434.
- (7) Jamison, C. R.; Overman, L. E. *Acc. Chem. Res.* **2016**, *49*, 1578–1586.
- (8) Lo, J. C.; Yabe, Y.; Baran, P. S. *J. Am. Chem. Soc.* **2014**, *136*, 1304–1307.
- (9) Lo, J. C.; Kim, D.; Pan, C.-M.; Edwards, J. T.; Yabe, Y.; Gui, J.; Qin, T.; Gutiérrez, S.; Giacoboni, J.; Smith, M. W.; *et al.* *J. Am. Chem. Soc.* **2017**, *139*, 2484–2503.
- (10) Togo, H.; Matsubayashi, S.; Yamazaki, O.; Yokoyama, M. *J. Org. Chem.* **2000**, *65*, 2816–2819.
- (11) Lackner, G. L.; Quasdorf, K. W.; Overman, L. E. *J. Am. Chem. Soc.* **2013**, *135*, 15342–15345.
- (12) Lackner, G. L.; Quasdorf, K. W.; Pratsch, G.; Overman, L. E. *J. Org. Chem.* **2015**, *80*, 6012–6024.
- (13) Nawrat, C. C.; Jamison, C. R.; Slutskyy, Y.; MacMillan, D. W. C.; Overman, L. E. *J. Am. Chem. Soc.* **2015**, *137*, 11270–11273.
- (14) Okada, K.; Okamoto, K.; Morita, N.; Okubo, K.; Oda, M. *J. Am. Chem. Soc.* **1991**, *113*, 9401–9402.
- (15) Chu, L.; Ohta, C.; Zuo, Z.; MacMillan, D. W. C. *J. Am. Chem. Soc.* **2014**, *136*, 10886–10889.
- (16) Pratsch, G.; Lackner, G. L.; Overman, L. E. *J. Org. Chem.* **2015**, *80*, 6025–6036.
- (17) Chinzei, T.; Miyazawa, K.; Yasu, Y.; Koike, T.; Akita, M. *RSC Adv* **2015**, *5*, 21297–21300.
- (18) Yang, J.; Zhang, J.; Qi, L.; Hu, C.; Chen, Y. *Chem. Commun.* **2015**, *51*, 5275–5278.

- (19) Gao, C.; Li, J.; Yu, J.; Yang, H.; Fu, H. *Chem. Commun.* **2016**, 52, 7292–7294.
- (20) Huan, F.; Chen, Q.-Y.; Guo, Y. *J. Org. Chem.* **2016**, 81, 7051–7063.
- (21) Giese, B. *Angew. Chem. Int. Ed. Engl.* **1983**, 22, 753–764.
- (22) Srikanth, G. S. C.; Castle, S. L. *Tetrahedron* **2005**, 61, 10377–10441.
- (23) Bouhadir, G.; Legrand, N.; Quiclet-Sire, B.; Zard, S. Z. *Tetrahedron Lett.* **1999**, 40, 277–280.
- (24) Binot, G.; Quiclet-Sire, B.; Saleh, T.; Zard, S. Z. *Synlett* **2003**, 0382–0386.
- (25) Quiclet-Sire, B.; Zard, S. Z. In *Radicals in Synthesis II*; Gansäuer, A., Ed.; Springer-Verlag: Berlin/Heidelberg, 2006; Vol. 264, pp. 201–236.
- (26) Zard, S. Z. *Angew. Chem. Int. Ed. Engl.* **1997**, 36, 672–685.
- (27) Heinrich, M. R.; Zard, S. Z. *Org. Lett.* **2004**, 6, 4969–4972.
- (28) Chatgililoglu, C.; Crich, D.; Komatsu, M.; Ryu, I. *Chem. Rev.* **1999**, 99, 1991–2070.
- (29) Brahmachari, G.; Mandal, L. C.; Roy, R.; Mondal, S.; Brahmachari, A. K. *Arch. Pharm. (Weinheim)* **2011**, 344, 5–19.
- (30) Müller, D. S.; Untiedt, N. L.; Dieskau, A. P.; Lackner, G. L.; Overman, L. E. *J. Am. Chem. Soc.* **2015**, 137, 660–663.
- (31) Slutskyy, Y.; Jamison, C. R.; Lackner, G. L.; Müller, D. S.; Dieskau, A. P.; Untiedt, N. L.; Overman, L. E. *J. Org. Chem.* **2016**, 81, 7029–7035.
- (32) Barton, D. H. R.; George, M. V.; Tomoeda, M. *J. Chem. Soc. Resumed* **1962**, 1967.
- (33) Hoyle, C. E.; Bowman, C. N. *Angew. Chem. Int. Ed.* **2010**, 49, 1540–1573.
- (34) Czaplyski, W. L.; Na, C. G.; Alexanian, E. J. *J. Am. Chem. Soc.* **2016**, 138, 13854–13857.
- (35) Quiclet-Sire, B.; Seguin, S.; Zard, S. Z. *Angew. Chem. Int. Ed.* **1998**, 37, 2864–2866.
- (36) Allais, F.; Boivin, J.; Nguyen, V. T. *Beilstein J. Org. Chem.* **2007**, 3, 46.
- (37) Harbeson, S. L.; Tung, R. D. In *Annual Reports in Medicinal Chemistry*; Elsevier, 2011; Vol. 46, pp. 403–417.

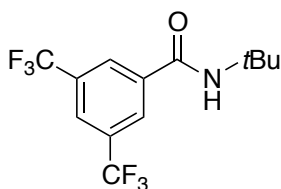
## APPENDIX A: SUPPORTING INFORMATION FOR CHAPTER 2

### General Methods and Materials

Infrared (IR) spectra were obtained using a Jasco 260 Plus Fourier transform infrared spectrometer. GC spectra were obtained using a Shimadzu GC-2010 gas chromatograph with a Shimadzu AOC-20s Autosampler, and Shimadzu SHRXI-5MS GC column. The results of the kinetic isotope study were analyzed using an Agilent Gas Chromatograph-Mass Spectrometer with a 6850 series GC system and a 5973 Network Mass Selective Detector. Proton and carbon magnetic resonance spectra ( $^1\text{H}$  NMR and  $^{13}\text{C}$  NMR) were recorded on a Bruker model DRX 400, or a Bruker AVANCE III 600 CryoProbe ( $^1\text{H}$  NMR at 400 or 600 MHz and  $^{13}\text{C}$  NMR at 100 or 151 MHz) spectrometer with solvent resonance as the internal standard ( $^1\text{H}$  NMR:  $\text{CDCl}_3$  at 7.26 ppm;  $^{13}\text{C}$  NMR:  $\text{CDCl}_3$  at 77.16 ppm).  $^1\text{H}$  NMR data are reported as follows: chemical shift, multiplicity (s = singlet, d = doublet, t = triplet, q = quartet, dd = doublet of doublets, ddd = doublet of doublet of doublets, td = triplet of doublets, tdd = triplet of doublet of doublets, qd = quartet of doublets, m = multiplet, br. s. = broad singlet, app = apparent), coupling constants (Hz), and integration. Mass spectra were obtained using a Thermo LTqFT mass spectrometer with electrospray introduction and external calibration. Thin layer chromatography (TLC) was performed on SiliaPlate 250 $\mu\text{m}$  thick silica gel plates provided by Silicycle. Visualization was accomplished with short wave UV light (254 nm), iodine, aqueous basic potassium permanganate solution, or aqueous acidic ceric ammonium molybdate solution followed by heating. Flash chromatography was performed using SiliaFlash P60 silica gel (40-63  $\mu\text{m}$ ) purchased from Silicycle. Tetrahydrofuran, diethyl ether, and dichloromethane were dried by passage through a column of neutral alumina under nitrogen prior to use. Irradiation of xanthylation reactions was

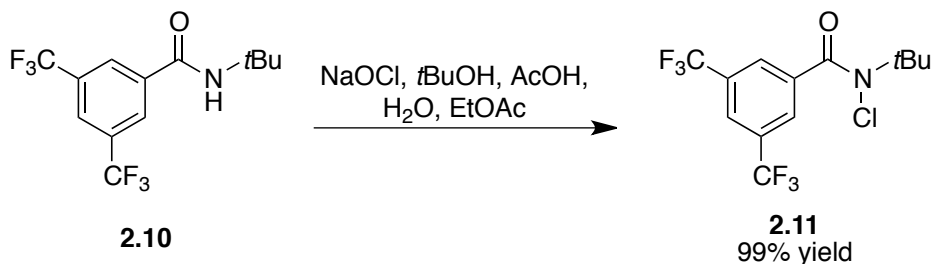
performed using either PAR38 Royal Blue 21W aquarium LED lamps (Model #6851) fabricated with high-power Cree XR-E LEDs as purchased from Ecoxotic ([www.ecoxotic.com](http://www.ecoxotic.com)) or Kessil KSH150B Blue 36W LED Grow Lights. UV light experiments were performed in a Luzchem LZC-ORG photoreactor containing UVA lamps. All other reagents were obtained from commercial sources and used without further purification unless otherwise noted.

### Xanthylamide Synthesis

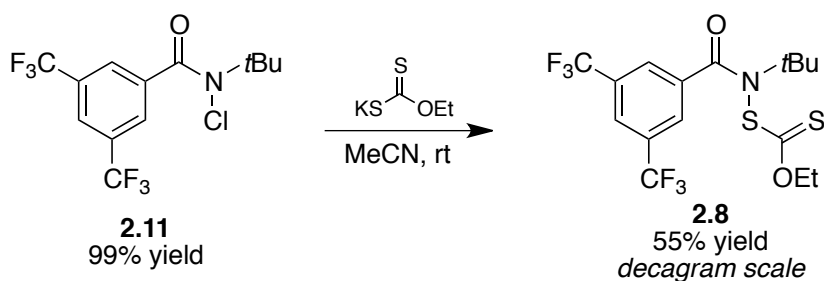


**2.10**

***N*-(*tert*-butyl)-3,5-bis(trifluoromethyl)benzamide (2.10):** Prepared similarly to previous reports from our lab.<sup>3,4</sup> To a solution of 3,5-bis(trifluoromethyl)benzoic acid (15 g, 58.11 mmol) in CH<sub>2</sub>Cl<sub>2</sub>/DMF (232 mL/1 mL) at 0 °C was added oxalyl chloride (9.85 mL, 116.23 mmol) dropwise, and the resulting solution was allowed to warm to rt overnight. The mixture was concentrated *in vacuo* and resuspended in THF (200 mL) and chilled to 0 °C. *t*-Butylamine (12.21 mL, 116.23 mmol) was added, and the mixture was warmed to rt and stirred overnight. The ammonium salts were filtered and the mixture was concentrated *in vacuo* and the residue suspended in Et<sub>2</sub>O (250 mL) and washed with 3M NaOH (1 x 200 mL), 1M HCl (1 x 200 mL), brine (1 x 200 mL), dried with MgSO<sub>4</sub> and concentrated to afford **2.10** as a pale yellow solid (16.12 g, 89% yield), which was used without purification.



***N*-(*tert*-butyl)-*N*-chloro-3,5-bis(trifluoromethyl)benzamide (2.11):** Prepared similarly to a previous report from our lab.<sup>4</sup> With the laboratory lights off, to a solution of amide (16.1 g) in EtOAc (296 mL) was added *t*BuOH (7.8 mL). To this solution was added a solution of AcOH (68 mL), NaOCl (172 mL), and H<sub>2</sub>O (103 mL) dropwise over 2 h via addition funnel. The mixture was stirred vigorously for 2 days, then diluted with CH<sub>2</sub>Cl<sub>2</sub> (200 mL) and quenched with sat. aq. NaHCO<sub>3</sub> (200 mL). The aqueous phase was extracted with CH<sub>2</sub>Cl<sub>2</sub> (3 x 300 mL), and the combined organic phase was washed with brine (1 x 500 mL), dried with MgSO<sub>4</sub>, and concentrated *in vacuo* followed by 1 day under high vacuum to afford chloroamide **2.11** as a yellow oil (14.2 g, 97% yield), which was used without any additional purification.



***N*-(*tert*-butyl)-*N*-((ethoxycarbonothioyl)thio)-3,5-bis(trifluoromethyl)benzamide (2.8):**

Adapted from an analogous literature procedure using *N*-chlorophthalimide.<sup>5</sup> With the laboratory and hood lights off, in a 2-neck, 5L round-bottom flask, potassium ethyl xanthate (6.55 g, 40.84 mmol) was suspended in MeCN (1.7 L). To this suspension was added a solution of chloroamide **2.11** (14.2 g, 40.84 mmol) in MeCN (350 mL) via cannula wire over 20 min. The round-bottom was foil wrapped and stirred for 16 h, at which point the

suspension was concentrated *in vacuo* and left under high-vacuum for 20 h. The residue was taken up in CH<sub>2</sub>Cl<sub>2</sub>/H<sub>2</sub>O (1:1, 2L total volume) and the layers were separated. The organic layer was washed with brine, dried with MgSO<sub>4</sub>, and concentrated *in vacuo*. The resultant orange solid was purified by careful flash column chromatography on a short, wide silica column (hexanes flush until the first yellow band had fully eluted, then 0–5% Et<sub>2</sub>O in hexanes) to afford xanthylamide **2.8** as a yellow solid (8.47 g, 48% yield):

**<sup>1</sup>H NMR (600 MHz, CDCl<sub>3</sub>)** δ 7.88 (s, 1H), 7.86 (s, 2H), 4.71 – 4.61 (m, 2H), 1.58 (s, 9H), 1.49 (t, *J* = 7.1 Hz, 3H).

**<sup>13</sup>C NMR (151 MHz, CDCl<sub>3</sub>)** δ 212.00, 172.59, 139.98, 131.60 (q, *J* = 33.8 Hz), 127.11 (d, *J* = 3.9 Hz), 123.69 (q, *J* = 3.7 Hz), 123.05 (q, *J* = 272.8 Hz), 70.84, 64.15, 28.94, 13.77.

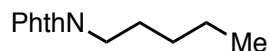
**IR (film)** 2981.41, 2938.02, 2360.44, 1680.66, 1368.25, 1279.59, 1183.11, 1136.83 cm<sup>-1</sup>.

**HRMS (ES+)** Exact mass calcd for C<sub>16</sub>H<sub>18</sub>F<sub>6</sub>NO<sub>2</sub>S<sub>2</sub> [M+H]<sup>+</sup>, 434.0677. Found 434.0686.

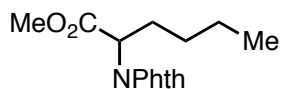
### Substrates for C-H Xanthylation

Cyclopentane, cyclohexane, cycloheptane, cyclooctane, adamantane, *trans*-decalin, norbornane, *n*-hexane, 2-methylanisole, 15-crown-5, amyl acetate, methyl hexanoate, 2-heptanone, (3aR)-(+)-sclareolide, (–)-ambroxide, 2-(1-adamantyl)-4-bromoanisole, and (+)-longifolene were obtained commercially and used without further purification.

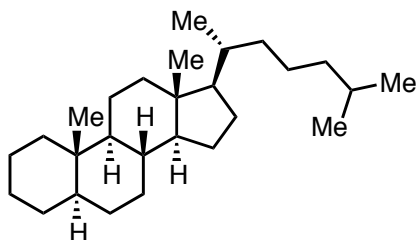
Tetrahydrofuran and 1,4-dioxane were degassed with argon over 3Å molecular sieves prior to use.



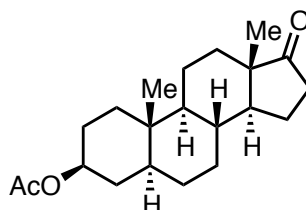
**2-Pentylisophthalonitrile** was prepared according to a literature procedure, and spectral data were in accordance with the literature values.<sup>3</sup>



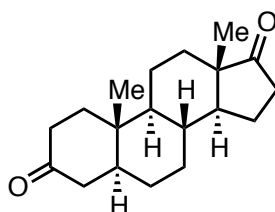
**Methyl 2-(1,3-dioxoisindolin-2-yl)hexanoate** was prepared according to a literature procedure, and spectral data were in accordance with the literature values.<sup>4</sup>



**Cholestane** was prepared according to a literature procedure, and spectral data were in accordance with the literature values.<sup>6</sup>



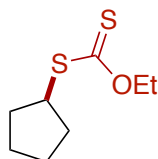
**Trans-androsterone acetate** was prepared according to a literature procedure, and spectral data were in accordance with the literature values.<sup>7</sup>



**5α-Androstenedione:** Pyridinium chlorochromate (PCC, 0.89 g, 4.2 mmol) was added to a solution of *trans*-androsterone (0.61 g, 2.1 mmol) in CH<sub>2</sub>Cl<sub>2</sub> (15 mL). After stirring for 12 h at rt, the mixture was filtered, and the filtrate was washed with saturated NaHSO<sub>3</sub> and brine, dried over anhydrous Na<sub>2</sub>SO<sub>4</sub>, and concentrated. The resulting green residue was purified by column chromatography (20 – 50% EtOAc in hexanes) to yield the product (0.56 g, 93% yield) as a white solid. Physical and spectral data were in accordance with literature data.<sup>8</sup>

## Independent Synthesis of Xanthate Standards

**General Procedure A:** To a suspension of potassium ethyl xanthate (1.5 equiv) in acetone (0.75 M wrt xanthate) was added alkyl bromide (1 equiv). The mixture was stirred at rt until consumption of the alkyl bromide as determined by GC-MS. The salts were removed by filtration and the filtrate concentrated. The residue was taken up in CH<sub>2</sub>Cl<sub>2</sub> and washed with H<sub>2</sub>O, brine, dried with MgSO<sub>4</sub>, and concentrated to afford the alkyl xanthate.



**2.12**

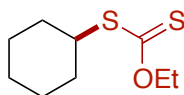
**S-cyclopentyl O-ethyl carbonodithioate (2.12):** Prepared from cyclopentyl bromide according to General Procedure A (1 mmol scale) as a yellow oil (154 mg, 81% yield):

**<sup>1</sup>H NMR (600 MHz, CDCl<sub>3</sub>)**  $\delta$  4.62 (q,  $J$  = 7.2 Hz, 2H), 3.95 – 3.83 (m, 1H), 2.20 – 2.11 (m, 2H), 1.73 – 1.67 (m, 2H), 1.63 – 1.58 (m, 4H), 1.41 (t,  $J$  = 7.1 Hz, 3H).

**<sup>13</sup>C NMR (151 MHz, CDCl<sub>3</sub>)**  $\delta$  215.26, 69.52, 48.28, 32.65, 24.95, 13.91.

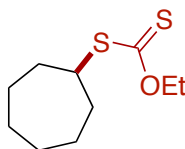
**IR (film)** 2958.27, 2867.63, 2265.95, 1445.39, 1363.43, 1212.04, 1111.76, 1052.94 cm<sup>-1</sup>.

**HRMS (ES+)** Exact mass calcd for C<sub>8</sub>H<sub>15</sub>OS<sub>2</sub> [M+H]<sup>+</sup>, 191.0559. Found 191.0563.



**2.13**

**S-cyclohexyl O-ethyl carbonodithioate (2.13)** was prepared according to a literature procedure, and spectral data were in accordance with the literature values.<sup>9, 10</sup>



**2.14**



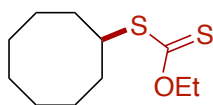
***S*-cycloheptyl *O*-ethyl carbonodithioate (2.14):** Prepared from cycloheptyl bromide according to General Procedure A (1 mmol scale) as a yellow oil (170.3 mg, 80% yield):

**<sup>1</sup>H NMR (600 MHz, CDCl<sub>3</sub>)** δ 4.62 (q, *J* = 7.1 Hz, 2H), 3.79 (dt, *J* = 9.3, 4.8 Hz, 1H), 2.10 – 2.04 (m, 2H), 1.73 – 1.65 (m, 4H), 1.62 – 1.50 (m, 6H), 1.40 (t, *J* = 7.1 Hz, 3H).

**<sup>13</sup>C NMR (151 MHz, CDCl<sub>3</sub>)** δ 214.86, 69.50, 50.56, 34.22, 28.27, 26.27, 13.91.

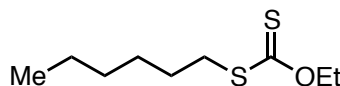
**IR (film)** 2981.41, 2927.41, 2853.17, 2359.48, 1457.92, 1210.11, 1110.80, 1051.98 cm<sup>-1</sup>.

**HRMS (ES<sup>+</sup>)** Exact mass calcd for C<sub>10</sub>H<sub>19</sub>OS<sub>2</sub> [M+H]<sup>+</sup>, 219.0872. Found 219.0877.



### 2.15

***S*-cyclooctyl *O*-ethyl carbonodithioate (2.15)** was prepared according to a literature procedure, and spectral data were in accordance with the literature values.<sup>11</sup>



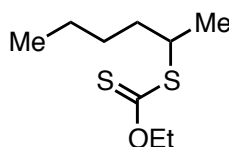
***O*-ethyl *S*-hexyl carbonodithioate:** Prepared from 1-bromohexane according to General Procedure A (1 mmol scale) as a yellow oil (164.2 mg, 80% yield):

**<sup>1</sup>H NMR (600 MHz, CDCl<sub>3</sub>)** δ 4.63 (q, *J* = 7.1 Hz, 2H), 3.10 (t, *J* = 7.5 Hz, 2H), 1.67 (q, *J* = 7.5 Hz, 2H), 1.43 – 1.37 (m, 5H), 1.32 – 1.26 (m, 4H), 0.88 (t, *J* = 6.8 Hz, 3H).

**<sup>13</sup>C NMR (151 MHz, CDCl<sub>3</sub>)** δ 215.29, 69.79, 36.01, 31.40, 28.67, 28.43, 22.60, 14.10, 13.90.

**IR (film)** 2956.34, 2928.38, 2856.06, 1457.92, 1363.43, 1218.79, 1111.76, 1051.01 cm<sup>-1</sup>.

**HRMS (ES<sup>+</sup>)** Exact mass calcd for C<sub>9</sub>H<sub>19</sub>OS<sub>2</sub> [M+H]<sup>+</sup>, 207.0872. Found 207.0872.



***O*-ethyl *S*-hexan-2-yl carbonodithioate:** Prepared from 2-bromohexane according to

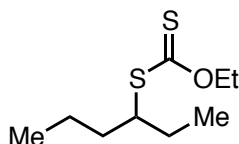
General Procedure A (1 mmol scale) as a yellow oil (388 mg, 84% yield):

**<sup>1</sup>H NMR (600 MHz, CDCl<sub>3</sub>)** δ 4.66 (q, *J* = 7.3 Hz, 2H), 3.77 – 3.68 (m, 1H), 1.75 – 1.66 (m, 1H), 1.66 – 1.55 (m, 1H), 1.47 – 1.30 (m, 10H), 0.96 – 0.90 (m, 3H).

**<sup>13</sup>C NMR (151 MHz, CDCl<sub>3</sub>)** δ 214.89, 69.62, 46.00, 35.68, 29.29, 22.62, 20.63, 14.12, 13.93.

**IR (film)** 2962.13, 2932.23, 2872.45, 2360.44, 2342.12, 1213.01, 1111.76, 1049.09 cm<sup>-1</sup>.

**HRMS (ES<sup>+</sup>)** Exact mass calcd for C<sub>9</sub>H<sub>19</sub>OS<sub>2</sub> [M+H]<sup>+</sup>, 207.0872. Found 207.0885.



***O*-ethyl *S*-hexan-3-yl carbonodithioate:** Prepared from 3-bromohexane according to

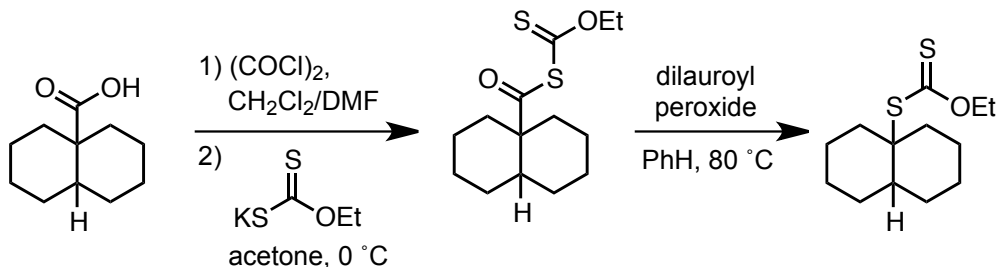
General Procedure A (1 mmol scale) as a yellow oil (190 mg, 85% yield):

**<sup>1</sup>H NMR (600 MHz, CDCl<sub>3</sub>)** δ 4.64 (q, *J* = 7.1 Hz, 2H), 3.72 – 3.65 (m, 1H), 1.79 – 1.71 (m, 1H), 1.70 – 1.56 (m, 3H), 1.48 – 1.38 (m, 5H), 1.02 – 0.97 (m, 3H), 0.94 – 0.88 (m, 3H).

**<sup>13</sup>C NMR (151 MHz, CDCl<sub>3</sub>)** δ 215.37, 69.75, 52.69, 35.80, 27.25, 20.20, 14.12, 13.95, 11.34.

**IR (film)** 2958.27, 2929.34, 2859.72, 1456.96, 1211.08, 1111.76, 1051.98 cm<sup>-1</sup>.

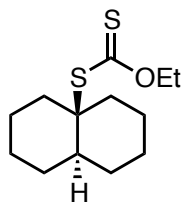
**HRMS (ES<sup>+</sup>)** Exact mass calcd for C<sub>9</sub>H<sub>19</sub>OS<sub>2</sub> [M+H]<sup>+</sup>, 207.0872. Found 207.0880.



***S*-(decahydronaphthalen-4a-yl) *O*-ethyl carbonodithioate:** A solution of

decahydronaphthalene-4a-carboxylic acid<sup>12</sup> (182 mg, 1 mmol) in CH<sub>2</sub>Cl<sub>2</sub> (5 mL) was treated

with oxalyl chloride (2 mmol, 0.17 mL) and DMF (1 drop) in a 25 mL round-bottom flask. After stirring at rt for 2 h, the reaction mixture was concentrated *in vacuo*, yielding the crude acid chloride which was used directly without further purification. To a solution of acid chloride in acetone (5 mL) at 0 °C was added potassium ethyl xanthate (152 mg, 0.95 mmol). After stirring for 2 h, the solution was concentrated, redissolved in CH<sub>2</sub>Cl<sub>2</sub>, and washed with H<sub>2</sub>O. The aqueous layer was extracted with CH<sub>2</sub>Cl<sub>2</sub> (x 2), and the combined organic layers were washed with brine, dried over MgSO<sub>4</sub>, and concentrated *in vacuo*. The resulting product was purified by flash column chromatography on silica (5% EtOAc in hexanes) to give a yellow oil (60.1 mg, 0.21 mmol, 21% yield), which was dissolved in benzene (0.42 mL) and heated at 80 °C with dilauroyl peroxide (4 mg, 5 mol %) overnight. The solution was concentrated *in vacuo* and the residue purified by flash column chromatography on silica (hexanes) to give the *trans*- (16.1 mg, 30% yield) and *cis*- (7.4 mg, 14% yield) isomers as off-white solids:



**trans**

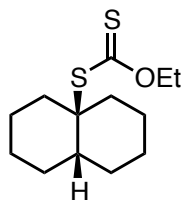
***S*-((4as,8as)-decahydronaphthalen-4a-yl) *O*-ethyl carbonodithioate (*trans*):**

**<sup>1</sup>H NMR (400 MHz, CDCl<sub>3</sub>)** δ 4.65 (q, *J* = 7.1 Hz, 2H), 2.58 (dt, *J* = 13.9, 3.9 Hz, 2H), 1.89 (qt, *J* = 13.2, 4.0 Hz, 2H), 1.81 – 1.71 (m, 2H), 1.60 – 1.49 (m, 3H), 1.50 – 1.38 (m, 4H), 1.38 – 1.15 (m, 7H).

**<sup>13</sup>C NMR (151 MHz, CDCl<sub>3</sub>)** δ 214.03, 69.55, 64.32, 48.19, 37.58, 28.98, 26.55, 22.43, 13.86.

**IR (film)** 2924.52, 2846.42, 1445.39, 1243.86, 1213.97, 1114.65, 1035.59, 933.34 cm<sup>-1</sup>.

**HRMS (ES+)** Exact mass calcd for C<sub>13</sub>H<sub>23</sub>OS<sub>2</sub> [M+H]<sup>+</sup>, 259.1185. Found 259.1192.



**cis**

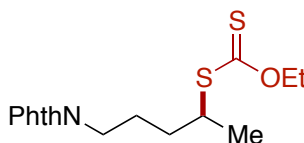
***S*-((4ar,8ar)-decahydronaphthalen-4a-yl) *O*-ethyl carbonodithioate (cis):**

**<sup>1</sup>H NMR (400 MHz, CDCl<sub>3</sub>)** δ 4.67 (q, *J* = 7.1 Hz, 2H), 2.16 – 1.97 (m, 5H), 2.16 – 1.37 (m, 15H).

**<sup>13</sup>C NMR (151 MHz, CDCl<sub>3</sub>)** δ 214.87, 69.42, 63.16, 38.77, 28.18, 22.87, 13.88.

**IR (film)** 2928.38, 2859.92, 1456.96, 1215.90, 1111.76, 1040.41, 970.02 cm<sup>-1</sup>.

**HRMS (ES+)** Exact mass calcd for C<sub>13</sub>H<sub>23</sub>OS<sub>2</sub> [M+H]<sup>+</sup>, 259.1185. Found 259.1198.



**2.26**

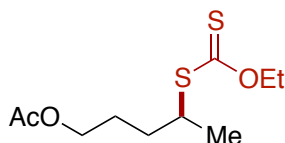
***S*-(5-(1,3-dioxisoindolin-2-yl)pentan-2-yl) *O*-ethyl carbonodithioate (2.26):** Prepared from 2-(4-bromopentyl)isoindoline-1,3-dione<sup>3</sup> according to General Procedure A (1 mmol scale) as a yellow oil (137.6 mg, 41% yield):

**<sup>1</sup>H NMR (600 MHz, CDCl<sub>3</sub>)** δ 7.85 – 7.82 (m, 2H), 7.73 – 7.70 (m, 2H), 4.61 (q, *J* = 7.2 Hz, 2H), 3.76 (q, *J* = 6.9 Hz, 1H), 3.72 – 3.66 (m, 2H), 1.85 – 1.71 (m, 3H), 1.69 – 1.62 (m, 1H), 1.40 (t, *J* = 7.1 Hz, 3H), 1.37 (d, *J* = 6.9 Hz, 3H).

**<sup>13</sup>C NMR (151 MHz, CDCl<sub>3</sub>)** δ 214.33, 168.49, 134.09, 132.17, 123.37, 69.78, 45.52, 37.75, 33.24, 26.29, 20.61, 13.92.

**IR (film)** 2934.16, 1772.26, 1714.41, 1615.09, 1466.60, 1396.21, 1213.01, 1048.12 cm<sup>-1</sup>.

**HRMS (ES+)** Exact mass calcd for C<sub>16</sub>H<sub>20</sub>NO<sub>3</sub>S<sub>2</sub> [M+H]<sup>+</sup>, 338.0879. Found 338.0897.



**2.27**

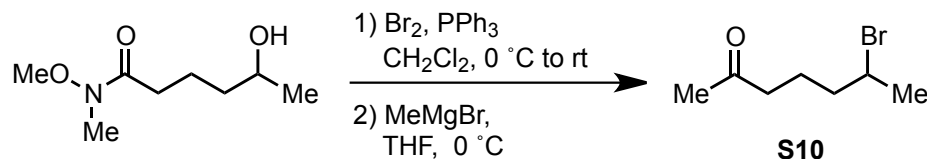
**4-((ethoxycarbonothioyl)thio)pentyl acetate (2.27):** Prepared from 4-chloropentyl acetate<sup>4</sup> according to General Procedure A (1 mmol scale) as a yellow oil (38.2 mg, 40% yield):

**<sup>1</sup>H NMR (600 MHz, CDCl<sub>3</sub>)**  $\delta$  4.63 (q,  $J$  = 7.1 Hz, 2H), 4.08 – 4.04 (m, 2H), 3.76 – 3.72 (m, 1H), 2.04 (s, 3H), 1.78 – 1.71 (m, 3H), 1.71 – 1.63 (m, 1H), 1.43 – 1.37 (m, 6H).

**<sup>13</sup>C NMR (151 MHz, CDCl<sub>3</sub>)**  $\delta$  214.36, 171.21, 69.77, 64.14, 45.56, 32.50, 26.24, 21.10, 20.57, 13.91.

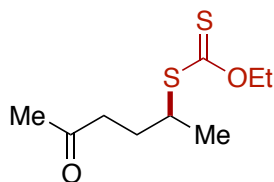
**IR (film)** 2959.23, 2868.59, 2360.44, 1739.48, 1365.35, 1237.11, 1111.76, 1048.12 cm<sup>-1</sup>.

**HRMS (ES<sup>+</sup>)** Exact mass calcd for C<sub>10</sub>H<sub>19</sub>O<sub>3</sub>S<sub>2</sub> [M+H]<sup>+</sup>, 251.0770. Found 251.0769.



**6-bromoheptan-2-one:** To a solution of triphenylphosphine (1.15 g, 4.4 mmol) in CH<sub>2</sub>Cl<sub>2</sub> (15 mL) at 0 °C was added bromine (225  $\mu$ L, 4.4 mmol) followed by a solution of 5-hydroxy-*N*-methoxy-*N*-methylhexanamide<sup>13</sup> (701 mg, 4 mmol) in CH<sub>2</sub>Cl<sub>2</sub> (5 mL). The mixture was warmed to room temperature and stirred overnight, after which it was quenched by the addition of H<sub>2</sub>O (20 mL). The layers were separated, and the aqueous phase was extracted with CH<sub>2</sub>Cl<sub>2</sub> (2 x 20 mL). The combined organic phases were dried with MgSO<sub>4</sub> and concentrated *in vacuo* to afford a yellow solid that was purified by flash column chromatography (30 – 40% EtOAc in hexanes) to afford 5-bromo-*N*-methoxy-*N*-methylhexanamide as a yellow oil (822 mg, 86% yield).

To a solution of 4-bromo-*N*-methoxy-*N*-methylpentanamide (200 mg, 0.84 mmol) in THF (3.5 mL) at 0 °C was added MeMgBr (0.56 mL, 1.68, 3M in Et<sub>2</sub>O) dropwise over 10 min. The mixture was maintained at 0 °C for 2 h and then quenched with 8 mL saturated aqueous NH<sub>4</sub>Cl. The aqueous phase was extracted with Et<sub>2</sub>O (3 x 10 mL), and the combined organic phase was washed with brine (20 mL), dried with MgSO<sub>4</sub>, and concentrated *in vacuo* to afford 5-bromohexan-2-one (84 mg, 52% yield) in accordance with literature data.



**2.28**

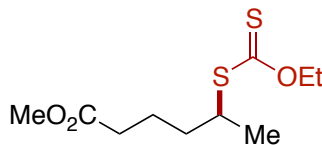
**O-ethyl S-(6-oxoheptan-2-yl) carbonodithioate (2.28):** Prepared from 5-bromohexan-2-one<sup>3</sup> according to General Procedure A (1 mmol scale) to afford xanthate **2.28** as a yellow oil (47.3 mg, 86% yield):

<sup>1</sup>H NMR (600 MHz, CDCl<sub>3</sub>) δ 4.63 (q, *J* = 6.8 Hz, 2H), 3.76 – 3.65 (m, 1H), 2.51 – 2.40 (m, 2H), 2.13 (s, 3H), 1.73 – 1.55 (m, 4H), 1.41 (t, *J* = 7.1 Hz, 3H), 1.37 (d, *J* = 6.9 Hz, 3H).

<sup>13</sup>C NMR (151 MHz, CDCl<sub>3</sub>) δ 214.57, 208.56, 69.74, 45.68, 43.24, 35.36, 30.08, 21.18, 20.40, 13.91.

IR (film) 2926.45, 1716.34, 1540.85, 1455.99, 1361.50, 1213.01, 1111.76, 1048.12 cm<sup>-1</sup>.

HRMS (ES<sup>+</sup>) Exact mass calcd for C<sub>10</sub>H<sub>19</sub>O<sub>2</sub>S<sub>2</sub> [M+H]<sup>+</sup>, 235.0821. Found 235.0838.



**2.29**

**Methyl 5-((ethoxycarbonothioyl)thio)hexanoate (2.29):** Prepared from methyl 5-

bromohexanoate<sup>3</sup> according to General Procedure A (1 mmol scale) as a yellow oil (128 mg, 51% yield):

**<sup>1</sup>H NMR (600 MHz, CDCl<sub>3</sub>)** δ 4.63 (q, *J* = 7.1 Hz, 2H), 3.72 (m, 1H), 3.66 (s, 3H), 2.33 (t, *J* = 7.2 Hz, 2H), 1.79 – 1.69 (m, 3H), 1.66 – 1.60 (m, 1H), 1.41 (t, *J* = 7.1 Hz, 3H), 1.37 (d, *J* = 6.9 Hz, 3H).

**<sup>13</sup>C NMR (151 MHz, CDCl<sub>3</sub>)** δ 214.49, 173.78, 69.73, 51.69, 45.57, 35.44, 33.78, 22.48, 20.44, 13.91.

**IR (film)** 2952.48, 2868.59, 1738.51, 1436.71, 1364.39, 1213.01, 1111.76, 1048.12 cm<sup>-1</sup>.

**HRMS (ES+)** Exact mass calcd for C<sub>10</sub>H<sub>19</sub>O<sub>3</sub>S<sub>2</sub> [M+H]<sup>+</sup>, 251.0770. Found 251.0770.

### Synthesis of Alkyl Xanthates via C–H Xanthylation

**General Procedure B:** A 1 dram vial was charged with xanthylamide **2.8** (1 equiv) in the dark (overhead laboratory lights turned off), fitted with a PTFE lined screw cap, and taken into the glovebox. The xanthylamide was dissolved in PhCF<sub>3</sub> (1M wrt substrate), and the resulting solution was sealed with Teflon tape and removed from the glovebox. Liquid substrate (1 equiv) was added by syringe, and the vial was placed in a 3D-printed holder (see below pictures). The holder was suspended above an Ecoxotic PAR38 23 W blue LED such that the bottom of each vial was directly aligned with and 1 cm above one of the five LEDs. A steady stream of nitrogen was blown over the top of the vials to keep the reaction temperature as close to room temperature as possible, and the apparatus was covered with aluminum foil. The reaction was irradiated until completion and then either diluted with CH<sub>2</sub>Cl<sub>2</sub> and added dodecane (1 equiv) for GC analysis or concentrated *in vacuo* and added hexamethyldisiloxane (0.17 equiv) for NMR analysis. When a standard could not be easily

prepared, the crude residue was purified by flash column chromatography to afford the alkyl xanthate products.

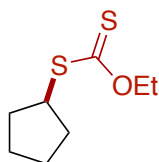
**General Procedure C:** A 1 dram vial was charged with xanthylamide **2.8** (1–3 equiv) in the dark (overhead laboratory lights turned off), fitted with a PTFE lined screw cap, and taken into the glovebox. The xanthylamide was dissolved in PhCF<sub>3</sub> (0.15 mL), and the resulting solution was sealed with Teflon tape and removed from the glovebox. Liquid substrate (0.15 mmol, 1 equiv) was added by syringe (note: solid substrate is added at the same time as xanthylamide outside the glovebox), and the vial was placed in a 3D-printed holder. The holder was suspended above an Ecoxotic PAR38 23 W blue LED such that the bottom of each vial was directly aligned with and 1 cm above one of the five LEDs, and the apparatus was covered with aluminum foil. The reaction was irradiated until completion and then either diluted with CH<sub>2</sub>Cl<sub>2</sub> and added dodecane (1 equiv) for GC analysis or concentrated *in vacuo* and added hexamethyldisiloxane (0.17 equiv) for NMR analysis. When a standard could not be easily prepared or for complex substrates, the crude residue was purified by flash column chromatography to afford the alkyl xanthate products.

**General Procedure D:** A 1 dram vial with a stir bar was charged with xanthylamide **2.8** (1–3 equiv) and solid substrate (1 equiv) in the dark (overhead laboratory lights turned off), fitted with a PTFE lined screw cap, and taken into the glovebox. The xanthylamide was dissolved in PhCF<sub>3</sub> or C<sub>6</sub>F<sub>6</sub> (1 M), and the resulting solution was sealed with Teflon tape and removed from the glovebox. The vial was suspended on a stir plate and irradiated with a Kessil Blue KSH150B 34W LED Grow Light from the side (2 cm away) with the apparatus covered by aluminum foil until completion. The reaction was then concentrated *in vacuo* or



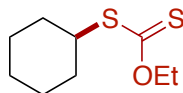
by passing a stream of nitrogen over the solution. The crude residue was purified by flash column chromatography to afford the alkyl xanthate products.

**General Procedure E:** A 1 dram vial with a stir bar was charged with xanthylamide **2.8** (3 equiv) and solid substrate (1 equiv) in the dark (overhead laboratory lights turned off), fitted with a PTFE lined screw cap, and taken into the glovebox. The xanthylamide was dissolved in MeCN or C<sub>6</sub>F<sub>6</sub> (1 M), and the resulting solution was sealed with Teflon tape and removed from the glovebox. The vial was placed directly on a stir plate maintained at 80 °C and irradiated with a Kessil Blue KSH150B 34W LED Grow Light from the side (2 cm away) with the apparatus covered by aluminum foil until completion. The reaction was then concentrated *in vacuo* or by passing a stream of nitrogen over the solution. The crude residue was purified by flash column chromatography to afford the alkyl xanthate products.



**2.12**

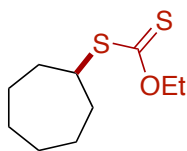
**S-cyclopentyl O-ethyl carbonodithioate (2):** Prepared according to General Procedure B (0.15 mmol scale) using cyclopentane and xanthylamide **2.8** (1 equiv), giving 59% NMR yield.



**2.13**

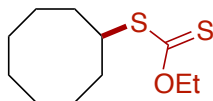
**S-cyclohexyl O-ethyl carbonodithioate (3):** Prepared according to General Procedure B (0.15 mmol scale) using cyclohexane and xanthylamide **2.8** (1 equiv), giving 77% NMR yield.

**Competition Experiment:** A 1 dram vial was charged with xanthylamide **2.8** (65 mg, 0.15 mmol) in the dark (overhead laboratory lights turned off), fitted with a PTFE lined screw cap, and was taken into the glovebox. The xanthylamide was dissolved in PhCF<sub>3</sub> (0.15 mL), and cyclohexane (81 uL, 0.75 mmol) and cyclohexane-d<sub>12</sub> (80.8 uL, 0.75 mmol) were added. The reaction mixture was sealed with Teflon tape, removed from the glovebox, and irradiated from below according to General Procedure B for 5 min. The reaction mixture was diluted with CH<sub>2</sub>Cl<sub>2</sub>, passed over a short silica plug, and analyzed using an Agilent Gas Chromatograph-Mass Spectrometer with a 6850 series GC system and a 5973 Network Mass Selective Detector to determine the ratio of non-deuterated to deuterated product ( $K_H/K_D = 6.3$ ).



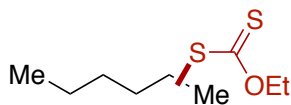
**2.14**

**S-cycloheptyl O-ethyl carbonodithioate (4):** Prepared according to General Procedure B (0.15 mmol scale) using cycloheptane and xanthylamide **2.8** (1 equiv), giving 73% NMR yield.



**2.15**

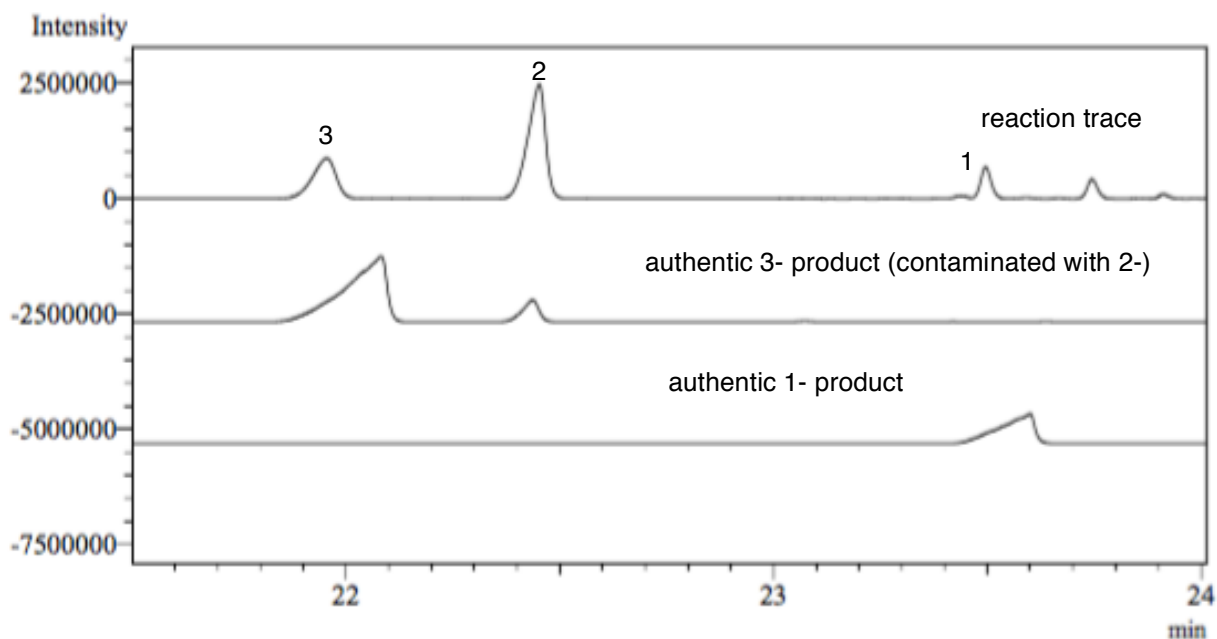
**S-cyclooctyl O-ethyl carbonodithioate (5):** Prepared according to General Procedure B (0.15 mmol scale) using cyclooctane and xanthylamide **2.8** (1 equiv), giving 85% NMR yield.



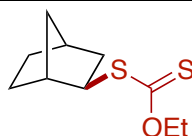
**2.16**

**Reaction with *n*-Hexane:** Prepared according to General Procedure B (0.15 mmol scale) using *n*-hexane and xanthylamide **2.8** (1 equiv), giving 64% combined NMR yield. The product distribution was determined by GC analysis and comparison to independently synthesized standards.

**Distribution of *n*-Hexane Xanthates**



Product	% area
1	6.6
2	63.7
3	29.7



**2.17**

***S*-(1*S*,2*S*,4*R*)-bicyclo[2.2.1]heptan-2-yl *O*-ethyl carbonodithioate (**7**):** Prepared according to General Procedure B (0.15 mmol scale) using norbornane (note: the norbornane was added

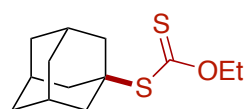
in the glovebox to prevent sublimation upon entering the glovebox) and xanthylamide **2.8** (1 equiv), giving 49% NMR yield. The residue was purified by flash column chromatography on silica (pentanes) to afford pure norbornyl xanthate as a yellow oil (4.9 mg, 15% yield).

**<sup>1</sup>H NMR (600 MHz, CDCl<sub>3</sub>)** δ 4.62 (q, *J* = 7.1 Hz, 2H), 3.57 – 3.50 (m, 1H), 2.41 (s, 1H), 2.31 (s, 1H), 1.83 (ddd, *J* = 13.3, 8.6, 2.4 Hz, 1H), 1.64 (tt, *J* = 12.3, 4.5 Hz, 1H), 1.56 – 1.51 (m, 1H), 1.46 – 1.34 (m, 6H), 1.26 – 1.20 (m, 2H).

**<sup>13</sup>C NMR (151 MHz, CDCl<sub>3</sub>)** δ 215.20, 69.55, 50.94, 43.00, 37.23, 36.53, 36.33, 29.03, 28.53, 13.96.

**IR (film)** 2955.38, 2870.52, 2359.48, 1453.10, 1213.97, 1138.76, 1110.80, 1056.80 cm<sup>-1</sup>.

**HRMS (ES<sup>+</sup>)** Exact mass calcd for C<sub>10</sub>H<sub>16</sub>OS<sub>2</sub>Na [M+Na]<sup>+</sup>, 239.0540. Found 239.1271.



**2.18**

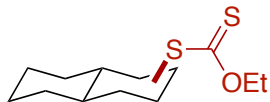
**S-adamantan-1-yl O-ethyl carbonodithioate (8):** Prepared according to General Procedure C (0.15 mmol scale) using adamantane and xanthylamide **2.8** (1 equiv), giving 70% NMR yield. The residue was purified by flash column chromatography on silica (pentanes) to afford an inseparable mixture of adamantyl xanthate and bisxanthate as a yellow oil (23.1 mg, 60% yield):

**<sup>1</sup>H NMR (600 MHz, CDCl<sub>3</sub>)** δ 4.66 (q, *J* = 7.1 Hz, 2H), 2.17 – 2.11 (m, 6H), 2.11 – 2.04 (m, 3H), 1.72 (d, *J* = 3.0 Hz, 6H), 1.48 (t, *J* = 7.1 Hz, 3H).

**<sup>13</sup>C NMR (151 MHz, CDCl<sub>3</sub>)** δ 214.45, 69.40, 54.65, 42.00, 36.32, 29.93, 13.87.

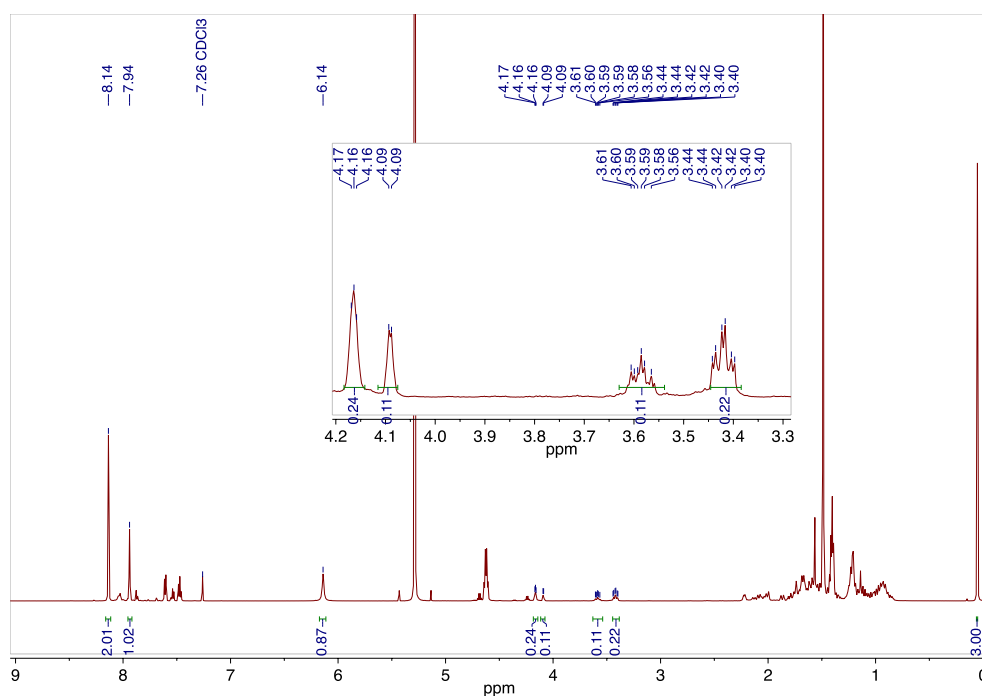
**IR (film)** 2908.13, 2850.27, 2360.44, 1453.10, 1366.32, 1219.76, 1112.73, 1027.87 cm<sup>-1</sup>.

**HRMS (ES<sup>+</sup>)** Exact mass calcd for C<sub>13</sub>H<sub>21</sub>OS<sub>2</sub> [M+H]<sup>+</sup>, 257.1028. Found 257.1036.

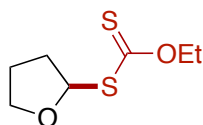
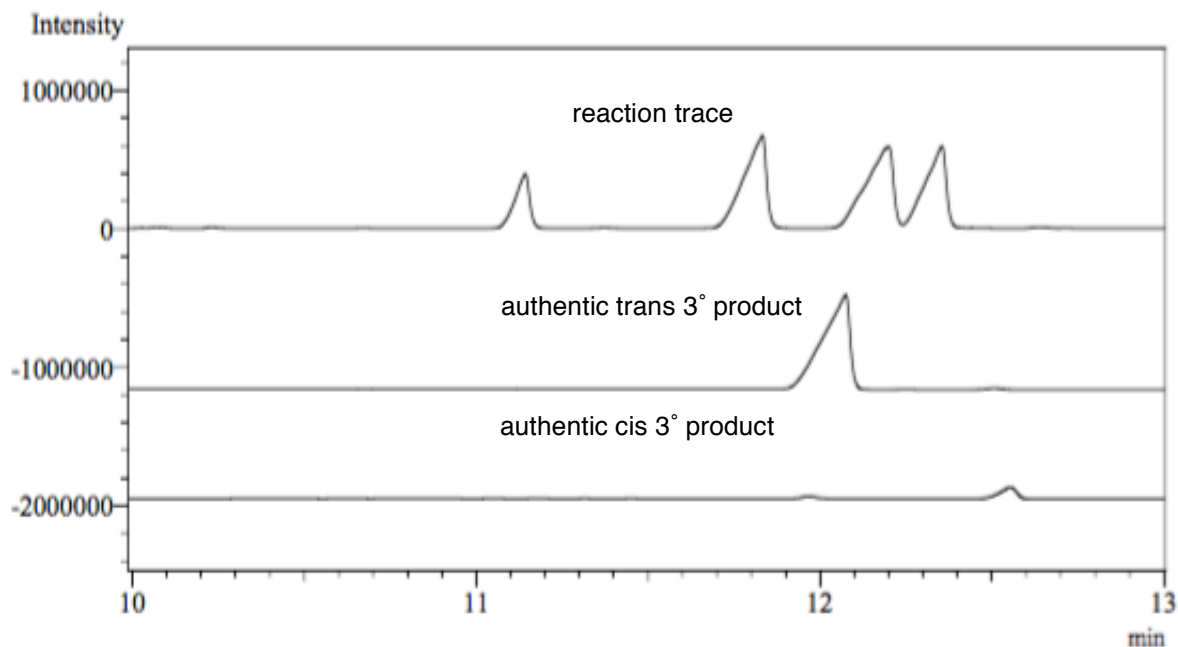


## 2.19

**Reaction with *trans*-decalin:** Prepared according to General Procedure C (0.15 mmol scale) using *trans*-decalin and xanthylamide **2.8** (1 equiv), giving 69% combined NMR yield of secondary xanthate products (as determined by analogy with our previous halogenation chemistry).<sup>3</sup>

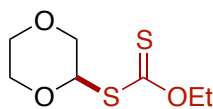


GC analysis was used to verify that no tertiary product was formed in the reaction.



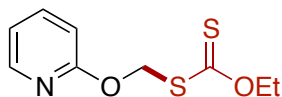
**2.20**

**O-ethyl S-(tetrahydrofuran-2-yl) carbonodithioate (10):** Prepared according to General Procedure B (0.15 mmol scale) using tetrahydrofuran and xanthylamide **2.8** (1 equiv), giving 54% NMR yield. Spectral data was in accordance with literature values.<sup>11</sup>



**2.21**

**S-(1,4-dioxan-2-yl) O-ethyl carbonodithioate (11):** Prepared according to General Procedure B (0.15 mmol scale) using dioxane and xanthylamide **2.8** (1 equiv), giving 50% NMR yield. Spectral data was in accordance with literature values.<sup>11</sup>



### 2.22

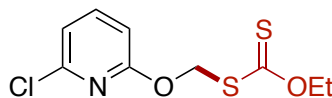
**O-ethyl S-((pyridin-2-yloxy)methyl) carbonodithioate (12):** Prepared according to General Procedure C (0.30 mmol scale) using 2-methoxypyridine and xanthylamide **2.8** (1 equiv), giving 55% NMR yield. The crude residue was purified by flash column chromatography to afford pure **12** as a yellow oil (35.1 mg, 51% yield):

**<sup>1</sup>H NMR (600 MHz, CDCl<sub>3</sub>)** δ 8.16 (dd, *J* = 5.0, 1.9 Hz, 1H) 7.60 (ddd, *J* = 8.7, 7.2, 2.1 Hz, 1H), 6.93 (ddd, *J* = 7.1, 5.1, 1.0 Hz, 1H), 6.81 (d, *J* = 8.3 Hz, 1H), 6.05 (s, 2H), 4.68 (q, *J* = 7.0 Hz, 2H), 1.42 (t, *J* = 7.1 Hz, 3H).

**<sup>13</sup>C NMR (151 MHz, CDCl<sub>3</sub>)** δ 213.24, 161.97, 146.62, 139.12, 117.96, 111.83, 70.48, 69.08, 13.87.

**IR (film)** 2980.45, 1471.42, 1434.78, 1279.54, 1230.36, 1141.65, 1054.87, 1008.59, 778.13 cm<sup>-1</sup>.

**HRMS (ES<sup>+</sup>)** Exact mass calcd for C<sub>9</sub>H<sub>12</sub>NO<sub>2</sub>S<sub>2</sub> [M+H]<sup>+</sup>, 230.0304. Found 230.0304.



### 2.23

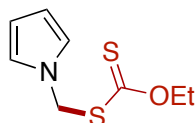
**S-(((6-chloropyridin-2-yl)oxy)methyl) O-ethyl carbonodithioate (13):** Prepared according to General Procedure C (0.15 mmol scale) using 2-chloro-6-methoxypyridine and xanthylamide **2.8** (1 equiv), giving 53% NMR yield. The crude residue was purified by flash column chromatography to afford pure **13** as a yellow oil (13.2 mg, 33% yield):

**<sup>1</sup>H NMR (600 MHz, CDCl<sub>3</sub>)** δ 7.55 (t, *J* = 7.8 Hz, 1H), 6.97 (d, *J* = 7.5 Hz, 1H), 6.73 (d, *J* = 8.1 Hz, 1H), 6.03 (s, 2H), 4.68 (q, *J* = 7.2 Hz, 2H), 1.42 (t, *J* = 7.1 Hz, 3H).

**$^{13}\text{C}$  NMR (151 MHz,  $\text{CDCl}_3$ )**  $\delta$  212.61, 161.72, 148.20, 141.24, 117.72, 109.99, 70.67, 69.56, 13.87.

**IR (film)** 2983.34, 1646.91, 1471.42, 1434.78, 1277.61, 1230.36, 1110.8, 1055.84, 1001.55  $\text{cm}^{-1}$ .

**HRMS (ES<sup>+</sup>)** Exact mass calcd for  $\text{C}_9\text{H}_{11}\text{ClNO}_2\text{S}_2$   $[\text{M}+\text{H}]^+$ , 263.9920. Found 264.2329.



**2.24**

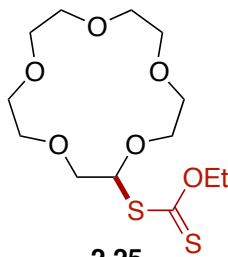
Prepared according to General Procedure C (0.15 mmol scale) using *N*-methylpyrrole and xanthylamide **2.8** (1 equiv). The crude residue was purified by flash column chromatography to afford pure **14** as a yellow oil (12.1 mg, 40% yield):

**$^1\text{H}$  NMR (400 MHz,  $\text{CDCl}_3$ )**  $\delta$  6.82 (d,  $J = 2.2$  Hz, 2H), 6.18 (d,  $J = 2.2$  Hz, 2H), 5.65 (s, 2H), 4.69 (q,  $J = 7.1$  Hz, 2H), 1.46 (t,  $J = 7.1$  Hz, 3H).

**$^{13}\text{C}$  NMR (151 MHz,  $\text{CDCl}_3$ )**  $\delta$  212.23, 121.34, 109.68, 70.78, 53.65, 13.88.

**IR (film)** 2922.41, 2856.06, 1682.59, 1489.74, 1278.57, 1225.54, 1045.23, 725.10  $\text{cm}^{-1}$ .

**HRMS (ES<sup>+</sup>)** Exact mass calcd for  $\text{C}_8\text{H}_{12}\text{NOS}_2$   $[\text{M}+\text{H}]^+$ , 202.0355. Found 202.0363.



**2.25**

***O*-ethyl *S*-1,4,7,10,13-pentaoxacyclopentadecan-2-yl carbonodithioate (**16**)**. Prepared according to General Procedure C (0.30 mmol scale) using 15-crown-5 and xanthylamide **2.8** (1 equiv), giving 67% NMR yield. The residue was purified by flash column chromatography on silica to afford pure crown ether xanthate **16** as a yellow oil (48.6 mg, 48% yield).

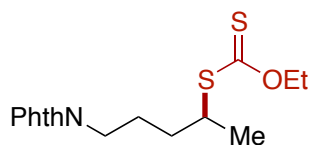


**$^1\text{H}$  NMR (600 MHz,  $\text{CDCl}_3$ )**  $\delta$  5.83 – 5.76 (m, 1H), 4.69 – 4.58 (m, 2H), 3.94 – 3.60 (m, 18H), 1.46 – 1.35 (m, 3H).

**$^{13}\text{C}$  NMR (151 MHz,  $\text{CDCl}_3$ )**  $\delta$  213.09, 90.60, 73.05, 70.94, 70.79, 70.76, 70.72, 70.70, 70.65, 70.03, 69.93, 69.76, 13.87.

**IR (film)** 2924.52, 2856.06, 1716.34, 1652.70, 1558.20, 1540.85, 1225.54, 1113.69, 1044.26  $\text{cm}^{-1}$ .

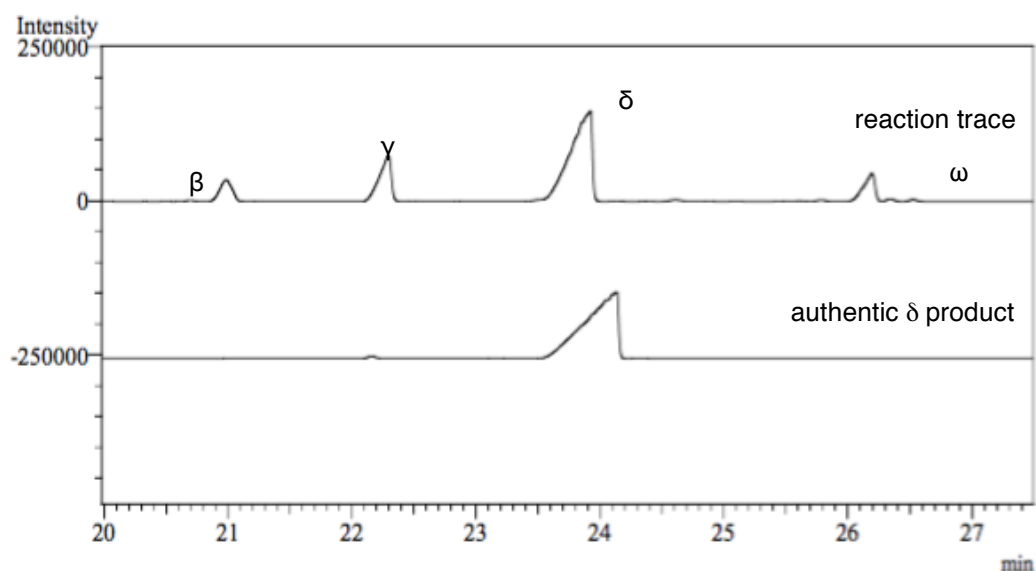
**HRMS (ES+)** Exact mass calcd for  $\text{C}_{13}\text{H}_{24}\text{O}_6\text{S}_2\text{Na}$   $[\text{M}+\text{Na}]^+$ , 363.0907. Found 363.0904.



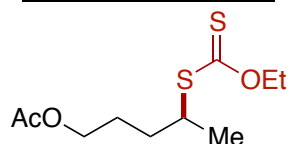
**2.26**

**Reaction with *N*-Pentylphthalimide:** Prepared according to General Procedure C (0.15 mmol scale) using *N*-pentylphthalimide (**S5**) and xanthylamide **2.8** (2 equiv), giving 68% combined GC yield of xanthate products (64% selectivity for major d product):

#### Distribution of *N*-Pentylphthalimide Xanthates



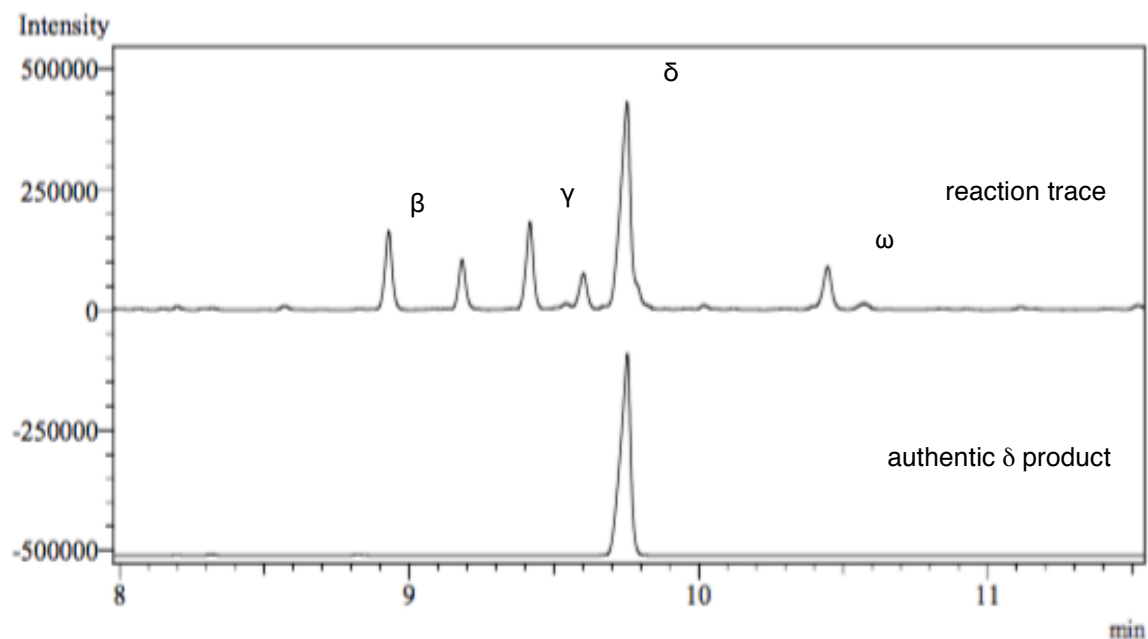
Product	% area
$\beta$	8.4
$\gamma$	17.8
$\delta$	63.7
$\omega$	10.1



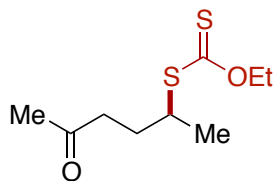
### 2.27

**Reaction with Amyl Acetate:** Prepared according to General Procedure C (0.15 mmol scale) using amyl acetate and xanthylamide **2.8** (2 equiv) with the addition of 2-chloropyridine (2.8 uL, 0.2 equiv) to minimize byproduct formation, giving 48% combined GC yield of xanthate products (58% selectivity for major  $\delta$  product):

### Distribution of Amyl Acetate Xanthates



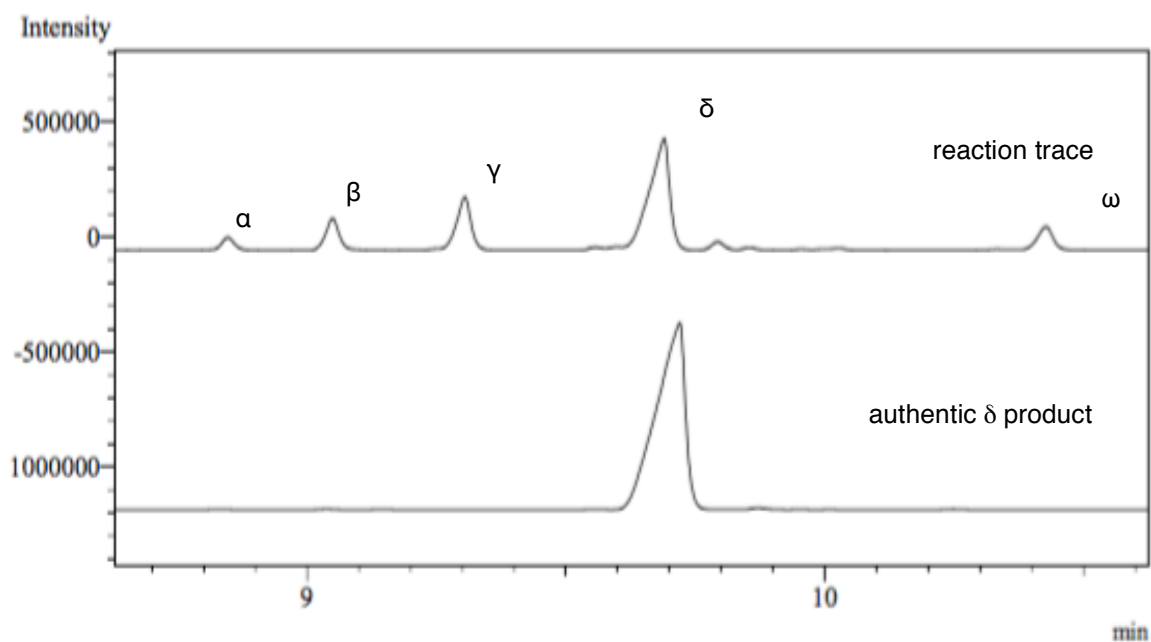
Product	% area
$\beta$	14.5
$\gamma$	17.2
$\delta$	58.3
$\omega$	10.0



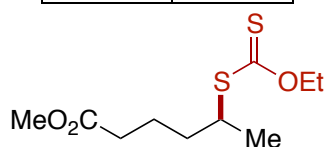
**2.28**

**Reaction with 2-Heptanone:** Prepared according to General Procedure C (0.15 mmol scale) using 2-heptanone and xanthylamide **2.8** (2 equiv) with the addition of 2-chloropyridine (2.8 uL, 0.2 equiv) to minimize byproduct formation, giving 47% combined GC yield of xanthate products (55% selectivity for major  $\delta$  product):

#### Distribution of 2-Heptanone Xanthates



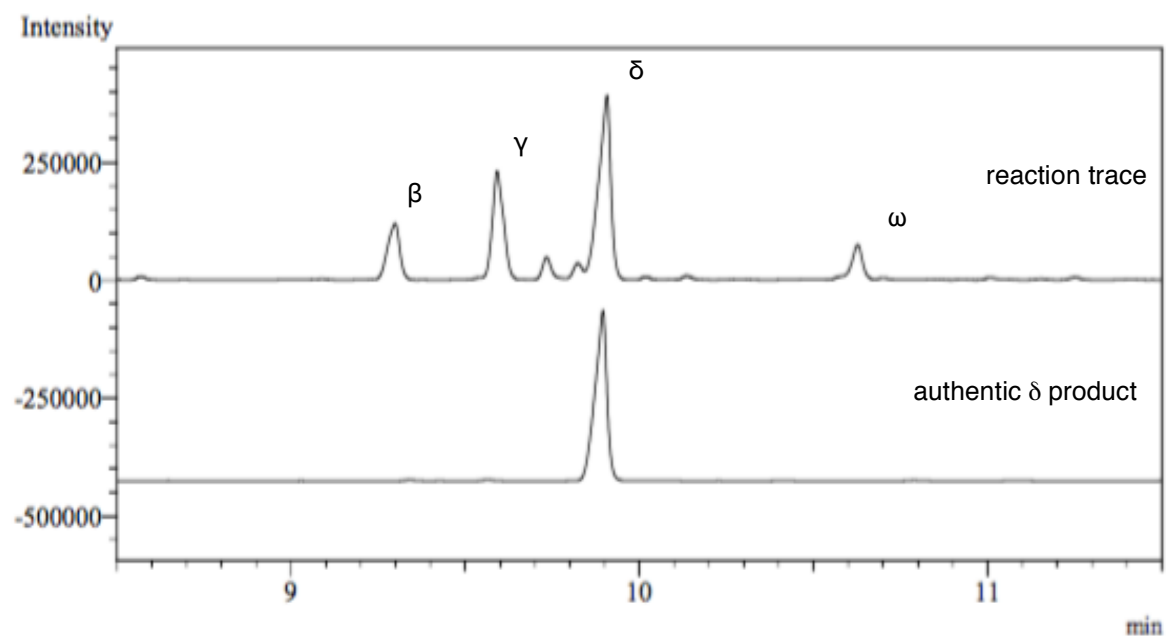
Product	% area
$\alpha$	4.1
$\beta$	10.2
$\gamma$	18.8
$\delta$	54.7
$\omega$	12.2



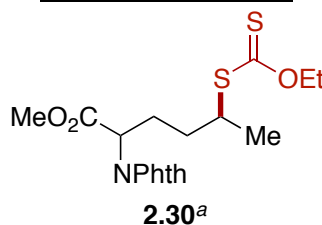
**2.29**

**Reaction with Methyl Hexanoate:** Prepared according to General Procedure C (0.15 mmol scale) using methyl hexanoate and xanthylamide **2.8** (2 equiv) with the addition of 2-chloropyridine (2.8 uL, 0.2 equiv) to minimize byproduct formation, giving 52% combined GC yield of xanthate products (53% selectivity for major  $\delta$  product):

#### Distribution of Methyl Hexanoate Xanthates



Product	% area
$\beta$	11.6
$\gamma$	26.9
$\delta$	53.2
$\omega$	8.3



**Reaction with *N*-Phthalimide Norleucine Methyl Ester:** Prepared according to General Procedure C (0.15 mmol scale) using *N*-phthalimide norleucine methyl ester and xanthylamide **2.8** (3 equiv). The crude residue was purified by flash column chromatography on silica (20% – 50% Et<sub>2</sub>O in hexanes) to afford the xanthate products as an amorphous solid (39 mg, 68% yield).

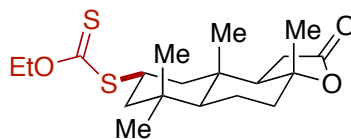
NMR Data listed for major products (mixture of diastereomers). NMR contains other regioisomers of xanthylation products, which exist both as diastereomers and rotamers and complicate the NMR spectrum.

**<sup>1</sup>H NMR (600 MHz, CDCl<sub>3</sub>)**  $\delta$  7.87 (d,  $J$  = 4.9 Hz, 2H), 7.76 (d,  $J$  = 3.0 Hz, 2H), 4.87 – 4.79 (m, 1H), 4.73 – 4.47 (m, 2H), 3.76 – 3.70 (m, 4H), 2.41 – 2.21 (m, 2H), 1.74 – 1.64 (m, 1H), 1.42 (s, 3H), 1.39 – 1.23 (m, 4H, overlap with other products).

**<sup>13</sup>C NMR (151 MHz, CDCl<sub>3</sub>)**  $\delta$  214.05, 169.58, 167.79, 167.75, 167.71, 135.82, 134.41, 134.37, 131.82, 125.63, 123.74, 69.79, 69.75, 52.98, 52.96, 51.99, 51.88, 45.24, 45.20, 35.47, 34.33, 32.81, 32.70, 30.41, 29.81, 28.35, 27.89, 26.59, 26.50, 20.55, 20.25, 14.37, 13.87, 13.85.

**IR (film)** 2926.45, 1772.26, 1748.16, 1716.34, 1652.70, 1540.85, 1387.53, 1219.76, 1047.16  $\text{cm}^{-1}$ .

**HRMS (ES+)** Exact mass calcd for  $\text{C}_{18}\text{H}_{22}\text{NO}_5\text{S}_2$   $[\text{M}+\text{H}]^+$ , 396.0934. Found 396.0954.



**2.31**

***O*-ethyl *S*-((3*aR*,5*aS*,8*S*,9*aS*,9*bR*)-3*a*,6,6,9*a*-tetramethyl-2-**

***oxododecahydronaphtho[2,1-*b*]furan-8-yl) carbonodithioate:*** Prepared according to

General Procedure C using sclareolide (1 mmol, 1 equiv) and xanthylamide **2.8** (1 mmol, 1 equiv) in  $\text{PhCF}_3$  (1 mL) giving 55% NMR yield. The crude residue was purified by flash column chromatography (10 – 20% EtOAc in hexanes) to afford pure **2.31** as an off-white solid (0.205 g, 55% yield, 91% yield brsm):

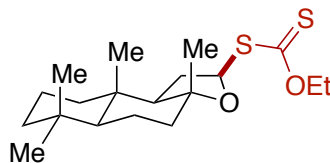
**$^1\text{H}$  NMR (600 MHz,  $\text{CDCl}_3$ )**  $\delta$  4.63 (q,  $J = 7.1$ , 2H), 4.01 (tt,  $J = 12.9$ , 3.6 Hz, 1H), 2.43 (t,  $J = 14.9$  Hz, 1H), 2.24 (dd,  $J = 16.3$ , 6.6 Hz, 1H), 2.09 (dt,  $J = 12.0$ , 3.2 Hz, 1H), 1.99 (dd,  $J = 14.7$ , 6.6 Hz, 1H), 1.90 (td,  $J = 13.0$ , 3.1 Hz, 3H), 1.69 (td,  $J = 12.6$ , 4.1 Hz, 1H), 1.41 (td,  $J = 7.2$ , 2.3 Hz, 3H), 1.36 – 1.31 (m, 4H), 1.26 – 1.23 (m, 1H), 1.17 (t,  $J = 12.4$  Hz, 1H), 1.11 (dd,  $J = 12.7$ , 2.5 Hz, 1H), 1.05 (s, 3H), 0.96 (s, 3H), 0.94 (s, 3H).

**$^{13}\text{C}$  NMR (151 MHz,  $\text{CDCl}_3$ )**  $\delta$  214.06, 176.37, 86.12, 69.89, 58.75, 56.22, 47.24, 45.23, 42.37, 38.57, 37.68, 35.16, 32.93, 28.74, 21.75, 21.27, 20.38, 15.59, 13.93.

**IR (film)** 2950.55, 2360.44, 2342.12, 1777.08, 1385.60, 1220.72, 1113.69, 1049.09  $\text{cm}^{-1}$ .

**HRMS (ES+)** Exact mass calcd for  $\text{C}_{19}\text{H}_{31}\text{O}_3\text{S}_2$   $[\text{M}+\text{H}]^+$ , 371.1709. Found 371.1704.

A gram-scale reaction was run with sclareolide (4 mmol, 1 equiv) and xanthylamide **1** (4 mmol, 1 equiv) using General Procedure D on 4 mmol scale (0.804 g, 54% yield).



### 2.32

***O*-ethyl *S*-((2*R*,3*aR*,5*aS*,9*aS*,9*bR*)-3*a*,6,6,9*a*-tetramethyldodecahydronaphtho[2,1-*b*]furan-2-yl) carbonodithioate (2.32):** The reaction was run according to General

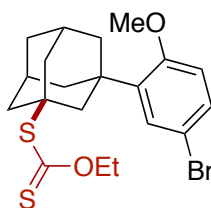
Procedure C for 4 hr on a 0.3 mmol scale (note: product decomposition occurs under reaction conditions after 4 hr). The mixture was concentrated *in vacuo* and extensively dried via high-vacuum. <sup>1</sup>H NMR of the crude reaction with an HMDS internal standard reveals an NMR yield of 80% with 1.2:1 dr. The solid residue was triturated with pentanes, and the solution was passed over a cotton plug and concentrated *in vacuo* to remove amide. The resultant residue was heated at 115 °C in a sand bath under high vacuum overnight to remove unreacted ambroxide, which is chromatographically inseparable from the xanthate products. Finally, the resultant residue was purified through rapid flash column chromatography on silica (5% EtOAc in hexanes, less than five minutes spent on the column) to afford pure ambroxide xanthates **2.32** as an inseparable mixture of diastereomers (34 mg, 32% yield):

**<sup>1</sup>H NMR (600 MHz, CDCl<sub>3</sub>)** δ 6.10 (t, *J* = 7.8 Hz, 0.32H), 5.96 (dd, *J* = 7.5 Hz, 1.1 Hz, 0.56H), 4.72 – 4.59 (m, 2H), 2.41 (td, *J* = 13.4, 7.6 Hz, 0.61H), 2.33 (dd, *J* = 12.8, 6.5 Hz, 0.37H), 2.01 – 1.94 (m, 1.53H), 1.88 (td, *J* = 13.1, 8.1 Hz, 0.48H), 1.81 – 1.74 (m, 1H), 1.69 – 1.56 (m, 3H), 1.48 – 1.40 (m, 6H), 1.30 – 1.15 (m, 5H), 1.10 – 1.03 (m, 1 H), 1.02 – 0.94 (m, 1H), 0.88 – 0.81 (m, 9H)

**<sup>13</sup>C NMR (151 MHz, CDCl<sub>3</sub>)** δ 213.85, 213.43, 86.06, 84.24, 83.29, 69.88, 69.44, 60.35, 58.51, 57.12, 57.07, 42.43, 40.02, 39.99, 39.96, 39.61, 36.40, 36.29, 33.65, 33.63, 33.21, 31.90, 29.90, 22.63, 22.40, 21.20, 21.18, 20.88, 20.57, 18.43, 15.58, 15.32, 13.94, 13.91.

**IR (film)** 2978.52, 2941.88, 1518.67, 1378.85, 1267.00, 1230.36, 1130.08, 992.20  $\text{cm}^{-1}$ .

**HRMS (ES+)** Exact mass calcd for  $\text{C}_{19}\text{H}_{32}\text{O}_2\text{S}_2\text{Na}$   $[\text{M}+\text{Na}]^+$ , 379.1736. Found 379.1784.



**2.33**

***S*-((1*s*,3*r*,5*R*,7*S*)-3-(5-bromo-2-methoxyphenyl)adamantan-1-yl) *O*-ethyl**

**carbonodithioate (2.33).** Prepared according to General Procedure D (0.15 mmol scale)

using 2-(1-adamantyl)-4-bromoanisole and xanthylamide **2.8** (1 equiv). The crude residue was purified by flash column chromatography to afford **2.33** as an off-white solid (33.8 mg, 51% yield) containing 5% of a minor regioisomer arising from functionalization on the methoxy group. Due to the nonpolar nature of the product, a minor amount of an inseparable impurity was isolated alongside the xanthylated products (annotated on  $^1\text{H}$  NMR spectrum):

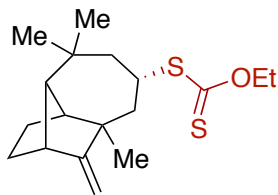
**$^1\text{H}$  NMR (600 MHz,  $\text{CDCl}_3$ )** 7.29 (d,  $J = 8.7$  Hz, 1H), 7.26 (br. s, 1H, underneath residual  $\text{CHCl}_3$ ), 6.75 (d,  $J = 8.6$  Hz, 1H), 4.67 (q,  $J = 7.2$  Hz, 2H), 3.82 (s, 3H), 2.45 (s, 1H), 2.27 – 2.23 (m, 2H), 2.19 – 2.13 (m, 7H), 1.91 (d,  $J = 12.4$  Hz, 2H), 1.74 – 1.69 (m, 2H), 1.46 (t,  $J = 7.2$  Hz, 3H).

**$^{13}\text{C}$  NMR (151 MHz,  $\text{CDCl}_3$ )**  $\delta$  214.15, 157.73, 138.80, 129.99, 129.67, 113.43, 113.38, 69.37, 55.41, 55.09, 43.89, 41.26, 39.31, 39.23, 35.76, 30.36, 13.94 (overlap of adamantyl carbons).

**IR (film)** IR 2915.84, 2853.17, 1744.30, 1483.46, 1455.03, 1234.22, 1133.94, 1112.73, 1046.19, 1027.87  $\text{cm}^{-1}$ .

**HRMS (ES+)** Exact mass calcd for  $\text{C}_{20}\text{H}_{26}\text{BrO}_2\text{S}_2$   $[\text{M}+\text{H}]^+$ , 441.0552. Found 441.0568.





### 2.34

***O*-ethyl *S*-((6*S*)-4,8,8-trimethyl-9-methylenedecahydro-1,4-methanoazulen-6-yl)**

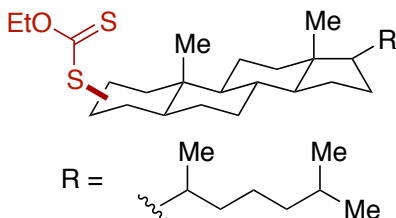
**carbonodithioate (2.34):** Prepared according to General Procedure C using (+)-longifolene (0.50 mmol, 1 equiv) and xanthylamide **2.8** (0.50 mmol, 1 equiv) with the exception that no solvent was used. The crude residue was purified by flash column chromatography to afford pure **2.34** as an off-white solid (87.6 mg, 54% yield):

**<sup>1</sup>H NMR (600 MHz, CDCl<sub>3</sub>)** δ 4.81 (s, 1H), 4.64 (qdd, *J* = 10.3, 7.2, 3.5 Hz, 2H), 4.55 (d, *J* = 2.1 Hz, 1H), 3.93 (td, *J* = 12.2, 6.2 Hz, 1H), 2.65 (d, *J* = 4.8 Hz, 1H), 2.19 (d, *J* = 3.7 Hz, 1H), 2.17 – 2.11 (m, 2H), 1.78 – 1.67 (m, 4H), 1.42 (tdd, *J* = 12.3, 5.8, 1.6 Hz, 6H), 1.12 (s, 3H), 1.03 (s, 3H), 0.93 (s, 3H).

**<sup>13</sup>C NMR (151 MHz, CDCl<sub>3</sub>)** δ 214.43, 166.47, 100.29, 69.66, 61.70, 48.39, 47.69, 44.92, 44.61, 43.96, 43.09, 34.06, 30.80, 30.36, 29.92, 29.60, 25.56, 14.04.

**IR (film)** 3063.37, 2955.38, 2867.63, 1655.59, 1364.39, 1213.01, 1111.76, 1051.98 cm<sup>-1</sup>.

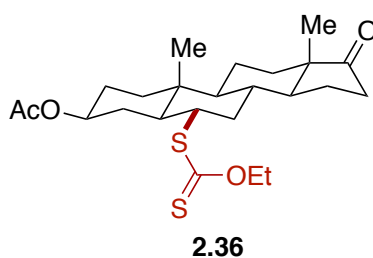
**HRMS (ES<sup>+</sup>)** Exact mass calcd for C<sub>18</sub>H<sub>28</sub>OS<sub>2</sub>Na [M+Na]<sup>+</sup>, 347.1474. Found 347.1474.



### 2.35

**Reaction with 5a-cholestane :** The xanthate was prepared according to General Procedure D (0.15 mmol scale) using cholestane and xanthylamide **2.8** (1 equiv), giving 60% NMR yield.

The resulting crude residue was dissolved in EtOH (1 mL) and treated with ethylene diamine (4 equiv). After 4 h the mixture was concentrated *in vacuo*, redissolved in Et<sub>2</sub>O (2 mL), and washed with 2M H<sub>2</sub>SO<sub>4</sub> (2 mL), brine (2 mL), dried over MgSO<sub>4</sub>, and concentrated *in vacuo* to afford **2.35** in 60% NMR yield.



**Reaction with *trans*-androsterone acetate:** Prepared according to General Procedure E (0.064 mmol scale) using *trans*-androsterone acetate and xanthylamide **2.8** (3 equiv) in C<sub>6</sub>F<sub>6</sub> for 24 h giving 63% NMR yield. The crude residue was purified by flash column chromatography to afford pure **2.36** as an off-white solid (16.1 mg, 56% yield):

**(3R,5S,8R,9S,10S,13S,14S)-2-((ethoxycarbonothioyl)thio)-10,13-dimethyl-17-oxohexadecahydro-1H-cyclopenta[a]phenanthren-3-yl acetate (2.36a):**

**<sup>1</sup>H NMR (600 MHz CDCl<sub>3</sub>)** δ 4.76 (td, *J* = 11.3, 5.1 Hz, 1H), 4.67 – 4.59 (m, 2H), 3.96 (td, *J* = 12.2, 4.3 Hz, 1H), 2.43 (dd, *J* = 19.3, 8.8 Hz, 1H), 2.33 (dd, *J* = 13.1, 4.3 Hz, 1H), 2.11 – 2.00 (m, 1H), 2.03 (s, 3H), 1.93 (ddd, *J* = 14.3, 8.5, 5.9 Hz, 1H), 1.84 – 1.77 (m, 3H), 1.66 – 1.61 (m, 1H), 1.56 – 1.46 (m, 2H), 1.42 (t, *J* = 7.2 Hz, 3H), 1.39 – 1.19 (m, 7H), 1.02 – 0.94 (m, 1H), 0.99 (s, 3H), 0.89 – 0.83 (m, 1H), 0.86 (s, 3H), 0.76 (td, *J* = 12.7, 4.0 Hz, 1H).

**<sup>13</sup>C NMR (151 MHz, CDCl<sub>3</sub>)** δ 221.27, 213.80, 170.61, 72.74, 70.01, 54.15, 51.32, 50.32, 47.88, 44.61, 44.54, 37.54, 35.95, 34.83, 34.59, 31.49, 30.71, 27.73, 21.89, 21.28, 20.63, 13.95, 12.42.

**(3S,5S,8R,9S,10R,13S,14S)-6-((ethoxycarbonothioyl)thio)-10,13-dimethyl-17-oxohexadecahydro-1H-cyclopenta[a]phenanthren-3-yl acetate (2.36b):**

**<sup>1</sup>H NMR (600 MHz, CDCl<sub>3</sub>)** δ 4.67 – 4.60 (m, 3H), 3.81 (td, *J* = 12.3, 4.1 Hz, 1H), 2.47 (dd, *J* = 19.4, 7.9 Hz, 1H), 2.31 (dt, *J* = 12.8, 4.0 Hz, 1H), 2.17 (ddt, *J* = 12.4, 4.6, 2.6 Hz, 1H), 2.13 – 2.03 (m, 2H), 2.04 (s, 3H), 1.97 – 1.92 (m, 1H), 1.90 – 1.79 (m, 2H), 1.78 – 1.69 (m, 2H), 1.56 – 1.50 (m, 2H), 1.45 (t, *J* = 7.0 Hz, 3H), 1.37 – 1.25 (m, 5H), 1.10 (td, *J* = 13.7, 4.0 Hz, 1H), 1.02 (s, 3H), 0.90 (s, 3H), 0.89 – 0.87 (m, 1H), 0.82 (td, *J* = 11.3, 3.9 Hz, 1H).

**<sup>13</sup>C NMR (151 MHz, CDCl<sub>3</sub>)** δ 220.77, 214.68, 170.67, 73.16, 70.15, 53.78, 51.13, 50.75, 48.72, 47.88, 38.58, 37.80, 36.75, 35.95, 35.64, 31.47, 30.44, 27.34, 21.76, 21.57, 20.58, 13.96, 12.95.

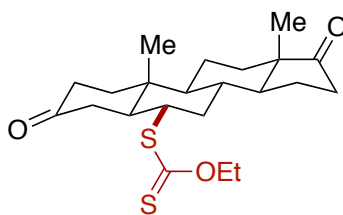
**IR (film)** 2943.8, 1771.30, 1734.66, 1652.70, 1540.85, 1239.04, 1047.16 cm<sup>-1</sup>.

**HRMS (ES<sup>+</sup>)** Exact mass calcd for C<sub>24</sub>H<sub>37</sub>O<sub>4</sub>S<sub>2</sub> [M+H]<sup>+</sup>, 453.2128. Found 453.2159.

Steroid regiochemistry assignments were made by converting the xanthate to the TEMPO adduct and oxidation to the corresponding ketone via the following procedure:

The starting xanthate was dissolved in PhCl (0.1 M) and stirred at 100 °C. TEMPO (6 equiv) and tris(trimethylsilyl)silane (3 equiv) were added in three portions over 48 h. The reaction mixture was stirred for an additional 24 hr, then was concentrated. The crude mixture was redissolved in CH<sub>2</sub>Cl<sub>2</sub> (0.1 M) and cooled to 0 °C, into which a solution of 3-chloroperbenzoic acid (2 equiv) dissolved in CH<sub>2</sub>Cl<sub>2</sub> was added dropwise. After the addition, the reaction mixture was stirred for 2 h, then quenched with saturated Na<sub>2</sub>S<sub>2</sub>O<sub>3</sub> and saturated NaHCO<sub>3</sub>. After stirring for 5 min at rt, EtOAc and 10% NaOH was added to the mixture. The organic layer was extracted and washed with brine, dried over anhydrous Na<sub>2</sub>SO<sub>4</sub>, filtered,

and concentrated. The spectroscopic data was then compared to the literature values to identify the regioisomer of xanthate functionalization.<sup>14</sup>



**2.37**

**S-((5S,6S,8R,9S,10R,13S,14S)-10,13-dimethyl-3,17-dioxohexadecahydro-1H-cyclopenta[a]phenanthren-6-yl) O-ethyl carbonodithioate (2.37):** Prepared according to General Procedure E (0.10 mmol scale) using 5 $\alpha$ -androstanedione and xanthylamide **2.8** (3 equiv) in MeCN for 3 days giving 38% NMR yield. A mix of the starting material and product was recovered by flash chromatography and resubjected to the reaction conditions. The resulting crude residue was purified by flash column chromatography to afford pure **2.37** as an off-white solid (18.0 mg, 44% yield):

**<sup>1</sup>H NMR (400 MHz, CDCl<sub>3</sub>)**  $\delta$  4.63 (q,  $J$  = 7.1 Hz, 2H), 3.89 (td,  $J$  = 12.4, 4.2 Hz, 1H), 2.71 (ddd,  $J$  = 15.5, 4.1, 2.0 Hz, 1H), 2.51 – 2.29 (m, 5H), 2.13 – 2.04 (m, 2H), 1.98 – 1.91 (m, 1H), 1.89 – 1.80 (m, 2H), 1.78 – 1.68 (m, 2H), 1.42 (t,  $J$  = 7.1 Hz, 3H), 1.36 – 1.22 (m, 4H), 1.19 (s, 3H), 1.10 – 1.03 (m, 2H), 0.91 (s, 3H), 0.90 – 0.84 (m, 1H).

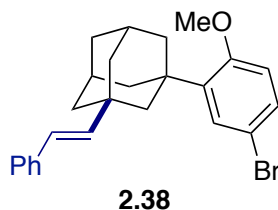
**<sup>13</sup>C NMR (151 MHz, CDCl<sub>3</sub>)**  $\delta$  220.49, 214.47, 210.66, 70.39, 53.40, 51.08, 50.83, 50.42, 47.84, 41.23, 38.12, 37.86, 37.82, 35.90, 35.65, 31.44, 21.80, 20.78, 13.98, 12.30.

**IR (film)** 2945.73, 2856.06, 1735.62, 1715.37, 1670.05, 1540.85, 1218.79, 1047.16 cm<sup>-1</sup>.

**HRMS (ES<sup>+</sup>)** Exact mass calcd for C<sub>22</sub>H<sub>33</sub>O<sub>3</sub>S<sub>2</sub> [M+H]<sup>+</sup>, 409.1866. Found 409.1885.

The site selectivity of xanthate functionalization was determined through a similar procedure as described above for *trans*-androsterone acetate.

## Further Derivatization of Xanthate Products



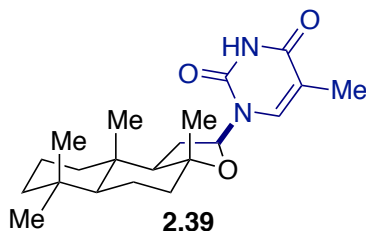
**(1*s*,3*r*,5*R*,7*S*)-1-(5-bromo-2-methoxyphenyl)-3-((*E*)-styryl)adamantane (2.38):** Adapted from the literature procedure.<sup>15</sup> To a solution of adamantyl bromoanisole xanthate **2.33** (30 mg, 0.068 mmol) and styryl ethyl sulfone (40 mg, 0.20 mmol) dissolved in PhCl (1.5 mL) and stirring at 130 °C, tert-butyl peroxide (10  $\mu$ L, 0.068 mmol) was added. Four more tert-butyl peroxide (5  $\mu$ L, 0.034 mmol) additions were added in the following 12 hours. After the last addition, the reaction was left stirring overnight. The resulting dark brown mixture was concentrated, and the product was isolated by flash column chromatography (pentanes) to yield styrene **2.38** as a white solid (15.8 mg, 55% yield). Due to the nonpolar nature of the product, it is contaminated with an inseparable grease impurity (annotated on the <sup>1</sup>H spectrum).

**<sup>1</sup>H NMR (600 MHz, CDCl<sub>3</sub>)**  $\delta$  7.39 – 7.36 (m, 2H), 7.32 – 7.26 (m, 4H, overlap with residual CHCl<sub>3</sub>), 7.21 – 7.17 (m, 1H), 6.74 (d,  $J$  = 8.6 Hz, 1H), 6.29 (d,  $J$  = 16.2 Hz, 1H), 6.16 (d,  $J$  = 16.3 Hz, 1H), 3.81 (s, 3H), 2.25 – 2.19 (m, 2H), 2.07 – 2.00 (m, 4H), 1.99 – 1.94 (m, 2H), 1.75 – 1.68 (m, 6H).

**<sup>13</sup>C NMR (151 MHz, CDCl<sub>3</sub>)**  $\delta$  157.97, 141.72, 140.13, 138.17, 129.86, 129.62, 128.62, 126.92, 126.12, 124.91, 113.40, 113.36, 55.37, 44.85, 41.62, 39.75, 37.89, 36.33, 36.21, 29.27 (peak overlap of adamantyl carbons).

**IR (film)** 2908.13, 2856.06, 1698.98, 1483.96, 1439.60, 1234.22, 1032.69, 805.14 cm<sup>-1</sup>.

**HRMS (ES<sup>+</sup>)** Exact mass calcd for C<sub>25</sub>H<sub>28</sub>BrO [M+H]<sup>+</sup>, 424.3932. Found 424.3903.



**5-methyl-1-((2*S*,3*aR*,5*aS*,9*aS*,9*bR*)-3*a*,6,6,9*a*-tetramethyldodecahydronaphtho[2,1-**

***b*]furan-2-yl)pyrimidine-2,4(1*H*,3*H*)-dione (2.39):** Adapted from the literature procedure.<sup>16</sup>

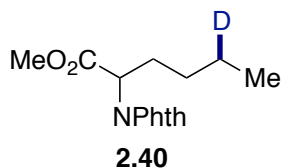
To a solution of ambroxide xanthate **2.32** (50 mg, 0.14 mmol) in PhMe (2.2 mL) at  $-10\text{ }^{\circ}\text{C}$  was added 5-methyl-2,4-bis((trimethylsilyl)oxy)pyrimidine (57 mg, 0.21 mmol)<sup>17</sup> followed by silver (I) triflate (54 mg, 0.21 mmol). The suspension was stirred at  $-10\text{ }^{\circ}\text{C}$  for 2 h then rt for 2 h. Some of the salts were filtered, and the suspension was diluted with EtOAc (5 mL), washed with  $\text{NaHCO}_3$  (2 x 5 mL), brine (5 mL), dried with  $\text{MgSO}_4$ , and concentrated *in vacuo*. The residue was purified by flash column chromatography on silica (40 – 50% EtOAc in hexanes) to afford thymine adduct **2.39** as a white solid (44.1 mg, 4:1 dr, 87% yield):

**$^1\text{H}$  NMR (600 MHz,  $\text{CDCl}_3$ )**  $\delta$  8.95 – 8.75 (br. m, 1H), 7.51 (s, 0.2H), 7.30 (s, 0.8H), 6.06 – 6.03 (m, 0.8H), 5.80 – 5.77 (m, 0.2H), 2.51 (dt,  $J = 9.6, 4.2\text{ Hz}$ , 0.2H), 2.31 (td,  $J = 13.6, 7.4\text{ Hz}$ , 0.8H), 2.10 – 2.02 (m, 1H), 1.96 – 1.90 (m, 3H), 1.87 – 1.82 (m, 1H), 1.78 – 1.54 (m, 4H), 1.49 – 1.37 (m, 4H), 1.37 – 1.27 (m, 1H), 1.26 – 1.20 (m, 3H), 1.05 – 0.97 (m, 2H), 0.90 (s, 3H), 0.86 – 0.81 (m, 6H).

**$^{13}\text{C}$  NMR (major diastereomer, 151 MHz,  $\text{CDCl}_3$ )**  $\delta$  164.02, 150.39, 135.65, 110.22, 87.26, 84.19, 58.70, 57.41, 42.36, 39.93, 39.65, 36.40, 33.58, 33.25, 31.26, 22.31, 21.20, 20.73, 18.35, 15.14, 12.97.

**IR (film)** 3170.40, 2927.41, 2867.63, 1697.05, 1682.59, 1472.38, 1380.78, 1271.82  $\text{cm}^{-1}$ .

**HRMS (ES<sup>+</sup>)** Exact mass calcd for  $\text{C}_{21}\text{H}_{33}\text{N}_2\text{O}_3$   $[\text{M}+\text{H}]^+$ , 361.2486. Found 361.2598.



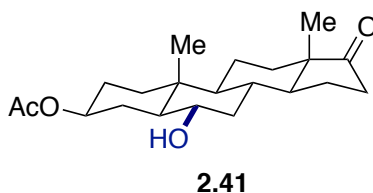
**Methyl 5-deutero-2-(1,3-dioxoisindolin-2-yl)hexanoate (2.40):** Adapted from the literature procedure.<sup>18</sup> In a 1 dram vial in the glovebox, to a solution of norleucine xanthate **2.30** (20 mg, 0.051 mmol) in DCE/MeOH-*d*<sub>4</sub> (0.2 mL/0.08 mL) was added triethylborane (0.25 mL, 0.25 mmol, 1M in hexanes). The vial was fitted with a Teflon-lined screw cap and sealed with Teflon tape. The vial headspace was purged with a dry O<sub>2</sub> balloon for 2 min and then stirred under an O<sub>2</sub> atmosphere for 48 h. The reaction mixture was diluted with DCM (1 mL), passed over a short silica plug, and concentrated. The residue was purified by flash column chromatography on silica (10% EtOAc in hexanes) to afford **2.40** as a pale yellow amorphous solid (10 mg, 71% yield). GC-MS analysis according to the literature revealed 85% D incorporation:

**<sup>1</sup>H NMR (600 MHz, CDCl<sub>3</sub>)** δ 7.87 (dt, *J* = 7.3, 3.9 Hz, 2H), 7.75 (dq, *J* = 7.8, 4.5, 4.0 Hz, 2H), 4.88 – 4.80 (m, 1H), 3.73 (s, 3H), 2.40 – 2.30 (m, 1H), 2.29 – 2.17 (m, 1H), 1.70 – 1.53 (m, 3H), 1.37 – 1.28 (m, 3H).

**<sup>13</sup>C NMR (151 MHz, CDCl<sub>3</sub>)** δ 170.14, 167.87, 167.75, 134.40, 134.32, 131.92, 123.78, 123.76, 123.69, 77.16, 63.49, 63.42, 52.86, 52.28, 33.32, 29.85, 28.48, 26.40, 14.40, 13.90.

**IR (film)** 2957.3, 2924.52, 2853.17, 1747.19, 1717.3, 1456.96, 1388.50, 1253.50 cm<sup>-1</sup>.

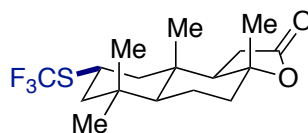
**HRMS (ES<sup>+</sup>)** Exact mass calcd for C<sub>15</sub>H<sub>17</sub>DNO<sub>4</sub> [M+H]<sup>+</sup>, 277.1292. Found 277.1315.



**(3*S*,5*S*,6*S*,8*R*,9*S*,10*R*,13*S*,14*S*)-6-hydroxy-10,13-dimethyl-17-oxohexadecahydro-1*H*-cyclopenta[*a*]phenanthren-3-yl acetate (2.41):** To a solution of steroidal xanthate **2.36b** (35 mg, 0.077 mmol) in PhCl (0.77 mL) stirring at 100 °C, TEMPO (72 mg, 0.23 mmol) and tris(trimethylsilyl)silane (72  $\mu$ L, 0.15 mmol) were added in three portions over 48 h. The reaction mixture was stirred for an additional 24 h, then concentrated. Zinc powder (0.203 g, 3.08 mmol), then a mixture of HOAc/THF/H<sub>2</sub>O (3:1:1, 1.9 mL) was added and heated at 70 °C overnight. The reaction mixture was filtered through a cotton plug and washed with EtOAc. The resulting filtrate was washed with saturated NaHCO<sub>3</sub>, water, dried over anhydrous Na<sub>2</sub>SO<sub>4</sub>, filtered, and concentrated. The crude material was purified by column chromatography (20 – 50% EtOAc in hexanes) to yield **2.41** (14.9 mg, 56% yield) as a white solid in accordance with the literature data.<sup>14</sup>

**<sup>1</sup>H NMR (600 MHz, CDCl<sub>3</sub>)**  $\delta$  4.67 (ddt,  $J$  = 16.4, 11.2, 4.9 Hz, 1H), 3.44 (td,  $J$  = 10.8, 4.5 Hz, 1H), 2.45 (dd,  $J$  = 19.4, 8.8 Hz, 1H), 2.22 (app d,  $J$  = 12.1, 1H), 2.15 – 2.04 (m, 2H), 2.02 (s, 3H), 1.95 (ddd,  $J$  = 14.1, 8.7, 5.8 Hz, 1H), 1.87 – 1.76 (m, 2H), 1.76 – 1.60 (m, 3H), 1.57 – 1.45 (m, 2H), 1.38 – 1.20 (m, 4H), 1.14 – 1.04 (m, 2H), 0.99 – 0.91 (m, 1H), 0.89 – 0.83 (m, 1H), 0.85 (s, 6H), 0.75 (td,  $J$  = 11.4, 4.0 Hz, 1H).

**<sup>13</sup>C NMR (151 MHz, CDCl<sub>3</sub>)**  $\delta$  221.00, 170.76, 73.48, 69.29, 53.85, 51.74, 51.18, 47.89, 40.54, 37.08, 36.54, 35.93, 34.01, 31.46, 28.39, 27.25, 21.89, 21.56, 20.48, 13.93, 13.46.



**2.42**

**(3*aR*,5*aS*,8*S*,9*aS*,9*bR*)-3*a*,6,6,9*a*-tetramethyl-8-**

**((trifluoromethyl)thio)decahydronaphtho[2,1-*b*]furan-2(3*aH*)-one (2.42):** Sclareolide

xanthate **2.31** (10 mg, 0.027 mmol) and ((2-phenylpropan-2-

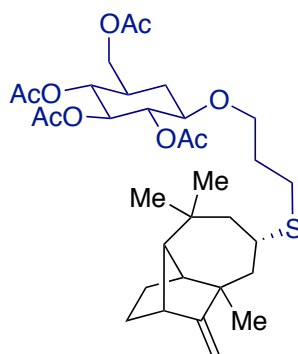


yl)oxy)(trifluoromethyl)sulfane<sup>19</sup> (19 mg, 0.081 mmol) were dissolved in PhCl (1.35 mL) and heated to 100 °C. DLP (5 mg, 0.014 mmol) was added every half-hour for a total of eight additions under an argon atmosphere. After the last addition, the reaction was stirred for another 30 minutes. The mixture was then concentrated, and the product was isolated by flash chromatography (10% EtOAc in hexanes) to yield **2.42** as a white solid in accordance with the literature data (6.7 mg, 71% yield).<sup>20</sup>

**<sup>1</sup>H NMR (600 MHz, CDCl<sub>3</sub>)** δ 3.52 (tt, *J* = 12.8, 3.8 Hz, 1H), 2.44 (dd, *J* = 16.2, 14.7 Hz, 1H), 2.27 (dd, *J* = 16.2, 6.5 Hz, 1H), 2.10 (dt, *J* = 12.0, 3.3 Hz, 1H), 1.99 (dd, *J* = 14.7, 6.5 Hz, 1H), 1.93 – 1.89 (m, 2H), 1.86 (ddd, *J* = 12.5, 3.7, 2.1 Hz, 1H), 1.70 (td, *J* = 12.6, 4.3 Hz, 1H), 1.42 – 1.31 (m, 1H), 1.34 (s, 3H), 1.21 (app t, *J* = 12.6 Hz, 1H), 1.10 (dd, *J* = 12.6, 2.9 Hz, 1H), 0.98 (s, 3H), 0.97 (s, 3H), 0.92 (s, 3H).

**<sup>13</sup>C NMR (151 MHz, CDCl<sub>3</sub>)** δ 176.19, 131.08 (q, *J* = 306.5 Hz), 86.00, 55.85, 49.14, 46.75, 38.53, 37.60, 37.23, 35.13, 32.98, 28.69, 21.76, 21.30, 20.38, 15.73.

**<sup>19</sup>F NMR (565 MHz, CDCl<sub>3</sub>)** δ -38.78.



**2.43**

**(6S)-4,8,8-trimethyl-9-methylenedecahydro-1,4-methanoazulene-6-thiol:** To a solution of xanthate **2.34** (57 mg, 0.18 mmol) in EtOH (0.9 mL) was added ethylene diamine (47 uL, 0.70 mmol), leading to persistence of a deep yellow color. After 4 h the mixture was concentrated *in vacuo*, redissolved in Et<sub>2</sub>O (2 mL), and washed with 2M H<sub>2</sub>SO<sub>4</sub> (2 mL), brine

(2 mL), dried over MgSO<sub>4</sub>, and concentrated *in vacuo* to afford the thiol as a yellow oil (42 mg, 99% yield), which was used directly without further purification:

**<sup>1</sup>H NMR (600 MHz, CDCl<sub>3</sub>)** δ 4.81 (s, 1H), 4.56 (s, 1H), 3.22 – 3.09 (m, 1H), 2.63 (d, *J* = 5.0 Hz, 1H), 2.14 (dd, *J* = 13.9, 11.6 Hz, 1H), 2.10 – 2.06 (m, 2H), 1.77 (dd, *J* = 13.6, 11.8 Hz, 1H), 1.74 – 1.69 (m, 1H), 1.67 (ddd, *J* = 12.4, 9.0, 3.2 Hz, 1H), 1.58 (d, *J* = 6.3 Hz, 1H), 1.44 – 1.37 (m, 2H), 1.28 (dq, *J* = 14.0, 1.5 Hz, 1H), 1.14 (ddd, *J* = 11.9, 9.0, 5.8 Hz, 1H), 1.01 (s, 3H), 1.01 (s, 3H), 0.90 (s, 3H).

**<sup>13</sup>C NMR (151 MHz, CDCl<sub>3</sub>)** δ 166.67, 100.20, 61.58, 55.13, 47.65, 47.51, 44.97, 44.31, 34.08, 33.79, 30.73, 30.13, 29.87, 29.60, 25.53.

**(2*R*,3*R*,4*S*,5*R*,6*R*)-2-(acetoxymethyl)-6-(3-(((6*S*)-4,8,8-trimethyl-9-methylenedecahydro-1,4-methanoazulen-6-yl)thio)propoxy)tetrahydro-2*H*-pyran-3,4,5-triyl triacetate (2.43):**

Adapted from the literature.<sup>21</sup> In a vial in the glovebox, thiol (27 mg, 0.11 mmol), allylglycoside (160 mg, 0.41 mmol), 2,2-dimethoxy-2-phenylacetophenone (3 mg, 0.011 mmol), and 4'-methoxyacetophenone (2 mg, 0.011 mmol) were dissolved in DMF (0.22 mL). The vial was sealed with a teflon-lined screw cap, sealed with Teflon tape, and placed in a UV-A box and irradiated for 22 h. The crude reaction mixture was diluted with EtOAc (2 mL), washed with H<sub>2</sub>O (5 x 2 mL), brine (2 x 2 mL), dried with MgSO<sub>4</sub>, and concentrated *in vacuo*. The yellow residue was purified by flash column chromatography on silica (20% EtOAc in hexanes) to afford thiol-ene adduct **2.43** as a white solid (36.5 mg, 62% yield):

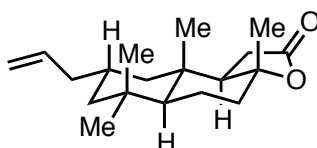
**<sup>1</sup>H NMR (600 MHz, CDCl<sub>3</sub>)** δ 5.46 (td, *J* = 9.8, 2.2 Hz, 1H), 5.07 – 5.04 (m, 2H), 4.87 (dd, *J* = 10.4, 3.7 Hz, 1H), 4.80 (s, 1H), 4.55 (s, 1H), 4.26 (dd, *J* = 12.4, 4.3 Hz, 1H), 4.09 (dd, *J* = 12.4, 2.2 Hz, 1H), 4.05 – 4.00 (m, 1H), 3.85 – 3.78 (m, 1H), 3.54 – 3.47 (m, 1H), 2.90 (td, *J* = 12.0, 6.1 Hz, 1H), 2.64 (d, *J* = 4.6 Hz, 1H), 2.62 – 2.55 (m, 3H), 2.10 (s, 3H), 2.06 (s, 3H),

2.02 (s, 3H), 2.01 (s, 3H), 1.63 – 1.57 (m, 4H), 1.29 – 1.22 (m, 7H), 1.02 (s, 3H), 1.00 (s, 3H), 0.93 (s, 3H).

<sup>13</sup>C NMR (151 MHz, CDCl<sub>3</sub>) δ 170.86, 170.31, 170.26, 169.77, 166.68, 100.18, 95.84, 70.94, 70.32, 68.60, 67.34, 67.02, 61.96, 61.55, 50.19, 47.75, 45.04, 43.97, 43.58, 38.27, 33.70, 31.71, 30.84, 30.17, 30.05, 29.63, 29.27, 26.90, 25.54, 20.94, 20.89, 20.80.

IR (film) 2926.45, 1750.08, 1455.99, 1367.28, 1225.54, 1168.65, 1036.55, 2351.77 cm<sup>-1</sup>.

HRMS (ES<sup>+</sup>) Exact mass calcd for C<sub>32</sub>H<sub>49</sub>O<sub>10</sub>S [M+H]<sup>+</sup>, 625.3041. Found 625.3156.



**(3aR,5aS,8S,9aS,9bR)-8-allyl-3a,6,6,9a-tetramethyldecahydronaphtho[2,1-b]furan**

**2(3aH)-one:** Adapted from the literature procedure.<sup>22</sup> In a 2 dram vial in a glovebox, sclareolide xanthate **2.31** (50 mg, 0.13 mmol), allyl ethyl sulfone (54 mg, 0.40 mmol), and dilauroyl peroxide (5.4 mg, 0.013 mmol) were dissolved in chlorobenzene (0.5 mL). The vial was fitted with a rubber septum, wrapped with Teflon tape, and placed under a balloon of argon once removed from the glovebox. The vial was heated at 100 °C, and additional dilauroyl peroxide was added every 30 minutes until the sclareolide xanthate had been consumed as determined by TLC (48.6 mg additional DLP). The crude reaction mixture was concentrated by passing a stream of nitrogen over the heated vial. The residue was purified via flash column chromatography on silica (10 – 20% EtOAc in hexanes) to afford allylated sclareolide as a clear oil (18 mg, 49% yield):

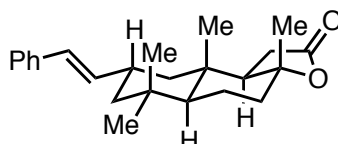
<sup>1</sup>H NMR (600 MHz, CDCl<sub>3</sub>) δ 5.79 – 5.71 (m, 1H), 5.00 – 4.97 (m, 2H), 2.75 – 2.70 (m, 1H), 2.40 (d, *J* = 17.9 Hz, 1H), 2.27 – 2.22 (m, 1H), 1.93 (t, *J* = 6.6 Hz, 2H), 1.78 – 1.72 (m,

1H), 1.66 – 1.57 (m, 4H), 1.54 – 1.41 (m, 4H), 1.32 (s, 3H), 1.22 – 1.18 (m, 1H), 0.91 (s, 6H), 0.87 (s, 3H).

**<sup>13</sup>C NMR (151 MHz, CDCl<sub>3</sub>)** δ 177.91, 137.09, 116.02, 85.83, 54.84, 51.65, 48.54, 47.47, 41.75, 36.80, 35.29, 33.76, 33.73, 32.59, 30.13, 28.61, 22.94, 18.41, 15.42.

**IR (film)** 3446.17, 2925.48, 1867.72, 1772.26, 1670.05, 1540.85, 1521.56, 1456.96 cm<sup>-1</sup>.

**HRMS (ES<sup>+</sup>)** Exact mass calcd for C<sub>19</sub>H<sub>31</sub>O<sub>2</sub> [M+H]<sup>+</sup>, 291.2319. Found 291.2339.



**(3aR,5aS,8S,9aS,9bR)-3a,6,6,9a-tetramethyl-8-((E)-styryl)decahydronaphtho[2,1-**

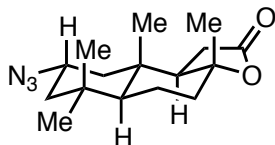
**b]furan-2(3aH)-one:** Adapted from the literature procedure.<sup>15</sup> To a solution of sclareolide xanthate **2.31** (32 mg, 0.086 mmol) and styryl ethyl sulfone (51 mg, 0.26 mmol) dissolved in PhCl (1.35 mL) and stirring at 130 °C, tert-butyl peroxide (10 μL, 0.068 mmol) was added. Four more tert-butyl peroxide (5 μL, 0.034 mmol) additions were added in the following 24 hours. After the last addition, the reaction was left stirring overnight. The resulting dark brown mixture was concentrated, and the product was isolated by flash column chromatography (10% EtOAc in hexanes) to yield the styrene as a yellow oil (22.2 mg, 73% yield):

**<sup>1</sup>H NMR (600 MHz, CDCl<sub>3</sub>)** δ 7.36 – 7.32 (m, 2H), 7.32 – 7.27 (t, *J* = 7.7 Hz, 2H), 7.22 – 7.17 (m, 1H), 6.37 (d, *J* = 15.9 Hz, 1H), 6.09 (dd, *J* = 15.9, 7.0 Hz, 1H), 2.75 (dd, *J* = 17.9, 7.9 Hz, 1H), 2.49 – 2.39 (m, 2H), 2.35 (ddd, *J* = 14.8, 5.0, 2.0 Hz, 1H), 1.80 (d, *J* = 7.9 Hz, 1H), 1.72 (dt, *J* = 12.6, 2.7 Hz, 1H), 1.67 – 1.55 (m, 2H), 1.50 (td, *J* = 13.6, 12.7, 4.8 Hz, 1H), 1.34 (s, 3H), 1.11 (app t, *J* = 12.8 Hz, 1H), 0.99 (s, 3H), 0.96 (s, 3H), 0.95 (s, 3H), 0.93 – 0.79 (m, 3H).

**<sup>13</sup>C NMR (151 MHz, CDCl<sub>3</sub>)** δ 177.78, 137.75, 135.70, 128.64, 128.09, 127.11, 126.04, 85.75, 54.80, 51.26, 48.09, 47.18, 36.71, 35.25, 33.73, 33.63, 32.56, 32.54, 30.14, 22.93, 18.38, 15.39.

**IR (film)** 2951.52, 1772.26, 1646.91, 1576.52, 1540.85, 1507.10, 1473.35, 1456.96 cm<sup>-1</sup>.

**HRMS (ES<sup>+</sup>)** Exact mass calcd for C<sub>24</sub>H<sub>33</sub>O<sub>2</sub> [M+H]<sup>+</sup>, 353.2475. Found 353.2507.

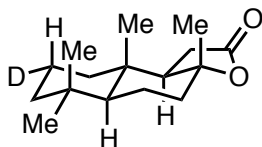


**(3aR,5aS,8S,9aS,9bR)-8-azido-3a,6,6,9a-tetramethyldecahydronaphtho[2,1-b]furan-**

**2(3aH)-one:** Adapted from the literature procedure.<sup>23</sup> In a 2 dram vial in a glovebox, sclareolide xanthate **2.31** (50 mg, 0.13 mmol), azide ethyl sulfone (55 mg, 0.40 mmol), and dilauroyl peroxide (5.4 mg, 0.013 mmol) were dissolved in chlorobenzene (0.5 mL). The vial was fitted with a rubber septum, wrapped with Teflon tape, and placed under a balloon of argon once removed from the glovebox. The vial was heated at 100 °C, and additional dilauroyl peroxide was added every 30 minutes until the sclareolide xanthate had been consumed as determined by TLC (48.6 mg additional DLP). The crude reaction mixture was concentrated by passing a stream of nitrogen over the heated vial. The residue was purified via flash column chromatography on silica (10 – 20% EtOAc in hexanes) to afford the azide as a yellow oil in a 5:1 diastereomeric mixture (28.2 mg, 74% yield) in accordance with the literature (NMR shifts are reported for the major diastereomer only):<sup>24</sup>

**<sup>1</sup>H NMR (major diastereomer, 600 MHz, CDCl<sub>3</sub>)** δ 3.61 (tt, *J* = 12.1, 4.2 Hz, 1H), 2.47 – 2.38 (m, 1H), 2.28 (dd, *J* = 16.1, 6.4 Hz, 1H), 2.12 – 2.07 (m, 1H), 2.01 (dd, *J* = 14.7, 6.4 Hz, 1H), 1.93 – 1.88 (m, 1H), 1.86 – 1.75 (m, 2H), 1.73 – 1.67 (m, 1H), 1.64 – 1.54 (m, 2H), 1.33 (s, 3H), 1.10 – 1.04 (m, 2H), 0.98 (s, 3H), 0.96 (s, 3H), 0.90 (s, 3H).

**<sup>13</sup>C NMR (major diastereomer, 151 MHz, CDCl<sub>3</sub>)** δ 176.30, 86.03, 58.76, 56.05, 54.02, 47.06, 44.61, 38.48, 37.09, 34.54, 33.11, 32.01, 28.73, 21.75, 20.30, 16.03.



**(3aR,5aS,8S,9aS,9bR)-8-deutero-3a,6,6,9a-tetramethyldecahydronaphtho[2,1-b]furan-**

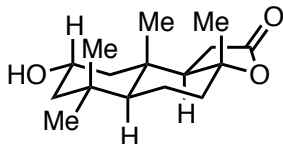
**2(3aH)-one (S16):** Adapted from the literature procedure.<sup>18</sup> In a 1 dram vial in the glovebox, to a solution of sclareolide xanthate **2.31** (40 mg, 0.11 mmol) in DCE/MeOH-*d*<sub>4</sub> (0.4 mL/0.2 mL) was added triethylborane (0.54 mL, 0.54 mmol, 1M in hexanes). The vial was fitted with a Teflon-lined screw cap and sealed with Teflon tape. The vial headspace was purged with a dry O<sub>2</sub> balloon for 2 min and then stirred under an O<sub>2</sub> atmosphere for 72 h. The reaction mixture was diluted with DCM (1 mL), passed over a short silica plug, and concentrated to afford the reduced product as a pale yellow amorphous solid (16 mg, 62% yield). GC-MS analysis according to the literature revealed 72% D incorporation:

**<sup>1</sup>H NMR (600 MHz, CDCl<sub>3</sub>)** δ 2.44 – 2.37 (m, 1H), 2.23 (dd, *J* = 16.3, 6.5 Hz, 1H), 2.07 (dt, *J* = 12.0, 3.3 Hz, 1H), 1.96 (dd, *J* = 14.9, 6.5 Hz, 1H), 1.89 – 1.85 (m, 1H), 1.73 – 1.60 (m, 2H), 1.44 – 1.36 (m, 2H), 1.33 (s, 3H), 1.22 – 1.14 (m, 2H), 1.08 – 1.02 (m, 1H), 0.99 – 0.93 (m, 1H), 0.91 (s, 3H), 0.88 (s, 3H), 0.83 (s, 3H).

**<sup>13</sup>C NMR (151 MHz, CDCl<sub>3</sub>)** δ 177.10, 86.58, 59.23, 56.75, 42.18, 39.51, 38.81, 36.15, 33.43, 33.31, 28.86, 21.71, 21.06, 20.68, 17.83 (t, *J* = 19.6 Hz), 15.21.

**IR (film)** 2926.45, 2869.56, 1844.58, 1773.23, 1716.34, 1540.85, 1497.45, 1456.96 cm<sup>-1</sup>.

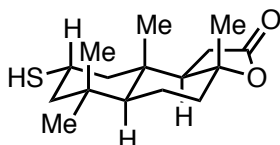
**HRMS (ES<sup>+</sup>)** Exact mass calcd for C<sub>16</sub>H<sub>26</sub>O<sub>2</sub>D [M+H]<sup>+</sup>, 252.2067. Found 252.2083.



**(3aR,5aS,8S,9aS,9bR)-8-hydroxy-3a,6,6,9a-tetramethyldecahydronaphtho[2,1-b]furan-2(3aH)-one (S17):** To a solution of sclareolide xanthate **2.31** (37 mg, 0.1 mmol) in PhCl (1 mL) stirring at 100 °C, TEMPO (94 mg, 0.6 mmol) and tris(trimethylsilyl)silane (93  $\mu$ L, 0.3 mmol) were added in three portions over 48 h. The reaction mixture was stirred for an additional 24 h, then concentrated. Zinc powder (262 mg, 4.0 mmol), then a mixture of HOAc/THF/H<sub>2</sub>O (3:1:1, 2.5 mL) was added and heated at 70 °C overnight. The reaction mixture was filtered through a cotton plug and washed with EtOAc. The resulting filtrate was washed with saturated NaHCO<sub>3</sub> and water, dried over anhydrous Na<sub>2</sub>SO<sub>4</sub>, filtered, and concentrated. The crude material was purified by flash column chromatography (20 – 50% EtOAc in hexanes) to yield the alcohol as a white solid in accordance with the literature data (16.2 mg, 61% yield).<sup>25</sup>

**<sup>1</sup>H NMR (600 MHz, CDCl<sub>3</sub>)**  $\delta$  3.98 (tt,  $J$  = 11.3, 4.3 Hz, 1H), 2.43 (dd,  $J$  = 16.2, 14.7 Hz, 1H), 2.26 (dd,  $J$  = 16.2, 6.4 Hz, 1H), 2.08 (dt,  $J$  = 11.9, 3.3 Hz, 1H), 2.00 (dd,  $J$  = 14.7, 6.4 Hz, 1H), 1.90 (dd,  $J$  = 14.2, 3.6 Hz, 1H), 1.86 – 1.79 (m, 2H), 1.69 (td,  $J$  = 12.6, 4.3 Hz, 1H), 1.52 (br. s, 1H), 1.41 – 1.31 (m, 1H), 1.32 (s, 3H), 1.15 (t,  $J$  = 12.1 Hz, 1H), 1.07 (dd,  $J$  = 12.7, 2.9 Hz, 1H), 0.99 – 0.94 (m, 7H), 0.88 (s, 3H).

**<sup>13</sup>C NMR (151 MHz, CDCl<sub>3</sub>)**  $\delta$  176.66, 86.27, 64.42, 58.98, 56.23, 51.47, 48.39, 38.56, 37.44, 34.86, 33.35, 28.84, 21.90, 21.76, 20.32, 16.29.



**(3a*R*,5a*S*,8*S*,9a*S*,9b*R*)-8-mercapto-3a,6,6,9a-tetramethyldecahydronaphtho[2,1-*b*]furan-**

**2(3a*H*)-one:** 4-Methyl piperidine (49  $\mu$ L, 0.40 mmol) was added to a solution of sclareolide xanthate **2.31** (37 mg, 0.10 mmol) dissolved in EtOH (0.5 mL) and was left stirring overnight at room temperature. The reaction mixture was then concentrated, and the thiol was isolated by flash column chromatography (30% EtOAc in hexanes) as a white solid (20.2 mg, 71% yield):

**<sup>1</sup>H NMR (600 MHz, CDCl<sub>3</sub>)**  $\delta$  2.97 (td,  $J$  = 10.7, 8.8, 6.3 Hz, 1H), 2.44 (app t,  $J$  = 15.4 Hz, 1H), 2.24 (dd,  $J$  = 16.2, 6.4 Hz, 1H), 2.09 (app d,  $J$  = 11.9 Hz, 1H), 2.00 (dd,  $J$  = 14.8, 6.5 Hz, 1H), 1.90 (dd,  $J$  = 14.5, 3.7 Hz, 1H), 1.86 – 1.77 (m, 2H), 1.70 (td,  $J$  = 12.6, 4.1 Hz, 1H), 1.65 (br. s, 1H), 1.40 – 1.31 (m, 1H), 1.33 (s, 3H), 1.25 (app t,  $J$  = 13.0 Hz, 1H), 1.10 (app t,  $J$  = 12.8 Hz, 2H), 0.95 (s, 3H), 0.94 (s, 3H), 0.87 (s, 3H).

**<sup>13</sup>C NMR (151 MHz, CDCl<sub>3</sub>)**  $\delta$  176.38, 86.21, 58.83, 56.08, 48.66, 46.01, 43.41, 38.54, 37.59, 35.04, 33.09, 28.77, 21.75, 21.55, 20.44, 16.04.

**IR (film)** 3445.21, 2947.66, 1772.26, 1646.91, 1540.85, 1473.35, 1033.66, 916.99 cm<sup>-1</sup>.

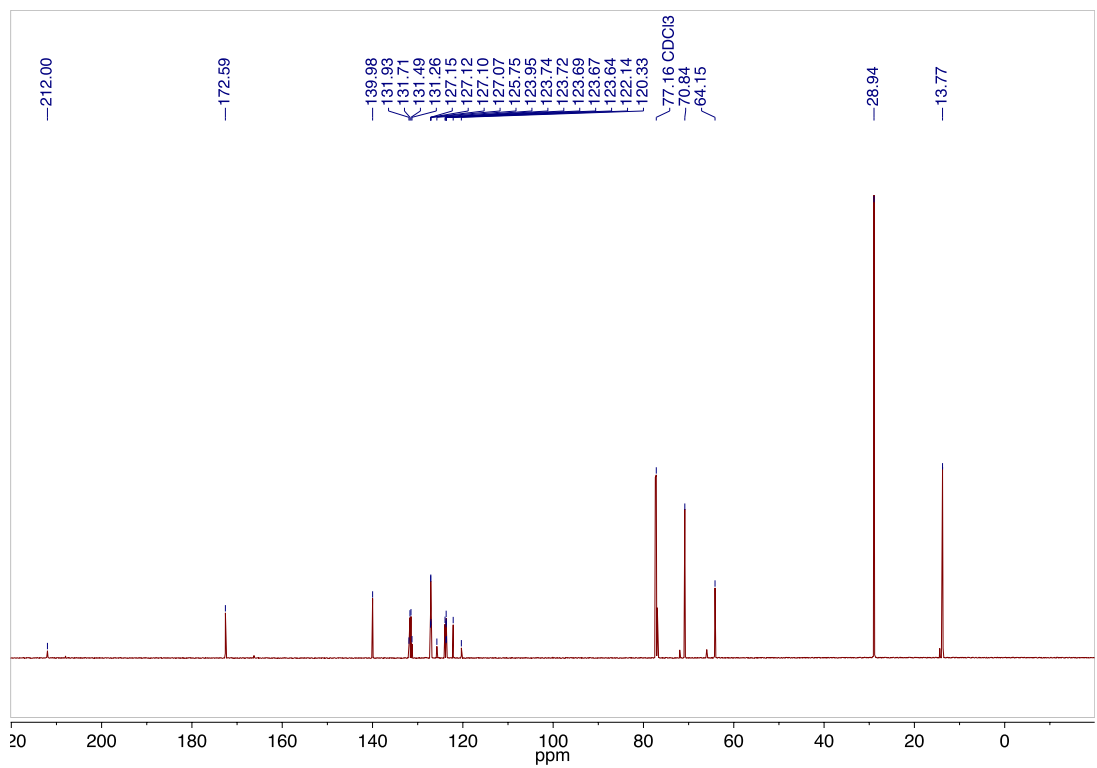
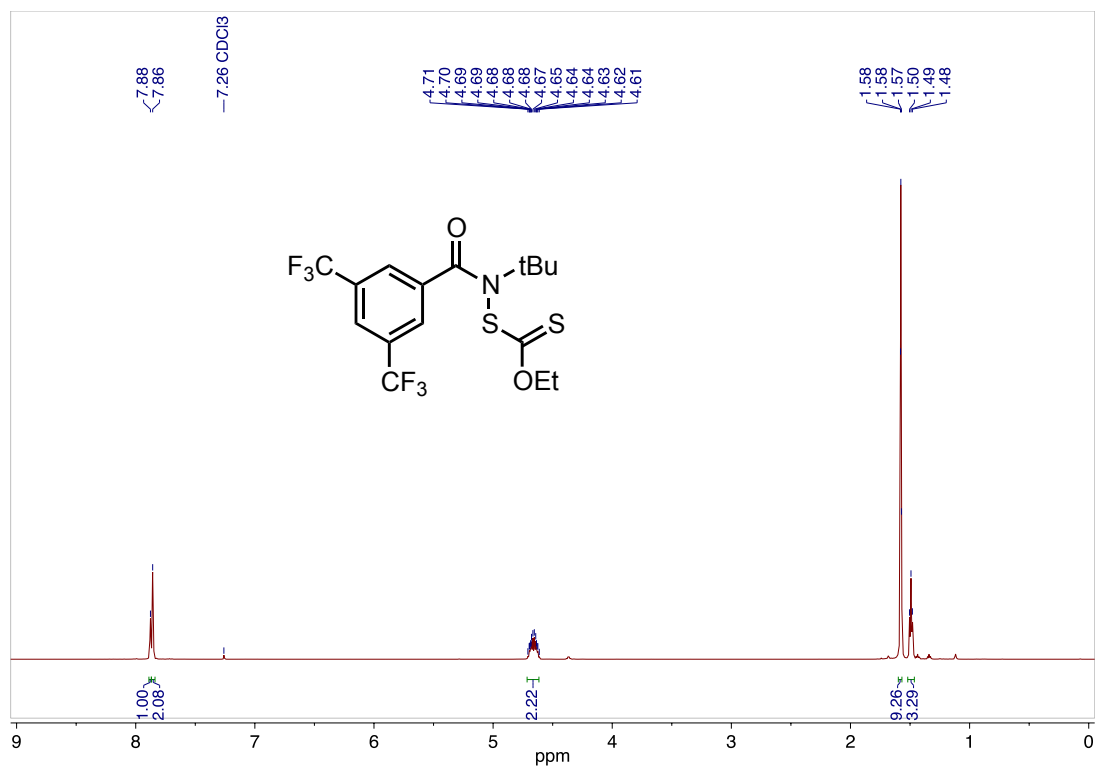
**HRMS (ES<sup>+</sup>)** Exact mass calcd for C<sub>32</sub>H<sub>53</sub>O<sub>4</sub>S<sub>2</sub> [2M+H]<sup>+</sup>, 565.3380. Found 565.3271.

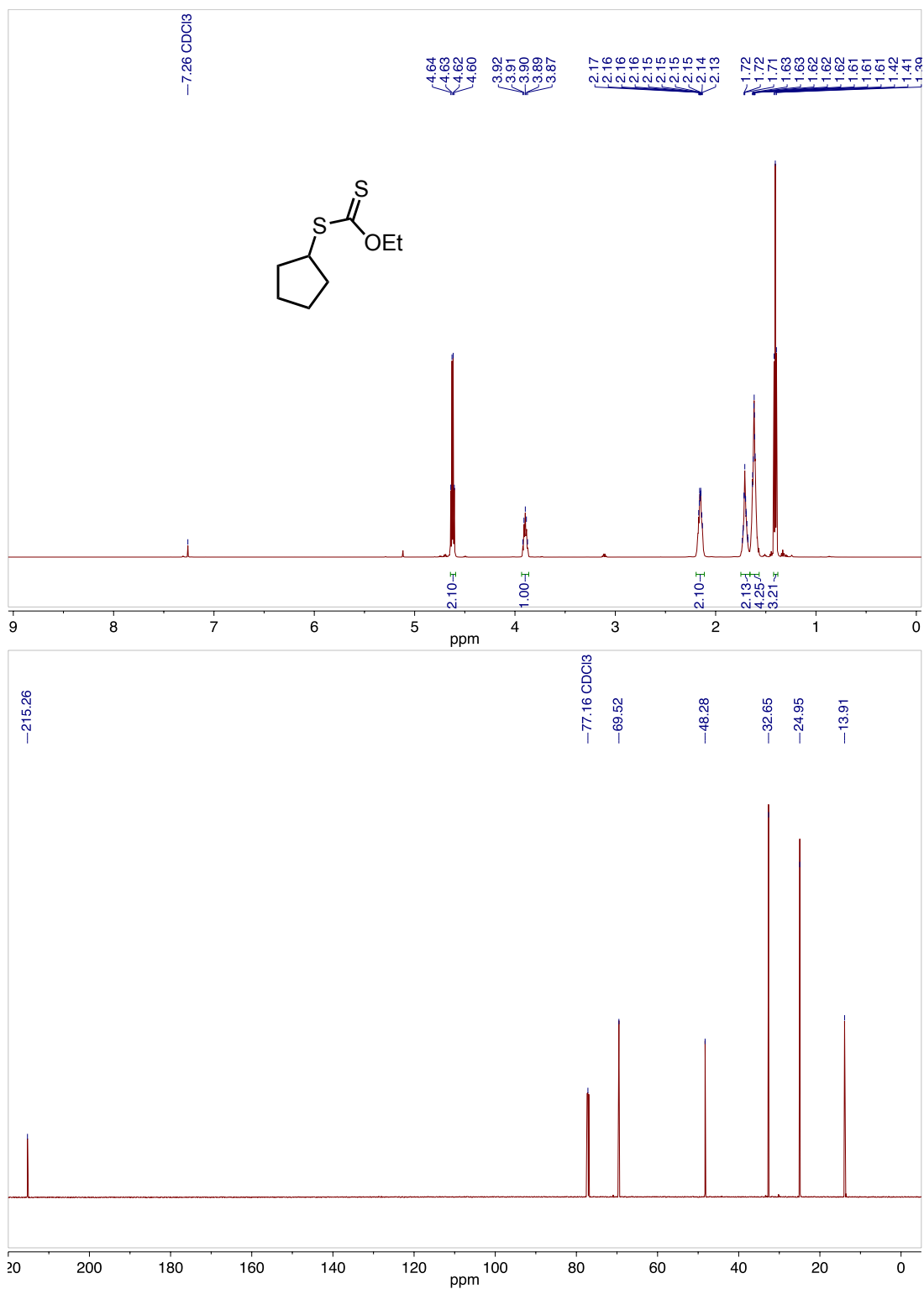


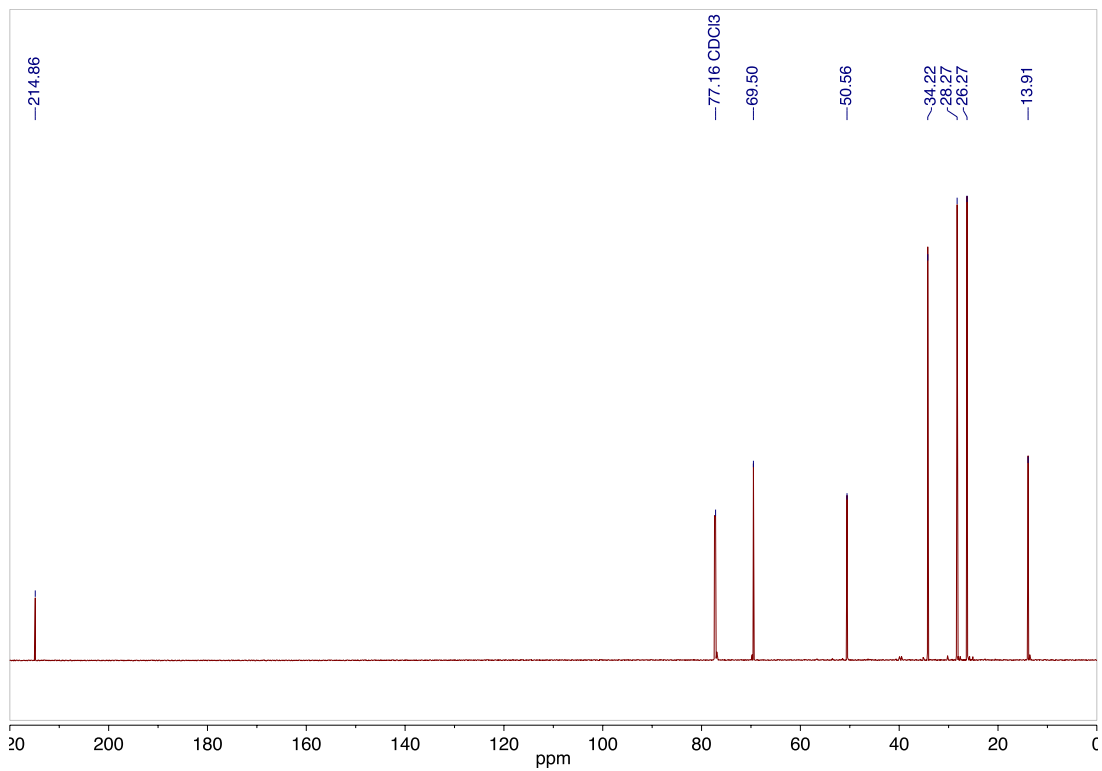
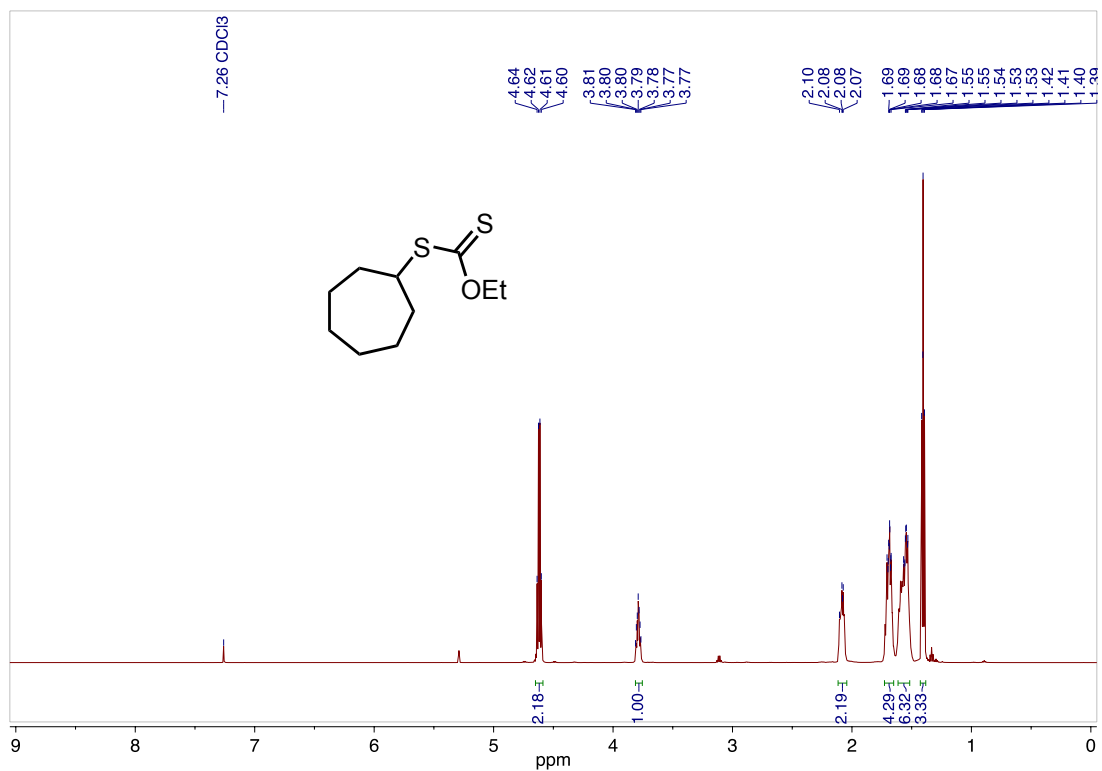
## REFERENCES

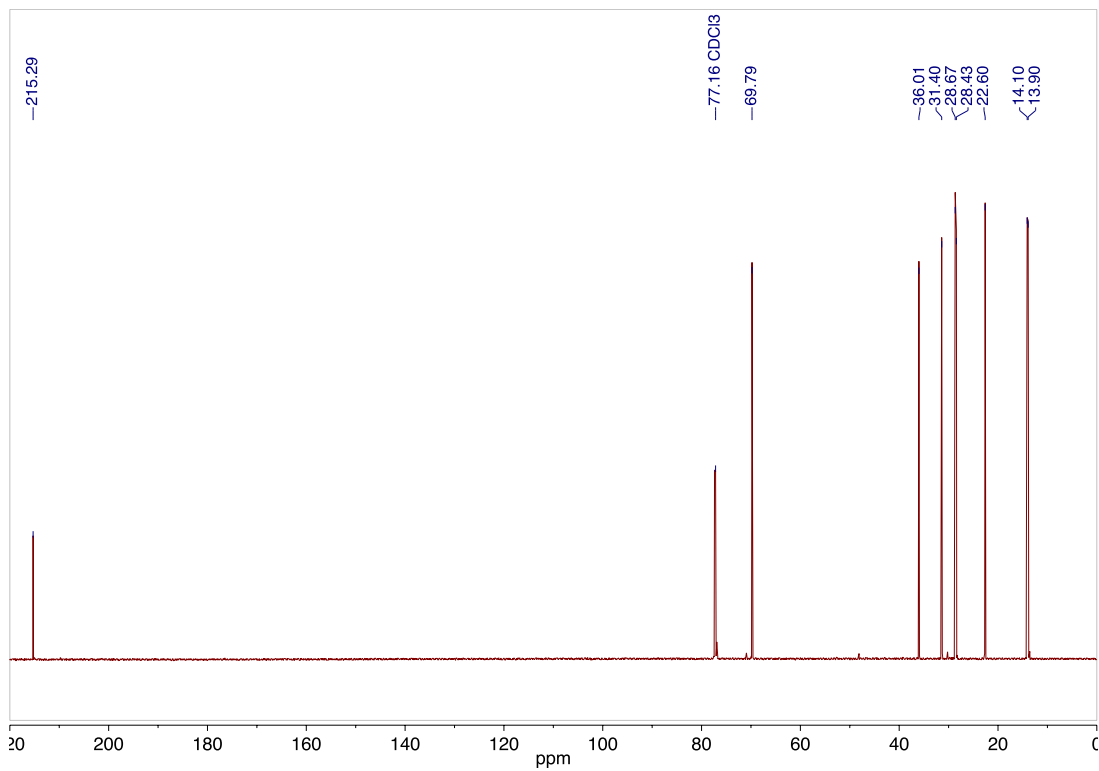
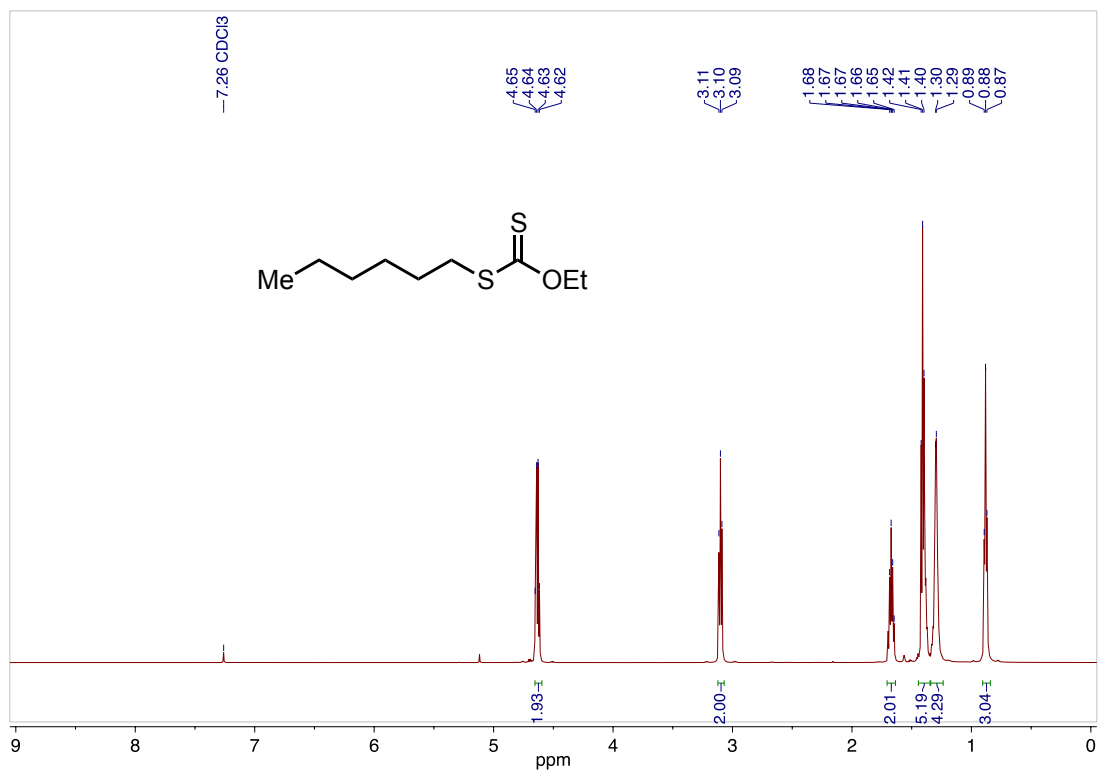
1. Molawi, K.; Schulte, T.; Siegenthaler, K. O.; Wetter, C.; Studer, A. *Chem. Eur. J.* **2005**, *11*, 2335.
2. Larouche-Gauthier, R.; Elford, T. G.; Aggarwal, V. K.; *J. Am. Chem. Soc.* **2011**, *133*, 16794.
3. Schmidt, V. A.; Quinn, R. K.; Brusoe, A. T.; Alexanian, E. J. *J. Am. Chem. Soc.* **2014**, *136*, 14389.
4. Quinn, R. K.; Könst, Z. A.; Michalak, S. E.; Schmidt, Y.; Szklarski, A. R.; Flores, A. R.; Nam, S.; Horne, D. A.; Vanderwal, C. D.; Alexanian, E. J. *J. Am. Chem. Soc.* **2016**, *138*, 696.
5. Kato, S.; Miyagawa, K.; Hattori, R.; Mizuta, M.; Ishida, M. *Synthesis*, **1981**, 746.
6. Xu, S.; Toyama, T.; Nakamura, J.; Arimoto, H. *Tetrahedron Lett.* **2010**, *51*, 4534.
7. Purushottamachar, P.; Njar, V. C. O. *Steroids* **2012**, *77*, 1530.
8. Zhang, W.; Pan, D.; Wu, A.; Shen, L. *Steroids* **2015**, *96*, 16.
9. Trimmell, D.; Stout, E. I.; Doane, W. M.; Russell, C. R.; Beringer, V.; Saul, M.; Van Gessel, G. *J. Org. Chem.* **1975**, *40*, 1337.
10. Gade, A. M.; Abelt, C. J. *Synthesis* **2007**, 2097.
11. Sato, A.; Yorimitsu, H.; Oshima, K. *Chem. Asian. J.* **2007**, *2*, 1568.
12. Bartlett, P. D.; Pincock, R. E.; Rolston, J. H.; Schindel, W. G.; Singer, L. A. *J. Am. Chem. Soc.* **1965**, *87*, 2590.
13. Zlotorzynska, M.; Zhai, H.; Sammis, G. M. *Org. Lett.* **2008**, *10*, 5083.
14. Canta, M.; Font, D.; Gómez, L.; Ribas, X.; Costas, M. *Adv. Synth. Catal.* **2014**, *356*, 818.
15. Bertrand, F.; Quiclet-Sire, B.; Zard, S. Z. *Angew. Chem. Int. Ed.* **1999**, *38*, 1943.
16. Jean-Baptiste, L.; Yemets, S.; Legay, R.; Lequeux, T. *J. Org. Chem.* **2006**, *71*, 2352.
17. Wang, S.; Wen, X.; Golen, J. A.; Arifin, J. F.; Rheingold, A. L. *Chem. Eur. J.* **2013**, *19*, 16104.
18. Allais, F.; Boivin, J.; Nguyen, V. T. *Beilstein J. Org. Chem.* **2007**, *3*, 46.

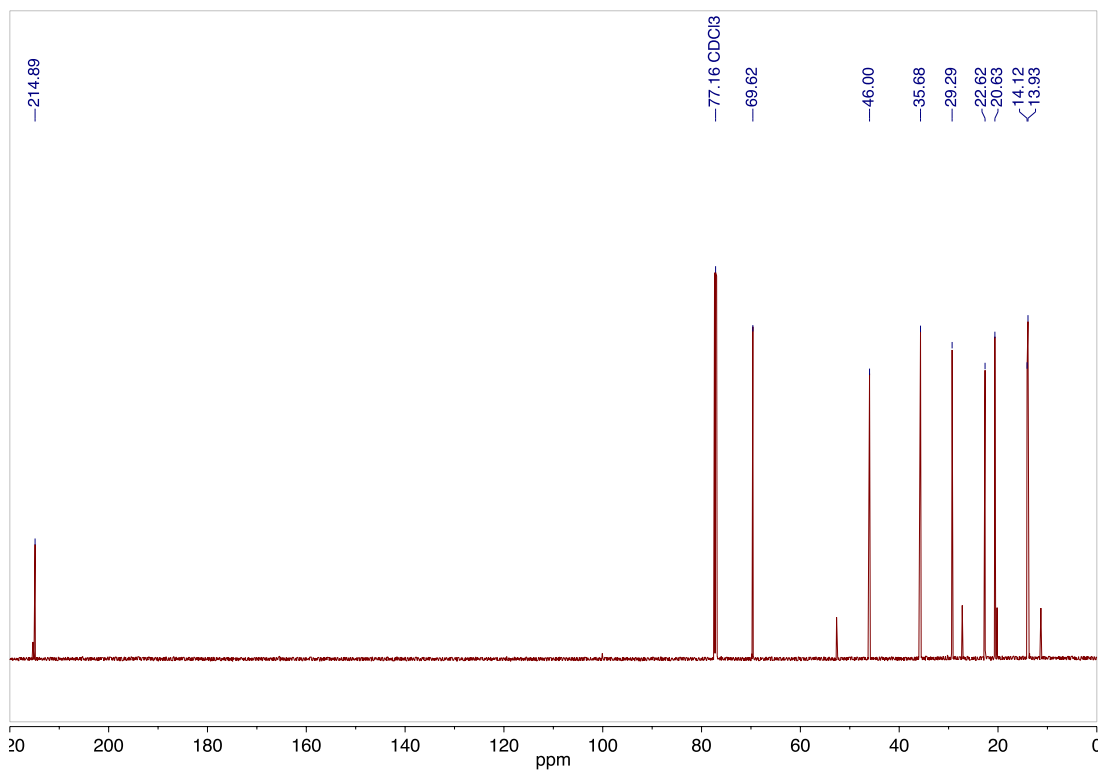
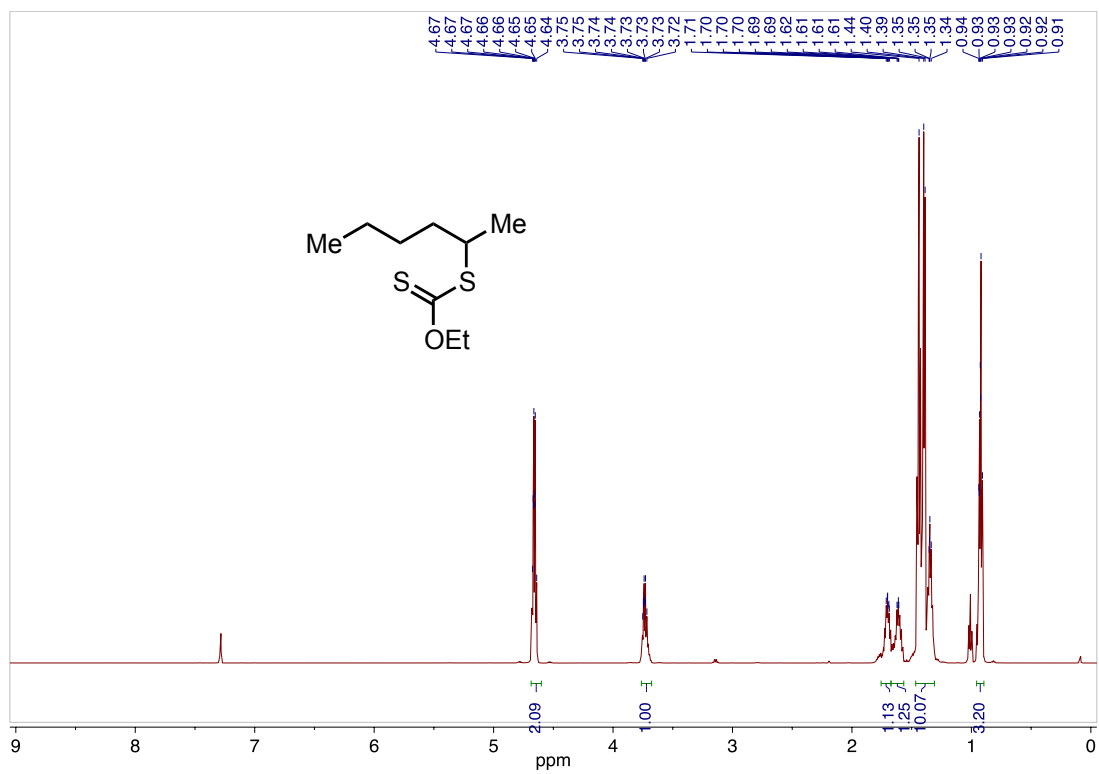
19. Shao, X.; Xu, C.; Lu, L.; Shen, Q. *J. Org. Chem.* **2015**, *80*, 3012.
20. Guo, S.; Zhang, X.; Tang, P. *Angew. Chem. Int. Ed.* **2015**, *54*, 4065.
21. Markey, L.; Giordani, S.; Scanlan, E. M. *J. Org. Chem.* **2013**, *78*, 4270.
22. Quiclet-Sire, B.; Seguin, S.; Zard, S. Z. *Angew. Chem. Int. Ed.* **1998**, *37*, 2864.
23. Ollivier, C.; Renaud, P. *J. Am. Chem. Soc.* **2000**, *122*, 6496.
24. Huang, X.; Bergsten, T. M.; Groves, J. T. *J. Am. Chem. Soc.* **2015**, *137*, 5300.
25. Gormisky, P. E.; White, M. C. *J. Am. Chem. Soc.* **2013**, *135*, 14052.

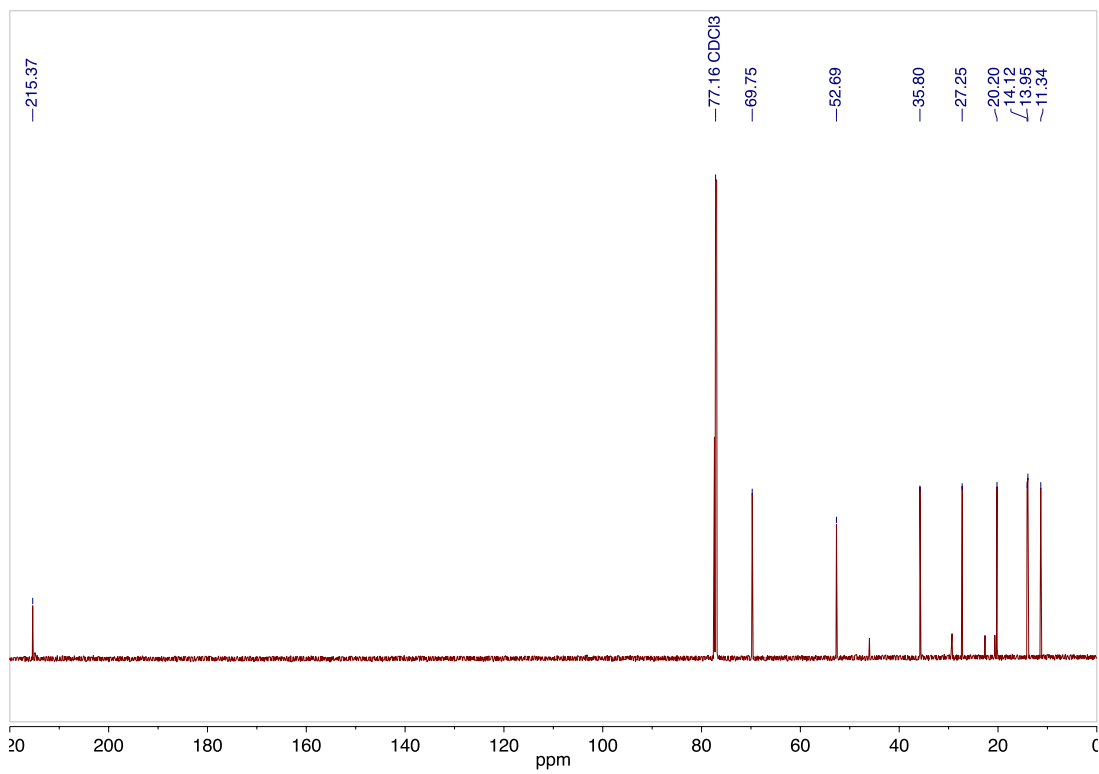
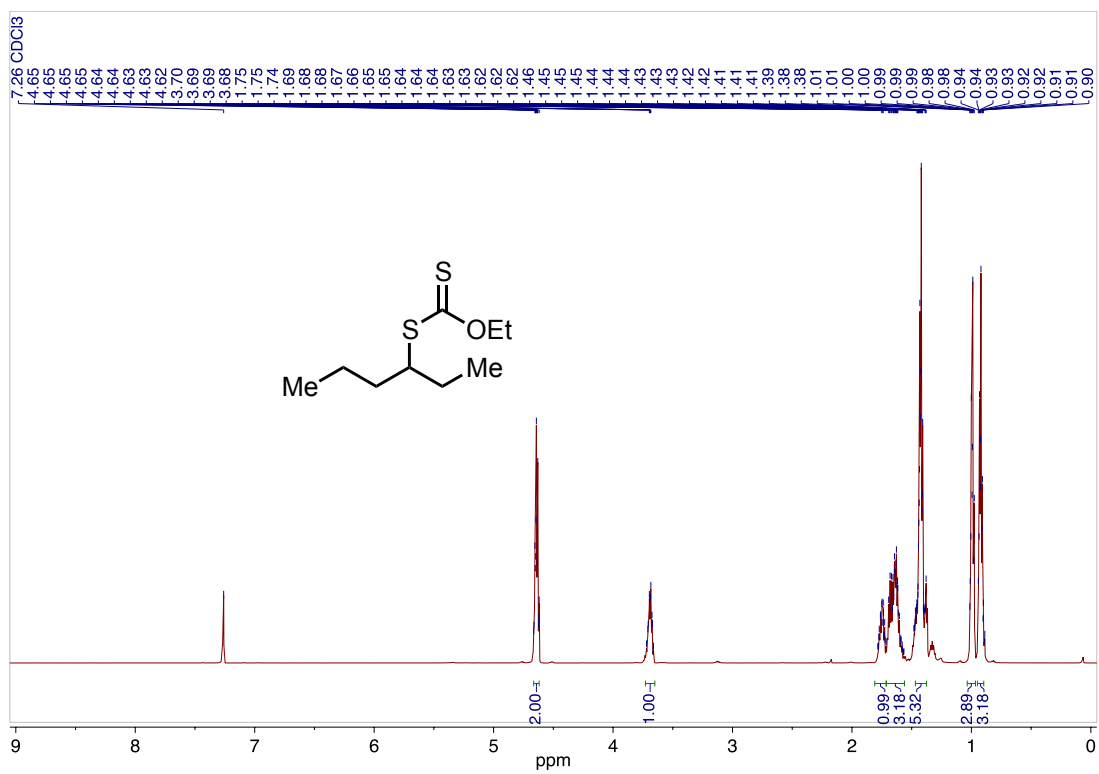




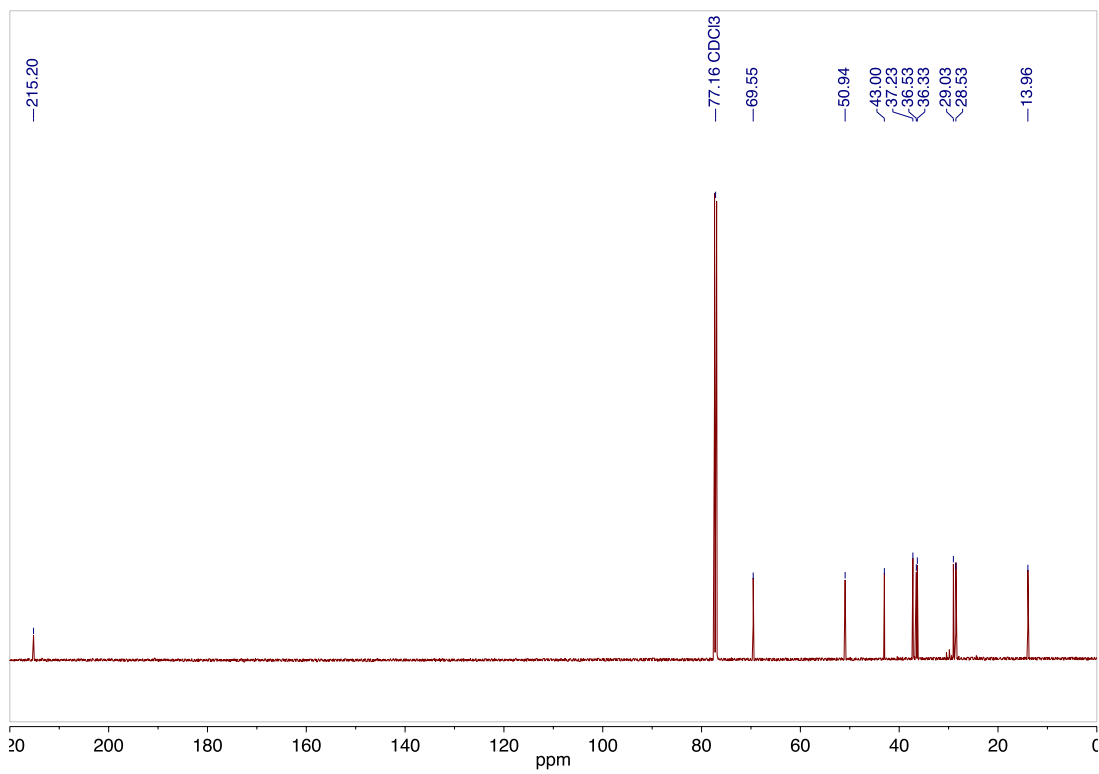
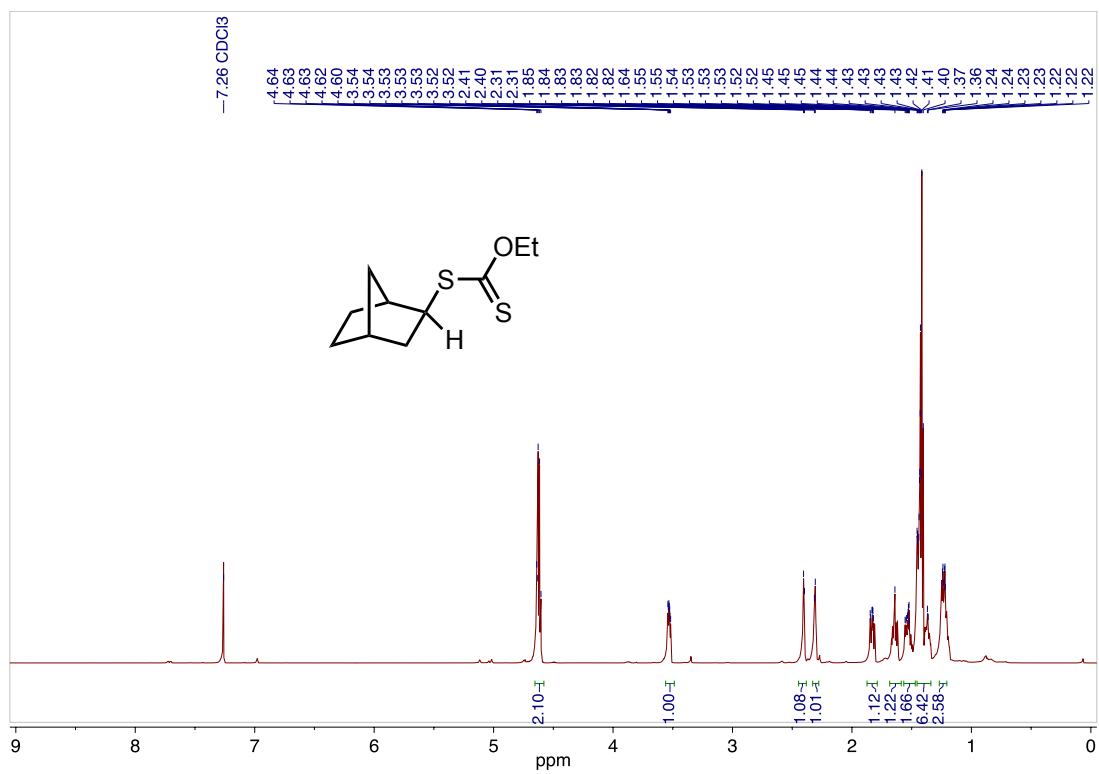


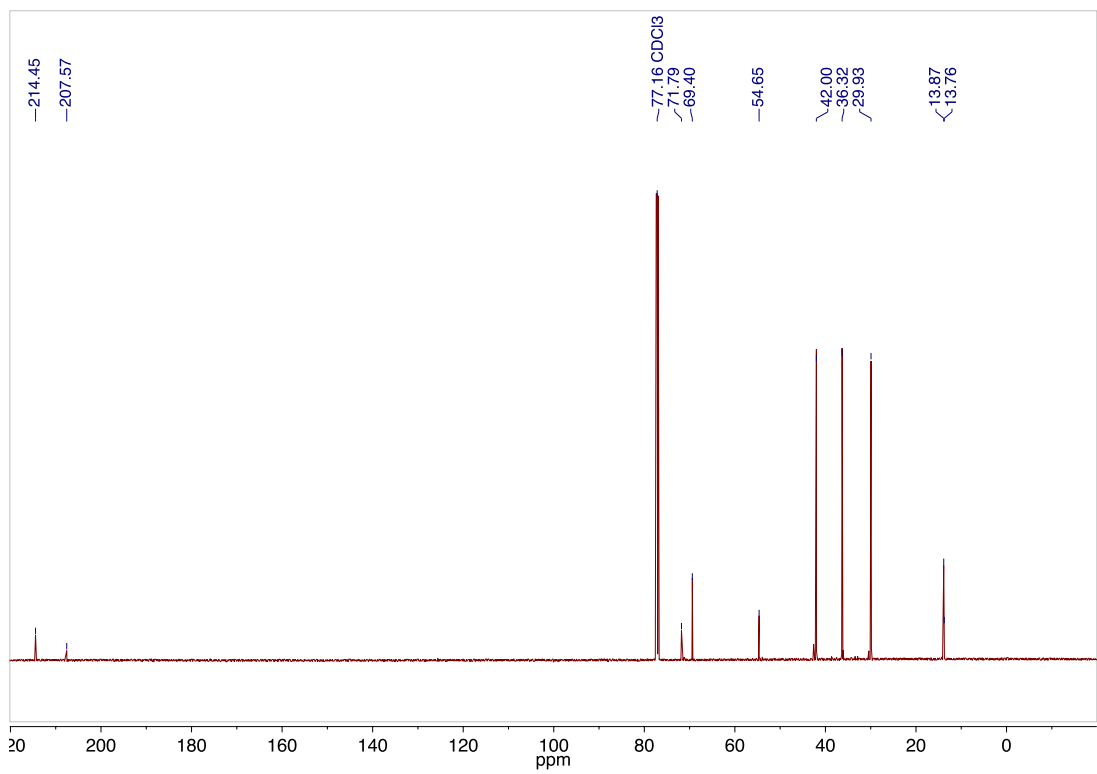
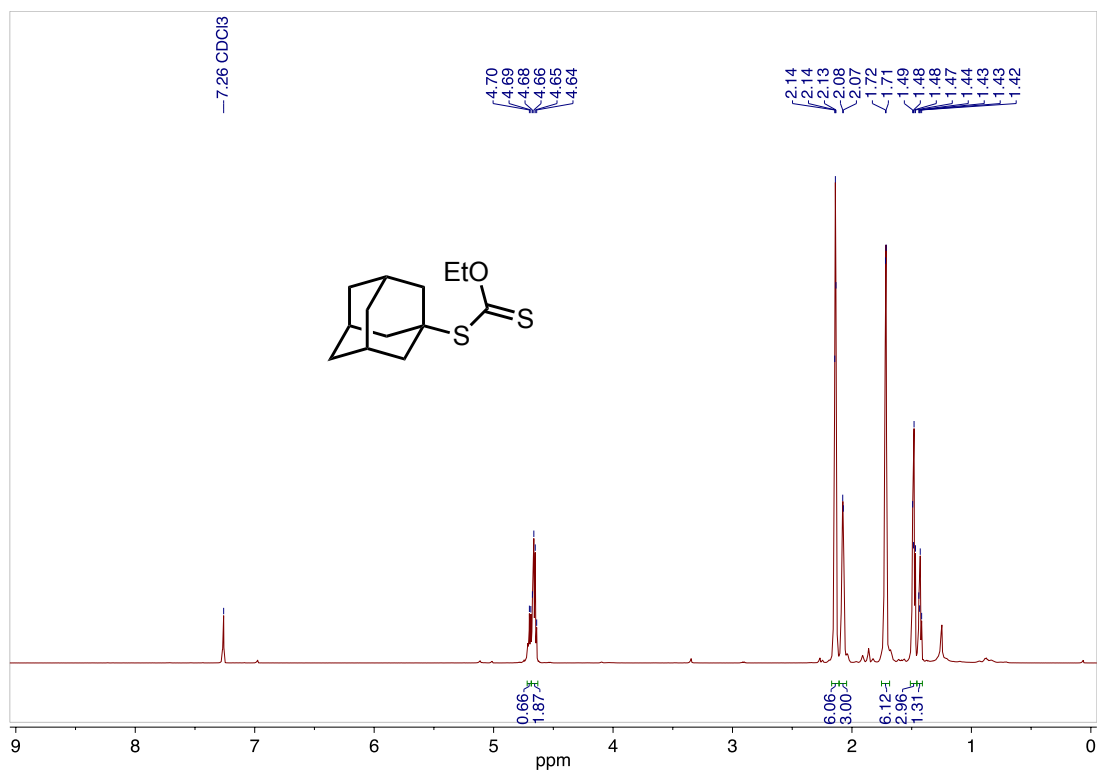


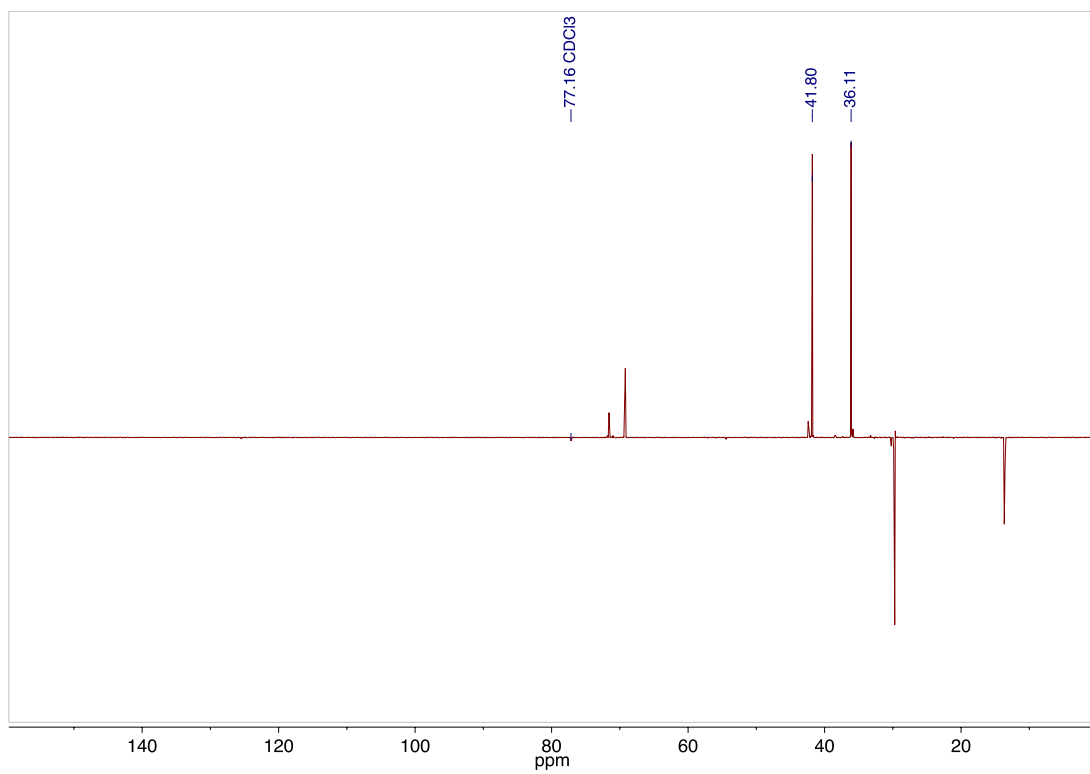


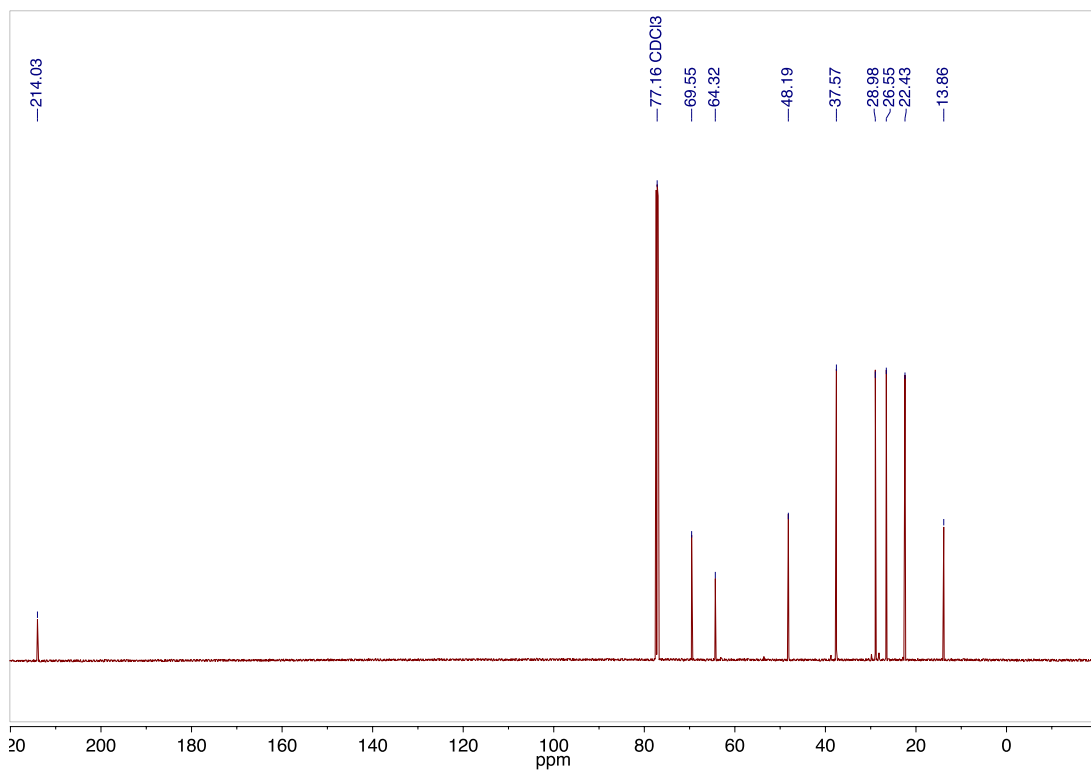
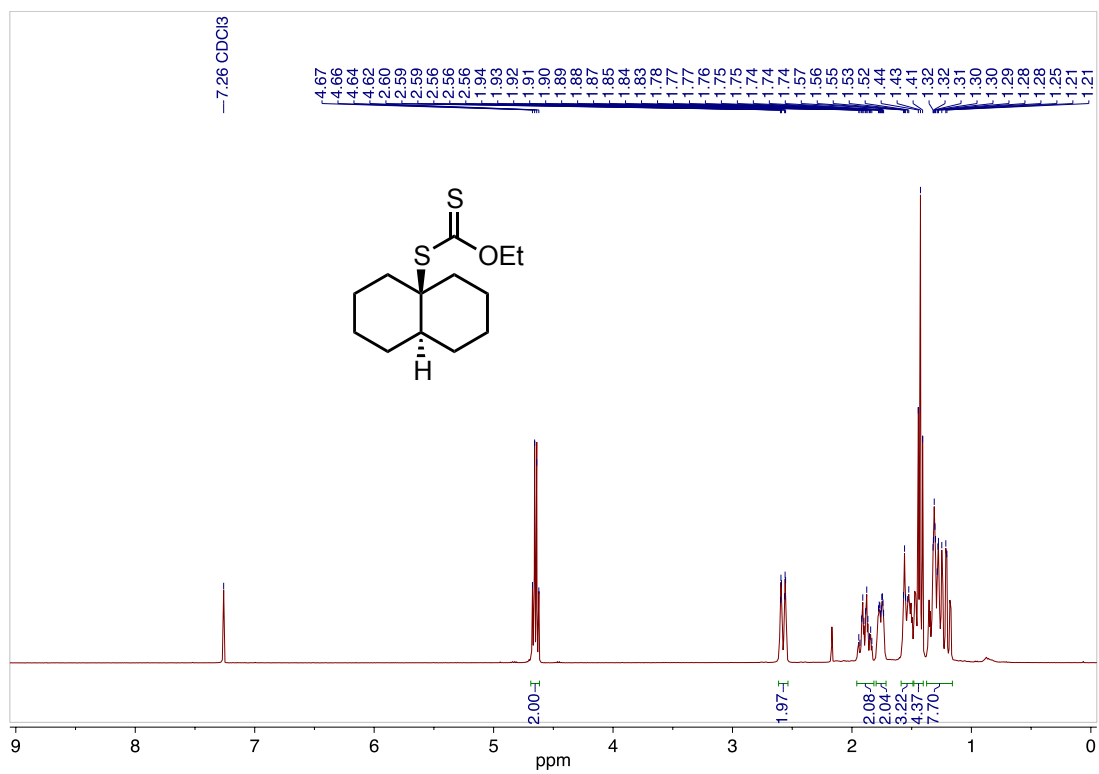


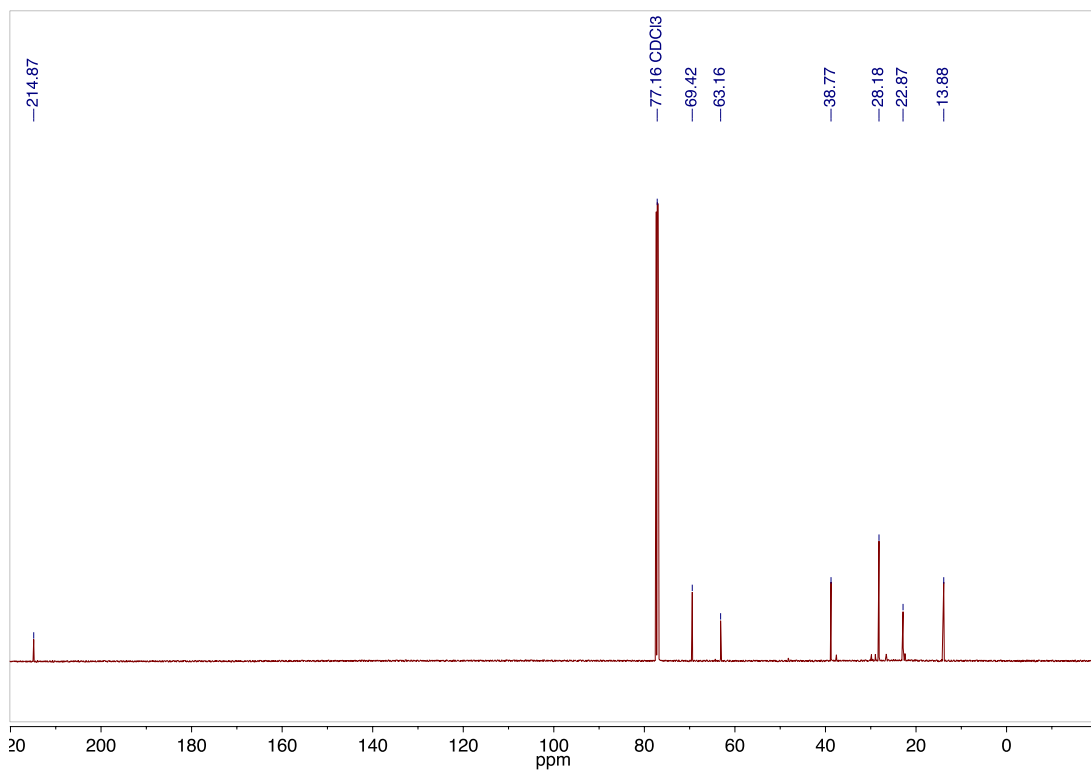
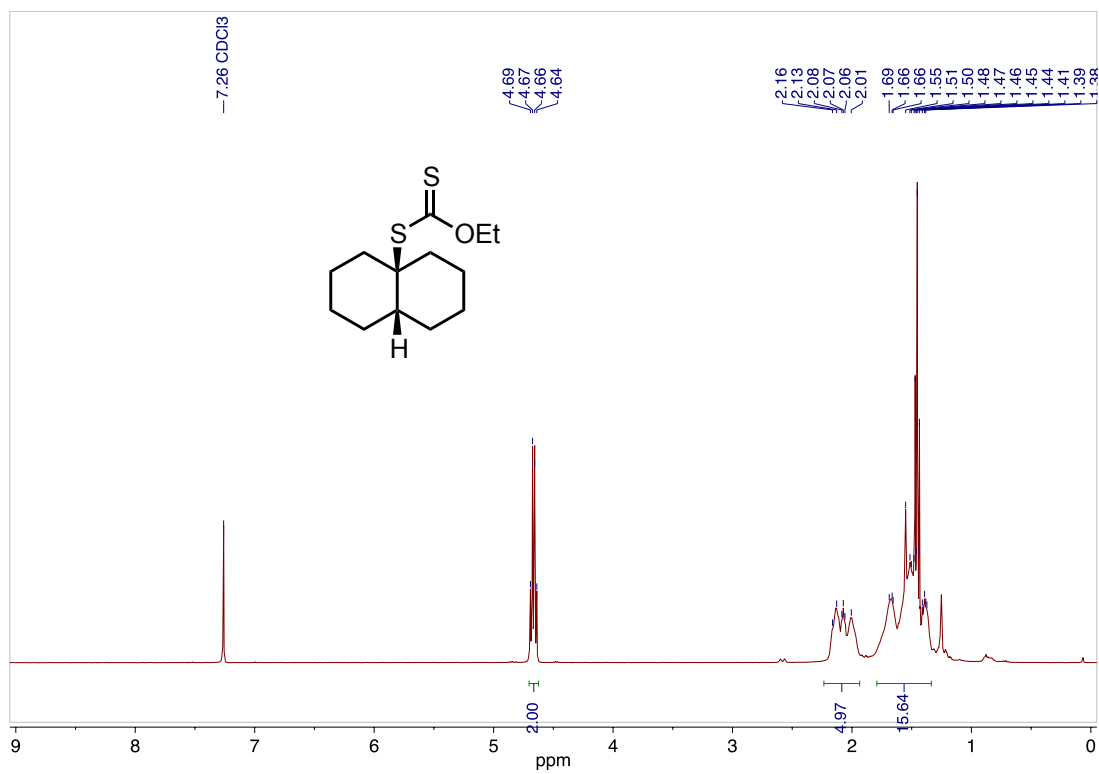


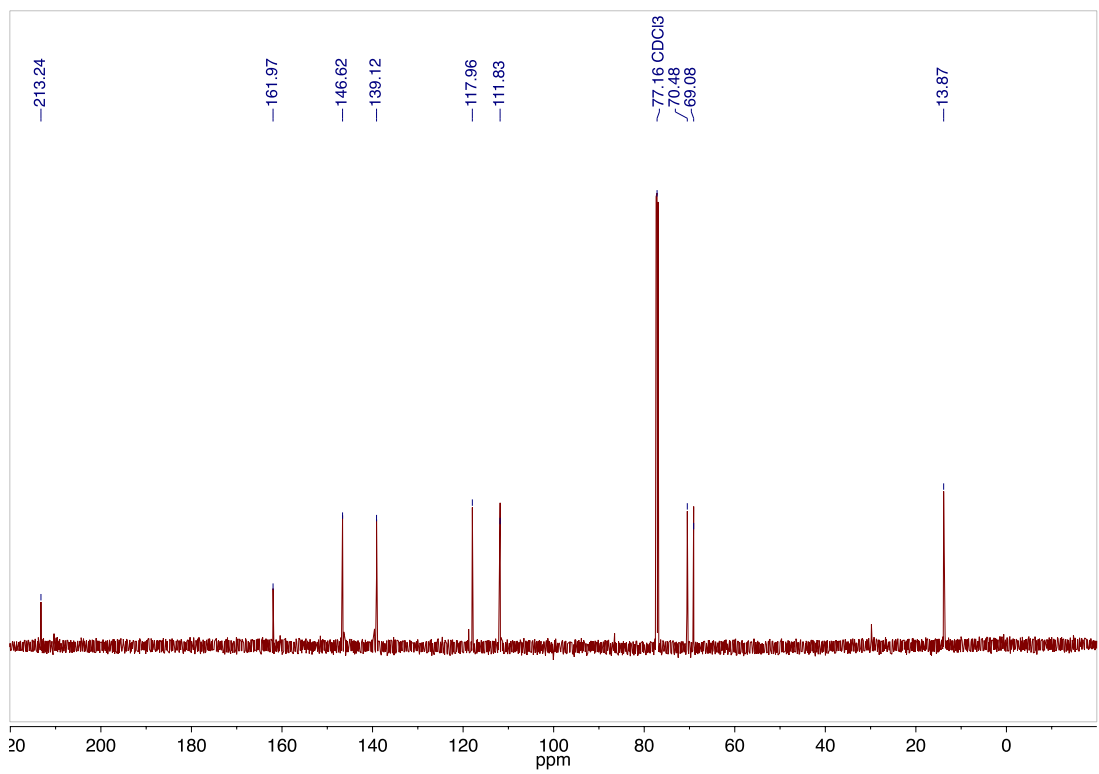
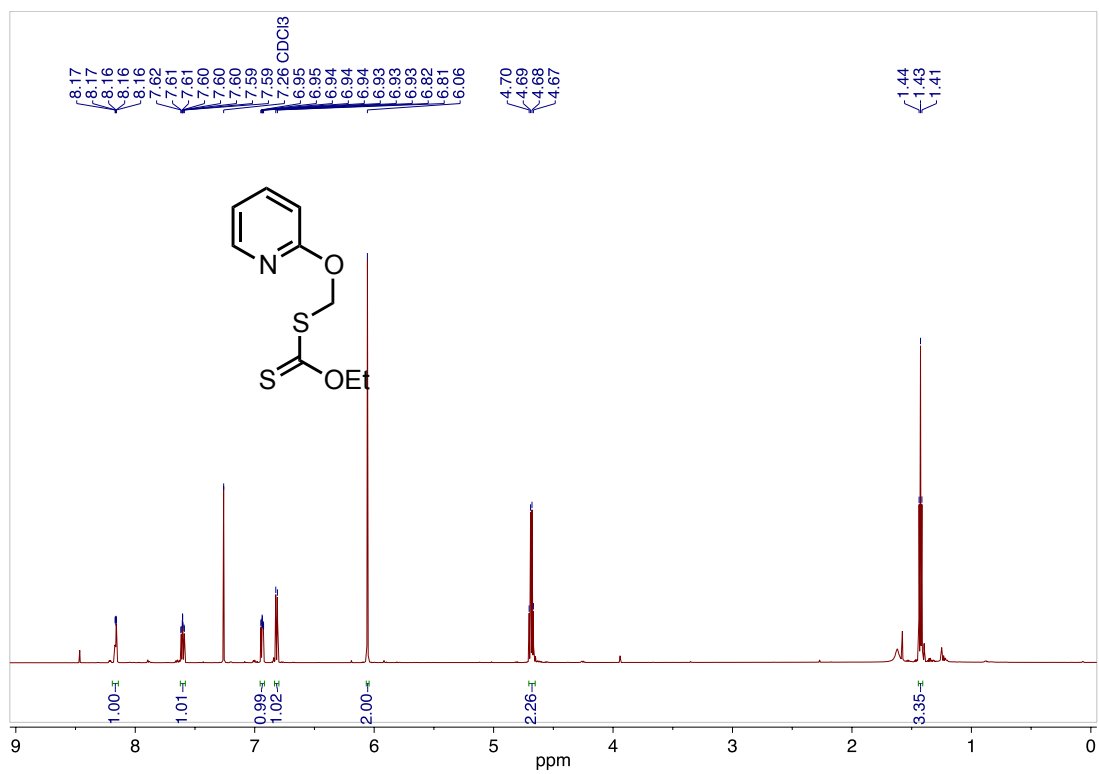


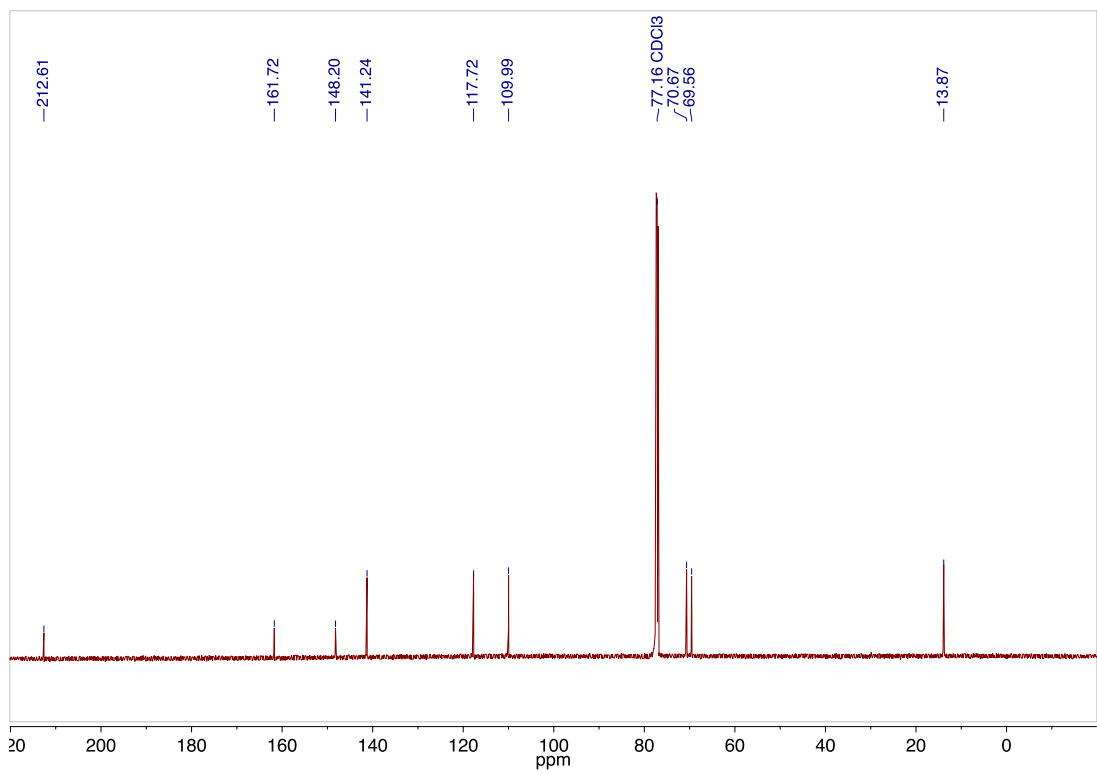
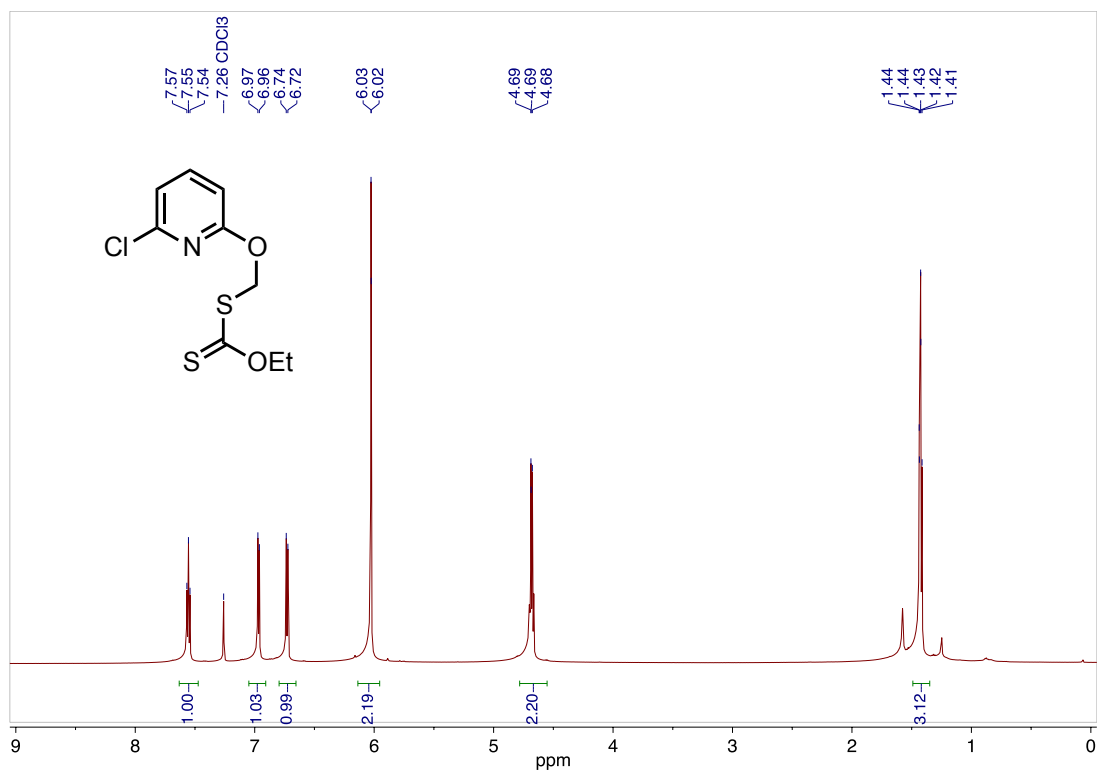




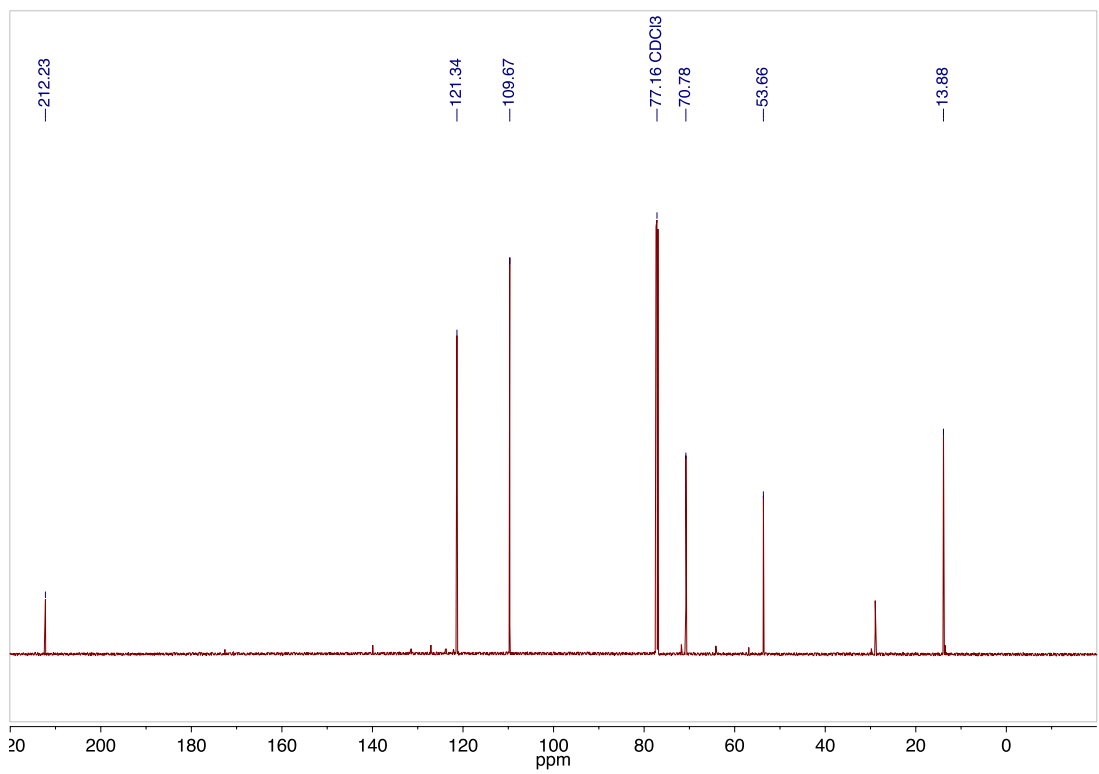
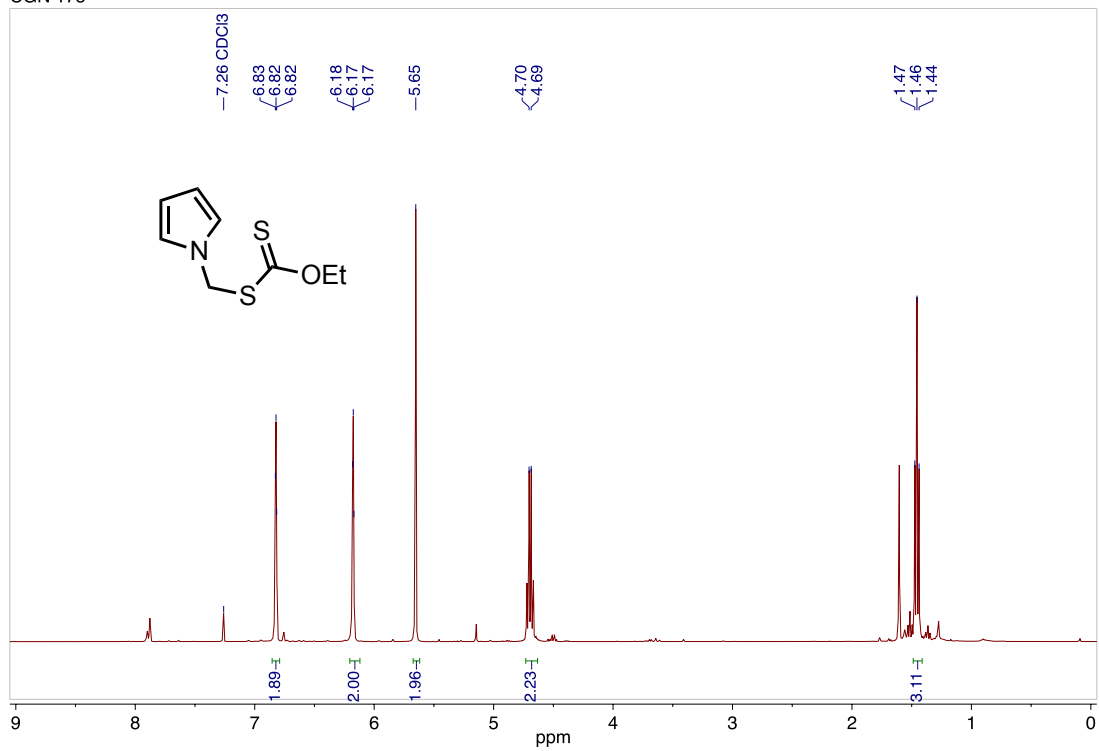




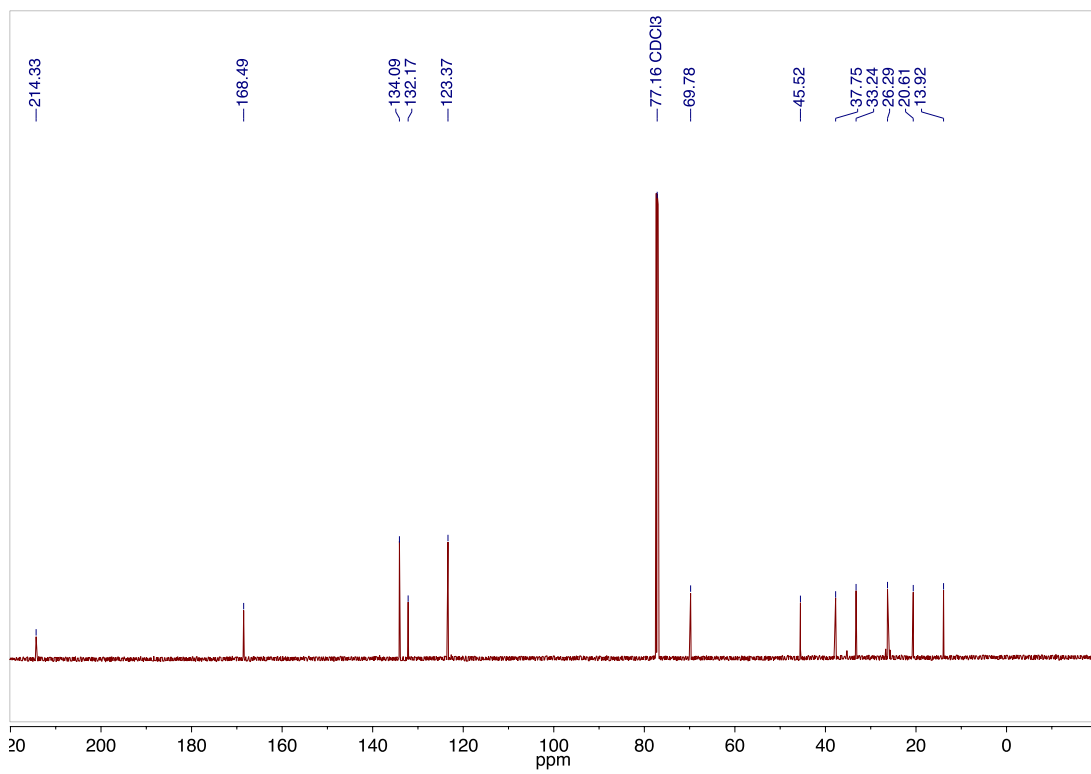
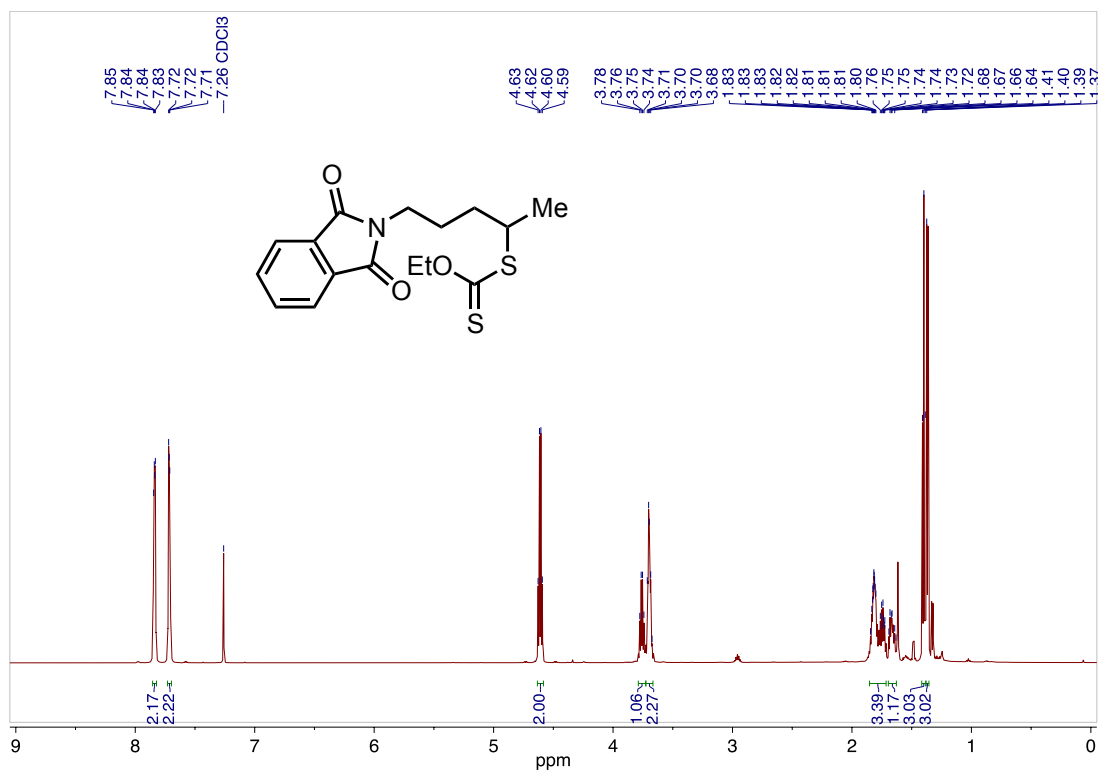


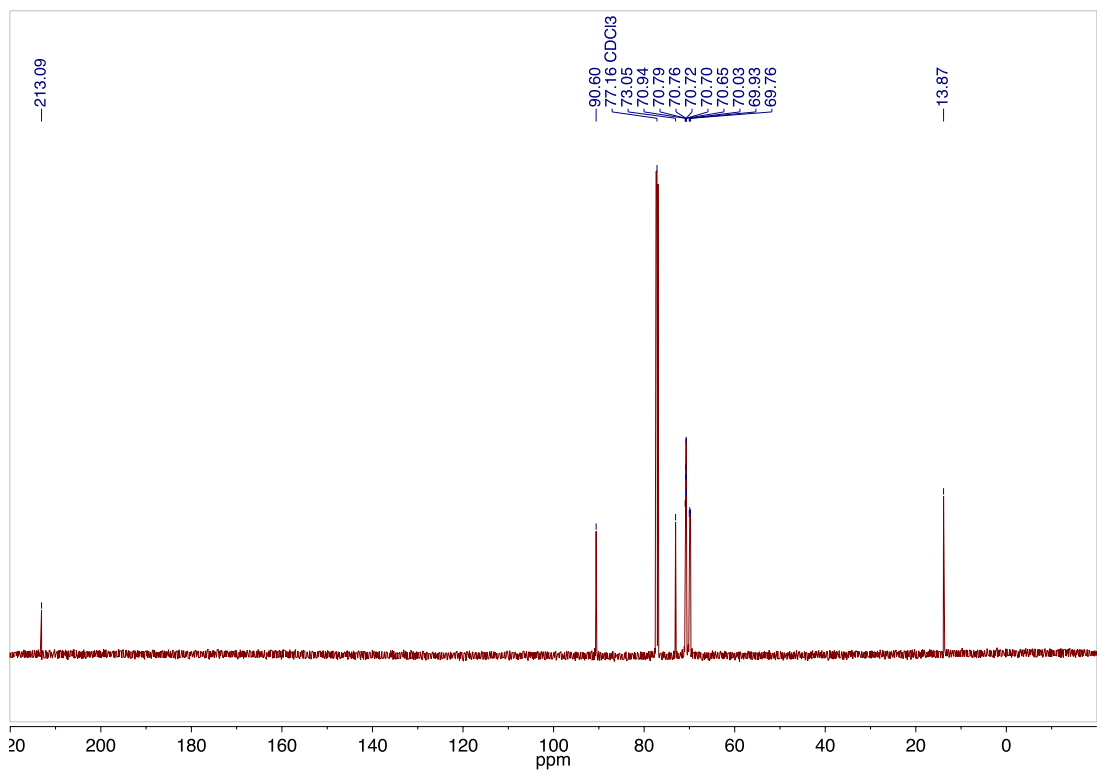
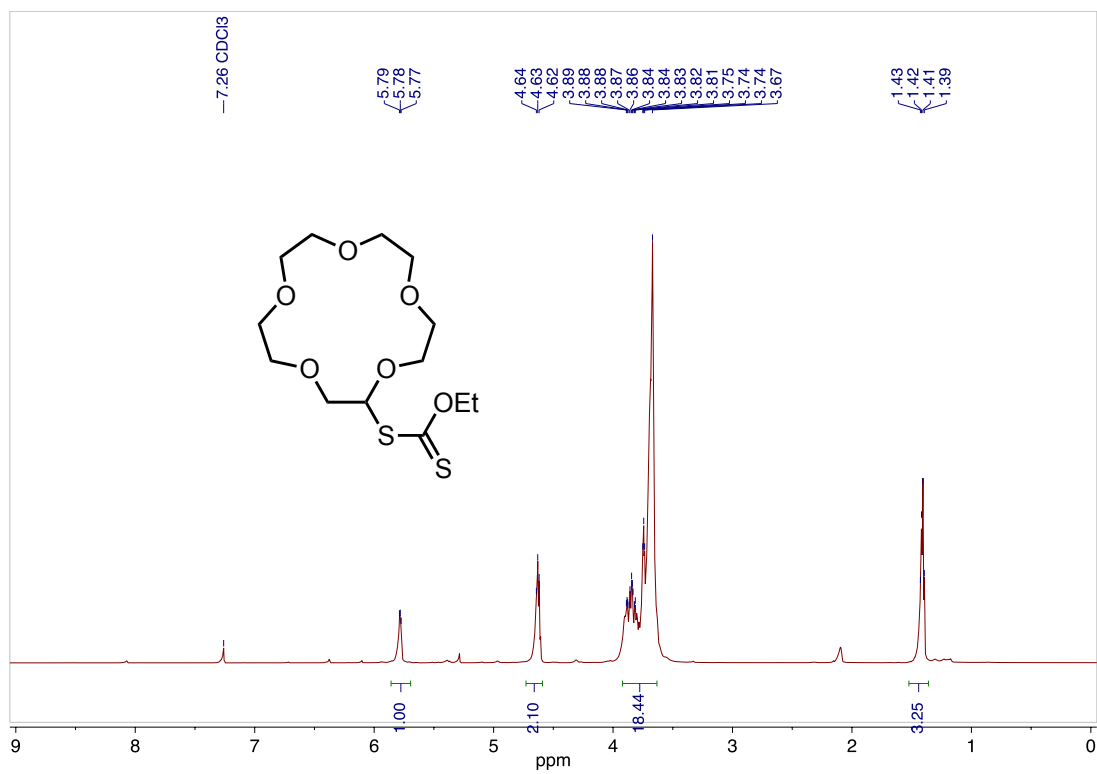


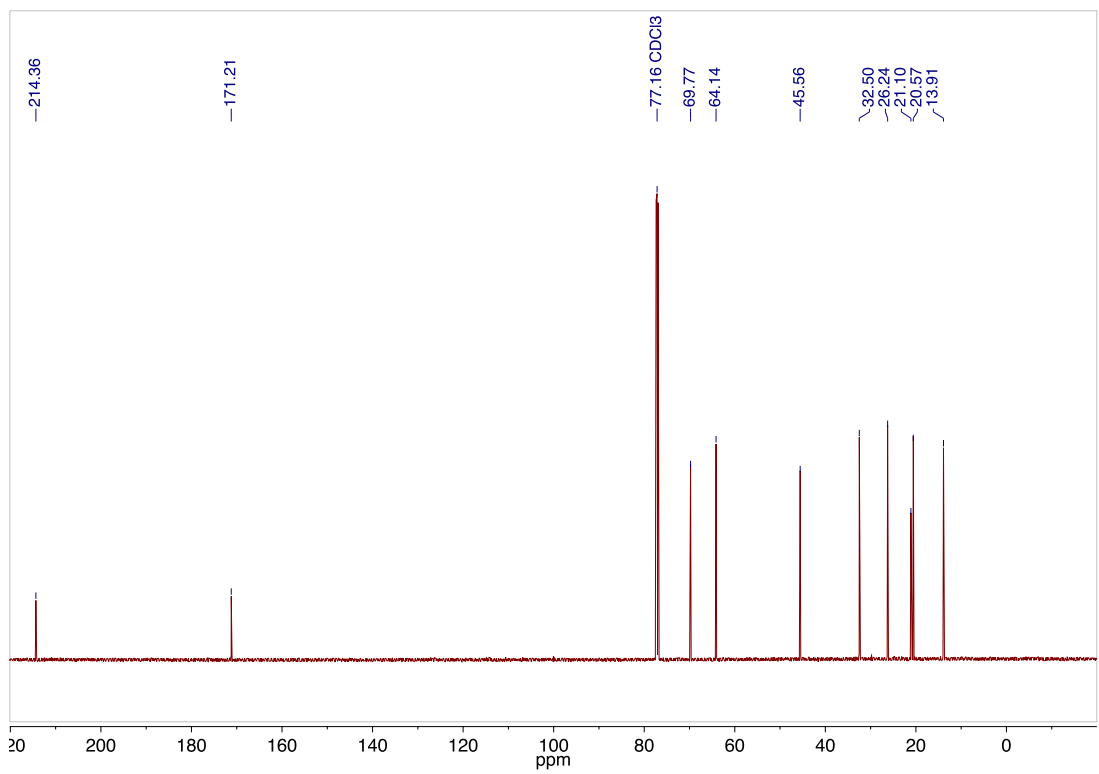
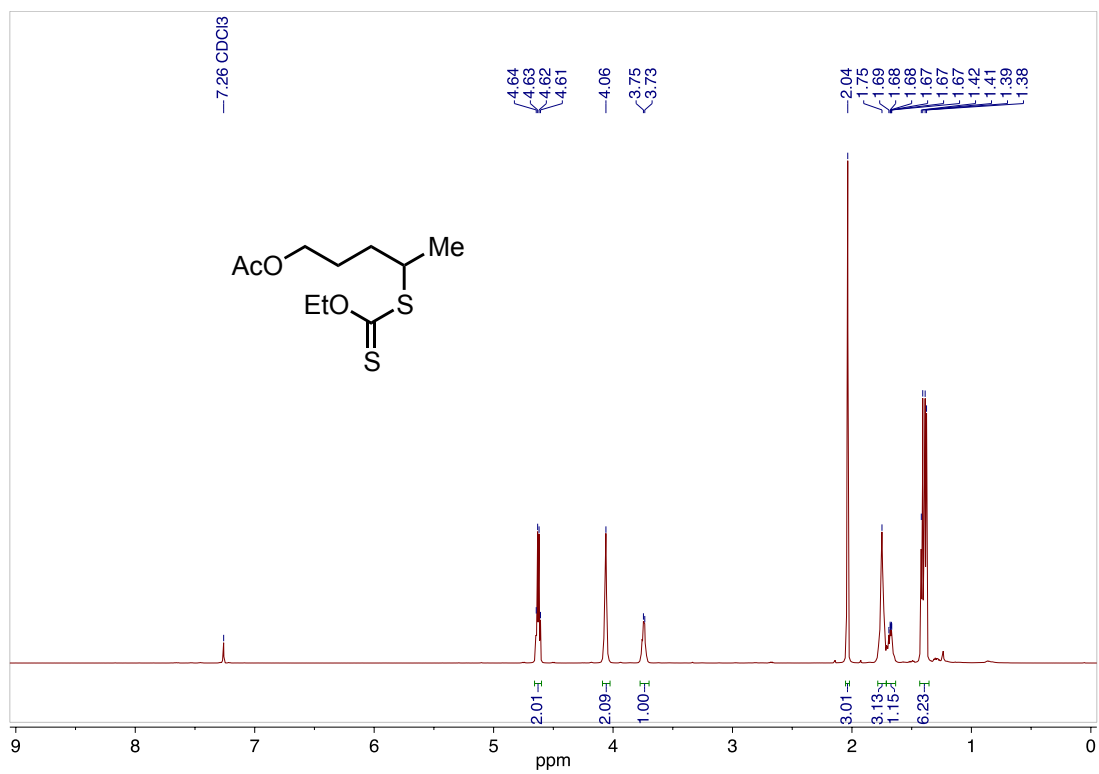
CGN 175

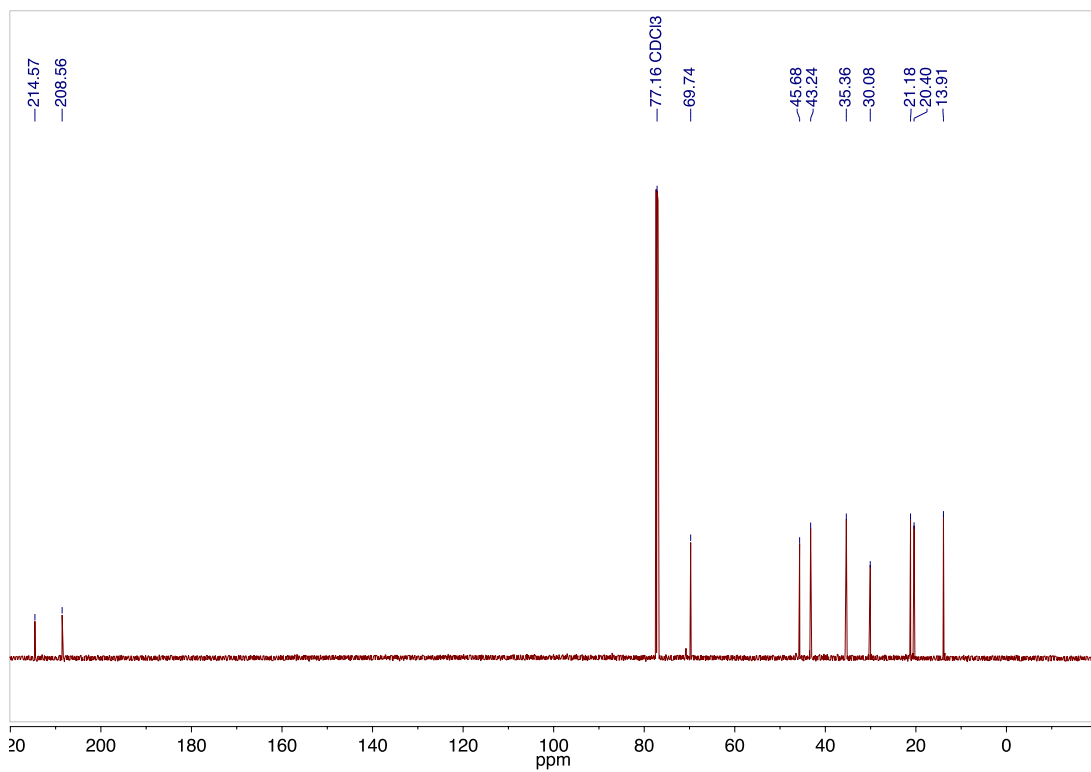
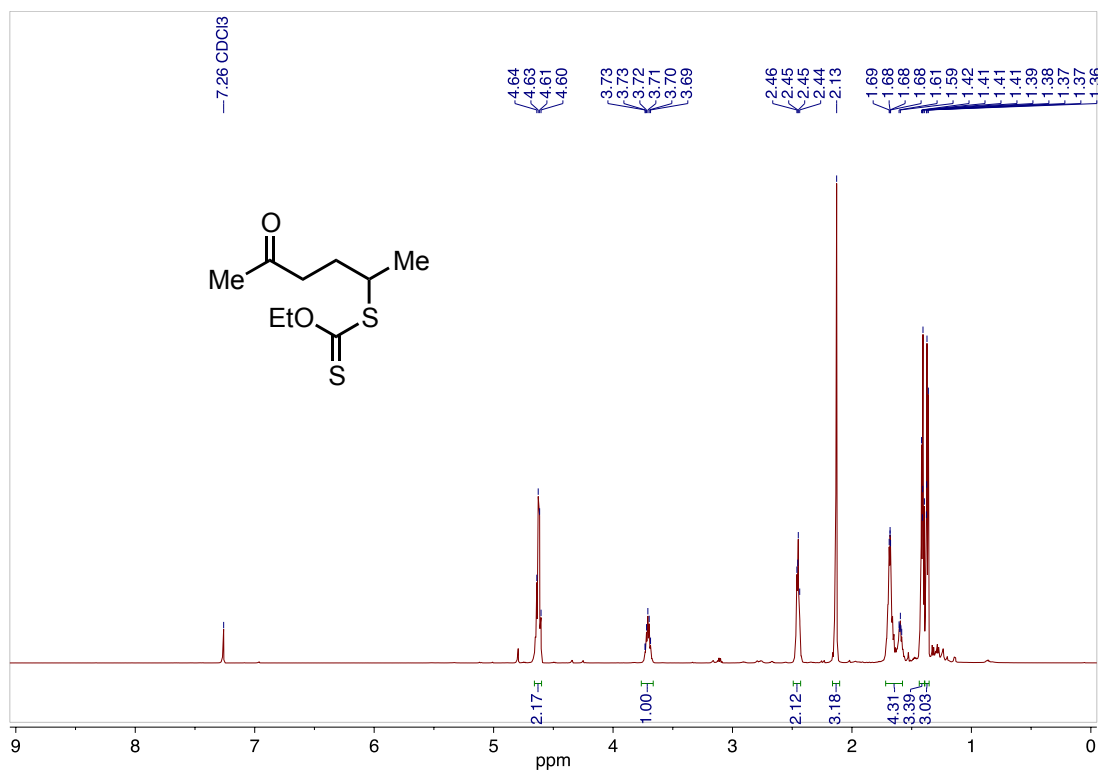


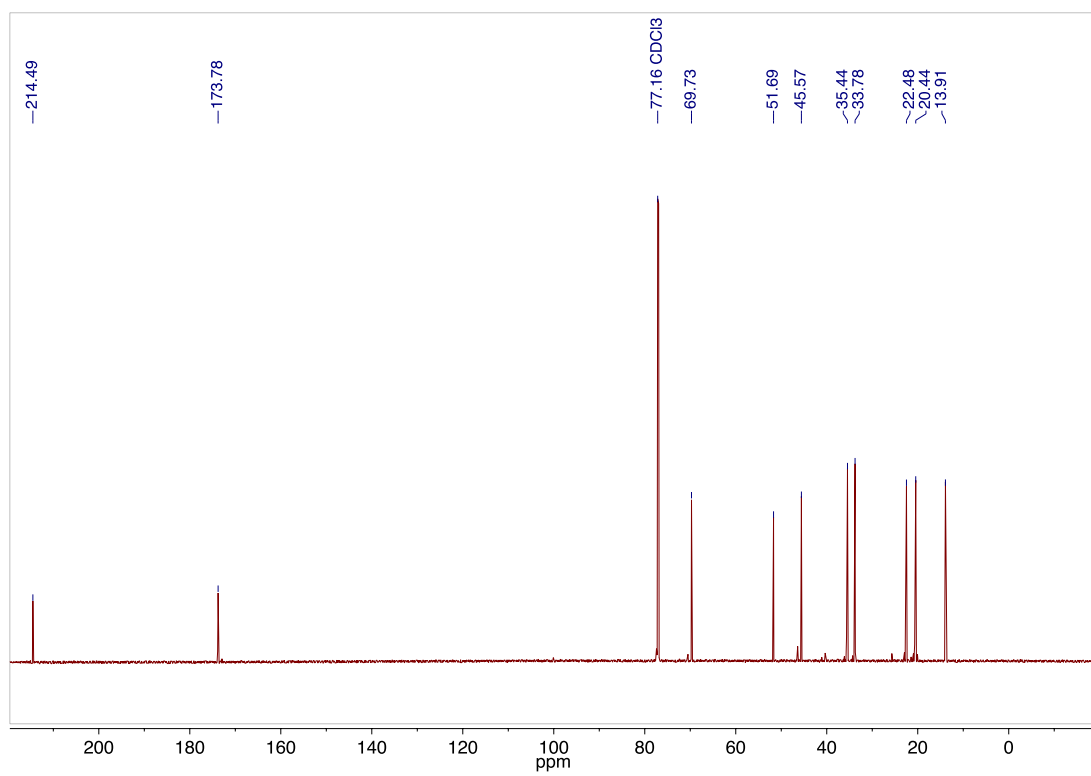
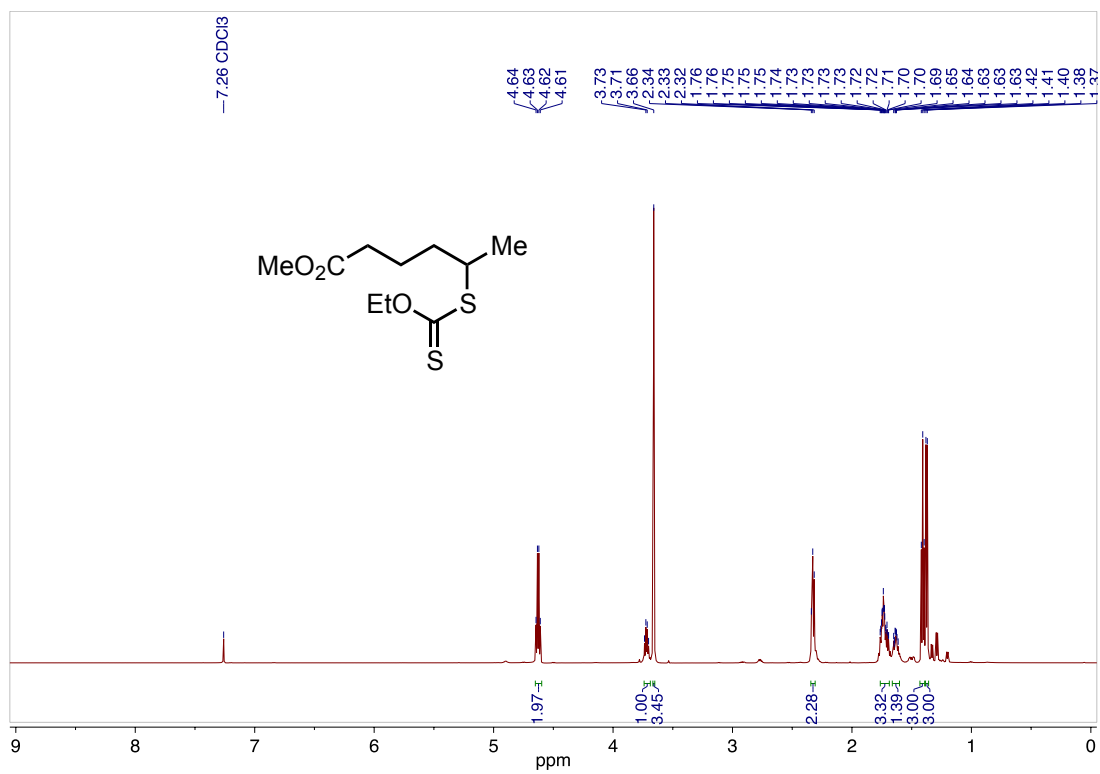


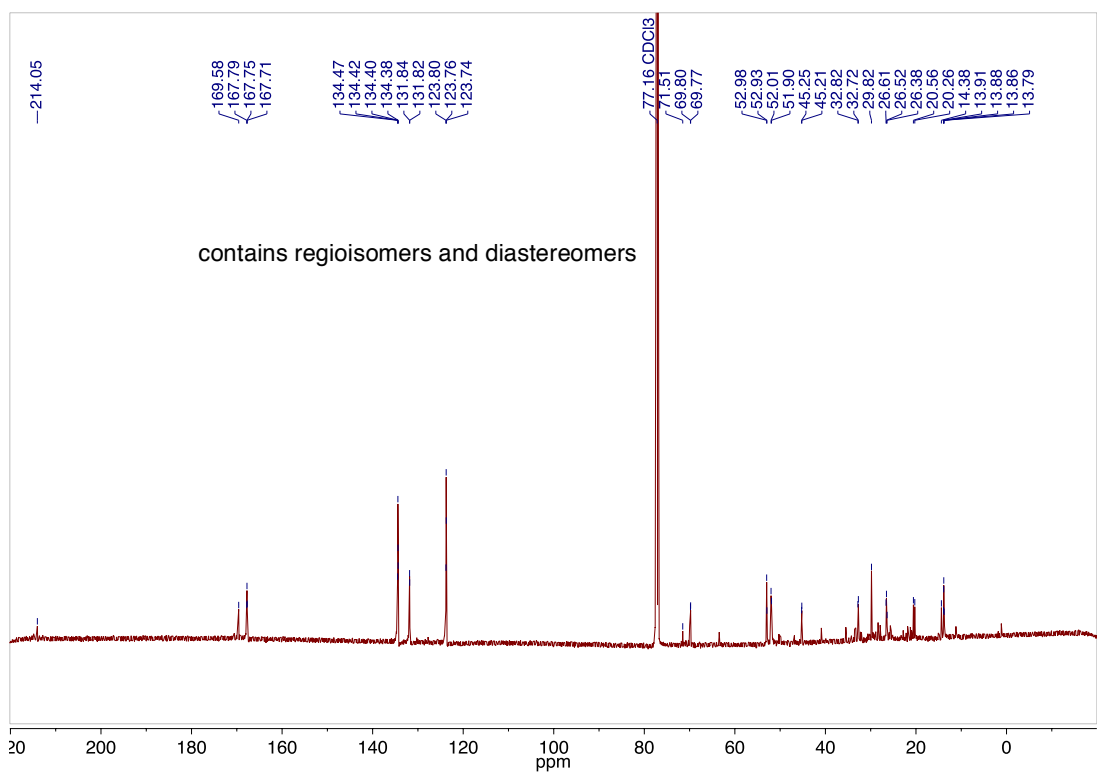
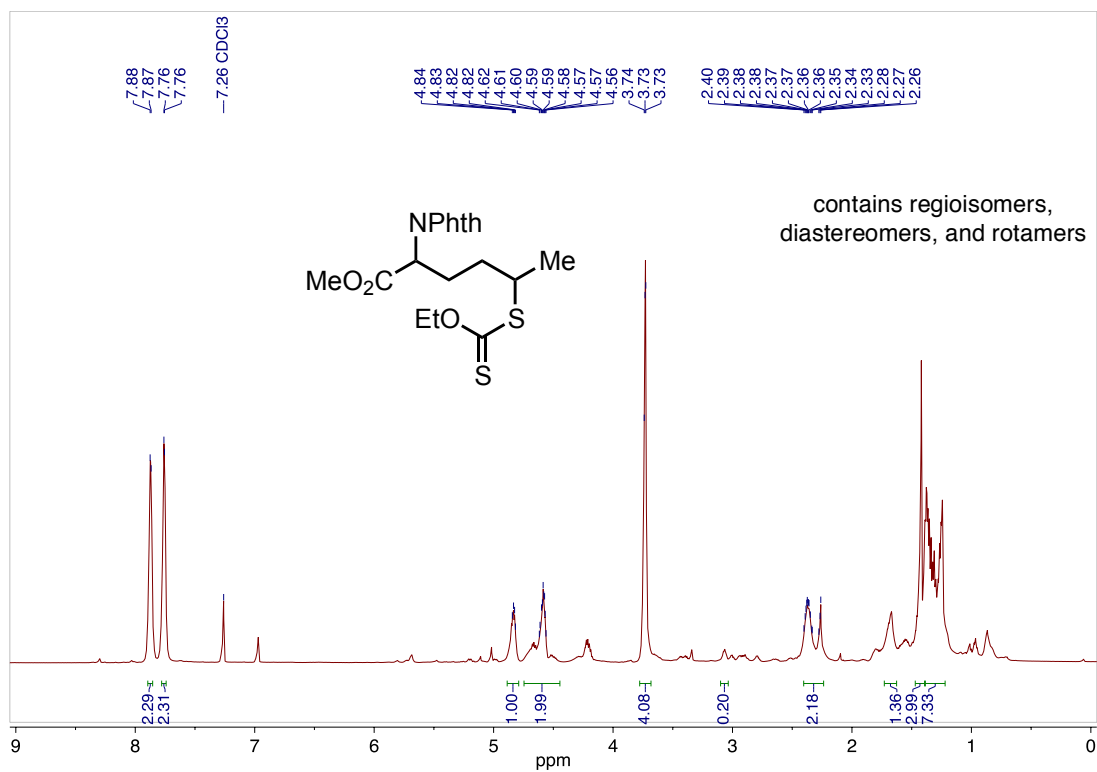


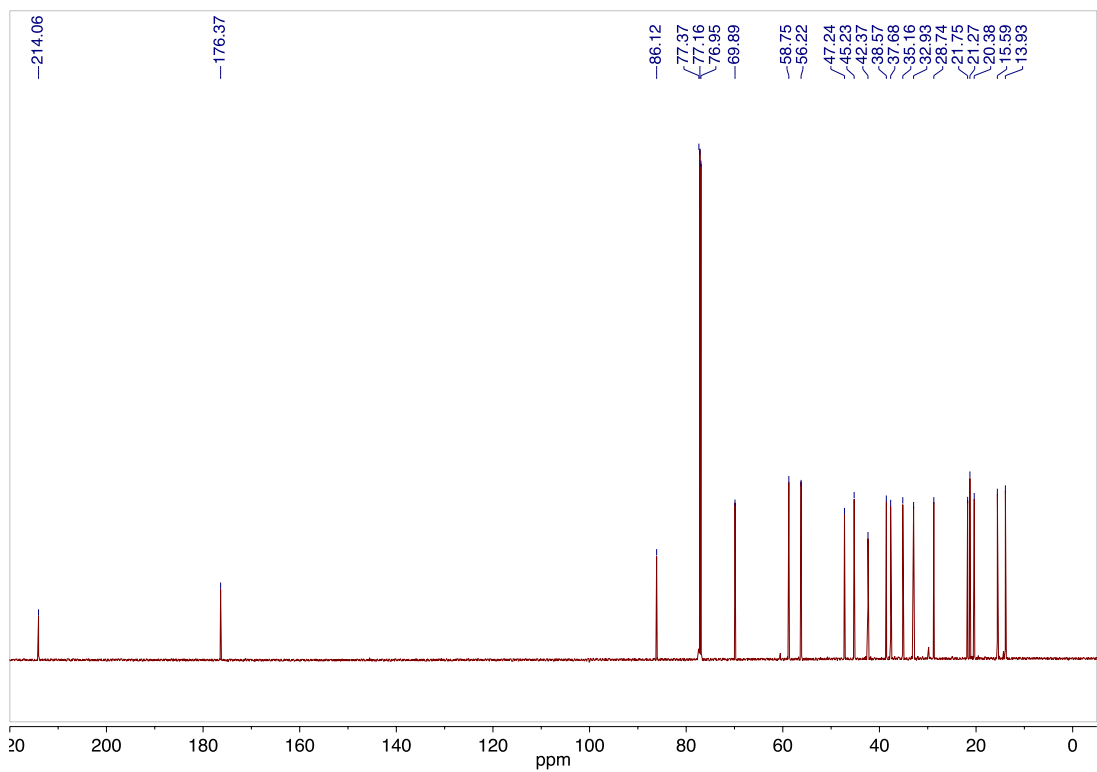
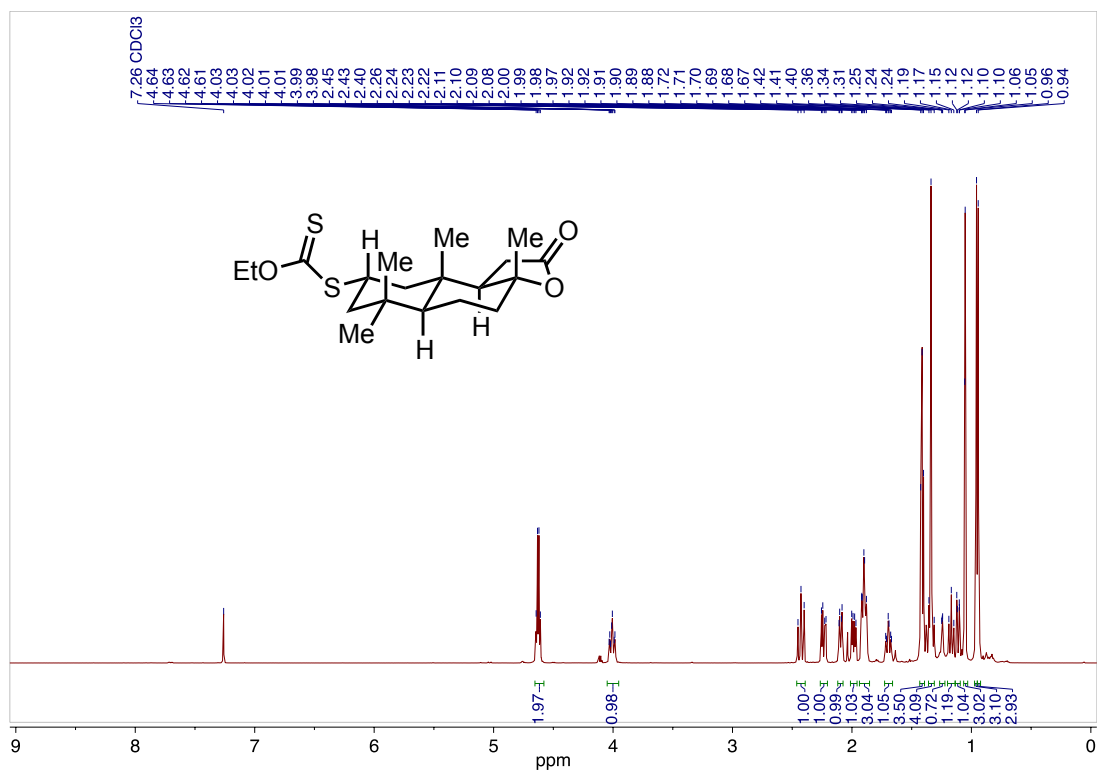




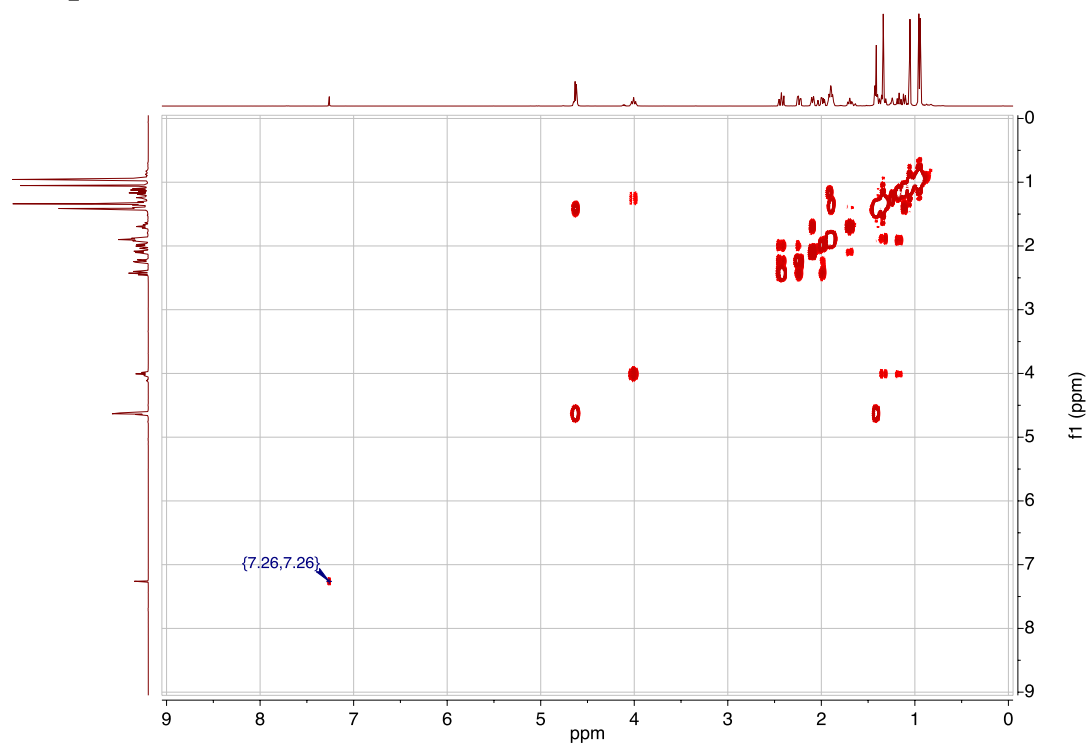




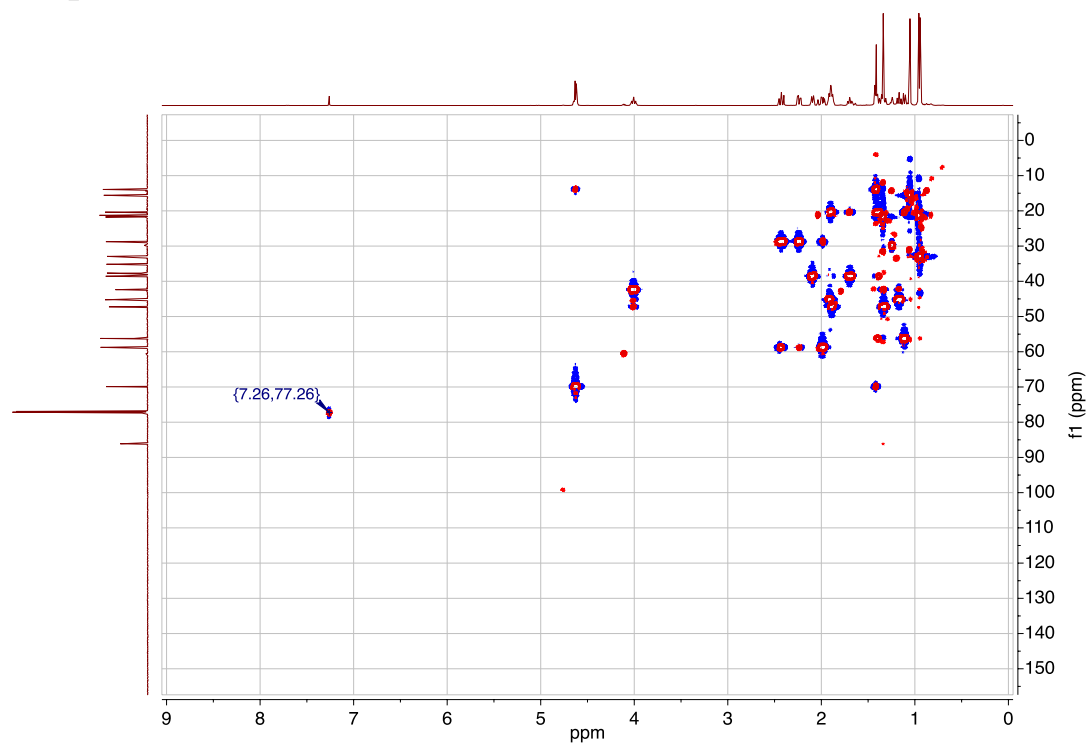




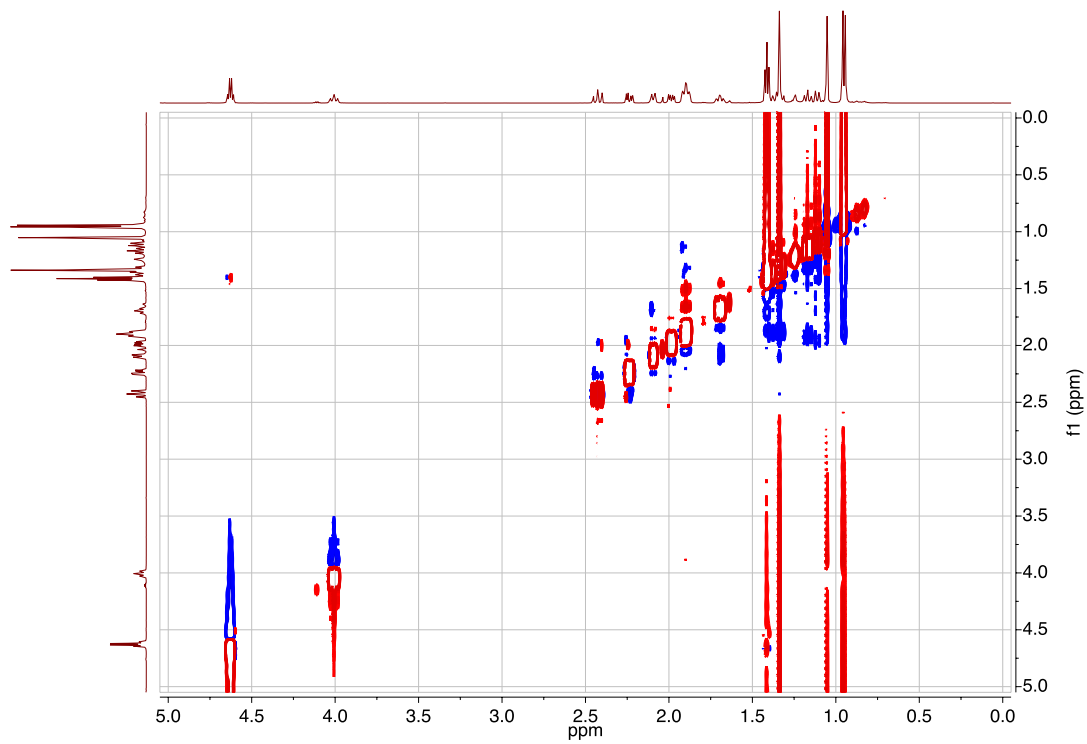
wlciv109\_36-54COSY

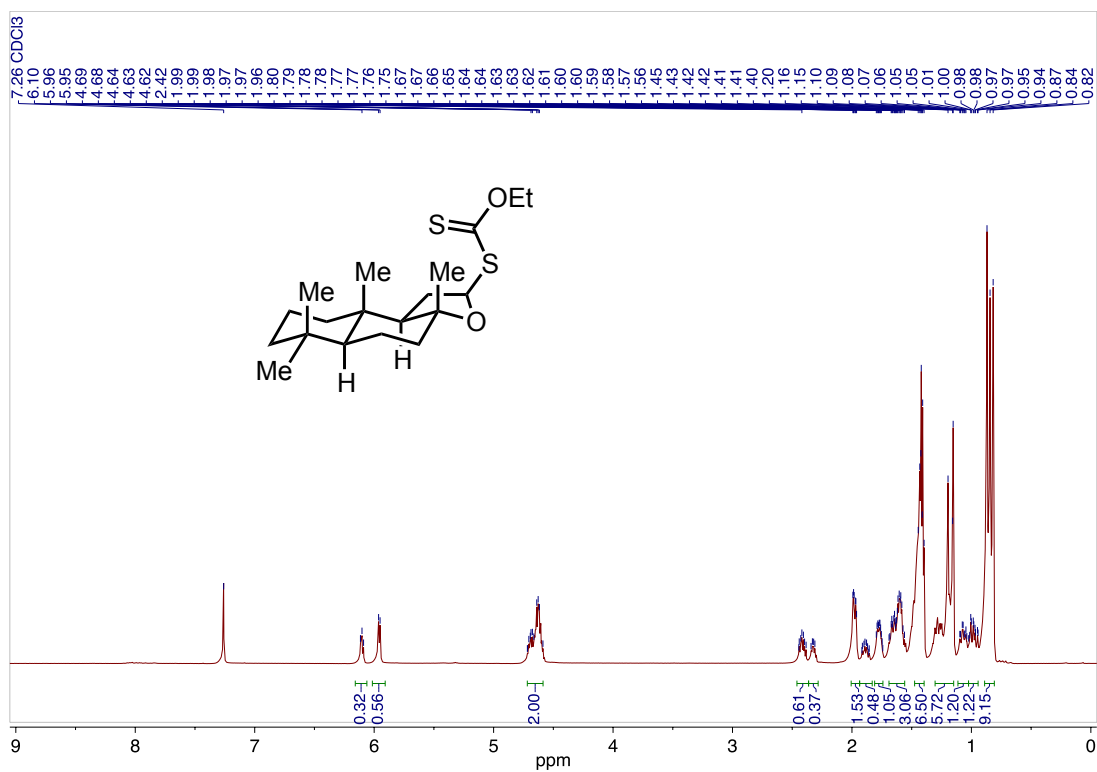


wlciv109\_36-54HSQC

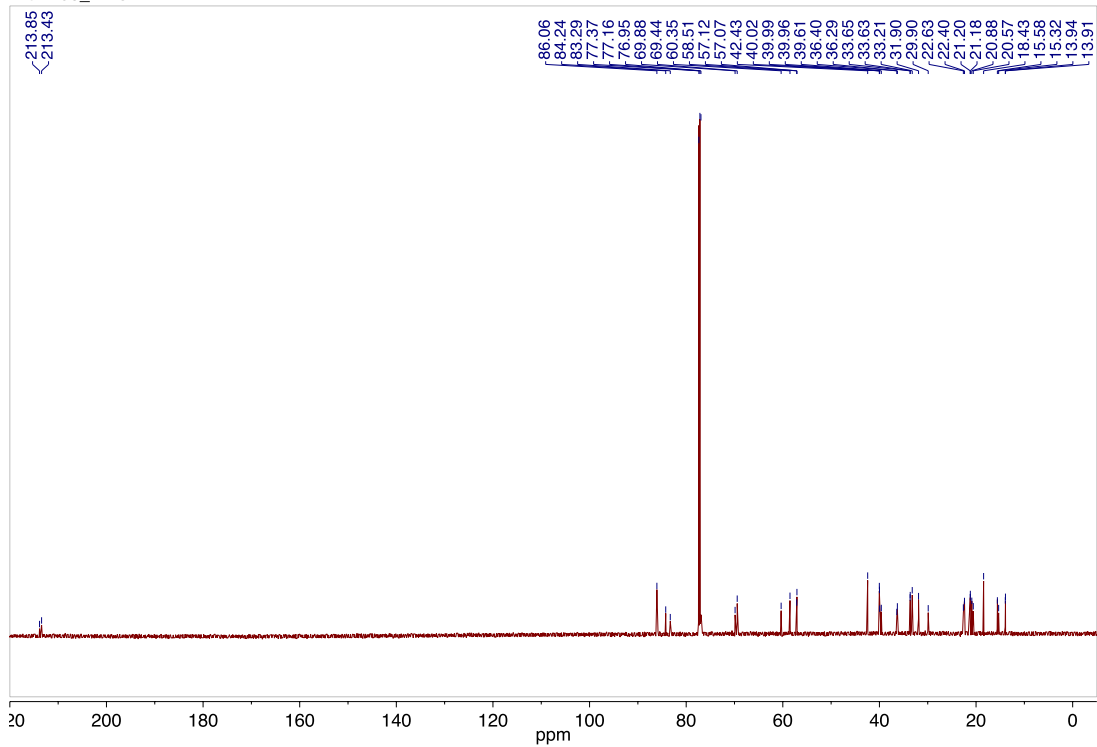


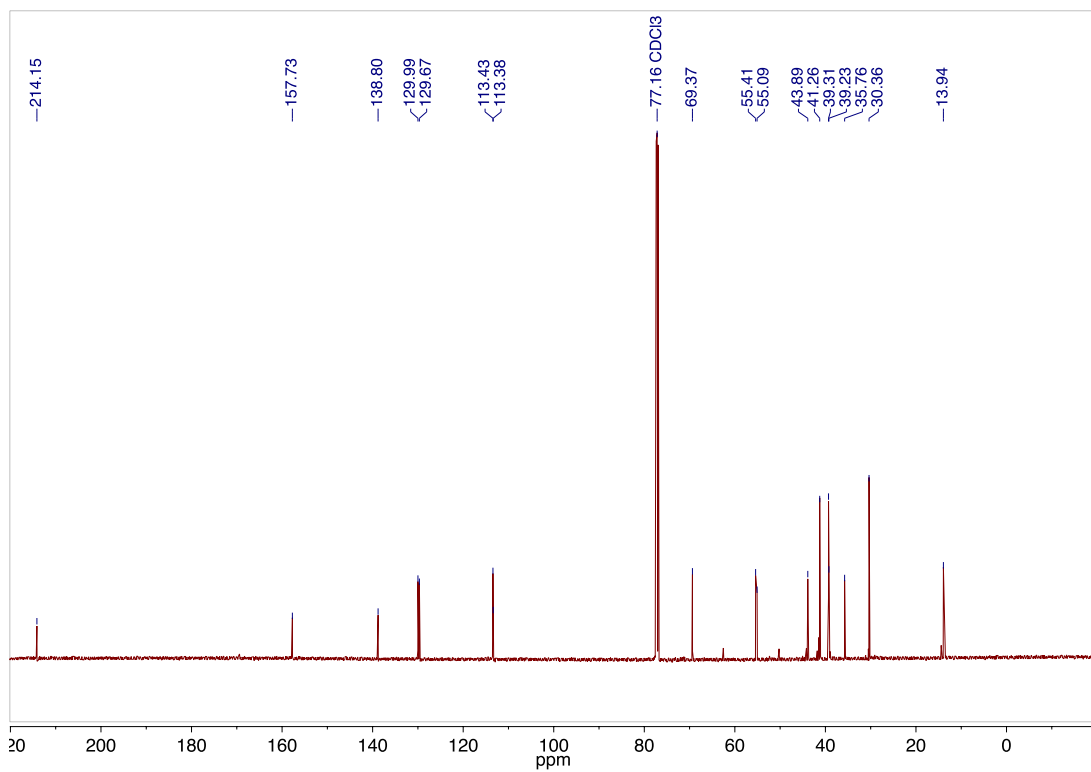
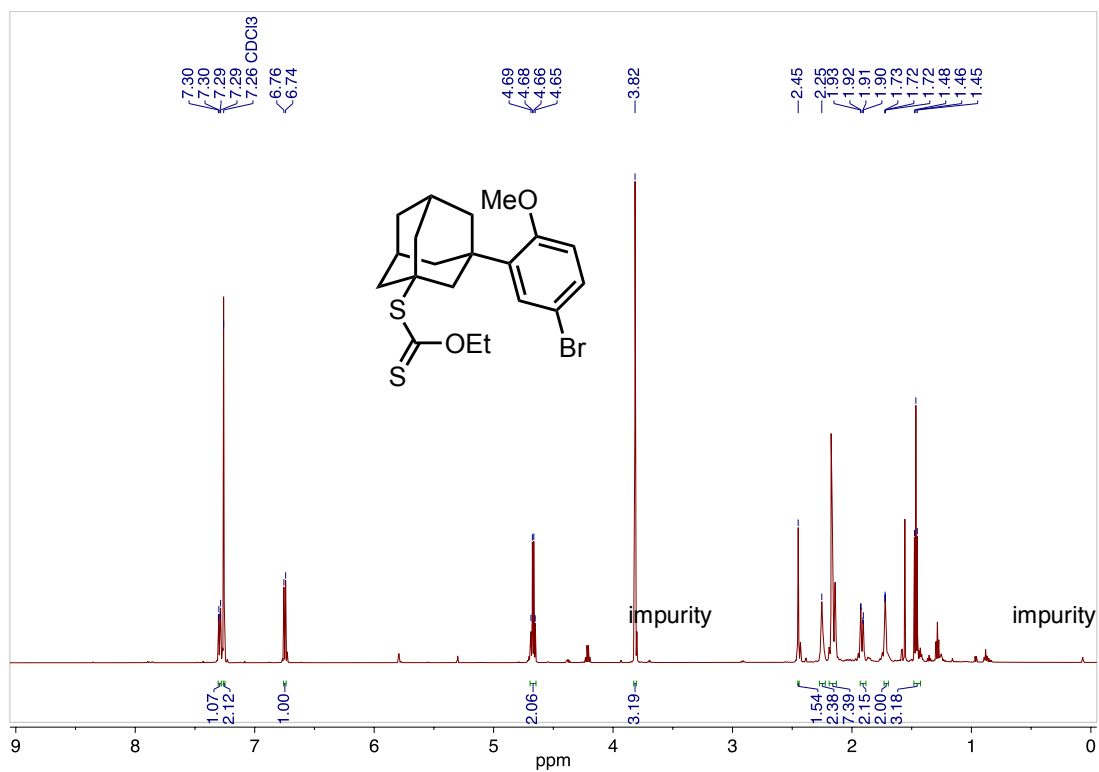




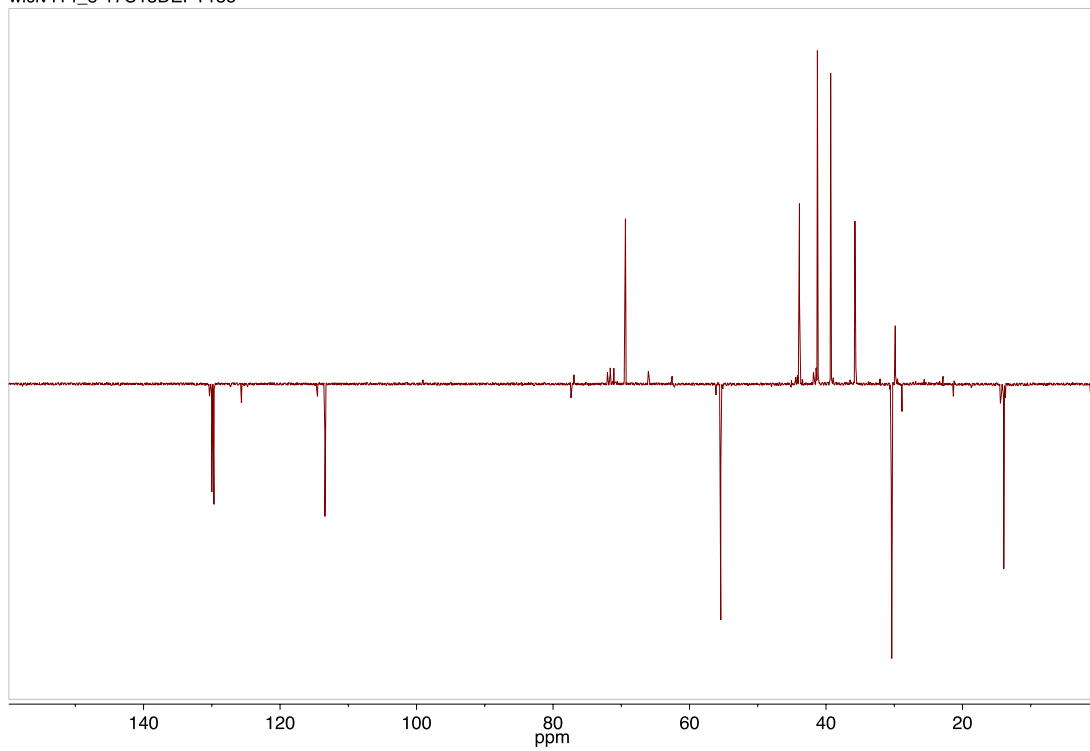


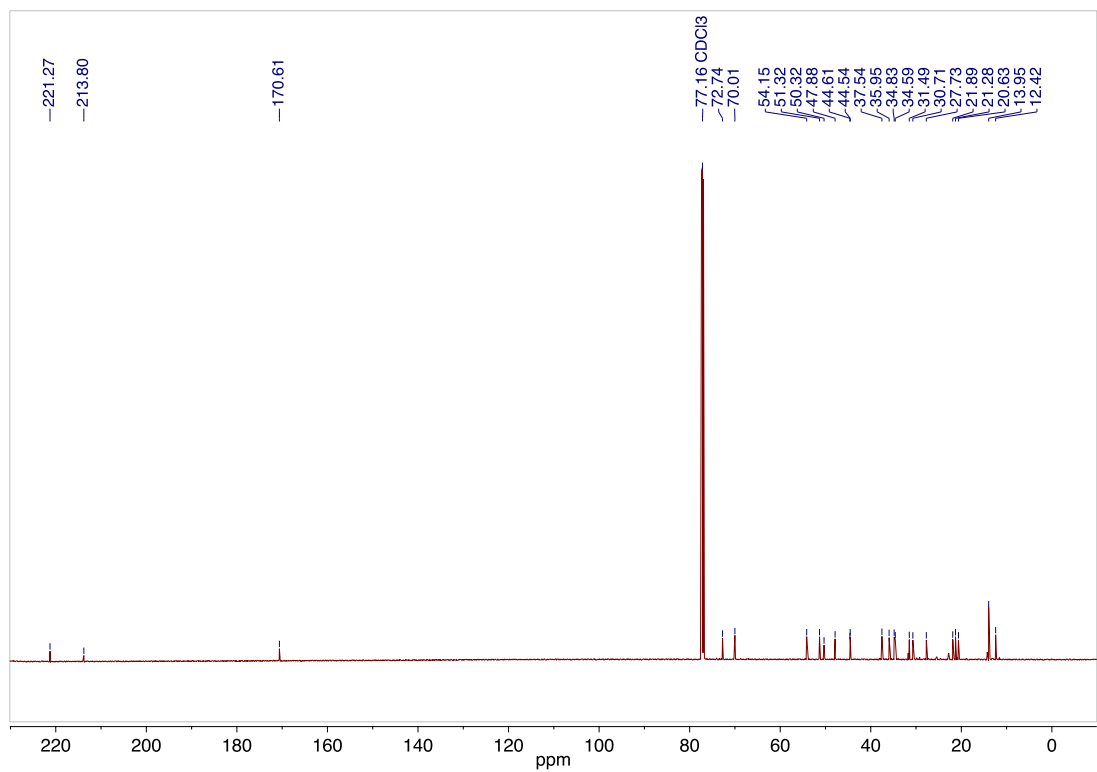
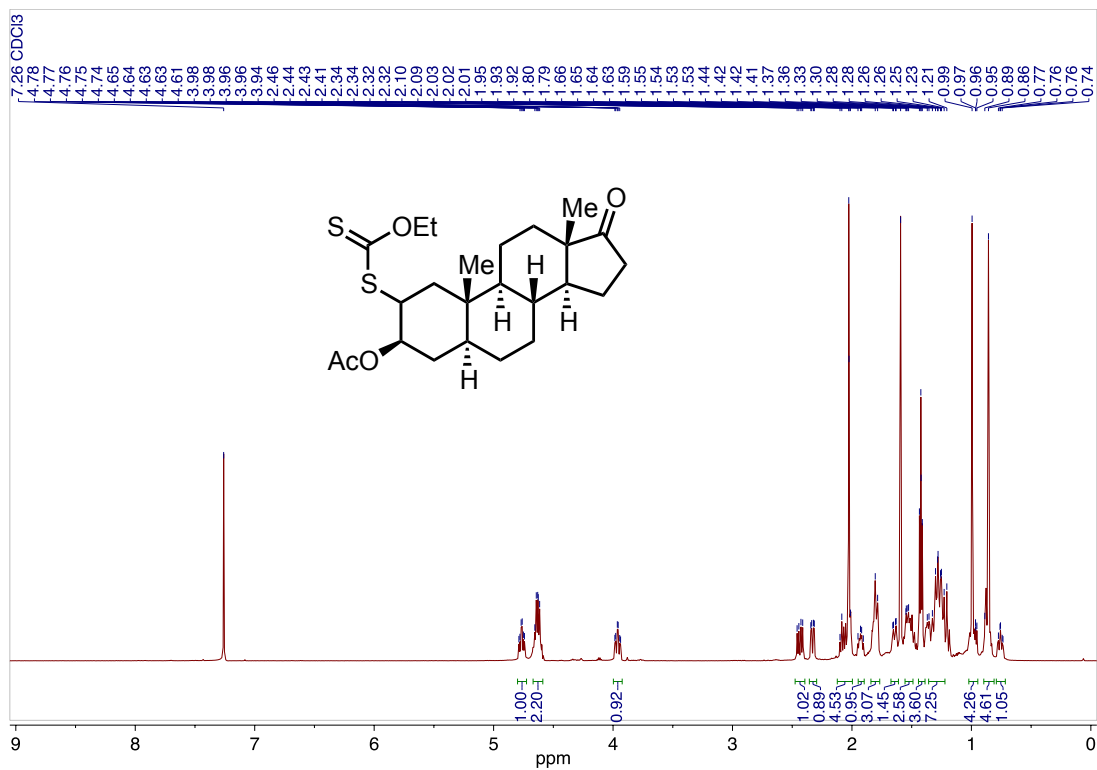
wlciv208\_1-2C



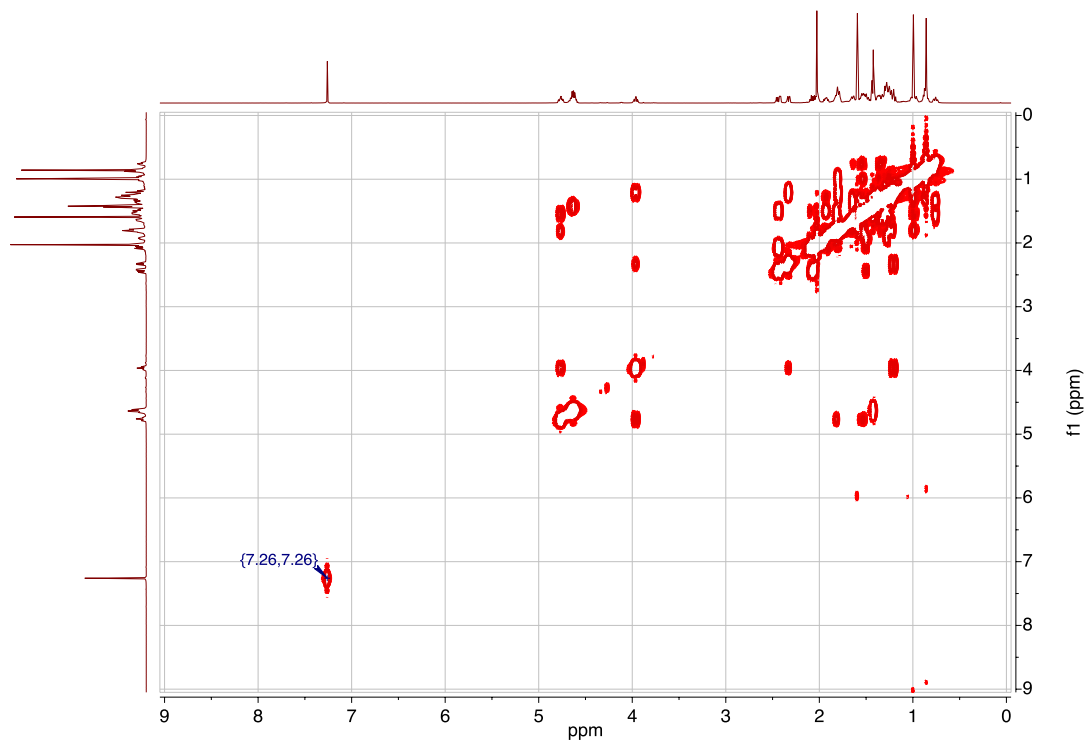


wlciv114\_8-17C13DEPT135

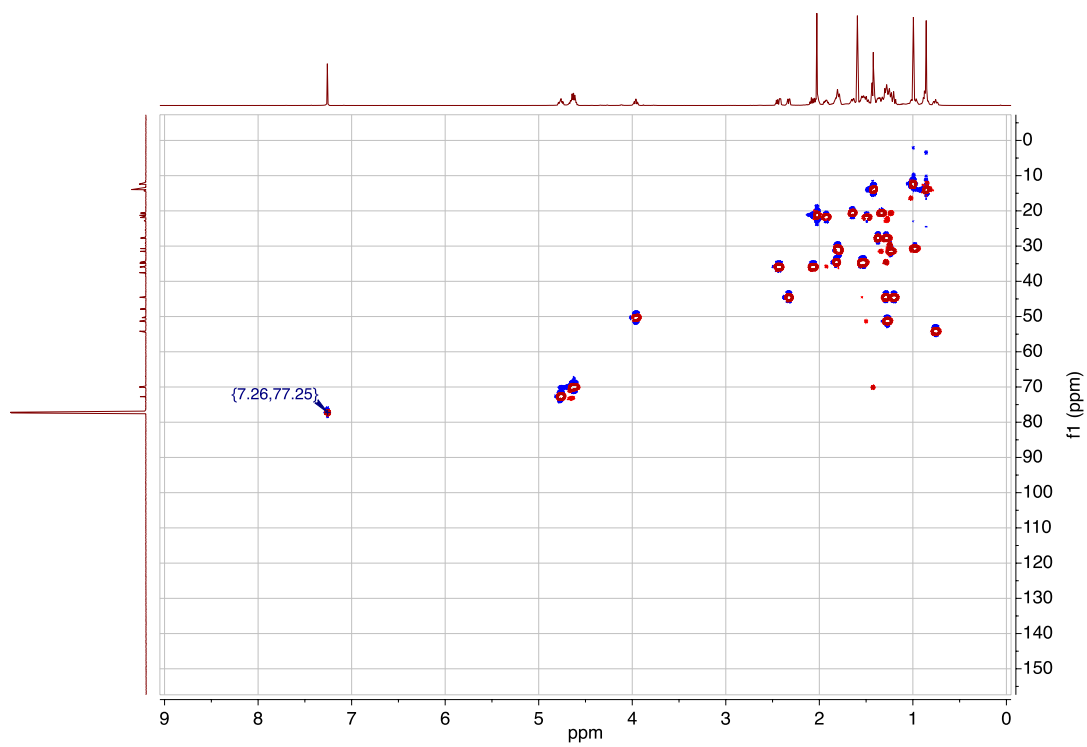




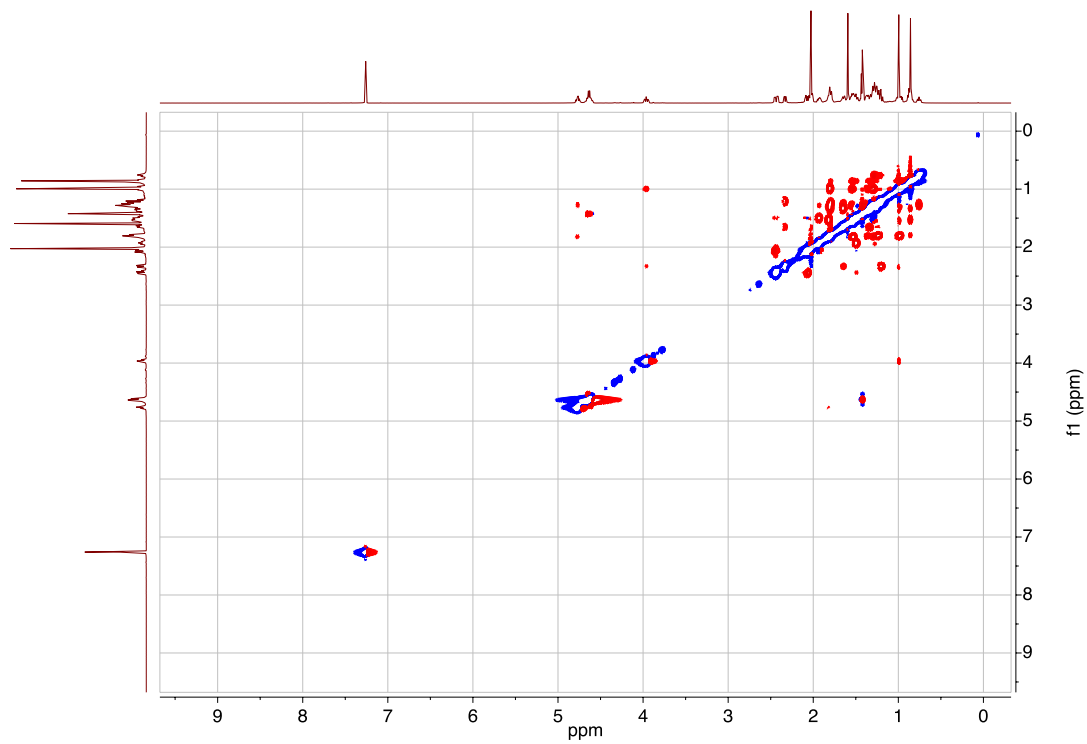
CGN 128A COSY

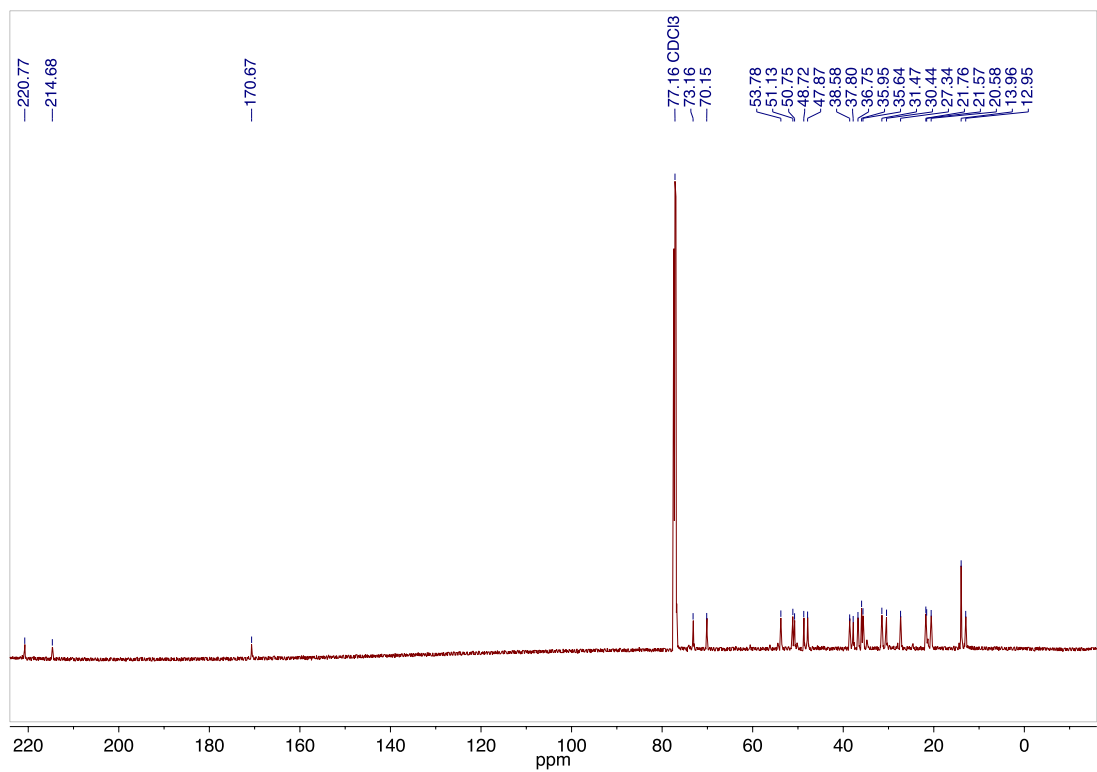
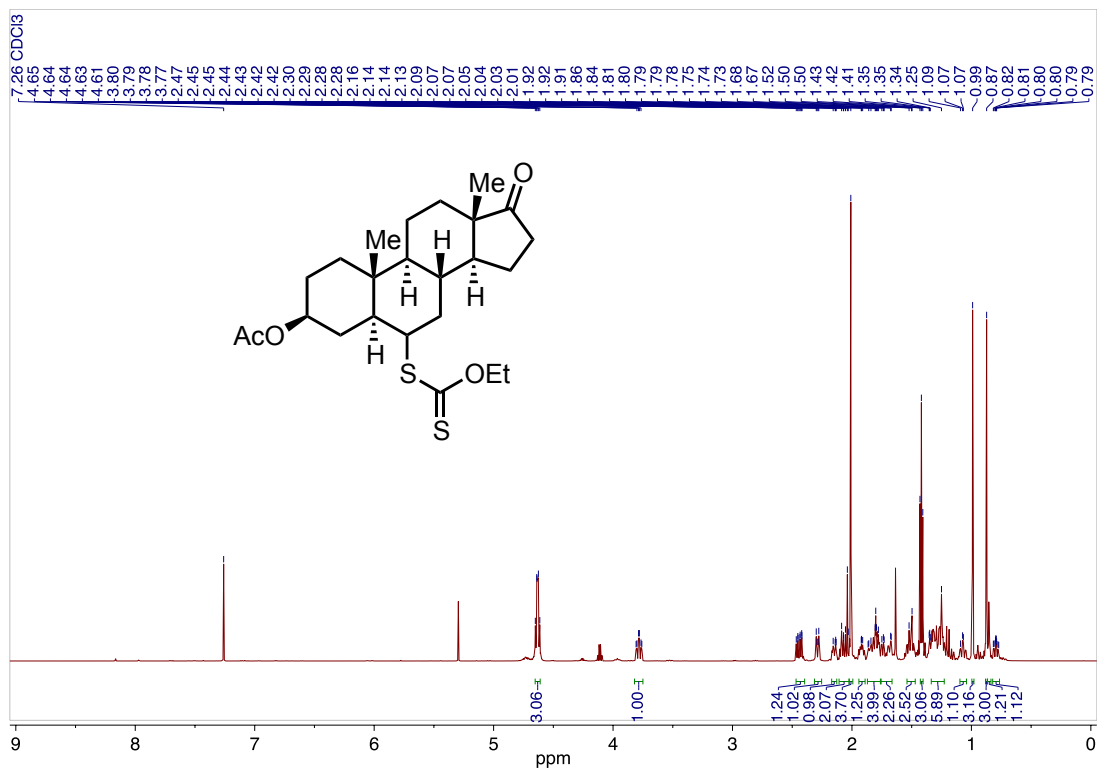


CGN 128A HSQC



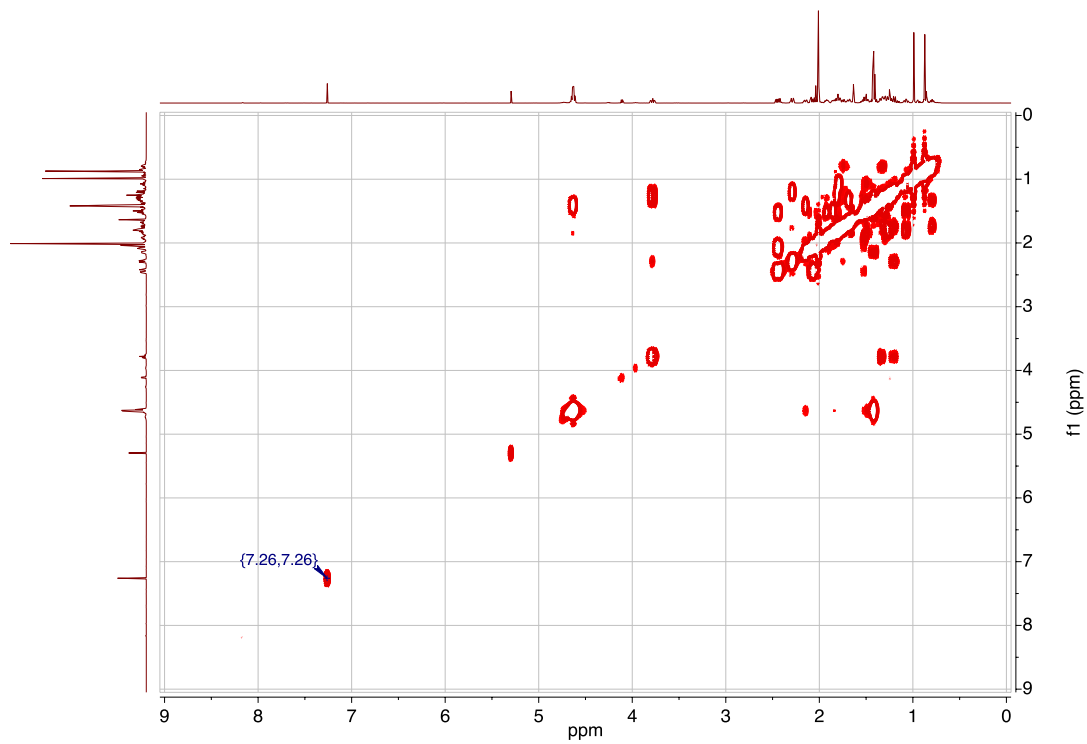
CGN 128A NOESY



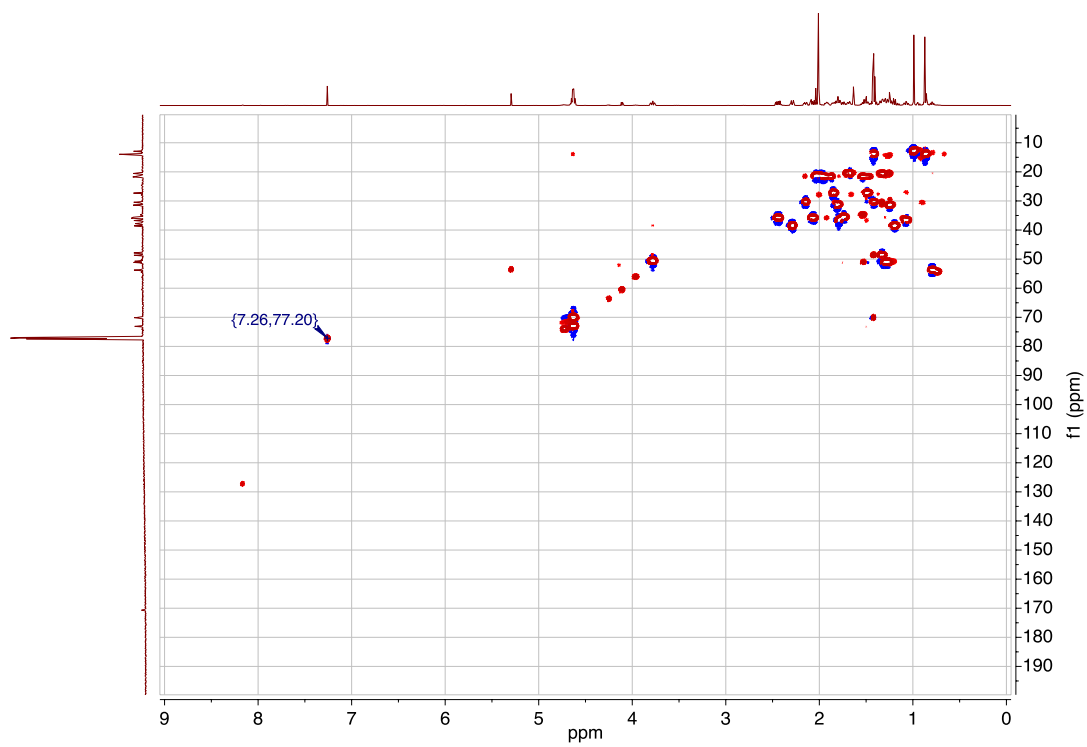


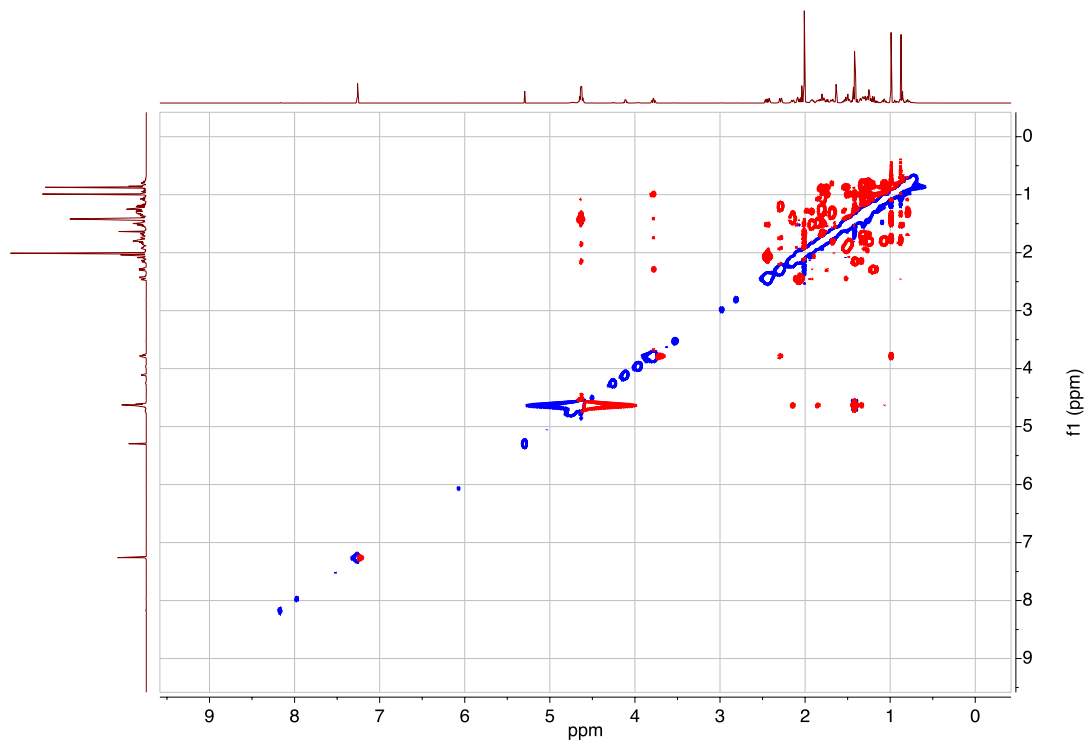


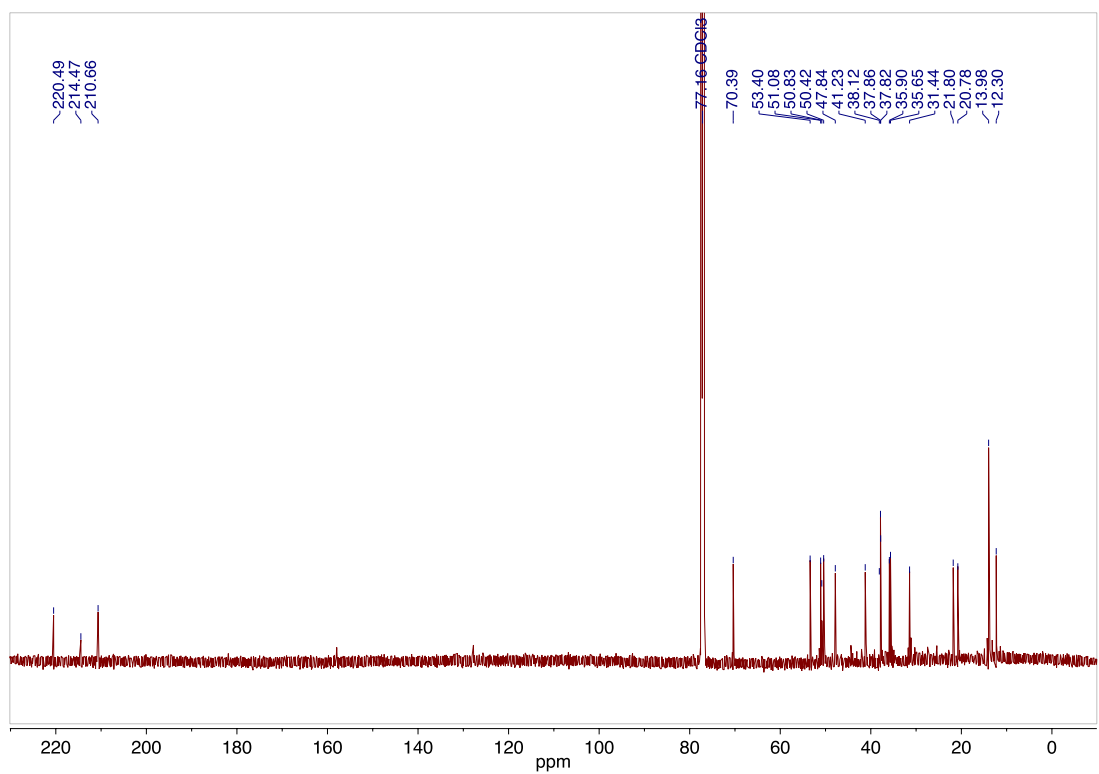
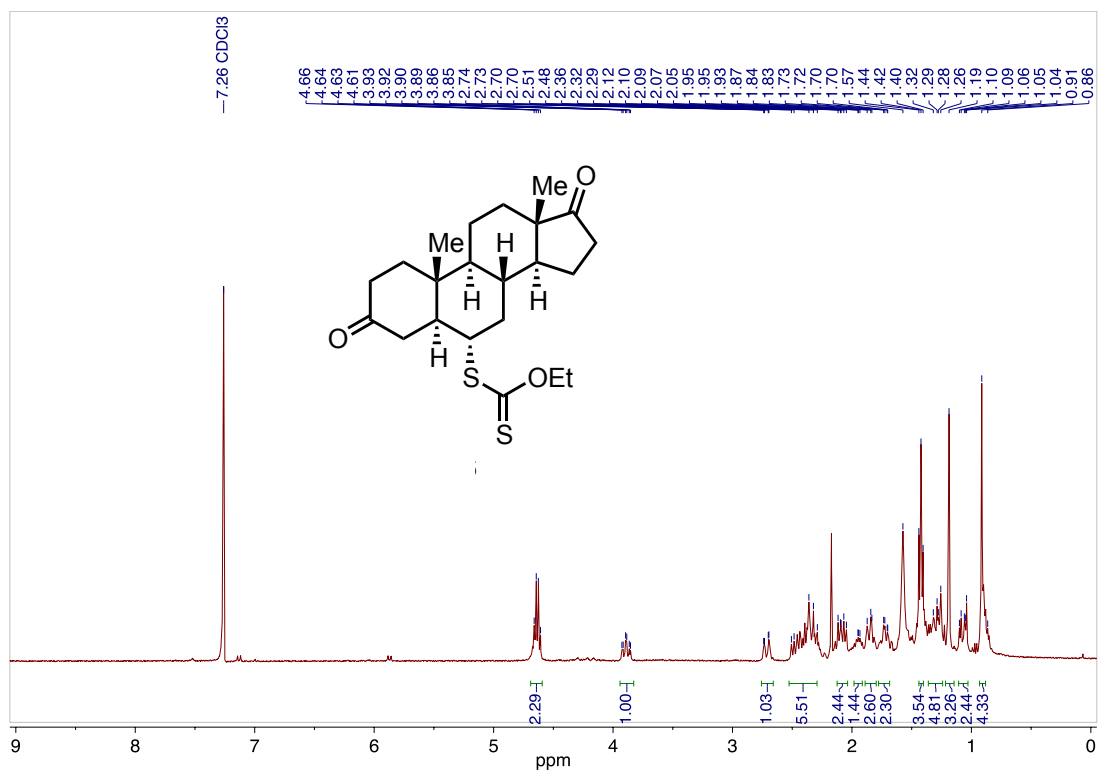
CGN 128B - COSY



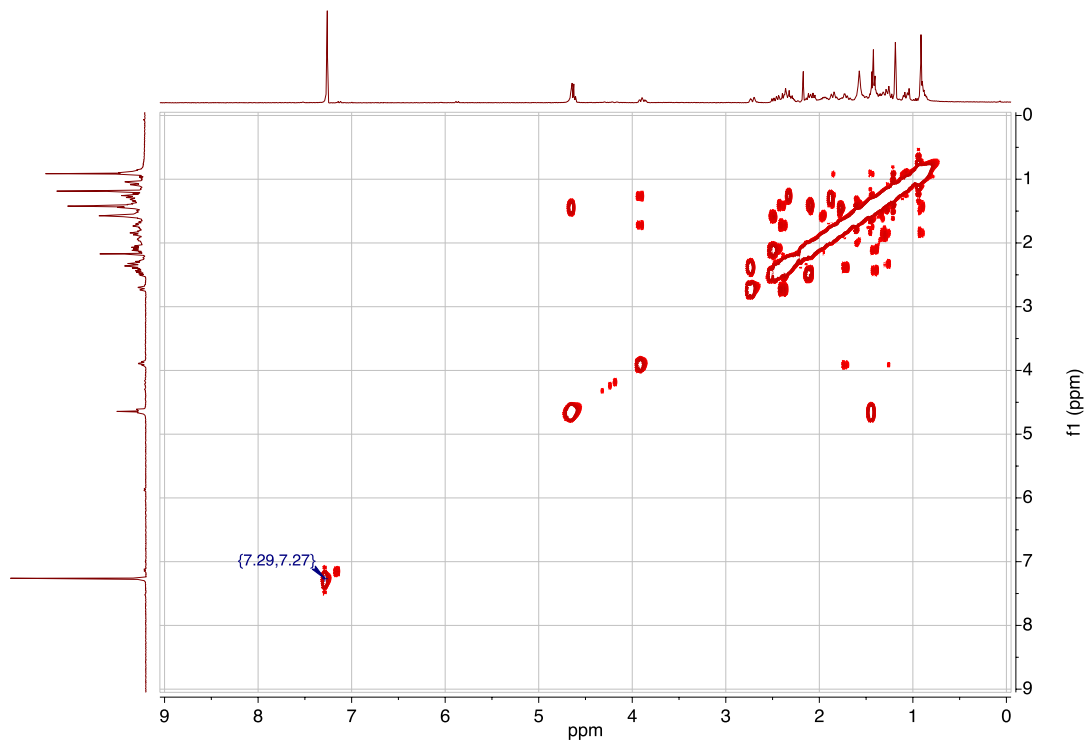
CGN 128B - HSQC



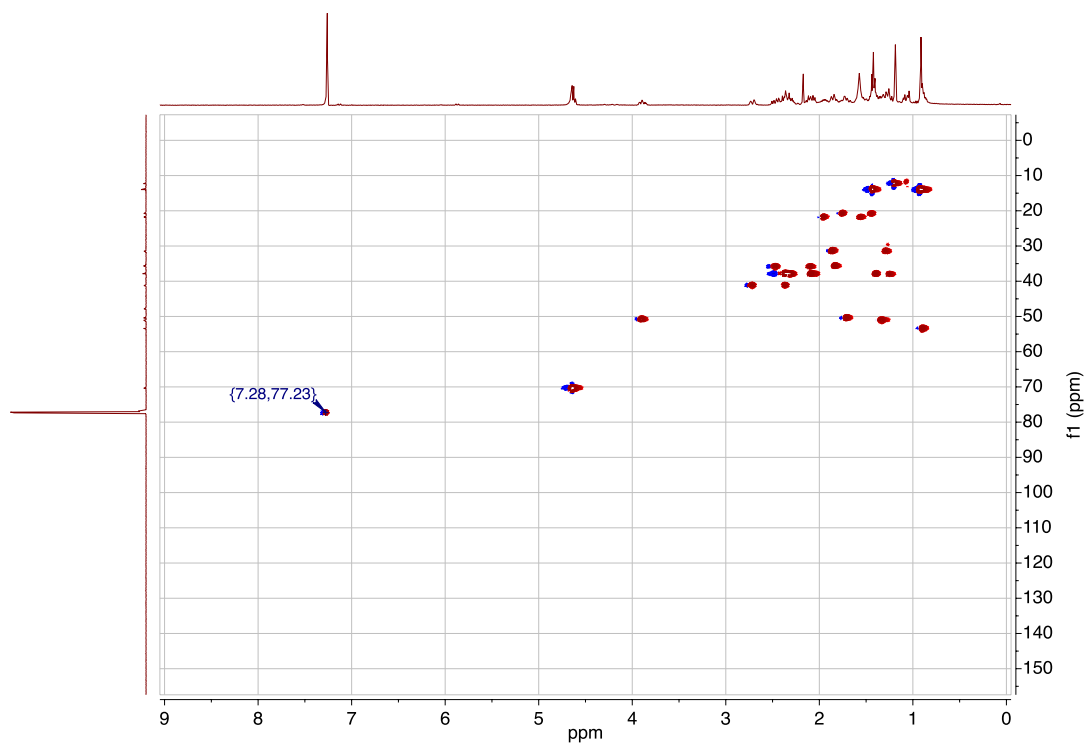


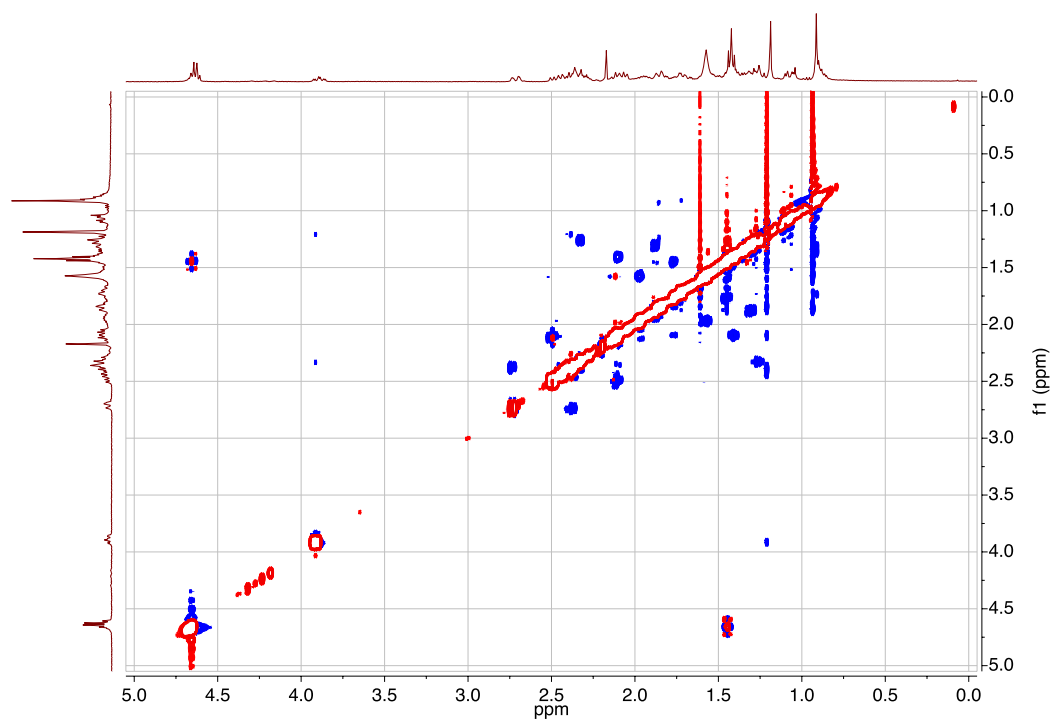


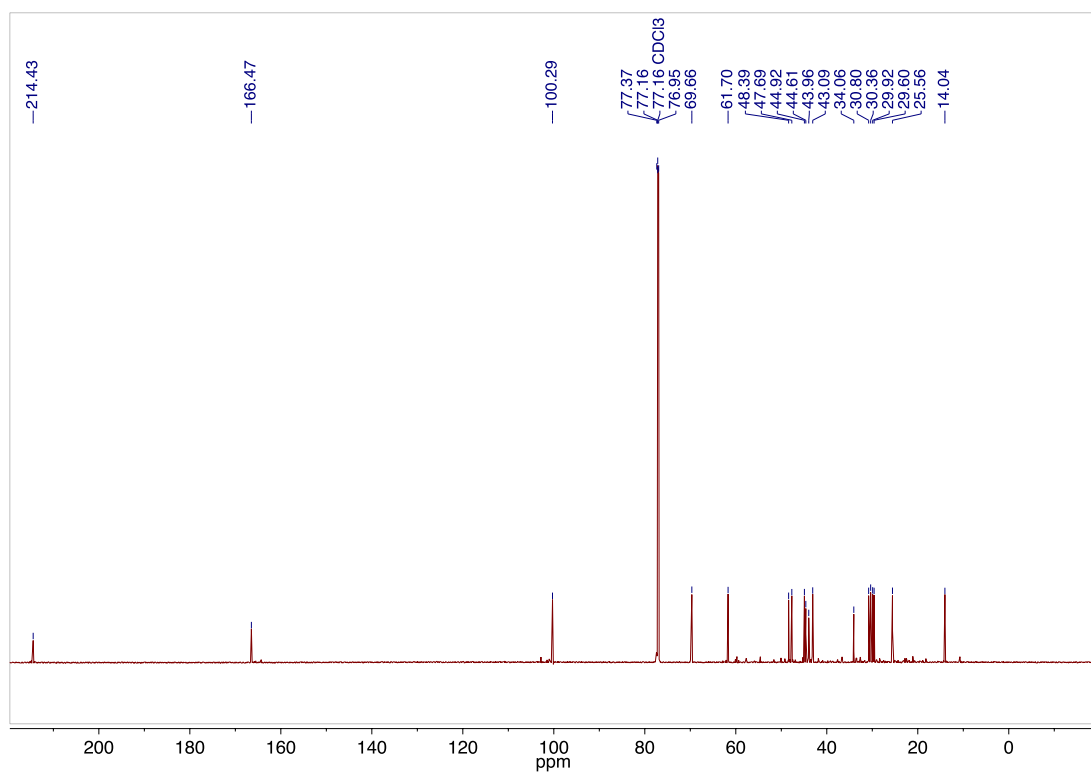
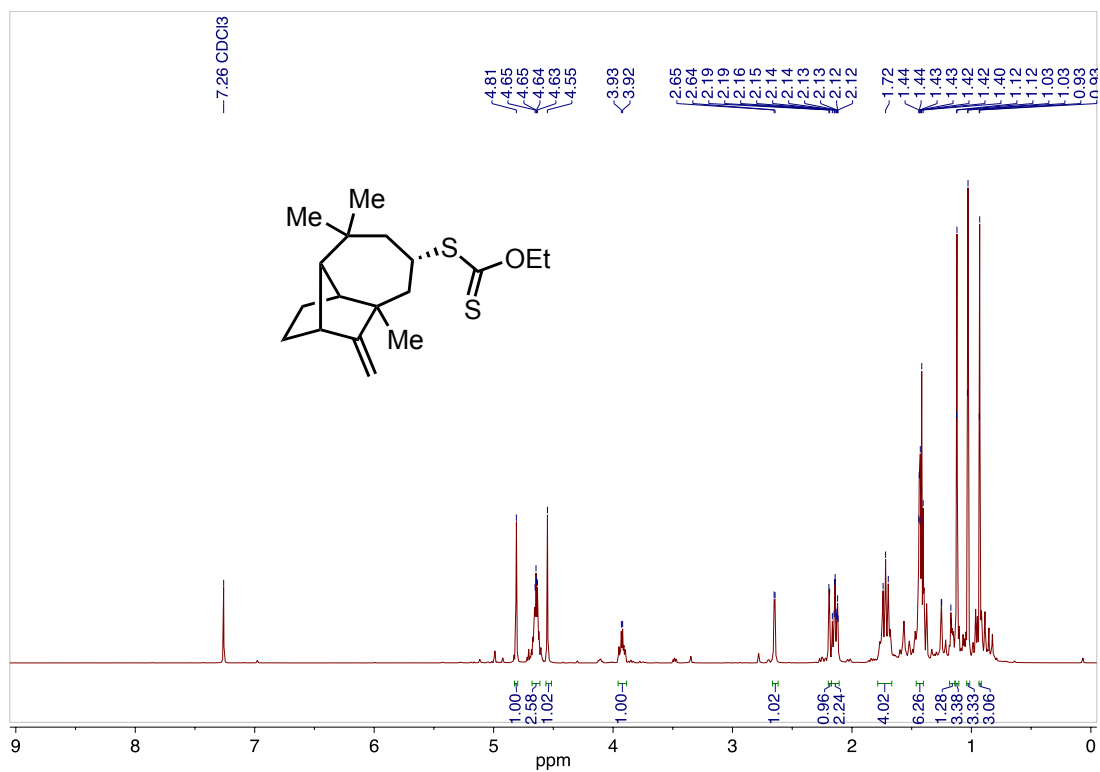
CGN diketone xanthate2 COSY



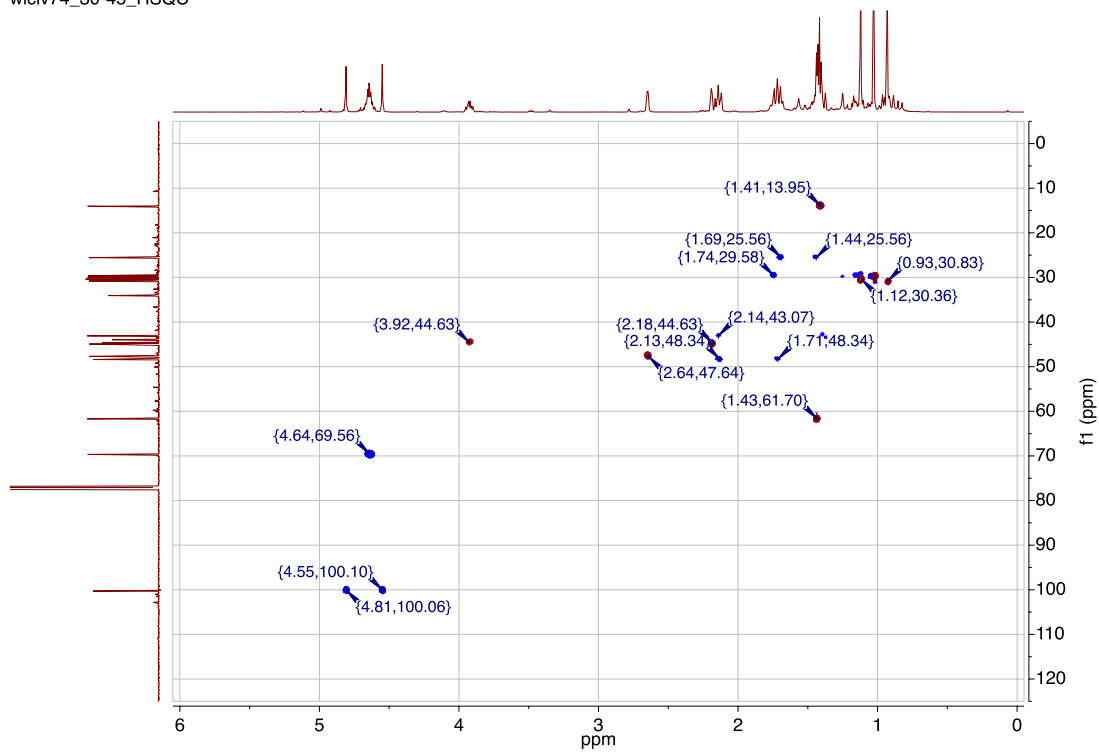
CGN diketone xanthate2 HSQC



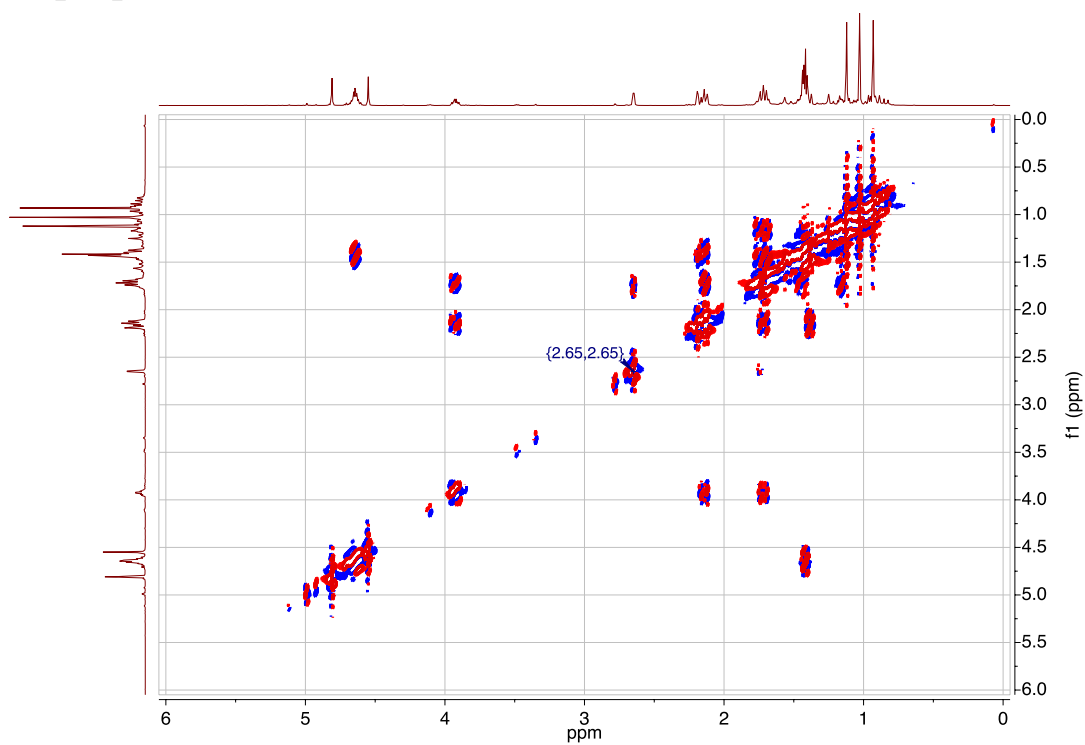




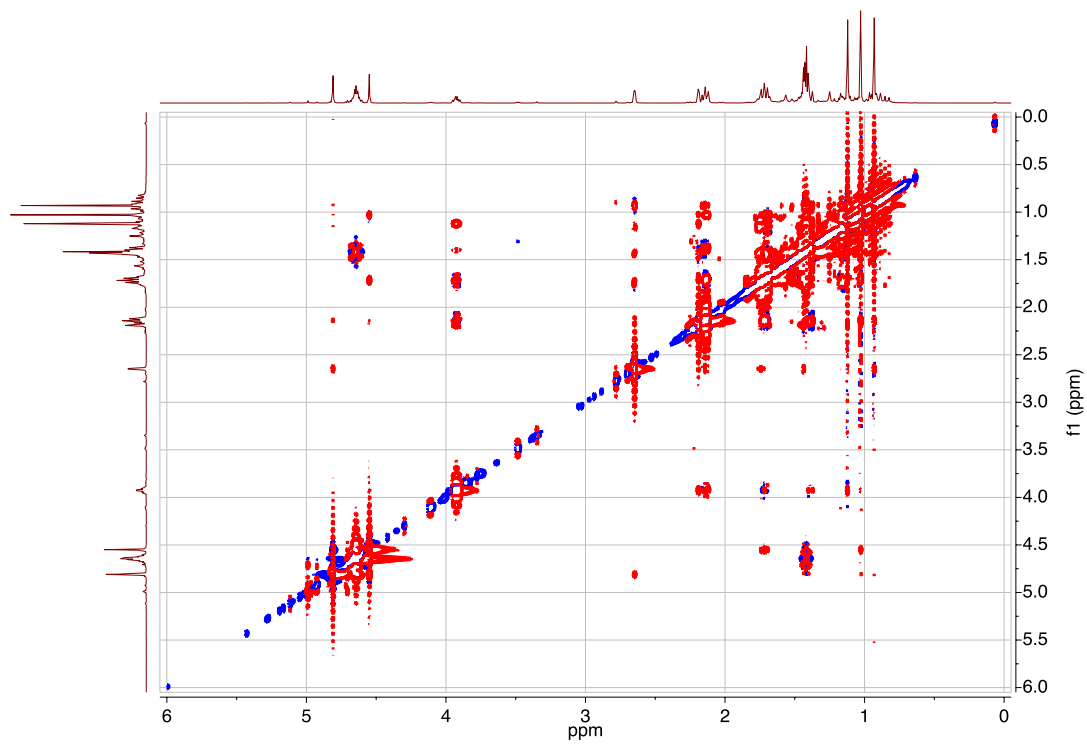
wlciv74\_30-45\_HSQC



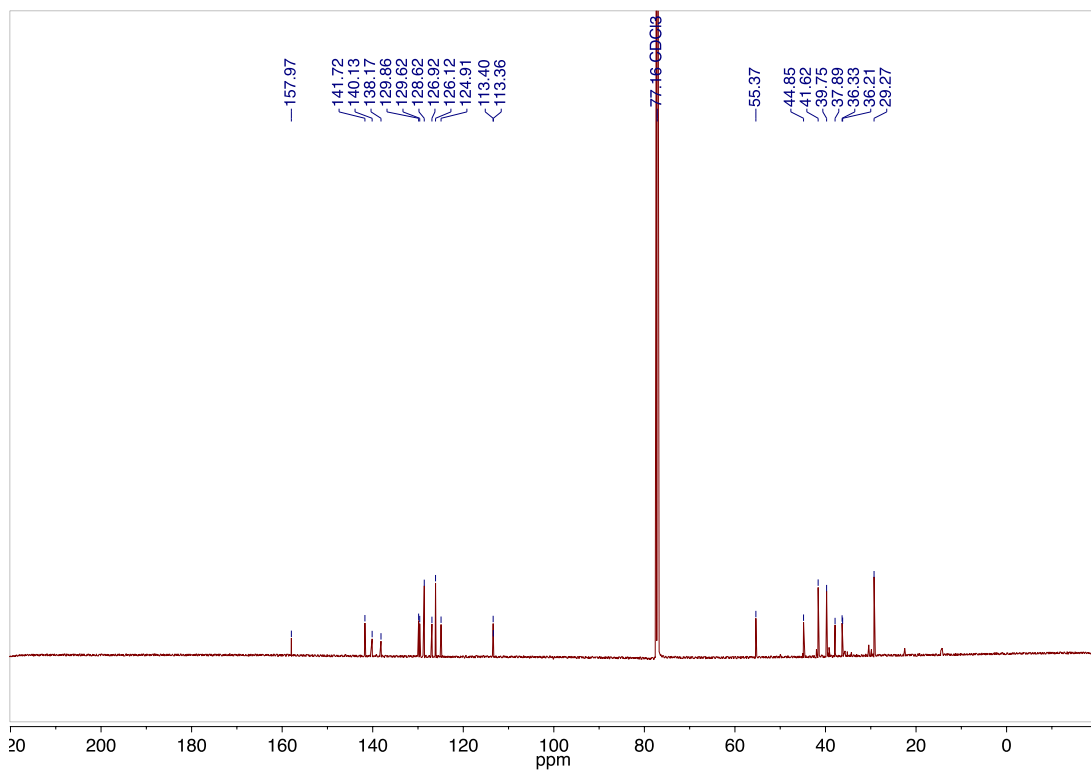
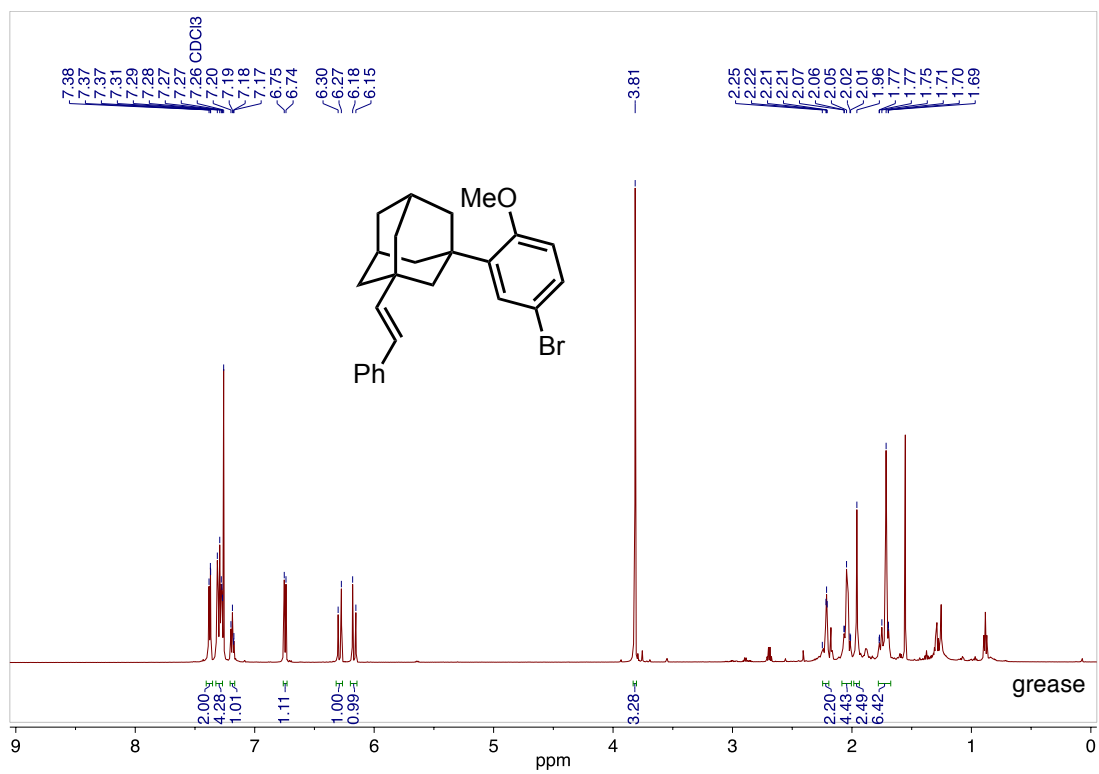
wlciv74\_30-45\_COSY

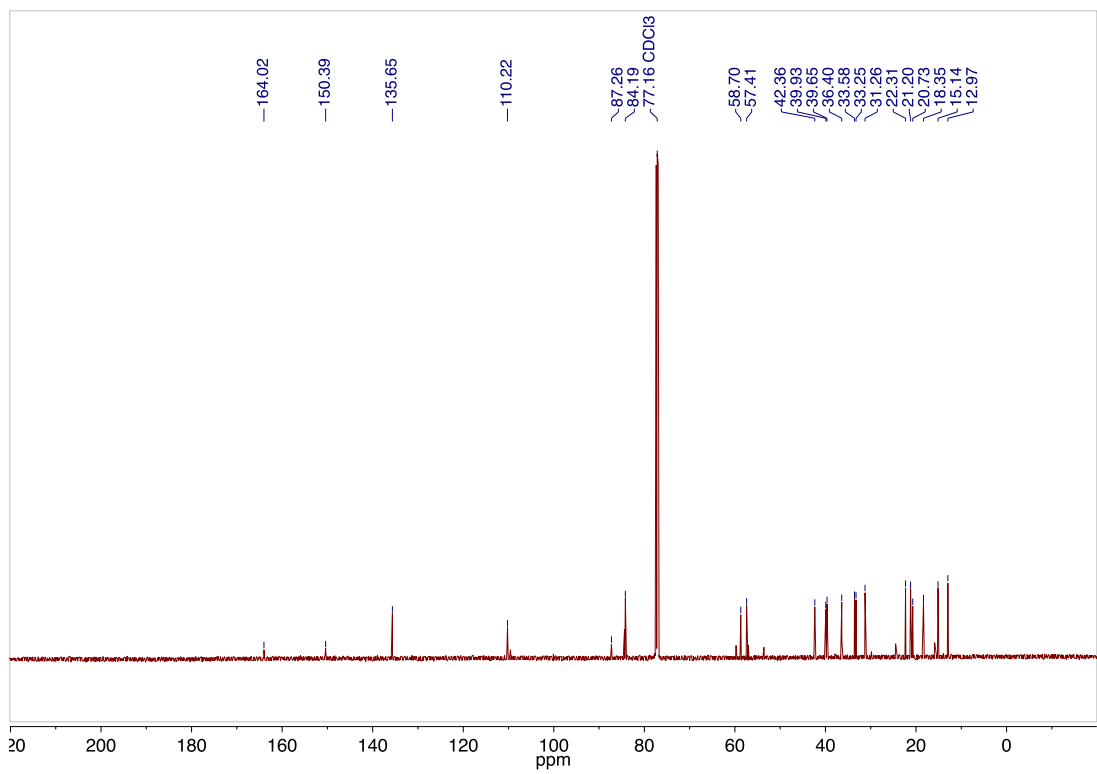
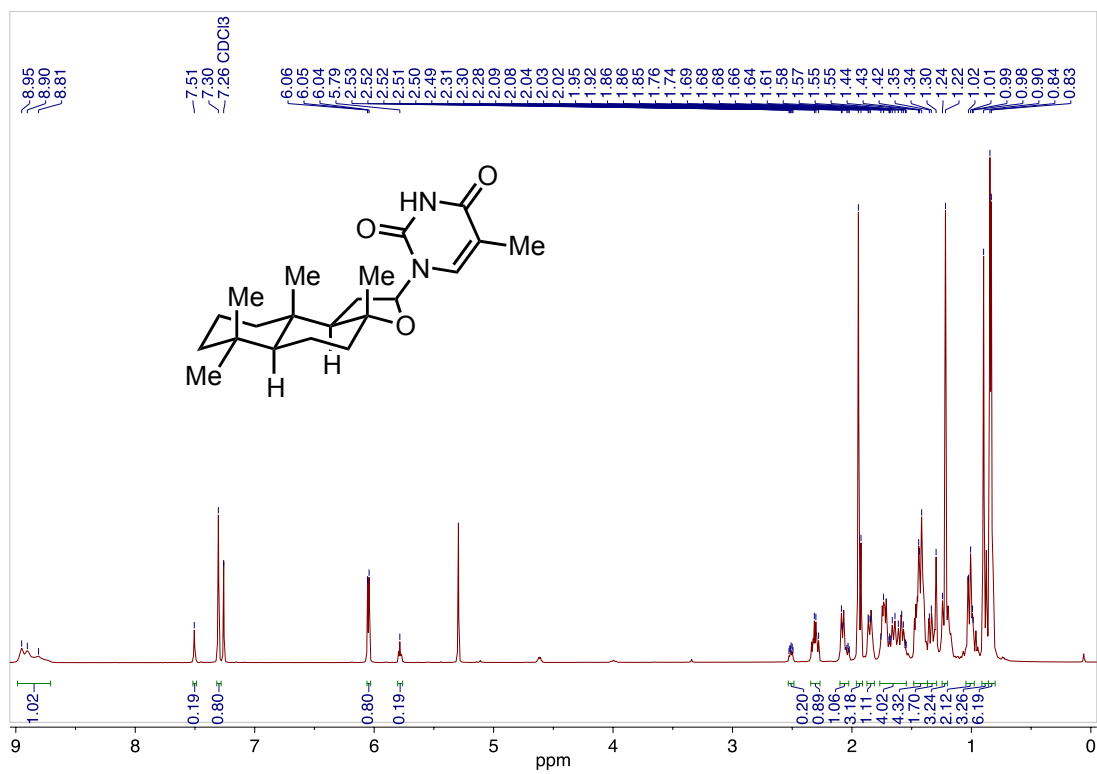


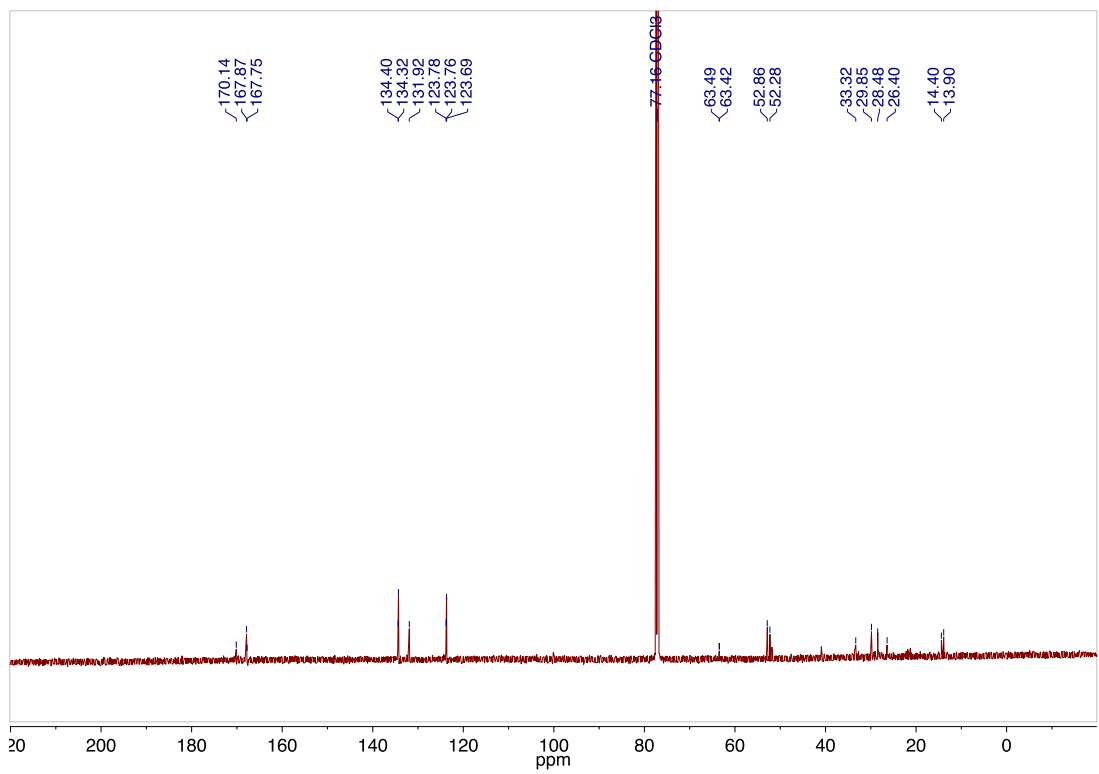
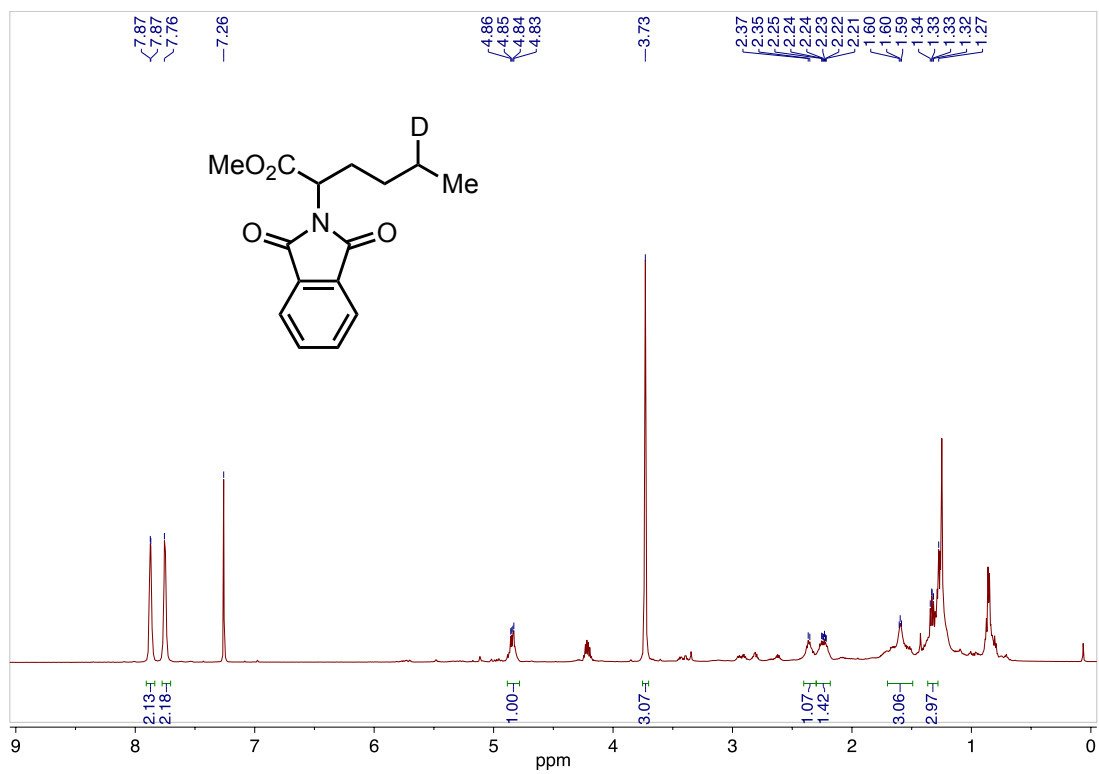
wlciv74\_30-45\_NOESY

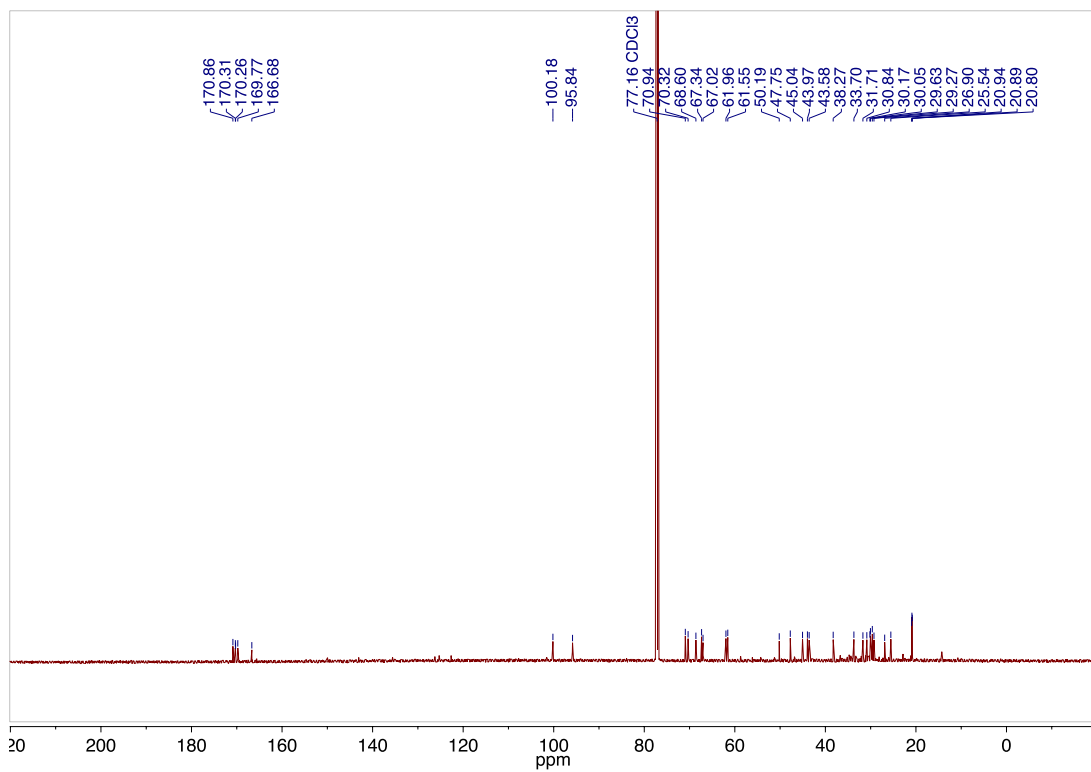
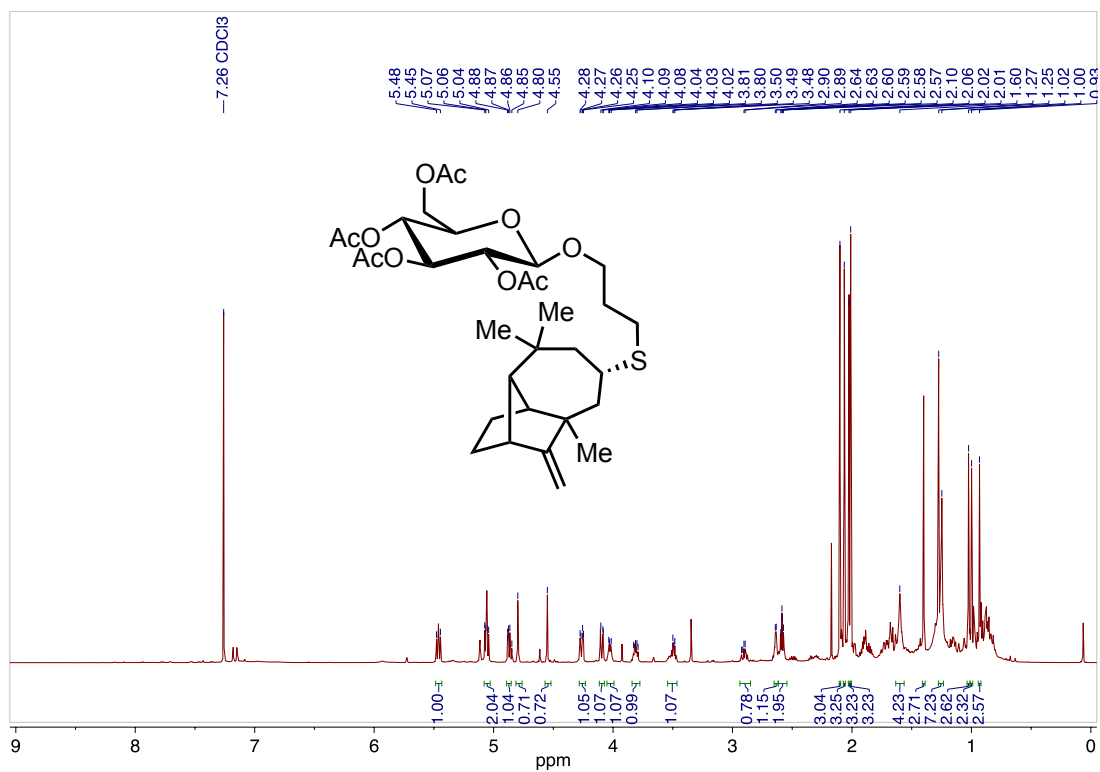


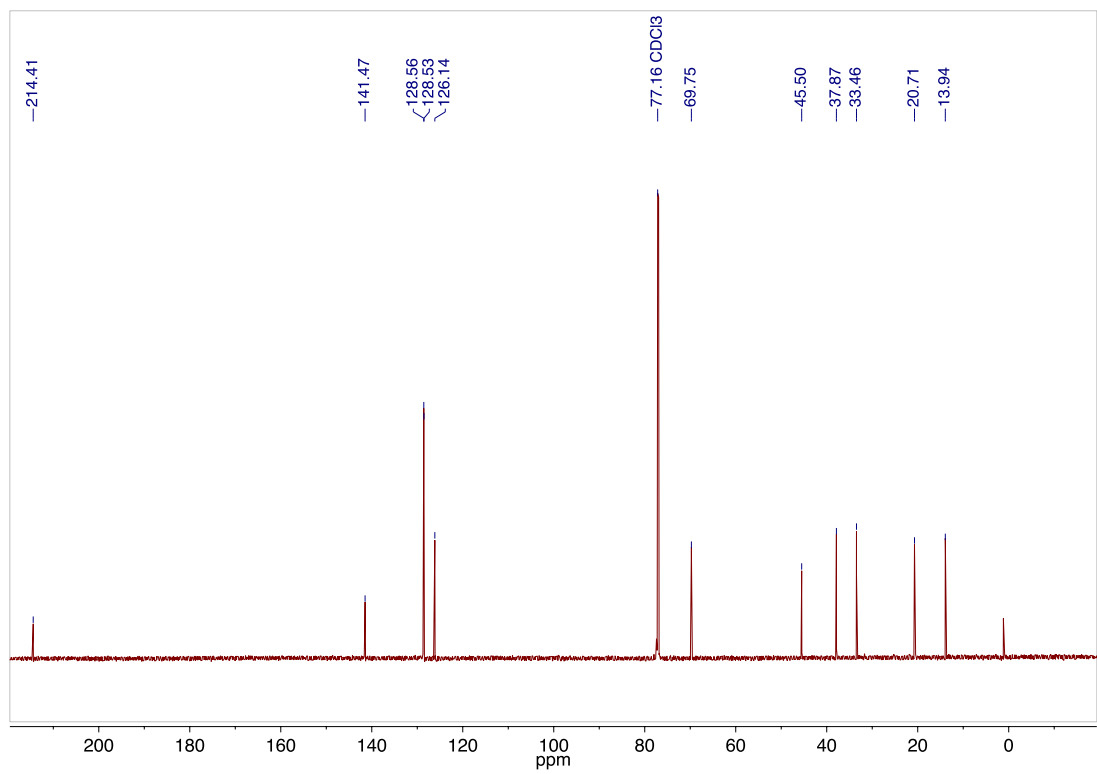
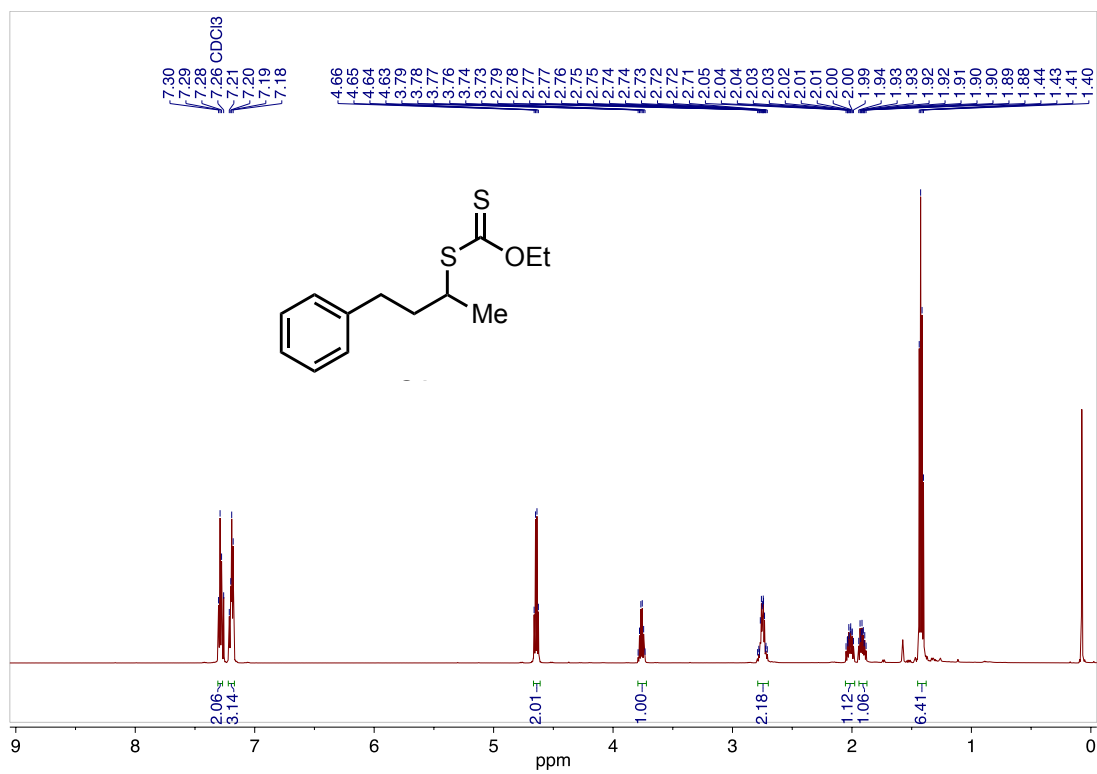


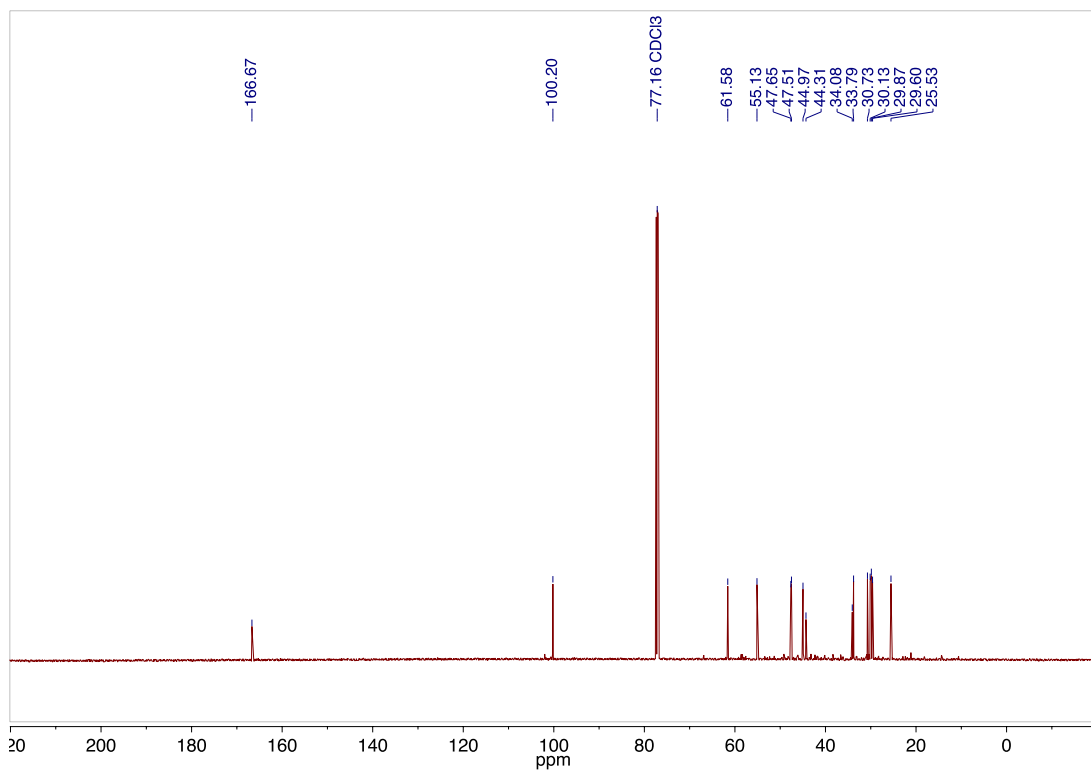
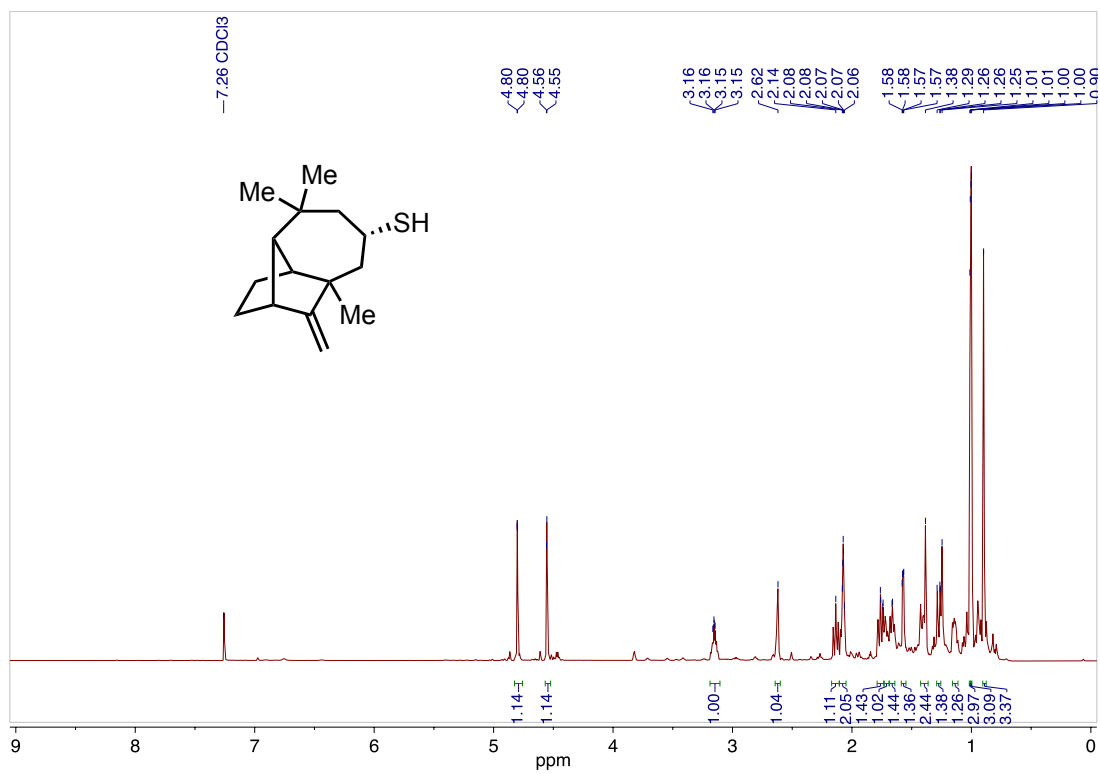


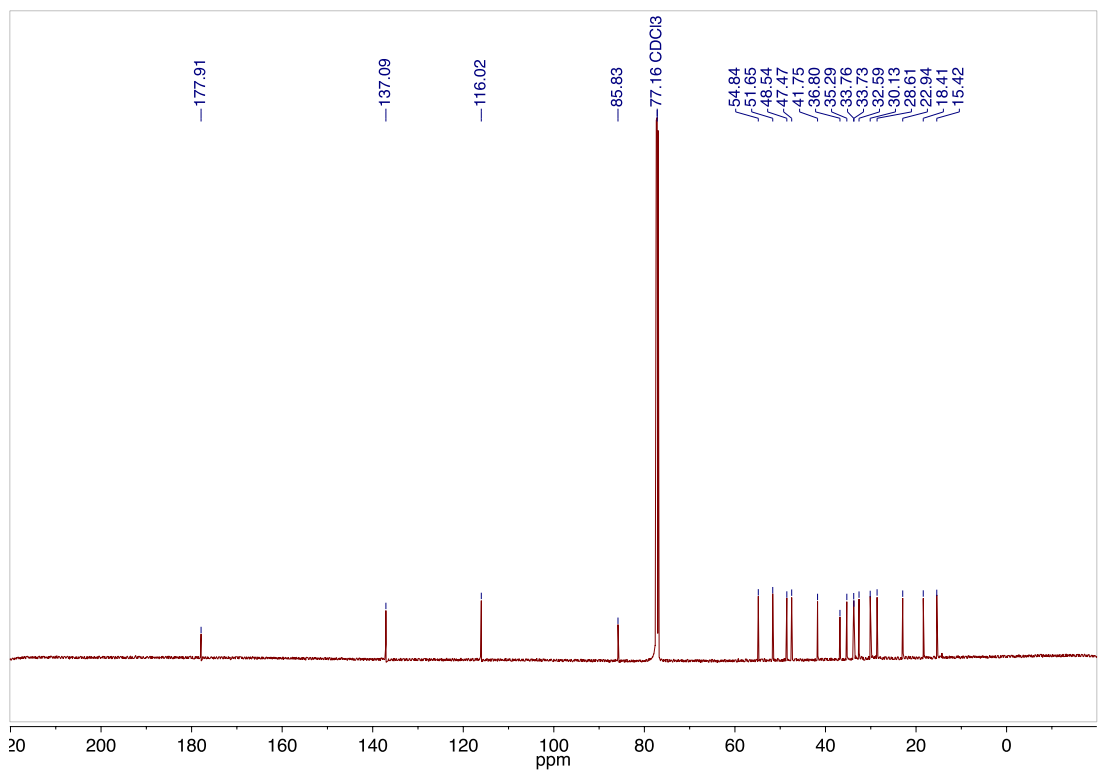
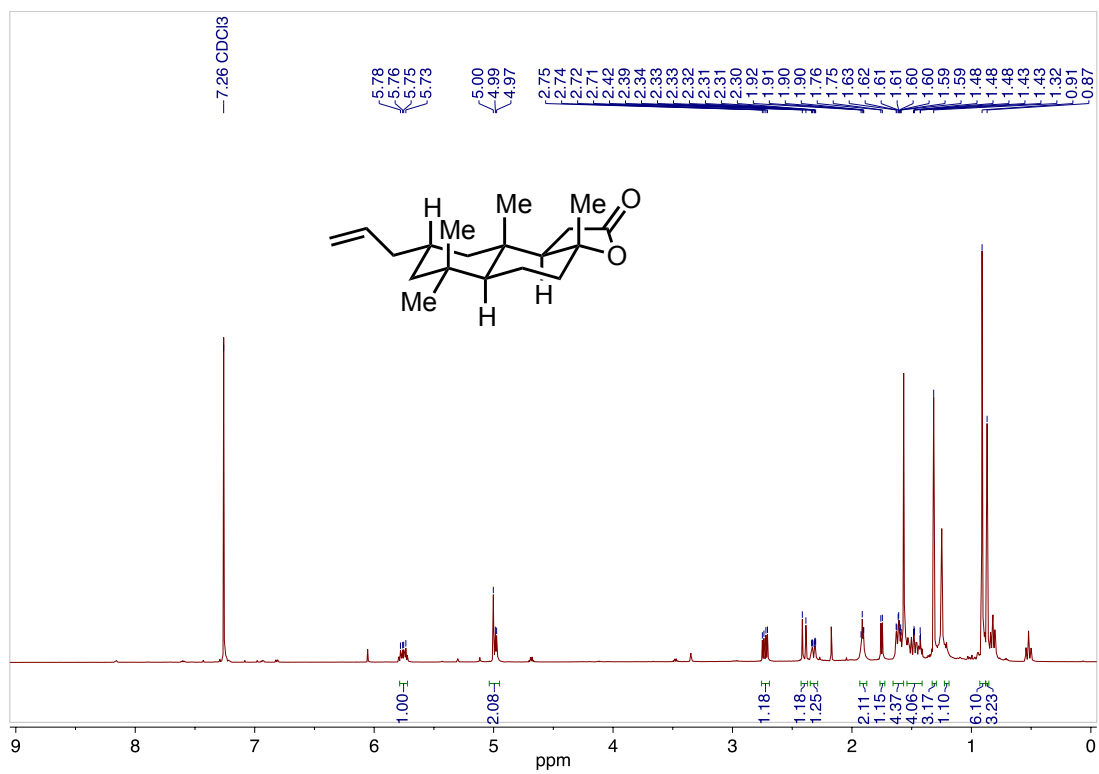


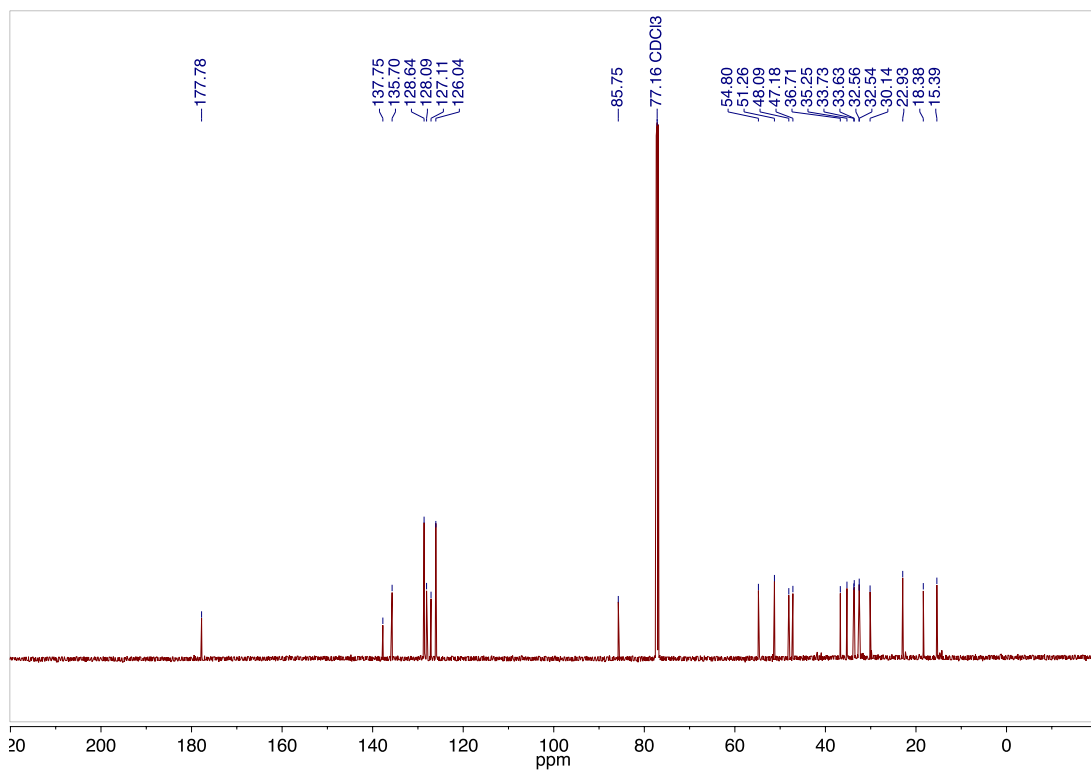
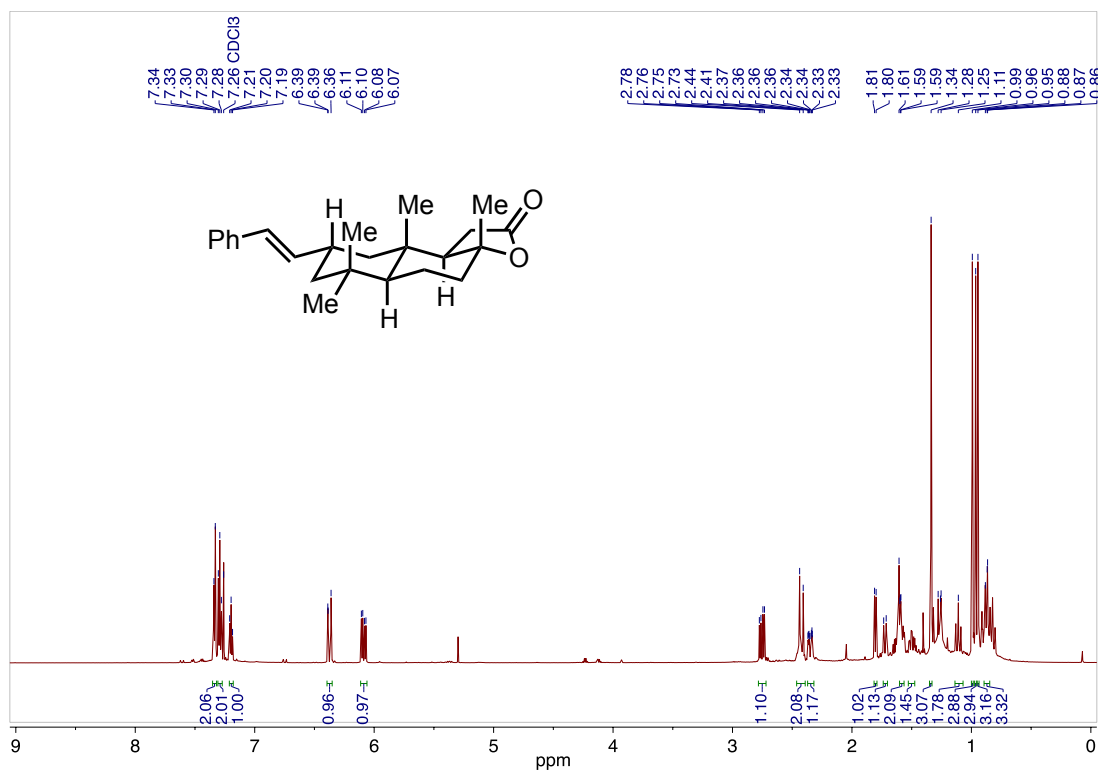




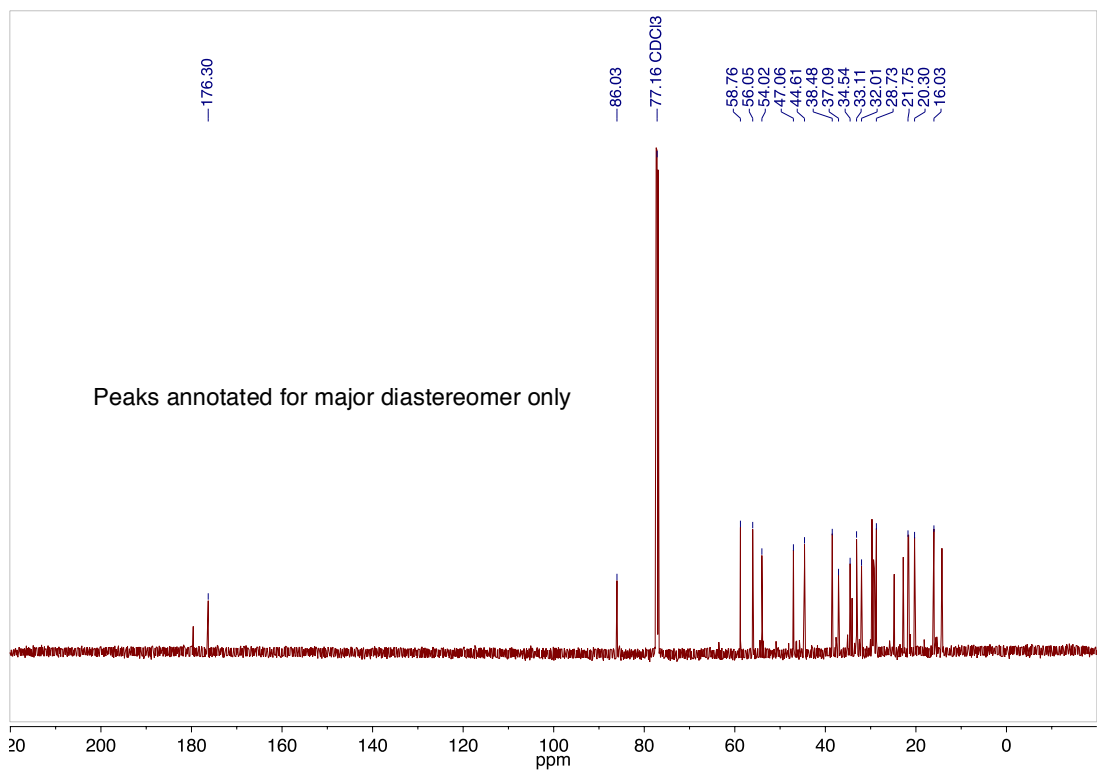
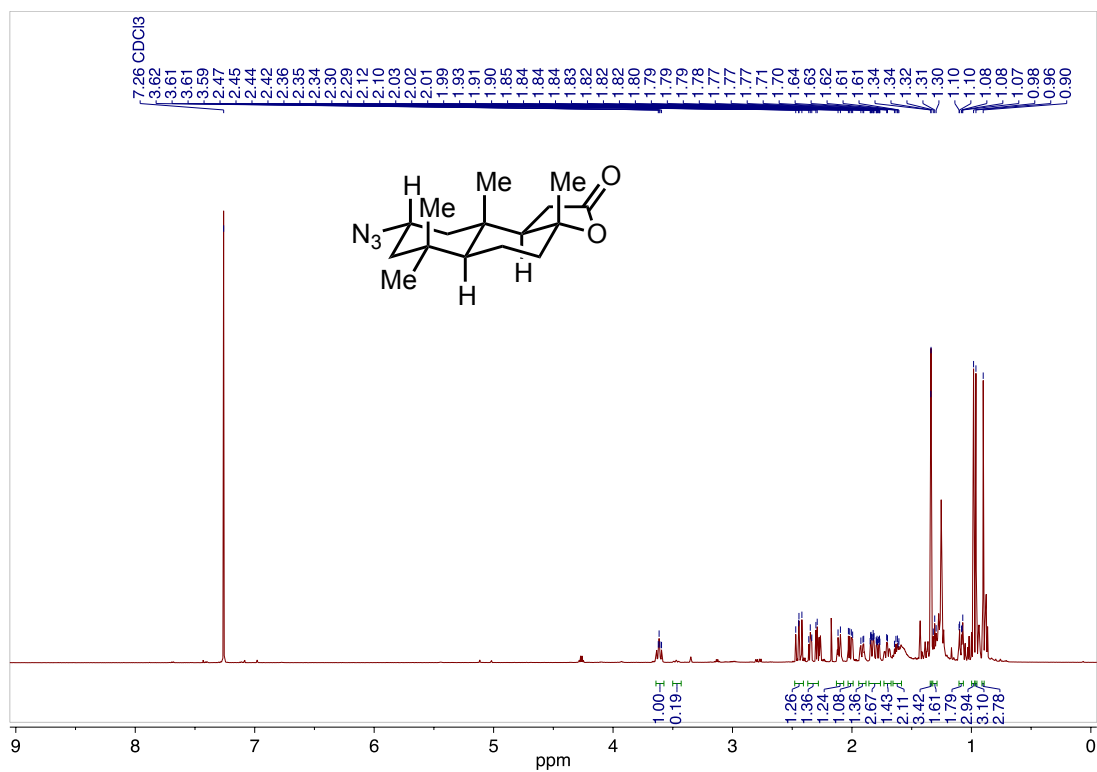


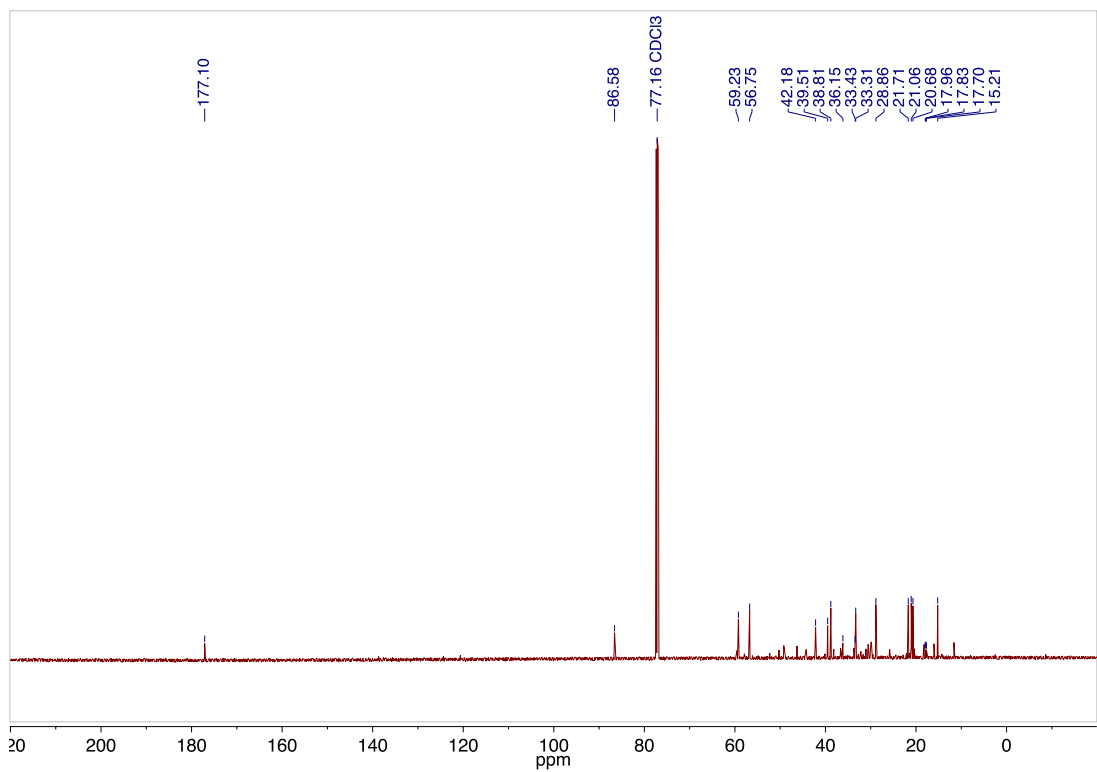
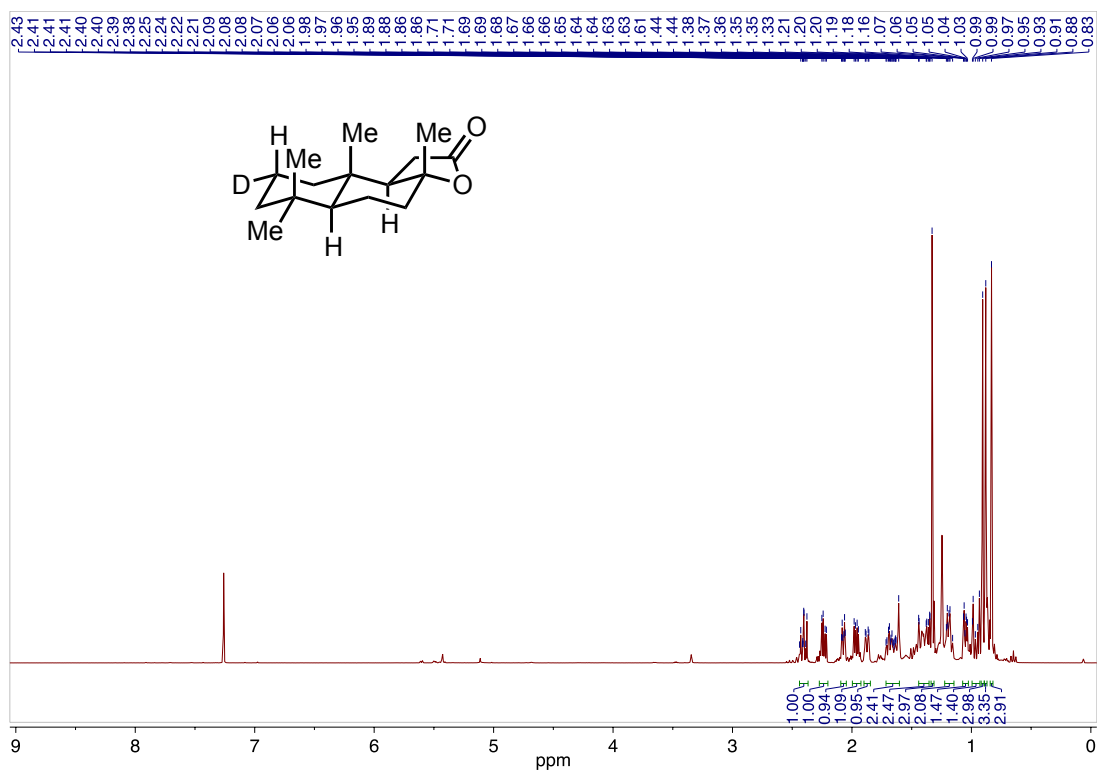
















## APPENDIX B: SUPPORTING INFORMATION FOR CHAPTER 3

### General Methods and Materials

All post-polymerization modifications were performed under inert atmosphere using standard glove box and Schlenk-line techniques. Xanthylamide<sup>1</sup> and TES-protected N-(2-[3,4-dihydroxyphenyl]ethyl)acrylamide<sup>2</sup> were prepared using previously reported methods. Predominantly (90%) 1,2-polybutadiene was purchased from Sigma-Aldrich and hydrogenated according to known procedure.<sup>3</sup> Hyperbranched polyethylene (13% branched) was obtained from collaborators and synthesized according to known procedure.<sup>4</sup> Low molecular weight polyethylene was obtained from Sigma-Aldrich and purified via two precipitations in methanol prior to use. Commercial polyolefins were obtained from their respective companies. The company and lot number are named in the individual procedures. 1,2-Dichlorobenzene was degassed with argon through three freeze-pump-thaw cycles. Trifluorotoluene was distilled over calcium hydride and stored in a glove box. Reagents, unless otherwise specified, were purchased and used without further purification.

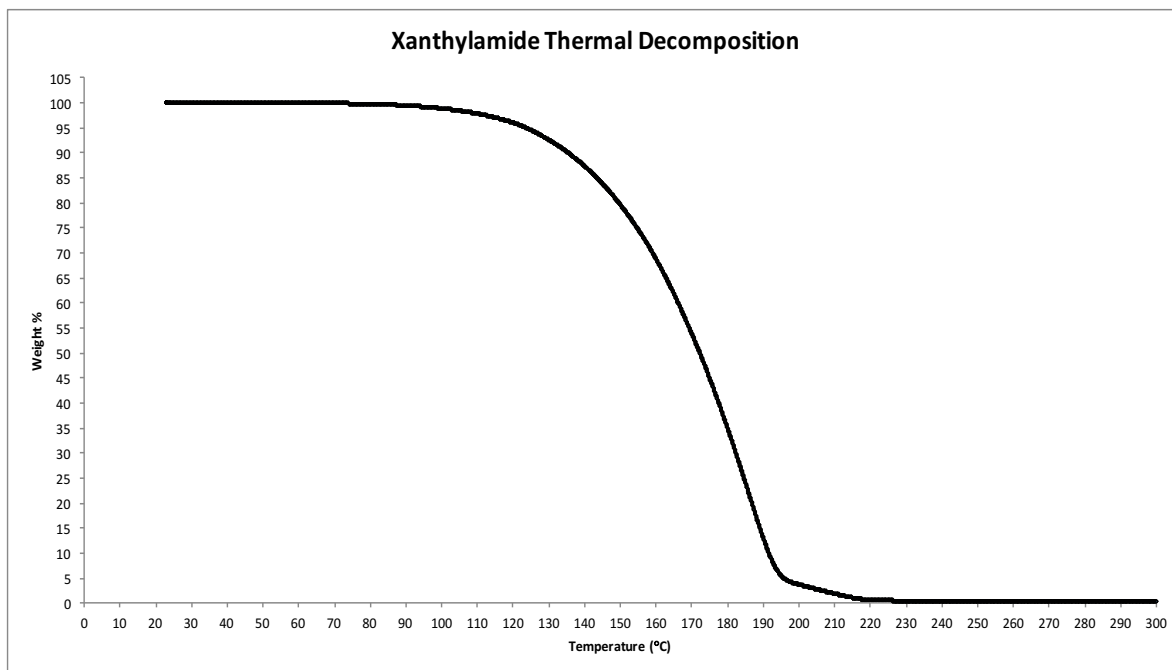
Proton and carbon magnetic resonance spectra (<sup>1</sup>H NMR and <sup>13</sup>C NMR) were recorded on a Bruker model DRX 400 MHz, Bruker 500 MHz, Varian Inova 600, or Bruker AVANCE III 600 MHz CryoProbe spectrometer with solvent resonance as the internal standard (<sup>1</sup>H NMR: CDCl<sub>3</sub> at 7.26 ppm; <sup>13</sup>C NMR: CDCl<sub>3</sub> at 77.16 ppm). <sup>1</sup>H NMR data are reported as follows: chemical shift, multiplicity (s = singlet, d = doublet, t = triplet, q = quartet, m = multiplet, dd = doublet of doublets, bs = broad singlet), coupling constants (Hz), and integration. Infrared (IR) spectra were obtained using PerkinElmer Frontier FT-IR spectrometer. Small molecule mass spectra obtained using a Thermo LTqFT mass

spectrometer with electrospray introduction and external calibration at the University of North Carolina's Department of Chemistry Mass Spectrometry Core Laboratory.

Gel permeation chromatography (GPC) spectra were obtained using Waters 2695 separations module liquid chromatograph, Waters 2414 refractive index detector at room temperature, and Waters 2996 photodiode array detector with styragel HR columns. Tetrahydrofuran was the mobile phase and the flow rate was set to 1 mL/min. The instrument was calibrated using polystyrene standards in the range of 580 to 892,800 Da. Low molecular weight polyethylene was analyzed with high-temperature GPC (140 °C, TCB stabilized with 0.0125% BHT) against polystyrene standards at the University of Akron. High density polyethylene and linear low density polyethylene were analyzed with high-temperature GPC (150 °C, TCB stabilized with 0.0125% BHT) against polyethylene standards at Cornell University.

Differential scanning calorimetry (DSC) was used to determine the thermal characteristics of the polyolefins and graft copolymers using a TA Instruments DSC (Discovery Series). The DSC measurements were performed on 2 – 10 mg of polymer samples at a temperature ramp rate of 10 °C/min unless otherwise noted. Data was taken from the second thermal scanning cycle. Thermal gravimetric analysis was obtained using a TA Instruments TGA (Discovery Series) in the temperature range of 40-600 °C at a temperature ramp rate of 10 °C/min. Gas chromatography (GC) spectra were obtained using a Shimadzu GC-2010 gas chromatograph with a Shimadzu AOC-20s Autosampler, and Shimadzu SHRXI-5MS GC column. Irradiation of xanthylation reactions was performed using Kessil KSH150B Blue 36W LED Grow Lights. UV light reactions were performed in a Luzchem LZC-ORG photoreactor containing UV-A lamps.

## Additional Data

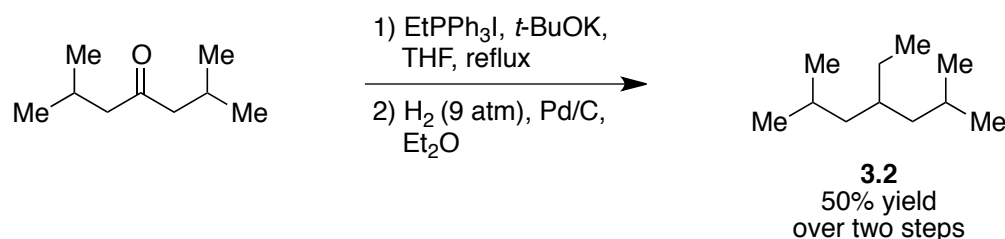


Thermal Gravimetric Analysis of xanthylamide reveals that xanthylamide is stable up to 135 °C, where 10% of the initial weight is lost.

### Independent Synthesis of Xanthate Standards

**Overview of experiment:** If tertiary xanthylation were observed, it would occur via the abstraction of a tertiary C–H bond by the amidyl radical to generate a tertiary radical, the presence of which could lead to  $\beta$ -scission of the polymer backbone with deleterious impact on the molecular weight of the final material. In order to confirm that no tertiary xanthylation occurs under the reaction conditions, we synthesized a small molecule model substrate, 4-ethyl-2,6-dimethylheptane (**S1**), and subjected it to xanthylation using xanthylamide **1**. The products of this reaction, multiple mono-xanthylated substrates that differ in site of xanthylation, were analyzed by gas chromatography against a tertiary xanthate standard (**S3**). The standard was independently synthesized via decarbonylation of the corresponding acyl xanthate to afford the single product regioisomer. In **Figure S5**, the products of xanthylation

of **S1** are shown not to contain any tertiary xanthylation product, as there was no compound eluted around 15.9 min, where the tertiary standard **S3** eluted.

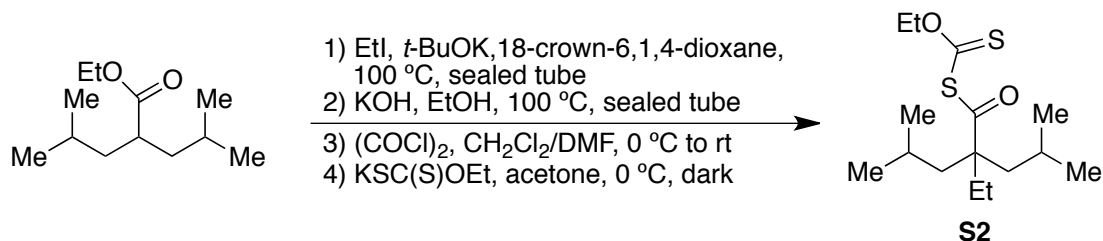


**Synthesis of model small molecule substrate 4-ethyl-2,6-dimethylheptane (3.2):** To a solution of ethyltriphenylphosphonium iodide (8.37 g, 20 mmol) in THF (66 mL) was added potassium *tert*-butoxide (2.24 g, 20 mmol) portionwise followed by 2,6-dimethylheptan-4-one (3.52 mL, 20 mmol). The resultant orange mixture was heated at reflux for 24 h, then cooled to room temperature, diluted with hexanes (100 mL), and stirred for 2 h. The mixture was passed through a pad of Celite and concentrated *in vacuo*. The product was then dissolved in hexanes, passed over a short silica pad, and concentrated *in vacuo* to yield the olefin (2.9 g, 94% yield), which was used without further purification.

To a solution of olefin (2.9 g, 18.8 mmol) in diethyl ether (2 mL) was added 10% palladium on carbon (600 mg). The reaction was pressurized with H<sub>2</sub> (9 atm) and stirred at room temperature overnight. After depressurization, the solution was passed over a pad of silica and Celite and carefully concentrated *in vacuo* to afford the alkane as a clear liquid (1.56 g, 53% yield):

**<sup>1</sup>H NMR (600 MHz, CDCl<sub>3</sub>)**  $\delta$  1.62 (dt,  $J$  = 13.6, 6.7 Hz, 2H), 1.39 – 1.32 (m, 1H), 1.28 – 1.22 (m, 2H), 1.08 (dt,  $J$  = 13.8, 6.9 Hz, 2H), 1.02 – 0.98 (m, 2H), 0.86 (d,  $J$  = 6.6 Hz, 12H), 0.82 (t,  $J$  = 7.4 Hz, 3H). **<sup>13</sup>C NMR (151 MHz, CDCl<sub>3</sub>)**  $\delta$  43.65, 33.81, 26.12, 25.20, 23.17, 22.82, 10.32. **HRGC-MS (EI)** Exact mass calcd for C<sub>9</sub>H<sub>18</sub> [M–C<sub>2</sub>H<sub>6</sub>]<sup>+</sup>, 126.1409. Found 126.1402.





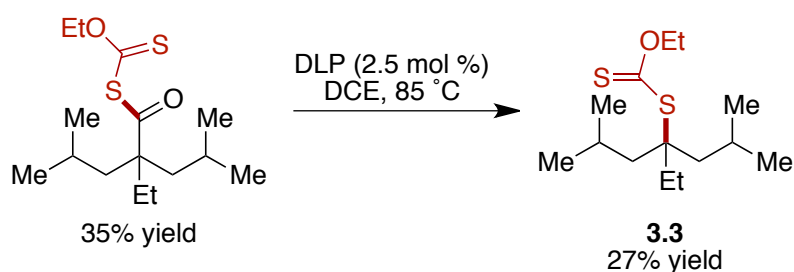
**Synthesis of tertiary xanthate standard:** To a solution of 4-methyl-2-(2-methylpropyl)-pentanoic acid ethyl ester<sup>1</sup> (1.5 g, 7.5 mmol) in 1,4-dioxane (8 mL) in a pressure tube was added 18-crown-6 (20 mg, 0.08 mmol), iodoethane (6 mL, 75 mmol), and potassium *tert*-butoxide (2.5 g, 22.5 mmol). The tube was sealed and heated at 100 °C for 16 h, then cooled to room temperature. The mixture was passed over a short silica plug and concentrated to afford the alkylated ester as a clear oil (1.7 g, 90% yield), which was used without further purification.

To a solution of the alkylated ester (1.7 g, 7.4 mmol) in ethanol (3 mL) in a pressure tube was added potassium hydroxide (2.5 g, 44.4 mmol). The tube was sealed and heated at 100 °C for 24 h, then cooled to room temperature. The mixture was washed 3x with Et<sub>2</sub>O to remove unreacted ester, acidified to pH 2 with concentrated hydrochloric acid, and then extracted 3x with Et<sub>2</sub>O. The combined organic extracts were dried with MgSO<sub>4</sub> and concentrated *in vacuo* to afford the acid as a pale brown oil (450 mg, 30% yield), which was used without further purification.

To a solution of acid (200 mg, 1 mmol) in CH<sub>2</sub>Cl<sub>2</sub> (4 mL) at 0 °C was added DMF (2 drops) followed by oxalyl chloride (169 µL, 2 mmol). The solution was warmed to room temperature and stirred for 4 h until effervescence ceased, after which it was concentrated *in vacuo*. The residue was taken up in acetone (4 mL) and cooled to 0 °C. Potassium ethyl xanthate (152 mg, 0.95 mmol) was added in one portion, and the suspension was stirred for 2 h at 0 °C and then concentrated *in vacuo*. The residue was dissolved in CH<sub>2</sub>Cl<sub>2</sub>/H<sub>2</sub>O, and the

aqueous phase was extracted 2x with CH<sub>2</sub>Cl<sub>2</sub>. The combined organic phases were washed with brine, dried with MgSO<sub>4</sub>, and concentrated *in vacuo*. The residue was purified by flash column chromatography (5% Et<sub>2</sub>O in hexanes) to afford the acyl xanthate as a bright yellow oil (105 mg, 35% yield):

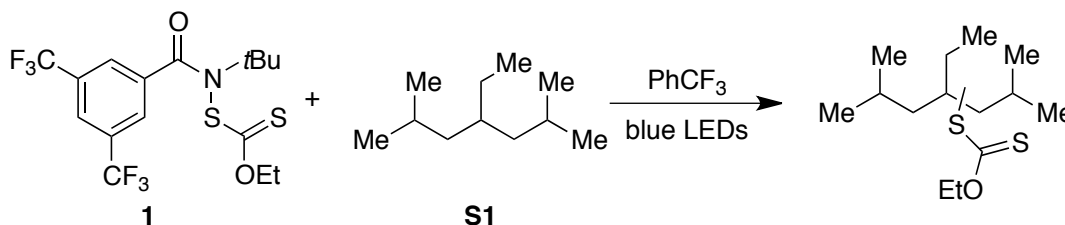
**<sup>1</sup>H NMR (400 MHz, CDCl<sub>3</sub>)** δ 4.63 (q, *J* = 7.0 Hz, 2H), 1.71 (q, *J* = 7.4 Hz, 2H), 1.65 – 1.56 (m, 3H), 1.54 (d, *J* = 6.3 Hz, 1H), 1.49 (d, *J* = 5.6 Hz, 1H), 1.47 – 1.38 (m, 4H), 0.89 (d, *J* = 6.5 Hz, 12H), 0.81 (t, *J* = 7.4 Hz, 3H). **<sup>13</sup>C NMR (101 MHz, CDCl<sub>3</sub>)** δ 205.42, 199.51, 70.78, 58.38, 44.39, 25.64, 24.54, 24.31, 24.07, 13.50, 8.01. **HRMS (ES<sup>+</sup>)** Exact mass calcd for C<sub>15</sub>H<sub>28</sub>O<sub>2</sub>S<sub>2</sub>Na [M+Na]<sup>+</sup>, 327.1423. Found 327.1418.



Acyl xanthate (50 mg, 0.16 mmol) was dissolved in 1,2-dichloroethane (0.2 mL) in an argon-filled glovebox and added dilauroyl peroxide (1.6 mg, 0.004 mmol). The vial was sealed with a Teflon-lined screw cap, sealed with Teflon tape, and placed under a balloon of argon outside the glovebox. The solution was heated at 85 °C for 30 min until bubbling ceased, after which the solution was cooled to room temperature and concentrated *in vacuo*. The residue was purified by flash column chromatography (0 – 5% Et<sub>2</sub>O in hexanes) to afford the tertiary xanthate as a pale yellow oil (12 mg, 27% yield) contaminated with an inseparable, xanthate-derived impurity. The NMR spectra are also complicated due to the presence of rotamers:

**<sup>1</sup>H NMR (400 MHz, CDCl<sub>3</sub>)** δ 4.67 – 4.65 (m, 2H), 1.81 – 1.76 (m, 4H), 1.68 – 1.64 (m, 2H), 1.50 – 1.42 (m, 8H), 0.95 (d, *J* = 6.5 Hz, 12H), 0.92 (t, *J* = 7.4 Hz, 3H).

$^{13}\text{C}$  NMR (151 MHz,  $\text{CDCl}_3$ )  $\delta$  214.86, 207.61, 71.80, 71.15, 69.40, 64.75, 44.89, 31.11, 29.86, 29.14, 25.26, 25.24, 24.67, 13.98, 13.77. **HRMS (ES+)** Exact mass calcd for  $\text{C}_{14}\text{H}_{29}\text{OS}_2$   $[\text{M}+\text{H}]^+$ , 277.1654. Found 277.1657.



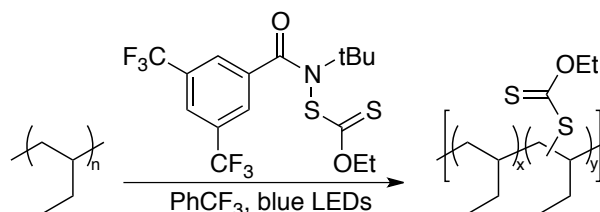
**Xanthylation of small molecule standard:** A 1 dram vial was charged with xanthylamide **1** (173 mg, 0.4 mmol), 4-ethyl-2,6-dimethylheptane **S1** (188 mg, 1.2 mmol), and  $\text{PhCF}_3$  (0.4 mL) in an argon-filled glovebox. The vial was fitted with a PTFE lined screw cap, sealed with Teflon tape, and removed from the glovebox. The vial suspended above an Ecoxotic PAR38 23 W blue LED such that the bottom of the vial was directly aligned with and 1 cm above one of the five LEDs, and the apparatus was covered with aluminum foil. The reaction was irradiated for 15 h and then diluted with  $\text{CH}_2\text{Cl}_2$  for GC analysis.

### Synthesis of Xanthylated Polyolefins via C–H Xanthylation

**General Procedure A (room temperature reactions):** The required amount of polyolefin, xanthylamide, and trifluorotoluene were added to a 1 dram reaction vial equipped with a magnetic stir bar under inert atmosphere. The reaction vial was sealed and placed on a magnetic stir plate. Two Kessil-brand “Tuna Blue” aquarium lights were placed 2 inches from the vial (Figure S6) and the reaction mixture was irradiated for 19h with the apparatus covered by aluminum foil. After completion of the reaction, the solution was concentrated *in vacuo* and precipitated in cold MeOH to yield the xanthylated polyolefin as a viscous liquid.

**General Procedure B (heated reactions neat or with solvent):** The required amount of polyolefin, xanthylamide, and optionally solvent were added to a 1 dram reaction vial

equipped with a magnetic stir bar under inert atmosphere. The reaction vial was sealed and placed on a magnetic stir plate in a small beaker of oil at the desired temperature (Figure S6). Two Kessil-brand “Tuna Blue” aquarium lights were placed 2 inches from the vial and the reaction mixture was irradiated for 19h with the apparatus covered by aluminum foil. After completion of the reaction, the solution was concentrated *in vacuo* and precipitated in cold MeOH to yield the xanthylated polyolefin as a viscous liquid.



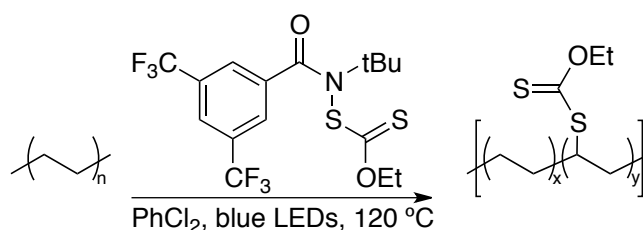
**Xanthylated Polyethylethylene:** Polyethylethylene ( $M_n = 3.6$  kg/mol, PDI = 1.23) and xanthylamide were reacted according to General Procedure A or B, both conditions yielded similar material (Figure S8). Polyethylethylene (56 mg, 0.89 mmol repeat unit) reacted with xanthylamide (193 mg, 0.45 mmol) in trifluorotoluene (2.25 mL) upon blue light irradiation for 19h. The resulting material was 15 mol % xanthylated polyethylethylene. Similar characterization data was obtained using other stoichiometric ratios of xanthylamide to repeat unit. See accompanying tables and figures for more information.

The following was gathered using 15 mol % xanthylated polyethylethylene:

**<sup>1</sup>H NMR (600 MHz, CDCl<sub>3</sub>)** δ 4.64 (bs), 3.98 (bs), 3.77 (bs), 3.69 (bs), 3.10 (bs), 1.64 (bs), 1.41 (t, J = 1 Hz), 1.25 (bs), 1.05 (bs), 0.83 (bs). **<sup>13</sup>C NMR (125 MHz, CDCl<sub>3</sub>)** δ 215.1, 69.6, 69.4, 41.4, 39.2, 39.0, 38.9, 38.5, 38.4, 37.9, 36.5, 36.1, 36.1, 36.1, 36.0, 34.7, 34.6, 33.8, 33.5, 33.4, 33.1, 32.9, 32.0, 31.6, 30.7, 30.3, 29.8, 29.4, 29.1, 29.0, 28.9, 28.6, 27.7, 26.9, 26.8, 26.7, 26.4, 26.1, 26.0, 25.9, 25.3, 23.3, 23.2, 22.7, 22.7, 22.6, 20.7, 20.5, 18.8, 14.3,

14.2, 14.1, 13.8, 12.0, 11.5, 10.9, 10.7, 10.5, 10.3, 10.2. **IR (neat, ATR,  $\text{cm}^{-1}$ )** 735, 907, 1007, 1051, 1111, 1143, 1210, 1279, 1379, 1461, 2855, 2874, 2918, 2959. **GPC (THF)**  $M_n$  = 4.8 kg/mol, PDI = 1.32, UV-Vis (nm) = 224, 283 at 33 min. **DSC ( $^{\circ}\text{C}$ ):**  $T_g$  =  $-27^{\circ}\text{C}$ .

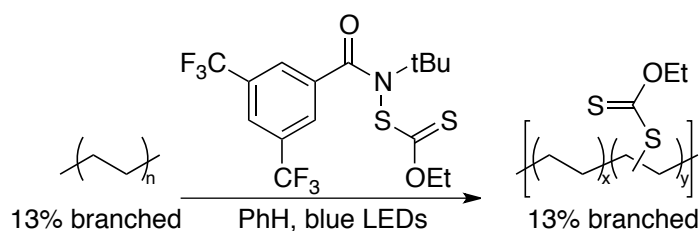
**Determination of percent functionalization of polyethylethylene:** Upon purification, the percent xanthylation of polyethylethylene can be determined through integration of the  $^1\text{H}$  NMR. Considering the composition of the polymer, the peaks between 0.8 – 1.6 ppm were set to total to 8 protons. The methylene protons of the ethoxy group that appear at 4.6 ppm are used to determine mol % xanthylation per repeat unit. Regioselectivity is determined by integration of the two signals corresponding to primary and secondary xanthylation. For instance, protons *alpha* to primary xanthates appear between 3.0 – 3.5 ppm and protons *alpha* to secondary xanthates appear between 3.5 – 4.0 ppm.



**Xanthylated Polyethylene:** Polyethylene ( $M_n$  = 4.5 kg/mol, PDI = 2.13, 50 mg, 1.79 mmol repeat unit) and xanthylamide (77 mg, 0.179 mmol) were reacted according to General Procedure B in dichlorobenzene (3.6 mL). The reaction yielded 9 mol % xanthylated polyethylene:

**$^1\text{H}$  NMR (600 MHz,  $\text{CDCl}_3$ )**  $\delta$  4.64 (q,  $J$  = 1 Hz), 3.69 (bs), 1.64 (bs), 1.57 (d,  $J$  = 3 Hz), 1.42 (t,  $J$  = 1 Hz), 1.38 (bs), 1.25 (bs), 0.89 (bs), 0.83 (bs).  **$^{13}\text{C}$  NMR (125 MHz,  $\text{CDCl}_3$ )**  $\delta$  215.2, 69.6, 51.5, 34.1, 29.8, 29.7, 29.6, 28.8, 26.8, 13.9. **IR (neat, ATR,  $\text{cm}^{-1}$ )** 2925, 2853, 1464, 1207, 1111, 1047. **GPC (TCB,  $140^{\circ}\text{C}$ )**  $M_n$  = 4.7 kg/mol, PDI = 2.20.

**Determination of percent functionalization of polyethylene:** Upon purification, the percent xanthylation of polyethylene can be determined through integration of the  $^1\text{H}$  NMR. Considering the composition of the polymer, the peaks between 0.8 – 1.6 ppm were set to total to 4 protons. The methylene protons of the ethoxy unit that appear at 4.6 ppm are used to determine mol % xanthylation per repeat unit.



**Xanthylated Hyperbranched Polyethylene:** Hyperbranched polyethylene<sup>4</sup> ( $M_n = 29$  kg/mol, PDI = 1.56, mg, 1.07 mmol repeat unit, 13% branched) and xanthylamide (23 mg, 0.05 mmol) were added to a reaction vial with a stir bar. The mixture was submitted to the glove box, where dry benzene was added (0.3 mL). The mixture was then stirred and irradiated with Kessil blue lights for 19h. The polymer was purified via precipitation in cold MeOH to yield xanthylated polyolefin. Similar characterization data was obtained using other stoichiometric ratios of xanthylamide to repeat unit. See accompanying tables and figures for more information.

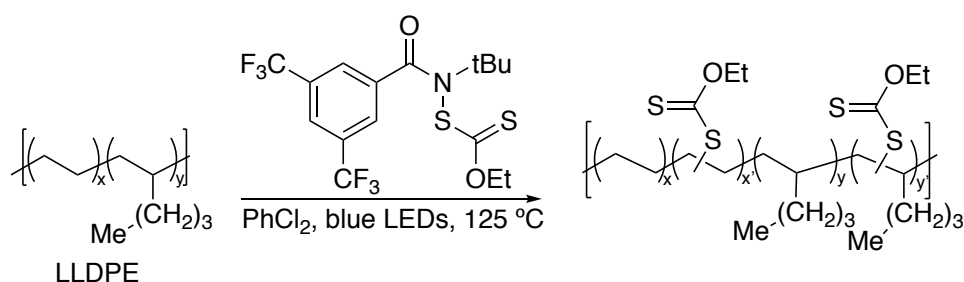
The following was gathered for 3 mol % xanthylated hyperbranched polyethylene:

**$^1\text{H}$  NMR (600 MHz,  $\text{CDCl}_3$ )**  $\delta$  4.64 (s), 3.78 (bs), 3.70 (bs), 3.13 (bs), 1.64 (bs), 1.56 (s), 1.51 (s), 1.42 (s), 1.22 (bs), 1.09 (bs), 0.89 (s), 0.84 (s).  **$^{13}\text{C}$  NMR (125 MHz,  $\text{CDCl}_3$ )**  $\delta$  215.1, 77.3, 77.0, 76.8, 69.5, 45.9, 39.3, 38.9, 37.8, 37.4, 37.2, 36.8, 36.7, 34.9, 34.4, 34.2, 33.7, 33.4, 33.3, 32.8, 32.4, 32.0, 32.0, 30.2, 30.1, 29.9, 29.8, 29.5, 29.4, 29.0, 28.8, 27.6, 27.2, 26.8, 25.9, 25.5, 23.8, 23.2, 23.1, 22.7, 20.5, 19.8, 19.3, 14.6, 14.2, 13.8, 11.4, 10.9. **IR**

(neat, ATR,  $\text{cm}^{-1}$ ) 2945, 2922, 2853, 1459, 1377, 1209, 1118, 1065, 1052, 722. GPC (THF)

$M_n = 34 \text{ kg/mol}$ , PDI = 1.66, UV-Vis (nm) = 228, 283 at 28 min.

**Determination of percent functionalization of hyperbranched polyethylene:** Upon purification, the percent xanthylation of hyperbranched polyethylene can be determined through integration of the  $^1\text{H}$  NMR. Considering the composition of the polymer, the peaks between 0.8 – 1.6 ppm were set to total to 4 protons. The methylene protons of the ethoxy unit that appear at 4.6 ppm are used to determine mol % xanthylation per repeat unit.

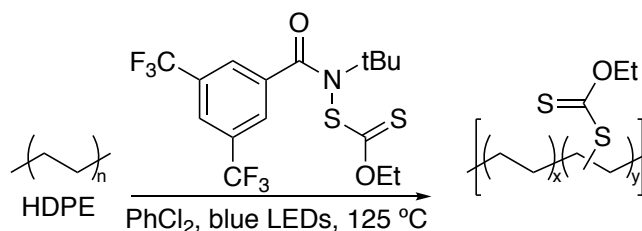


**Xanthylated Linear Low Density Polyethylene:** DOW<sup>TM</sup> DNDA-1081 NT 7 Linear Low Density Polyethylene Resin ( $M_n = 8.1 \text{ kg/mol}$ , PDI = 3.77, 112 mg, 3.29 mmol repeat unit) and xanthylamide (143 mg, 0.329 mmol) were reacted according to General Procedure B in dichlorobenzene (6.6 mL). The material was washed with THF three times to purify the polyolefin rather than purifying by precipitation. The reaction yielded 4 mol % xanthylated linear low density polyethylene:

$^1\text{H}$  NMR (500 MHz,  $\text{C}_2\text{D}_2\text{Cl}_4$ , 110 °C)  $\delta$  4.73 (bs), 3.75 (bs), 1.73 (bs), 1.55 (bs), 1.47 (bs), 1.34 (bs), 0.96 (bs). IR (neat, ATR,  $\text{cm}^{-1}$ ) 3325, 2919, 2850, 1647, 1551, 1464, 1380, 1366, 1301, 1278, 1208, 1151, 1145, 1110, 1050, 720. GPC (TCB, 150 °C)  $M_n = 13 \text{ kg/mol}$ , PDI = 3.58.

**Determination of percent functionalization of linear low density polyethylene:** Upon purification, the percent xanthylation of linear low density polyethylene can be determined

through integration of the  $^1\text{H}$  NMR. Considering the composition of the polymer, the peaks between 0.9 – 1.8 ppm were set to total to 4 protons. The methylene protons of the ethoxy unit that appear at 4.6 ppm are used to determine mol % xanthylation per repeat unit.

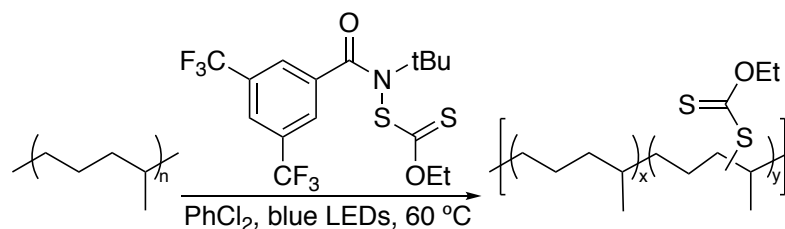


**Xanthylated High Density Polyethylene:** ExxonMobil<sup>TM</sup> High Density Polyethylene ( $M_n$  = 15.0 kg/mol, PDI = 3.25, 89 mg, 3.18 mmol repeat unit) and xanthylamide (138 mg, 0.318 mmol) were reacted according to General Procedure B in dichlorobenzene (6.4 mL). The material was washed with THF three times to purify the polyolefin rather than purifying by precipitation. The reaction yielded 5 mol % xanthylated high density polyethylene:

$^1\text{H}$  NMR (500 MHz,  $\text{C}_2\text{D}_2\text{Cl}_4$ , 110 °C)  $\delta$  4.72 (bs), 3.75 (bs), 1.73 (bs), 1.47 (bs), 1.35 (bs), 0.96 (bs). IR (neat, ATR,  $\text{cm}^{-1}$ ) 2917, 2849, 1466, 1464, 1207, 1144, 1110, 1049, 720. GPC (TCB, 150 °C)  $M_n$  = 15.4 kg/mol, PDI = 4.13.

**Determination of percent functionalization of high density polyethylene:** Upon purification, the percent xanthylation of high density polyethylene can be determined through integration of the  $^1\text{H}$  NMR. Considering the composition of the polymer, the peaks between 0.9 – 1.8 ppm were set to total to 4 protons. The methylene protons of the ethoxy unit that appear at 4.6 ppm are used to determine mol % xanthylation per repeat unit.



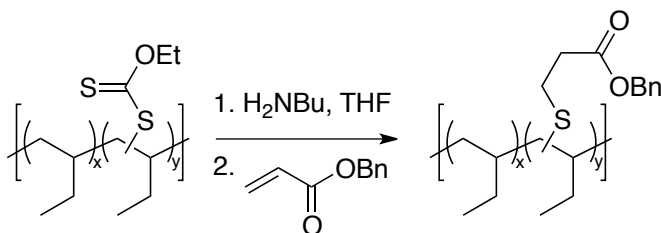


**Xanthylated Ethylene/Propylene Copolymer:** Kraton™ G1750 VO ethylene/propylene copolymer ( $M_n = 463$  kg/mol, PDI = 1.13, 37 mg, 0.5 mmol repeat unit), xanthylamide (23 mg, 0.05 mmol), and dichlorobenzene (2.0 mL) were added to a one dram reaction vial equipped with a magnetic stir bar under inert atmosphere. The reaction vial was sealed and placed on a magnetic stir plate in a small beaker of oil at 60 °C, suspended 1 inch above the hot plate. Two Kessil-brand “Tuna Blue” aquarium lights were placed 2 inches from the oil bath and the reaction mixture was irradiated for 16h. After completion of the reaction, the solution was precipitated in cold MeOH to yield the xanthylated polyolefin. The reaction yielded 3 mol % xanthylated ethylene/propylene copolymer:

**$^1\text{H}$  NMR (600 MHz,  $\text{CDCl}_3$ )**  $\delta$  4.64 (q), 3.85 (bs), 3.79 (bs), 3.74 (bs), 3.14 (bs), 1.68 (bs), 1.59 (bs), 1.37 (bs), 1.25 (bs), 1.07 (bs), 0.84 (bs), 0.07 (bs). **IR (neat, ATR,  $\text{cm}^{-1}$ )** 2939, 2926, 2859, 1463, 1378, 1262, 1212, 1116, 1112, 1052, 804, 739. **GPC (THF)**  $M_n = 490$  kg/mol, PDI = 1.23, UV-Vis (nm) = 228, 283 at 24 min.

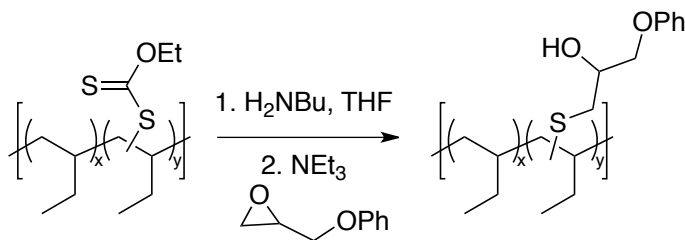
**Determination of percent functionalization of ethylene/propylene copolymer:** Upon purification, the percent xanthylation of poly(ethylene-*alt*-propylene) can be determined through integration of the  $^1\text{H}$  NMR. Considering the composition of the polymer, the peaks between 0.8 – 1.7 ppm were set to total to 10 protons. The methylene protons of the ethoxy unit that appear at 4.6 ppm are used to determine mol % xanthylation per repeat unit.

#### Further Derivatization of Xanthate Products



**Thiol-acrylate procedure:** A solution of 13 mol % xanthylated polyethylethylene (66 mg, 0.15 mmol xanthate) in 1 mL THF and butylamine were separately degassed with argon for 30 min. Butylamine (38  $\mu$ L, 0.38 mmol) was added to the polymer solution at room temperature and allowed to stir at room temperature overnight. Benzyl acrylate (0.11 mL, 0.77 mmol) was degassed with argon for 30 min and then added to the solution. The mixture was left to stir overnight at room temperature. The reaction was concentrated *in vacuo* and the desired polymer was collected through precipitation in cold MeOH:

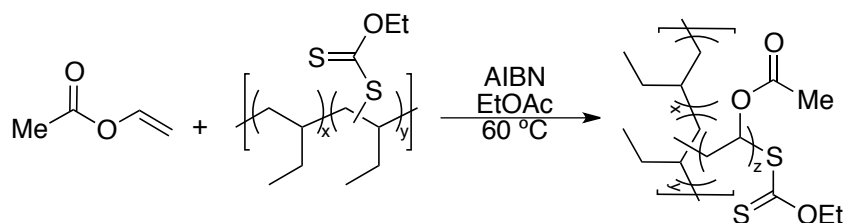
**$^1\text{H}$  NMR (600 MHz,  $\text{CDCl}_3$ )**  $\delta$  7.35 (m, 5H,  $J = 3$  Hz), 5.14 (s, 2H), 2.79 (bs, 2H), 2.65 (bs, 2H), 1.27 (bs), 0.89 (t), 0.84 (bs).  **$^{13}\text{C}$  NMR (125 MHz,  $\text{CDCl}_3$ )**  $\delta$  172, 136, 129, 128.4, 128.3, 128.2, 66, 49, 39, 38, 36, 35, 33, 32, 27, 26, 25, 23, 14, 11, 10. **IR (neat, ATR,  $\text{cm}^{-1}$ )** 696, 735, 751, 803, 1029, 1140, 1183, 1215, 1238, 1279, 1347, 1379, 1459, 1740, 2855, 2874, 2919, 2959. **GPC (THF)**  $M_n = 5.9$  kg/mol, PDI = 1.32, UV-Vis (nm) = 214 at 33 min.



**Thiol-epoxy procedure:** To a 1-dram vial, 13 mol % xanthylated polyethylethylene (84 mg, 0.20 mmol xanthate) in THF (1 mL) was added and degassed with argon for 30 min. Degassed butylamine (48  $\mu$ L, 0.49 mmol) was added to the solution. The reaction was stirred at room temperature for 20 hours. Glycidyl phenyl ether (0.14 mL, 0.98 mmol) and

triethylamine (0.14 mL, 0.98 mmol) were degassed and added to the reaction and stirred at room temperature for 24 h. The solution was concentrated *in vacuo* and precipitated in MeOH to afford the desired polymer:

**<sup>1</sup>H NMR (CDCl<sub>3</sub>, 600 MHz)** δ 7.28 (t, 2H, J = 1 Hz), 6.96 (t, 1H, J = 1 Hz), 6.92 (d, 2H, J = 1 Hz), 4.07 (bs, 1H), 4.04 (bs, 2H), 3.38 (bs, 0.15H), 2.92 (t, 0.23H), 2.84 (bs, 0.92H), 2.77 (t, 0.41H), 2.72 (bs, 0.88H), 2.55 (bs, 0.33H), 1.59 (bs, 2H), 1.25 (bs, 43H), 1.05 (bs, 13H), 0.82 (bs, 27H). **<sup>13</sup>C NMR (CDCl<sub>3</sub>, 125 MHz)** δ 158, 130, 121, 115, 70, 69, 50, 45, 39, 38, 36, 33, 27, 26, 23, 14, 11, 10. **IR (neat, ATR, cm<sup>-1</sup>):** 690, 747, 752, 815, 910, 1043, 1079, 1143, 1173, 1245, 1280, 1300, 1380, 1461, 1496, 1589, 1601, 2856, 2874, 2921, 2959. **GPC (THF):** M<sub>n</sub> = 6.5 kg/mol, PDI = 1.28, UV-Vis (nm) = 272 at 33 min.



**RAFT polymerization of vinyl acetate:** A reaction vial was charged with vinyl acetate (0.90 mL, 9.79 mmol), AIBN (2.5 mg, 0.015 mmol), and 14 mol % xanthylated polyethylethylene (63 mg, 0.15 mmol xanthate) in EtOAc (0.9 mL) and degassed by 4 freeze-pump-thaw cycles. The reaction was sealed and placed in an oil bath at 60 °C. After 18 h, the reaction was stopped by cooling in an ice bath. The reaction was concentrated *in vacuo* and the resulting polymer was purified through multiple washes with hexanes to yield a clear, viscous oil:

**<sup>1</sup>H NMR (600 MHz, CDCl<sub>3</sub>)** δ 4.91 (bs), 4.85 (bs), 4.61 (bs), 2.00 (t, J = 2 Hz), 1.82 (bs), 1.82 (bs), 1.73 (bs), 1.23 (bs), 0.94 (bs), 0.86 (d, J = 1 Hz), 0.82 (t, J = 1 Hz), 0.80 (bs). **<sup>13</sup>C NMR (125 MHz, CDCl<sub>3</sub>)** δ 170.5, 170.4, 170.3, 170.3, 68.0, 67.9, 66.9, 66.7, 66.7, 66.6,

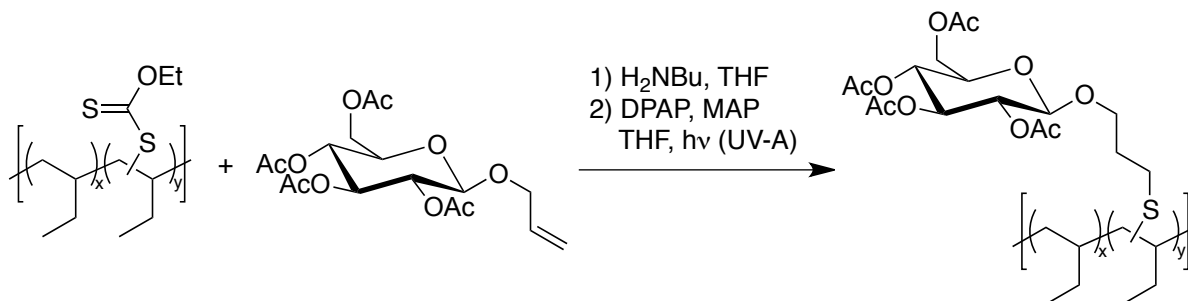
66.3, 66.0, 39.9, 39.5, 39.1, 38.7, 36.0, 34.6, 34.5, 33.4, 31.6, 29.0, 25.3, 25.2, 22.6, 21.1, 21.0, 20.9, 20.8, 20.7, 18.8, 14.1, 13.8, 11.4. **IR (neat, ATR,  $\text{cm}^{-1}$ )** 606, 632, 735, 797, 947, 1020, 1045, 1112, 1230, 1371, 1437, 1732, 2855, 2872, 2925, 2961. **GPC (THF)**  $M_n$  = 16.7 kg/mol, PDI = 2.00, UV-Vis (nm) = 221, 282 at 33 min. **DSC ( $^{\circ}\text{C}$ , 40  $^{\circ}\text{C}/\text{min}$ )**  $T_g$  (2 observed) = -50.64 and 26.37  $^{\circ}\text{C}$ .



**Trifluoromethylthiolation procedure:** In a 2-dram vial, 12 mol % xanthylated polyethylethylene (50 mg, 0.084 mmol xanthate), ((2-phenylpropan-2-yl)oxy)(trifluoromethyl)sulfane<sup>5</sup> (60 mg, 0.25 mmol), and dilauroyl peroxide (16 mg, 0.04 mmol) were dissolved in chlorobenzene (4 mL) in an argon-filled glovebox. The vial was sealed with a Teflon-lined screw cap, sealed with Teflon tape, and heated at 100  $^{\circ}\text{C}$  under a balloon of argon. Additional dilauroyl peroxide (16 mg, 0.04 mmol) was added every 30 minutes for a total of eight additions. After the last addition, the reaction mixture was heated for an additional 30 minutes, then cooled to room temperature and concentrated *in vacuo*. The polymer was purified via precipitation three times from methanol to afford trifluoromethylthiolated polyethylethylene as a yellow solid (29 mg, 60% yield):

**$^1\text{H}$  NMR (600 MHz,  $\text{CDCl}_3$ )**  $\delta$  3.48 (bs), 3.26 (q,  $J$  = 7.66 Hz), 1.56 (bs), 1.25 (bs), 1.05 (bs), 0.83 (bs).  **$^{13}\text{C}$  NMR (151 MHz,  $\text{CDCl}_3$ )**  $\delta$  134.57, 132.79, 132.54, 130.77, 130.52, 125.16, 39.29, 39.25, 39.19, 39.10, 39.02, 38.97, 38.63, 38.53, 36.23, 36.19, 36.17, 36.14, 33.63, 33.53, 33.49, 32.09, 32.08, 31.11, 30.87, 29.86, 29.82, 29.81, 29.53, 26.79, 26.55, 26.14, 26.03, 25.95, 23.35, 22.86, 14.30, 10.83, 10.79, 10.75, 10.72, 10.62, 10.45, 10.34.  **$^{19}\text{F}$**

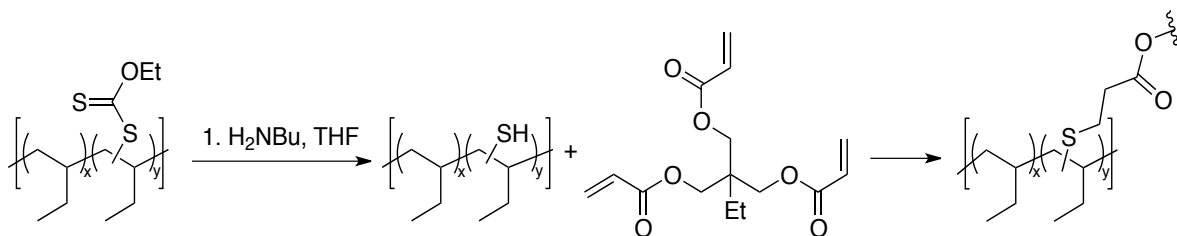
**NMR (376 MHz, CDCl<sub>3</sub>)**  $\delta$  -39.41, -39.56, -39.81, -39.86, -39.88, -40.20, -40.25, -40.34, -41.93, -41.96. **IR (neat, ATR, cm<sup>-1</sup>)** 2962, 2924, 2857, 1463, 1381, 1264, 1114, 742. **GPC (THF)**  $M_n$  = 5.2 kg/mol, PDI = 1.22, UV-Vis (nm) = 212 at 33 min.



**Thiol-ene procedure:** In a 1-dram vial, 11 mol % xanthylated polyethylethylene (60 mg, 0.095 mmol xanthate) was dissolved in THF (1 mL) in an argon-filled glovebox. The vial was fitted with a rubber septum, sealed with Teflon tape, and removed from the glovebox. Butylamine (94  $\mu$ L, 0.95 mmol) was added, causing a deep yellow color to persist. The solution was stirred for 20 h and then concentrated to dryness *in vacuo* and further dried via high-vacuum. The vial was brought back into the glovebox, and the residue was added to a 20 mL scintillation vial containing the allyl glycoside<sup>6</sup> (111 mg, 0.29 mmol), 2,2-dimethoxy-2-phenylacetophenone (2.3 mg, 0.009 mmol), 4'-methoxyacetophenone (1.4 mg, 0.009 mmol), and THF (15 mL). The scintillation vial was sealed with Teflon tape, removed from the glovebox, and irradiated with UV-A light for 24 h. The solution was concentrated *in vacuo* and washed with methanol ten times to afford the thiol-ene polymer adduct as a yellow solid (38 mg, 43% yield):

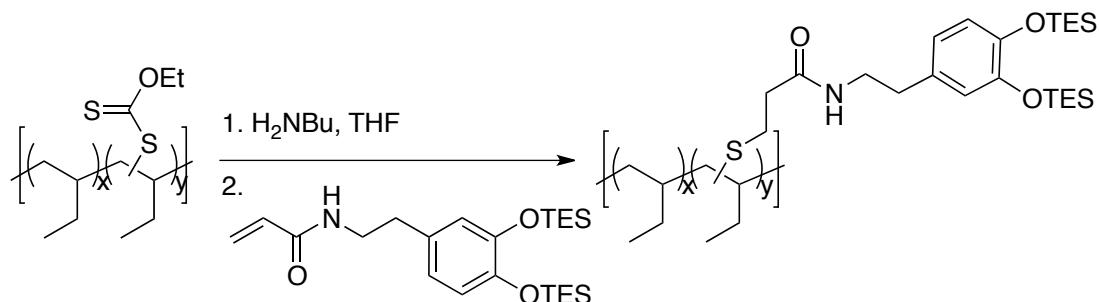
**<sup>1</sup>H NMR (600 MHz, CDCl<sub>3</sub>)**  $\delta$  5.23 – 5.16 (m), 5.12 – 5.03 (m), 5.01 – 4.95 (s), 4.55 (d,  $J$  = 8.0 Hz), 4.49 (d,  $J$  = 8.0 Hz), 4.34 (dd,  $J$  = 13.2, 4.8 Hz), 4.29 – 4.24 (m), 4.12 (dd,  $J$  = 11.1, 3.5 Hz), 3.93 (bs), 3.71 – 3.66 (m), 3.62 (bs), 3.48 (bs), 2.54 (bs), 2.08 (s), 2.04 (s), 2.02 (s), 2.00 (s), 1.25 (bs), 1.04 (bs), 0.82 (bs). **<sup>13</sup>C NMR (126 MHz, CDCl<sub>3</sub>)**  $\delta$  170.81, 170.42,

169.54, 169.47, 101.10, 99.69, 72.99, 71.93, 71.43, 70.17, 68.55, 62.07, 51.02, 39.20, 38.59, 36.23, 33.59, 30.86, 29.86, 26.75, 26.11, 23.34, 20.89, 20.82, 20.76, 14.34, 10.79, 10.50. **IR** ( $\text{cm}^{-1}$ ) 2962, 2926, 1758, 1464, 1381, 1226, 1045. **GPC (THF)**  $M_n$  = 6.2 kg/mol, PDI = 1.32, UV-Vis (nm) = 212 at 33 min.



**Thiol-triacrylate procedure:** With a trifunctional acrylate, the goal was to generate a perfectly elastomeric network of the polyolefin. A solution of 14 mol % xanthylated polyethylethylene (50 mg, 0.098 mmol xanthate, 1 equiv) in THF (0.7 mL) was degassed with argon for 30 min. Degassed butylamine (12  $\mu\text{L}$ , 0.12 mmol, 1.2 equiv) was added to the reaction mixture and allowed to stir at RT overnight. Trimethylolpropane triacrylate (11  $\mu\text{L}$ , 0.039 mmol, 1.2 equiv per functional group) was degassed with argon for 30 min and then added to the solution. The mixture was left to stir overnight at RT. The reaction was concentrated *in vacuo*. After the reaction, the resulting material was an insoluble polymer network. Analysis by IR confirmed the expected carbonyl peaks and the lack of xanthate absorbances, demonstrating that the desired reaction went to completion.  $^1\text{H}$  and  $^{13}\text{C}$  NMR could not be conducted as the material was insoluble in all solvents:

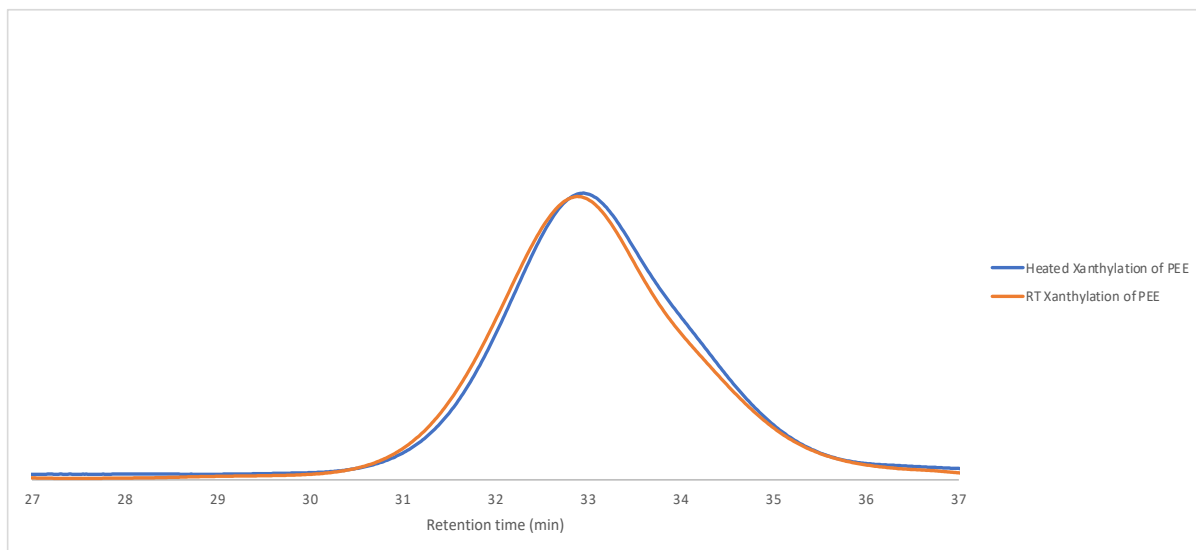
**IR (neat, ATR,  $\text{cm}^{-1}$ ):** 2959, 2915, 2858, 2855, 1740, 1461, 1379, 1279, 1241, 1174, 1142, 1070, 1016, 994, 913, 782.



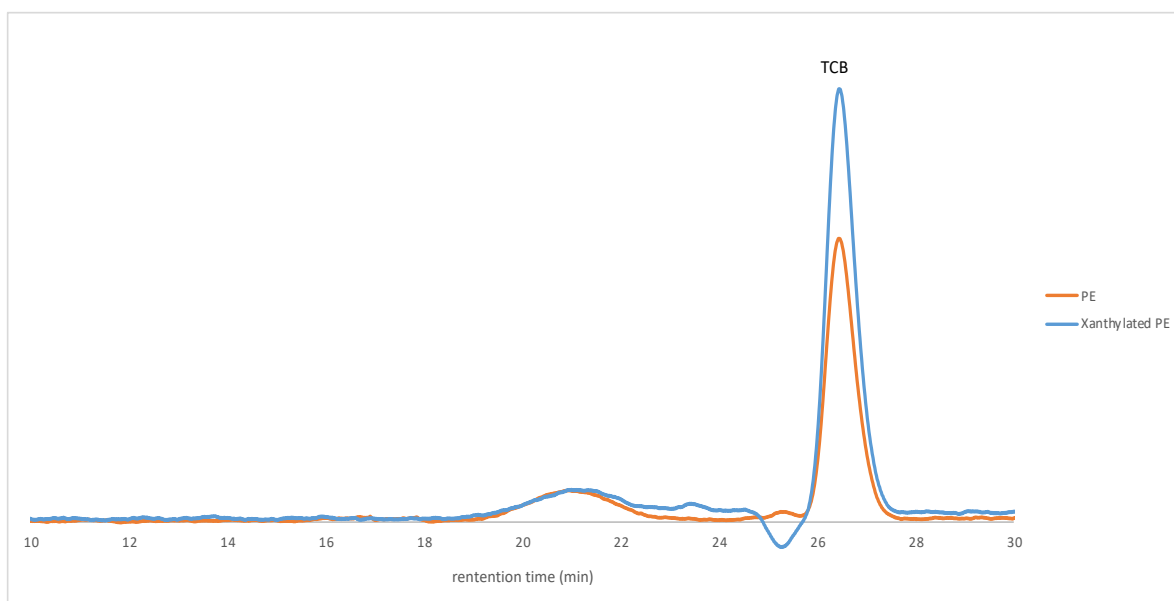
**Thiol-acrylamide procedure:** A solution of 14 mol % xanthylated polyethylethylene (47 mg, 0.11 mmol xanthate) in THF (0.8 mL) was bubbled with argon for 30 min. Degassed butylamine (28  $\mu\text{L}$ , 0.29 mmol) was added to the reaction mixture and the solution was allowed to stir RT overnight. TES-protected N-(2-[3,4-dihydroxyphenyl]ethyl)acrylamide<sup>6</sup> (249 mg, 0.57 mmol) in THF (0.5 mL) was degassed with argon for 30 min and then added to the solution. The mixture was left to stir overnight at RT. The reaction was concentrated *in vacuo*. The desired polymer was collected through precipitation in cold MeOH as a clear, viscous oil:

**$^1\text{H}$  NMR (600 MHz,  $\text{CDCl}_3$ )**  $\delta$  6.73 (m,  $J = 2$  Hz), 6.63 (m,  $J = 2$  Hz), 3.66 (bs), 3.45 (bs), 2.89 (bs), 2.83 (bs), 2.77 (bs), 2.68 (bs), 2.51 (bs), 2.39 (bs), 1.60 (bs), 1.25 (bs), 1.05 (bs), 0.98 (bs), 0.83 (bs), 0.76 (bs), 0.74 (bs), 0.73 (bs).  **$^{13}\text{C}$  NMR (125 MHz,  $\text{CDCl}_3$ )**  $\delta$  146.8, 121.0, 120.5, 39.1, 38.4, 36.1, 33.4, 30.7, 29.7, 26.0, 23.2, 14.2, 10.4, 6.7, 5.1, 5.1, 1.0. **IR ( $\text{cm}^{-1}$ )** 2959, 2918, 2874, 2854, 1740, 1649, 1512, 1461, 1379, 1279, 1279, 1262, 1240, 1143, 1052, 1019, 801, 749. **GPC (THF)**  $M_n = 6.7$  kg/mol, PDI = 1.44, UV-Vis (nm) = 225, 280 at 33 min.

## GPC Overlays



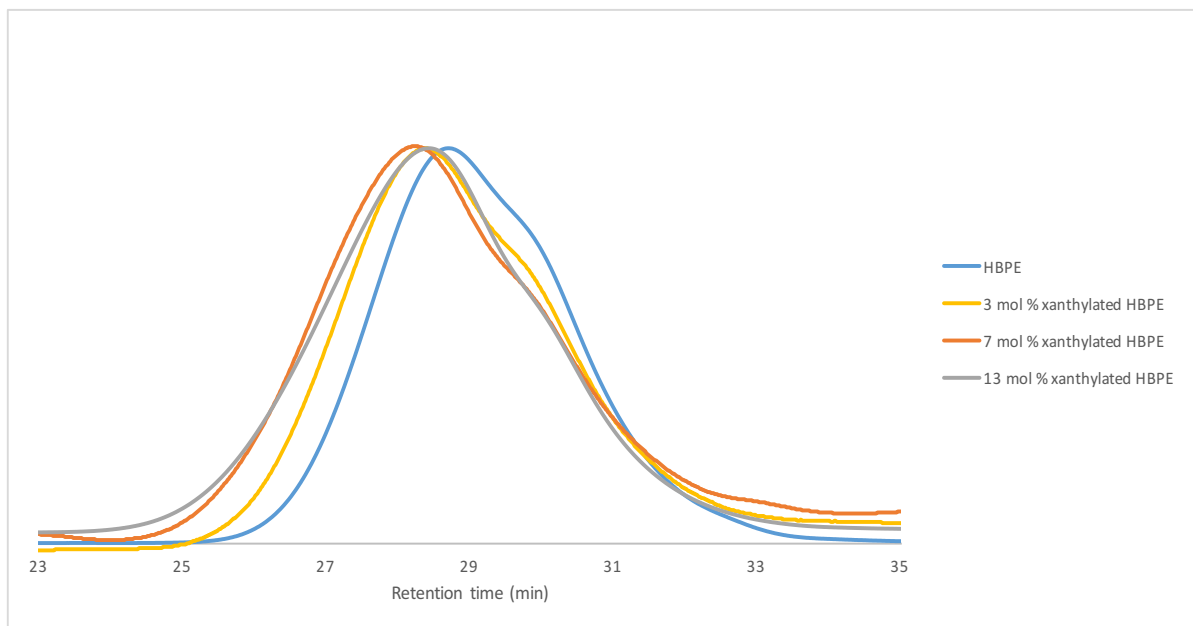
GPC overlay of polyethylethylene after xanthylation reaction at room temperature (orange,  $M_n = 4.5$  kg/mol, PDI = 1.31) or at 120 °C in 1,2-dichlorobenzene (blue,  $M_n = 4.6$  kg/mol, PDI = 1.33). Heating the reaction mixture did not significantly alter the molecular weight or dispersity. This indicates that General Procedure A and General Procedure B deliver similar polymer products.



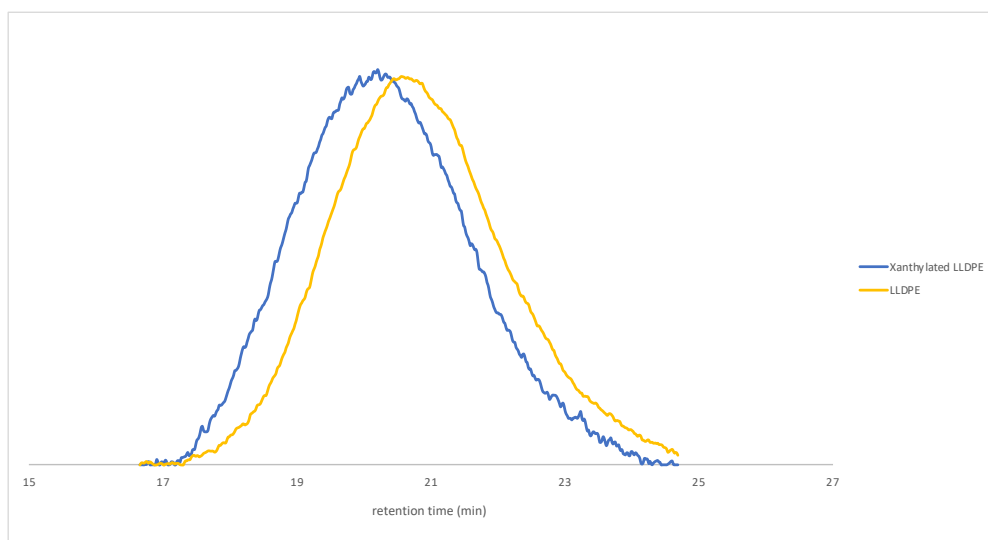
High temperature size exclusion chromatography of low molecular weight polyethylene. At a



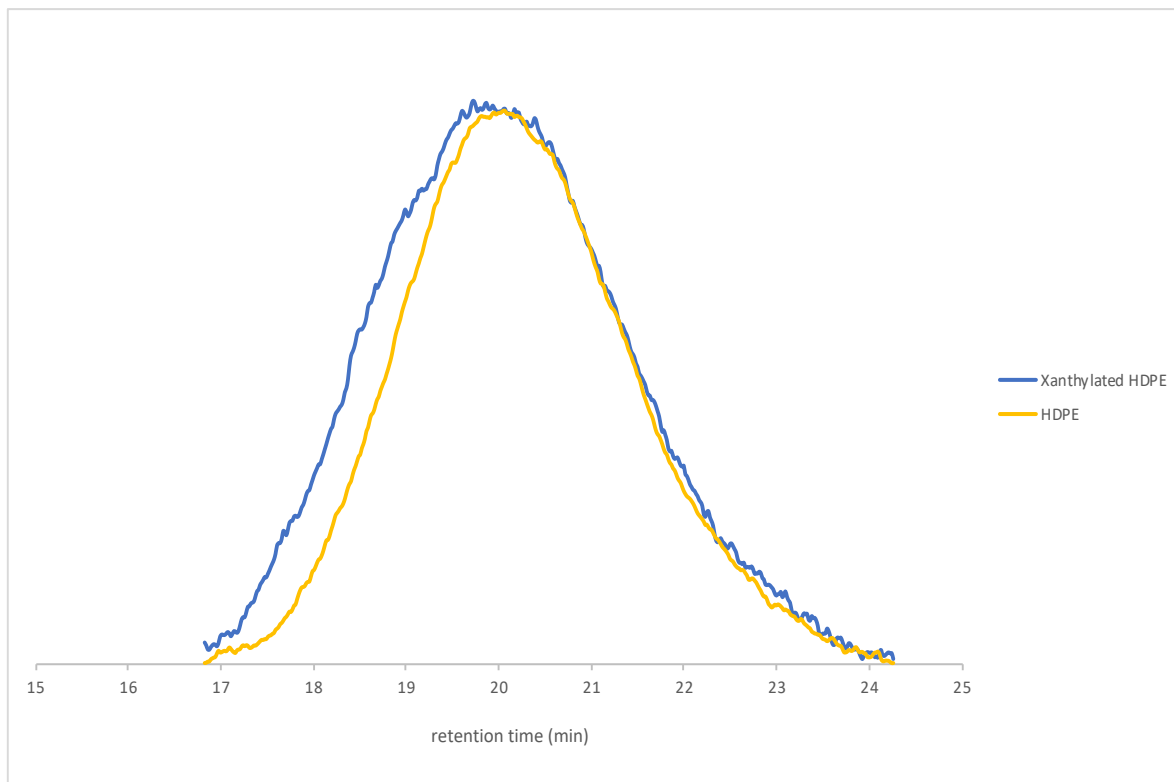
retention time of 21 min, high temperature GPC at 140 °C in TCB of polyethylene after xanthylation ( $M_n = 4.7$  kg/mol, PDI = 2.2) mimics the same molecular weight distribution as the parent material ( $M_n = 4.5$  kg/mol, PDI = 2.1).



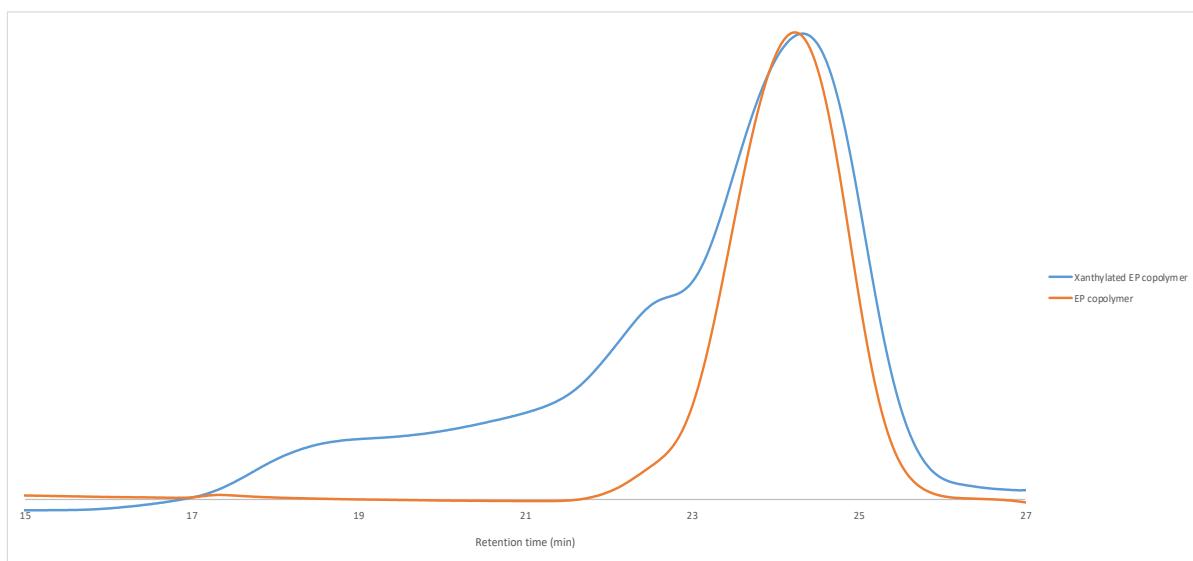
Xanthylated hyperbranched polyethylene ( $M_n = 29$  kg/mol, PDI = 1.56) shifted to a higher molecular weight upon 3 mol % xanthylation ( $M_n = 34$  kg/mol, PDI = 1.66) and 7 mol % xanthylation ( $M_n = 36$  kg/mol, PDI = 1.82), but maintained nearly the same MWD.



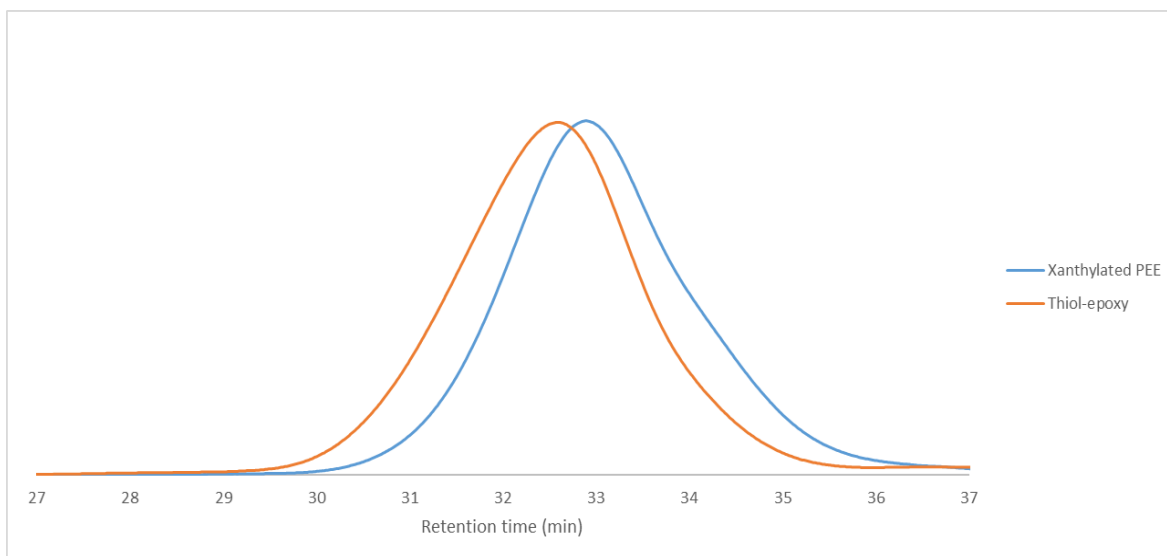
High temperature size exclusion chromatography of LLDPE before and after xanthylation. High temperature GPC at 150 °C in TCB of linear low density polyethylene ( $M_n = 8.1$  kg/mol, PDI = 3.77, left) reveals that upon xanthylation the molecular weight distribution of the polyolefin is retained ( $M_n = 13$  kg/mol, PDI = 3.58, right). This indicates that C–H xanthylation is a viable post-polymerization modification for commodity polyolefins.



High temperature size exclusion chromatography of HDPE before and after xanthylation. High temperature GPC at 150 °C in TCB of high density polyethylene prior to xanthylation ( $M_n = 15.0$  kg/mol, PDI = 3.25, left) and after xanthylation have very similar molecular weight distributions ( $M_n = 15.4$  kg/mol, PDI = 4.13, right).

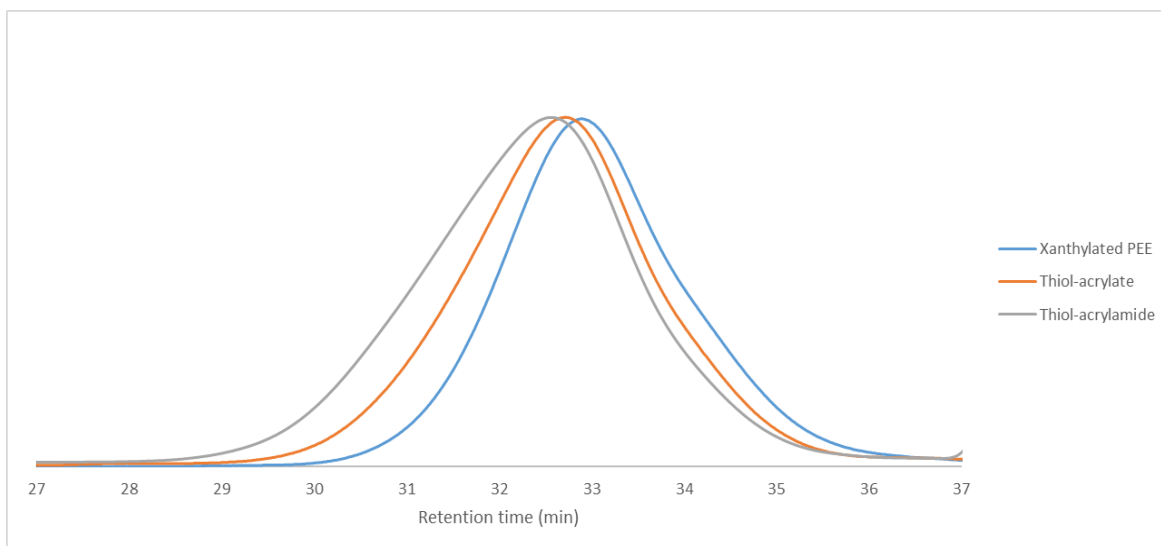


The main population of ethylene/propylene copolymer ( $M_n = 463$  kg/mol,  $M_w = 521$  kg/mol), when xanthylated, demonstrated a broadening of MWD toward higher molecular weight but remained a soluble elastomeric material ( $M_n = 521$  kg/mol,  $M_w = 605$  kg/mol).

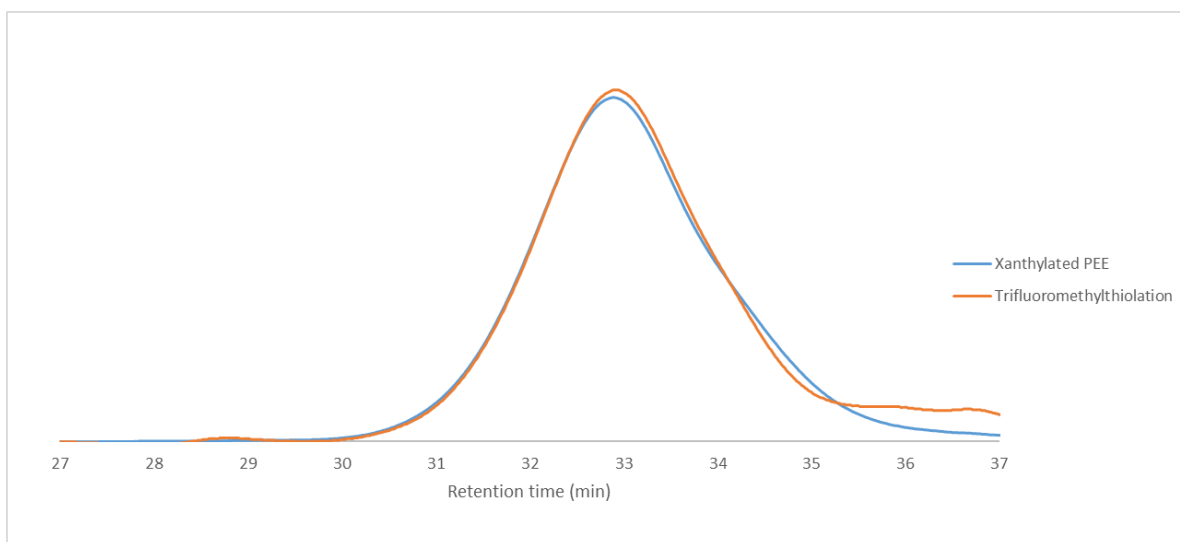


Xanthylated polyethylethylene ( $M_n = 4.9$  kg/mol,  $PDI = 1.28$ ) was transformed using glycidyl phenyl ether. Adding more mass to the polymer backbone, the molecular weight of the polyolefin increased, but the dispersity remained unchanged ( $M_n = 6.5$  kg/mol,  $PDI =$

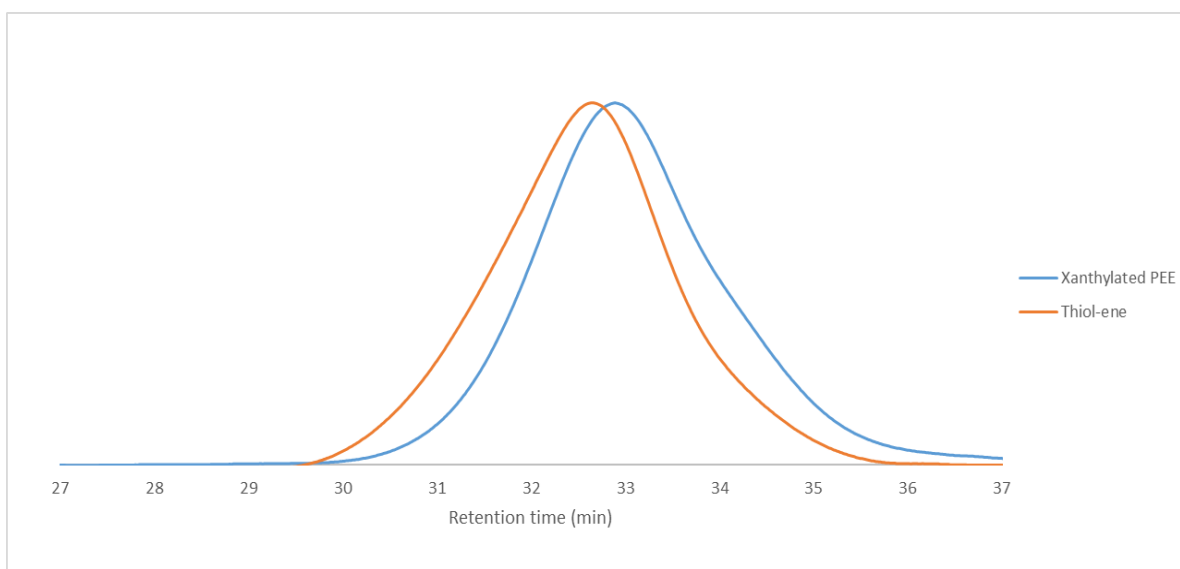
1.28). The UV-Vis spectrum demonstrated the conversion of xanthate to thiol through the disappearance of the xanthate absorption at 283 nm and the appearance of aromatic absorptions at 272 nm.



Xanthylated polyethylethylene ( $M_n = 4.9$  kg/mol, PDI = 1.28) was transformed using a thiol-Michael addition with benzyl acrylate and a dopamide-derived acrylamide. The result of thiol-acrylate reaction showed  $M_n = 5.9$  kg/mol and PDI = 1.32, so the molecular weight distribution was relatively unchanged. The reaction with a catechol-containing acrylamide resulted in a well defined polymer ( $M_n = 6.7$  kg/mol, PDI = 1.44).

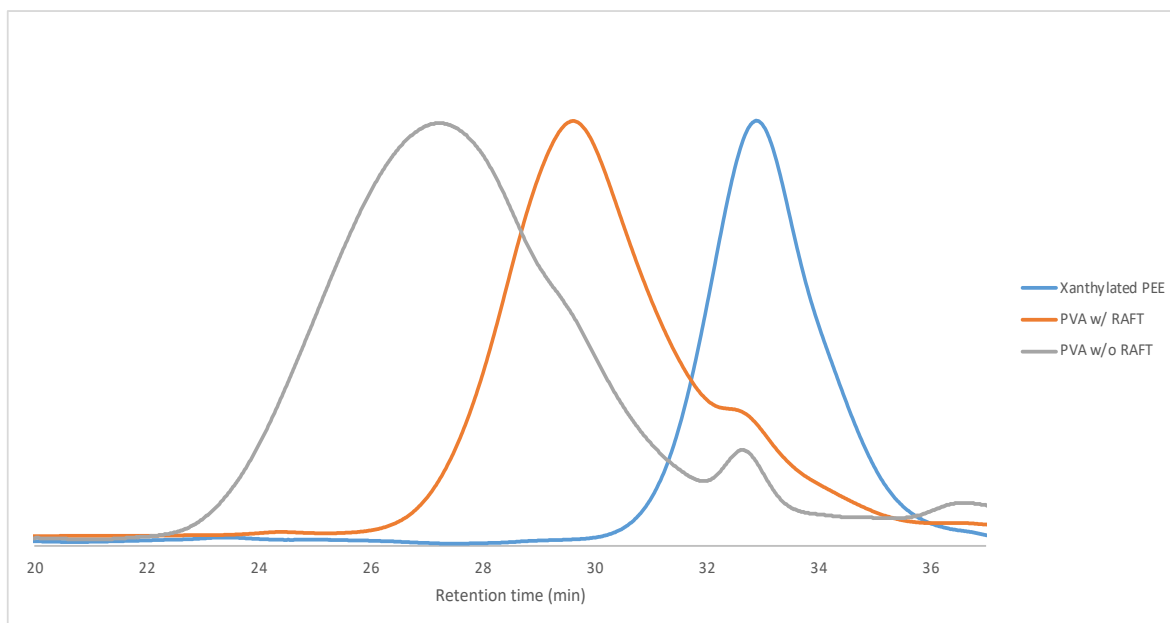


Even in radical-based transformations, such as trifluoromethylthiolation shown above, we were able to control the molecular weight distribution. The xanthylated material ( $M_n = 4.9$  kg/mol, PDI = 1.26) had nearly the identical molecular weight distribution as the final trifluoromethylthiolated material ( $M_n = 5.2$  kg/mol, PDI = 1.22).



Photochemical thiol-ene reactions occur via radical pathways. Xanthylated polyethylethylene ( $M_n = 5.0$  kg/mol, PDI = 1.25) underwent controlled conversion from the xanthate to thiol and then subsequent thiol-ene reaction with an allylglycoside without significant change in

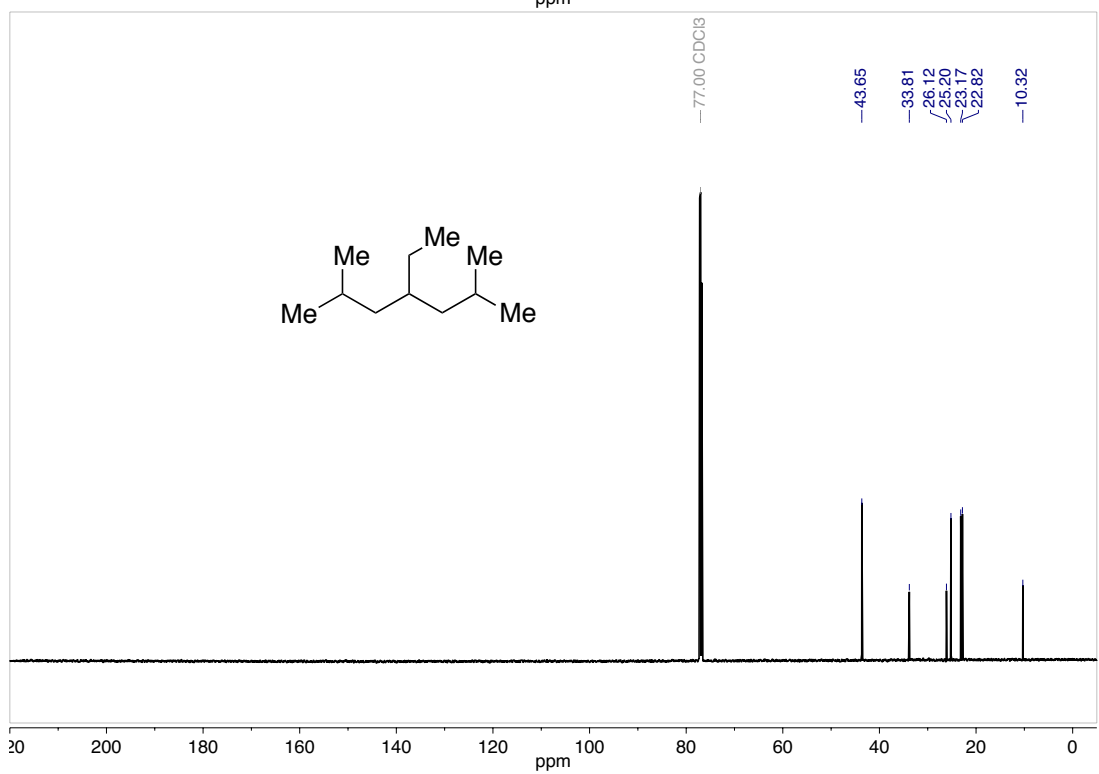
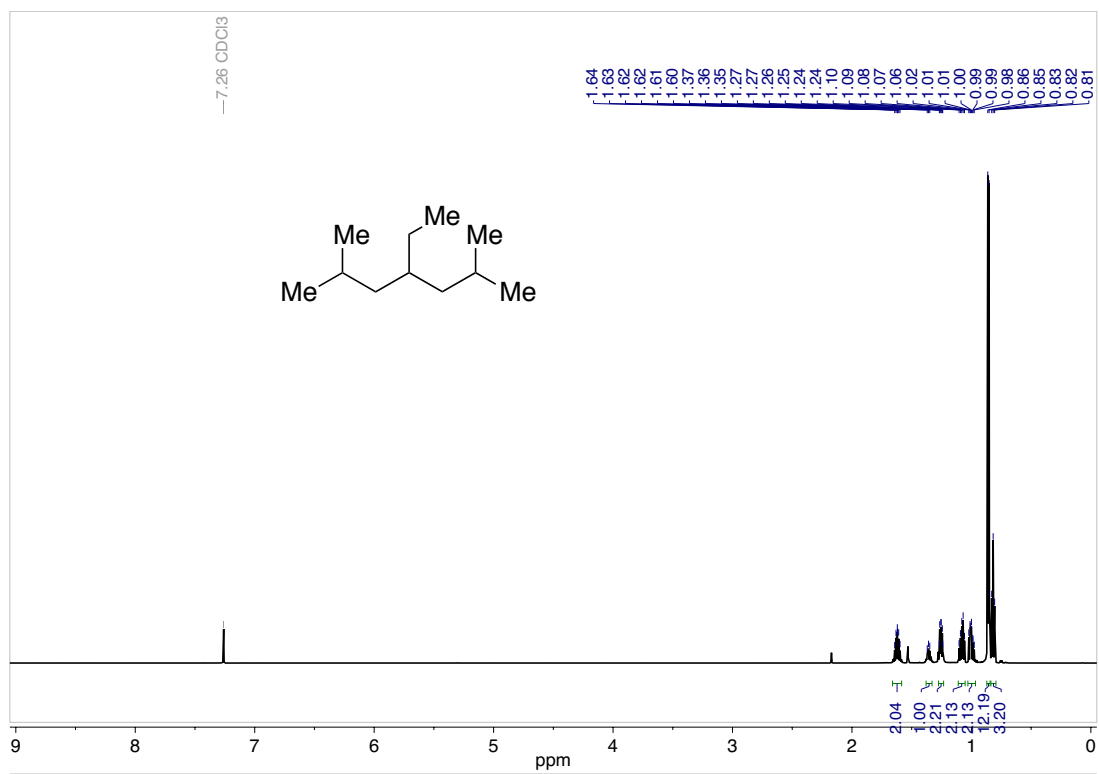
dispersity ( $M_n = 6.2$  kg/mol,  $PDI = 1.32$ ). As expected, the molecular weight of the polyolefin increased, as a large protected saccharide was added.



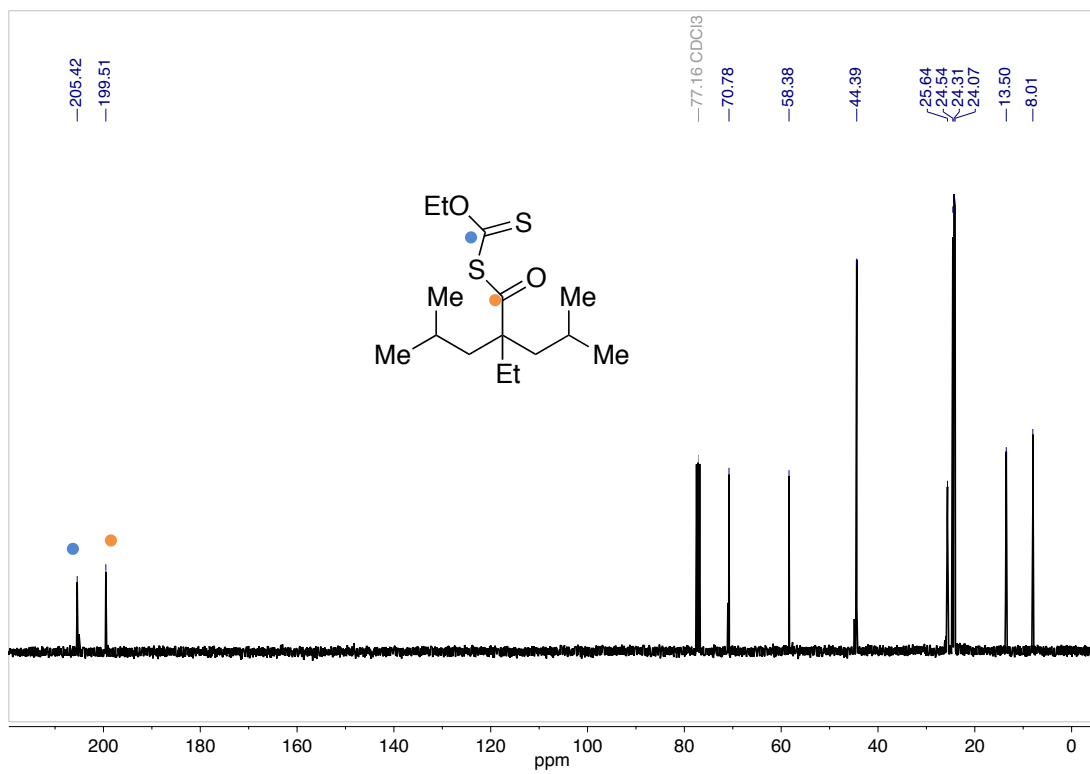
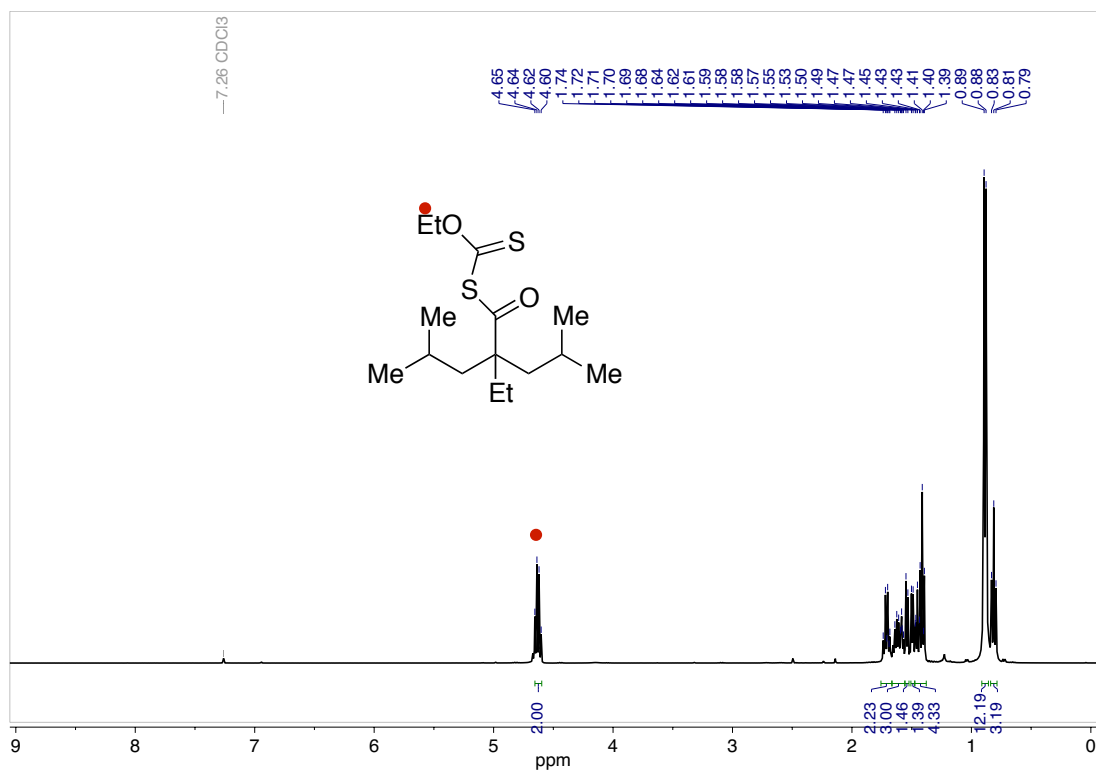
GPC overlay comparing the free-radical polymerization of vinyl acetate with and without including a macromolecular chain-transfer agent. The grey trace is the result of a free radical polymerization of vinyl acetate initiated by AIBN and run at 80 °C for 19 hours ( $M_n = 52$  kg/mol,  $PDI = 3.07$ ). The blue trace is a sample of xanthylated PEE containing 14 mol% xanthate moieties. The orange trace is the result of the RAFT polymerization of vinyl acetate initiated with AIBN and run in the presence of xanthylated PEE. The resulting poly(ethylethylene-*graft*-vinyl acetate) ( $M_n = 17$  kg/mol,  $PDI = 2.00$ ) displays peaks in the  $^1\text{H}$  and  $^{13}\text{C}$  NMR commensurate with the graft polymer structure. Furthermore, the DSC demonstrates two distinct  $T_g$  values representing the polyolefin (-50.6 °C) and the poly(vinyl acetate) (26.4 °C).

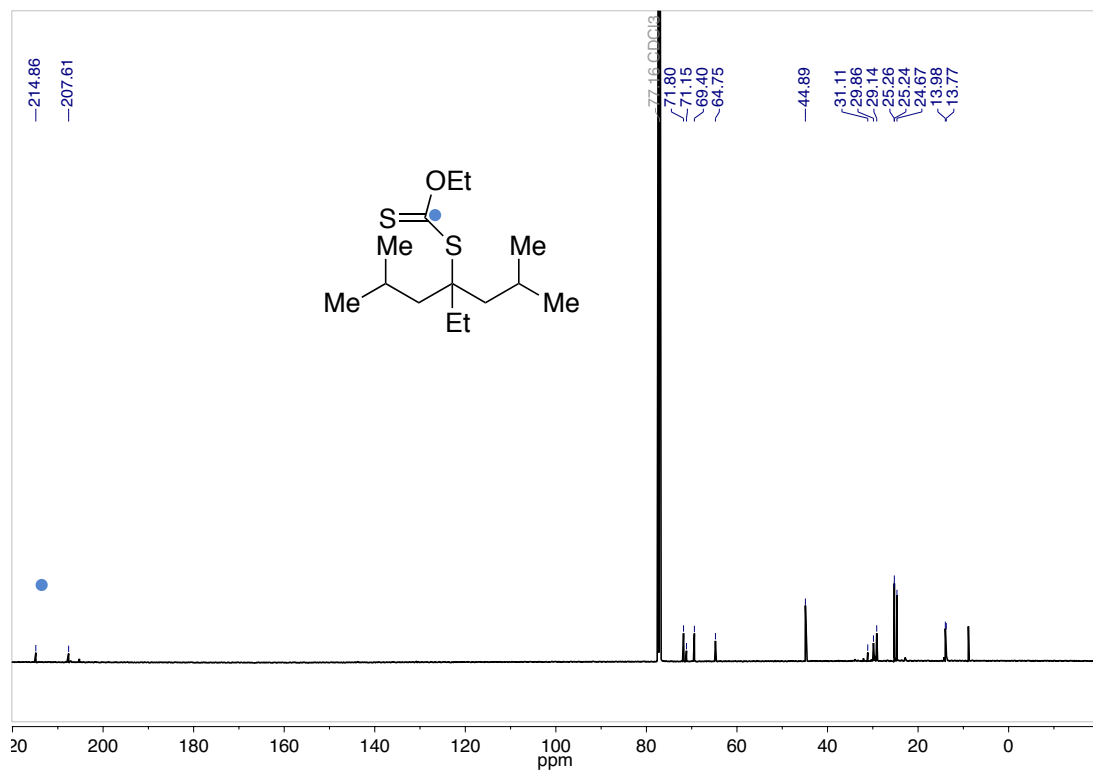
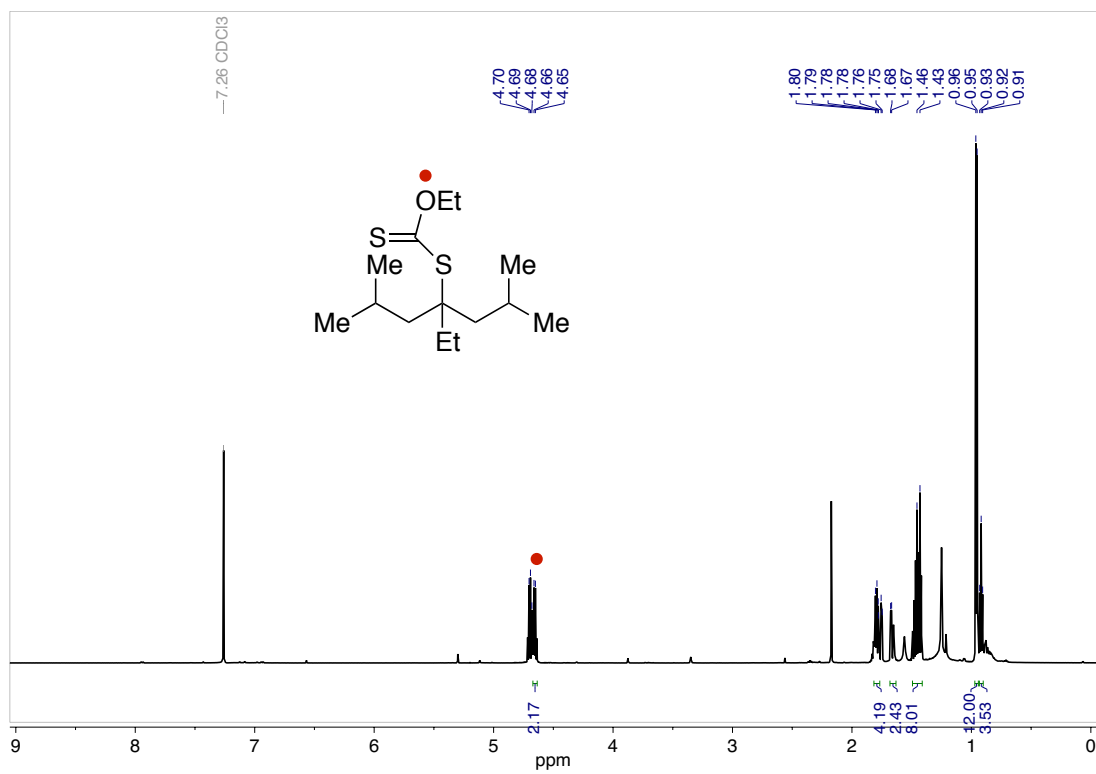
## REFERENCES

1. Czaplyski, W. L.; Na, C. G.; Alexanian, E. J. *J. Am. Chem. Soc.*, **2016**, *138* (42), 13854–13857.
2. Nishida, J.; Kobayashi, M.; Takahara, A. *ACS Macro Lett.*, **2013**, *2* (2), 112–115.
3. Kondo, Y.; Garcia-Cuadrado, D.; Hartwig, J. F.; Boen, N. K.; Wagner, N. L.; Hillmyer, M. A. *J. Am. Chem. Soc.* **2002**, *124* (7), 1164.
4. Bézier, D.; Daugulis, O.; Brookhart, M. *Organometallics* **2014**, *63* (5), 887-893.
5. Shao, X.; Xu, C.; Lu, L.; Shen, Q. *J. Org. Chem.* **2015**, *80*, 3012.
6. Markey, L.; Giordani, S.; Scanlan, E. M. *J. Org. Chem.* **2013**, *78*, 4270.

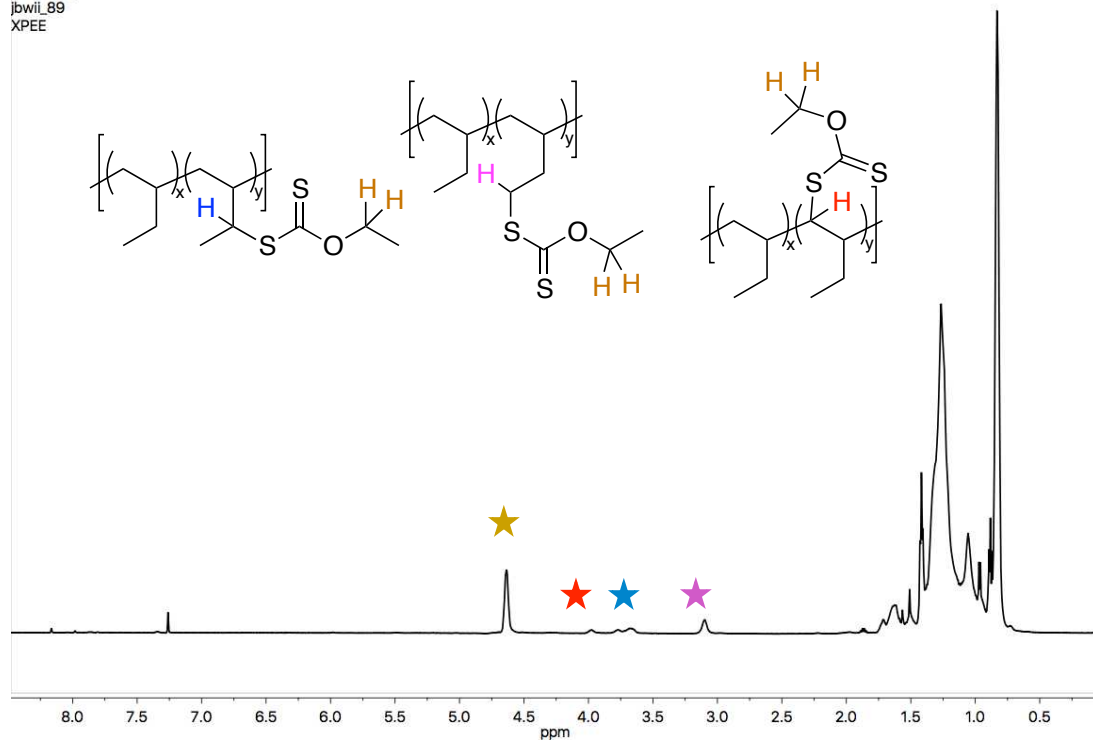




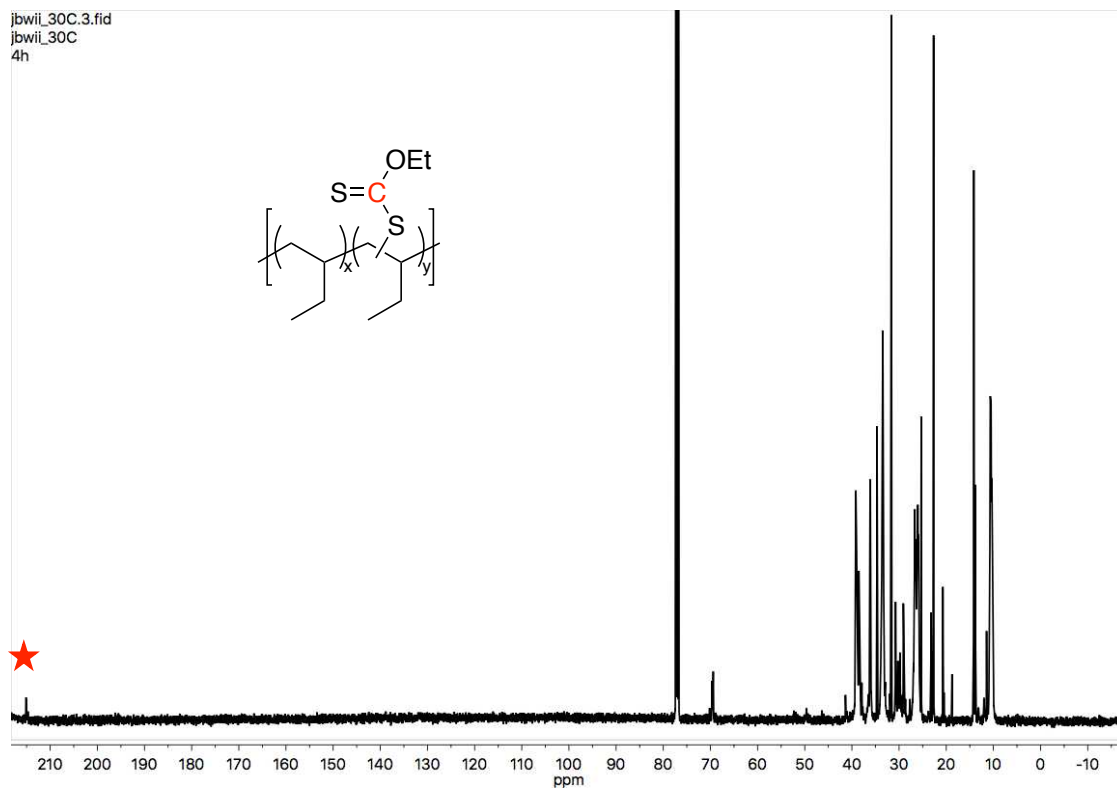




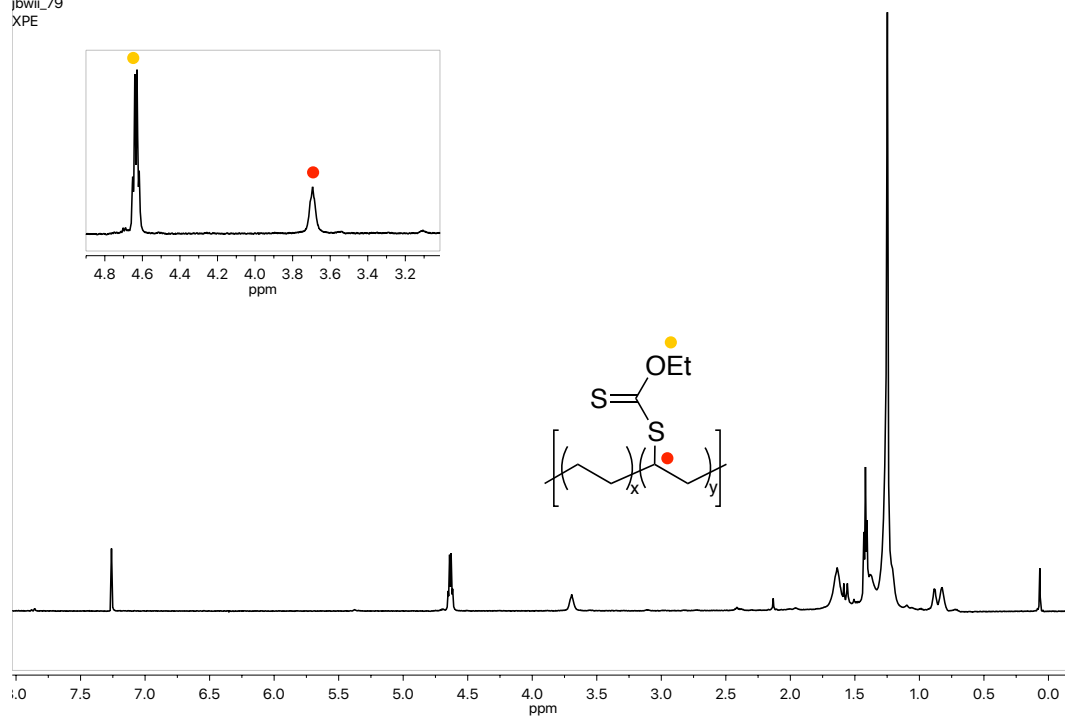
PROTON\_01  
jbwil\_89  
XPPE



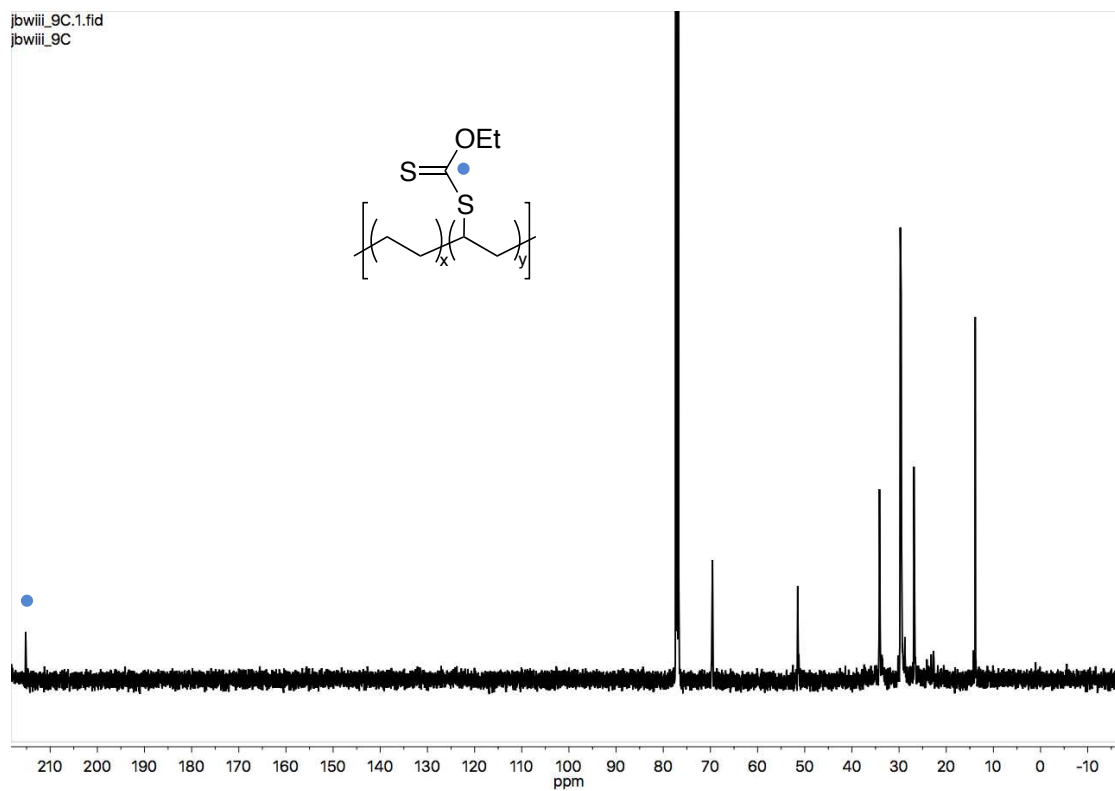
jbwil\_30C.3.fid  
jbwil\_30C  
4h



PROTON\_01  
jbwil\_79  
XPE

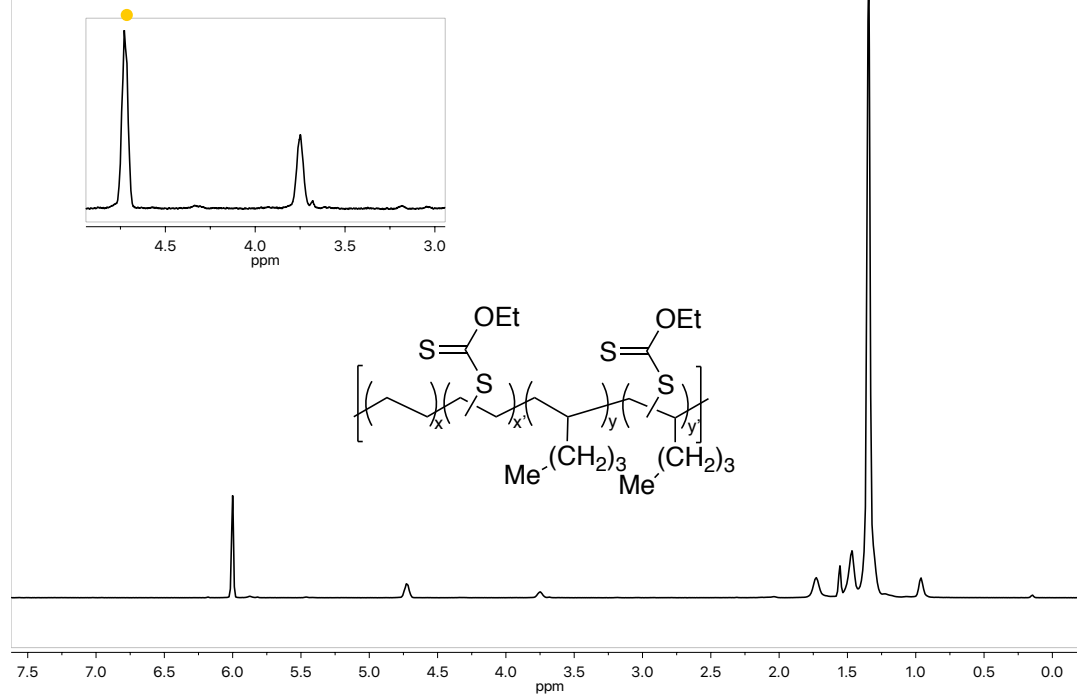


jbwil\_9C.1.fid  
jbwil\_9C

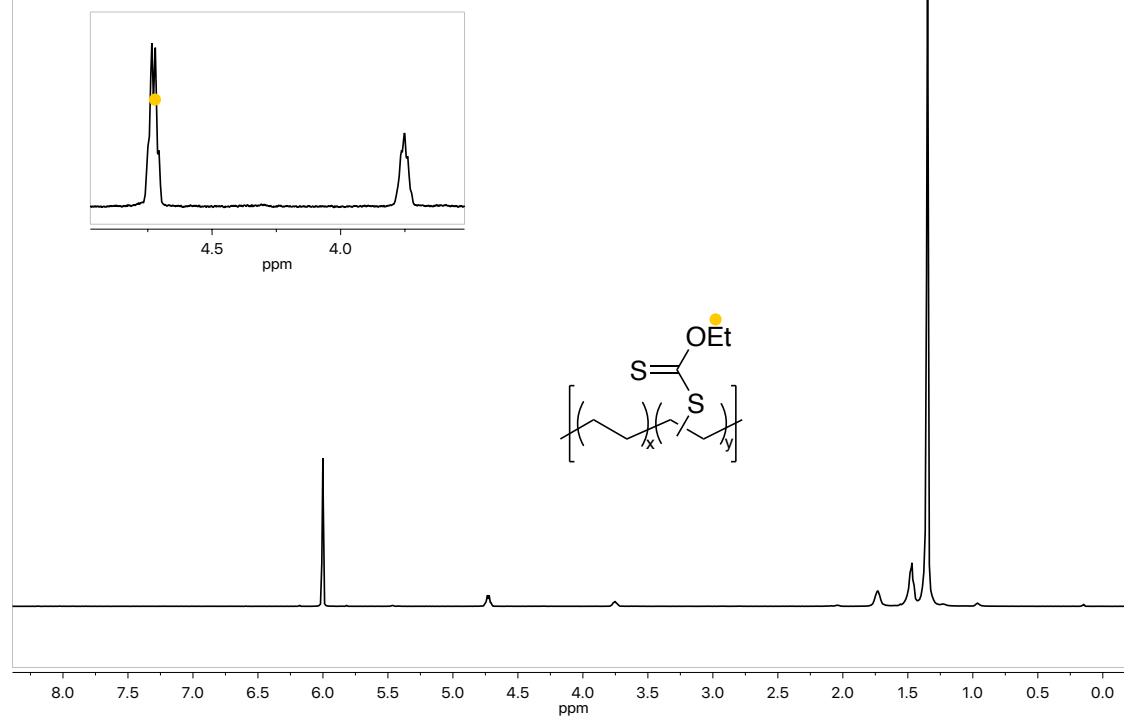


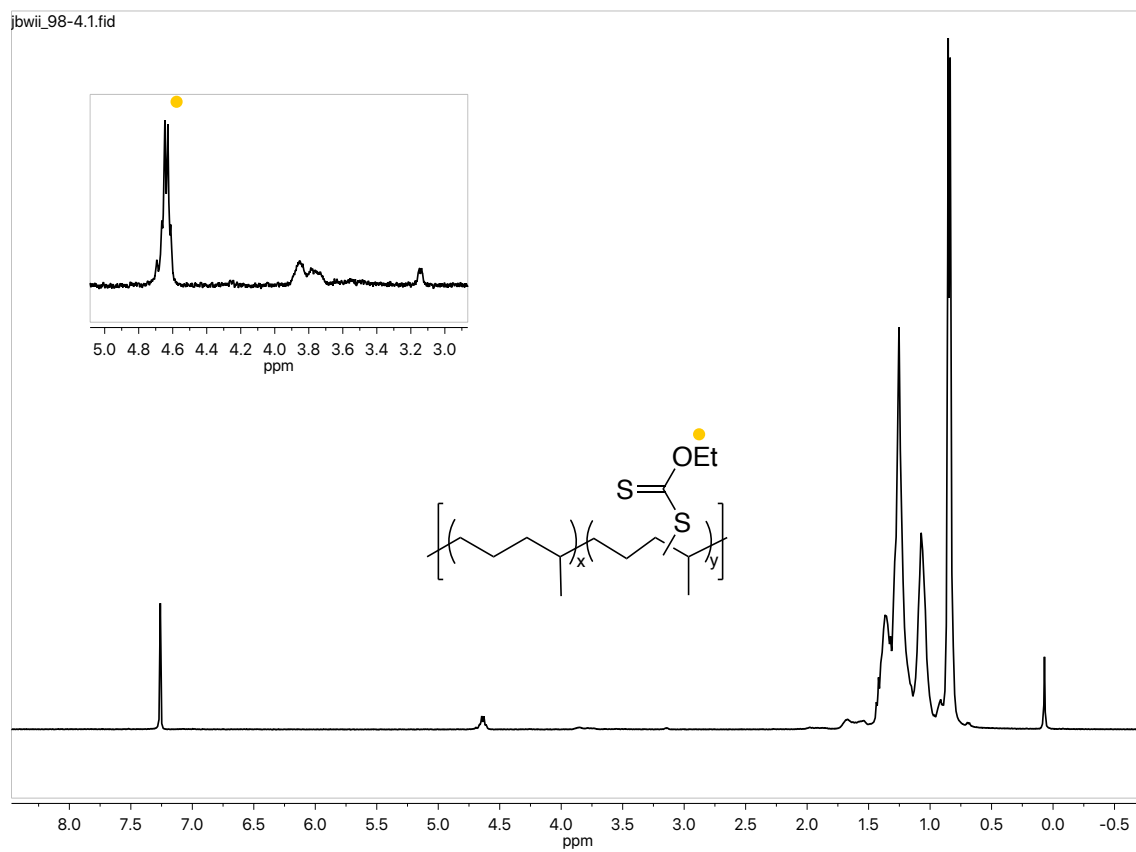


jbwiii\_85-2.2.fid  
 jbwiii\_85-2  
 XDND at 110 C



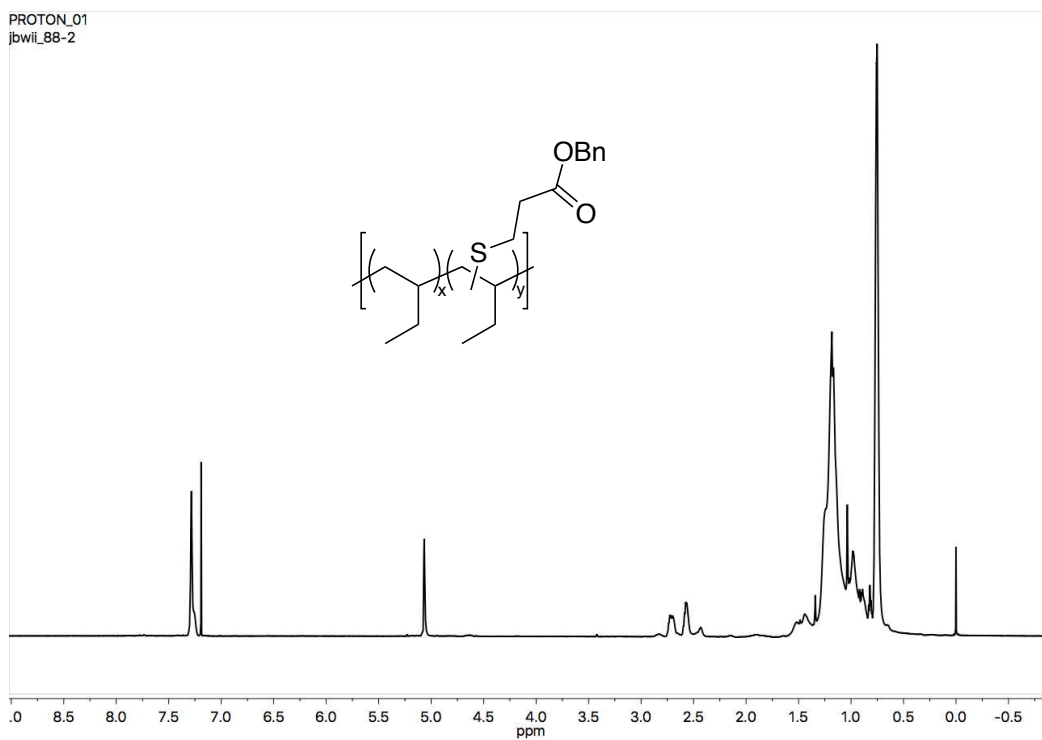
jbwiii\_86-2.1.fid  
 jbwiii\_86-2  
 XHDPE at 110 C



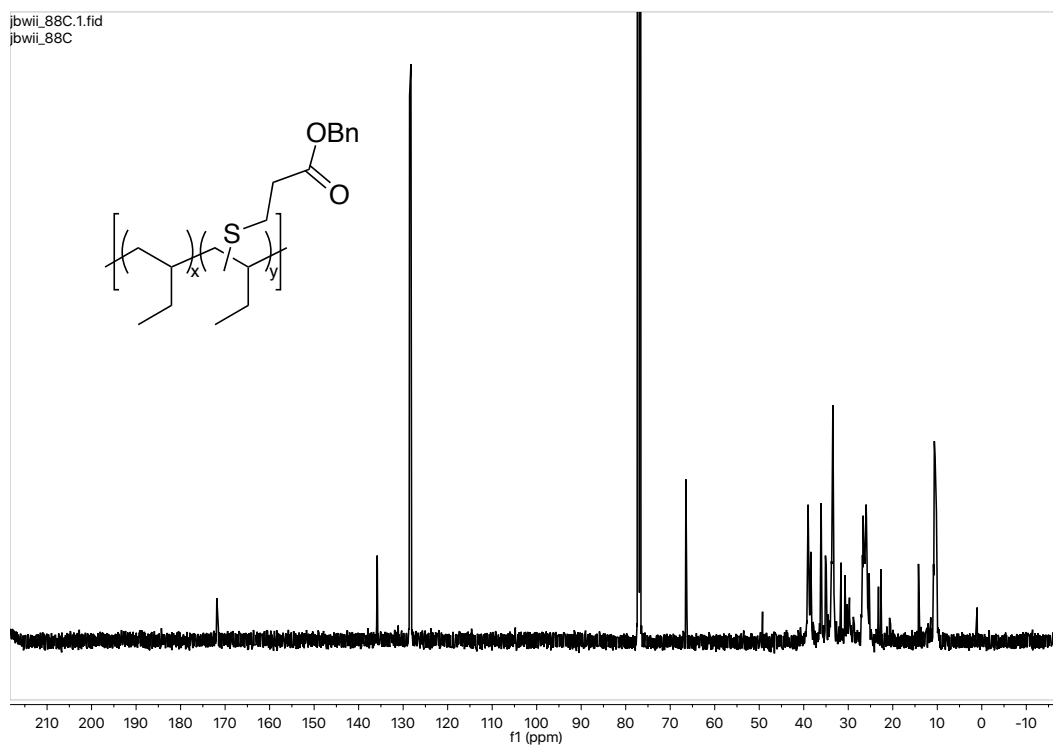




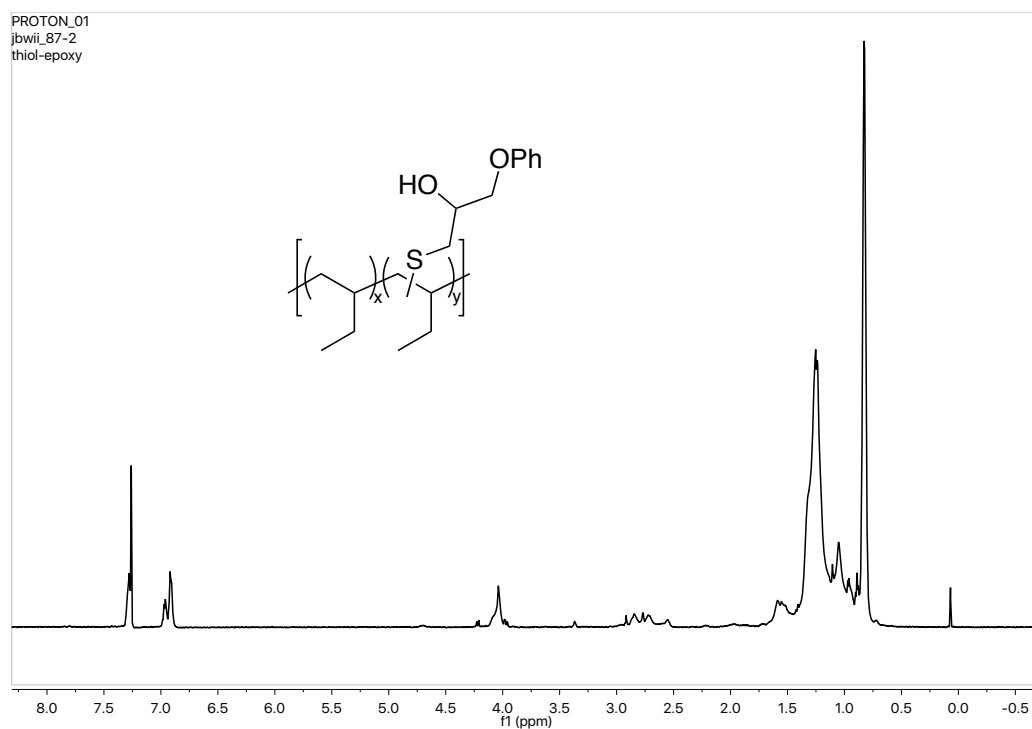
PROTON\_01  
jbwii\_88-2



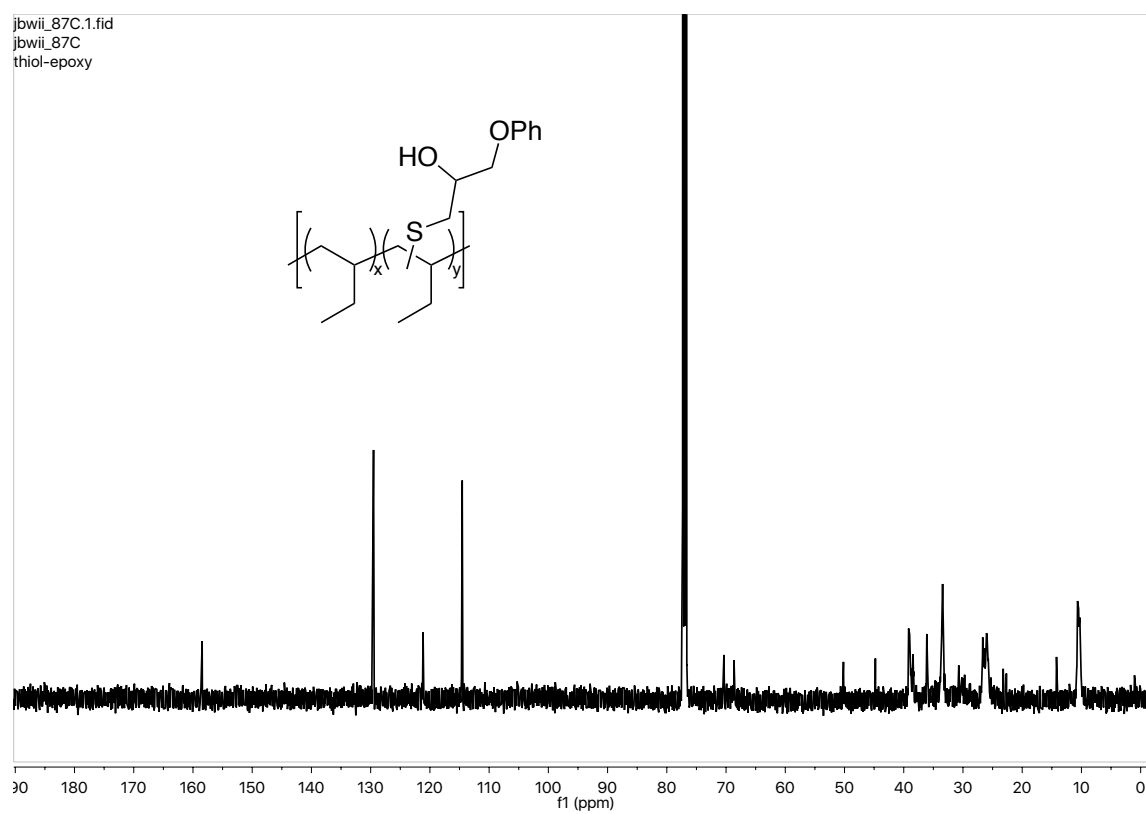
jbwii\_88C.1.fid  
jbwii\_88C



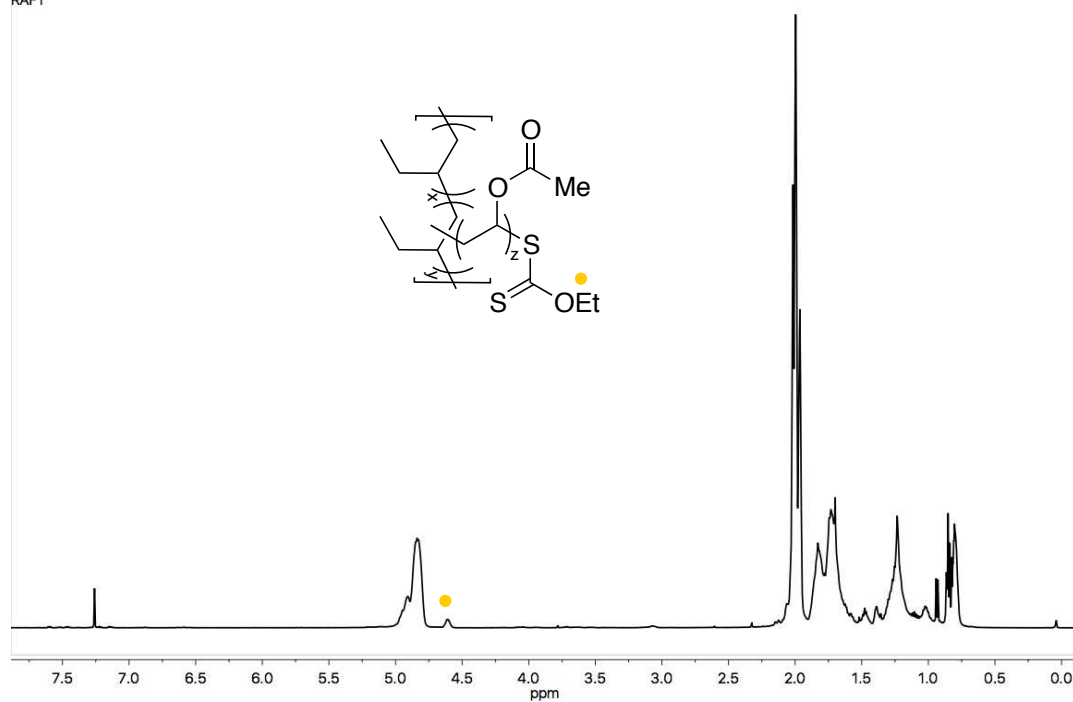
PROTON\_01  
jbwii\_87-2  
thiol-epoxy



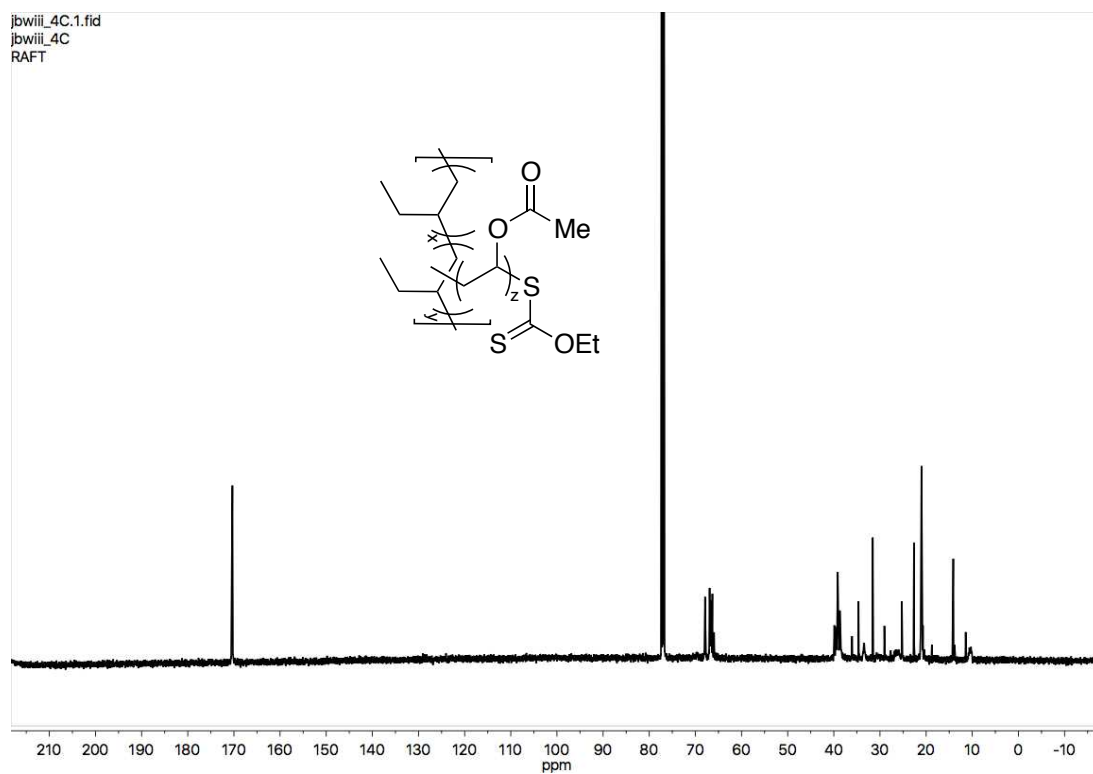
jbwii\_87C:1.fid  
jbwii\_87C  
thiol-epoxy

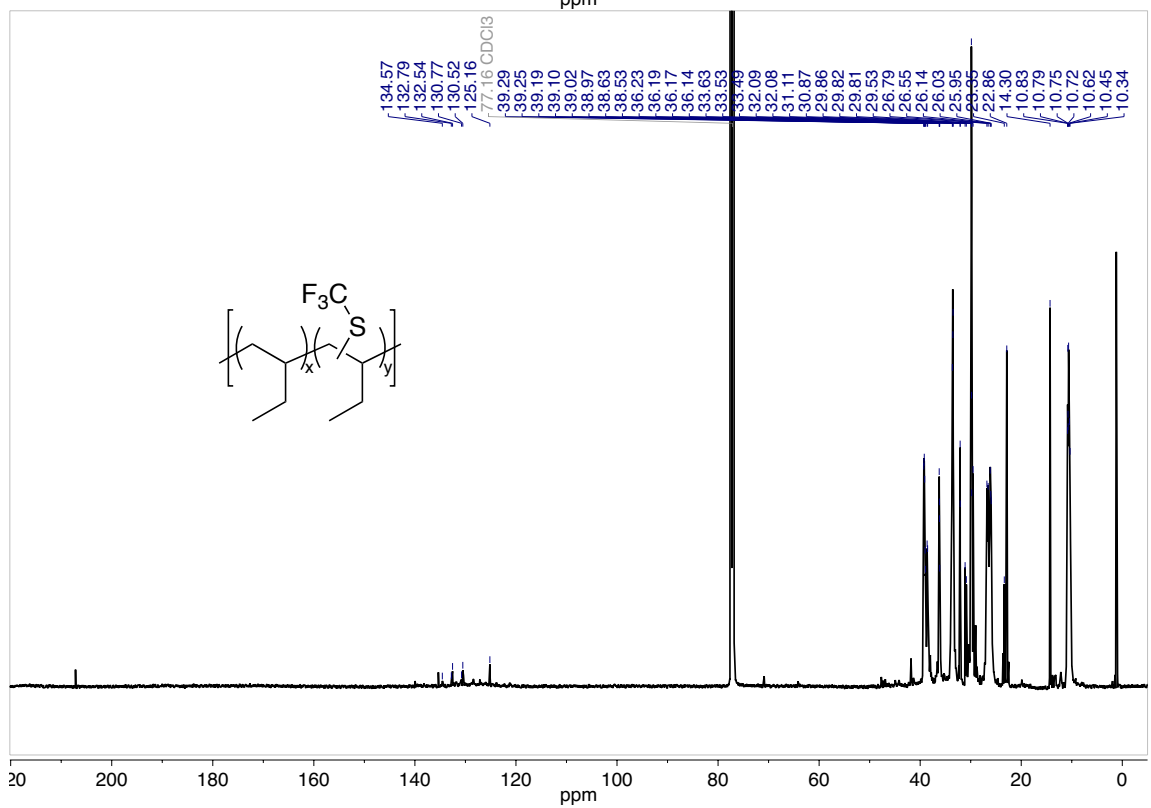
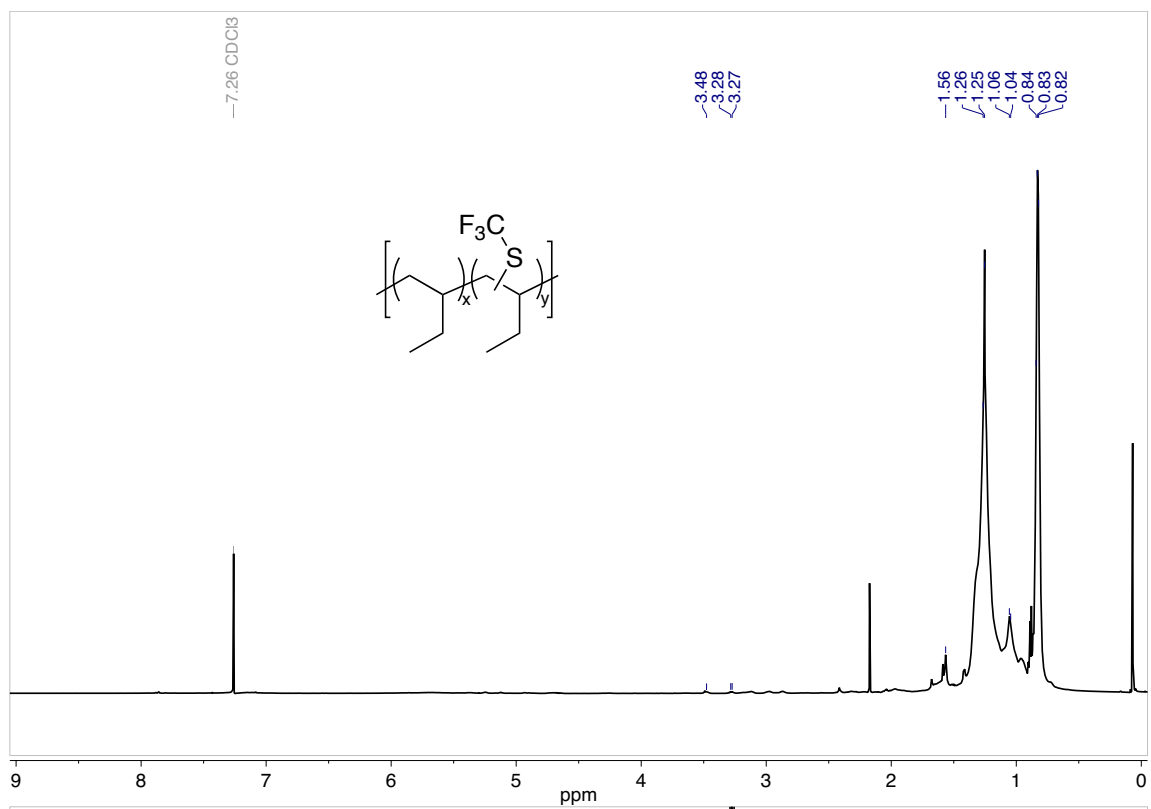


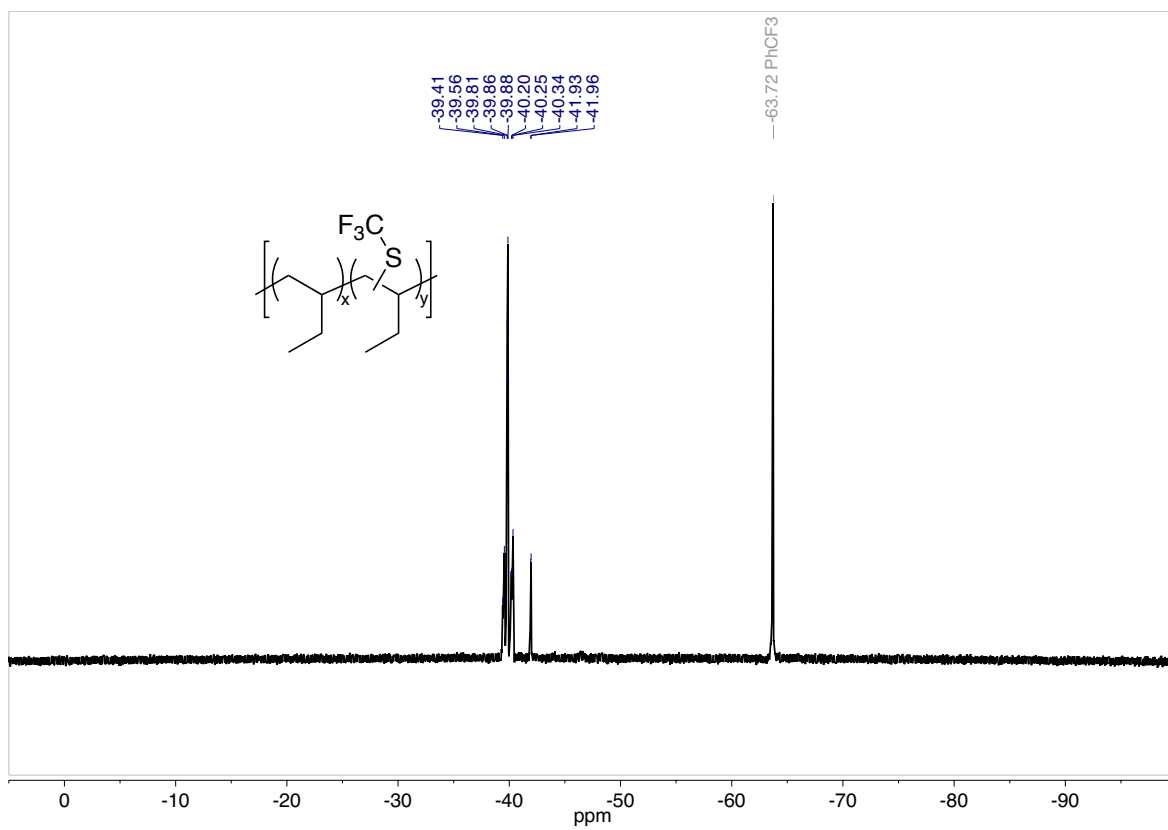
Cruzer/jbwiii\_4-2  
JBWIII\_4  
RAFT

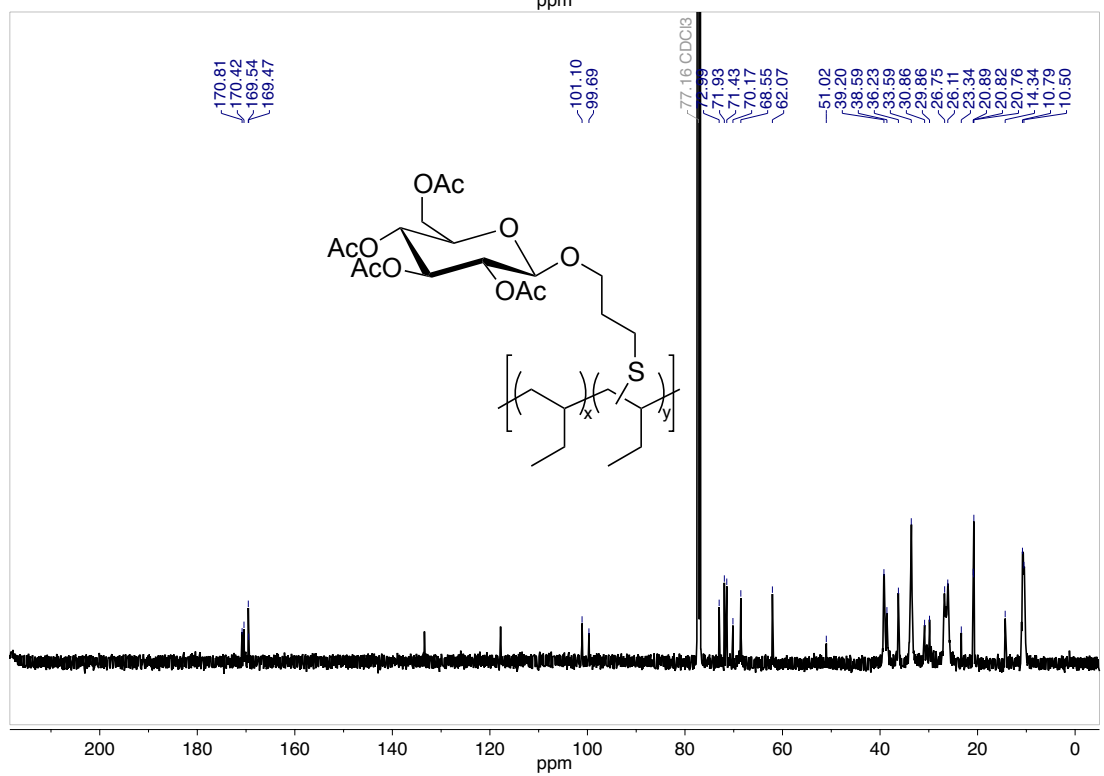
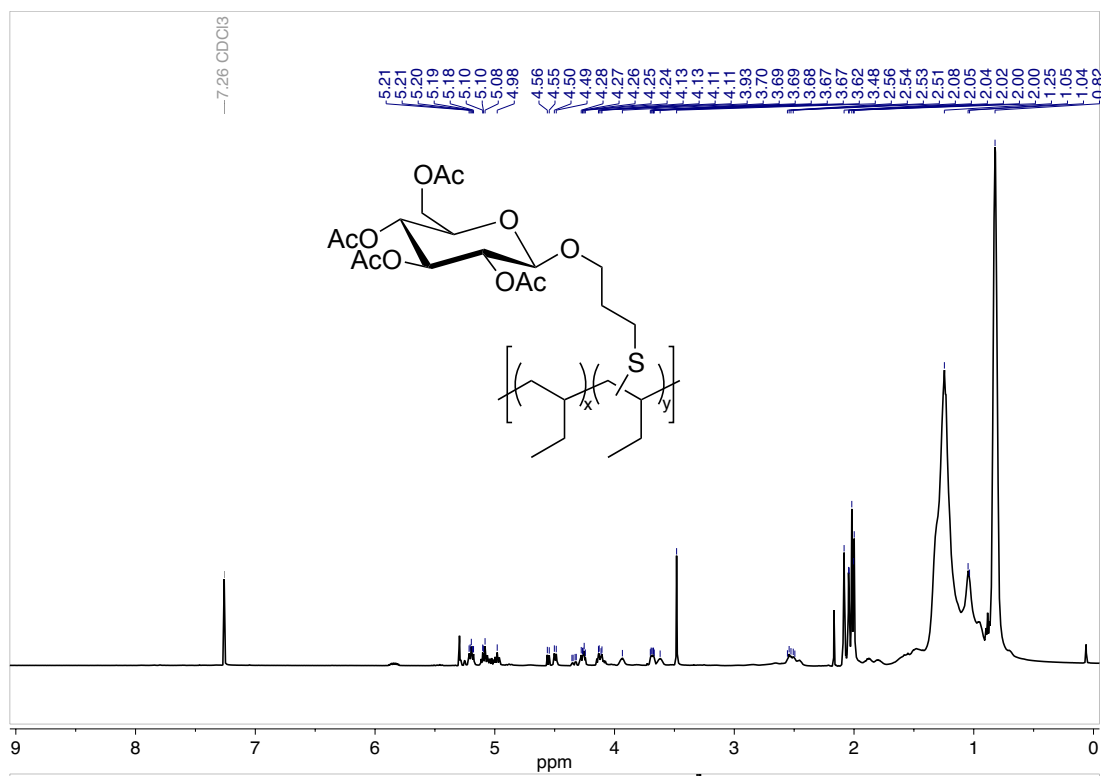


jbwiii\_4C.1.fid  
jbwiii\_4C  
RAFT

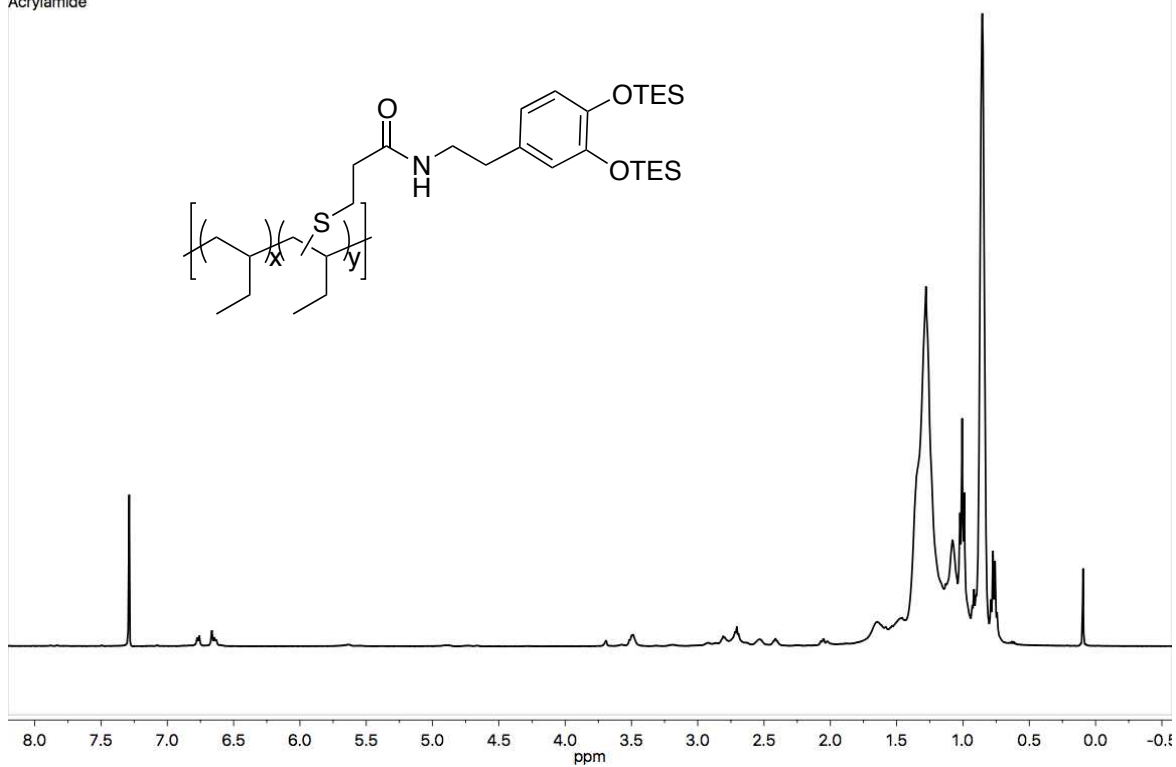




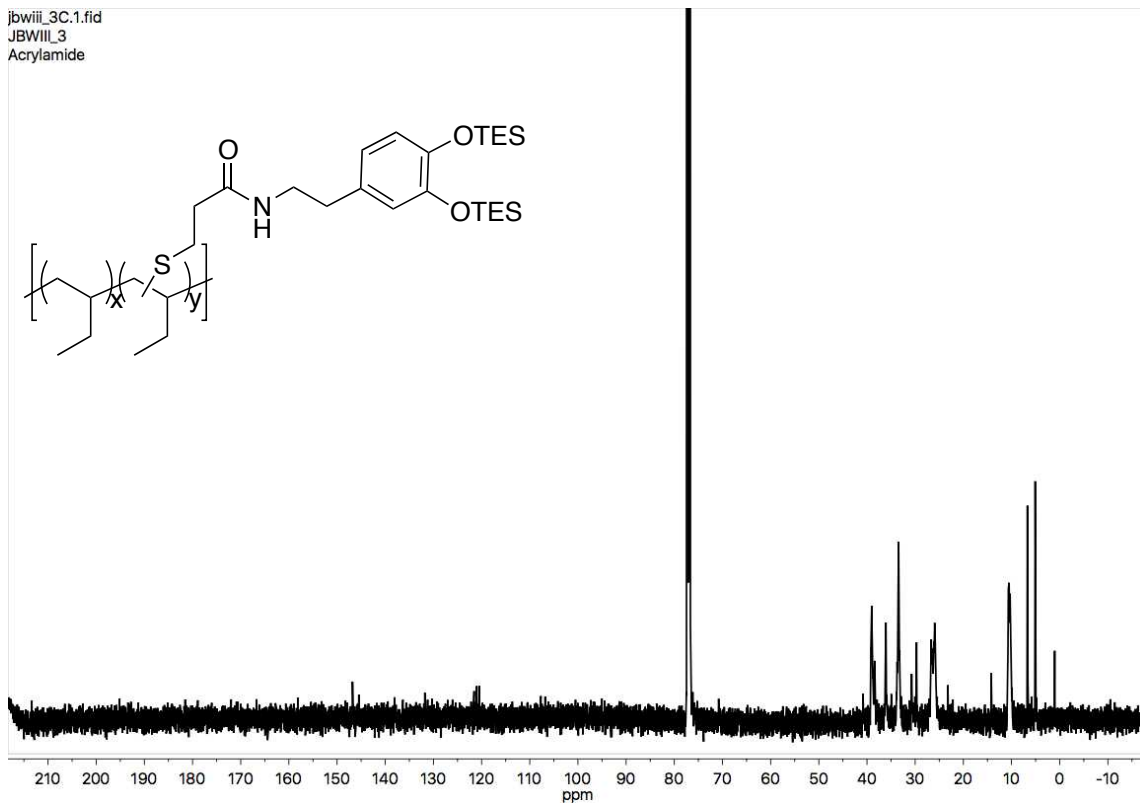




jbwiii\_3.1.fid  
JBWIII\_3  
Acrylamide



jbwiii\_3C.1.fid  
JBWIII\_3  
Acrylamide



## APPENDIX C: SUPPORTING INFORMATION FOR CHAPTER 4

### General Methods and Materials

Proton and carbon magnetic resonance spectra ( $^1\text{H}$  NMR and  $^{13}\text{C}$  NMR) were recorded on a Bruker model DRX 400 or a Bruker Avance III 600 CryoProbe( $^1\text{H}$  NMR at 400 MHz and 600 MHz and  $^{13}\text{C}$  NMR at 100 and 151 MHz) spectrometer. Chemical shifts for protons are reported in parts per million downfield from tetramethylsilane and are referenced to residual protium in the solvent ( $^1\text{H}$  NMR:  $\text{CHCl}_3$  at 7.26 ppm). Chemical shifts for carbons are reported in parts per million downfield from tetramethylsilane and are referenced to the carbon resonances of the solvent peak ( $^{13}\text{C}$  NMR:  $\text{CDCl}_3$  at 77.16 ppm). Chemical shifts for fluorines are referenced to fluorobenzene as an internal standard ( $^{19}\text{F}$  NMR:  $\text{C}_6\text{H}_5\text{F}$  at  $-113.15$  ppm).  $^1\text{H}$  NMR data are reported as follows: chemical shift, multiplicity (s = singlet, d = doublet, t = triplet, q = quartet, sept = septet, oct = octet, dd = doublet of doublets, ddt = doublet of doublet of triplets, ddd = doublet of doublet of doublets, dddd = doublet of doublet of doublet of doublets, m = multiplet, and prefixed br = broad), coupling constants (Hz), and integration.

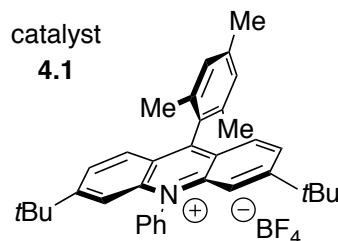
High resolution mass spectra (HRMS) were obtained using a Thermo LTqFT mass spectrometer with electrospray ionization or atmospheric pressure chemical ionization in positive mode. Gas chromatography (GC) was performed on an Agilent 6850 series instrument equipped with a split-mode capillary injection system and Agilent 5973 network mass spec detector (MSD). Thin layer chromatography (TLC) was performed on SiliaPlate 250  $\mu\text{m}$  thick silica gel plates provided by Silicycle. Visualization was accomplished with short wave UV light (254 nm), cerium ammonium molybdate, *p*-anisaldehyde, or potassium permanganate solution followed by heating. Flash chromatography was performed using



SiliaFlash P60 silica gel (40-63  $\mu\text{m}$ ) purchased from Silicycle. Irradiation of photochemical reactions was carried out using a PAR38 blue aquarium LED lamp (Model #6851) fabricated with high-power Cree LEDs as purchased from Ecoxotic ([www.ecoxotic.com](http://www.ecoxotic.com)) or Kessil KSH150B Blue 36W LED Grow Lights with standard borosilicate glass vials purchased from Fischer Scientific. For all photolyses, reactions were stirred using a PTFE coated magnetic stir bar on a magnetic stir plate. Yield refers to isolated yield of analytically pure material unless otherwise noted. NMR yields were determined using hexamethyldisiloxane as an internal standard. Tetrahydrofuran, diethyl ether, and dichloromethane were dried by passage through a column of neutral alumina under nitrogen prior to use. All other reagents were obtained from commercial sources and used without further purification unless otherwise noted.

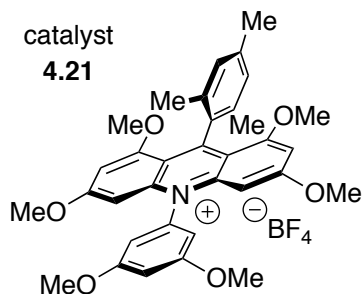
### Preparation of Photocatalysts and Reagents

4-Acetamidobenzenesulfonyl azide, *N*-fluorobenzenesulfonimide, diethyl bromomalonate, and *N*-Chlorosuccinimide were used as purchased. Methyl acrylate and methyl vinyl ketone were purchased from commercial sources, deoxygenated via multiple freeze-pump-thaw cycles, purified by vacuum transfer, and stored at  $-35\text{ }^{\circ}\text{C}$  under in an argon-filled glovebox prior to use.



### 9-Mesityl-3,6-di-*tert*-butyl-10-phenylacridinium tetrafluoroborate (*t*-Bu<sub>2</sub>-Mes-Acr<sup>+</sup>)

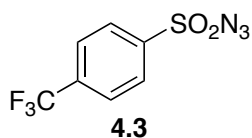
(4.1) was prepared as previously reported by the Nicewicz lab. The spectral data matched the values reported in the literature.<sup>1</sup>



**10-(3,5-Dimethoxyphenyl)-9-mesityl-1,3,6,8-tetramethoxyacridin-10-ium**

**tetrafluoroborate (OMe<sub>6</sub>-Mes-Acr<sup>+</sup>) (4.21)** was prepared as previously reported by our lab.

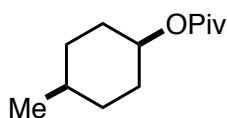
The spectral data matched the values reported in the literature.<sup>2</sup>



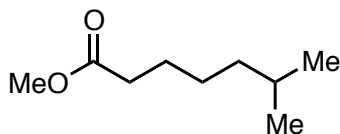
**4-(Trifluoromethyl)benzenesulfonyl azide (4.3)** was prepared as previously reported. The spectral data matched the values reported in the literature.<sup>3</sup>

**Preparation of Substrates**

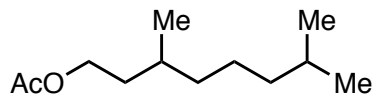
Cyclohexane, cycloheptane, cyclooctane, *trans*-decalin, adamantane, *n*-propylbenzene, *t*-butyl cyclohexane, isopropylbenzene, 3,7-dimethyl-1-octanol, 2-(1-adamantyl)-4-bromoanisole, and 5- $\alpha$ -cholestan-3-one were used as purchased.



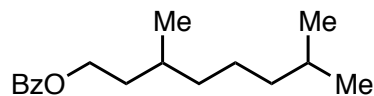
**Cis-4-methylcyclohexyl pivalate** was prepared according to a published procedure; spectral data were in agreement with literature values.<sup>4</sup>



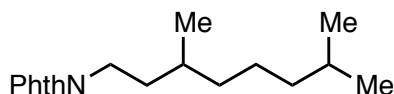
**Methyl 6-methylheptanoate** was prepared according to a published procedure; spectral data were in agreement with literature values.<sup>5</sup>



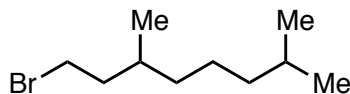
**3,7-Dimethyloctyl acetate** was prepared according to a published procedure; spectral data were in agreement with literature values.<sup>6</sup>



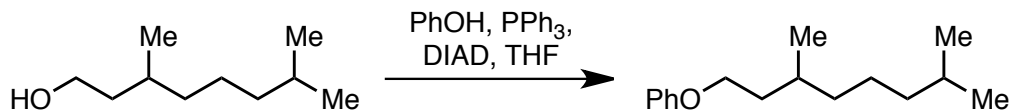
**3,7-Dimethyloctyl benzoate** was prepared according to a published procedure; spectral data were in agreement with literature values.<sup>7</sup>



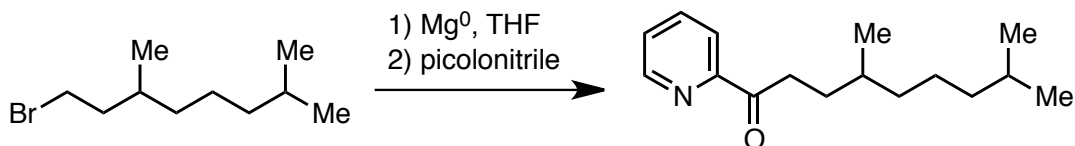
**2-(3,7-Dimethyloctyl)isoindoline-1,3-dione** was prepared according to a published procedure; spectral data were in agreement with literature values.<sup>8</sup>



**1-Bromo-3,7-dimethyloctane** was prepared according to a published procedure; spectral data were in agreement with literature values.<sup>6</sup>



**((3,7-Dimethyloctyl)oxy)benzene:** To a solution of phenol (1 g, 10.6 mmol) and triphenylphosphine (6.1 g, 23.4 mmol) in THF (100 mL) at 0 °C was added 3,7-dimethyloctanol (4.47 mL, 23.4 mmol) followed by DIAD (4.6 mL, 23.4 mmol). The solution was warmed to rt overnight, the concentrated *in vacuo*. The residue was triturated with hexanes, and the solution was concentrated *in vacuo* and purified by flash column chromatography (0 – 5% EtOAc in hexanes) affording the product as a colorless liquid (990 mg, 40% yield). Spectral data were in agreement with literature values.<sup>9</sup>

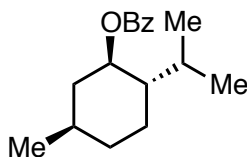


**4,8-Dimethyl-1-(pyridin-2-yl)nonan-1-one:** To a suspension of magnesium (100 mg, 4.1 mmol) and an iodine crystal in THF (2 mL) was added 1-bromo-3,7-dimethyloctane (995 mg, 4.5 mmol) in THF (7 mL) dropwise. Gentle heating to facilitate initiation was accomplished with a heat gun. Subsequently, picolonitrile (395 mL, 4.1 mmol) was added at room temperature and stirred overnight. The reaction was quenched with 1M HCl, stirred for 3 hours, and then quenched with aqueous NaHCO<sub>3</sub>. The solution was extracted three times with EtOAc, and the combined organic layers were washed with brine, dried with MgSO<sub>4</sub>, and concentrated *in vacuo*. The resultant oil was purified by flash column chromatography (10–20% EtOAc/Hex) affording the product in a 17% yield (170 mg):

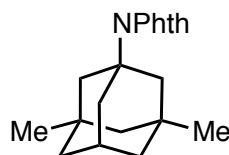
**<sup>1</sup>H NMR** (600 MHz, CDCl<sub>3</sub>) δ 8.63 (d, *J* = 5.0 Hz, 1H), 7.98 (d, *J* = 7.8 Hz, 1H), 7.83 – 7.66 (m, 1H), 7.40 (dd, *J* = 7.6, 4.8 Hz, 1H), 3.24 – 3.05 (m, 2H), 1.84 – 1.70 (m, 1H), 1.48 (ddt, *J* = 19.7, 13.4, 6.5 Hz, 3H), 1.33 – 1.16 (m, 2H), 1.10 (h, *J* = 6.7, 5.4 Hz, 4H), 0.88 (d, *J* = 6.3 Hz, 3H) 0.81 (d, *J* = 6.7 Hz, 6H).

**<sup>13</sup>C NMR** (151 MHz, CDCl<sub>3</sub>) δ 202.45, 153.65, 148.94, 136.86, 126.97, 121.78, 39.36, 37.14, 35.48, 32.69, 31.03, 28.03, 24.81, 22.78, 22.68, 19.66.

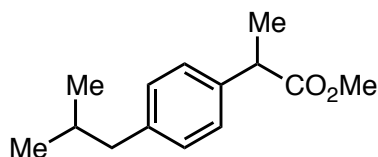
**HRMS** (ESI): calculated for C<sub>16</sub>H<sub>26</sub>NO [M+H]<sup>+</sup> = 248.2009; found 248.2010.



**(1R,2S,5R)-2-Isopropyl-5-methylcyclohexyl benzoate** was prepared according to a published procedure; spectral data were in agreement with literature values.<sup>10</sup>

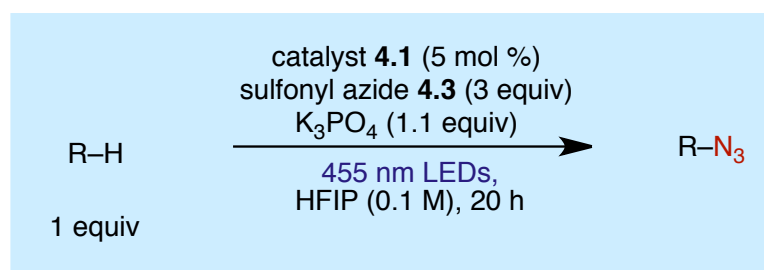


**2-(3,5-Dimethyladamantan-1-yl)isoindoline-1,3-dione** was prepared according to a published procedure; spectral data were in agreement with literature values.<sup>11</sup>

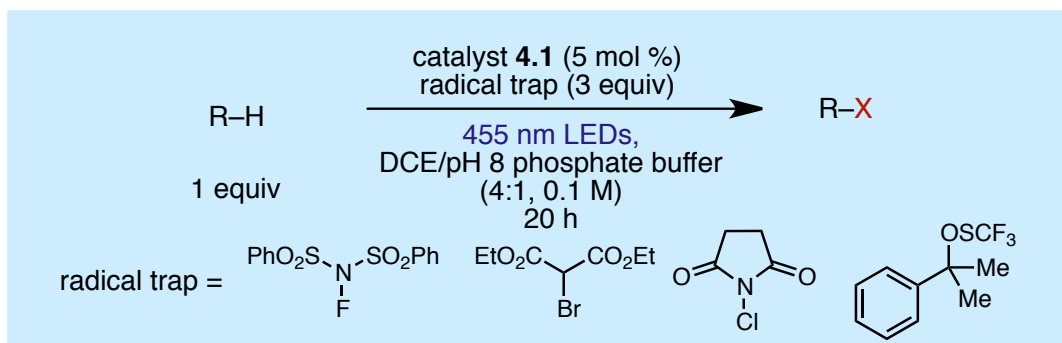


**Methyl 2-(4-isobutylphenyl)propanoate** was prepared according to a published procedure; spectral data were in agreement with literature values.<sup>12</sup>

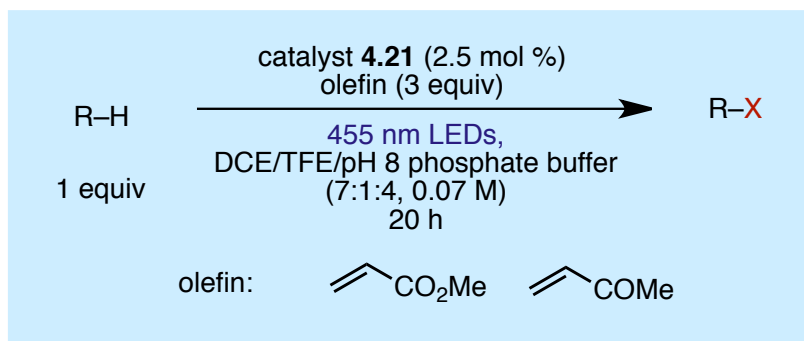
### Products of Aliphatic C–H Functionalization



**General Procedure A (Azidation):** In an argon-filled glovebox, a 1 dram vial with a Teflon-coated magnetic stir bar was charged with *t*Bu<sub>2</sub>-Mes-Acr<sup>+</sup> **4.1** (0.05 equiv), 4-(trifluoromethyl)benzenesulfonyl azide (3 equiv), K<sub>3</sub>PO<sub>4</sub> (1.1 equiv), and the alkane substrate (1 equiv). Hexafluoroisopropanol (HFIP) was added (0.1 M wrt alkane), and the vial was sealed with a Teflon-lined septum screw cap. The vial was positioned on a stir plate approximately 2 – 3 cm from a Par38 LED lamp supplying blue light ( $\lambda = 440\text{-}460$  nm). After irradiation for 20 hours, the reaction mixture was passed over a short plug of silica and concentrated *in vacuo*. The residue was analyzed by <sup>1</sup>H NMR or purified by column chromatography on silica gel with the eluent noted for each substrate.

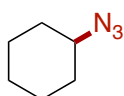


**General Procedure B (Halogenation and Trifluoromethylthiolation):** In an argon-filled glovebox, a 1 dram vial with a Teflon-coated magnetic stir bar was charged with *t*Bu<sub>2</sub>-Mes-Acr<sup>+</sup> **4.1** (0.05 equiv), radical trap (3 equiv), and the alkane substrate (1 equiv). 1,2-Dichloroethane (DCE) was added (0.125 M wrt alkane), and the vial was sealed with a Teflon-lined septum screw cap. Upon removal from the glovebox, 4 M pH 8 phosphate buffer was added (0.25 \* amount of DCE added such that total solvent amount is 0.1 M wrt alkane). The vial was positioned on a stir plate approximately 2 – 3 cm from a Par38 LED lamp supplying blue light ( $\lambda = 440\text{--}460\text{ nm}$ ). After irradiation for 4 – 20 hours, the reaction mixture was passed over a short plug of silica and concentrated *in vacuo*. The residue was analyzed by <sup>1</sup>H NMR or purified by column chromatography on silica gel with the eluent noted for each substrate.



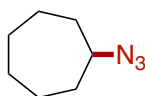
**General Procedure C (Alkylation):** In an argon-filled glovebox, a 1 dram vial with a Teflon-coated magnetic stir bar was charged with OMe<sub>6</sub>-Mes-Acr<sup>+</sup> **4.21** (0.0025 equiv), olefin (3 equiv), and the alkane substrate (1 equiv). A mixture of DCE and 2,2,2-

trifluoroethanol (TFE) was added (7:1, 0.125 M wrt alkane), and the vial was sealed with a Teflon-lined septum screw cap. Upon removal from the glovebox, 4 M pH 8 phosphate buffer was added (0.5 \* amount of organic solvent mixture added such that total solvent amount is 0.07 M wrt alkane). For methyl acrylate as the olefin, the vial was positioned on a stir plate approximately 2 – 3 cm from a Par38 LED lamp supplying blue light ( $\lambda = 440\text{-}460$  nm). For methyl vinyl ketone as the olefin, the vial was positioned on a stir plate approximately 2 cm from two Kessil KSH150B Blue 36W LED Grow Lights supplying blue light. After irradiation for 20 hours, the reaction mixture was passed over a short plug of silica and concentrated *in vacuo*. The residue was analyzed by  $^1\text{H}$  NMR or purified by column chromatography on silica gel with the eluent noted for each substrate.



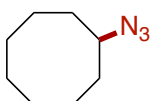
**4.4**

**Azidocyclohexane (4.4):** Prepared according to General Procedure A (0.1 mmol scale) using cyclohexane, giving 58% yield by  $^1\text{H}$  NMR. The spectra matched literature values.<sup>13</sup>



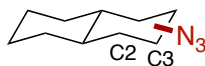
**4.5**

**Azidocycloheptane (4.5):** Prepared according to General Procedure A (0.1 mmol scale) using cycloheptane, giving 57% yield by  $^1\text{H}$  NMR. The spectra matched literature values.<sup>14</sup>



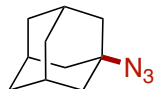
**4.6**

**Azidocyclooctane (4.6):** Prepared according to General Procedure A (0.1 mmol scale) using cyclooctane, giving 70% yield by  $^1\text{H}$  NMR. The spectra matched literature values.<sup>6</sup>



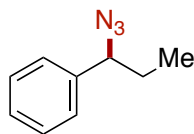
#### 4.7

**(2*R*,4*aR*,8*aR*)-2-Azidodecahydronaphthalene (4.7):** Prepared according to General Procedure A (0.1 mmol scale) using *trans*-decalin, giving 57% yield by  $^1\text{H}$  NMR and a 1.4:1 ratio of C3:C2. The spectra matched literature values.<sup>13</sup>



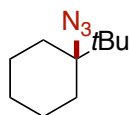
#### 4.8

**1-Azidoadamantane (4.8):** Prepared according to General Procedure A (0.1 mmol scale) using adamantane, giving 75% yield by  $^1\text{H}$  NMR. The spectra matched literature values.<sup>13</sup>



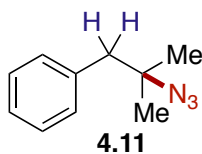
#### 4.9

**(1-Azidopropyl)benzene (4.9):** Prepared according to General Procedure A (0.1 mmol scale) using *n*-propylbenzene, giving 46% yield by  $^1\text{H}$  NMR. The spectra matched literature values.<sup>13</sup>



#### 4.10

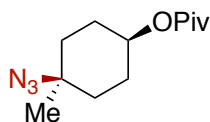
**1-Azido-1-(*tert*-butyl)cyclohexane (4.10):** Prepared according to General Procedure A (0.1 mmol scale) using *tert*-butylcyclohexane, giving 51% yield by  $^1\text{H}$  NMR. The spectra matched literature values.<sup>6</sup>



#### 4.11



**(2-Azido-2-methylpropyl)benzene (4.11).** Prepared according to General Procedure A (0.1 mmol scale) using isopropylbenzene, giving 46% combined yield by  $^1\text{H}$  NMR (1.3:1 site selectivity favoring the tertiary product). The spectra matched literature values.<sup>15</sup>



**4.12**

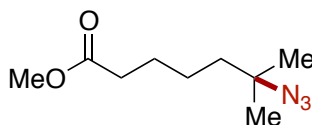
**(1s,4s)-4-Azido-4-methylcyclohexyl pivalate (4.12):** Prepared according to General Procedure A (0.1 mmol scale) using *cis*-4-methylcyclohexyl pivalate.  $^1\text{H}$  NMR analysis of the crude reaction indicated a dr of 1.4:1 with a total NMR yield of 45%. The residue was purified by column chromatography on silica gel (0 to 10% Et<sub>2</sub>O/Hexanes) to afford **4.12** (6.3 mg, 24% yield). Characterization data reported for a single isolated diastereomer:

$^1\text{H}$  NMR (600 MHz, CDCl<sub>3</sub>)  $\delta$  4.68 (tt,  $J$  = 9.8, 4.2 Hz, 1H), 1.85 – 1.71 (m, 4H), 1.68 (m, 2H), 1.52 – 1.43 (m, 2H), 1.32 (s, 3H), 1.19 (s, 9H).

$^{13}\text{C}$  NMR (151 MHz, CDCl<sub>3</sub>)  $\delta$  178.21, 71.02, 60.54, 38.86, 34.28, 27.35, 27.29, 27.23.

HRMS (APCI): calculated for C<sub>12</sub>H<sub>21</sub>N<sub>3</sub>O<sub>2</sub>Na [M+Na]<sup>+</sup> = 262.1526; found 262.1436.

IR (film) cm<sup>-1</sup> 2921.63, 2850.27, 2100.10, 1716.34, 1698.02, 1507.10, 1296.92.



**4.13**

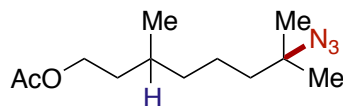
**Methyl 6-azido-6-methylheptanoate (4.13):** Prepared according to General Procedure A (0.1 mmol scale) using methyl 6-methylheptanoate. The crude residue was purified by column chromatography on silica gel (0 to 10% Et<sub>2</sub>O/Hexanes) to afford **4.13** (14.2 mg, 71% yield):

$^1\text{H}$  NMR (600 MHz, CDCl<sub>3</sub>)  $\delta$  3.74 – 3.63 (m, 3H), 2.36 – 2.28 (m, 2H), 1.66 – 1.59 (m, 2H), 1.52 – 1.44 (m, 2H), 1.38 (dd,  $J$  = 7.4, 4.1 Hz, 2H), 1.24 (dd,  $J$  = 4.2, 2.4 Hz, 6H).

$^{13}\text{C}$  NMR (151 MHz,  $\text{CDCl}_3$ )  $\delta$  174.07, 61.59, 51.64, 41.21, 34.04, 26.09, 25.26, 23.94.

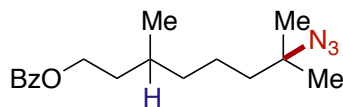
HRMS (ESI): calculated for  $\text{C}_9\text{H}_{17}\text{N}_3\text{O}_2\text{Na}$   $[\text{M}+\text{Na}]^+ = 222.1213$ ; found 222.1218.

IR (film)  $\text{cm}^{-1}$  2949.59, 2869.56, 2096.24, 1740.44, 1463.71, 1370.18, 1252.54.



**4.14**

**7-Azido-3,7-dimethyloctyl acetate (4.14):** Prepared according to General Procedure A (0.1 mmol scale) using 3,7-dimethyloctyl acetate. The crude residue was purified by column chromatography on silica gel (0 to 10%  $\text{Et}_2\text{O}$ /Hexanes) to give **4.14** in 73% yield and a 4:1 ratio of 3° isomers. The spectra matched literature values.<sup>6</sup>



**4.15**

**7-Azido-3,7-dimethyloctyl benzoate (4.15):** Prepared according to General Procedure A (0.1 mmol scale) using 3,7-dimethyloctyl benzoate. The crude residue was purified by column chromatography on silica gel (0 to 10%  $\text{Et}_2\text{O}$ /Hexanes) to afford **4.15** (27.7 mg, 91% yield, 3:1 ratio of 3° isomers). Characterization data reported for major isomer:

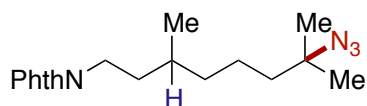
$^1\text{H}$  NMR (600 MHz,  $\text{CDCl}_3$ )  $\delta$  8.06 – 8.02 (m, 2H), 7.60 – 7.53 (m, 1H), 7.45 (d,  $J = 7.8$  Hz, 2H), 4.40 – 4.32 (m, 2H), 1.85 – 1.78 (m, 1H), 1.70 – 1.63 (m, 1H), 1.62 – 1.57 (m, 1H), 1.49 – 1.30 (m, 5H), 1.25 (s, 6H), 1.23 – 1.15 (m, 1H), 1.00 – 0.97 (m, 3H).

$^{13}\text{C}$  NMR (151 MHz,  $\text{CDCl}_3$ )  $\delta$  166.81, 132.97, 130.63, 129.67, 128.48, 63.57, 61.79, 41.81, 37.27, 35.69, 30.08, 26.17, 26.14, 21.73, 19.66.

HRMS (ESI): calculated for  $\text{C}_{17}\text{H}_{25}\text{N}_3\text{O}_2\text{Na}$   $[\text{M}+\text{H}]^+ = 326.1839$ ; found 326.1840.

IR (film)  $\text{cm}^{-1}$  2959.23, 2131.92, 2098.17, 1719.23, 1406.82, 1275.68, 1176.36.

The reaction was also performed on 1 mmol scale in a scintillation vial with irradiation from 1 Ecoxotic lamp for 2 days and purified to afford **4.15** (182 mg, 60% yield). The decrease in yield is likely due to reduced light penetration through the thicker-walled scintillation vial.



**4.16**

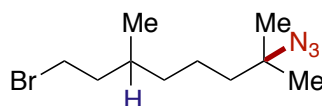
**2-(7-Azido-3,7-dimethyloctyl)isoindoline-1,3-dione (4.16):** Prepared according to General Procedure A (0.1 mmol scale) using 2-(3,7-dimethyloctyl)isoindoline-1,3-dione. The crude residue was purified by column chromatography on silica gel (0 to 10% Et<sub>2</sub>O/Hexanes) to afford **4.16** (24.7 mg, 72% yield, 3:1 ratio of 3° isomers). Characterization data reported for major isomer:

**<sup>1</sup>H NMR** (600 MHz, CDCl<sub>3</sub>) δ 7.83 (dd, *J* = 5.4, 3.0 Hz, 2H), 7.70 (dd, *J* = 5.4, 3.1 Hz, 2H), 3.70 (dq, *J* = 7.5, 2.9 Hz, 2H), 1.73 – 1.67 (m, 1H), 1.58 – 1.42 (m, 4H), 1.41 – 1.28 (m, 3H), 1.24 (s, 6H), 1.21 – 1.13 (m, 1H), 0.98 (d, *J* = 5.9 Hz, 3H).

**<sup>13</sup>C NMR** (151 MHz, CDCl<sub>3</sub>) δ 168.53, 133.97, 132.35, 123.28, 61.80, 41.67, 37.07, 36.38, 35.61, 30.73, 26.13, 26.10, 21.63, 19.43.

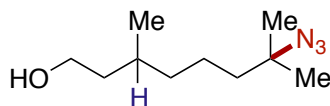
**HRMS** (ESI): calculated for C<sub>18</sub>H<sub>24</sub>N<sub>4</sub>O<sub>2</sub>Na [M+Na]<sup>+</sup> = 351.1792; found 351.1797.

**IR (film)** cm<sup>-1</sup> 2955.38, 2870.52, 2098.17, 1772.26, 1715.37, 1321.14, 1266.04.



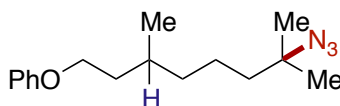
**4.17**

**7-Azido-1-bromo-3,7-dimethyloctane (4.17):** Prepared according to General Procedure A (0.1 mmol scale) using 1-bromo-3,7-dimethyloctane. The crude residue was purified by column chromatography on silica gel (0 to 10% Et<sub>2</sub>O/Hexanes) to afford **4.17** in 67% yield and a 3:1 ratio of 3° isomers. The spectra matched literature values.<sup>6</sup>



**4.18**

**7-Azido-3,7-dimethyloctan-1-ol (4.18):** Prepared according to General Procedure A (0.1 mmol scale) using 3,7-dimethyl-1-octanol to afford **4.18** in 63% yield and a 2.7:1 ratio of 3° isomers. The spectra matched literature values.<sup>6</sup>



**4.19**

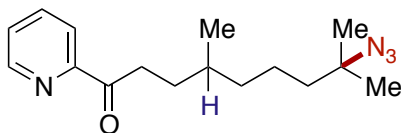
**((7-Azido-3,7-dimethyloctyl)oxy)benzene (4.19):** Prepared according to General Procedure A (0.1 mmol scale) using ((3,7-dimethyloctyl)oxy)benzene. The crude residue was purified by column chromatography on silica gel (0 to 10% Et<sub>2</sub>O/Hexanes) to afford **4.19** (8.6 mg, 31% yield by <sup>1</sup>H NMR, 2.1:1 ratio of 3° isomers). The product was characterized as an inseparable mixture from an impurity:

**<sup>1</sup>H NMR** (600 MHz, CDCl<sub>3</sub>) δ 7.30 – 7.26 (m, 2H), 6.95 – 6.91 (m, 1H), 6.91 – 6.87 (m, 2H), 4.04 – 3.95 (m, 2H), 2.05 – 1.94 (m, 1H), 1.83 (dtd, *J* = 13.8, 7.0, 5.3 Hz, 1H), 1.74 – 1.65 (m, 1H), 1.64 – 1.55 (m, 2H), 1.50 – 1.43 (m, 2H), 1.39 – 1.32 (m, 3H), 1.29 – 1.23 (m, 6H), 1.00 – 0.94 (m, 3H).

**<sup>13</sup>C NMR** (151 MHz, CDCl<sub>3</sub>) δ 129.56, 128.86, 120.64, 114.64, 66.17, 61.84, 41.82, 37.38, 36.33, 29.92, 26.19, 22.72, 21.75, 19.71.

**HRMS** (ESI): calculated for C<sub>16</sub>H<sub>25</sub>N<sub>3</sub>ONa [M+Na]<sup>+</sup> = 298.1890; found 298.1896.

**IR (film)** cm<sup>-1</sup> 2929.34, 2870.52, 2098.17, 1558.20, 1540.85, 1520.60, 1244.83.



**4.20**

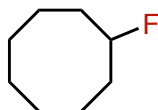
**8-Azido-4,8-dimethyl-1-(pyridin-2-yl)nonan-1-one (4.20):** Prepared according to General Procedure A (0.1 mmol scale) using 4,8-dimethyl-1-(pyridin-2-yl)nonan-1-one. The crude residue was purified by column chromatography on silica gel (0 to 10% Et<sub>2</sub>O/Hexanes) to afford **4.20** (11.2 mg, 39% yield, 3:1 ratio of 3° isomers):

**<sup>1</sup>H NMR** (600 MHz, CDCl<sub>3</sub>) δ 8.68 (ddd, *J* = 4.8, 1.7, 0.9 Hz, 1H), 8.04 (dt, *J* = 7.9, 1.1 Hz, 1H), 7.83 (td, *J* = 7.7, 1.7 Hz, 1H), 7.50 – 7.43 (m, 1H), 3.25 – 3.18 (m, 2H), 1.83 – 1.75 (m, 1H), 1.58 – 1.51 (m, 3H), 1.50 – 1.43 (m, 2H), 1.43 – 1.31 (m, 2H), 1.25 (s, 6H), 1.21 – 1.17 (m, 1H), 0.95 (d, *J* = 6.4 Hz, 3H).

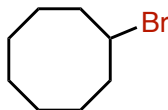
**<sup>13</sup>C NMR** (151 MHz, CDCl<sub>3</sub>) δ 202.52, 153.69, 149.06, 137.01, 127.14, 121.93, 61.87, 41.86, 37.18, 35.53, 32.67, 31.03, 26.17, 26.14, 21.84, 19.66.

**HRMS** (ESI): calculated for C<sub>16</sub>H<sub>24</sub>N<sub>4</sub>ONa [M+Na]<sup>+</sup> = 311.1843; found 311.1852.

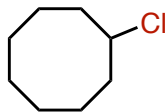
**IR (film)** cm<sup>-1</sup> 2933.20, 2869.56, 2097.21, 1698.02, 1540.85, 1520.60, 1321.00, 1267.69.



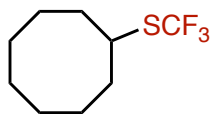
**Fluorocyclooctane.** Prepared according to General Procedure B (0.1 mmol scale) using cyclooctane as the substrate and NFSI as the radical trap with 4 hours of irradiation, affording 64% yield by <sup>19</sup>F NMR. The spectra matched literature values.<sup>16</sup>



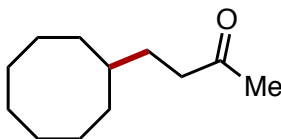
**Bromocyclooctane.** Prepared according to General Procedure B (0.1 mmol scale) using cyclooctane as the substrate and diethyl bromomalonate as the radical trap with 20 hours of irradiation, affording 60% yield by <sup>1</sup>H NMR. The spectra matched literature values.<sup>17</sup>



**Chlorocyclooctane.** Prepared according to General Procedure B (0.1 mmol scale) using cyclooctane as the substrate and NCS as the radical trap with 20 hours of irradiation, affording 32% yield by  $^1\text{H}$  NMR. The spectra matched literature values.<sup>18</sup>



**Cyclooctyl(trifluoromethyl)sulfane.** Prepared according to General Procedure B (0.1 mmol scale) using cyclooctane as the substrate and ((2-phenylpropan-2-yl)oxy)(trifluoromethyl)sulfane<sup>19</sup> as the radical trap with 4 hours of irradiation. The title compound cyclooctyl(trifluoromethyl)sulfane was afforded in 30% yield by  $^1\text{H}$  NMR. The spectra matched literature values.<sup>20</sup>



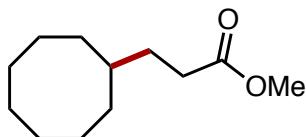
**4-Cyclooctylbutan-2-one.** Prepared according to General Procedure C using cyclooctane as the substrate and methyl vinyl ketone as the alkene. The title compound was afforded in 76% yield by  $^1\text{H}$  NMR. The title compound was purified by column chromatography on silica gel to afford 4-cyclooctylbutan-2-one (13.8 mg, 74% yield):

$^1\text{H}$  NMR (600 MHz,  $\text{CDCl}_3$ )  $\delta$  2.45 – 2.38 (m, 2H), 2.14 (s, 3H), 1.69 – 1.61 (m, 2H), 1.60 – 1.54 (m, 5H), 1.52 – 1.38 (m, 8H), 1.26 (dtd,  $J = 14.0, 8.6, 2.8$  Hz, 2H).

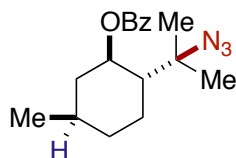
$^{13}\text{C}$  NMR (151 MHz,  $\text{CDCl}_3$ )  $\delta$  209.79, 42.17, 37.06, 32.31, 32.08, 30.02, 27.38, 26.42, 25.57.

**HRMS** (ESI): calculated for  $\text{C}_{12}\text{H}_{22}\text{ONa}$   $[\text{M}+\text{Na}]^+ = 205.1563$ ; found 205.1563.

**IR (film)**  $\text{cm}^{-1}$  2923.56, 2854.13, 1717.30, 1455.99, 1361.50.



**Methyl 3-cyclooctylpropanoate:** Prepared according to General Procedure C using cyclooctane as the substrate and methyl acrylate as the alkene. The residue was purified by column chromatography on silica gel to give methyl 3-cyclooctylpropanoate in 43% yield. The spectra matched literature values.<sup>21</sup>



**4.22**

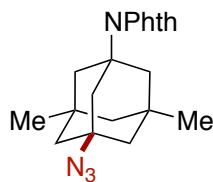
**(1R,2S,5R)-2-(2-Azidopropan-2-yl)-5-methylcyclohexyl benzoate (4.22):** Prepared according to General Procedure A (0.1 mmol scale) using (1R,2S,5R)-2-isopropyl-5-methylcyclohexyl benzoate. The crude residue was purified by column chromatography on silica gel (0 to 10% Et<sub>2</sub>O/Hexanes) to afford **4.22** (16.3 mg, 54% yield):

**<sup>1</sup>H NMR** (600 MHz, CDCl<sub>3</sub>) δ 8.07 (d, *J* = 7.8 Hz, 2H), 7.61 – 7.51 (m, 1H), 7.50 – 7.39 (m, 2H), 5.10 (td, *J* = 11.5, 10.9, 4.4 Hz, 1H), 2.10 (d, *J* = 12.3 Hz, 1H), 2.07 – 1.99 (m, 1H), 1.85 (td, *J* = 11.6, 10.9, 3.6 Hz, 1H), 1.78 – 1.70 (m, 1H), 1.66 – 1.52 (m, 1H), 1.29 (d, *J* = 4.9 Hz, 6H), 1.24 – 1.10 (m, 2H), 1.02 – 0.95 (m, 1H), 0.93 (dd, *J* = 6.6, 2.0 Hz, 3H).

**<sup>13</sup>C NMR** (151 MHz, CDCl<sub>3</sub>) δ 165.84, 133.05, 130.77, 129.77, 128.53, 74.01, 63.74, 49.31, 41.48, 34.24, 31.38, 26.70, 25.32, 24.64, 21.86.

**HRMS** (ESI): calculated for C<sub>17</sub>H<sub>23</sub>N<sub>3</sub>O<sub>2</sub>Na [M+Na]<sup>+</sup> = 324.1683; found 324.1678.

**IR (film)** cm<sup>-1</sup> 2958.27, 2872.45, 2131.92, 2102.03, 1715.37, 1322.93, 1276.65.



**4.23**

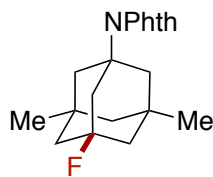
**2-(3-Azido-5,7-dimethyladamantan-1-yl)isoindoline-1,3-dione (4.23):** Prepared according to General Procedure A (0.1 mmol scale) using 2-(3,5-dimethyladamantan-1-yl)isoindoline-1,3-dione. The crude residue was purified by column chromatography on silica gel (0 to 10% Et<sub>2</sub>O/Hexanes) to afford **4.23** (19.3 mg, 55% yield):

**<sup>1</sup>H NMR** (600 MHz, CDCl<sub>3</sub>)  $\delta$  7.76 (dd,  $J$  = 5.4, 3.0 Hz, 2H), 7.68 (dd,  $J$  = 5.5, 3.0 Hz, 2H), 2.45 (s, 2H), 2.14 (s, 4H), 1.61 – 1.54 (m, 2H), 1.44 (d,  $J$  = 11.9 Hz, 2H), 1.26 (dt,  $J$  = 12.7, 2.3 Hz, 1H), 1.20 – 1.10 (m, 1H), 0.99 (s, 6H).

**<sup>13</sup>C NMR** (151 MHz, CDCl<sub>3</sub>)  $\delta$  169.60, 134.04, 131.87, 122.86, 61.90, 60.79, 49.20, 46.57, 44.99, 42.78, 34.02, 29.55.

**HRMS** (ESI): calculated for C<sub>20</sub>H<sub>23</sub>N<sub>4</sub>O<sub>2</sub> [M+H]<sup>+</sup> = 351.1833; found 351.1816.

**IR (film)** cm<sup>-1</sup> 2900.55, 2862.81, 2090.46, 1706.69, 1540.85, 1316.18, 1247.72.



**4.24**

**2-(3-Fluoro-5,7-dimethyladamantan-1-yl)isoindoline-1,3-dione (4.24).** Prepared according to General Procedure B (0.1 mmol scale) using 2-(3,5-dimethyladamantan-1-yl)isoindoline-1,3-dione as the substrate and NFSI as the radical trap with 4 hours of irradiation. The residue was purified by column chromatography on silica gel to afford **4.24** (28.2 mg, 86% yield). Minor amounts of secondary fluorination product are also present:



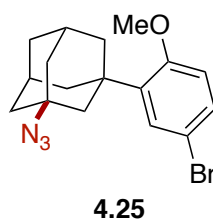
**<sup>1</sup>H NMR** (600 MHz, CDCl<sub>3</sub>) δ 7.76 (dd, *J* = 5.4, 3.1 Hz, 2H), 7.68 (dd, *J* = 5.5, 3.0 Hz, 2H), 2.60 – 2.57 (m, 2H), 2.18 – 2.13 (m, 2H), 2.08 (ddd, *J* = 12.4, 2.4, 1.2 Hz, 2H), 1.70 – 1.64 (m, 2H), 1.58 – 1.53 (m, 2H), 1.23 (ddt, *J* = 12.8, 4.1, 2.2 Hz, 1H), 1.16 (dt, *J* = 12.7, 2.3 Hz, 1H), 1.01 (s, 6H).

**<sup>13</sup>C NMR** (151 MHz, CDCl<sub>3</sub>) δ 169.57, 134.03, 131.84, 122.86, 93.50 (d, *J* = 183.7 Hz), 62.51 (d, *J* = 12.1 Hz), 49.18 (d, *J* = 1.5 Hz), 47.73 (d, *J* = 16.6 Hz), 45.01 (d, *J* = 1.5 Hz), 43.95 (d, *J* = 21.1 Hz), 34.91 (d, *J* = 10.6 Hz), 29.34.

**<sup>19</sup>F NMR** (400 MHz, CDCl<sub>3</sub>) δ –135.68.

**HRMS** (ESI): calculated for C<sub>20</sub>H<sub>22</sub>FNO<sub>2</sub> [M+H]<sup>+</sup> = 328.1707; found 328.1720.

**IR (film)** cm<sup>–1</sup> 2925.48, 2906.20, 1771.30, 1707.66, 1456.96, 1316.18, 717.39.



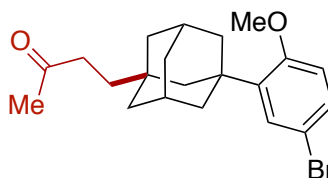
**1-Azido-3-(5-bromo-2-methoxyphenyl)adamantane (4.25):** Prepared according to General Procedure A (0.1 mmol scale) using 2-(1-adamantyl)-4-bromoanisole. The crude residue was purified by column chromatography on silica gel (0 to 10% Et<sub>2</sub>O/Hexanes) to give **4.25** in 40% yield by <sup>1</sup>H NMR due to the product being inseparable from an impurity:

**<sup>1</sup>H NMR** (600 MHz, CDCl<sub>3</sub>) δ 7.34 – 7.31 (m, 1H), 7.28 (s, 1H), 6.77 (d, *J* = 8.7 Hz, 1H), 3.84 (d, *J* = 3.8 Hz, 3H), 2.34 (dq, *J* = 6.5, 3.2 Hz, 2H), 2.14 (d, *J* = 5.9 Hz, 2H), 2.07 (dt, *J* = 12.9, 2.8 Hz, 2H), 1.97 (q, *J* = 14.5, 12.6 Hz, 2H), 1.86 (d, *J* = 3.3 Hz, 3H), 1.76 – 1.65 (m, 2H).

**<sup>13</sup>C NMR** (151 MHz, CDCl<sub>3</sub>) δ 157.75, 138.48, 130.07, 129.73, 113.49, 112.42, 59.92, 55.61, 55.40, 44.02, 43.89, 41.00, 39.72, 39.69, 39.11, 35.48, 30.31.

**HRMS** (APCI): calculated for  $C_{17}H_{20}N_3OBrNa$   $[M+Na]^+ = 384.0682$ ; found 384.0738.

**IR (film)**  $cm^{-1}$  2912.95, 2865.06, 2089.49, 1558.20, 1496.49, 1234.22.



**4.26**

**4-((1*r*,3*s*,5*R*,7*S*)-3-(5-bromo-2-methoxyphenyl)adamantan-1-yl)butan-2-one (4.26).**

Prepared according to General Procedure C using 2-(1-adamantyl)-4-bromoanisole as the substrate and methyl vinyl ketone as the alkene. The residue was purified by column chromatography on silica gel to afford **4.26** (17.6 mg, 45% yield):

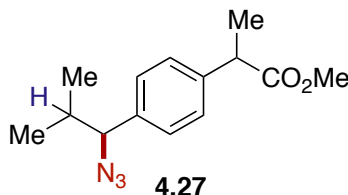
**$^1H$  NMR** (600 MHz,  $CDCl_3$ )  $\delta$  7.27 – 7.24 (m, 2H), 6.73 (d,  $J = 9.3$  Hz, 1H), 3.80 (s, 3H), 2.44 – 2.37 (m, 2H), 2.15 (s, 3H), 2.14 – 2.11 (m, 2H), 1.98 – 1.94 (m, 3H), 1.85 – 1.68 (m, 4H), 1.65 – 1.57 (m, 2H), 1.47 (d,  $J = 2.7$  Hz, 3H), 1.46 – 1.41 (m, 2H).

**$^{13}C$  NMR** (151 MHz,  $CDCl_3$ )  $\delta$  209.98, 157.96, 140.29, 129.81, 129.58, 113.49, 113.39, 55.36, 44.98, 41.59, 39.97, 38.02, 37.81, 37.66, 36.51, 32.84, 30.08, 29.38.

**HRMS** (ESI): calculated for  $C_{21}H_{27}BrO_2Na$   $[M+Na]^+ = 413.1087$ ; found 413.1082.

**IR (film)**  $cm^{-1}$  2904.27, 2848.35, 1716.34, 1520.61, 1473.35, 1234.22, 1027.87.

The reaction was also performed on 1 mmol scale in a scintillation vial with irradiation from 2 Kessil lamps for 2 days and purified to afford **4.26** (152 mg, 39% yield).



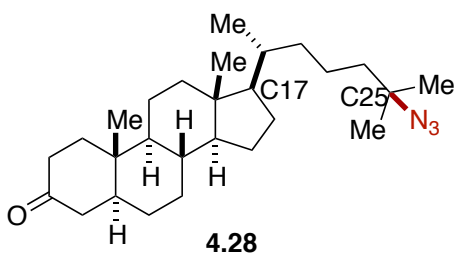
**4.27**

**Methyl 2-(4-(2-azido-2-methylpropyl)phenyl)propanoate (4.27):** Prepared according to General Procedure A (0.1 mmol scale) using methyl 2-(4-isobutylphenyl)propanoate.  $^1H$  NMR analysis of the crude reaction mixture revealed a 1.1:1 ratio of benzylic to tertiary

azide isomers. The residue was purified by column chromatography on silica gel (0 to 10% Et<sub>2</sub>O/Hexanes) to afford **4.27** (14.8 mg, 57% yield). Characterization data are reported for the previously unreported tertiary isomer; both benzylic azide diastereomers are also present as impurities in the product.<sup>13</sup>

**<sup>1</sup>H NMR** (600 MHz, CDCl<sub>3</sub>) δ 7.30 (d, *J* = 8.1 Hz, 1H), 7.25 – 7.20 (m, 2H), 7.16 (d, *J* = 8.1 Hz, 1H), 3.72 (m, 1H), 3.66 (s, 3H), 2.74 (s, 2H), 1.50 (dd, *J* = 7.2, 5.5 Hz, 3H), 1.26 (s, 6H).  
**<sup>13</sup>C NMR** (151 MHz, CDCl<sub>3</sub>) δ 175.17, 139.10, 135.81, 130.87, 127.34, 61.96, 52.17, 47.22, 45.19, 26.06, 18.73.

**IR (film)** cm<sup>-1</sup> 2958.27, 2936.09, 2099.14, 1739.48, 1456.96, 1210.11.



**(5*S*,8*R*,9*S*,10*S*,13*R*,14*S*,17*R*)-17-((*R*)-6-Azido-6-methylheptan-2-yl)-10,13-dimethyltetradecahydro-1*H*-cyclopenta[*a*]phenanthren-3(2*H*)-one (4.28):**

Prepared according to General Procedure A (0.1 mmol scale) using 5- $\alpha$ -cholestan-3-one. The crude residue was purified by column chromatography on silica gel (0 to 10% Et<sub>2</sub>O/Hexanes) to afford **4.28** (13.8 mg, 37% yield), favoring functionalization at the C25 and C17 tertiary positions (approximately 1:1). The <sup>13</sup>C spectrum is complicated due to the presence of minor secondary azidation products:

**<sup>1</sup>H NMR** (600 MHz, CDCl<sub>3</sub>) δ 2.41 – 2.34 (m, 1H), 2.32 – 2.23 (m, 2H), 2.11 – 2.05 (m, 1H), 2.04 – 1.95 (m, 2H), 1.86 – 1.60 (m, 3H), 1.60 – 1.46 (m, 5H), 1.46 – 1.29 (m, 8H), 1.28 – 1.19 (m, 1H), 1.25 (s, 3H), 1.19 – 1.04 (m, 4H), 1.04 – 0.98 (m, 1H), 1.01 (d, *J* = 1.4 Hz, 3H), 0.97 – 0.85 (m, 7.5H), 0.85 – 0.77 (m, 1H), 0.77 – 0.71 (m, 1H), 0.68 (s, 1.5H).

**<sup>13</sup>C NMR** (151 MHz, CDCl<sub>3</sub>) δ 212.34, 212.31, 80.95, 61.93, 56.44, 56.42, 56.33, 53.97, 53.95, 46.86, 44.89, 44.86, 44.80, 42.78, 42.75, 42.07, 42.02, 40.07, 40.05, 39.66, 38.72, 38.36, 38.33, 38.28, 36.30, 35.94, 35.85, 35.80, 35.74, 35.56, 31.89, 31.87, 31.82, 29.14, 29.13, 29.01, 28.39, 28.17, 28.13, 26.23, 26.16, 25.75, 24.39, 24.37, 23.99, 22.97, 22.92, 22.71, 22.65, 21.60, 21.36, 20.91, 18.82, 18.75, 14.80, 14.75, 12.23, 11.63, 11.59.

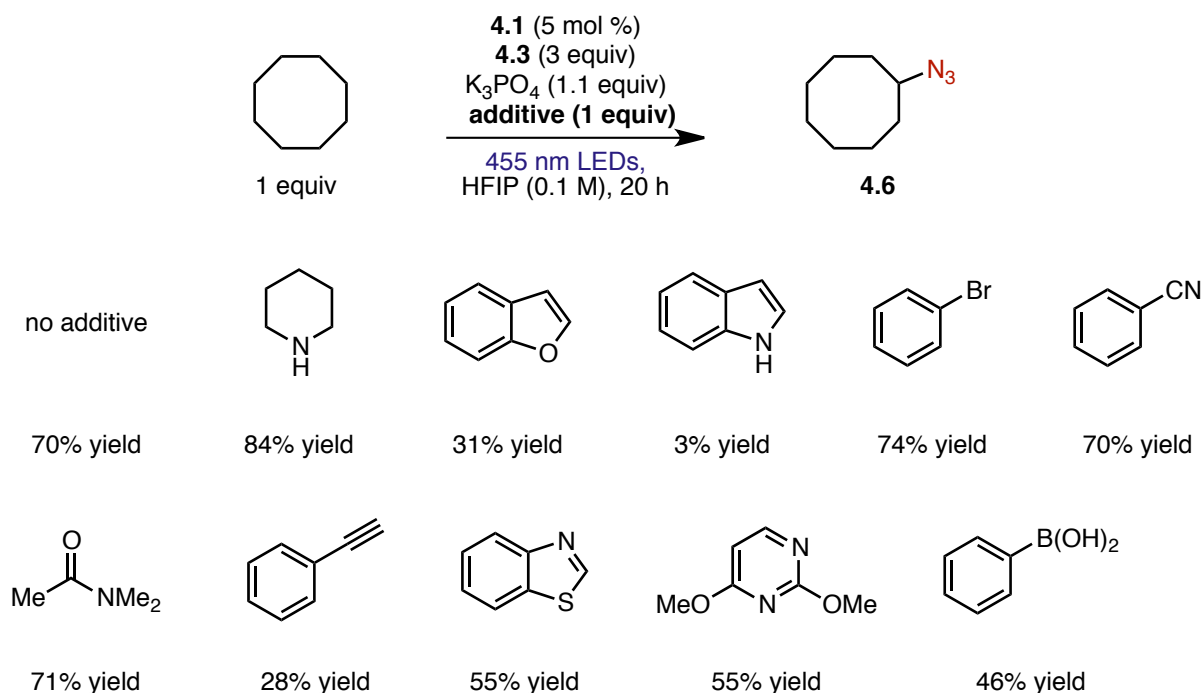
**HRMS** (ESI): calculated for C<sub>27</sub>H<sub>45</sub>N<sub>3</sub>ONa [M+Na]<sup>+</sup> = 450.3455; found 450.3469.

**IR (film)** cm<sup>-1</sup> 2932.23, 2866.62, 2098.17, 1715.37, 1455.99, 1267.97.

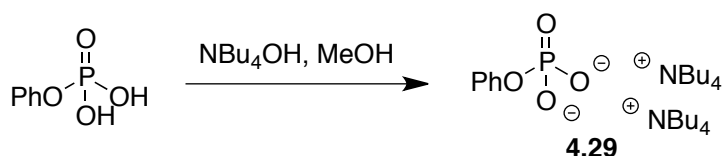
The singlet at δ 0.68 ppm corresponds to the methyl at C13, and this signal is underintegrated (1.5H instead of 3H), indicating that the methyl has been shifted for one of the azidation products. Since there is only trace secondary azidation, the methyl at C13 cannot be shifted from azidation at C12 and instead arises from tertiary azidation at C17. Additionally, the isopropyl methyl signals that lie between 0.85 and 0.90 ppm are underintegrated and there is a new signal at 1.25 ppm corresponding to azidation of the isopropyl group at C25. This signal integrates to 3H instead of 6H, however, indicating that it is only from one of the two products.

### **Robustness Screen**

Below are the results from a robustness screen surveying several different additives containing useful functionality or pharmaceutically relevant heterocycles. Yields of the cyclooctane azidation product **4.6** are given below each additive.



### Mechanistic Studies



**Di(tetrabutylammonium) phenyl phosphate (4.29):** To a solution of phenyl dihydrogen phosphate<sup>22</sup> (1.22 g, 7 mmol) in methanol (7 mL) was added tetrabutylammonium hydroxide in methanol (1M, 14 mL, 14 mmol). The solution was stirred overnight and then concentrated *in vacuo*. The resultant oil was dried via high vacuum for one week to afford **4.29** as an amorphous solid. The compound is extremely hygroscopic and unstable outside of an inert atmosphere.<sup>23</sup>

**$^1H$  NMR** (600 MHz,  $CDCl_3$ )  $\delta$  7.19 – 7.10 (m, 2H), 7.06 (t,  $J = 7.8$  Hz, 1H), 6.97 (d,  $J = 8.0$  Hz, 1H), 3.31 – 3.25 (m, 16H), 1.63 – 1.55 (m, 16H), 1.39 (q,  $J = 7.4$  Hz, 16H), 0.94 (t,  $J = 7.3$  Hz, 24H).

**$^{13}C$  NMR** (151 MHz,  $CDCl_3$ )  $\delta$  129.12, 128.85, 118.14, 116.11, 58.96, 24.20, 19.82, 13.79.

As determined by cyclic voltammetry, the oxidation potential of **4.29** was  $E_{p/2} = + 0.87$  V vs SCE in MeCN. Phosphate esters including **4.29** are known to be unstable for prolonged periods in MeCN.<sup>23</sup>

### **Stern-Volmer Quenching:**

Emission lifetime measurements were taken at ambient temperature using a Edinburgh FLS920 spectrometer and fit to single exponential decay according to a modification of the method previously described by our laboratory.<sup>24</sup> Measurements were made by the time-correlated single photon counting (TCSPC) capability of the instrument with pulsed excitation light (444.2 nm, typical pulse width = 95 ps) generated by a Edinburgh EPL-445 ps pulsed laser diode operating at a repetition rate of 5 MHz. The maximum emission channel count rate was less than 5% of the laser channel count rate, and each data set collected greater than 10000 counts on the maximum channel. The lifetime of fluorescence was determined by reconvolution fit with the instrument response function using the Edinburgh FS900 software. In all cases, after reconvolution, fluorescence decay was satisfactorily fit with a monoexponential function of the form:

$$I_t = I_0 e^{-t/\tau}$$

where  $I$  is the intensity (counts), and  $t$  is the mean lifetime of fluorescence.

Stern-Volmer analysis on the quenching of fluorescence lifetime was carried out in DCE or HFIP with detection at 500 nm (15 nm bandwidth), where the concentration of acridinium was  $1.6 \times 10^{-5}$  M. The quenching constant was determined with quencher concentrations in the range of 0 M to  $2.0 \times 10^{-2}$  M. Bimolecular quenching constants,  $k_q$ , were determined from the corresponding Stern-Volmer constant.<sup>25</sup> Quenching constants were determined for ***t*-Bu<sub>2</sub>-Mes-Acr<sup>+</sup>** with sulfonyl azide **4.3**, sodium 1,1,1,3,3,3-hexafluoroisopropoxide, and dibasic

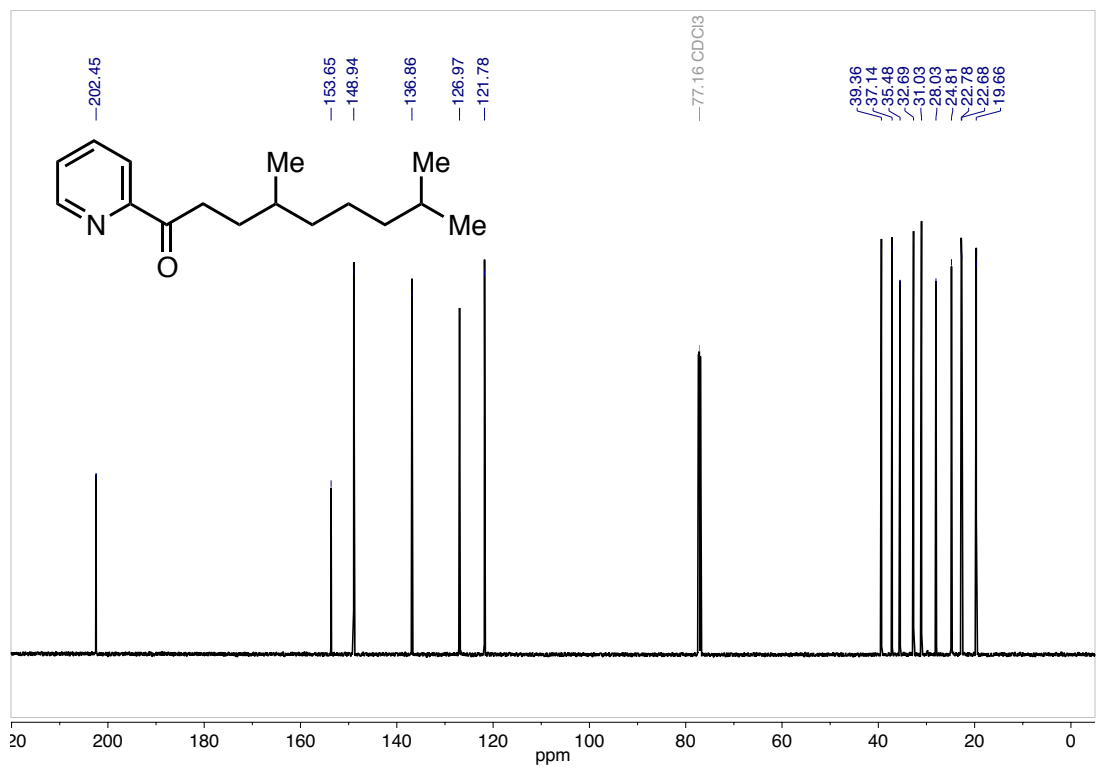
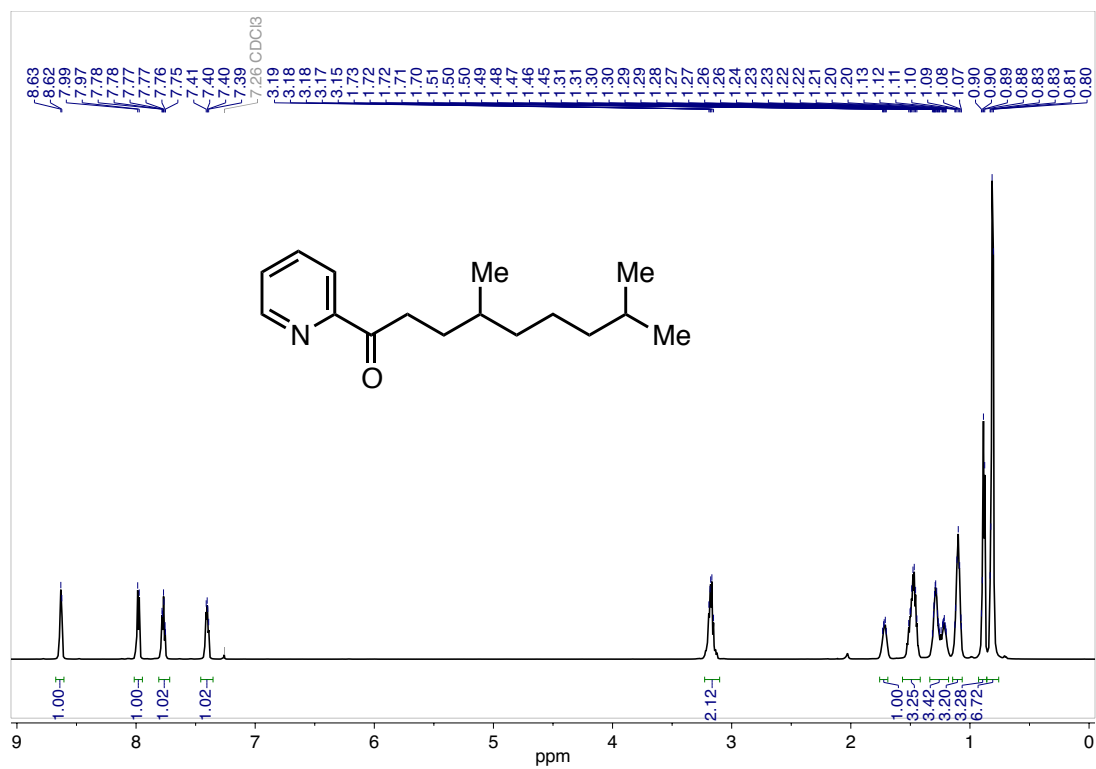
phosphate **4.29**. Comparison of UV-Vis absorption spectra taken before and after lifetime quenching studies verified that the acridinium was unchanged. UV-Vis spectra were taken on a Hewlett-Packard 8453 Chemstation spectrophotometer.

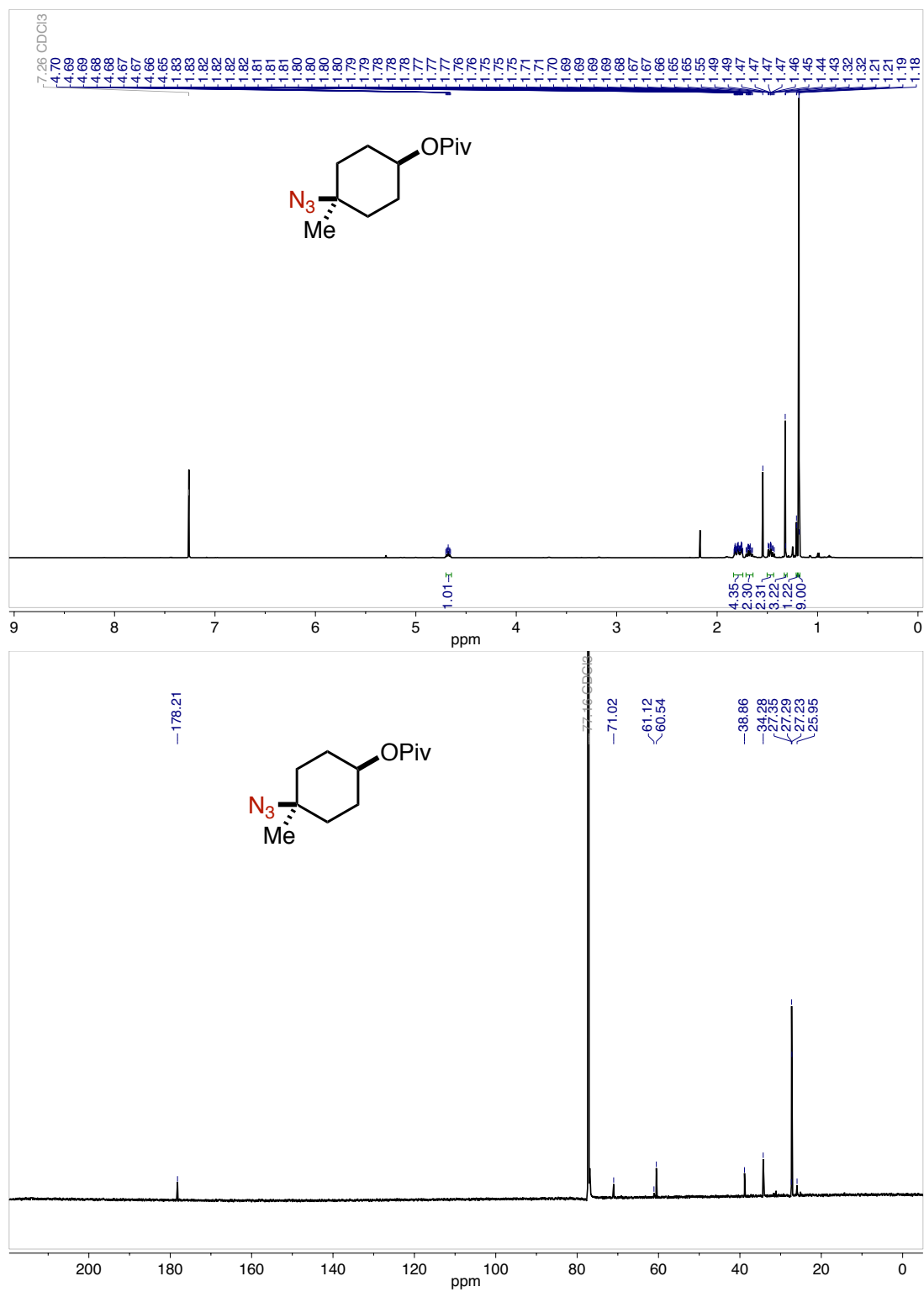
## REFERENCES

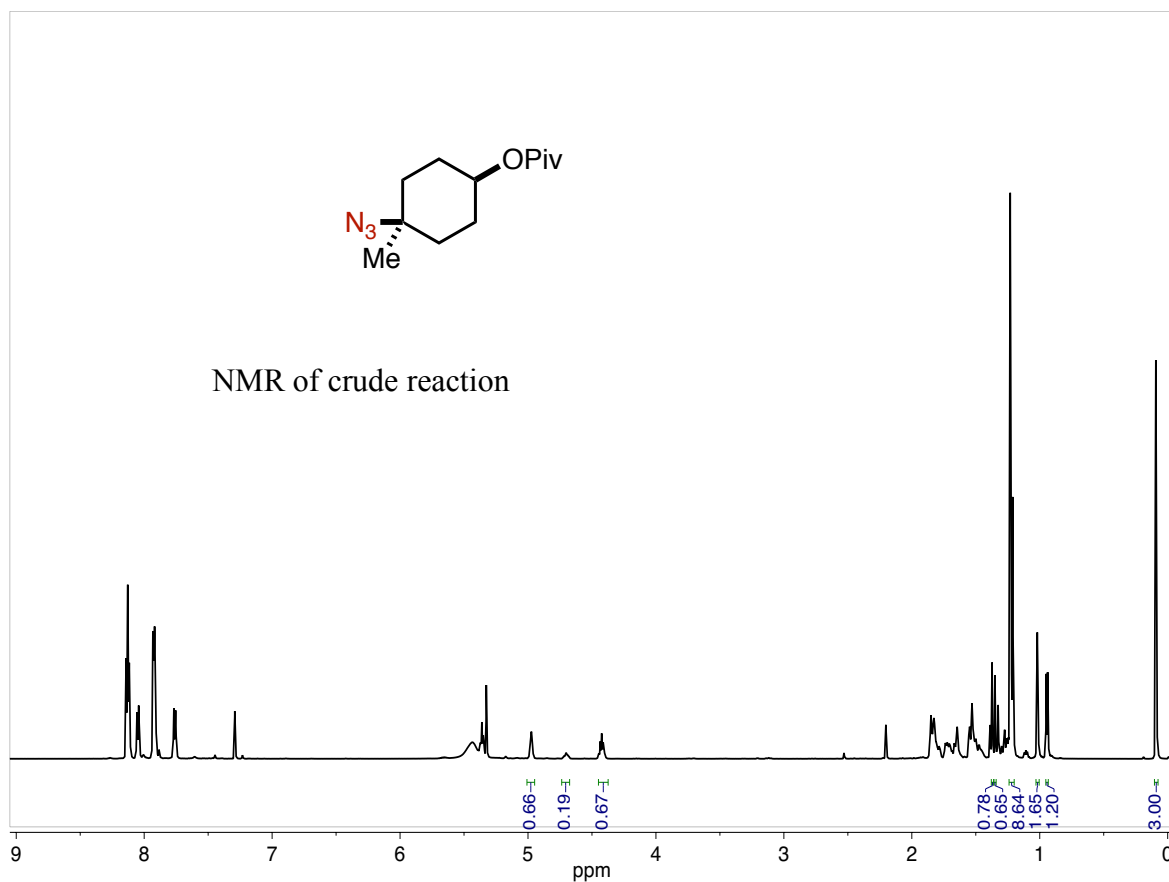
- (1) Romero, N. A.; Margrey, K. A.; Tay, N. E.; Nicewicz, D. A. *Science* **2015**, *349*, 1326–1330.
- (2) Joshi-Pangu, A.; Lévesque, F.; Roth, H. G.; Oliver, S. F.; Campeau, L.-C.; Nicewicz, D.; DiRocco, D. A. *J. Org. Chem.* **2016**, *81*, 7244–7249.
- (3) Chuprakov, S.; Malik, J. A.; Zibinsky, M.; Fokin, V. V. *J. Am. Chem. Soc.* **2011**, *133*, 10352–10355.
- (4) Shen, D.; Miao, C.; Wang, S.; Xia, C.; Sun, W. *Org. Lett.* **2014**, *16*, 1108–1111.
- (5) Dickschat, J. S.; Bruns, H.; Riclea, R. *Beilstein J. Org. Chem.* **2011**, *7*, 1697–1712.
- (6) Sharma, A.; Hartwig, J. F. *Nature* **2015**, *517*, 600–604.
- (7) Fung, Y.-S.; Yan, S.-C.; Wong, M.-K. *Org. Biomol. Chem.* **2012**, *10*, 3122.
- (8) Mukherjee, S.; Maji, B.; Tlahuext-Aca, A.; Glorius, F. *J. Am. Chem. Soc.* **2016**, *138*, 16200–16203.
- (9) Skattebøl, L.; Stenstrøm, Y.; Syvertsen, C. *J. Agric. Food Chem.* **2004**, *52*, 6944–6949.
- (10) Dander, J. E.; Weires, N. A.; Garg, N. K. *Org. Lett.* **2016**, *18*, 3934–3936.
- (11) Schmidt, V. A.; Quinn, R. K.; Brusoe, A. T.; Alexanian, E. J. *J. Am. Chem. Soc.* **2014**, *136*, 14389–14392.
- (12) Bogdan, A. R.; Poe, S. L.; Kubis, D. C.; Broadwater, S. J.; McQuade, D. T. *Angew. Chem. Int. Ed.* **2009**, *48*, 8547–8550.
- (13) Huang, X.; Bergsten, T. M.; Groves, J. T. *J. Am. Chem. Soc.* **2015**, *137*, 5300–5303.
- (14) Klich, K.; Pyta, K.; Kubicka, M. M.; Ruszkowski, P.; Celewicz, L.; Gajecka, M.; Przybylski, P. *J. Med. Chem.* **2016**, *59*, 7963–7973.
- (15) Dryzhakov, M.; Hellal, M.; Wolf, E.; Falk, F. C.; Moran, J. *J. Am. Chem. Soc.* **2015**, *137*, 9555–9558.
- (16) L’Heureux, A.; Beaulieu, F.; Bennett, C.; Bill, D. R.; Clayton, S.; LaFlamme, F.; Mirmehrabi, M.; Tadayon, S.; Tovell, D.; Couturier, M. *J. Org. Chem.* **2010**, *75*, 3401–3411.
- (17) Manabe, Y.; Kitawaki, Y.; Nagasaki, M.; Fukase, K.; Matsubara, H.; Hino, Y.; Fukuyama, T.; Ryu, I. *Chem. - Eur. J.* **2014**, *20*, 12750–12753.



- (18) Combe, S. H.; Hosseini, A.; Parra, A.; Schreiner, P. R. *J. Org. Chem.* **2017**, *82*, 2407–2413.
- (19) Shao, X.; Xu, C.; Lu, L.; Shen, Q. *Acc. Chem. Res.* **2015**, *48*, 1227–1236.
- (20) Wu, H.; Xiao, Z.; Wu, J.; Guo, Y.; Xiao, J.-C.; Liu, C.; Chen, Q.-Y. *Angew. Chem. Int. Ed.* **2015**, *54*, 4070–4074.
- (21) van Bruggen, E.; Boelens, H.; Rijkens, F. *Recl. Trav. Chim. Pays-Bas* **2010**, *86*, 958–960.
- (22) Cohen, A.; Bergel Franz; Frank Atherton Ratcliffe; Alexander Todd Robertus; Harry Openshaw Tacon; John Wynne Haworth. US2490573 (A).
- (23) Friedman, J. M.; Freeman, S.; Knowles, J. R. *J. Am. Chem. Soc.* **1988**, *110*, 1268–1275.
- (24) Romero, N. A.; Nicewicz, D. A. *J. Am. Chem. Soc.* **2014**, *136*, 17024–17035.

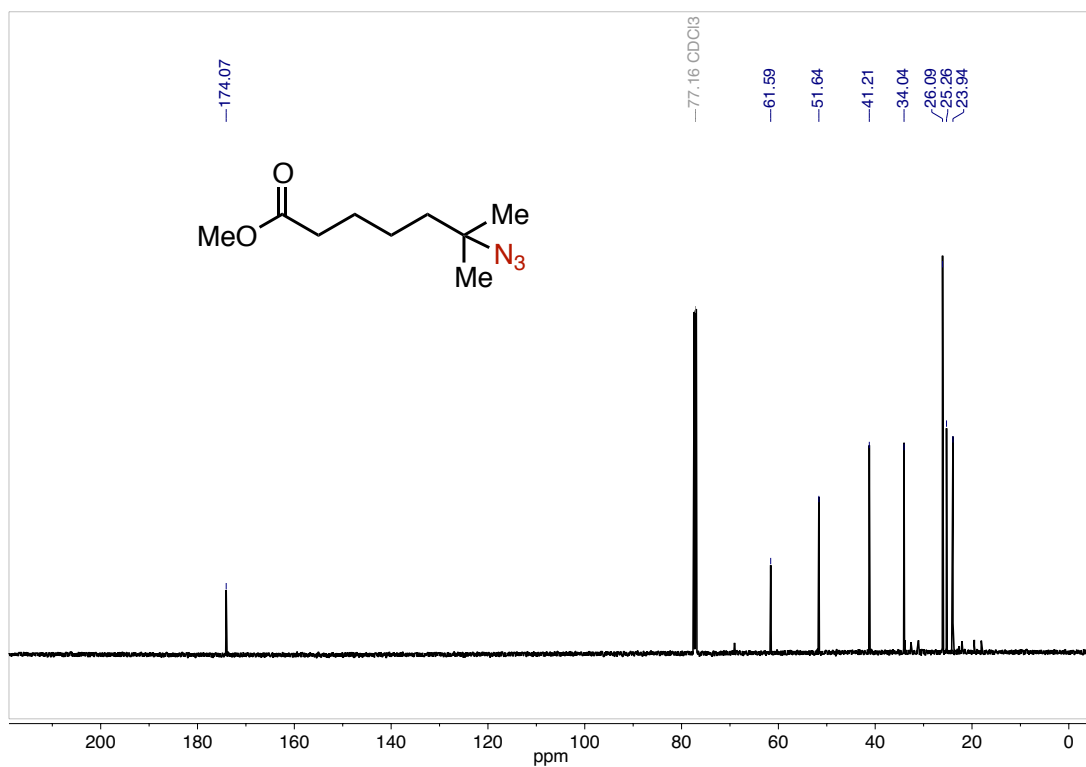
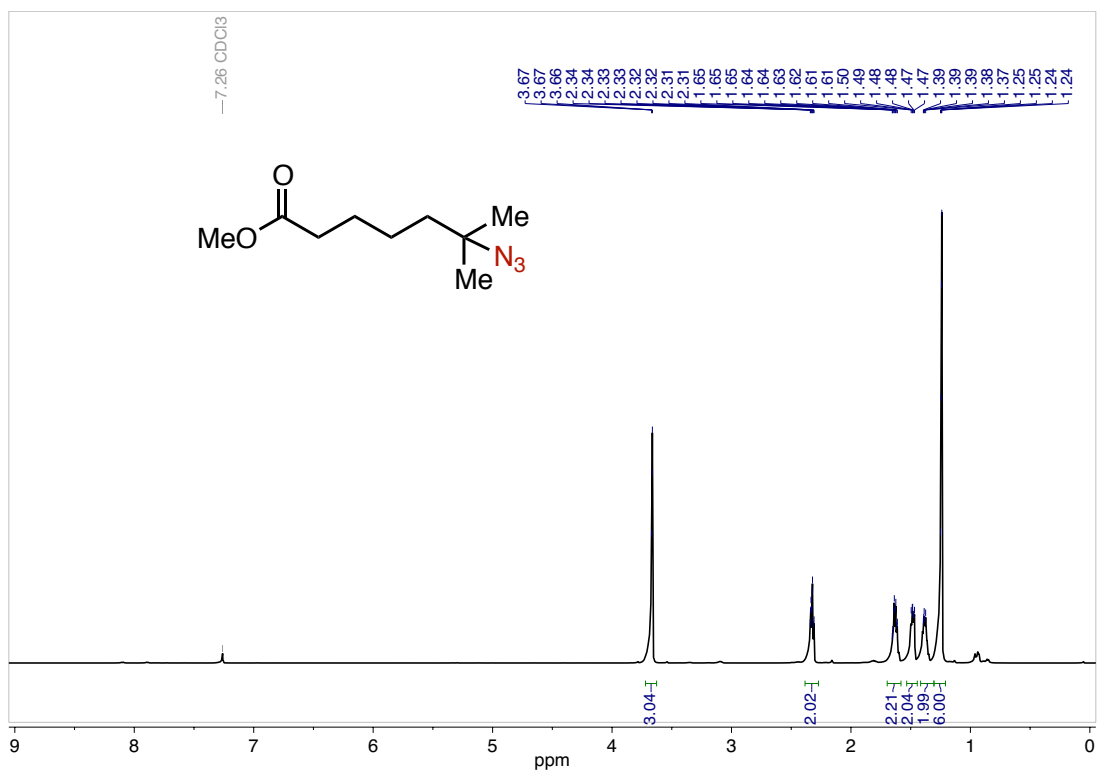


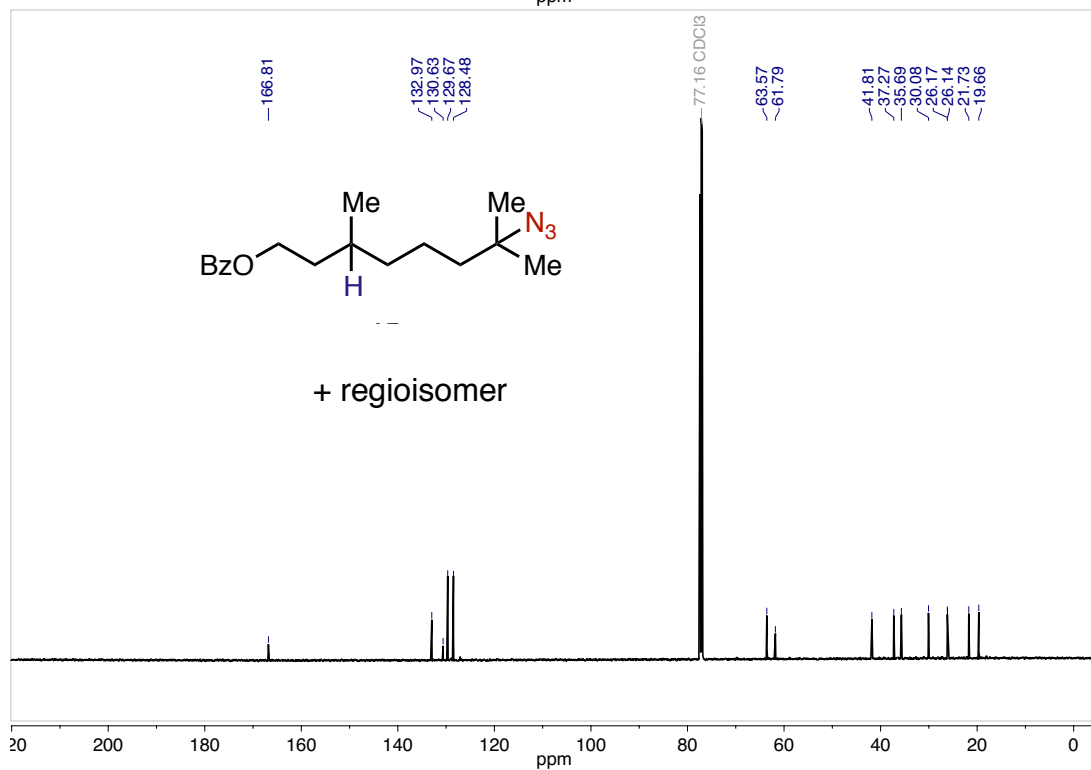
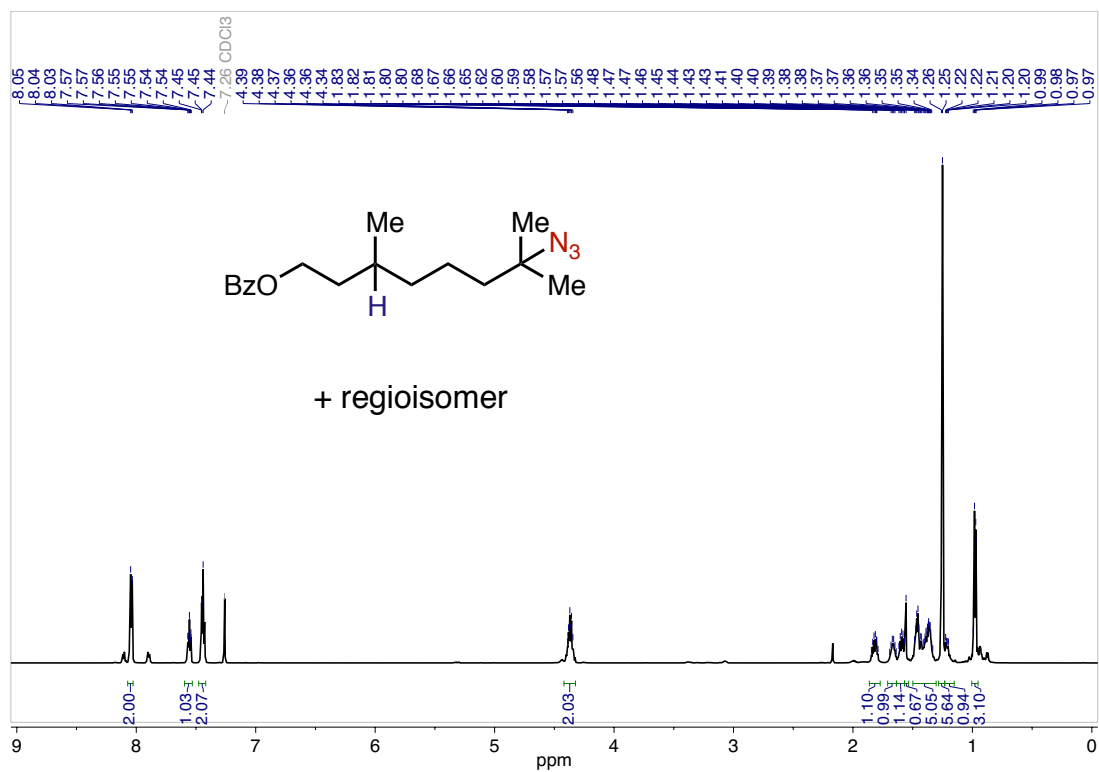




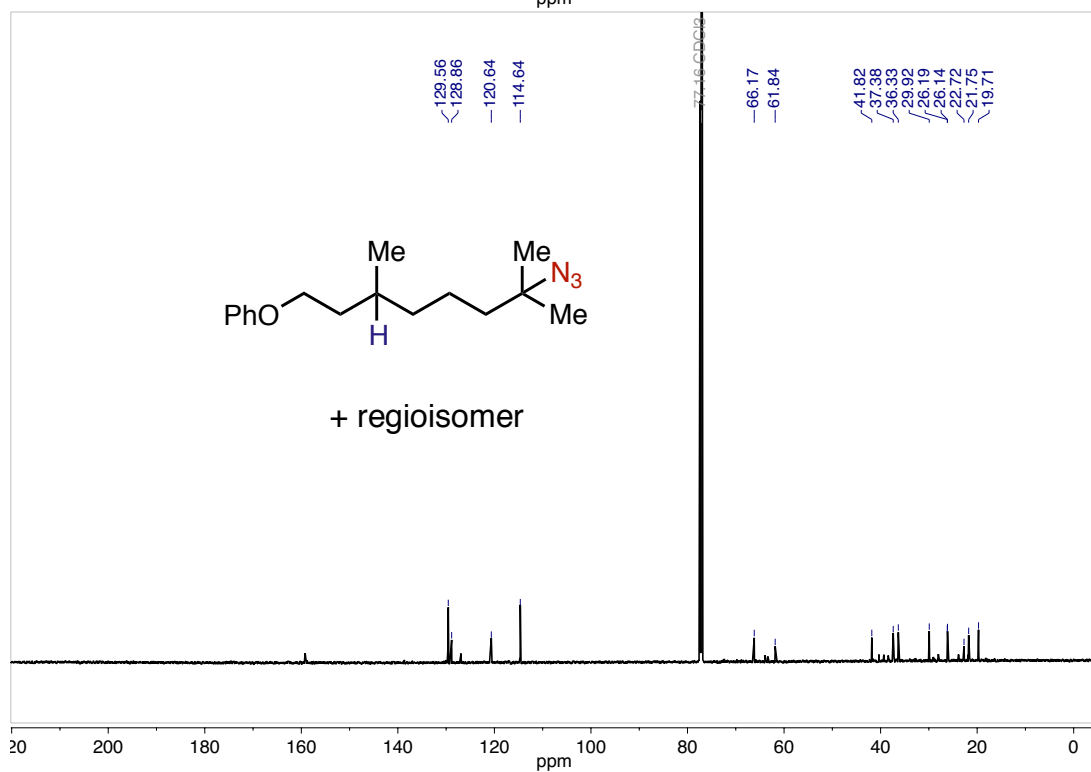
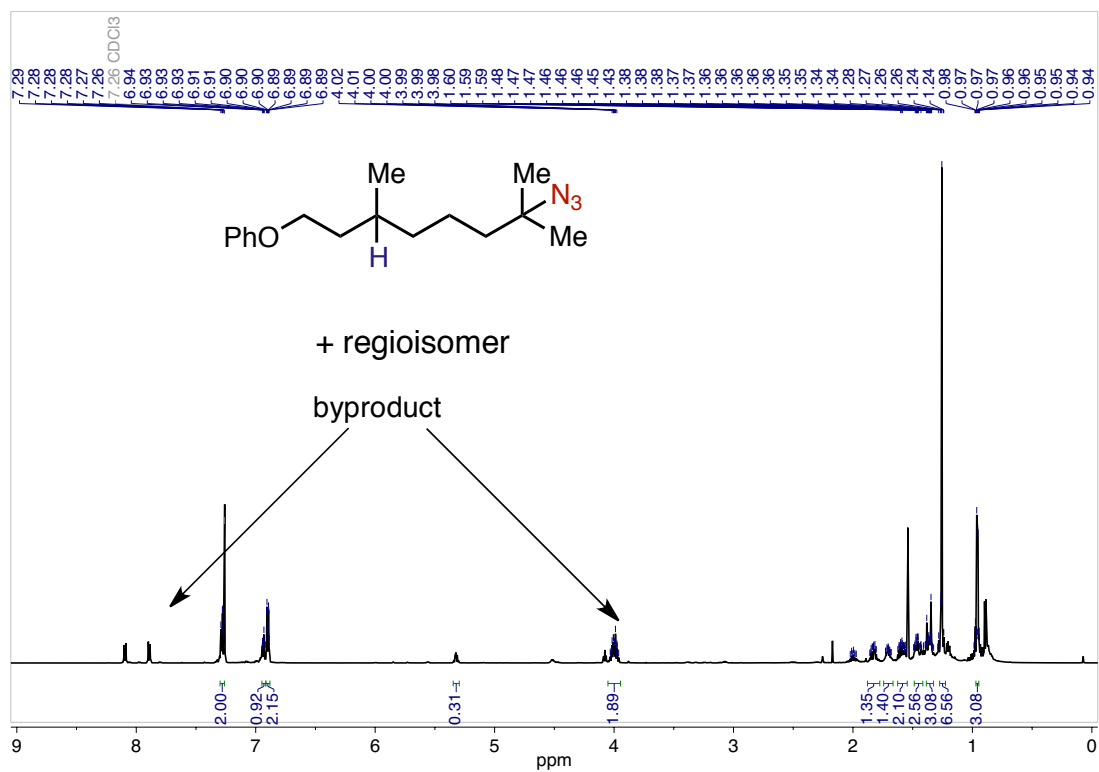
The methyl doublet below 1.0 ppm indicates 40% remaining starting material. The peaks at 5.0 ppm and 4.7 ppm correspond to both diastereomers of product, but the starting material also has a peak at 5.0 ppm. Subtraction of 40% from the peak at 5.0 ppm gives 26% yield of one diastereomer and 19% yield of the other, for a combined NMR yield of 45% and a dr

1.4:1.

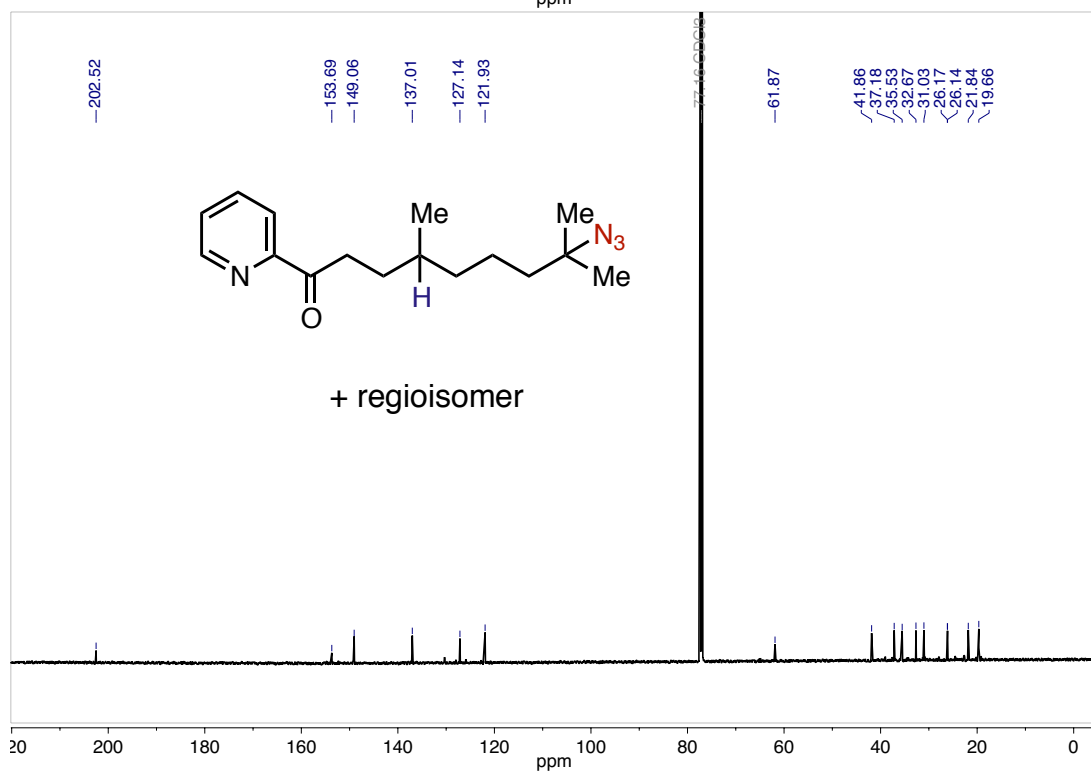
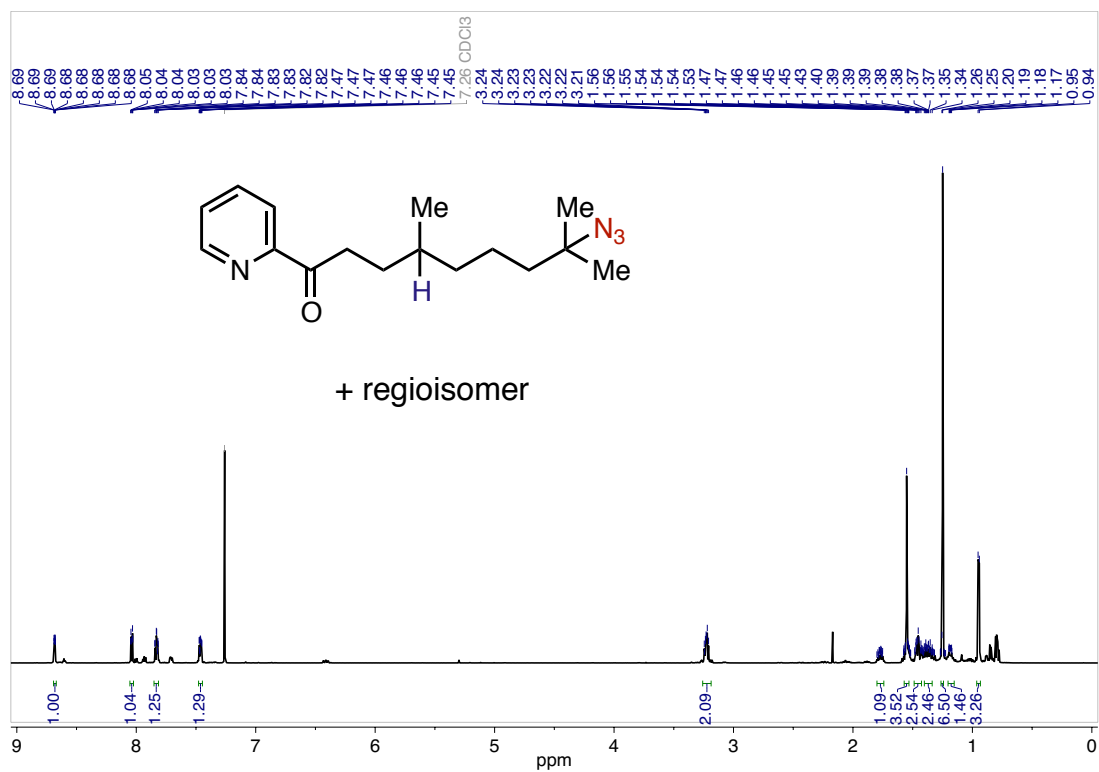


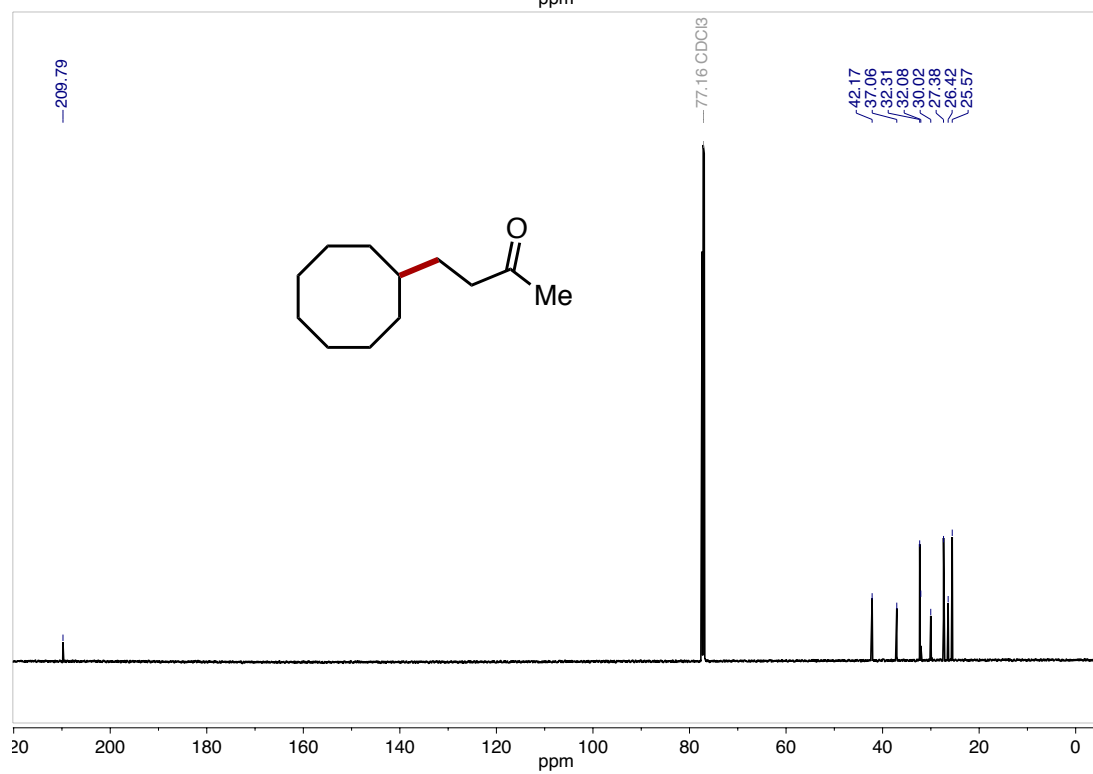
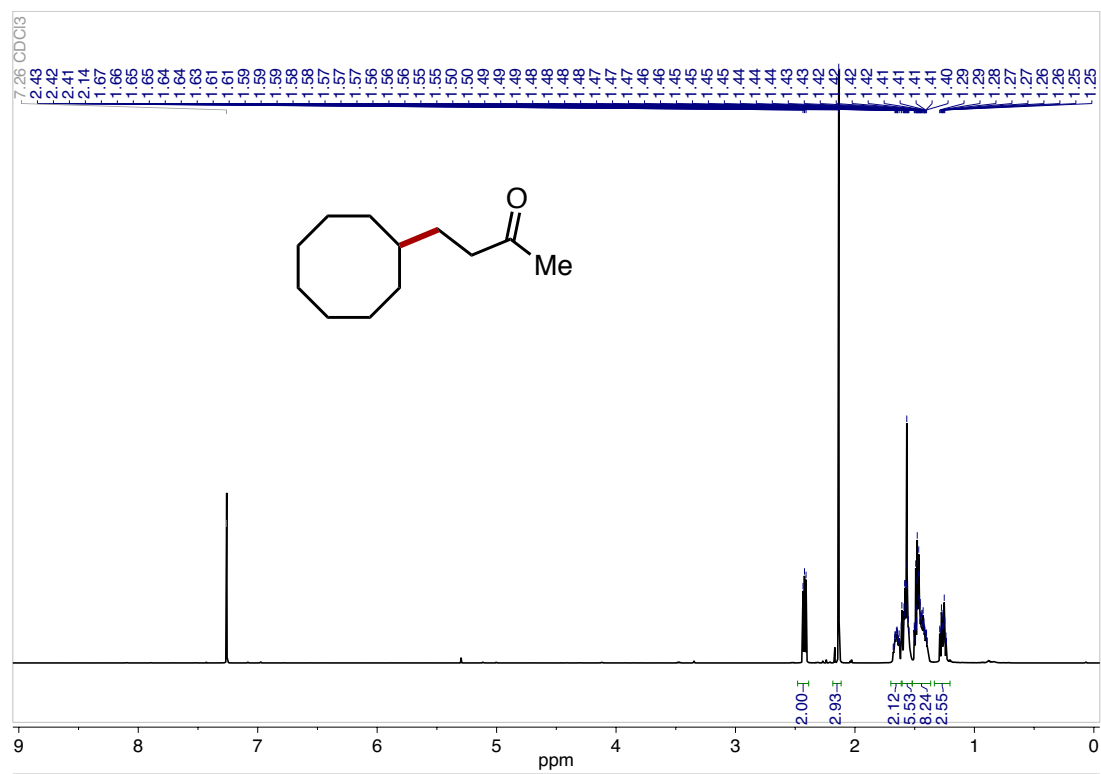


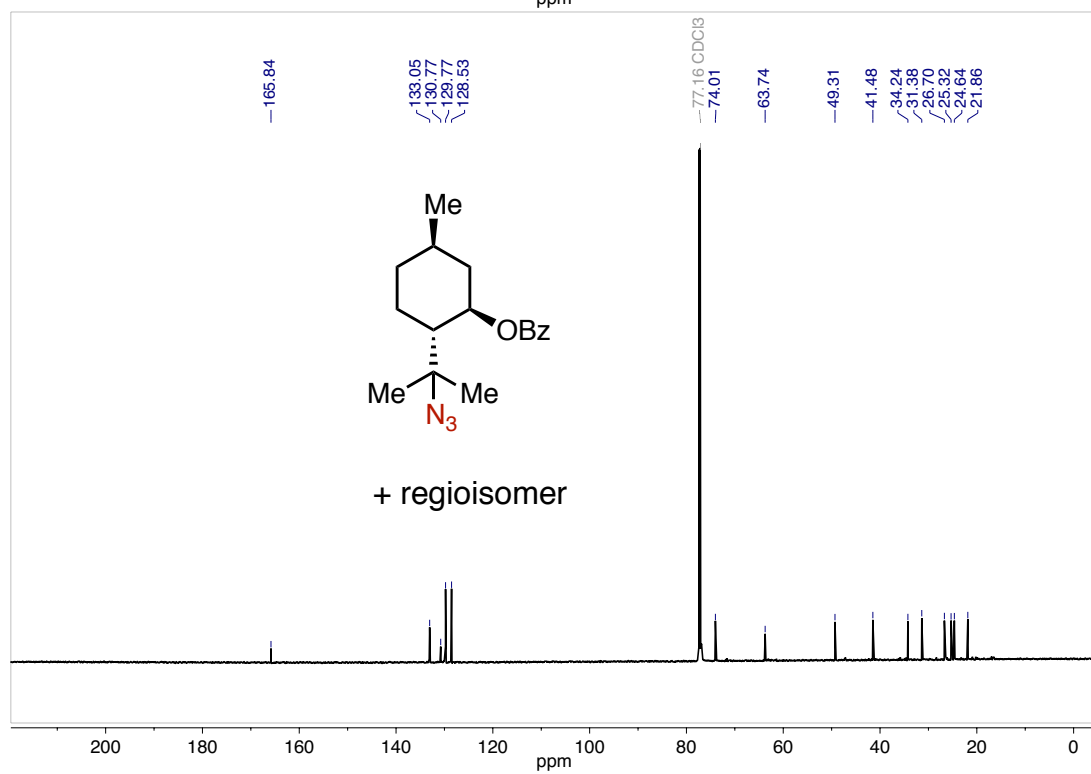
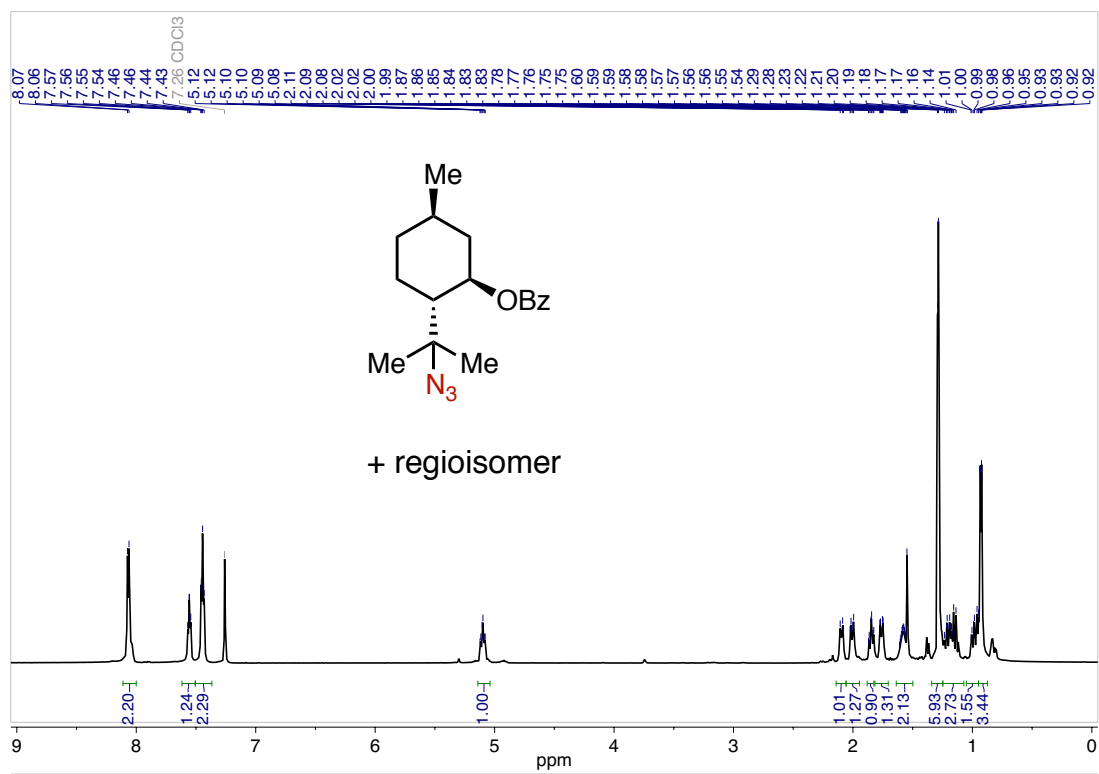


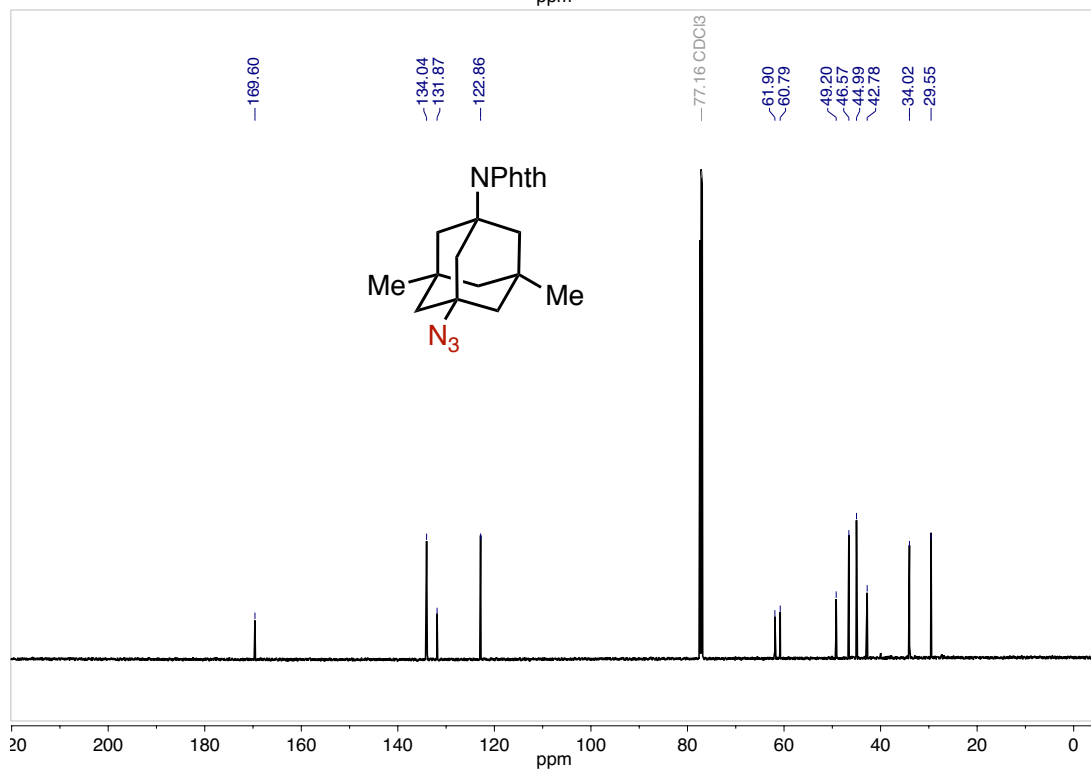
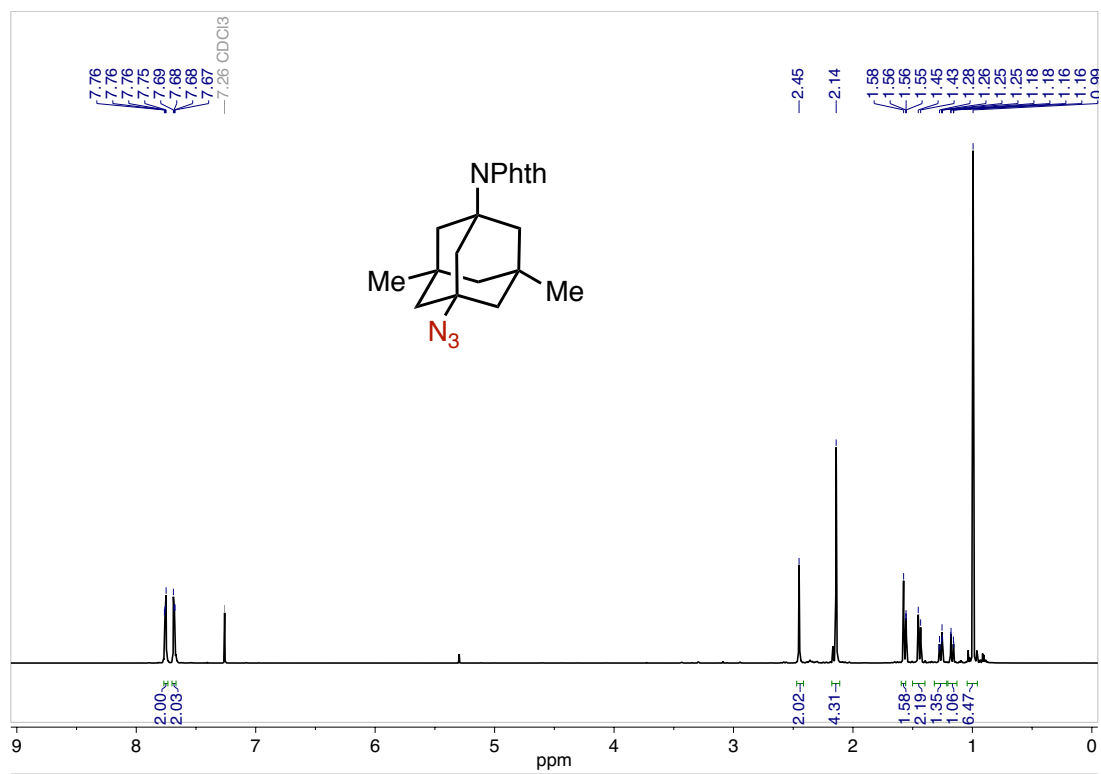


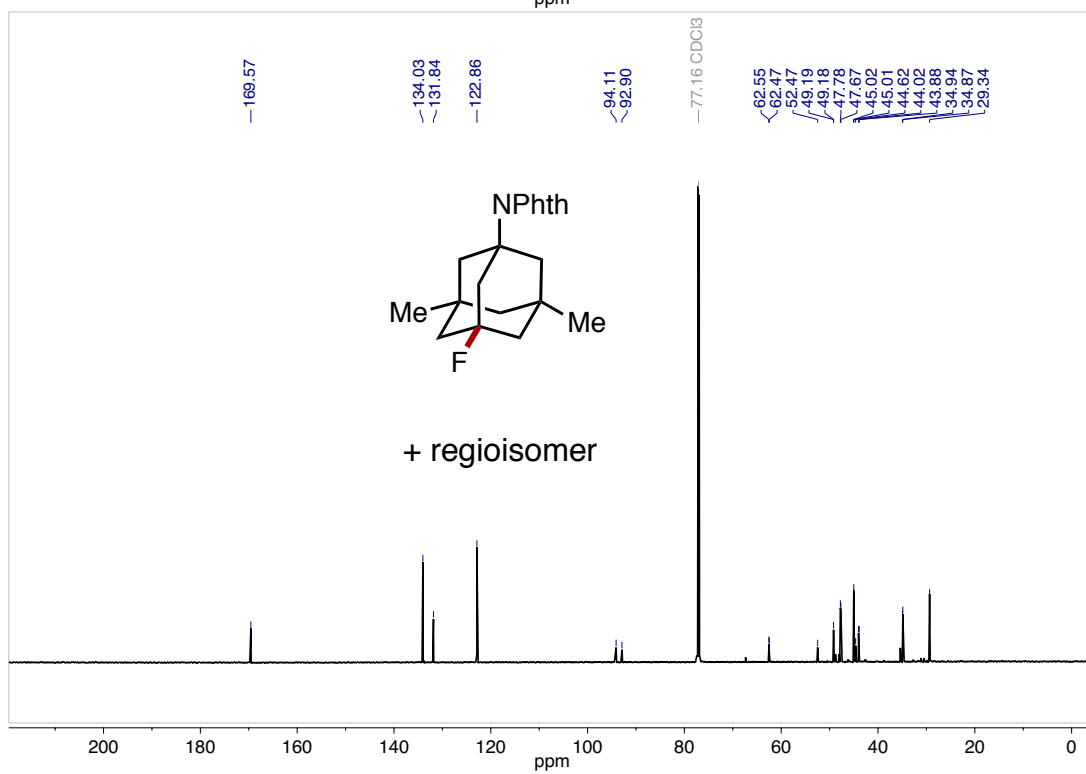
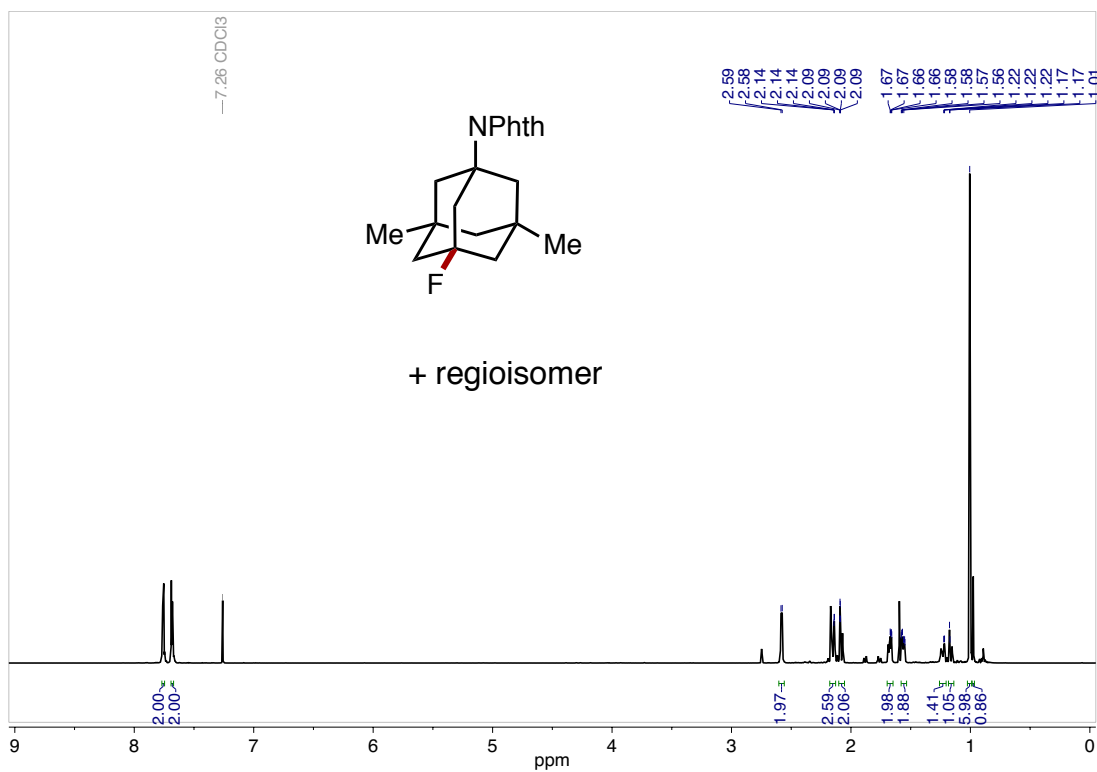


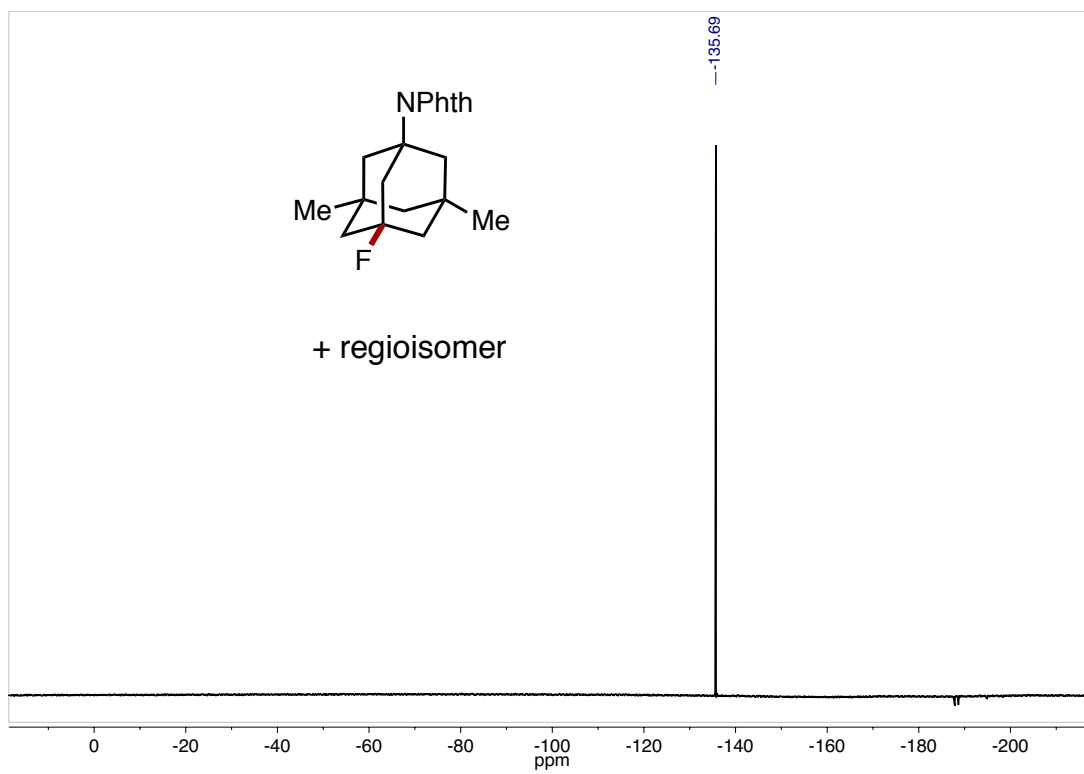


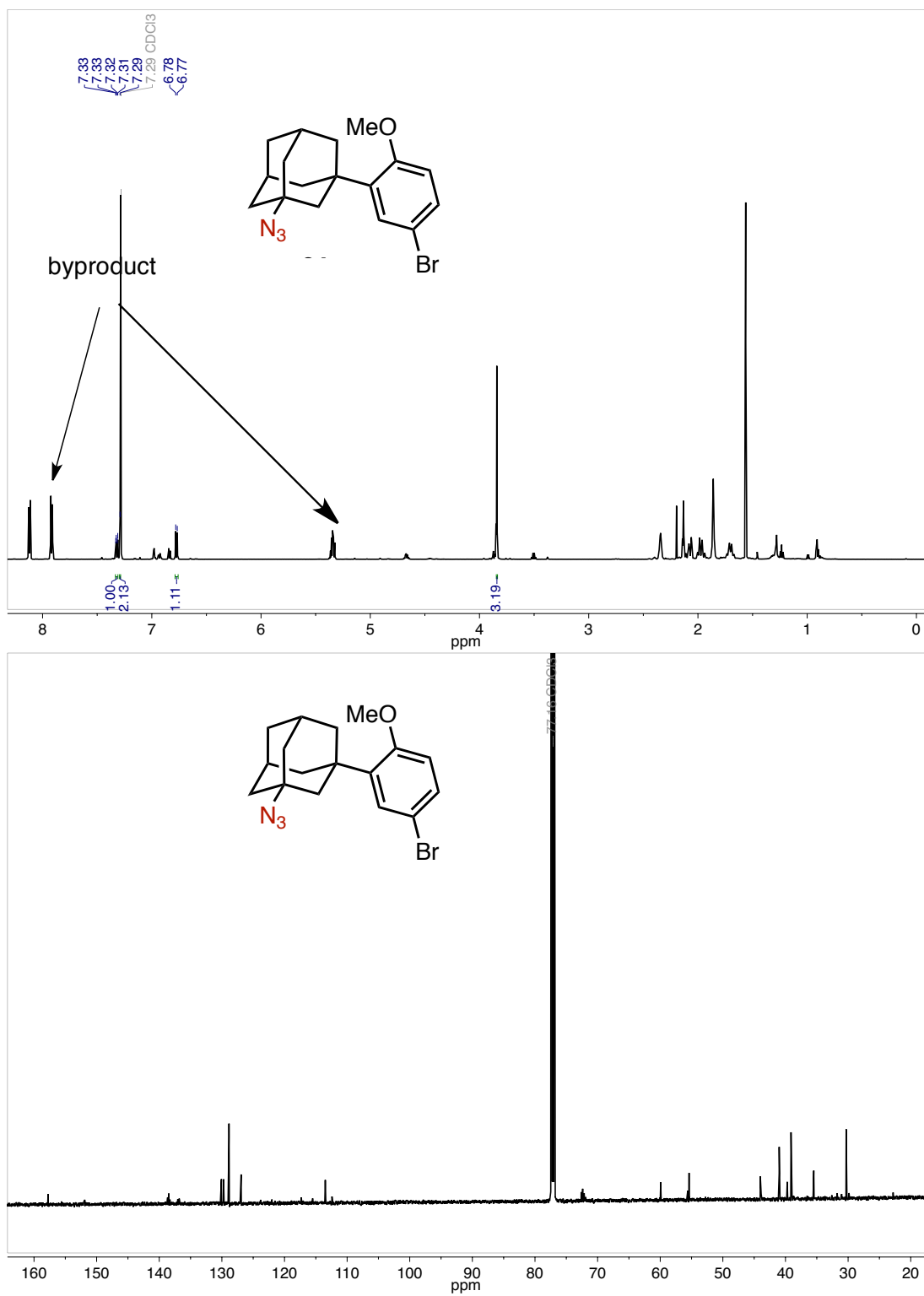


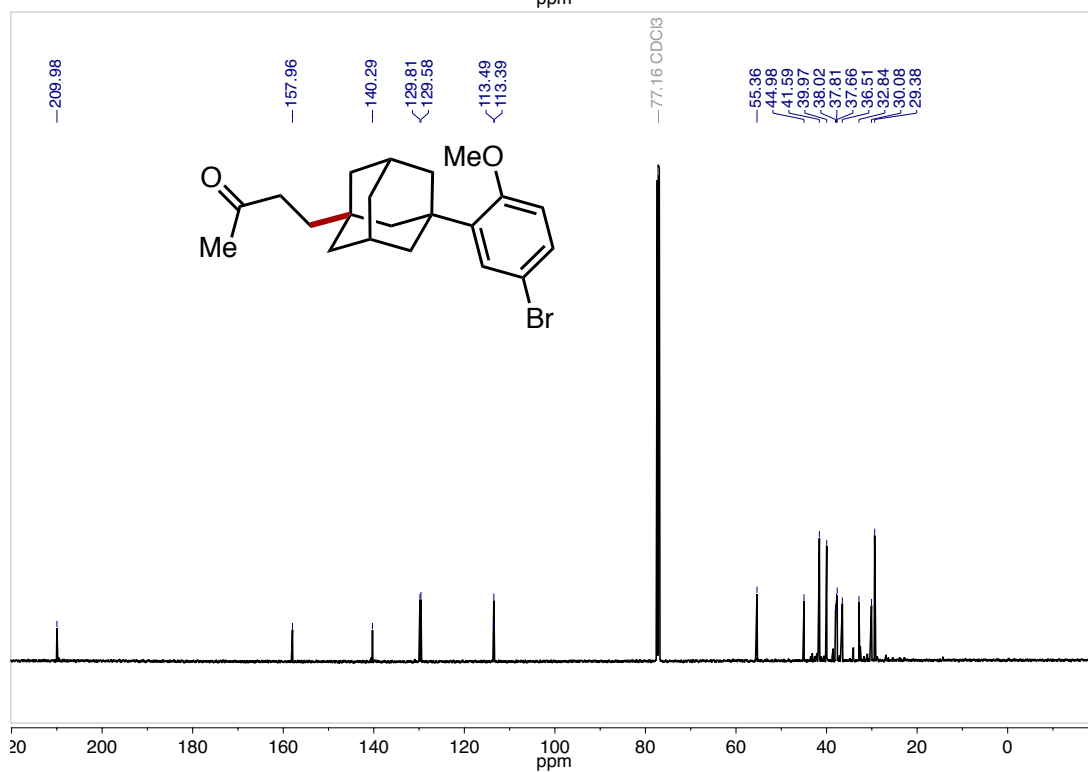
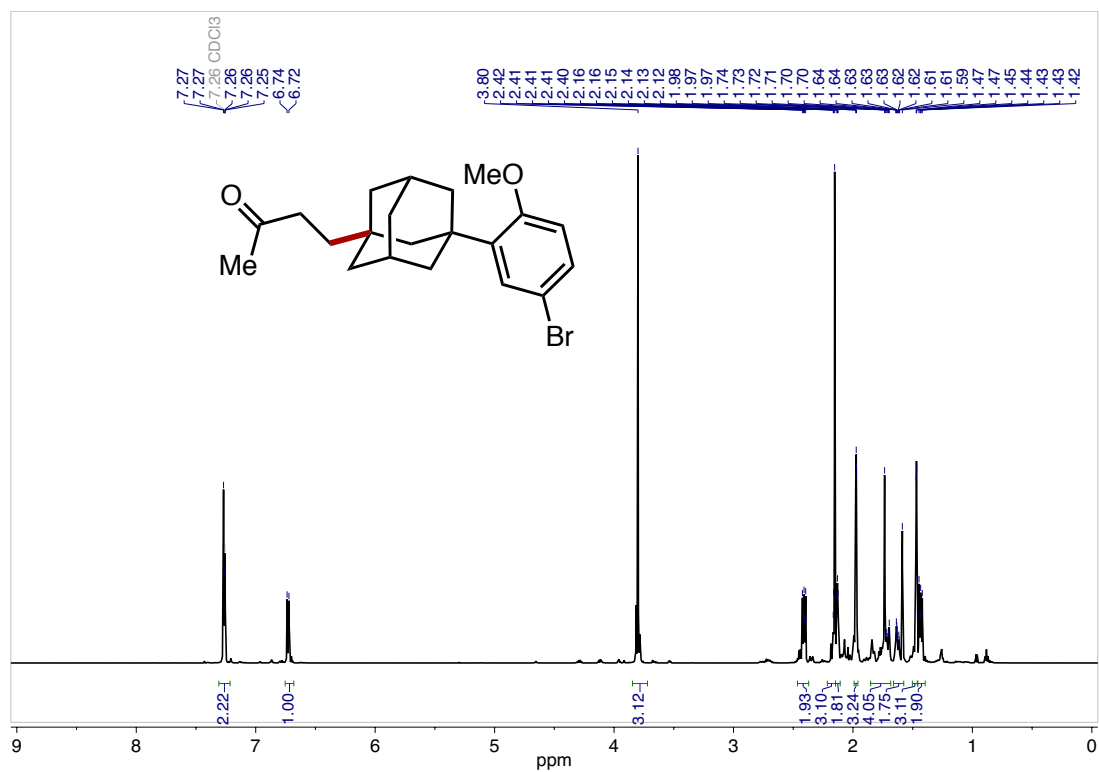




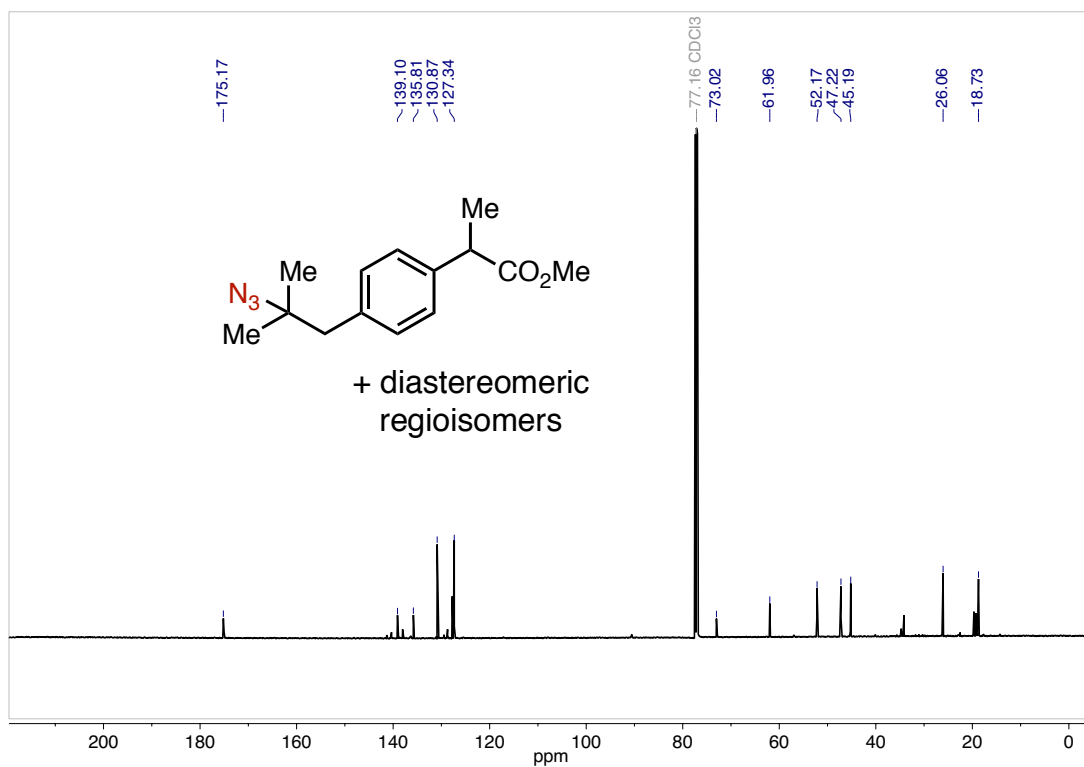
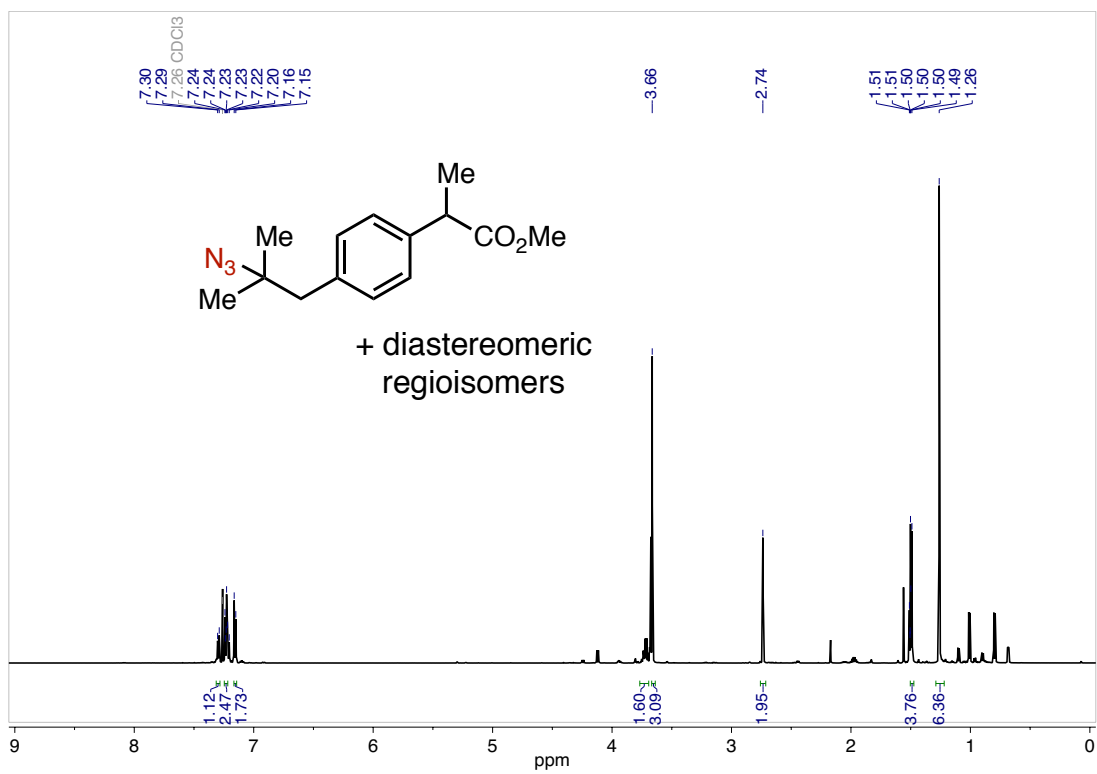


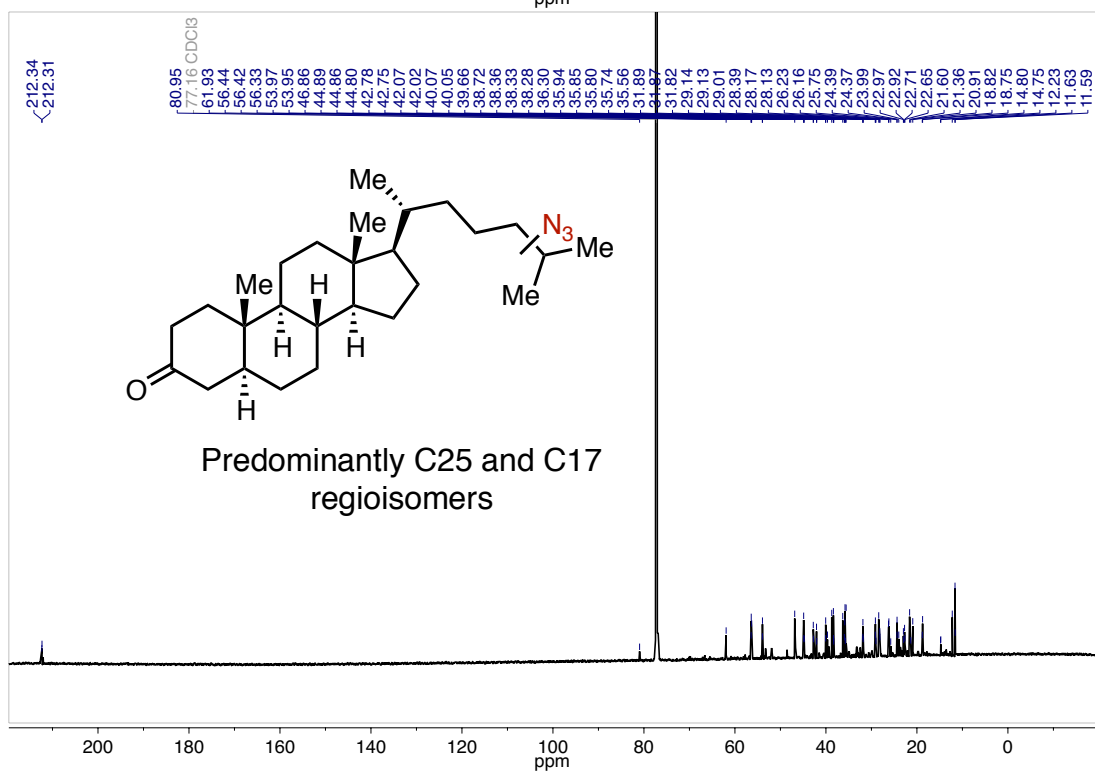
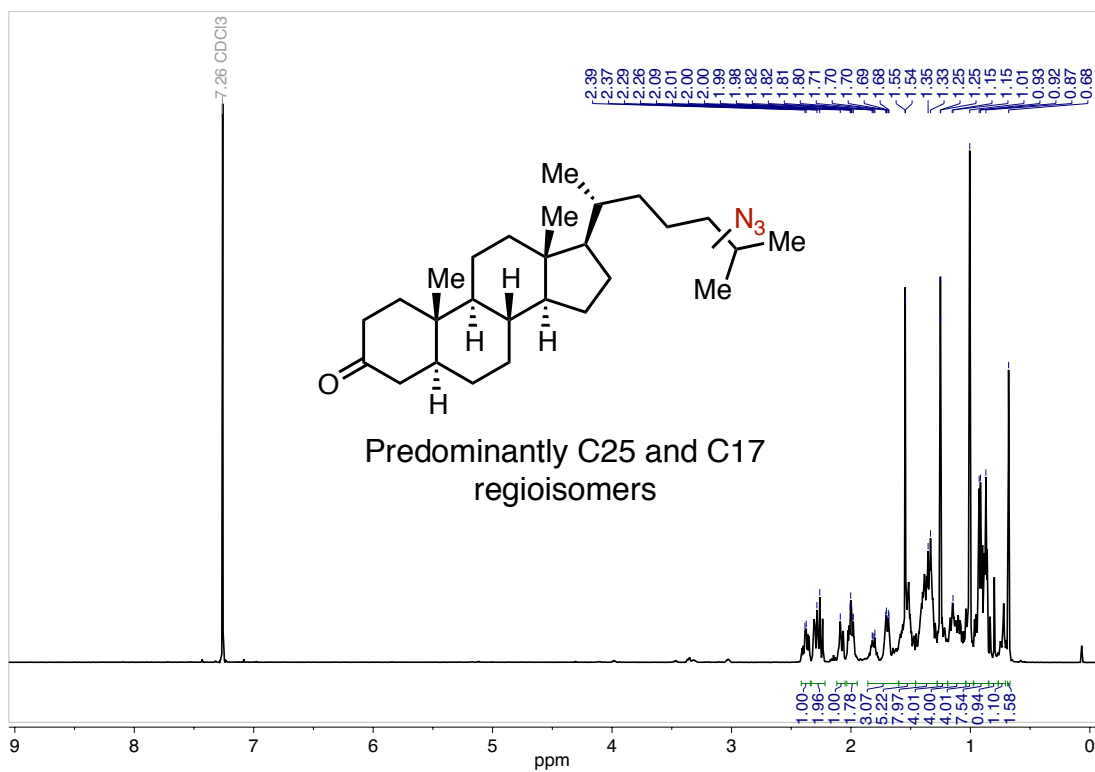


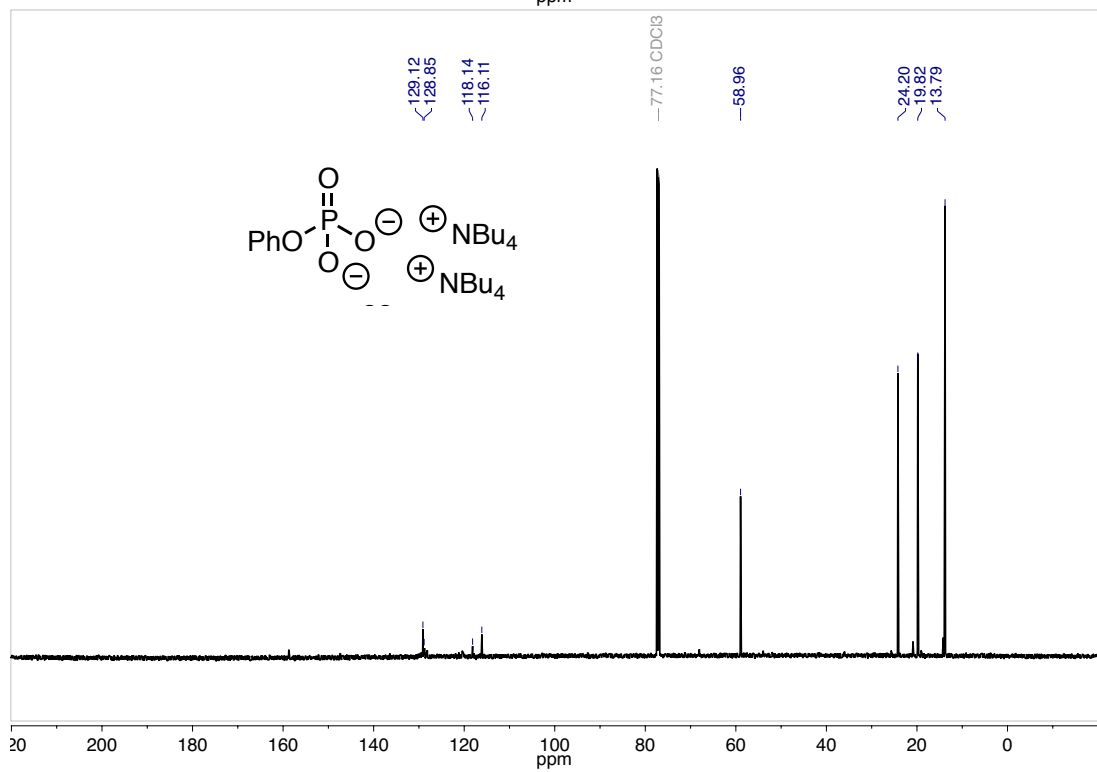
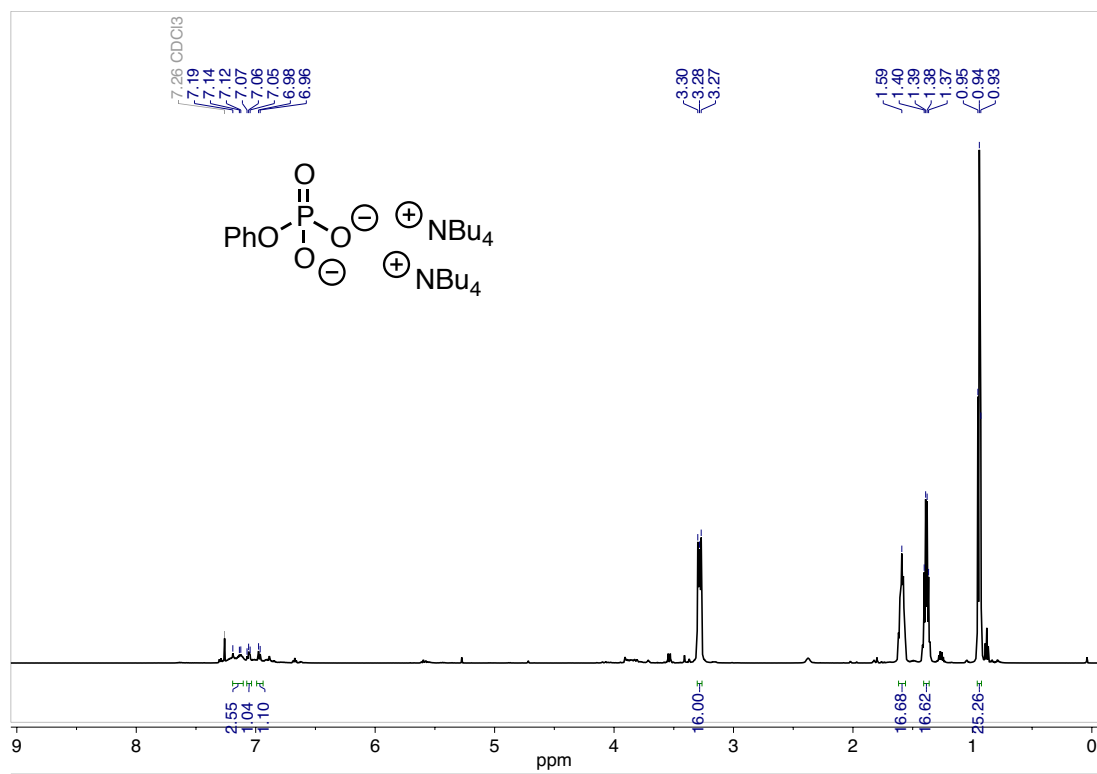












## APPENDIX D: SUPPORTING INFORMATION FOR CHAPTER 5

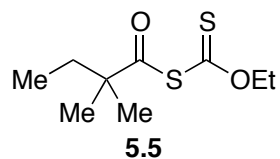
### General Methods and Materials

Infrared (IR) spectra were obtained using a Jasco 260 Plus Fourier transform infrared spectrometer. GC-MS data were obtained using an Agilent Gas Chromatograph-Mass Spectrometer with a 6850 series GC system and a 5973 Network Mass Selective Detector. Proton and carbon magnetic resonance spectra ( $^1\text{H}$  NMR and  $^{13}\text{C}$  NMR) were recorded on a Bruker model DRX 400, or a Bruker AVANCE III 600 CryoProbe ( $^1\text{H}$  NMR at 400 or 600 MHz and  $^{13}\text{C}$  NMR at 100 or 151 MHz) spectrometer with solvent resonance as the internal standard ( $^1\text{H}$  NMR  $\text{CDCl}_3$  at 7.26 ppm;  $^{13}\text{C}$  NMR  $\text{CDCl}_3$  at 77.16 ppm).  $^1\text{H}$  NMR data are reported as follows: chemical shift, multiplicity (s = singlet, d = doublet, t = triplet, q = quartet, dd = doublet of doublets, ddd = doublet of doublet of doublets, td = triplet of doublets, tdd = triplet of doublet of doublets, qd = quartet of doublets, m = multiplet, br. s. = broad singlet), coupling constants (Hz), and integration. Mass spectra were obtained using a Thermo LTqFT mass spectrometer with electrospray introduction and external calibration. Thin layer chromatography (TLC) was performed on SiliaPlate 250 $\mu\text{m}$  thick silica gel plates provided by Silicycle. Visualization was accomplished with short wave UV light (254 nm), iodine, aqueous basic potassium permanganate solution, or aqueous acidic ceric ammonium molybdate solution followed by heating. Flash chromatography was performed using SiliaFlash P60 silica gel (40-63  $\mu\text{m}$ ) purchased from Silicycle. Tetrahydrofuran, diethyl ether, and dichloromethane were dried by passage through a column of neutral alumina under nitrogen prior to use. All other reagents were obtained from commercial sources and used without further purification unless otherwise noted.

## Acyl Xanthate Synthesis

**General Procedure A:** To a solution of carboxylic acid (1 equiv) in  $\text{CH}_2\text{Cl}_2$  (0.25 M) was added DMF (2 drops). The solution was cooled to  $0\text{ }^\circ\text{C}$  and oxalyl chloride (2 equiv) was added. The mixture was warmed to rt and stirred for 2 – 20 hr until full conversion of the acid by TLC. The mixture was concentrated *in vacuo*, redissolved in acetone (0.25 M), and cooled to  $0\text{ }^\circ\text{C}$ . Potassium ethyl xanthate (0.95 equiv) was added in one portion (note: addition of excess potassium ethyl xanthate with respect to acid chloride leads to decomposition of the resultant acyl xanthate), and the mixture was stirred at  $0\text{ }^\circ\text{C}$  until full conversion of the acid chloride by TLC. The mixture was concentrated *in vacuo*, redissolved in  $\text{CH}_2\text{Cl}_2$ , washed with  $\text{H}_2\text{O}$ , brine, dried with  $\text{MgSO}_4$ , and concentrated *in vacuo*. The residue was purified by flash column chromatography to afford the acyl xanthate.

**General Procedure B:** To a solution of NaOH (6 equiv) in  $\text{H}_2\text{O}$  (4M with respect to NaOH) was added ester (1 equiv) in MeOH (0.55M with respect to ester). The mixture was heated to reflux overnight, then cooled to rt and adjusted to pH 2 with 1M HCl. The solution was extracted 3x with  $\text{CH}_2\text{Cl}_2$ , and the combined organic phases were washed with brine, dried with  $\text{MgSO}_4$ , and concentrated *in vacuo* to yield the carboxylic acid, which was used without further purification.



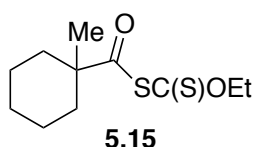
**(*O*-ethyl carbonothioic) 2,2-dimethylbutanoic thioanhydride (5.5).** Prepared from 2,2-dimethylbutyric acid (43 mmol) according to General Procedure A. Purified by flash column chromatography on silica (2% EtOAc in hexanes) to afford **5.5** as a yellow liquid (6.03 g, 70% yield):

**<sup>1</sup>H NMR (600 MHz, CDCl<sub>3</sub>)** δ 4.66 (dq, *J* = 14.1, 6.9, 6.3 Hz, 2H), 1.66 – 1.57 (m, 2H), 1.50 – 1.42 (m, 3H), 1.24 – 1.13 (m, 6H), 0.93 – 0.83 (m, 3H).

**<sup>13</sup>C NMR (151 MHz, CDCl<sub>3</sub>)** δ 204.94, 198.21, 70.99, 70.98, 51.65, 33.46, 24.30, 13.56, 9.00.

**IR (film)** 2969.84, 1732.73, 1717.30, 1472.38, 1256.40, 1040.41, 933.37 cm<sup>-1</sup>.

**HRMS (ES<sup>+</sup>)** Exact mass calcd for C<sub>9</sub>H<sub>16</sub>O<sub>2</sub>S<sub>2</sub>Na [M+Na]<sup>+</sup>, 243.0484. Found 243.0484.



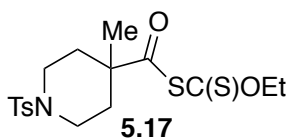
**(*O*-ethyl carbonothioic) 1-methylcyclohexanecarboxylic thioanhydride (5.15).** Prepared from 1-methyl-1-cyclohexanecarboxylic acid (14 mmol) according to General Procedure A. Purified by flash column chromatography on silica (2% EtOAc in hexanes) to afford **5.15** as a yellow liquid (2.63 g, 80% yield):

**<sup>1</sup>H NMR (600 MHz, CDCl<sub>3</sub>)** δ 4.67 (qd, *J* = 7.1, 1.4 Hz, 2H), 1.98 (dt, *J* = 13.4, 4.3 Hz, 2H), 1.58 – 1.39 (m, 8H), 1.36 – 1.26 (m, 3H), 1.21 (d, *J* = 1.3 Hz, 3H).

**<sup>13</sup>C NMR (151 MHz, CDCl<sub>3</sub>)** δ 205.45, 198.24, 71.00, 52.26, 35.31, 25.48, 22.80, 13.62.

**IR (film)** 2931.27, 2856.06, 1717.30, 1455.99, 1254.47, 1037.52, 931.45 cm<sup>-1</sup>.

**HRMS (ES<sup>+</sup>)** Exact mass calcd for C<sub>11</sub>H<sub>18</sub>O<sub>2</sub>S<sub>2</sub>Na [M+Na]<sup>+</sup>, 269.0640. Found 269.0641.



**(*O*-ethyl carbonothioic) 4-methyl-1-tosylpiperidine-4-carboxylic thioanhydride (5.17).**

To a solution of 1-*tert*-butyl 4-methyl 4-(pent-4-en-1-yl)piperidine-1,4-dicarboxylate<sup>1</sup> (3 g, 11.7 mmol) in CH<sub>2</sub>Cl<sub>2</sub> (30 mL) was added trifluoroacetic acid (4.5 mL, 58.3 mmol). The reaction mixture was stirred at rt overnight and quenched with 2M aqueous NaOH (40 mL).

The aqueous phase was extracted with 3x CH<sub>2</sub>Cl<sub>2</sub>, and the combined organic layers were washed with brine, dried with MgSO<sub>4</sub>, and concentrated *in vacuo* to afford the deprotected piperidine as a yellow oil (1.49 g, 81%) which was used without further purification.

To a solution of *p*-toluenesulfonyl chloride (1.9 g, 10 mmol) in CH<sub>2</sub>Cl<sub>2</sub> (20 mL) was added methyl 4-(pent-4-en-1-yl)piperidine-4-carboxylate (1.49 g, 9.5 mmol) in CH<sub>2</sub>Cl<sub>2</sub> (10 mL), and the solution was cooled to 0 °C. Triethylamine (3.3 mL, 23.7 mmol) was added, and the mixture was warmed to rt overnight. The reaction was concentrated *in vacuo* and taken up in EtOAc and H<sub>2</sub>O. The aqueous layer was extracted with EtOAc, and the combined organic layers were washed 2x with 1M HCl, brine, dried over MgSO<sub>4</sub>, and concentrated *in vacuo* to yield the tosyl-protected piperidine as a yellow solid (2.6 g, 89% yield).

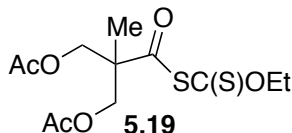
The resultant methyl 4-(pent-4-en-1-yl)-1-tosylpiperidine-4-carboxylate (2.5 g, 8.0 mmol) was converted to the acid according to General Procedure B (2.2 g, 94% yield) without purification and then to the acyl xanthate according to General Procedure A (3.36 mmol scale). Purified by flash column chromatography on silica (20% EtOAc in hexanes) to afford **5.17** as a yellow solid (856 mg, 64% yield):

**<sup>1</sup>H NMR (600 MHz, CDCl<sub>3</sub>)** δ 7.59 (d, *J* = 8.0 Hz, 2H), 7.30 (d, *J* = 8.1 Hz, 2H), 4.58 (q, *J* = 7.1 Hz, 2H), 3.40 (dt, *J* = 12.2, 4.5 Hz, 2H), 2.61 (ddd, *J* = 12.9, 10.6, 2.8 Hz, 2H), 2.41 (s, 3H), 2.19 – 2.10 (m, 2H), 1.63 (ddd, *J* = 14.3, 10.6, 4.0 Hz, 2H), 1.36 (t, *J* = 7.1 Hz, 3H), 1.21 (s, 3H).

**<sup>13</sup>C NMR (151 MHz, CDCl<sub>3</sub>)** δ 203.19, 197.11, 143.71, 133.02, 129.84, 127.64, 71.20, 49.76, 43.25, 34.12, 25.70, 21.61, 13.43.

**IR (film)** 2969.84, 2929.34, 1717.30, 1374.03, 1351.86, 1165.76, 1053.91 cm<sup>-1</sup>.

**HRMS (ES<sup>+</sup>)** Exact mass calcd for C<sub>17</sub>H<sub>24</sub>NO<sub>4</sub>S<sub>3</sub> [M+H]<sup>+</sup>, 402.0862. Found 402.0859.



**3-acetoxy-2-(acetoxymethyl)-2-methylpropanoic (*O*-ethyl carbonothioic) thioanhydride**

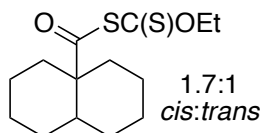
**(5.19).** Prepared from 2,2-bis(acetoxymethyl)propionic acid<sup>2</sup> (1 g, 4.6 mmol) according to General Procedure A. Purified by flash column chromatography on silica to afford **5.19** as a yellow liquid (886 mg, 60% yield):

**<sup>1</sup>H NMR (600 MHz, CDCl<sub>3</sub>)** δ 4.68 (q, *J* = 7.1 Hz, 2H), 4.26 – 4.19 (m, 4H), 2.07 (s, 6H), 1.47 (t, *J* = 7.1 Hz, 3H), 1.31 (s, 3H).

**<sup>13</sup>C NMR (151 MHz, CDCl<sub>3</sub>)** δ 202.13, 193.72, 170.47, 71.45, 65.38, 54.32, 20.86, 17.66, 13.61.

**IR (film)** 2984.3, 1748.16, 1715.37, 1470.46, 1375.96, 1237.11, 1042.34, 913.13 cm<sup>-1</sup>.

**HRMS (ES<sup>+</sup>)** Exact mass calcd for C<sub>12</sub>H<sub>18</sub>O<sub>6</sub>S<sub>2</sub>Na [M+Na]<sup>+</sup>, 345.0437. Found 345.0434.



**5.21**

**(*O*-ethyl carbonothioic) decahydronaphthalene-4a-carboxylic thioanhydride (5.21).**

Prepared according to a previous report from our lab<sup>3</sup> (2.7 mmol scale) and purified by flash column chromatography on silica (hexanes) to afford **5.21** as a yellow liquid (474 mg, 60%, 1.7:1 dr). <sup>13</sup>C NMR spectrum complicated due to ring inversion of the *cis* isomer.

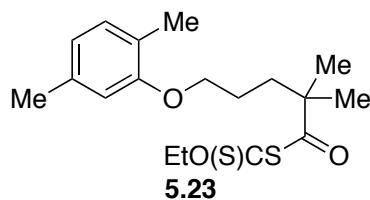
**<sup>1</sup>H NMR (600 MHz, CDCl<sub>3</sub>)** δ 4.67 – 4.63 (m, 2H), 2.17 – 2.03 (m, 1H), 1.76 – 1.64 (m, 2H), 1.62 – 1.42 (m, 15H), 1.35 – 1.26 (m, 2H).

**<sup>13</sup>C NMR (151 MHz, CDCl<sub>3</sub>)** δ 206.00, 205.02, 200.03, 198.63, 70.87, 57.31, 56.59, 38.49, 36.21, 36.15, 28.78, 27.93 (br.), 26.45, 23.10, 22.59 (br.), 13.56.

**IR (film)** 2929.34, 2863.77, 1730.80, 1464.67, 1251.58, 1043.30 cm<sup>-1</sup>.



**HRMS (ES+)** Exact mass calcd for  $C_{14}H_{22}O_2S_2Na$   $[M+Na]^+$ , 309.0954. Found 309.0937.



**5-(2,5-dimethylphenoxy)-2,2-dimethylpentanoic (*O*-ethyl carbonothioic) thioanhydride**

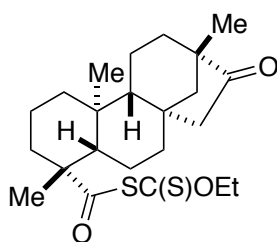
**(5.23).** Prepared from gemfibrozil (10 mmol) according to General Procedure A. Purified by flash column chromatography on silica (2 – 5% EtOAc in hexanes) to afford **5.23** as a yellow oil (2.25 g, 63% yield):

**$^1H$  NMR (600 MHz,  $CDCl_3$ )**  $\delta$  7.01 (d,  $J$  = 7.4 Hz, 1H), 6.66 (d,  $J$  = 8.0 Hz, 1H), 6.61 (d,  $J$  = 1.6 Hz, 1H), 4.68 (q,  $J$  = 7.1 Hz, 2H), 3.93 (tt,  $J$  = 3.7, 2.0 Hz, 2H), 2.31 (s, 3H), 2.19 (s, 3H), 1.81 – 1.77 (m, 4H), 1.48 (t,  $J$  = 7.1 Hz, 3H), 1.28 (s, 6H).

**$^{13}C$  NMR (151 MHz,  $CDCl_3$ )**  $\delta$  204.65, 198.28, 156.91, 136.59, 130.43, 123.65, 120.86, 111.93, 71.13, 67.59, 51.19, 37.32, 24.91 (coincidental overlap), 21.55, 15.95, 13.63.

**IR (film)** 2968.87, 2868.59, 1748.16, 1716.34, 1508.06, 1456.96, 1263.15, 1040.41  $cm^{-1}$ .

**HRMS (ES+)** Exact mass calcd for  $C_{18}H_{26}O_3S_2Na$   $[M+Na]^+$ , 377.1216. Found 377.1212.



**(*O*-ethyl carbonothioic) (4*R*,4*aS*,6*aR*,9*S*,11*aR*,11*bS*)-4,9,11*b*-trimethyl-8-oxotetradecahydro-6*a*,9-methanocyclohepta[*a*]naphthalene-4-carboxylic thioanhydride**

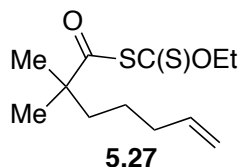
**(5.25).** Prepared from isosteviol<sup>4</sup> (3.14 mmol) according to General Procedure A. Purified by flash column chromatography on silica (10% EtOAc in hexanes) to afford **5.25** as a thick yellow oil (751 mg, 63% yield):

**<sup>1</sup>H NMR (600 MHz, CDCl<sub>3</sub>)** δ 4.58 (qd, *J* = 7.1, 2.0 Hz, 2H), 2.56 (dd, *J* = 18.6, 3.8 Hz, 1H), 2.07 (dq, *J* = 15.0, 2.7 Hz, 1H), 1.83 – 1.57 (m, 7H), 1.55 – 1.27 (m, 9H), 1.22 – 1.09 (m, 7H), 0.92 – 0.82 (m, 4H), 0.75 (s, 3H).

**<sup>13</sup>C NMR (151 MHz, CDCl<sub>3</sub>)** δ 222.13, 204.87, 197.07, 70.88, 58.12, 54.42, 54.03, 53.09, 48.57, 48.32, 41.47, 39.52, 39.36, 38.11, 37.41, 37.14, 29.25, 21.64, 20.33, 19.80, 19.03, 15.08, 13.47.

**IR (film)** 2929.34, 2848.35, 1737.55, 1716.34, 1698.98, 1472.38, 1252.54, 1041.37 cm<sup>-1</sup>.

**HRMS (ES<sup>+</sup>)** Exact mass calcd for C<sub>23</sub>H<sub>34</sub>O<sub>3</sub>S<sub>2</sub>Na [M+Na]<sup>+</sup>, 445.1842. Found 445.1875.



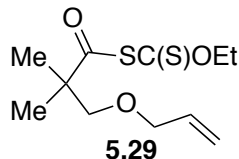
**(*S*-ethyl carbonothioic) 2,2-dimethylhept-6-enoic thioanhydride (5.27).** Prepared from 2,2-dimethylhept-6-enoic acid<sup>5</sup> (1 g, 6.4 mmol) according to General Procedure A. Purified by flash column chromatography on silica (2% EtOAc in hexanes) to afford **5.27** as a yellow liquid (1.36 g, 81% yield):

**<sup>1</sup>H NMR (600 MHz, CDCl<sub>3</sub>)** δ 5.75 (ddt, *J* = 16.9, 10.0, 6.5 Hz, 1H), 5.03 – 4.91 (m, 2H), 4.66 (q, *J* = 7.0 Hz, 2H), 2.03 (q, *J* = 7.0 Hz, 2H), 1.59 – 1.53 (m, 2H), 1.49 – 1.43 (m, 3H), 1.40 – 1.32 (m, 2H), 1.25 – 1.15 (m, 6H).

**<sup>13</sup>C NMR (151 MHz, CDCl<sub>3</sub>)** δ 204.86, 198.21, 138.18, 115.04, 71.02, 51.30, 40.14, 34.02, 24.82, 23.83, 13.59.

**IR (film)** 2974.66, 2938.02, 1732.73, 1716.34, 1507.10, 1257.36, 1042.34 cm<sup>-1</sup>.

**HRMS (ES<sup>+</sup>)** Exact mass calcd for C<sub>12</sub>H<sub>21</sub>O<sub>2</sub>S<sub>2</sub>Na [M+Na]<sup>+</sup>, 283.0797. Found 283.0798.



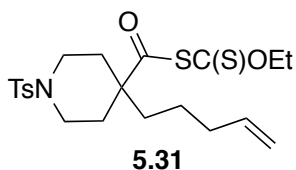
**3-(allyloxy)-2,2-dimethylpropanoic (S-ethyl carbonothioic) thioanhydride (5.29).** Methyl 3-(allyloxy)-2,2-dimethylpropanoate (1.3 g, 7.6 mmol)<sup>6</sup> was converted to the acid according to General Procedure B (966 mg, 81% yield) without purification and then to the acyl xanthate according to General Procedure A (750 mg, 4.7 mmol). Purified by flash column chromatography on silica (5% EtOAc in hexanes) to afford **5.29** as a yellow oil (893 mg, 76% yield):

**<sup>1</sup>H NMR (600 MHz, CDCl<sub>3</sub>)** δ 5.90 – 5.82 (m, 1H), 5.31 – 5.23 (m, 1H), 5.17 (dq, *J* = 10.4, 1.5 Hz, 1H), 4.68 (q, *J* = 7.1 Hz, 2H), 3.98 (dt, *J* = 5.5, 1.5 Hz, 2H), 3.45 (s, 2H), 1.47 (t, *J* = 7.1 Hz, 3H), 1.25 (s, 6H).

**<sup>13</sup>C NMR (151 MHz, CDCl<sub>3</sub>)** δ 204.96, 196.89, 134.52, 117.23, 76.24, 72.53, 71.11, 52.45, 22.37, 13.66.

**IR (film)** 3079.76, 2978.52, 2857.02, 1747.19, 1716.34, 1258.32, 1043.30, 907.34 cm<sup>-1</sup>.

**HRMS (ES<sup>+</sup>)** Exact mass calcd for C<sub>11</sub>H<sub>18</sub>O<sub>3</sub>S<sub>2</sub>Na [M+Na]<sup>+</sup>, 285.0590. Found 285.0588.



**(S-ethyl carbonothioic) 4-(pent-4-en-1-yl)-1-tosylpiperidine-4-carboxylic thioanhydride (5.31).** To a solution of 1-*tert*-butyl 4-methyl 4-(pent-4-en-1-yl)piperidine-1,4-dicarboxylate (7.32 g, 23.5 mmol)<sup>7</sup> in CH<sub>2</sub>Cl<sub>2</sub> (50 mL) was added trifluoroacetic acid (9 mL, 117 mmol). The solution was stirred overnight and then quenched with 2M NaOH, and the organic layer was washed with brine, dried over MgSO<sub>4</sub>, and concentrated *in vacuo* to afford a residue which was used without purification (3.32 g, 67% yield).

The resultant methyl 4-(pent-4-en-1-yl)piperidine-4-carboxylate (3.32 g, 15.7 mmol) and *p*-toluenesulfonyl chloride (3.14 g, 16.5 mmol) were dissolved in CH<sub>2</sub>Cl<sub>2</sub> (52 mL). NEt<sub>3</sub> (5.5 mL, 39.3 mmol) was added, and the mixture was stirred overnight and then quenched with 1M HCl. The organic layer was separated, and the aqueous phase was extracted with EtOAc. The combined organic layers were washed with brine, dried over MgSO<sub>4</sub>, and concentrated *in vacuo*. The resultant residue was dissolved in EtOAc, passed over a short silica plug, and concentrated *in vacuo* to afford an orange oil that was used without further purification (3.77 g, 66% yield).

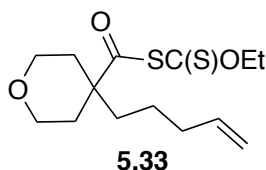
The resultant methyl 4-(pent-4-en-1-yl)-1-tosylpiperidine-4-carboxylate (1.5 g, 4.1 mmol) was converted to the acid according to General Procedure B (1.19 g, 82% yield) without purification and then to the acyl xanthate according to General Procedure A (1.42 mmol). Purified by flash column chromatography on silica (10 – 20% EtOAc in hexanes) to afford **5.31** as a yellow solid (390 mg, 60% yield):

**<sup>1</sup>H NMR (600 MHz, CDCl<sub>3</sub>)** δ 7.58 (d, *J* = 7.9 Hz, 2H), 7.30 (d, *J* = 7.9 Hz, 2H), 5.74 – 5.63 (m, 1H), 4.99 – 4.91 (m, 2H), 4.60 – 4.53 (m, 2H), 3.56 (dd, *J* = 12.2, 4.1 Hz, 2H), 2.45 – 2.39 (m, 5H), 2.20 – 2.10 (m, 2H), 2.04 – 1.95 (m, 2H), 1.65 – 1.58 (m, 2H), 1.57 – 1.47 (m, 2H), 1.36 – 1.23 (m, 5H).

**<sup>13</sup>C NMR (151 MHz, CDCl<sub>3</sub>)** δ 203.32, 196.73, 143.69, 137.64, 132.97, 129.84, 127.64, 115.38, 71.14, 53.58, 43.42, 39.63, 33.62, 32.95, 22.54, 21.61, 13.39.

**IR (film)** 2938.02, 2860.88, 1732.73, 1716.34, 1568.81, 1257.36, 1167.69, 1040.41 cm<sup>-1</sup>.

**HRMS (ES<sup>+</sup>)** Exact mass calcd for C<sub>21</sub>H<sub>30</sub>NO<sub>4</sub>S<sub>3</sub> [M+H]<sup>+</sup>, 456.1331. Found 456.1380.



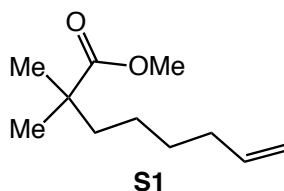
**(*S*-ethyl carbonothioic) 4-(pent-4-en-1-yl)tetrahydro-2*H*-pyran-4-carboxylic thioanhydride (5.33).** Prepared from 4-(pent-4-en-1-yl)tetrahydro-2*H*-pyran-4-carboxylic acid<sup>8</sup> (4.7 mmol) according to General Procedure A. Purified by flash column chromatography on silica (5% EtOAc in hexanes) to afford **5.33** as a yellow liquid (905 mg, 61% yield):

**<sup>1</sup>H NMR (600 MHz, CDCl<sub>3</sub>)** δ 5.78 – 5.71 (m, 1H), 5.04 – 4.95 (m, 2H), 4.69 (q, *J* = 7.1 Hz, 2H), 3.80 (dt, *J* = 12.1, 4.0 Hz, 2H), 3.52 (ddd, *J* = 12.0, 10.8, 2.4 Hz, 2H), 2.10 – 2.00 (m, 4H), 1.64 – 1.56 (m, 4H), 1.48 (d, *J* = 7.1 Hz, 3H), 1.38 – 1.32 (m, 2H).

**<sup>13</sup>C NMR (151 MHz, CDCl<sub>3</sub>)** δ 204.10, 197.16, 137.96, 115.35, 71.26, 64.91, 53.61, 39.88, 34.13, 33.84, 22.50, 13.64.

**IR (film)** 2938.02, 2859.92, 1732.73, 1716.34, 1254.47, 1110.80, 1040.41, 935.31 cm<sup>-1</sup>.

**HRMS (ES<sup>+</sup>)** Exact mass calcd for C<sub>14</sub>H<sub>22</sub>O<sub>3</sub>S<sub>2</sub>Na [M+Na]<sup>+</sup>, 325.0903. Found 325.0903.



**Methyl 2,2-dimethyloct-7-enoate (S1).** To a solution of diisopropylamine (4.3 mL, 30.4 mmol) in THF (101 mL) at 0 °C was added *n*-BuLi in hexanes (26.6 mmol). The solution was stirred at 0 °C for 10 min, warmed to rt for 10 min, then chilled to –78 °C. Methyl isobutyrate (2.9 mL, 25.3 mmol) was added dropwise, and the solution stirred for 20 min. 6-Bromo-1-hexene was added (4.1 mL, 30.4 mmol), and the solution was allowed to warm to rt overnight. The reaction mixture was then concentrated *in vacuo* and partitioned between Et<sub>2</sub>O and 1M HCl. The aqueous phase was extracted with Et<sub>2</sub>O 3x, and the combined organic layers were dried with MgSO<sub>4</sub> and concentrated *in vacuo*. The residue was purified by flash

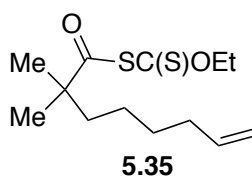
column chromatography on silica (5% EtOAc in hexanes) to afford **S1** as a colorless liquid (2.86 g, 61% yield):

**<sup>1</sup>H NMR (600 MHz, CDCl<sub>3</sub>)** δ 5.80 – 5.71 (m, 1H), 4.99 – 4.87 (m, 2H), 3.62 (s, 3H), 2.05 – 1.97 (m, 2H), 1.51 – 1.45 (m, 2H), 1.37 – 1.28 (m, 2H), 1.23 – 1.08 (m, 8H).

**<sup>13</sup>C NMR (151 MHz, CDCl<sub>3</sub>)** δ 178.59, 138.88, 114.44, 77.16, 51.70, 42.34, 40.69, 33.68, 29.36, 25.25, 24.49.

**IR (film)** 2937.06, 2859.92, 1732.73, 1641.13, 1473.35, 1192.76, 1152.26 cm<sup>-1</sup>.

**HRMS (ES<sup>+</sup>)** Exact mass calcd for C<sub>11</sub>H<sub>20</sub>O<sub>2</sub>Na [M+Na]<sup>+</sup>, 207.1356. Found 207.1365.



**(S-ethyl carbonothioic) 2,2-dimethyloct-7-enoic thioanhydride (5.35).** Methyl 2,2-dimethyloct-7-enoate (2.2 g, 12 mmol) was converted to the acid according to General Procedure B (2.0 g, quant.) without purification and then to the acyl xanthate according to General Procedure A (1.09 g, 6.4 mmol). Purified by flash column chromatography on silica (2% EtOAc in hexanes) to afford **5.35** as a yellow liquid (1.34 g, 76% yield):

**<sup>1</sup>H NMR (600 MHz, CDCl<sub>3</sub>)** δ 5.78 – 5.71 (m, 1H), 4.96 (dt, *J* = 17.1, 1.9 Hz, 1H), 4.90 (ddt, *J* = 10.2, 2.2, 1.1 Hz, 1H), 4.65 (q, *J* = 7.1 Hz, 2H), 2.02 (q, *J* = 7.1 Hz, 2H), 1.57 – 1.50 (m, 2H), 1.44 (t, *J* = 7.1, 3H), 1.35 (p, *J* = 7.4 Hz, 2H), 1.29 – 1.22 (m, 2H), 1.18 (s, 6H).

**<sup>13</sup>C NMR (151 MHz, CDCl<sub>3</sub>)** δ 204.83, 198.16, 138.57, 114.60, 70.93, 51.32, 40.50, 33.51, 29.22, 24.77, 24.00, 13.54.

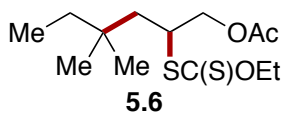
**IR (film)** 2974.66, 2936.09, 1732.73, 1716.34, 1540.85, 1257.36, 1042.34 cm<sup>-1</sup>.

**HRMS (ES<sup>+</sup>)** Exact mass calcd for C<sub>13</sub>H<sub>22</sub>O<sub>2</sub>S<sub>2</sub>Na [M+Na]<sup>+</sup>, 297.0953. Found 297.0953.

## Quaternary Center-Forming Reactions

**General Procedure C (intermolecular reactions):** To a 1-dram vial with a magnetic stir bar was added acyl xanthate (1 equiv) and dilauroyl peroxide (0.1 equiv). The vial was brought into the glovebox, and olefin (2 equiv) was added, followed by 1,2-dichloroethane (1 M). The vial was fitted with a rubber septum cap, sealed with Teflon tape, and removed from the glovebox. The vial was placed under a balloon of argon and heated at 85 °C for 2 h. If tertiary xanthate remained by TLC (generally a spot with a higher  $R_f$  than the desired addition product), the vial was cooled to rt and brought back into the glovebox. Additional DLP (0.1 equiv) was added, and the reaction was heated at 85 °C for an additional 4 h, then cooled to rt. If tertiary xanthate remained by TLC, further DLP (0.1 equiv) was added as described above, followed by additional heating. After tertiary xanthate consumption, the reaction mixture was cooled to rt, concentrated, and purified by flash column chromatography.

**General Procedure D (intramolecular reactions):** To a 1-dram vial with a magnetic stir bar was added acyl xanthate (1 equiv) and dilauroyl peroxide (0.1 equiv). The vial was brought into the glovebox, and 1,2-dichloroethane (1 M) was added. The vial was fitted with a rubber septum cap, sealed with Teflon tape, and removed from the glovebox. The vial was placed under a balloon of argon and heated at 85 °C for 2 h. If tertiary xanthate remained by TLC (generally a spot with a higher  $R_f$  than the desired addition product), the vial was cooled to rt and brought back into the glovebox. Additional DLP (0.1 equiv) was added, and the reaction was heated at 85 °C for an additional 4 h, then cooled to rt, concentrated, and purified by flash column chromatography.



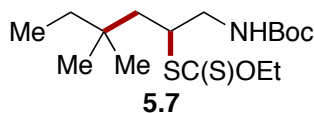
**2-((ethoxycarbonothioyl)thio)-4,4-dimethylhexyl acetate (5.6).** Prepared using acyl xanthate **5.5** (0.91 mmol scale) and allyl acetate according to General Procedure C with one addition of DLP. Purified by flash column chromatography on silica (5% EtOAc in hexanes) to afford **5.6** as a yellow oil (164 mg, 62% yield):

**<sup>1</sup>H NMR (600 MHz, CDCl<sub>3</sub>)** δ 4.67 – 4.58 (m, 2H), 4.19 – 4.11 (m, 2H), 3.97 – 3.90 (m, 1H), 2.05 (s, 3H), 1.59 – 1.47 (m, 2H), 1.43 – 1.37 (m, 3H), 1.32 – 1.19 (m, 2H), 0.89 (d, *J* = 3.4 Hz, 6H), 0.81 (td, *J* = 7.5, 2.1 Hz, 3H).

**<sup>13</sup>C NMR (151 MHz, CDCl<sub>3</sub>)** δ 213.46, 170.88, 70.11, 67.24, 45.10, 41.01, 34.40, 33.65, 26.82, 26.66, 20.98, 13.87, 8.51.

**IR (film)** 2962.13, 1747.19, 1462.74, 1380.78, 1364.39, 1224.58, 1047.16 cm<sup>-1</sup>.

**HRMS (ES<sup>+</sup>)** Exact mass calcd for C<sub>13</sub>H<sub>24</sub>O<sub>3</sub>S<sub>2</sub>Na [M+Na]<sup>+</sup>, 315.1065. Found 315.1057.



**tert-butyl (2-((ethoxycarbonothioyl)thio)-4,4-dimethylhexyl)carbamate (5.7).** Prepared using acyl xanthate **5.5** (0.45 mmol scale) and *N*-Boc allylamine according to General Procedure C with three additions of DLP. Purified by flash column chromatography on silica (5% EtOAc in hexanes) to afford **5.7** as a yellow oil (95 mg, 61% yield):

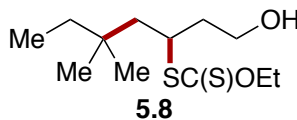
**<sup>1</sup>H NMR (600 MHz, CDCl<sub>3</sub>)** δ 4.84 (br. t, *J* = 6.5 Hz, 1H), 4.69 – 4.58 (m, 2H), 3.81 (p, *J* = 5.9 Hz, 1H), 3.45 (dt, *J* = 13.0, 6.2 Hz, 1H), 3.27 (dt, *J* = 13.4, 6.4 Hz, 1H), 1.52 (d, *J* = 5.6 Hz, 2H), 1.47 (s, 1H), 1.42 (s, 11H), 1.31 – 1.24 (m, 2H), 0.90 (d, *J* = 2.0 Hz, 6H), 0.81 (t, *J* = 7.5 Hz, 3H).

**<sup>13</sup>C NMR (151 MHz, CDCl<sub>3</sub>)** δ 214.21, 156.10, 79.49, 70.12, 47.47, 46.13, 41.90, 34.58, 33.75, 28.50, 26.75, 26.72, 13.94, 8.59.

**IR (film)** 3365.17, 2964.05, 1716.34, 1698.98, 1507.10, 1219.76, 1048.12 cm<sup>-1</sup>.



**HRMS (ES+)** Exact mass calcd for  $C_{16}H_{31}NO_3S_2Na$   $[M+Na]^+$ , 372.1643. Found 372.1638.



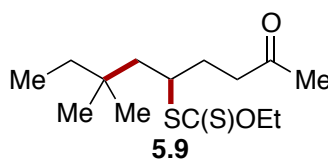
***O*-ethyl *S*-(1-hydroxy-5,5-dimethylheptan-3-yl) carbonodithioate (5.8).** Prepared using acyl xanthate **5.5** (0.5 mmol scale) and homoallyl alcohol according to General Procedure C with two additions of DLP. Purified by flash column chromatography on silica (5 – 20% EtOAc in hexanes) to afford **5.8** as a yellow liquid (82 mg, 62% yield):

**$^1H$  NMR (600 MHz,  $CDCl_3$ )**  $\delta$  4.66 – 4.59 (m, 2H), 3.92 – 3.86 (m, 1H), 3.75 – 3.69 (m, 1H), 3.68 – 3.63 (m, 1H), 2.16 (br. s, 1H), 2.01 – 1.95 (m, 1H), 1.84 – 1.78 (m, 1H), 1.68 (dd,  $J$  = 15.0, 7.6 Hz, 1H), 1.49 (dd,  $J$  = 15.1, 3.5 Hz, 1H), 1.41 (t,  $J$  = 7.1 Hz, 3H), 1.32 – 1.22 (m, 2H), 0.90 (d,  $J$  = 2.3 Hz, 6H), 0.80 (t,  $J$  = 7.5 Hz, 3H).

**$^{13}C$  NMR (151 MHz,  $CDCl_3$ )**  $\delta$  216.12, 70.27, 59.92, 45.87, 44.55, 41.21, 34.63, 33.96, 26.81, 26.74, 13.93, 8.57.

**IR (film)** 3365.17, 2961.16, 1463.71, 1387.53, 1213.97, 1050.05  $cm^{-1}$ .

**HRMS (ES+)** Exact mass calcd for  $C_{12}H_{24}O_2S_2Na$   $[M+Na]^+$ , 287.1116. Found 287.1108.



***S*-(7,7-dimethyl-2-oxononan-5-yl) *O*-ethyl carbonodithioate (5.9).** Prepared using acyl xanthate **5.5** (0.5 mmol scale) and 5-hexen-2-one according to General Procedure C with two additions of DLP. Purified by flash column chromatography on silica (2% EtOAc in hexanes) to afford **5.9** as a yellow liquid (88 mg, 61% yield):

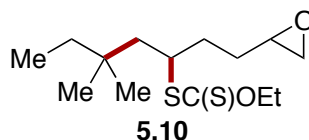
**$^1H$  NMR (600 MHz,  $CDCl_3$ )**  $\delta$  4.64 – 4.56 (m, 2H), 3.76 (tdd,  $J$  = 8.1, 5.1, 3.7 Hz, 1H), 2.63 – 2.56 (m, 1H), 2.54 – 2.48 (m, 1H), 2.11 (s, 3H), 2.07 – 2.00 (m, 1H), 1.85 – 1.78 (m, 1H),

1.61 (dd,  $J = 15.0, 7.5$  Hz, 1H), 1.43 – 1.36 (m, 4H), 1.30 – 1.21 (m, 2H), 0.88 (d,  $J = 2.6$  Hz, 6H), 0.79 (t,  $J = 7.5$  Hz, 3H).

$^{13}\text{C}$  NMR (151 MHz,  $\text{CDCl}_3$ )  $\delta$  214.53, 208.07, 69.89, 46.76, 45.42, 40.64, 34.62, 33.85, 31.45, 30.13, 26.81, 26.71, 13.91, 8.57.

IR (film) 2961.16, 1717.3, 1456.96, 1387.53, 1213.01, 1048.12  $\text{cm}^{-1}$ .

HRMS (ES+) Exact mass calcd for  $\text{C}_{14}\text{H}_{26}\text{O}_2\text{S}_2\text{Na}$   $[\text{M}+\text{Na}]^+$ , 313.1267. Found 313.1269.



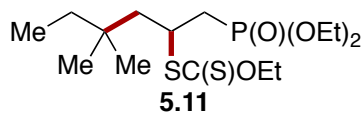
***S*-(5,5-dimethyl-1-(oxiran-2-yl)heptan-3-yl) *O*-ethyl carbonodithioate (5.10).** Prepared using acyl xanthate **5.5** (0.5 mmol scale) and 1,2-epoxy-5-hexene according to General Procedure C with two additions of DLP. Purified by flash column chromatography on silica (2% EtOAc in hexanes) to afford **5.10** as a yellow liquid (89 mg, 61% yield, 1.1:1 dr):

$^1\text{H}$  NMR (600 MHz,  $\text{CDCl}_3$ )  $\delta$  4.61 (qd,  $J = 7.1, 1.8$  Hz, 2H), 3.82 – 3.77 (m, 0.53H), 3.76 – 3.71 (m, 0.47H), 2.94 – 2.87 (m, 1H), 2.75 – 2.71 (m, 1H), 2.48 – 2.44 (m, 1H), 1.90 – 1.54 (m, 5H), 1.45 – 1.37 (m, 4H), 1.31 – 1.20 (m, 2H), 0.88 (d,  $J = 3.3$  Hz, 6H), 0.79 (t,  $J = 7.5$  Hz, 3H).

$^{13}\text{C}$  NMR (151 MHz,  $\text{CDCl}_3$ )  $\delta$  214.55, 69.76, 52.08, 51.98, 47.14, 47.13, 46.86, 46.77, 44.69, 44.67, 34.70, 34.19, 33.87, 33.76, 33.74, 29.87, 29.47, 26.84, 26.72, 13.92, 8.56.

IR (film) 2961.16, 2878.24, 1456.96, 1387.53, 1213.01, 1111.76, 1050.05  $\text{cm}^{-1}$ .

HRMS (ES+) Exact mass calcd for  $\text{C}_{14}\text{H}_{26}\text{O}_2\text{S}_2\text{Na}$   $[\text{M}+\text{Na}]^+$ , 313.1267. Found 313.1275.



***S*-(1-(diethoxyphosphoryl)-4,4-dimethylhexan-2-yl) *O*-ethyl carbonodithioate (5.11).**

Prepared using acyl xanthate **5.5** (0.91 mmol scale) and diethyl allylphosphonate according

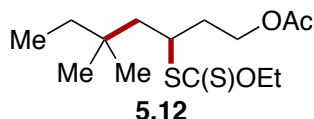
to General Procedure C with three additions of DLP. Purified by flash column chromatography on silica (35% EtOAc in hexanes) to afford **5.11** as a yellow oil (145 mg, 43% yield):

**<sup>1</sup>H NMR (600 MHz, CDCl<sub>3</sub>)** δ 4.59 (qd, *J* = 7.1, 1.1 Hz, 2H), 4.13 – 4.01 (m, 4H), 3.94 (dtdd, *J* = 12.0, 9.6, 3.6, 1.8 Hz, 1H), 2.35 (ddd, *J* = 20.0, 15.3, 3.6 Hz, 1H), 2.11 (ddd, *J* = 16.6, 15.3, 9.7 Hz, 1H), 1.93 (dd, *J* = 15.4, 2.4 Hz, 1H), 1.53 (dd, *J* = 15.3, 9.5 Hz, 1H), 1.38 (t, *J* = 7.1 Hz, 3H), 1.32 – 1.18 (m, 8H), 0.87 (d, *J* = 2.2 Hz, 6H), 0.77 (t, *J* = 7.5 Hz, 3H).

**<sup>13</sup>C NMR (151 MHz, CDCl<sub>3</sub>)** δ 213.44, 69.73, 61.76 (d, *J* = 7.6 Hz), 61.67 (d, *J* = 6.0 Hz), 43.36 (d, *J* = 3.0 Hz), 41.86 (d, *J* = 1.5 Hz), 34.86, 34.21 (d, *J* = 134.4 Hz), 33.65, 26.80, 26.64, 16.51 (d, *J* = 1.5 Hz), 16.47 (d, *J* = 1.5 Hz), 13.83, 8.45.

**IR (film)** 2963.09, 1472.38, 1390.42, 1222.65, 1047.16, 961.34 cm<sup>-1</sup>.

**HRMS (ES<sup>+</sup>)** Exact mass calcd for C<sub>15</sub>H<sub>31</sub>O<sub>4</sub>PS<sub>2</sub> [M+H]<sup>+</sup>, 371.1479. Found 371.1489.



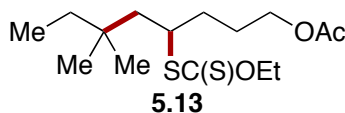
**3-((ethoxycarbonothioyl)thio)-5,5-dimethylheptyl acetate (5.12).** Prepared using acyl xanthate **5.5** (0.5 mmol scale) and homoallyl acetate according to General Procedure C with two additions of DLP. Purified by flash column chromatography on silica (2% EtOAc in hexanes) to afford **5.12** as a yellow liquid (105 mg, 69% yield):

**<sup>1</sup>H NMR (600 MHz, CDCl<sub>3</sub>)** δ 4.66 – 4.58 (m, 2H), 4.20 – 4.08 (m, 2H), 3.82 (qd, *J* = 6.8, 3.5 Hz, 1H), 2.07 – 1.98 (m, 5H), 1.65 – 1.59 (m, 1H), 1.53 – 1.46 (m, 1H), 1.43 – 1.38 (m, 3H), 1.33 – 1.22 (m, 2H), 0.89 (d, *J* = 7.7 Hz, 6H), 0.80 (t, *J* = 7.5 Hz, 3H).

**<sup>13</sup>C NMR (151 MHz, CDCl<sub>3</sub>)** δ 214.05, 171.04, 69.85, 62.06, 44.71, 44.00, 36.46, 34.70, 33.85, 26.77, 26.68, 21.11, 13.90, 8.55.

**IR (film)** 2962.13, 1742.37, 1456.96, 1365.35, 1231.33, 1048.12 cm<sup>-1</sup>.

**HRMS (ES+)** Exact mass calcd for  $C_{14}H_{26}O_3S_2Na$   $[M+Na]^+$ , 329.1216. Found 329.1221.



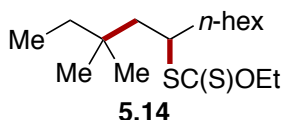
**4-((ethoxycarbonothioyl)thio)-6,6-dimethyloctyl acetate (5.13).** Prepared using acyl xanthate **5.5** (0.5 mmol scale) and 4-pentenyl acetate according to General Procedure C with two additions of DLP. Purified by flash column chromatography on silica (2% EtOAc in hexanes) to afford **5.13** as a yellow liquid (104 mg, 65% yield):

**$^1H$  NMR (600 MHz,  $CDCl_3$ )**  $\delta$  4.61 (q,  $J = 7.1$  Hz, 2H), 4.07 – 4.01 (m, 2H), 3.77 – 3.71 (m, 1H), 2.02 (s, 3H), 1.76 – 1.68 (m, 4H), 1.58 (dd,  $J = 15.1, 7.8$  Hz, 1H), 1.46 – 1.38 (m, 4H), 1.30 – 1.22 (m, 2H), 0.88 (s, 6H), 0.80 (t,  $J = 7.5$  Hz, 3H).

**$^{13}C$  NMR (151 MHz,  $CDCl_3$ )**  $\delta$  214.58, 171.16, 69.74, 64.26, 46.78, 44.69, 34.70, 34.17, 33.77, 26.86, 26.73, 25.88, 21.07, 13.92, 8.57.

**IR (film)** 2961.16, 1741.41, 1472.38, 1364.39, 1238.08, 1214.93, 1049.09  $cm^{-1}$ .

**HRMS (ES+)** Exact mass calcd for  $C_{15}H_{28}O_3S_2Na$   $[M+Na]^+$ , 343.1372. Found 343.1366.



**S-(3,3-dimethyltridecan-5-yl) O-ethyl carbonodithioate (5.14).** Prepared using acyl xanthate **5.5** (0.5 mmol scale) and 1-octene according to General Procedure C with two additions of DLP.  $^1H$  NMR of the crude reaction mixture with HMDS as internal standard indicated 80% yield of the addition product. Purified by flash column chromatography on silica (hexanes) to afford **5.14** as a pale yellow liquid (96 mg, 88% yield) contaminated with inseparable DLP-xanthate (~18%):

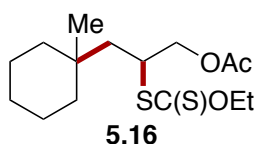
**$^1H$  NMR (600 MHz,  $CDCl_3$ )**  $\delta$  4.66 – 4.59 (m, 2H), 3.75 – 3.69 (m, 0.80H, product CH), 3.11 – 3.07 (m, 0.35H, DLP xanthate  $CH_2$ ), 1.70 – 1.63 (m, 2H), 1.58 – 1.53 (m, 0.87H), 1.48

– 1.43 (m, 0.86H), 1.42 – 1.34 (m, 5H), 1.32 – 1.22 (m, 10H), 0.90 – 0.84 (m, 8H), 0.83 – 0.77 (m, 3H).

**$^{13}\text{C}$  NMR (151 MHz,  $\text{CDCl}_3$ )**  $\delta$  215.25, 214.92, 69.75, 69.74, 69.50, 69.49, 47.27, 44.62, 37.89, 36.00, 34.77, 33.74, 32.01, 31.88, 29.70, 29.68, 29.57, 29.44, 29.35, 29.23, 29.00, 28.46, 26.91, 26.76, 26.73, 22.79, 22.73, 22.72, 14.23, 14.20, 13.93, 13.90, 8.58.

**IR (film)** 2925.48, 2854.13, 1456.96, 1212.04, 1111.76, 1051.01  $\text{cm}^{-1}$ .

**HRMS (ES+)** Exact mass calcd for  $\text{C}_{16}\text{H}_{33}\text{OS}_2$   $[\text{M}+\text{H}]^+$ , 305.1967. Found 305.1993.



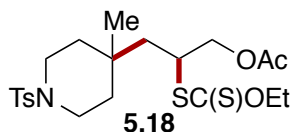
**2-((ethoxycarbonothioyl)thio)-3-(1-methylcyclohexyl)propyl acetate (5.16).** Prepared using acyl xanthate **5.15** (0.8 mmol scale) and allyl acetate according to General Procedure C with one addition of DLP. Purified by flash column chromatography on silica (5% EtOAc in hexanes) to afford **5.16** as a pale yellow oil (160 mg, 62% yield):

**$^1\text{H}$  NMR (600 MHz,  $\text{CDCl}_3$ )**  $\delta$  4.64 (qd,  $J = 7.1, 5.8$  Hz, 2H), 4.21 – 4.14 (m, 2H), 3.99 (tdd,  $J = 6.6, 5.4, 3.7$  Hz, 1H), 2.07 (s, 3H), 1.62 – 1.53 (m, 2H), 1.47 – 1.40 (m, 8H), 1.35 – 1.24 (m, 5H), 0.96 (s, 3H).

**$^{13}\text{C}$  NMR (151 MHz,  $\text{CDCl}_3$ )**  $\delta$  213.54, 171.01, 70.18, 67.37, 44.67, 37.97, 37.89, 33.61, 26.41, 22.13, 22.08, 21.08, 13.94.

**IR (film)** 2910.06, 1748.16, 1558.20, 1496.49, 1225.54, 1050.30  $\text{cm}^{-1}$ .

**HRMS (ES+)** Exact mass calcd for  $\text{C}_{15}\text{H}_{26}\text{O}_3\text{S}_2\text{Na}$   $[\text{M}+\text{Na}]^+$ , 341.1221. Found 341.1215.



**2-((ethoxycarbonothioyl)thio)-3-(4-methyl-1-tosylpiperidin-4-yl)propyl acetate (5.18).**

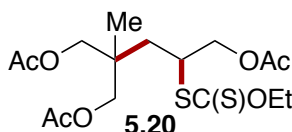
Prepared using acyl xanthate **5.17** (0.5 mmol scale) and allyl acetate according to General Procedure C with one addition of DLP. Purified by flash column chromatography on silica (25% EtOAc in hexanes) to afford **5.18** (144 mg, 61% yield):

**<sup>1</sup>H NMR (600 MHz, CDCl<sub>3</sub>)** δ 7.64 (dd, *J* = 8.5, 2.8 Hz, 2H), 7.36 – 7.30 (m, 2H), 4.68 – 4.57 (m, 2H), 4.17 – 4.06 (m, 2H), 3.97 – 3.90 (m, 1H), 3.29 – 3.19 (m, 2H), 2.80 – 2.71 (m, 2H), 2.43 (s, 3H), 2.02 (s, 3H), 1.66 – 1.39 (m, 9H), 0.88 (s, 3H).

**<sup>13</sup>C NMR (151 MHz, CDCl<sub>3</sub>)** δ 212.86, 170.75, 143.59, 133.29, 129.78, 127.76, 70.44, 66.98, 44.44, 42.25, 42.18, 41.45, 36.57, 36.24, 31.64, 23.15, 21.69, 20.96, 13.89.

**IR (film)** 2927.41, 2852.20, 1743.33, 1350.89, 1226.50, 1162.87, 1050.05 cm<sup>-1</sup>.

**HRMS (ES<sup>+</sup>)** Exact mass calcd for C<sub>21</sub>H<sub>31</sub>NO<sub>5</sub>S<sub>3</sub>Na [M+Na]<sup>+</sup>, 496.1262. Found 496.1267.



**2-(acetoxymethyl)-4-((ethoxycarbonothioyl)thio)-2-methylpentane-1,5-diyl diacetate**

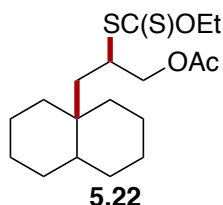
**(5.20).** Prepared using acyl xanthate **5.19** (0.5 mmol scale) and allyl acetate according to General Procedure C with one addition of DLP. Purified by flash column chromatography on silica (20% EtOAc in hexanes) to afford **5.20** as a yellow oil (135 mg, 68% yield):

**<sup>1</sup>H NMR (600 MHz, CDCl<sub>3</sub>)** δ 4.65 – 4.58 (m, 2H), 4.18 – 4.11 (m, 2H), 4.03 (tt, *J* = 7.0, 4.5 Hz, 1H), 3.98 – 3.87 (m, 4H), 2.07 – 2.00 (m, 9H), 1.74 – 1.69 (m, 2H), 1.39 (t, *J* = 7.1 Hz, 3H), 1.01 (s, 3H).

**<sup>13</sup>C NMR (151 MHz, CDCl<sub>3</sub>)** δ 212.60, 170.84, 170.82, 170.69, 70.45, 67.78, 67.68, 66.97, 44.37, 37.48, 34.67, 20.93, 20.92, 20.89, 19.44, 13.82.

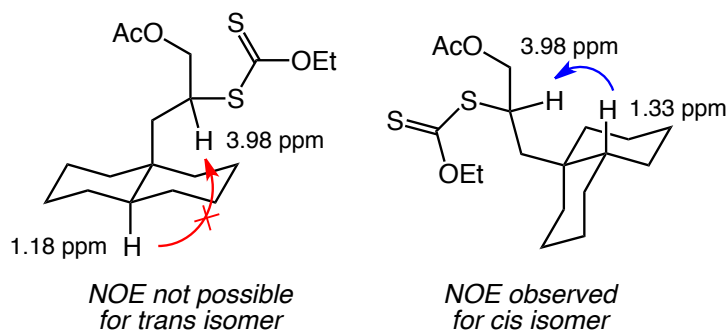
**IR (film)** 2976.59, 1743.33, 1456.96, 1380.78, 1232.29, 1045.23 cm<sup>-1</sup>.

**HRMS (ES<sup>+</sup>)** Exact mass calcd for C<sub>16</sub>H<sub>26</sub>O<sub>7</sub>S<sub>2</sub>Na [M+Na]<sup>+</sup>, 417.1012. Found 417.1009.



**3-(decahydronaphthalen-4a-yl)-2-((ethoxycarbonothioyl)thio)propyl acetate (5.22).**

Prepared using acyl xanthate **5.21** (0.5 mmol scale) and allyl acetate according to General Procedure C with one addition of DLP. Purified by flash column chromatography on silica (2% EtOAc in hexanes) to afford **5.22** as a yellow oil (89.4 mg, 50% yield, 2.7:1 *cis:trans*). The *cis* and *trans* isomers were identified as such by use of DEPT-135, HSQC, and NOESY NMR experiments. From the DEPT-135, methyl and methine carbons were identified as occurring at 47.56, 44.82, 44.32, 39.79, 21.06, and 13.90 ppm, with the latter two peaks being assigned as the methyl group of the acetate and xanthate respectively. Based on HSQC correlations, the carbons occurring at 44.82 and 44.32 ppm can be assigned as the methine carbons at which the xanthate group is attached in both isomers of product. The remaining two carbon signals then correspond to the bridgehead methines of the two decalin isomers. Based on HSQC correlations, the carbon signal at 47.56 ppm correlates to a proton at 1.18 ppm, and the carbon signal at 39.79 ppm correlates to a proton at 1.33 ppm. An NOE is observed between the proton at 1.33 ppm and the proton at 3.98 ppm (methine adjacent to the xanthate group), but not between the proton at 1.18 ppm and the proton at 3.98 ppm. This indicates that the proton at 1.33 ppm is the *cis* bridgehead methine, and the *cis* product is major.



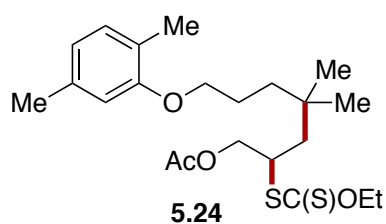
However, due to peak overlap, the exact *cis:trans* ratio could not be accurately determined by NMR, so it was determined by GC–MS analysis:

**<sup>1</sup>H NMR (600 MHz, CDCl<sub>3</sub>)** δ 4.67 – 4.58 (m, 2H), 4.21 – 4.13 (m, 2H), 4.00 – 3.92 (m, 1H), 2.08 – 2.05 (m, 3H), 1.87 – 1.61 (m, 4H), 1.57 – 1.38 (m, 10H), 1.34 – 0.83 (m, 8H).

**<sup>13</sup>C NMR (151 MHz, CDCl<sub>3</sub>)** δ 213.52, 170.96, 170.93, 70.14, 70.12, 67.53, 47.56, 44.82, 44.32, 39.79, 38.46, 37.49, 37.45, 36.74, 36.18, 28.41, 28.36, 27.68, 27.62, 26.91, 26.90, 25.29, 22.11, 22.07, 21.89, 21.62, 21.06, 13.90.

**IR (film)** 2925.48, 2861.84, 1747.19, 1455.99, 1223.61, 1049.09.

**HRMS (ES<sup>+</sup>)** Exact mass calcd for C<sub>18</sub>H<sub>30</sub>O<sub>3</sub>S<sub>2</sub>Na [M+Na]<sup>+</sup>, 381.1529. Found 381.1569.



**7-(2,5-dimethylphenoxy)-2-((ethoxycarbonothioyl)thio)-4,4-dimethylheptyl acetate**

**(5.24).** Prepared using acyl xanthate **5.23** (0.5 mmol scale) and allyl acetate according to General Procedure C with one addition of DLP. Purified by flash column chromatography on silica (5 – 10% EtOAc in hexanes) to afford **5.24** as a yellow oil (146 mg, 68% yield):

**<sup>1</sup>H NMR (600 MHz, CDCl<sub>3</sub>)** δ 7.01 (d, *J* = 7.4 Hz, 1H), 6.67 (d, *J* = 7.5 Hz, 1H), 6.63 (d, *J* = 1.6 Hz, 1H), 4.65 (qq, *J* = 7.7, 3.6 Hz, 2H), 4.23 – 4.15 (m, 2H), 4.04 – 3.98 (m, 1H), 3.95

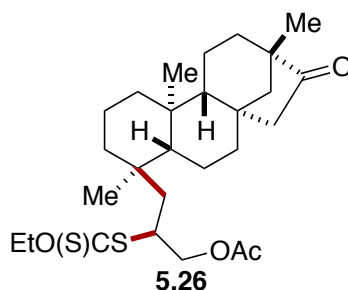


– 3.88 (m, 2H), 2.32 (s, 3H), 2.19 (s, 3H), 2.07 (s, 3H), 1.80 – 1.73 (m, 2H), 1.63 (qd,  $J = 15.2, 5.5$  Hz, 2H), 1.47 – 1.40 (m, 5H), 1.00 (s, 6H).

$^{13}\text{C}$  NMR (151 MHz,  $\text{CDCl}_3$ )  $\delta$  213.37, 170.90, 157.07, 136.56, 130.38, 123.61, 120.72, 111.99, 70.20, 68.39, 67.25, 45.16, 41.30, 38.26, 33.48, 27.41, 27.27, 24.39, 21.54, 20.99, 15.96, 13.89.

IR (film) 2955.38, 1746.23, 1508.06, 1472.38, 1224.58, 1046.19  $\text{cm}^{-1}$ .

HRMS (ES+) Exact mass calcd for  $\text{C}_{22}\text{H}_{34}\text{O}_4\text{S}_2\text{Na}$   $[\text{M}+\text{Na}]^+$ , 449.1797. Found 449.1785.

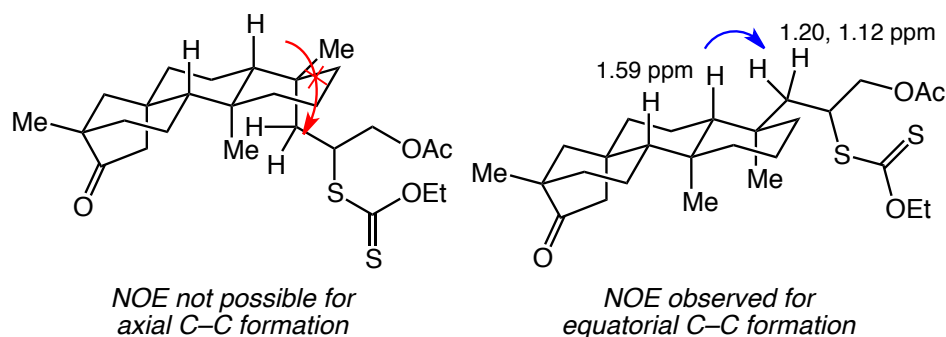


**2-((ethoxycarbonothioyl)thio)-3-((4*S*,4*aR*,6*aR*,9*S*,11*aR*,11*bR*)-4,9,11*b*-trimethyl-8-oxotetradecahydro-6*a*,9-methanocyclohepta[*a*]naphthalen-4-yl)propyl acetate (5.26).**

Prepared using acyl xanthate **5.25** (0.5 mmol scale) and allyl acetate according to General Procedure C with one addition of DLP. Purified by flash column chromatography on silica (10% EtOAc in hexanes) to afford **5.26** as a yellow oil (166 mg, 67% yield, 1.1:1 dr).

The relative stereochemistry at the new quaternary stereocenter was determined using DEPT-135,  $^1\text{H}$ – $^1\text{H}$  COSY, HSQC, and NOESY NMR experiments. According to the literature,<sup>9</sup> the bridgehead methine at the C5 position occurs at 57.15 ppm for the parent isosteviol. In the acyl xanthate **21**, the peak is 58.12 ppm, and upon formation of the new quaternary center, the two product diastereomers display this peak at 55.70 and 55.57 ppm (they are verified as being methine peaks via DEPT-135 analysis). Based on HSQC correlations, these carbons at 55.70 and 55.57 ppm are attached to protons at 1.21 and 1.13 ppm. The methine at which the

xanthate group is attached occurs at 4.06 – 3.96 ppm in the  $^1\text{H}$  spectrum, and through  $^1\text{H}$ – $^1\text{H}$  COSY, this peak is correlated to the multiplet from 4.17 – 4.08 (the methylene adjacent to the acetate group) and a multiplet centered at 1.60 ppm (the methylene adjacent to the quaternary center). An NOE is observed between the peak at 1.59 ppm and the peaks at 1.20 and 1.12 ppm, which is only possible for the equatorial addition product (as shown below).

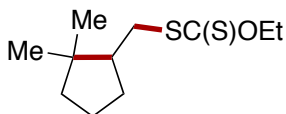


**$^1\text{H}$  NMR (600 MHz,  $\text{CDCl}_3$ )**  $\delta$  4.68 – 4.58 (m, 2H), 4.18 – 4.13 (m, 1H), 4.13 – 4.07 (m, 1H), 4.07 – 3.97 (m, 1H), 2.65 (ddd,  $J = 18.5, 8.4, 3.9$  Hz, 1H), 2.07 – 2.01 (m, 3H), 1.78 – 1.70 (m, 1H), 1.68 – 1.39 (m, 16H), 1.38 – 1.11 (m, 5H), 1.04 – 0.92 (m, 4H), 0.90 – 0.77 (m, 7H).

**$^{13}\text{C}$  NMR (151 MHz,  $\text{CDCl}_3$ )**  $\delta$  222.84, 222.77, 213.76, 213.34, 170.86, 70.19, 67.54, 67.38, 55.70, 55.57, 54.60, 54.50, 53.39, 51.92, 49.01, 48.89, 48.82, 44.67, 44.64, 43.46, 43.43, 41.05, 40.54, 39.46, 39.31, 38.98, 38.88, 37.90, 37.82, 37.69, 37.31, 36.86, 36.81, 36.73, 21.31, 21.12, 21.02, 20.99, 20.53, 20.07, 20.04, 20.02, 19.96, 19.95, 17.95, 17.86, 15.62, 15.45, 13.98, 13.90.

**IR (film)** 2927.41, 2848.35, 1455.99, 1402.96, 1224.58, 1048.12  $\text{cm}^{-1}$ .

**HRMS (ES+)** Exact mass calcd for  $\text{C}_{27}\text{H}_{43}\text{O}_4\text{S}_2$   $[\text{M}+\text{H}]^+$ , 495.2597. Found 495.2624.



**5.28**

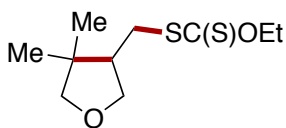
***S*-((2,2-dimethylcyclopentyl)methyl) *S*-ethyl carbonodithioate (5.28).** Prepared using acyl xanthate **5.27** (1.54 mmol scale) according to General Procedure D with one addition of DLP.  $^1\text{H}$  NMR yield with HMDS as an internal standard indicated 82% NMR yield of 5-exo product. Purified by flash column chromatography on silica (hexanes) to afford **5.28** as a yellow liquid (275 mg, 77% yield) contaminated with inseparable DLP-xanthate (~10% by  $^1\text{H}$  NMR):

**$^1\text{H}$  NMR (600 MHz,  $\text{CDCl}_3$ )**  $\delta$  4.64 (qd,  $J = 7.1, 1.1$  Hz, 2H), 3.33 (dd,  $J = 12.8, 4.0$  Hz, 1H), 2.79 (dd,  $J = 12.8, 11.0$  Hz, 1H), 1.99 – 1.91 (m, 1H), 1.74 (tdd,  $J = 10.7, 7.9, 4.0$  Hz, 1H), 1.65 – 1.53 (m, 2H), 1.47 – 1.35 (m, 6H), 1.06 (s, 3H), 0.84 (s, 3H).

**$^{13}\text{C}$  NMR (151 MHz,  $\text{CDCl}_3$ )**  $\delta$  215.48, 69.87, 48.18, 42.02, 41.49, 37.97, 30.72, 28.17, 21.89, 21.30, 13.97.

**IR (film)** 2953.45, 2867.63, 1463.71, 1366.32, 1213.97, 1111.76, 1050.05  $\text{cm}^{-1}$ .

**HRMS (ES+)** Exact mass calcd for  $\text{C}_{11}\text{H}_{21}\text{OS}_2$   $[\text{M}+\text{H}]^+$ , 233.1028. Found 233.1034.



**5.30**

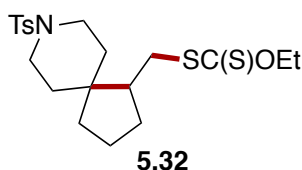
***S*-((4,4-dimethyltetrahydrofuran-3-yl)methyl) *S*-ethyl carbonodithioate (5.30).** Prepared using acyl xanthate **5.29** (1.5 mmol scale) according to General Procedure D with one addition of DLP. Purified by flash column chromatography on silica (2% EtOAc in hexanes) to afford **5.30** as a yellow liquid (253 mg, 71% yield):

**<sup>1</sup>H NMR (600 MHz, CDCl<sub>3</sub>)** δ 4.65 (qd, *J* = 7.1, 1.0 Hz, 2H), 4.10 (dd, *J* = 8.6, 7.9 Hz, 1H), 3.62 – 3.57 (m, 2H), 3.54 – 3.50 (m, 1H), 3.36 (dd, *J* = 13.3, 4.6 Hz, 1H), 2.91 (dd, *J* = 13.3, 10.5 Hz, 1H), 2.27 – 2.20 (m, 1H), 1.43 (t, *J* = 7.1 Hz, 3H), 1.12 (s, 3H), 1.03 (s, 3H).

**<sup>13</sup>C NMR (151 MHz, CDCl<sub>3</sub>)** δ 214.43, 81.48, 72.80, 70.23, 47.54, 41.51, 35.01, 25.04, 20.81, 13.95.

**IR (film)** 2959.23, 2926.45, 2867.63, 1465.63, 1390.42, 1215.90, 1048.12 cm<sup>-1</sup>.

**HRMS (ES<sup>+</sup>)** Exact mass calcd for C<sub>10</sub>H<sub>18</sub>O<sub>2</sub>S<sub>2</sub>Na [M+Na]<sup>+</sup>, 257.0641. Found 257.0652.



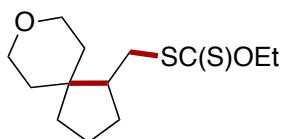
***S*-ethyl *S*-((8-tosyl-8-azaspiro[4.5]decan-1-yl)methyl) carbonodithioate (5.32).** Prepared using acyl xanthate **5.31** (0.5 mmol scale) according to General Procedure D with two additions of DLP. Purified by flash column chromatography on silica (10 – 20% EtOAc in hexanes) to afford **5.32** as a pale yellow oil (158 mg, 74% yield):

**<sup>1</sup>H NMR (600 MHz, CDCl<sub>3</sub>)** δ 7.64 (d, *J* = 8.5 Hz, 2H), 7.32 (d, *J* = 8.0 Hz, 2H), 4.62 (qd, *J* = 7.1, 1.3 Hz, 2H), 3.63 – 3.54 (m, 2H), 3.32 (dd, *J* = 13.0, 3.7 Hz, 1H), 2.70 (dd, *J* = 13.0, 11.3 Hz, 1H), 2.49 – 2.41 (m, 5H), 1.95 – 1.86 (m, 2H), 1.75 (dddd, *J* = 11.1, 9.2, 7.4, 3.6 Hz, 1H), 1.66 – 1.48 (m, 4H), 1.41 (t, *J* = 7.1 Hz, 3H), 1.38 – 1.20 (m, 4H).

**<sup>13</sup>C NMR (151 MHz, CDCl<sub>3</sub>)** δ 214.86, 143.57, 133.24, 129.76, 127.76, 70.01, 47.76, 44.15, 43.16, 42.87, 37.14, 35.91, 34.45, 30.00, 29.57, 21.68, 21.30, 13.95.

**IR (film)** 2938.98, 2864.74, 1351.86, 1215.9, 1164.79, 1050.05 cm<sup>-1</sup>.

**HRMS (ES<sup>+</sup>)** Exact mass calcd for C<sub>20</sub>H<sub>29</sub>NO<sub>3</sub>S<sub>3</sub>Na [M+Na]<sup>+</sup>, 450.1202. Found 450.1202.



**5.34**

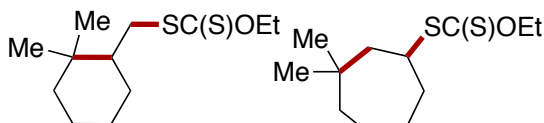
***S*-(8-oxaspiro[4.5]decan-1-ylmethyl) *S*-ethyl carbonodithioate (5.34).** Prepared using acyl xanthate **5.33** (0.5 mmol scale) according to General Procedure D with two additions of DLP. Purified by flash column chromatography on silica (5 – 10% EtOAc in hexanes) to afford **5.34** as a yellow oil (89 mg, 65% yield):

**<sup>1</sup>H NMR (600 MHz, CDCl<sub>3</sub>)** δ 4.64 (q, *J* = 7.1, 2H), 3.88 – 3.82 (m, 2H), 3.53 (dtd, *J* = 17.0, 11.7, 2.3 Hz, 2H), 3.43 (dd, *J* = 12.9, 3.6 Hz, 1H), 2.79 (dd, *J* = 12.9, 11.3 Hz, 1H), 1.99 – 1.92 (m, 1H), 1.91 – 1.83 (m, 2H), 1.79 – 1.73 (m, 1H), 1.71 – 1.55 (m, 3H), 1.52 – 1.46 (m, 1H), 1.43 – 1.36 (m, 4H), 1.26 – 1.19 (m, 1H), 1.18 – 1.14 (m, 1H).

**<sup>13</sup>C NMR (151 MHz, CDCl<sub>3</sub>)** δ 215.13, 70.00, 65.81, 64.81, 48.69, 42.89, 37.42, 37.29, 34.80, 31.14, 30.01, 21.58, 13.98.

**IR (film)** 2952.48, 2850.27, 1540.85, 1520.60, 1214.93, 1048.12 cm<sup>-1</sup>.

**HRMS (ES<sup>+</sup>)** Exact mass calcd for C<sub>13</sub>H<sub>22</sub>O<sub>2</sub>S<sub>2</sub>Na [M+Na]<sup>+</sup>, 297.0954. Found 297.0963.



**5.36**

**5.37**

***S*-((2,2-dimethylcyclohexyl)methyl) *S*-ethyl carbonodithioate (32) & *S*-(2,2-dimethylcycloheptyl) *S*-ethyl carbonodithioate (5.35).** Prepared using acyl xanthate **31** (0.5 mmol scale) according to General Procedure D with two additions of DLP. Purified by flash column chromatography on silica (hexanes) to afford **5.36** and **5.37** (5.7:1) as a pale yellow oil (86 mg, 70% yield):

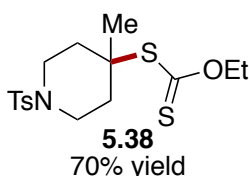
**<sup>1</sup>H NMR (600 MHz, CDCl<sub>3</sub>)** δ 4.64 (q, *J* = 7.2 Hz, 2H), 3.68 (tdd, *J* = 10.7, 3.0, 1.9 Hz, 0.14H), 3.53 (dd, *J* = 13.3, 2.8 Hz, 0.84H), 2.60 (dd, *J* = 13.3, 11.2 Hz, 0.85H), 2.19 – 2.13

(m, 0.16H), 1.80 – 1.62 (m, 2H), 1.54 – 1.35 (m, 7H), 1.26 – 1.07 (m, 3H), 1.04 – 1.00 (m, 3H), 0.92 (s, 0.50H), 0.85 (s, 2.50H).

<sup>13</sup>C NMR (151 MHz, CDCl<sub>3</sub>) δ 215.48, 214.52, 69.91, 69.54, 48.28, 46.53, 46.00, 42.04, 41.75, 38.29, 36.86, 33.93, 33.71, 32.06, 30.62, 29.38, 29.24, 27.61, 26.35, 22.88, 22.38, 19.71, 13.99.

IR (film) 2926.45, 2857.02, 1447.31, 1214.93, 1111.76, 1048.12 cm<sup>-1</sup>.

HRMS (ES+) Exact mass calcd for C<sub>12</sub>H<sub>22</sub>OS<sub>2</sub>Na [M+Na]<sup>+</sup>, 269.1005. Found 269.1012.



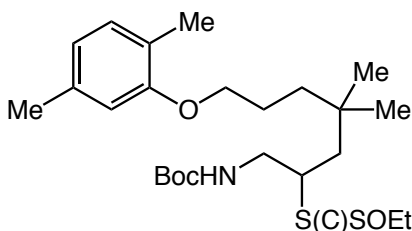
**O-ethyl S-(4-methyl-1-tosylpiperidin-4-yl) carbonodithioate (5.38).** To a round bottom flask in the glovebox, acyl xanthate **5.31** (856 mg, 2.13 mmol) and dilauroyl peroxide (42 mg, 0.11 mmol) were dissolved in DCE (4 mL). The flask was fitted with a reflux condenser and a rubber septum cap, sealed with Teflon tape, and removed from the glovebox. The flask was placed under a balloon of argon and heated at 85 °C for 2 h, then cooled to rt. The reaction was concentrated *in vacuo*, suspended in MeOH (5 mL), and decanted to afford **5.38** as a white solid (630 mg, 79% yield):

<sup>1</sup>H NMR (600 MHz, CDCl<sub>3</sub>) δ 7.64 – 7.60 (m, 2H), 7.34 – 7.31 (m, 2H), 4.63 (q, *J* = 7.1 Hz, 2H), 3.50 – 3.43 (m, 2H), 2.78 – 2.70 (m, 2H), 2.45 (s, 3H), 2.21 – 2.14 (m, 2H), 1.78 (ddd, *J* = 14.8, 11.0, 4.1 Hz, 2H), 1.59 (s, 3H), 1.44 (t, *J* = 7.1 Hz, 3H).

<sup>13</sup>C NMR (151 MHz, CDCl<sub>3</sub>) δ 212.23, 143.93, 133.12, 129.99, 127.68, 69.90, 53.22, 42.69, 36.41, 28.52, 21.73, 13.85.

IR (film) 2981.41, 2926.45, 2855.10, 1341.25, 1230.36, 1185.04, 1040.41 cm<sup>-1</sup>.

HRMS (ES+) Exact mass calcd for C<sub>16</sub>H<sub>23</sub>NO<sub>3</sub>S<sub>3</sub>Na [M+Na]<sup>+</sup>, 396.0733. Found 396.0764



***tert*-butyl (7-(2,5-dimethylphenoxy)-2-(((ethylthio)carbonyl)thio)-4,4-**

**dimethylheptyl)carbamate.** Prepared using acyl xanthate starting material (2.82 mmol

scale) and *N*-Boc allylamine according to General Procedure C with three additions of DLP.

Purified by flash column chromatography on silica (5 – 10% EtOAc in hexanes) followed by heating at 80 °C under high vacuum (to sublime coeluting *N*-Boc allylamine) afforded the

product as a thick yellow oil (826 mg, 61% yield). NMR spectra complicated due to presence of rotamers:

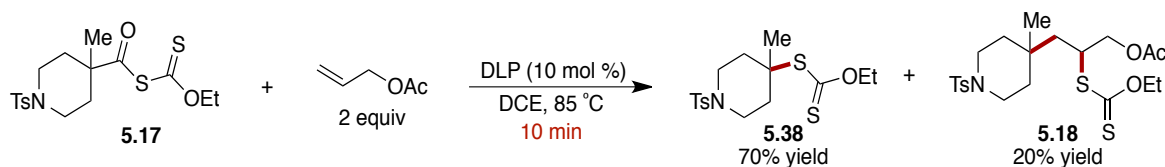
**<sup>1</sup>H NMR (600 MHz, CDCl<sub>3</sub>)** δ 7.02 (d, *J* = 7.4 Hz, 1H), 6.67 (d, *J* = 7.5 Hz, 1H), 6.64 (s, 1H), 4.99 (br. t, *J* = 6.3 Hz, 1H), 4.69 – 4.61 (m, 2H), 3.95 – 3.88 (m, 3H), 3.77 – 3.73 (m, 0.08H), 3.51 – 3.41 (m, 0.94H), 3.36 – 3.23 (m, 0.89H), 3.13 – 3.03 (m, 0.03H), 2.34 (s, 3H), 2.21 (s, 3H), 1.82 – 1.74 (m, 2H), 1.65 – 1.56 (m, 2H), 1.53 – 1.40 (m, 14H), 1.01 (s, 6H).

**<sup>13</sup>C NMR (151 MHz, CDCl<sub>3</sub>)** δ 213.83, 156.92, 155.93, 136.28, 130.19, 123.40, 120.53, 111.81, 79.20, 69.91, 68.23, 47.28, 45.94, 41.79, 38.22, 33.34, 28.33, 27.19, 27.12, 24.24, 21.40, 15.86, 13.75.

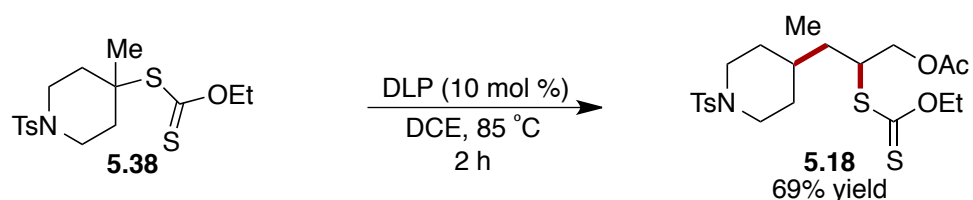
**IR (film)** 3366.14, 2956.34, 2868.59, 1715.37, 1508.06, 1252.54, 1168.65, 1048.12 cm<sup>-1</sup>.

**HRMS (ES<sup>+</sup>)** Exact mass calcd for C<sub>25</sub>H<sub>41</sub>NO<sub>4</sub>S<sub>2</sub>Na [M+Na]<sup>+</sup>, 506.2370. Found 506.2369.

### Mechanistic Experiments

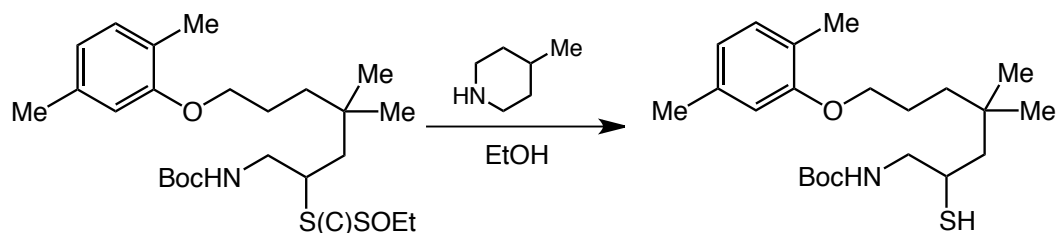


Short reaction time: To a 1-dram vial with a magnetic stir bar was added acyl xanthate **5.17** (201 mg, 0.5 mmol) and dilauroyl peroxide (20 mg, 0.05 mmol). The vial was brought into the glovebox, and allyl acetate (108  $\mu$ L, 1 mmol) was added, followed by 1,2-dichloroethane (0.5 mL). The vial was fitted with a rubber septum cap, sealed with Teflon tape, and removed from the glovebox. The vial was placed under a balloon of argon and heated at 85  $^{\circ}$ C for 10 minutes, cooled to rt, and concentrated. Based on  $^1$ H NMR analysis with hexamethyldisiloxane (HMDS) as internal standard, there was 70% tertiary xanthate **5.38** and 20% addition product **5.18** in the reaction mixture.



Use of isolated tertiary xanthate: To a 1-dram vial with a magnetic stir bar was added tertiary xanthate **5.38** (187 mg, 0.5 mmol) and dilauroyl peroxide (20 mg, 0.05 mmol). The vial was brought into the glovebox, and allyl acetate (108  $\mu$ L, 1 mmol) was added, followed by 1,2-dichloroethane (0.5 mL). The vial was fitted with a rubber septum cap, sealed with Teflon tape, and removed from the glovebox. The vial was placed under a balloon of argon and heated at 85  $^{\circ}$ C for 2 h, cooled to rt, and concentrated. Based on  $^1$ H NMR analysis with hexamethyldisiloxane (HMDS) as internal standard, 69% addition product **5.18** in the reaction mixture.

### Further Derivatization of Xanthate Products





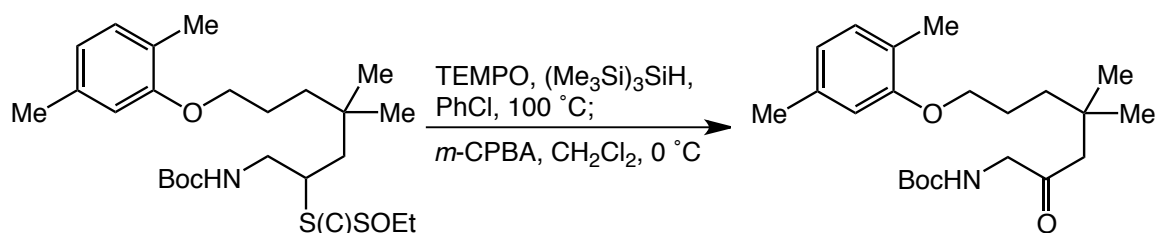
**tert-butyl (7-(2,5-dimethylphenoxy)-2-mercapto-4,4-dimethylheptyl)carbamate.** To a solution of xanthate (200 mg, 0.41 mmol) in EtOH (2 mL) was added 4-methylpiperidine (200  $\mu$ L, 1.7 mmol). The mixture was stirred for 4 h then concentrated *in vacuo*. The residue was purified by flash column chromatography on silica (10 – 15% EtOAc in hexanes) to afford the thiol as a clear oil (139 mg, 85% yield). NMR spectra complicated due to presence of rotamers:

**$^1\text{H}$  NMR (600 MHz,  $\text{CDCl}_3$ )**  $\delta$  7.00 (d,  $J$  = 7.4 Hz, 1H), 6.67 – 6.64 (m, 1H), 6.62 (dd,  $J$  = 7.3, 1.6 Hz, 1H), 5.20 – 5.08 (m, 0.25H), 5.03 – 4.99 (m, 0.62H), 3.96 – 3.88 (m, 2H), 3.75 (d,  $J$  = 5.9 Hz, 0.17H), 3.36 (dd,  $J$  = 10.0, 5.1 Hz, 0.82H), 3.01 (dt,  $J$  = 13.9, 7.1 Hz, 1.44H), 2.31 (s, 3H), 2.18 (s, 3H), 1.82 – 1.70 (m, 2H), 1.59 – 1.54 (m, 1.63H), 1.50 – 1.40 (m, 13H), 0.98 (d,  $J$  = 10.1 Hz, 6H).

**$^{13}\text{C}$  NMR (151 MHz,  $\text{CDCl}_3$ )**  $\delta$  157.10, 155.97, 136.56, 130.37, 123.64, 120.69, 112.03, 79.59, 68.45, 50.06, 47.38, 38.57, 36.76, 33.43, 28.51, 27.58, 27.46, 24.39, 21.56, 15.99.

**IR (film)** 3354.57, 2955.38, 1715.37, 1509.03, 1266.04, 1170.58, 1130.08  $\text{cm}^{-1}$ .

**HRMS (ES<sup>+</sup>)** Exact mass calcd for  $\text{C}_{22}\text{H}_{37}\text{O}_3\text{SNa}$   $[\text{M}+\text{Na}]^+$ , 418.2387. Found 418.2395.



**tert-butyl (7-(2,5-dimethylphenoxy)-4,4-dimethyl-2-oxoheptyl)carbamate.** Prepared as per our C–H xanthylation work.<sup>3</sup> In the glovebox, xanthate (48 mg, 0.1 mmol), TEMPO (31 mg, 0.2 mmol), and tris(trimethylsilyl)silane (31  $\mu$ L, 0.1 mmol) were dissolved in PhCl (1 mL) in a 1-dram vial. The vial was fitted with a rubber septum cap, sealed with Teflon tape, and removed from the glovebox. The vial was placed under a balloon of argon and heated at

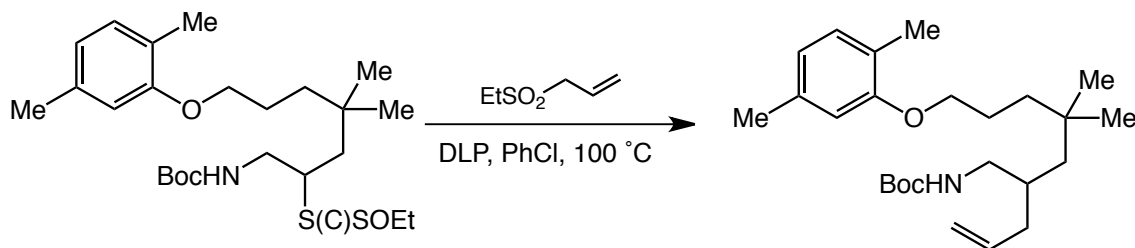
100 °C for 24 h, after which it was cooled to rt, brought back into the glovebox, and additional TEMPO (31 mg, 0.2 mmol) and tris(trimethylsilyl)silane (31  $\mu$ L, 0.1 mmol) were added. The reaction mixture was heated at 100 °C for 24 h, cooled to rt, and again brought back into the glovebox, where additional TEMPO (31 mg, 0.2 mmol) and tris(trimethylsilyl)silane (31  $\mu$ L, 0.1 mmol) were added. The reaction mixture was heated at 100 °C for 24 h, cooled to rt, concentrated *in vacuo*, redissolved in CH<sub>2</sub>Cl<sub>2</sub> (1 mL), and cooled to 0 °C. A solution of *m*-CPBA (35 mg, 0.2 mmol) in CH<sub>2</sub>Cl<sub>2</sub> (0.5 mL) was added to the reaction mixture, and the color turned from clear red to a cloudy yellow-orange. The mixture was stirred at 0 °C for 2 hr, then quenched with a saturated aqueous solution of sodium thiosulfate (1 mL), then saturated aqueous NaHCO<sub>3</sub> (1 mL). The organic layer was separated, and the aqueous layer was extracted with EtOAc. The combined organic layers were washed with saturated aqueous sodium thiosulfate, dried with MgSO<sub>4</sub>, and concentrated *in vacuo*. The resultant red-yellow residue was purified by flash column chromatography on silica (20% EtOAc in hexanes) to afford the alcohol as a clear viscous oil (24 mg, 65% yield). NMR spectra complicated due to presence of rotamers:

**<sup>1</sup>H NMR (600 MHz, CDCl<sub>3</sub>)**  $\delta$  7.00 (d, *J* = 7.4 Hz, 1H), 6.66 (d, *J* = 7.5 Hz, 1H), 6.61 (d, *J* = 1.6 Hz, 1H), 5.25 (br. s, 1H), 3.99 (d, *J* = 4.7 Hz, 2H), 3.92 (t, *J* = 6.4 Hz, 2H), 2.34 (s, 2H), 2.31 (s, 3H), 2.17 (s, 3H), 1.78 – 1.71 (m, 2H), 1.51 – 1.46 (m, 2H), 1.45 (s, 9H), 1.04 (s, 6H).

**<sup>13</sup>C NMR (151 MHz, CDCl<sub>3</sub>)**  $\delta$  205.26, 157.04, 155.65, 136.59, 130.40, 123.65, 120.76, 112.04, 79.86, 68.24, 52.38, 50.36, 38.61, 33.79, 28.45, 27.41, 24.47, 21.55, 15.94.

**IR (film)** 3421.10, 2955.38, 1731.76, 1715.37, 1508.06, 1366.32, 1265.07, 1159.01 cm<sup>-1</sup>.

**HRMS (ES<sup>+</sup>)** Exact mass calcd for C<sub>24</sub>H<sub>34</sub>NO<sub>4</sub>Na [M+Na]<sup>+</sup>, 400.2482. Found 400.2469.



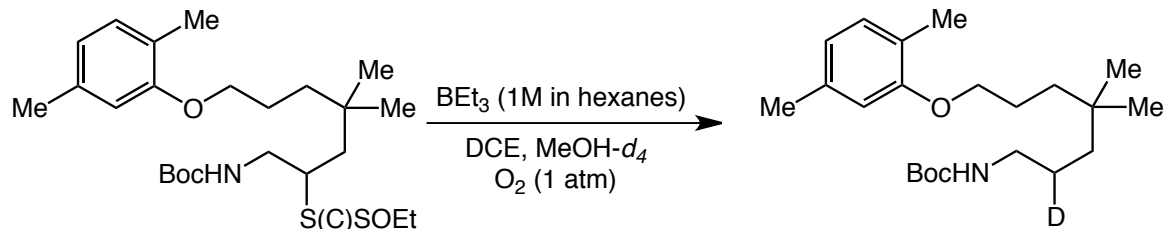
***tert*-butyl (2-allyl-7-(2,5-dimethylphenoxy)-4,4-dimethylheptyl)carbamate.** In the glovebox in a 1 dram vial, xanthate (48 mg, 0.1 mmol), ethyl allyl sulfone (40 mg, 0.3 mmol), and DLP (4 mg, 0.01 mmol) were dissolved in PhCl (0.4 mL). The vial was fitted with a rubber septum cap, sealed with Teflon tape, and removed from the glovebox. The vial was placed under a balloon of argon and heated at 100 °C for 30 min, after which it was cooled to rt and more DLP (4 mg, 0.01 mmol) was added. The mixture was heated at 100 °C for 30 min, and the additions were repeated until 0.1 mmol total DLP had been added. The reaction was heated overnight, then cooled to rt and concentrated to afford an orange residue that was purified by flash column chromatography on silica (5 – 20% EtOAc in hexanes) to afford allylated product as a clear oil (24.7 mg, 61% yield). NMR spectra complicated due to presence of rotamers, contaminated with silicone grease impurity:

**<sup>1</sup>H NMR (600 MHz, CDCl<sub>3</sub>)** δ 7.00 (d, *J* = 7.4 Hz, 1H), 6.65 (d, *J* = 7.4 Hz, 1H), 6.62 (s, 1H), 5.82 – 5.74 (m, 1H), 5.08 – 4.98 (m, 2H), 4.59 – 4.47 (m, 1H), 4.29 (q, *J* = 7.1 Hz, 0.5H), 3.91 (t, *J* = 6.5 Hz, 2H), 3.10 – 2.98 (m, 2.5H), 2.31 (s, 3H), 2.17 (s, 3H), 2.12 – 2.04 (m, 1 H), 1.94 (dt, *J* = 7.5, 1.3 Hz, 0.5H), 1.85 (ddt, *J* = 10.5, 7.9, 3.8 Hz, 0.5H), 1.78 – 1.65 (m, 3H), 1.45 – 1.41 (m, 10H), 1.38 – 1.34 (m, 2H), 0.92 – 0.90 (m, 5H), 0.85 (s, 1H).

**<sup>13</sup>C NMR (151 MHz, CDCl<sub>3</sub>)** δ 157.16, 156.18, 136.71, 136.58, 130.39, 123.67, 120.69, 116.84, 112.06, 79.15, 68.66, 50.64, 46.49, 45.43, 43.13, 38.93, 34.16, 33.40, 33.02, 32.03, 28.57, 27.38, 27.26, 27.07, 24.44, 23.59, 22.83, 21.57, 15.99, 15.32, 14.28.

**IR (film)** 2925.48, 2856.06, 1716.74, 1568.81, 1507.10, 1435.74 cm<sup>-1</sup>.

**HRMS (ES+)** Exact mass calcd for  $C_{25}H_{41}NO_3Na$   $[M+Na]^+$ , 426.2979. Found 426.2993.



***tert*-butyl (2-deutero-7-(2,5-dimethylphenoxy)-4,4-dimethylheptyl)carbamate.** Prepared

by a modified procedure from Boivin<sup>10</sup> as per our C–H xanthylation work.<sup>3</sup> To a solution of xanthate (48 mg, 0.1 mmol) in DCE/ $MeOH-d_4$  (0.4 mL/0.16 mL) in a 1-dram vial was added  $BEt_3$  (0.5 mL, 0.5 mmol, 1M in hexanes). The solution was sparged with  $O_2$  for 5 min, and then left under a balloon of  $O_2$  for 48 hr. The mixture was passed over a short silica plug, eluted with EtOAc, and then concentrated *in vacuo*. The residue was purified by flash column chromatography on silica (10% EtOAc in hexanes) to afford the reduced product as a colorless amorphous solid (24.6 mg, 67% yield). GC-MS analysis according to the literature revealed 61% D incorporation. NMR spectra complicated due to presence of rotamers:

**$^1H$  NMR (600 MHz,  $CDCl_3$ )** 7.00 (d,  $J = 7.4$  Hz, 1H), 6.65 (d,  $J = 7.5$  Hz, 1H), 6.62 (s, 1H), 4.56 – 4.49 (m, 1H), 3.91 (t,  $J = 6.5$  Hz, 2H), 3.09 – 2.99 (m, 1.5H), 2.31 (s, 3H), 2.16 (s, 3H), 1.78 – 1.72 (m, 2H), 1.51 – 1.41 (m, 9H), 1.38 – 1.29 (m, 3.5H), 1.17 – 1.12 (m, 1.5H), 0.93 – 0.86 (m, 7H).

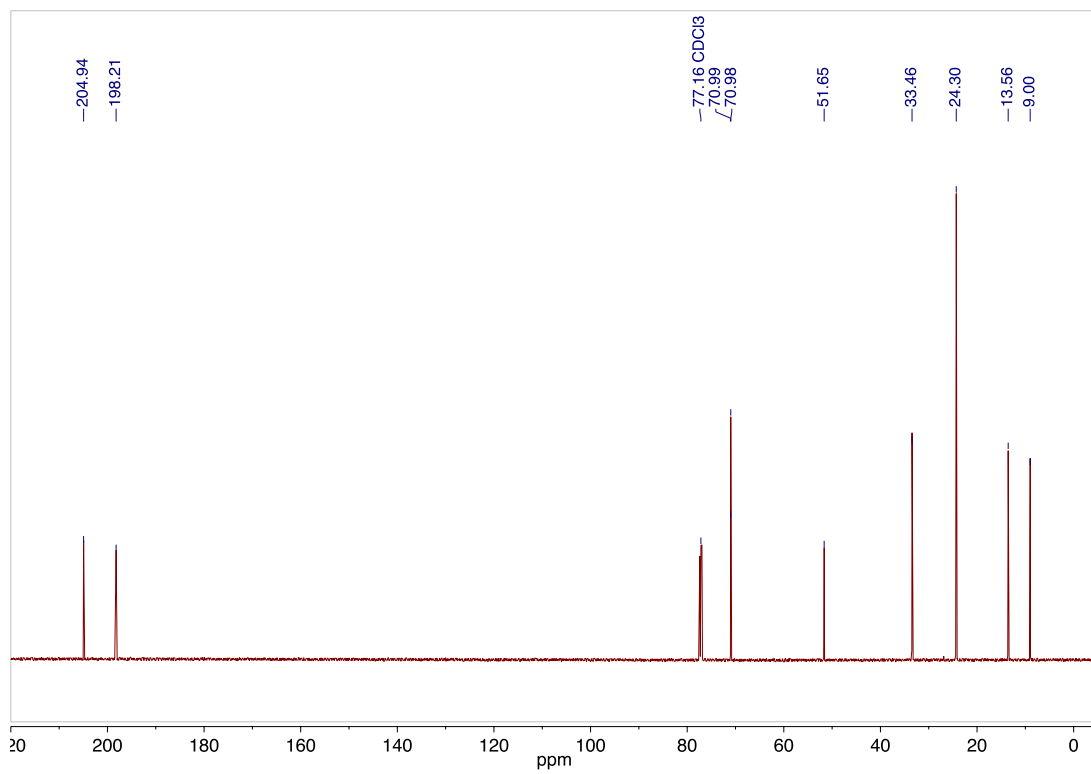
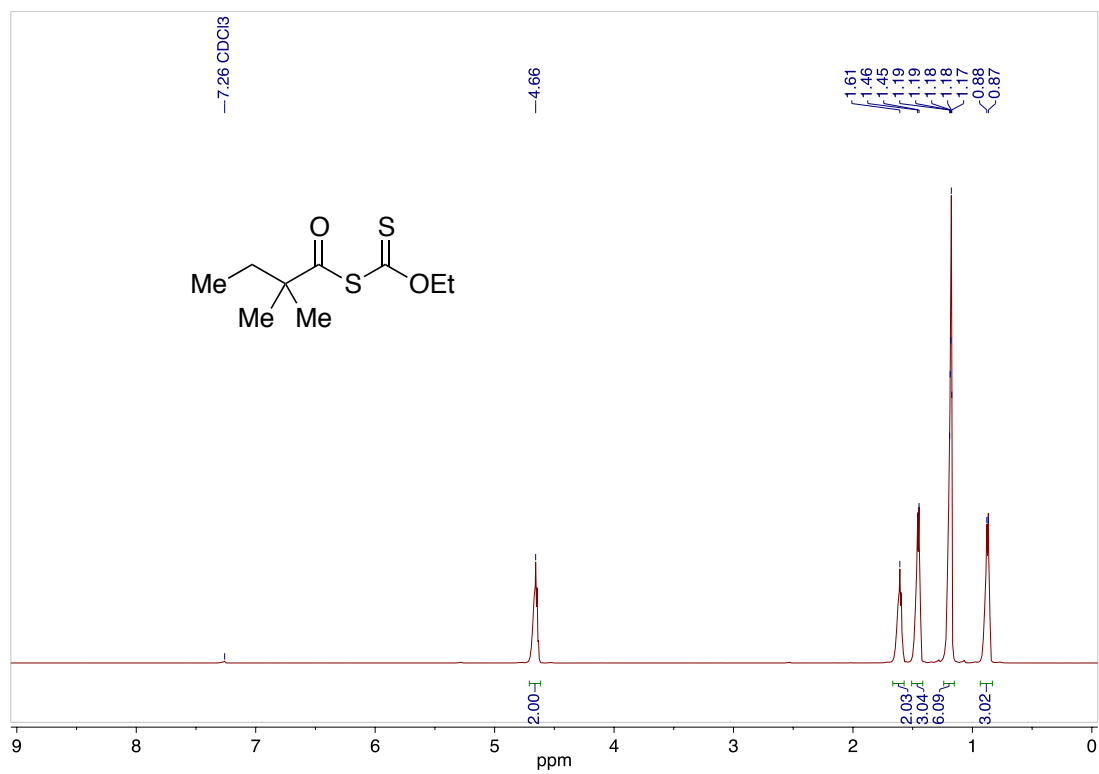
**$^{13}C$  NMR (151 MHz,  $CDCl_3$ )**  $\delta$  157.17, 156.26, 136.58, 130.38, 123.67, 120.68, 112.06, 79.09, 68.69, 45.06, 43.58, 38.99, 35.67, 33.37, 28.58, 27.22, 27.35, 27.18, 26.80, 24.47, 21.57, 15.98, 11.17.

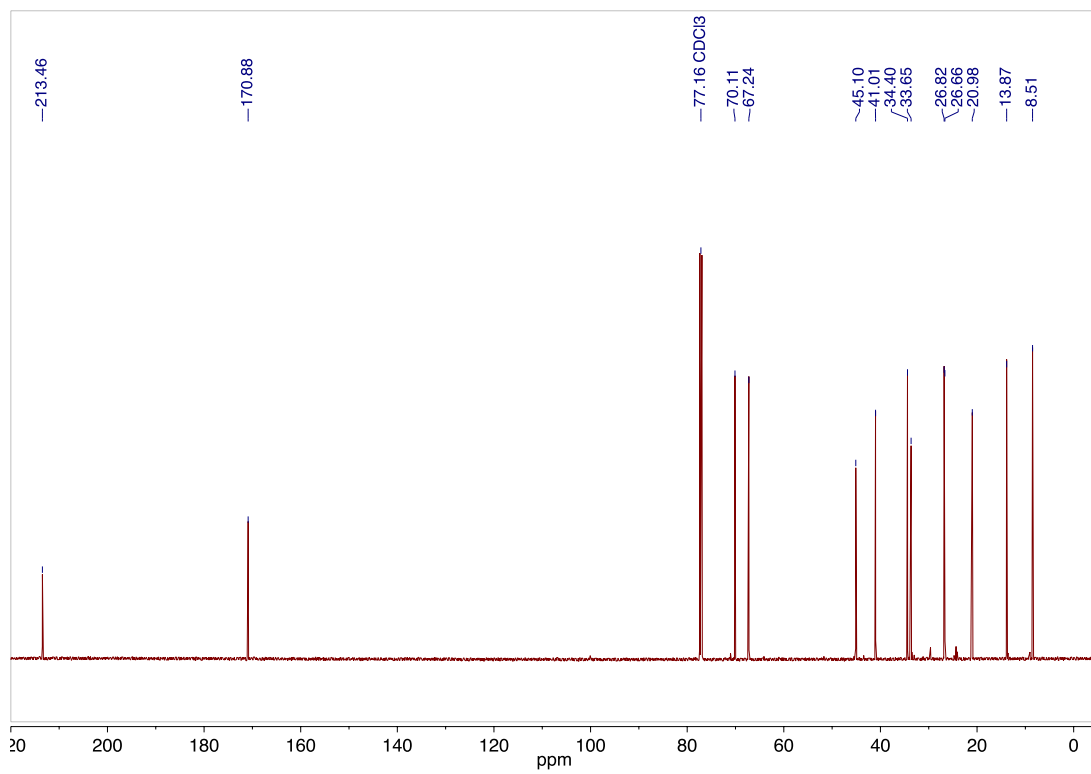
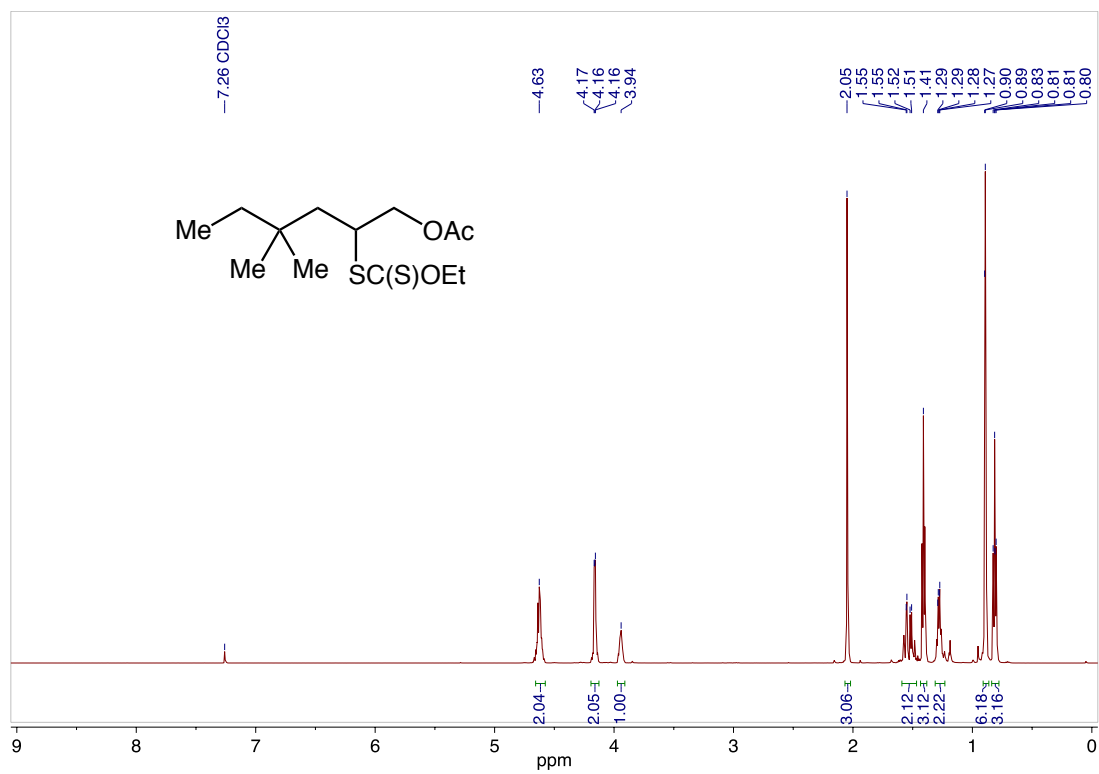
**IR (film)** 2956.34, 2883.06, 2444.33, 1716.45, 1652.70, 1540.85, 1488.78  $cm^{-1}$ .

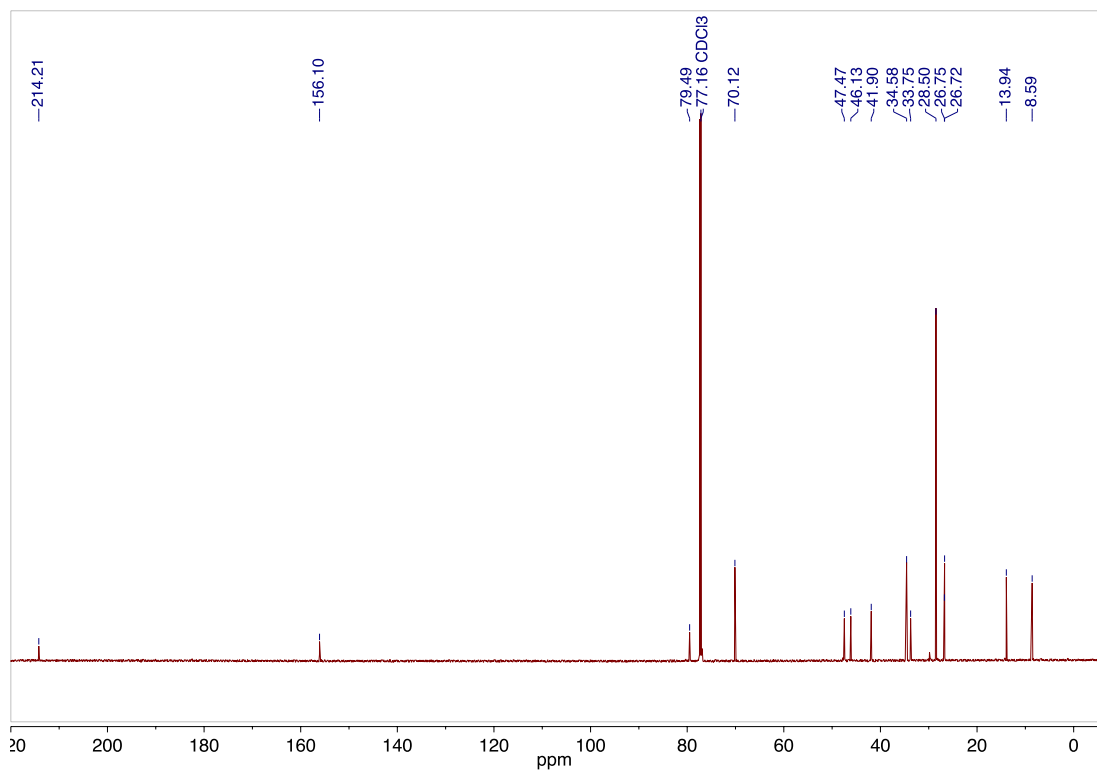
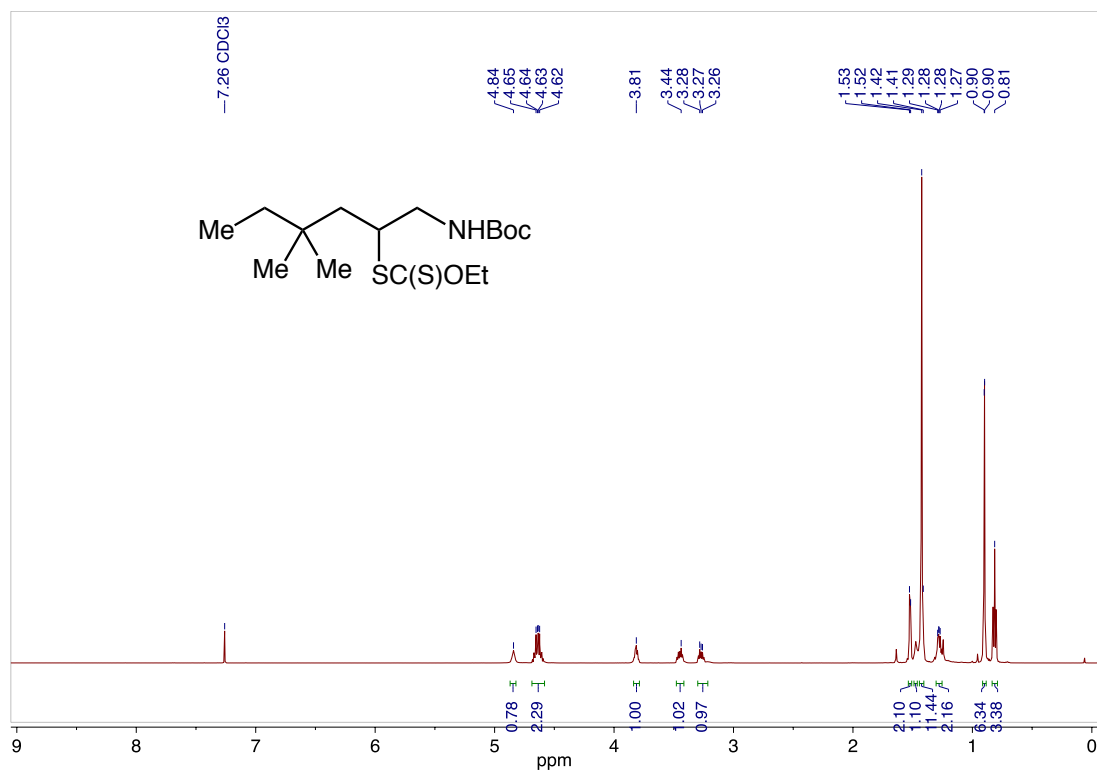
**MS (ES+)** Exact mass calcd for  $C_{22}H_{36}DNO_3$   $M^+$ , 364.28. Found 364.30.

## REFERENCES

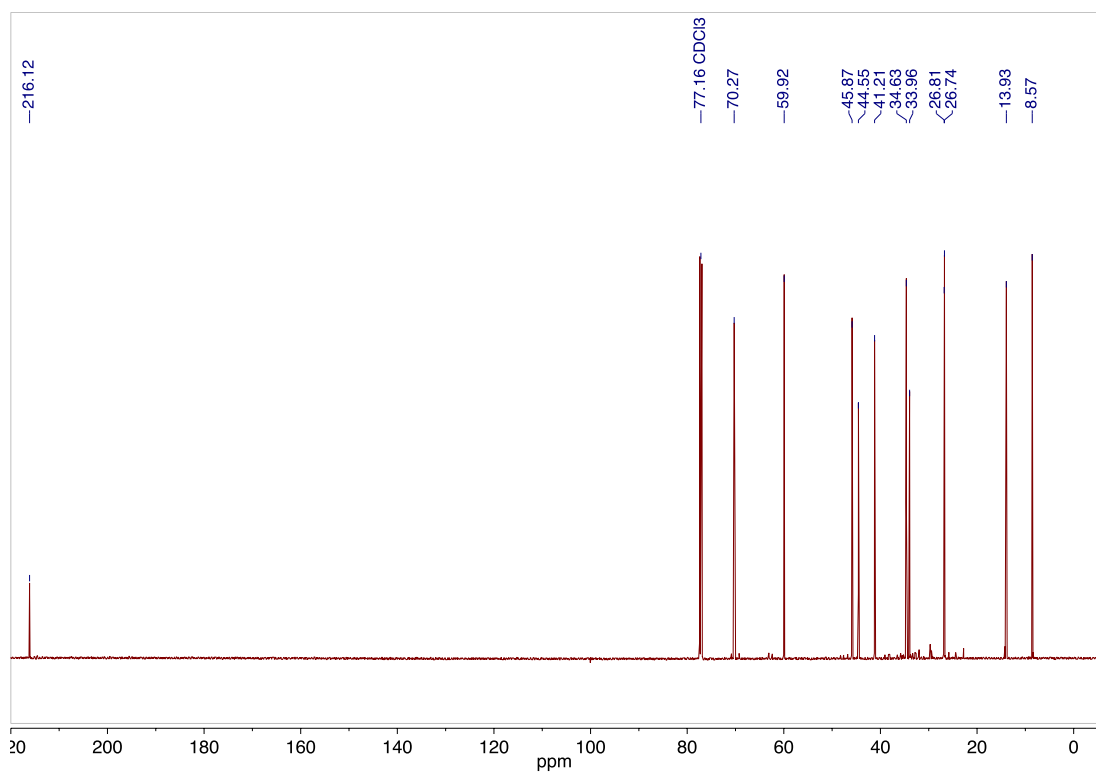
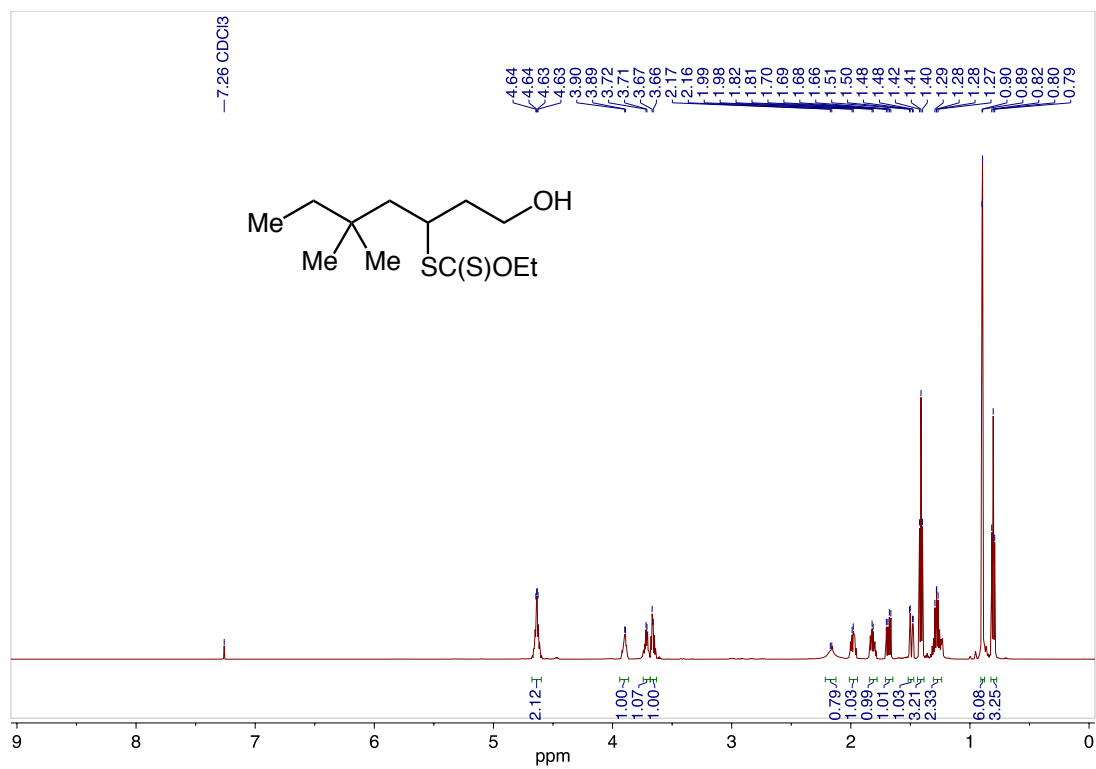
- (1) Renslo, A. R.; Atuegbu, A.; Herradura, P.; Jaishankar, P.; Ji, M.; Leach, K. L.; Huband, M. D.; Dermeyer, M. R.; Wu, L.; Vara Prasad, J. V. N.; *et al. Bioorg. Med. Chem. Lett.* **2007**, *17*, 5036–5040.
- (2) Ihre, H.; Hult, A.; Söderlind, E. *J. Am. Chem. Soc.* **1996**, *118*, 6388–6395.
- (3) Czaplyski, W. L.; Na, C. G.; Alexanian, E. J. *J. Am. Chem. Soc.* **2016**, *138*, 13854–13857.
- (4) Hutt, O. E.; Doan, T. L.; Georg, G. I. *Org. Lett.* **2013**, *15*, 1602–1605.
- (5) Walborsky, H. M.; Topolski, M.; Hamdouchi, C.; Pankowski, J. *J. Org. Chem.* **1992**, *57*, 6188–6191.
- (6) Barnes, D.; Chopra, R.; Cohen, S. L.; Fu, J.; Kato, M.; Lu, P.; Seepersaud, M.; Zhang, W. WO 2011/131709 A1, April 5, 2013.
- (7) Boto, A.; Hernández, R.; de León, Y.; Murguía, J. R.; Rodriguez-Afonso, A. *Eur. J. Org. Chem.* **2005**, *2005*, 673–682.
- (8) Hu, F.; Shao, X.; Zhu, D.; Lu, L.; Shen, Q. *Angew. Chem. Int. Ed.* **2014**, *53*, 6105–6109.
- (9) Avent, A. G.; Hanson, J. R.; De Oliveira, B. H. *Phytochemistry* **1990**, *29*, 2712–2715.
- (10) Allais, F.; Boivin, J.; Nguyen, V. T. *Beilstein J. Org. Chem.* **2007**, *3*, 46.

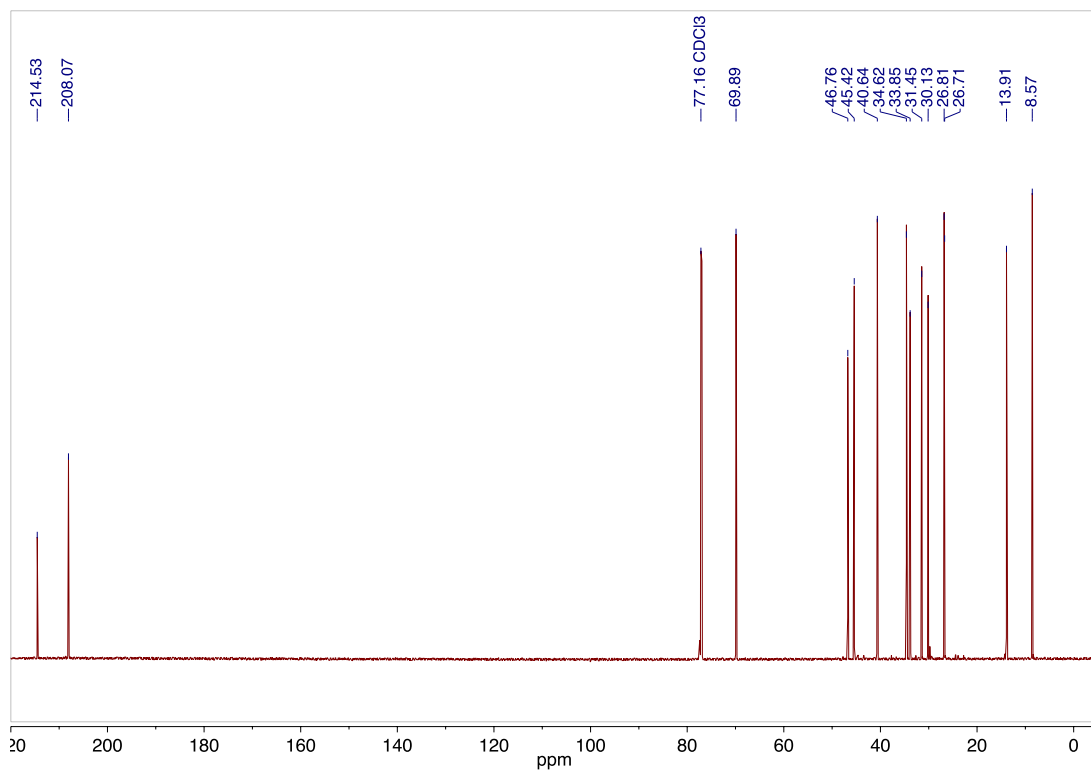
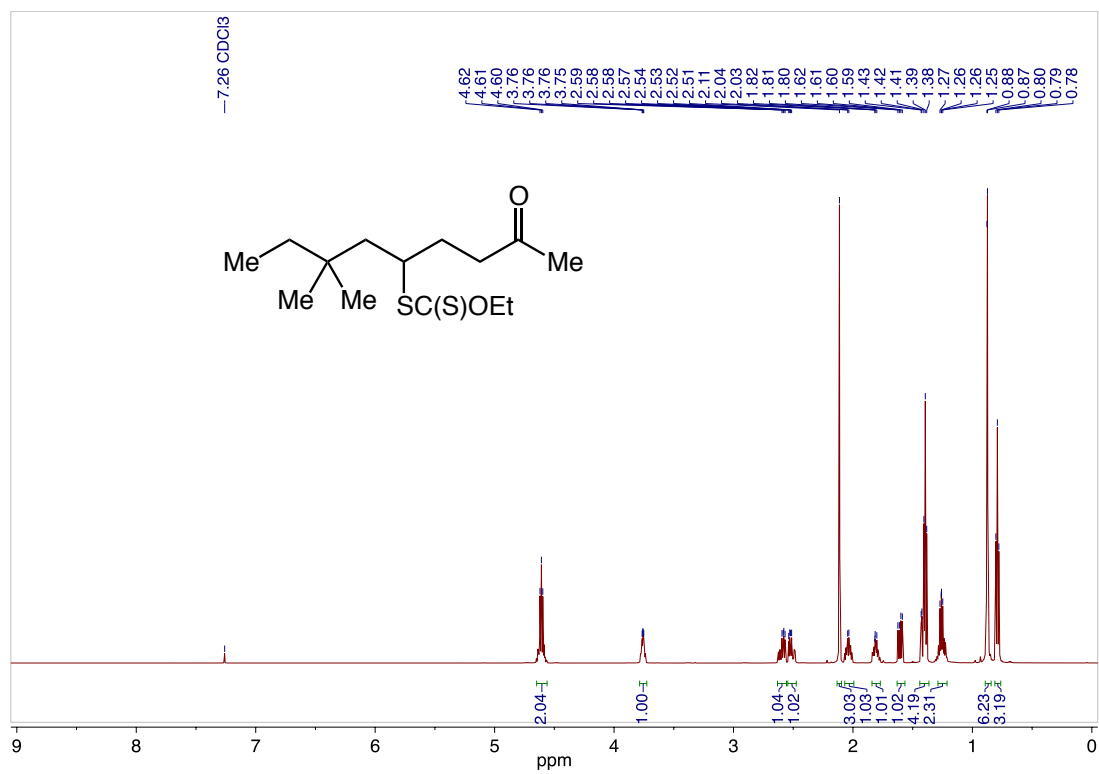


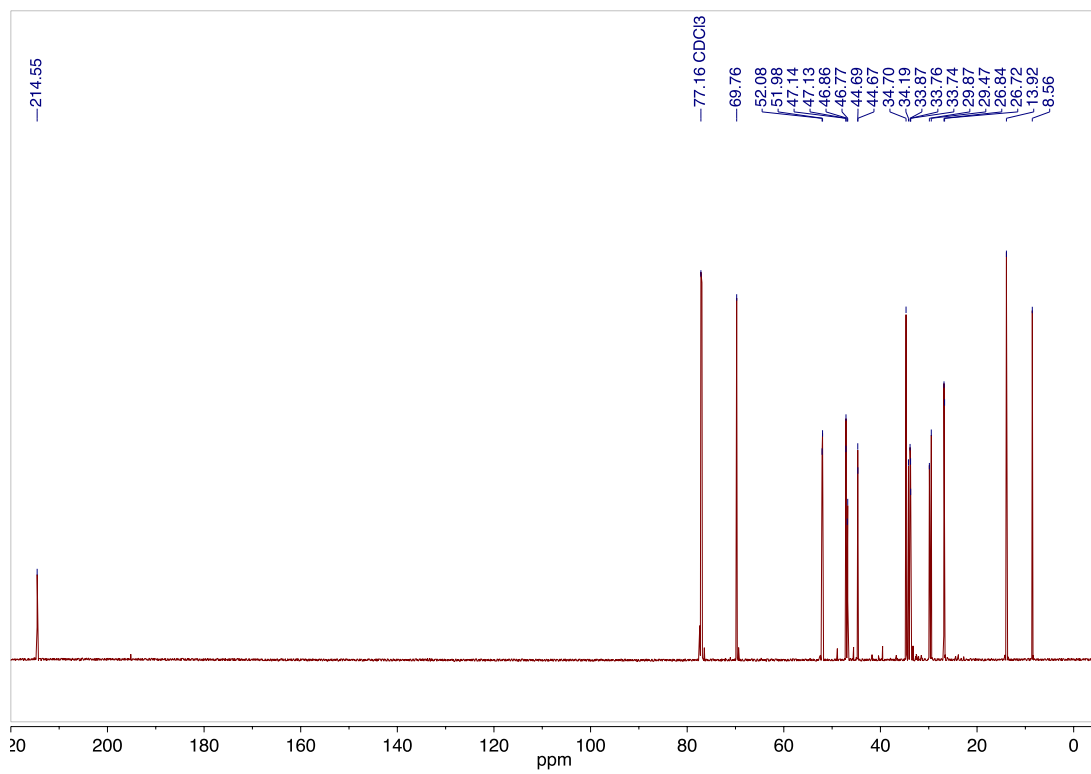
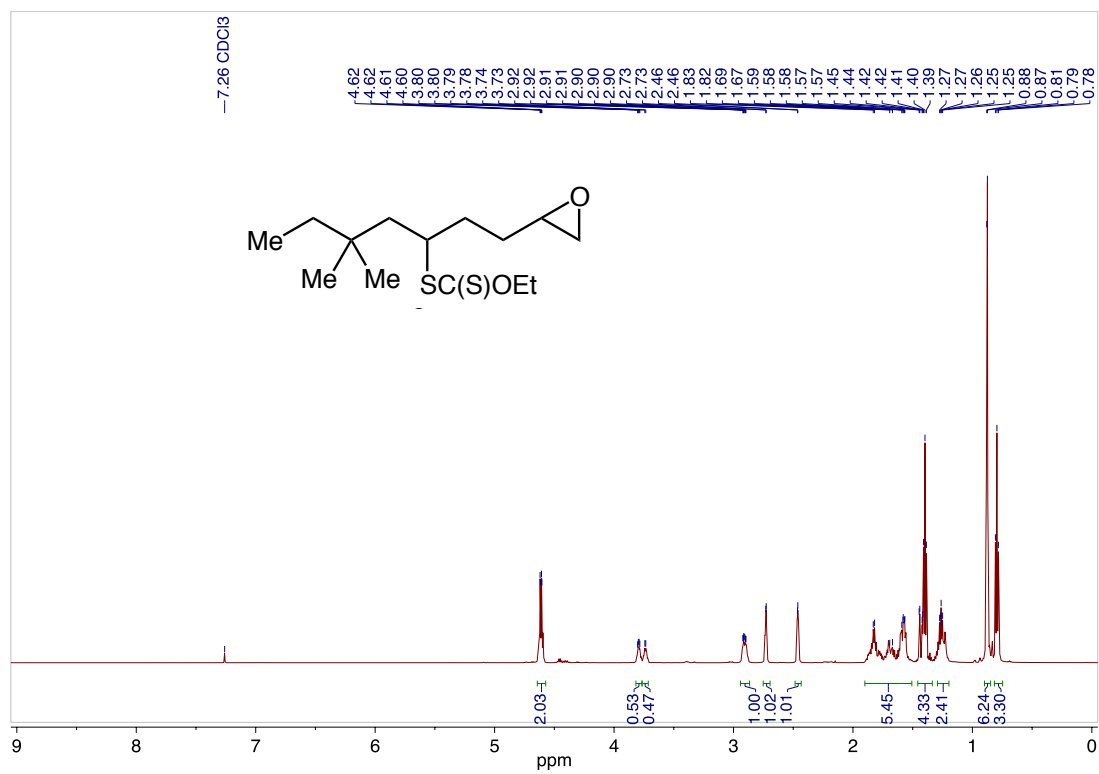


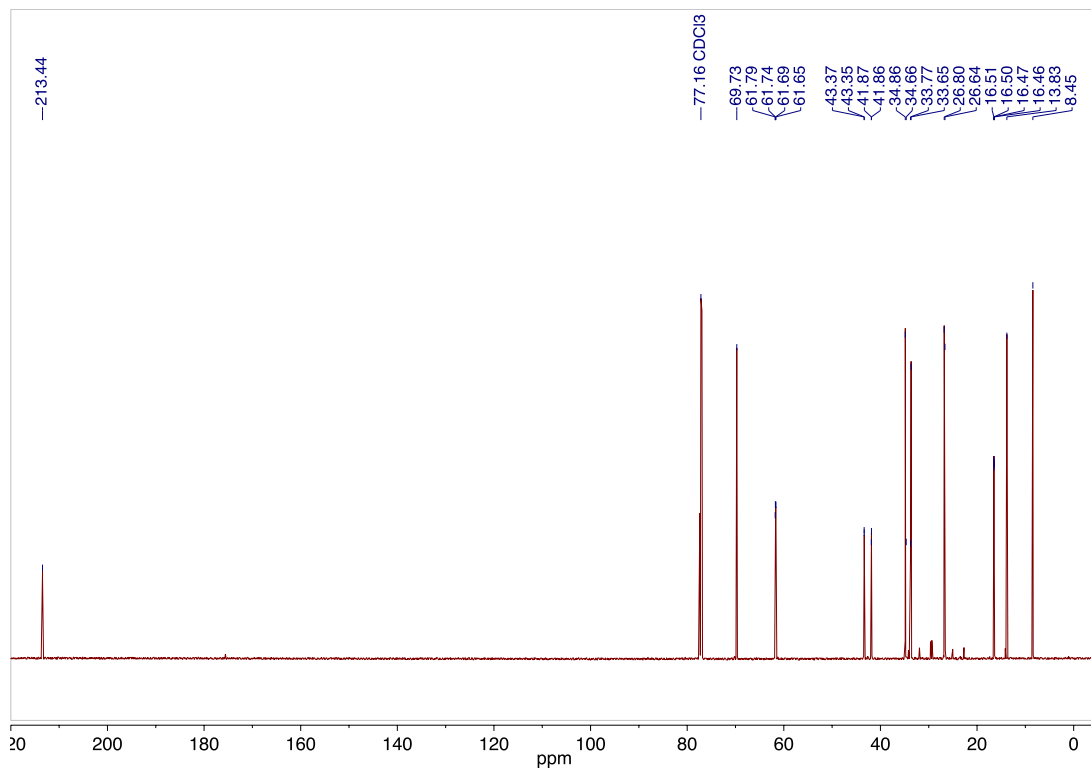
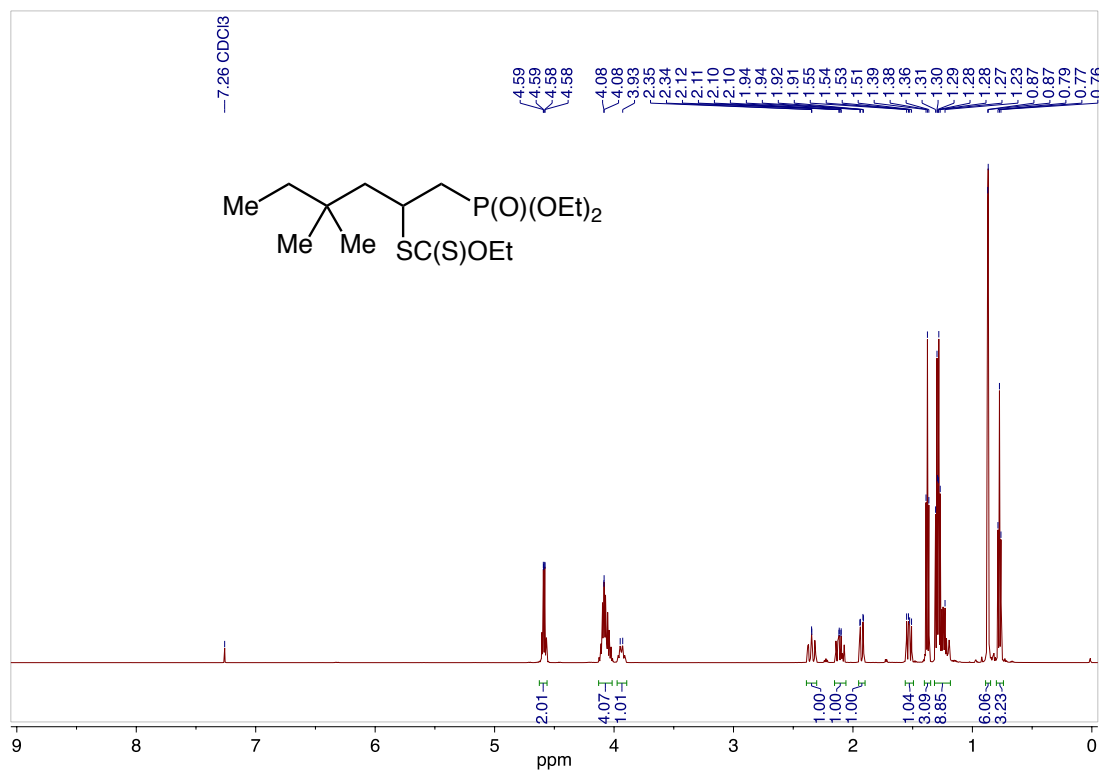


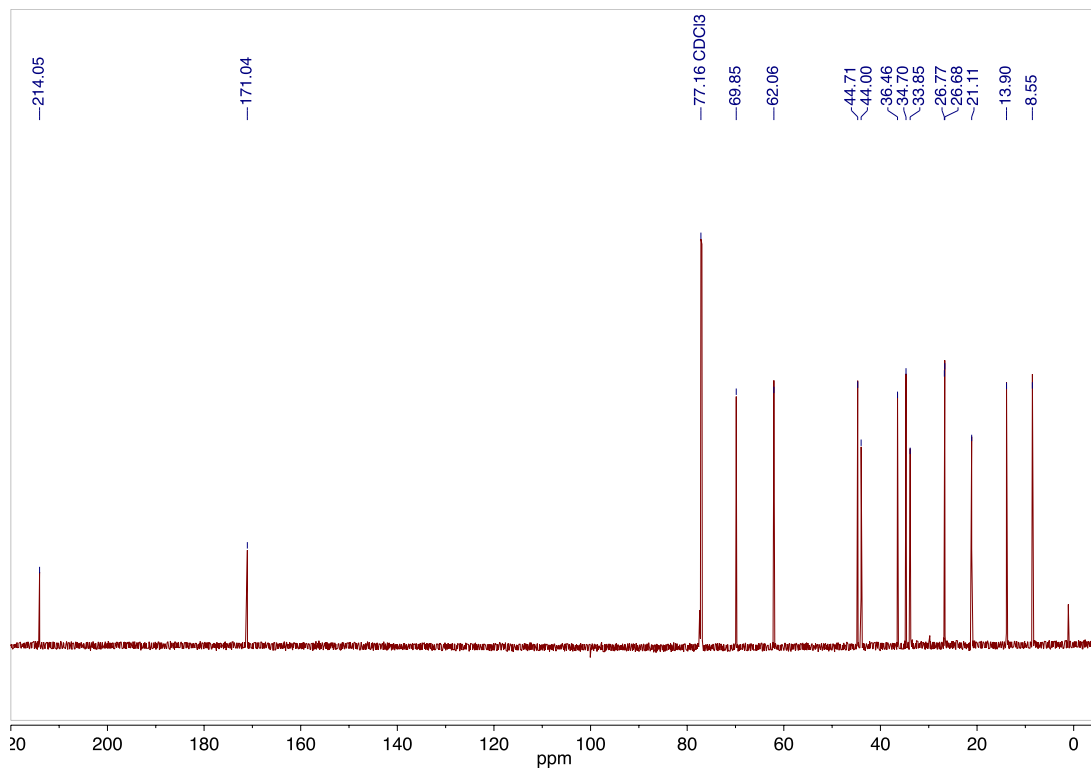
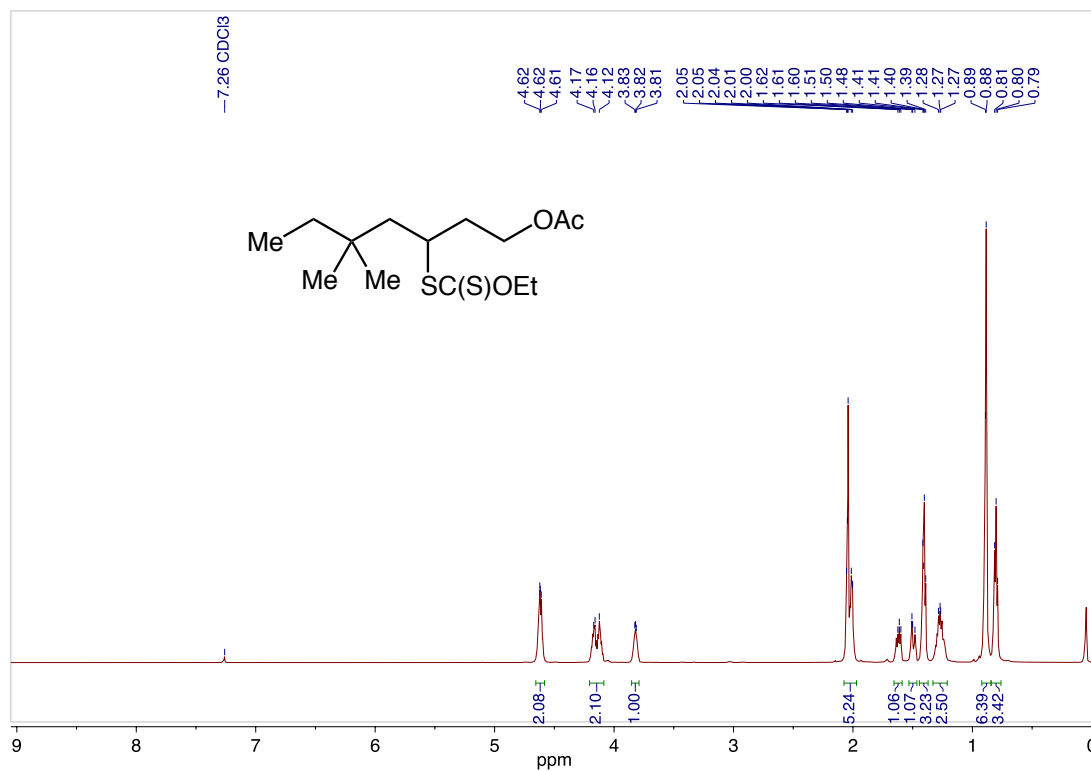


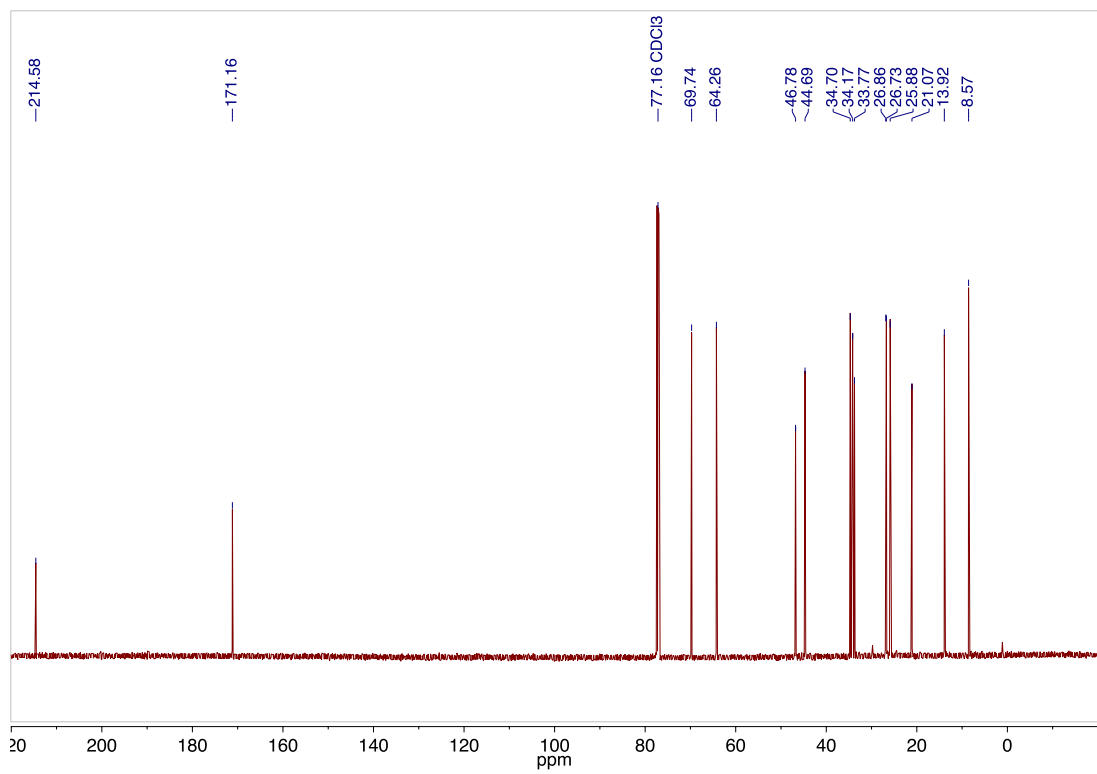
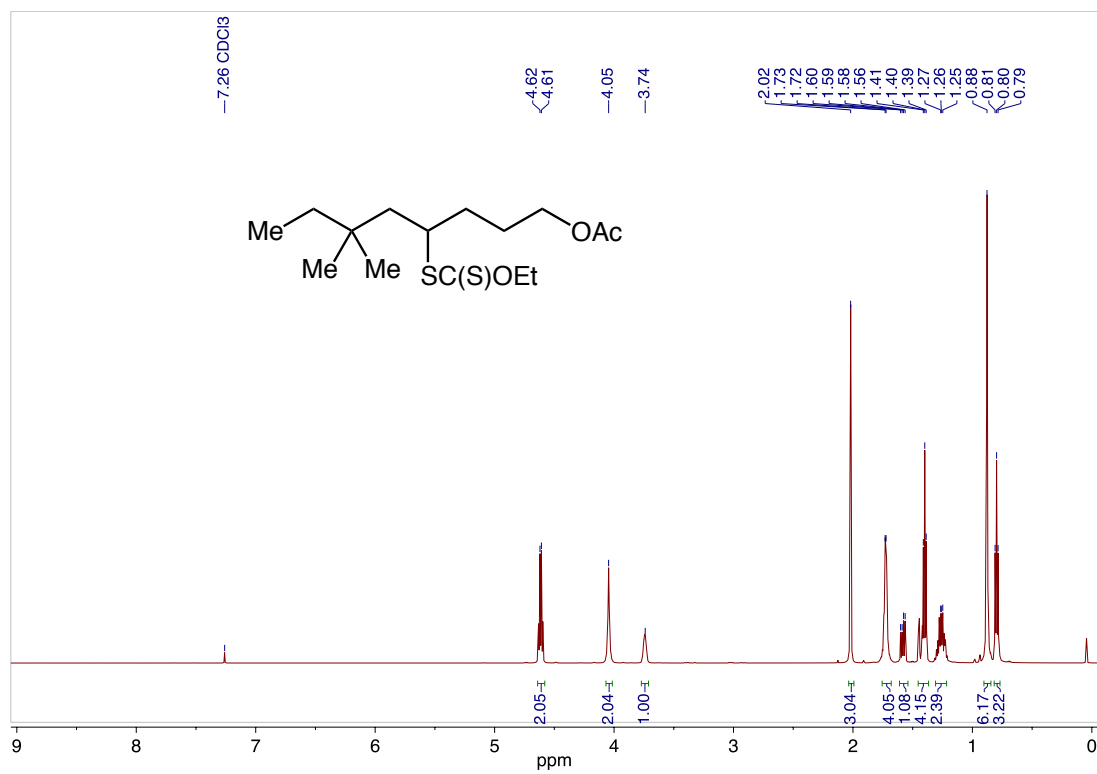


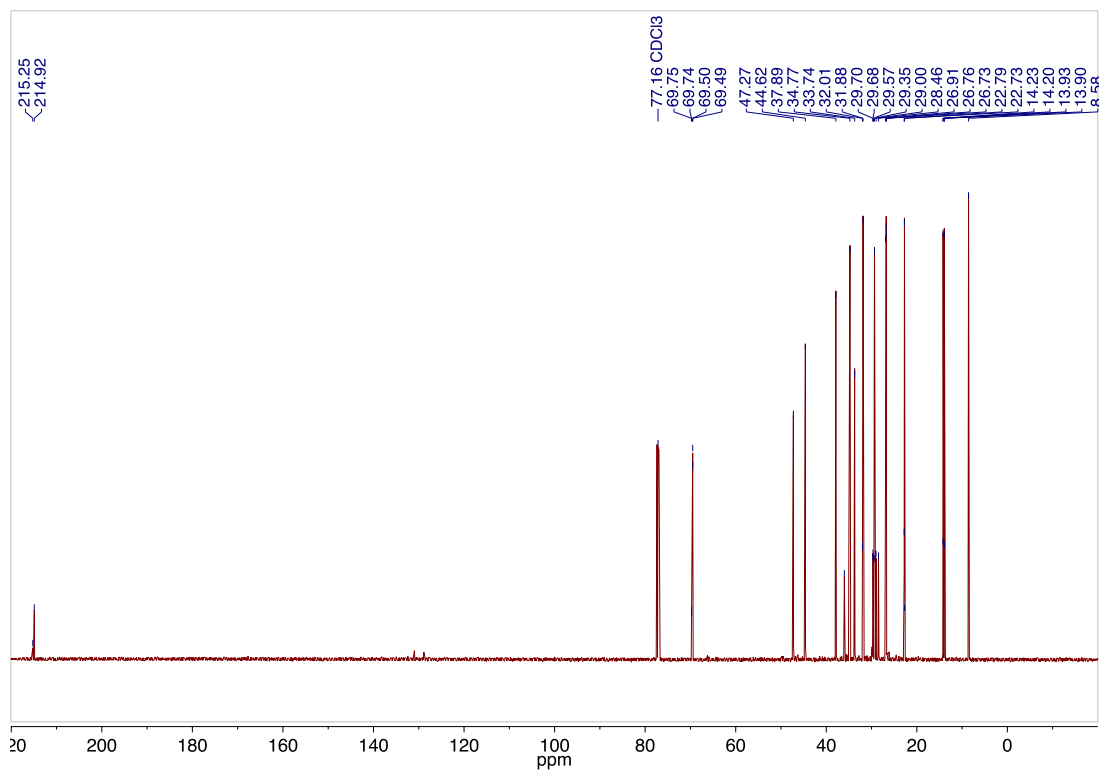
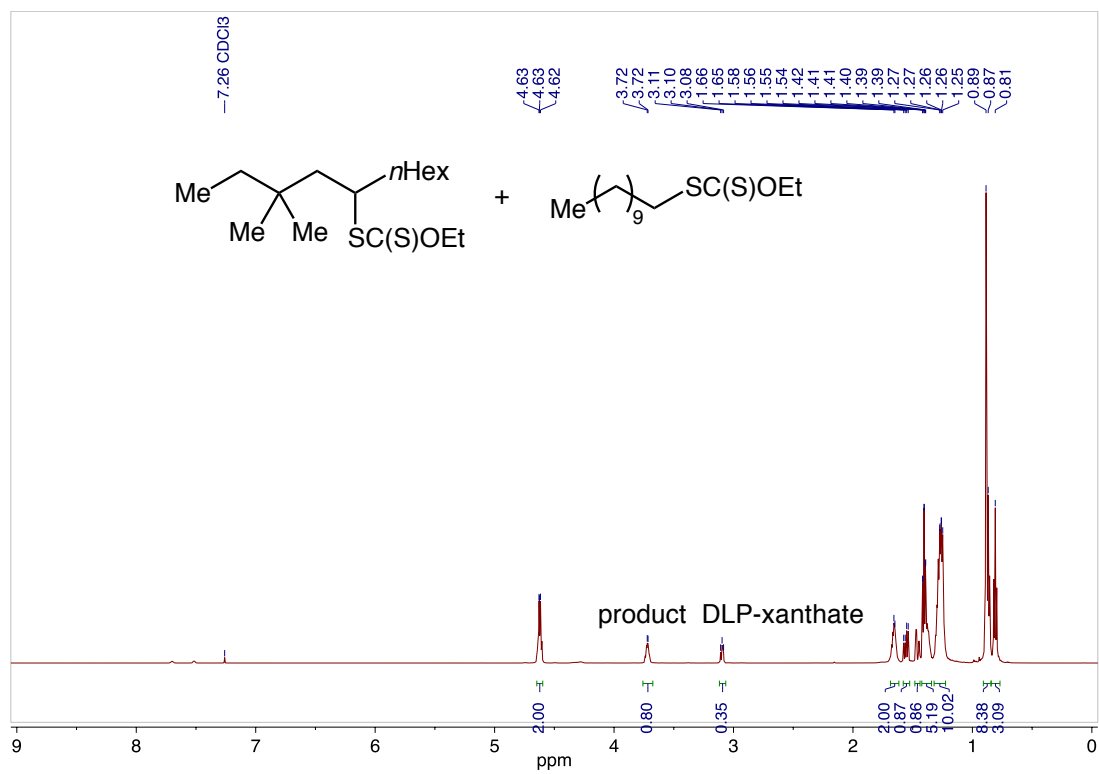


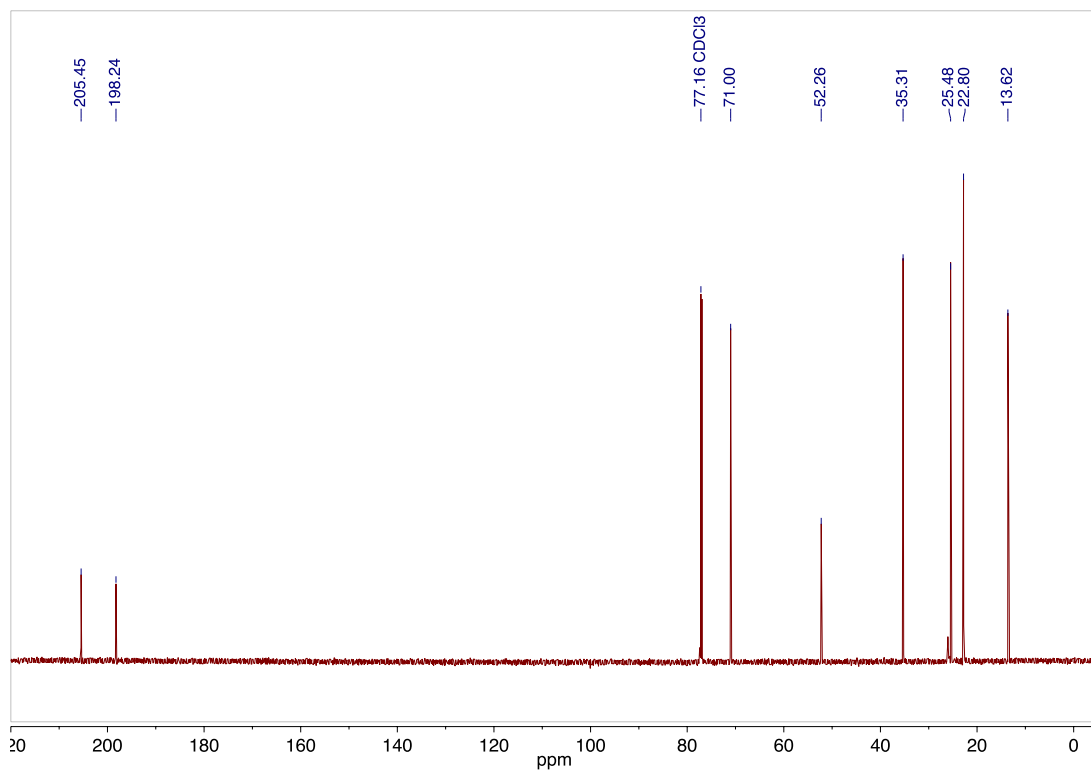
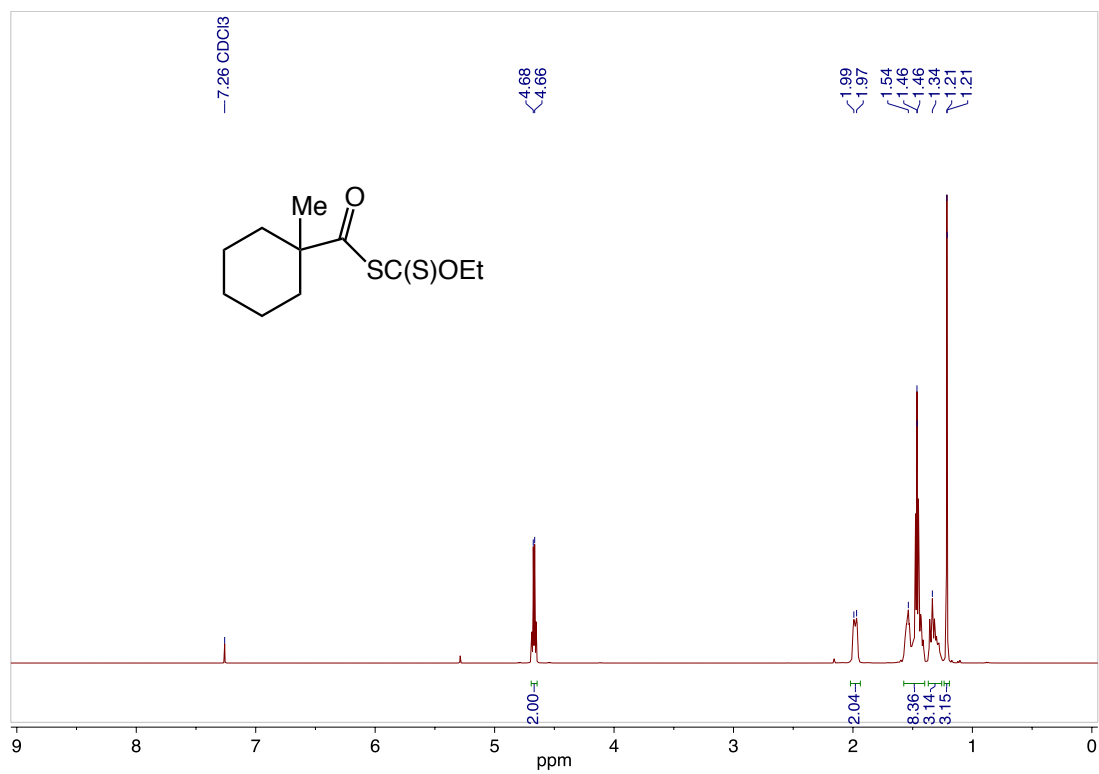




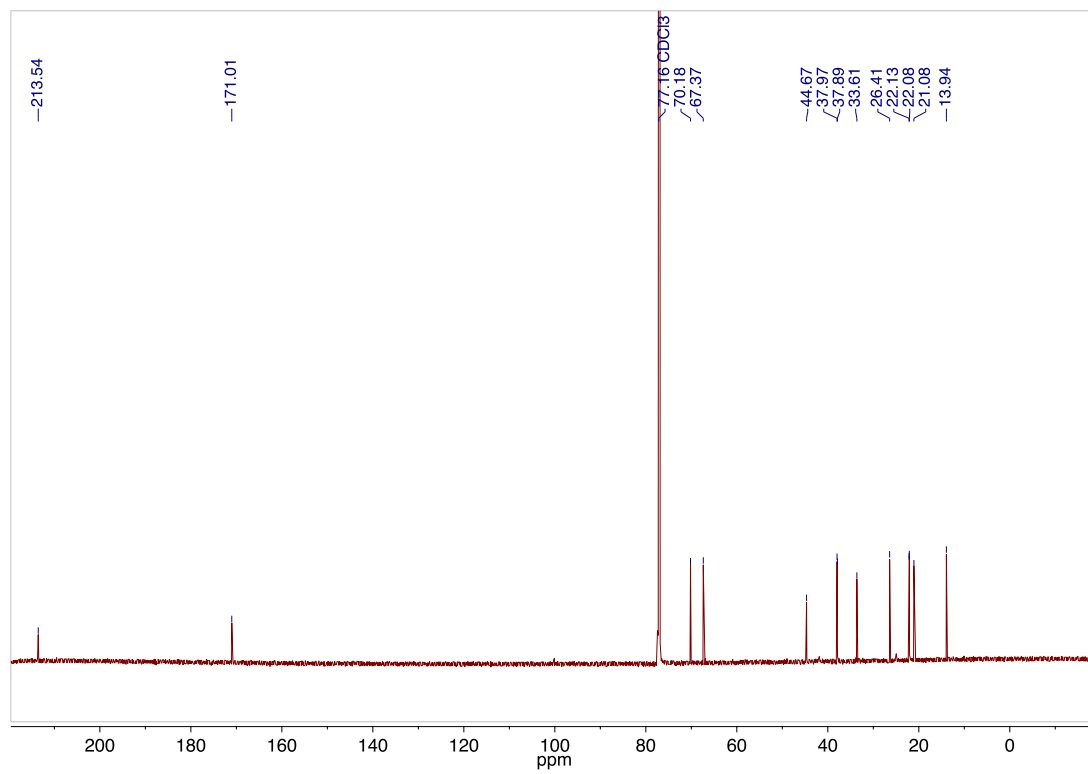
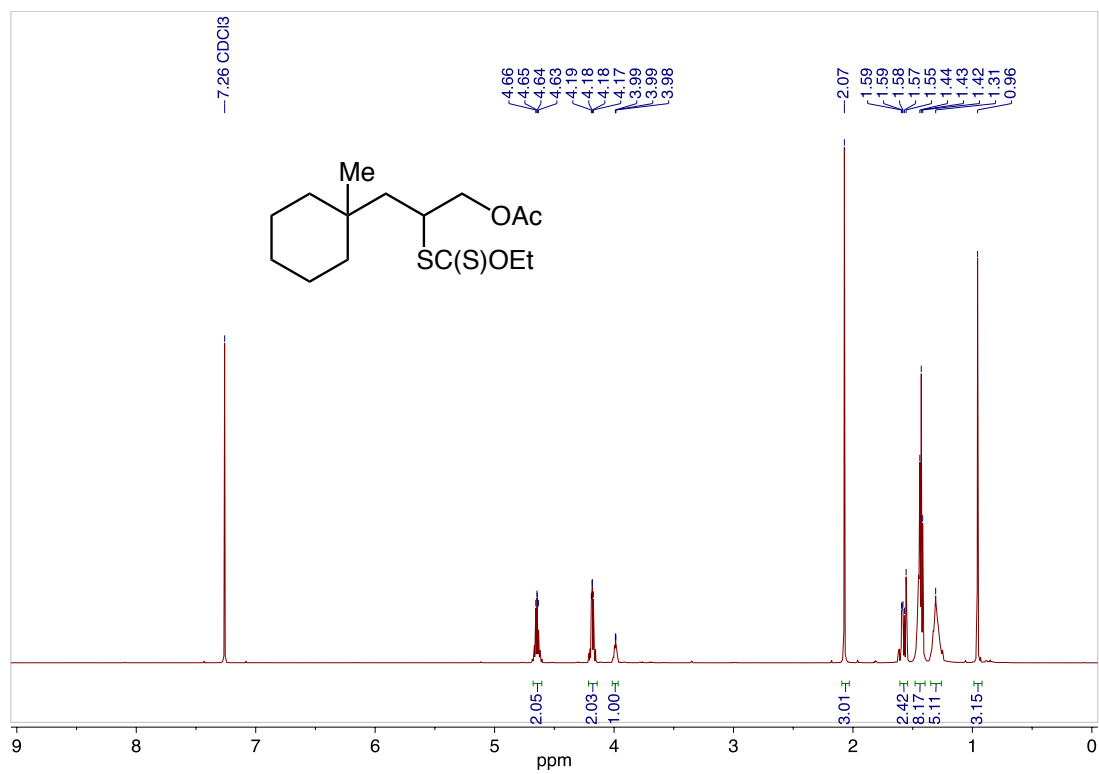


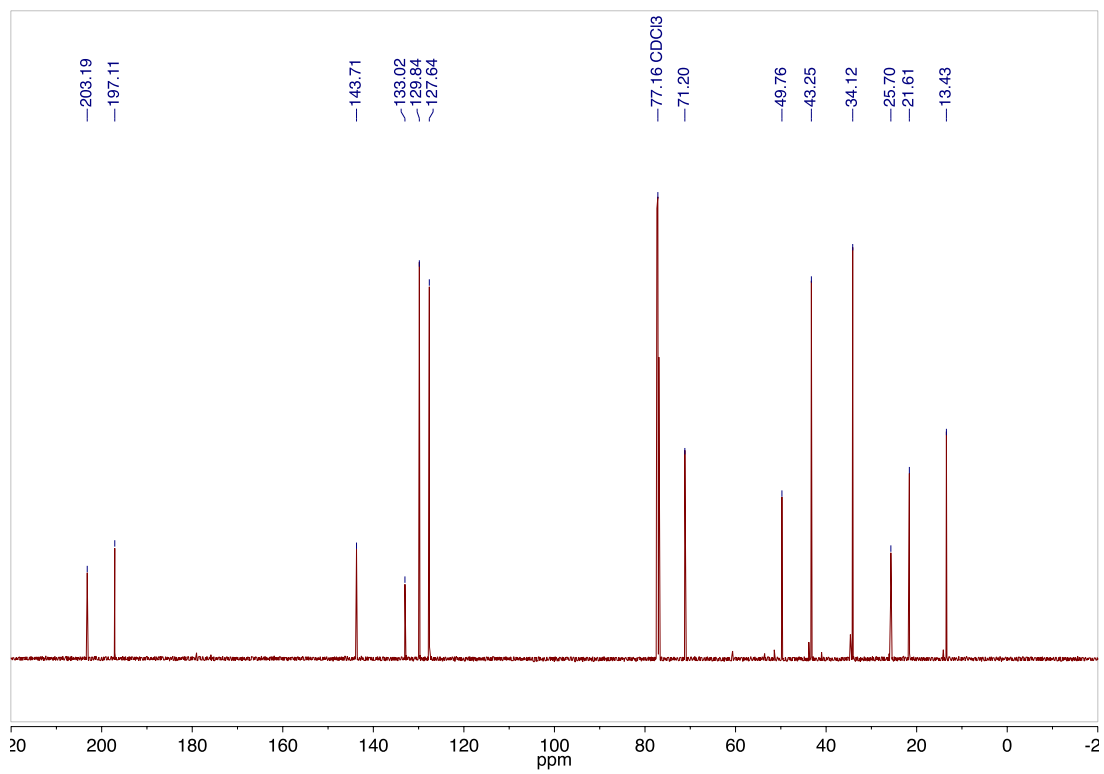
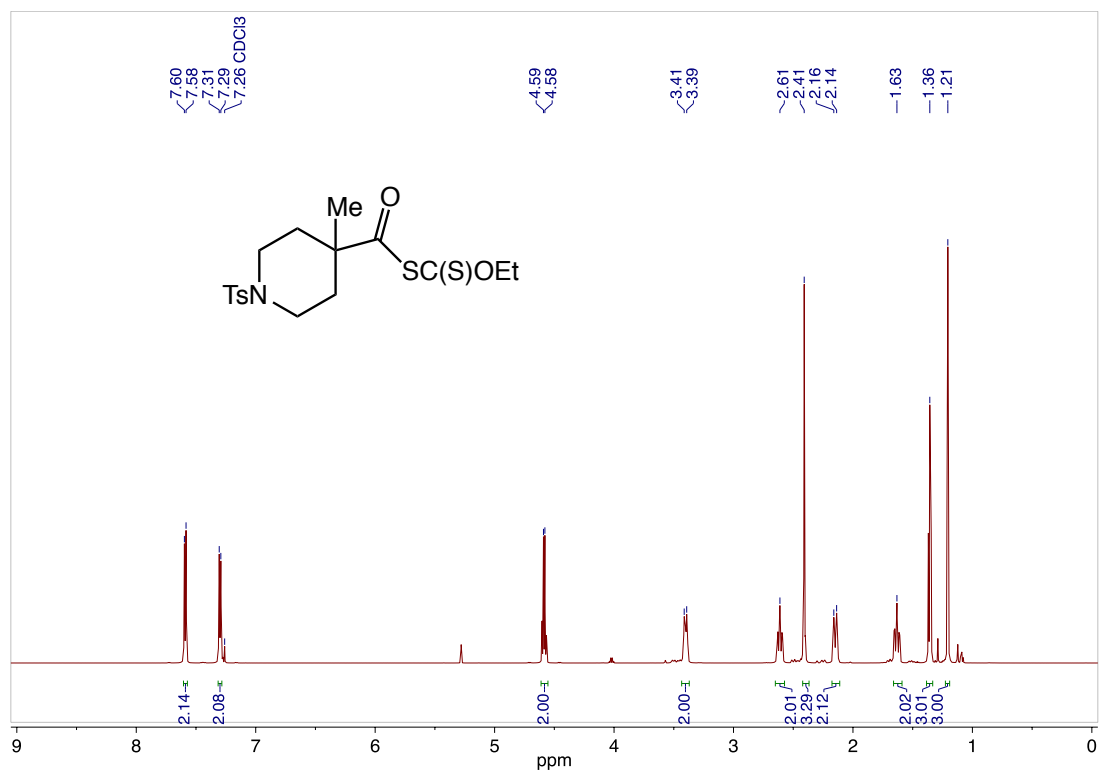


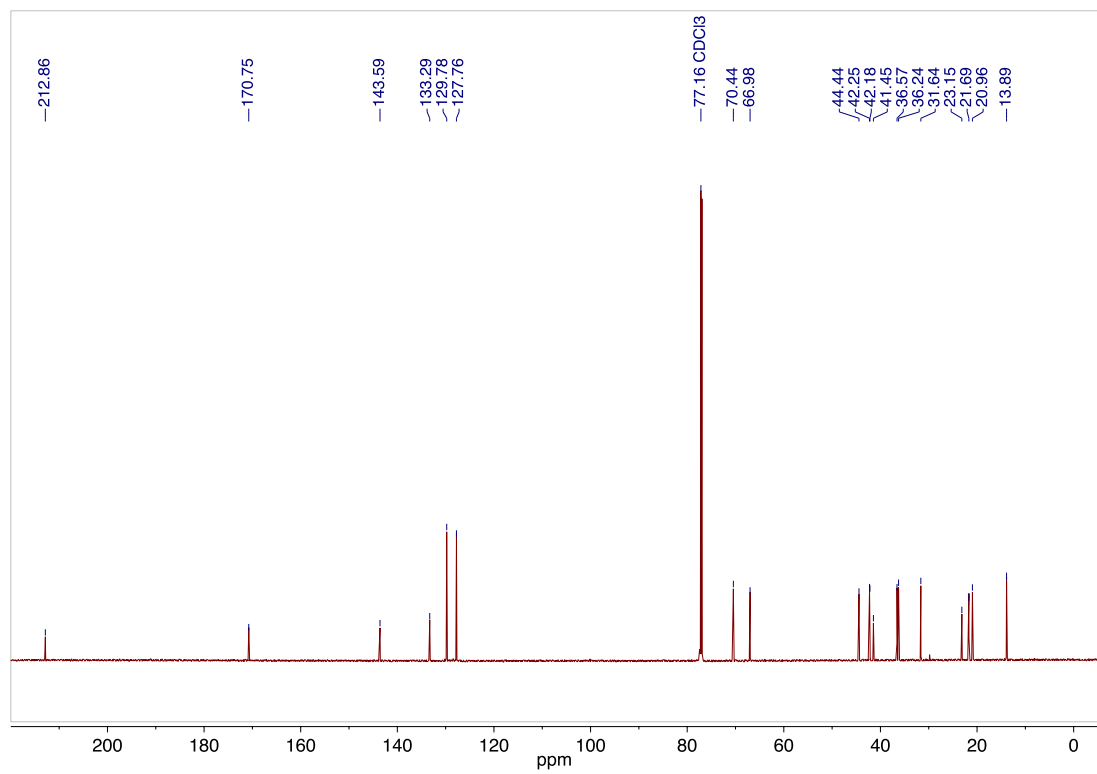
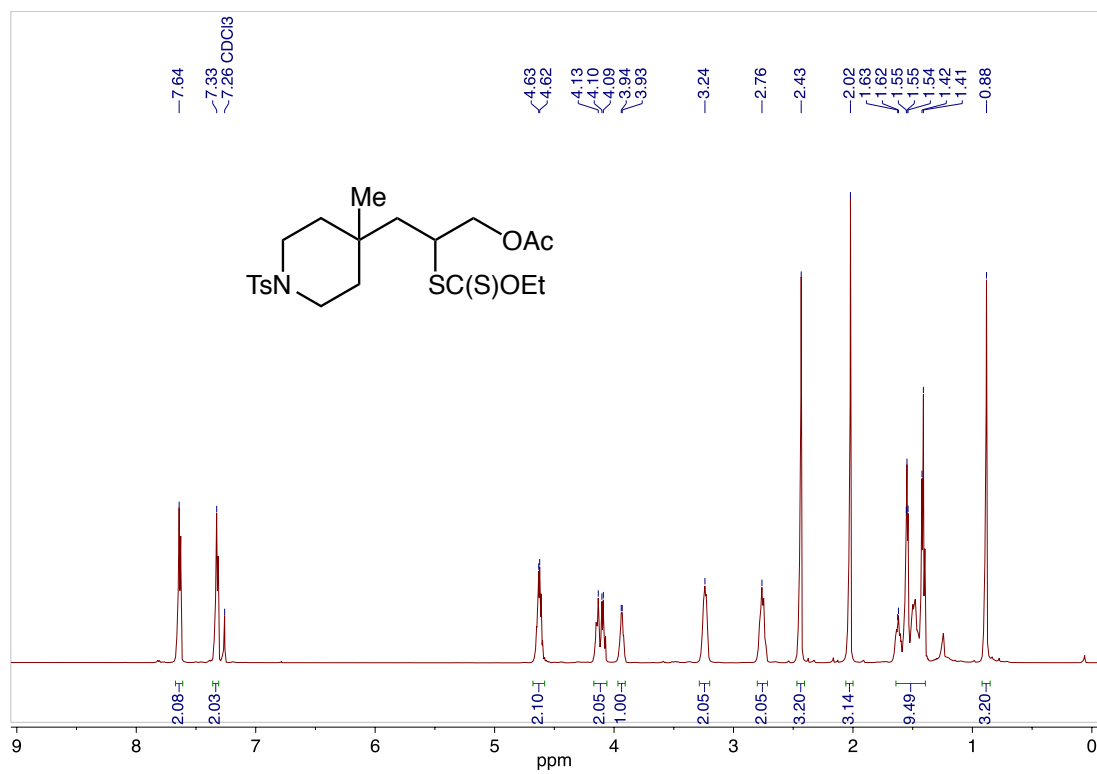


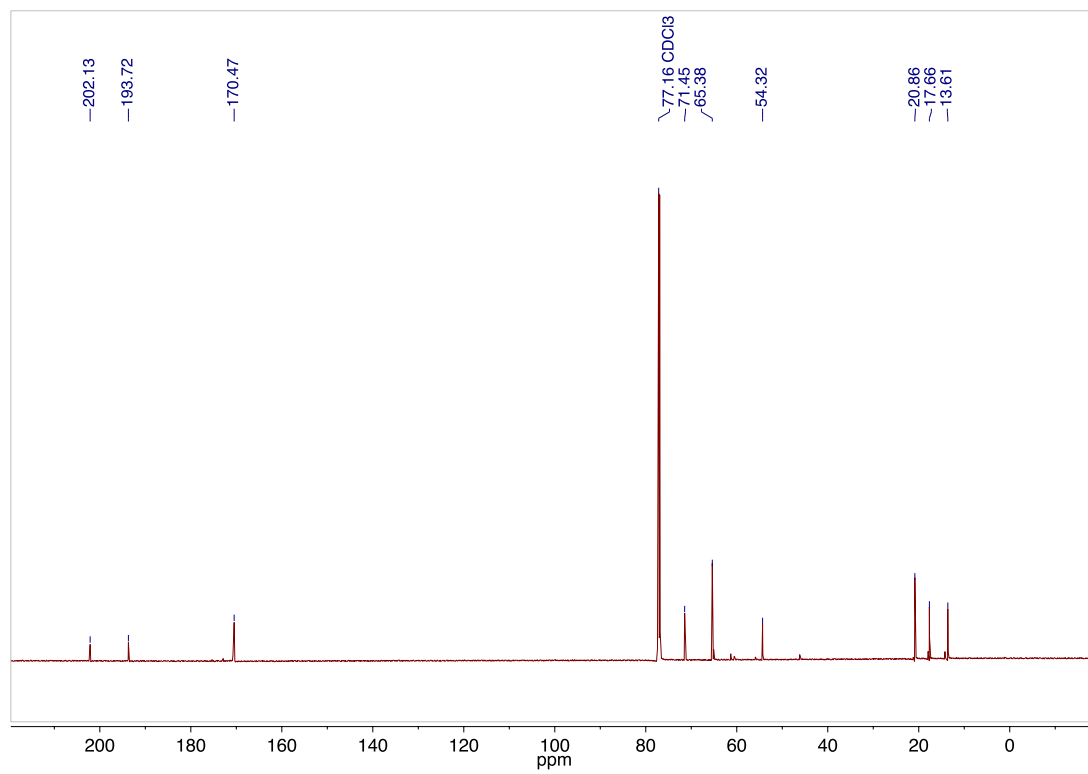
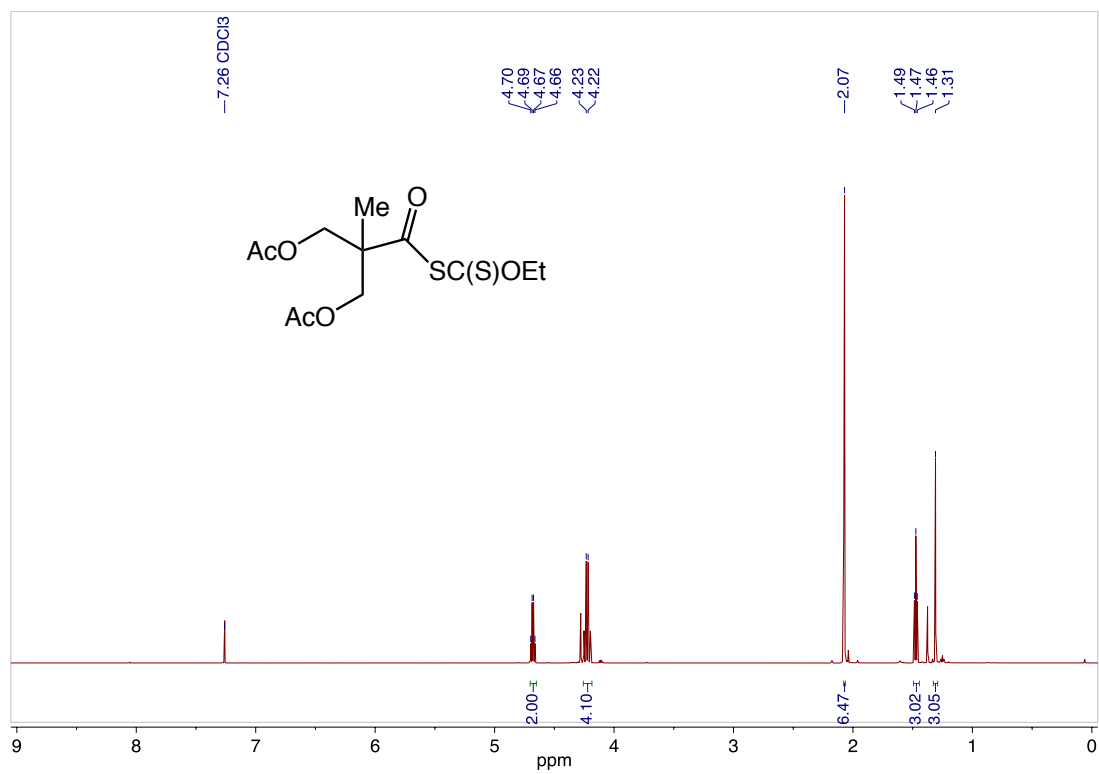


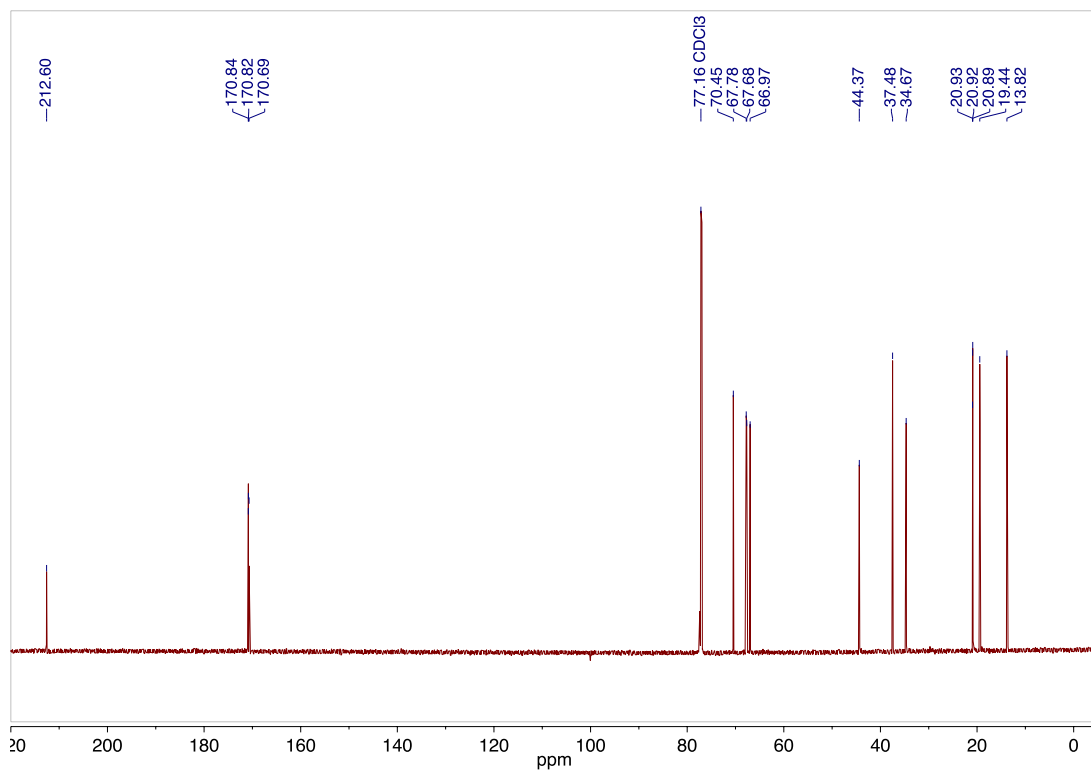
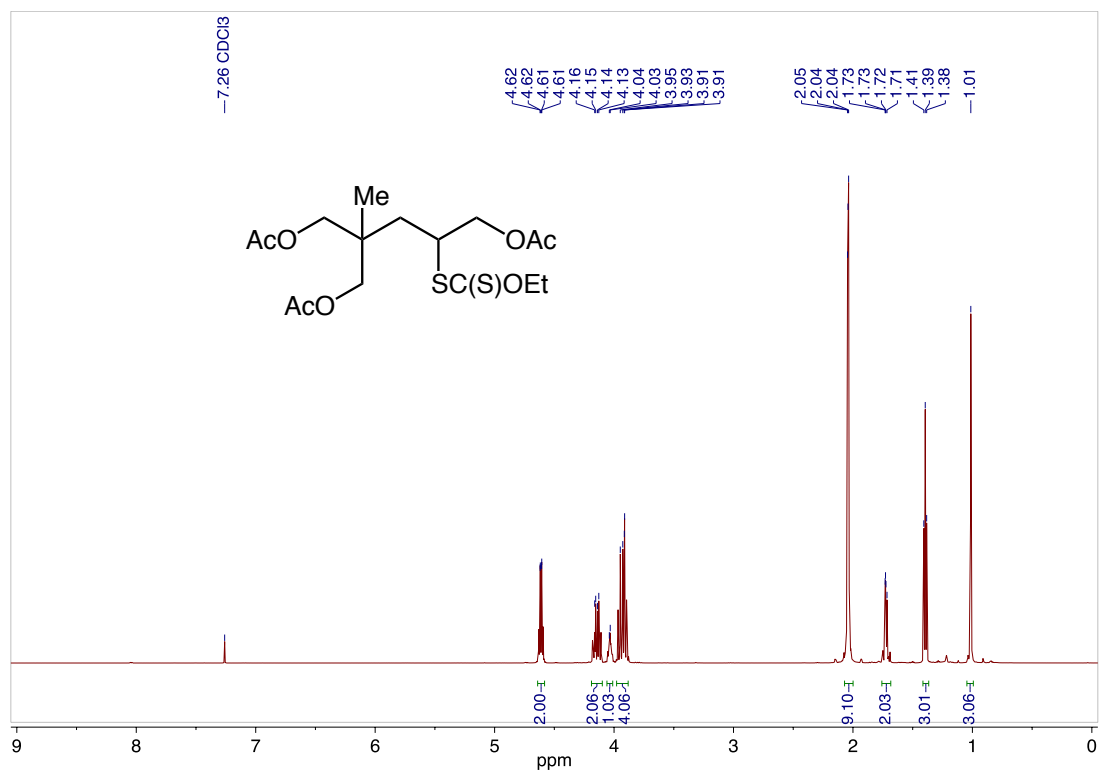


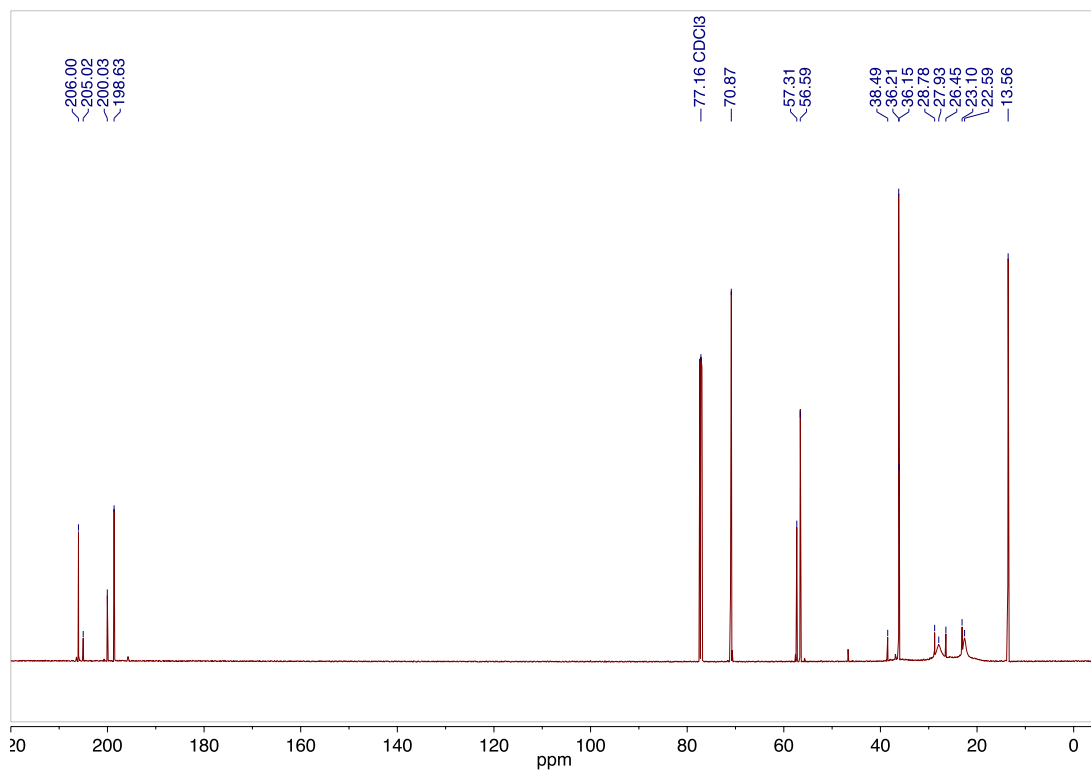
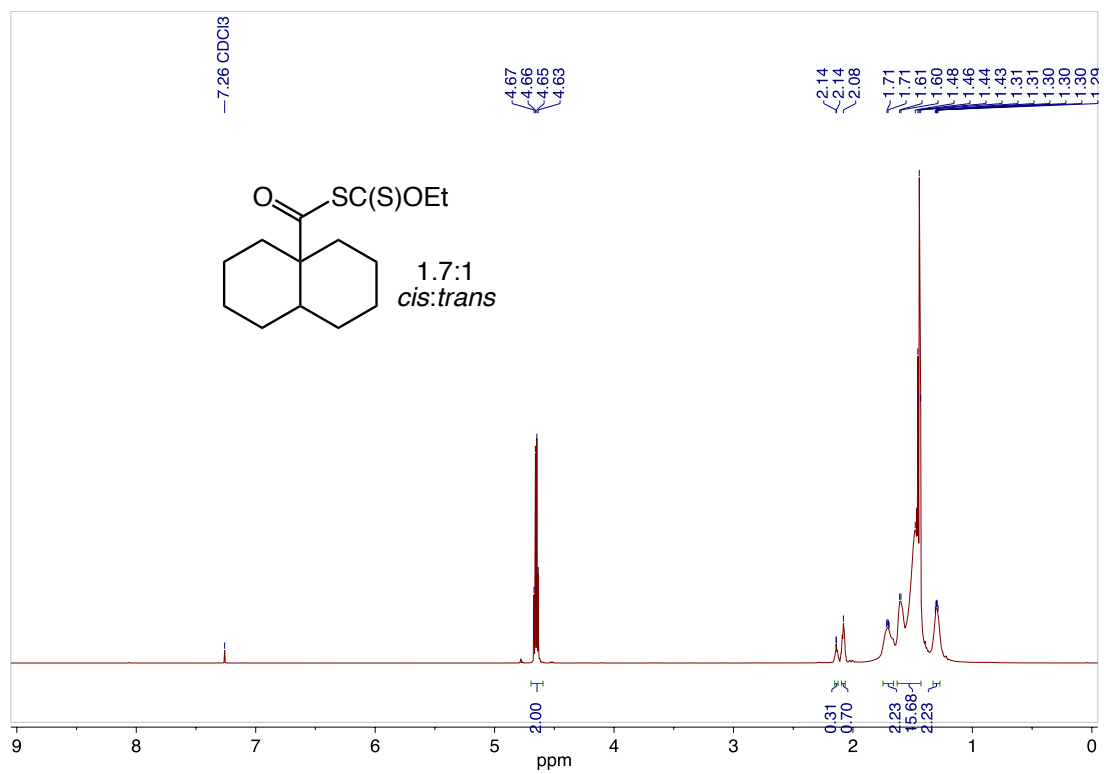


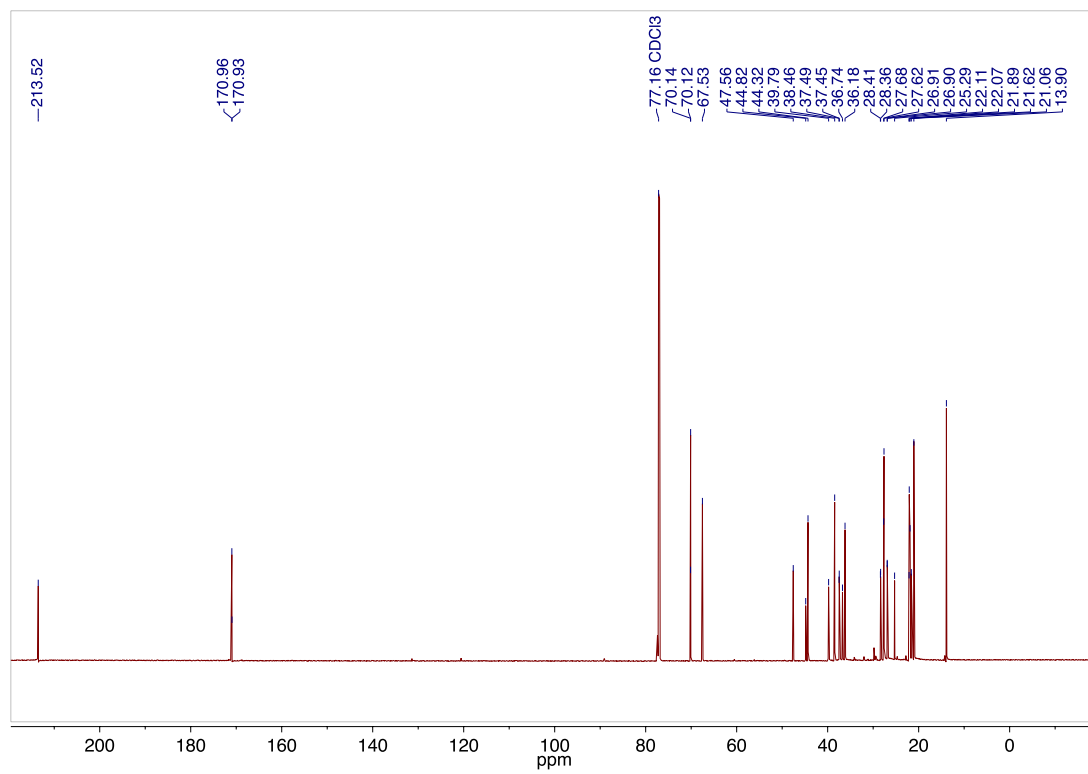
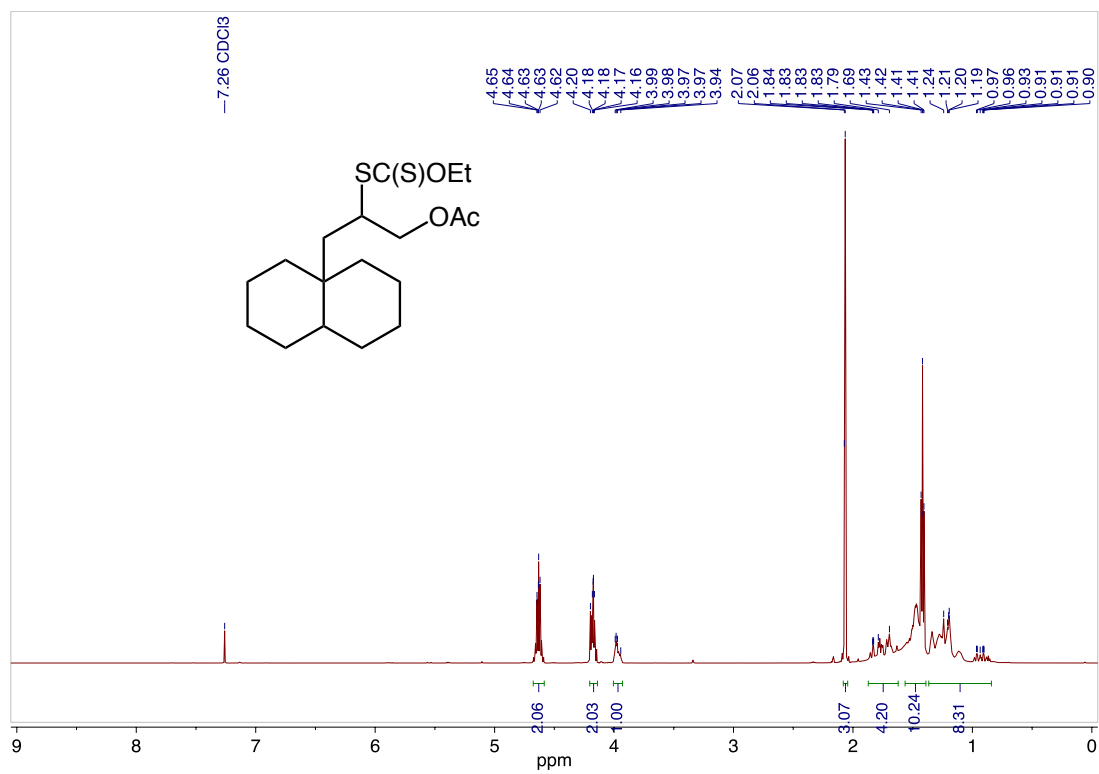




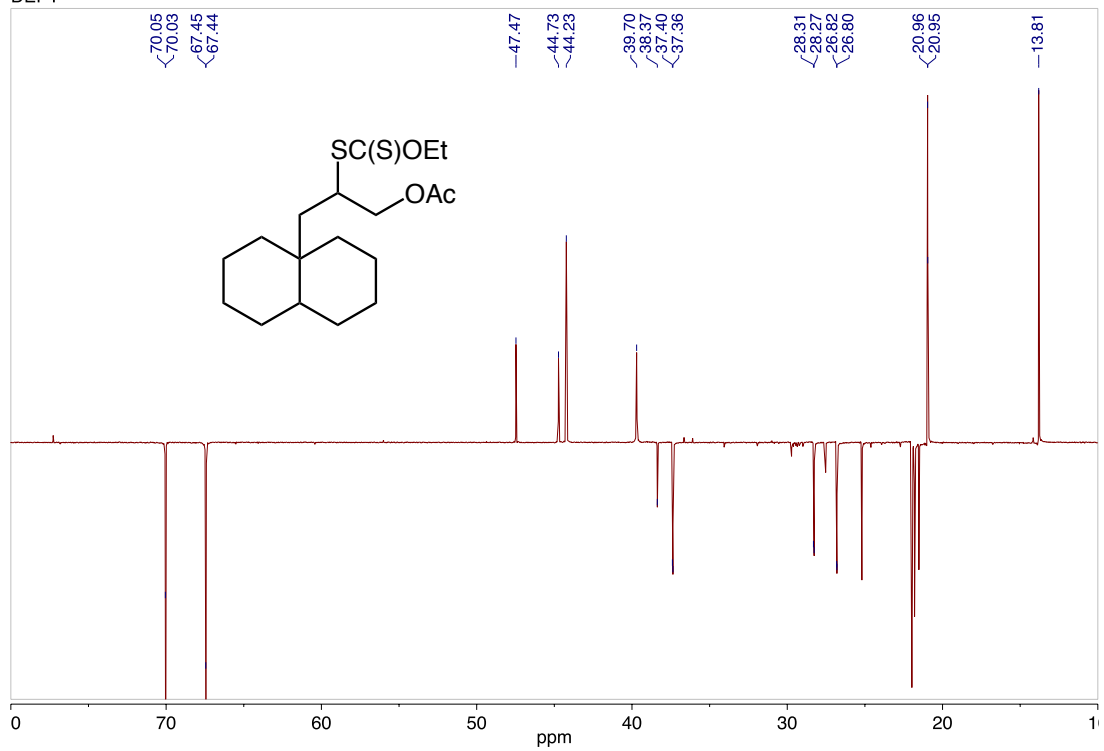




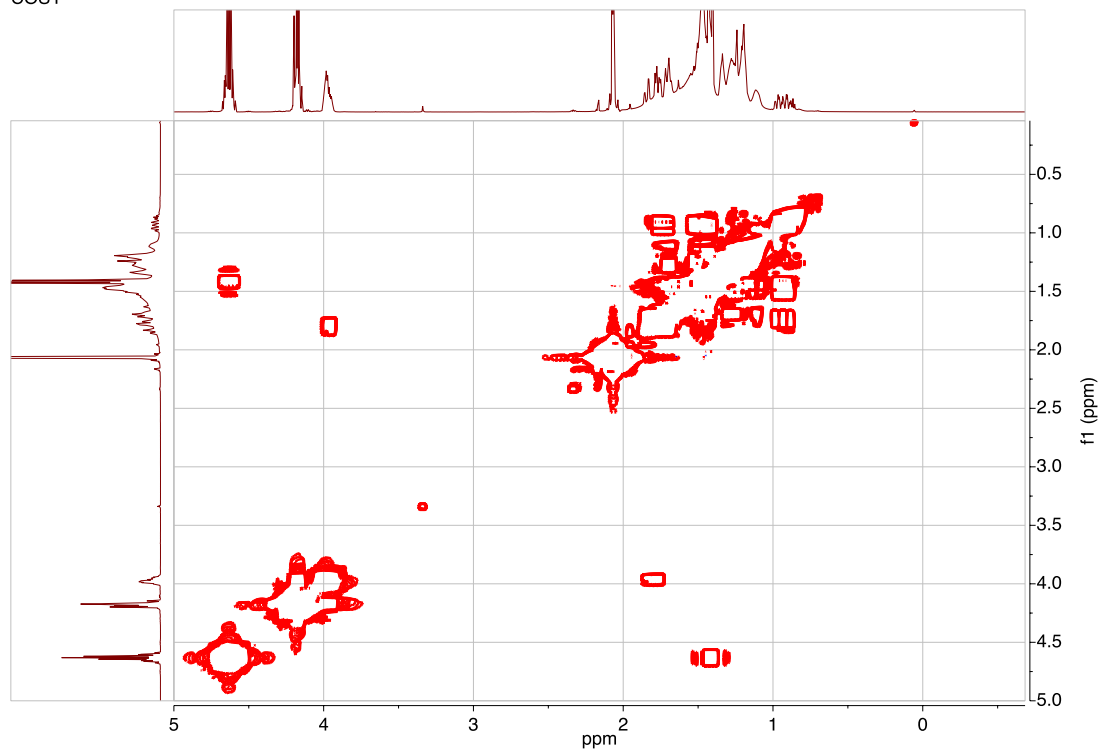




DEPT

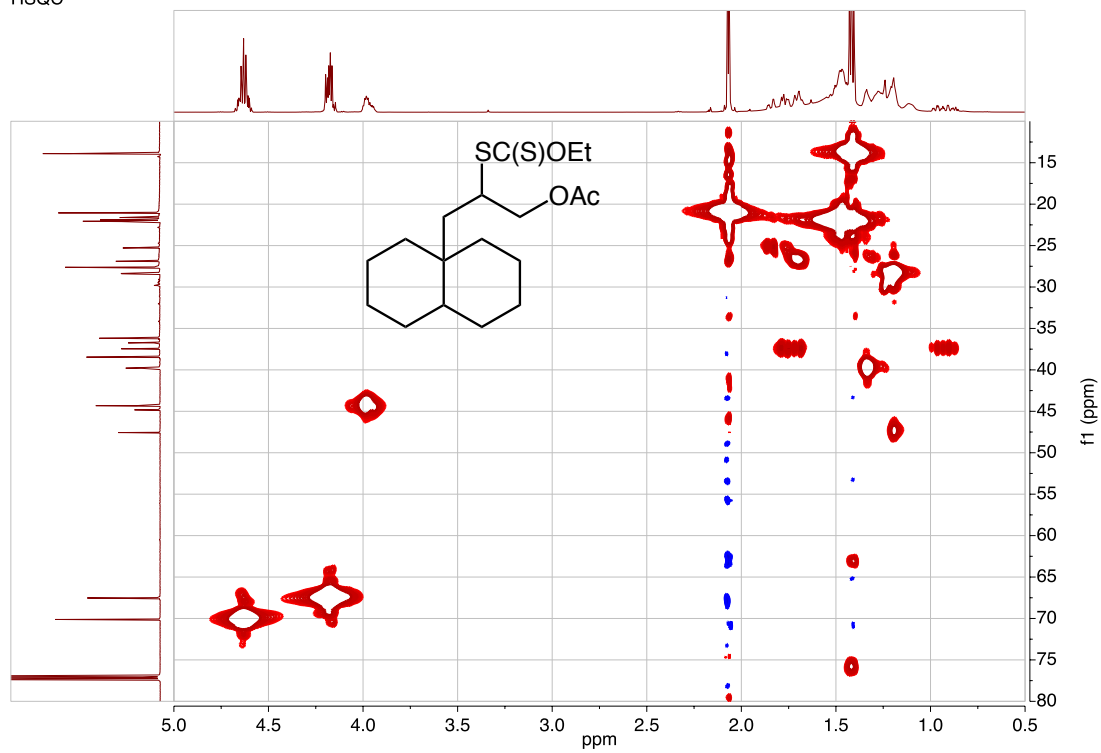


COSY

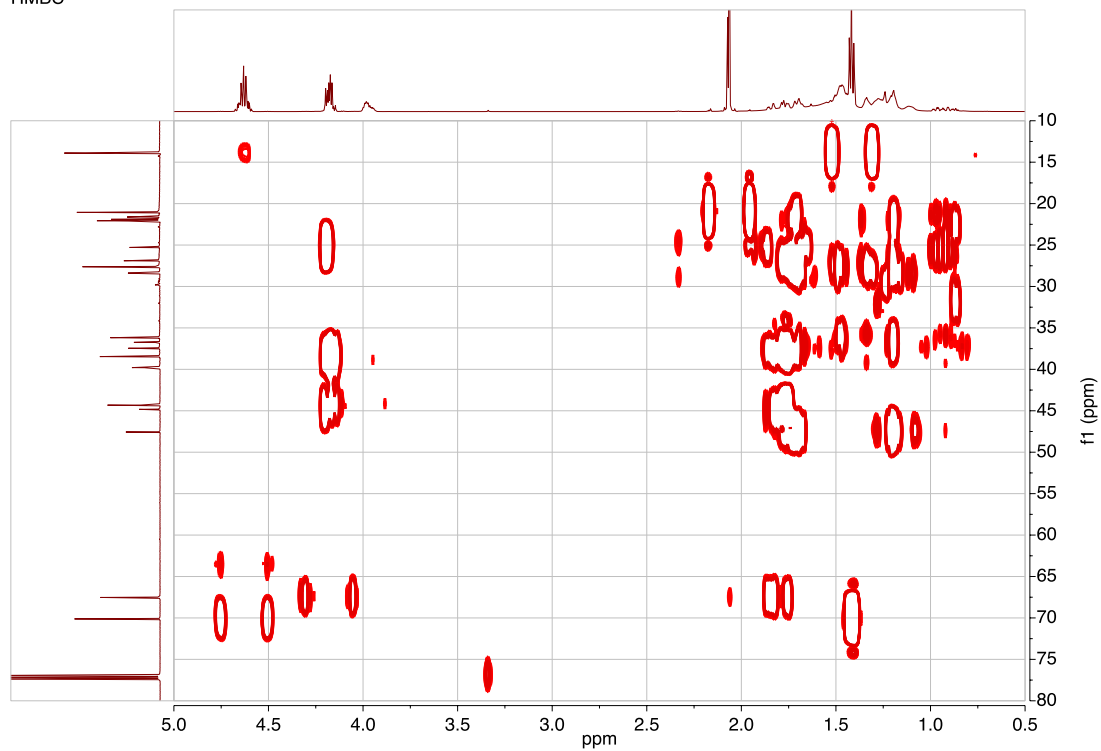




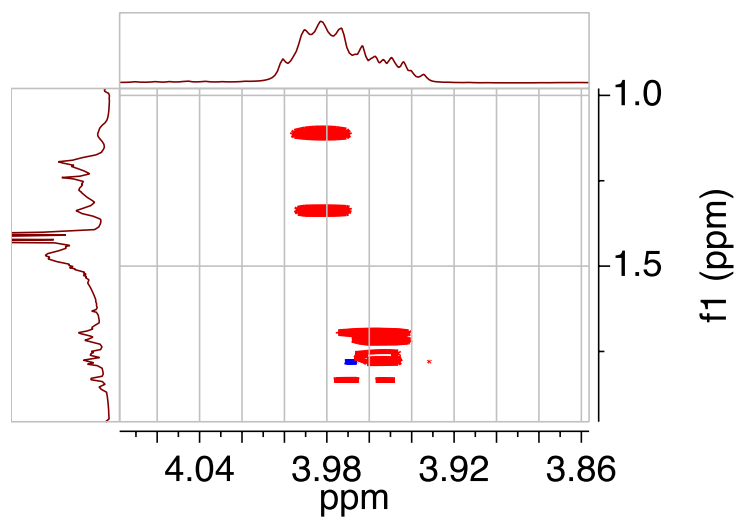
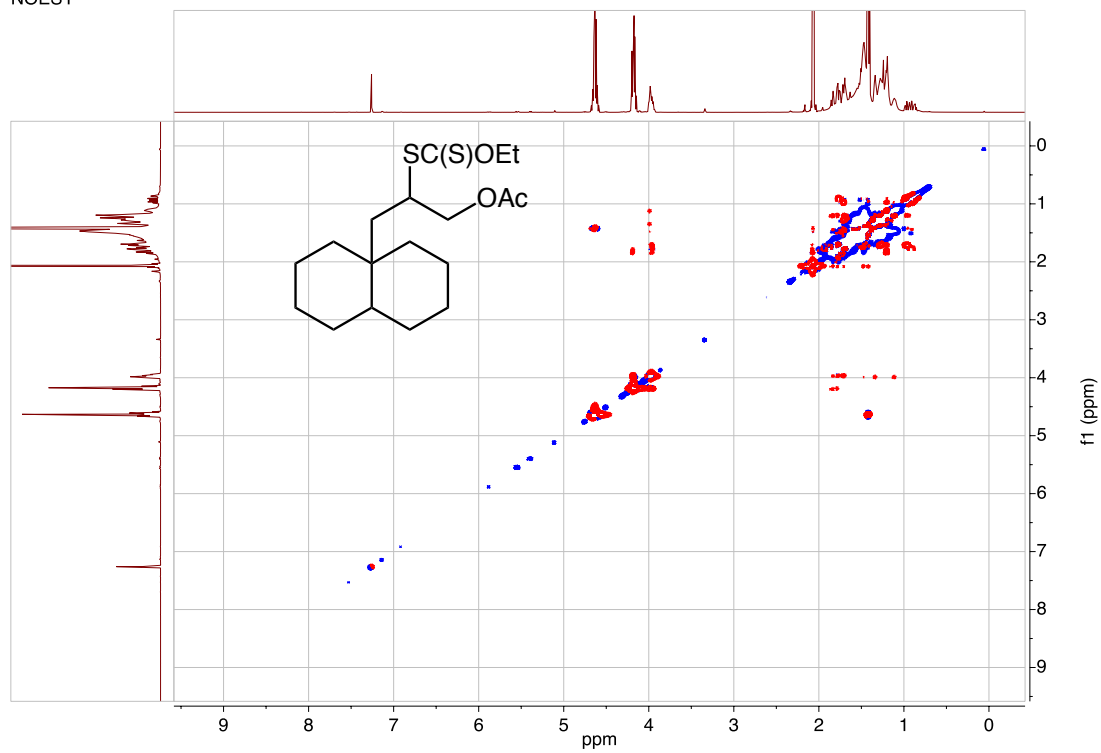
HSQC

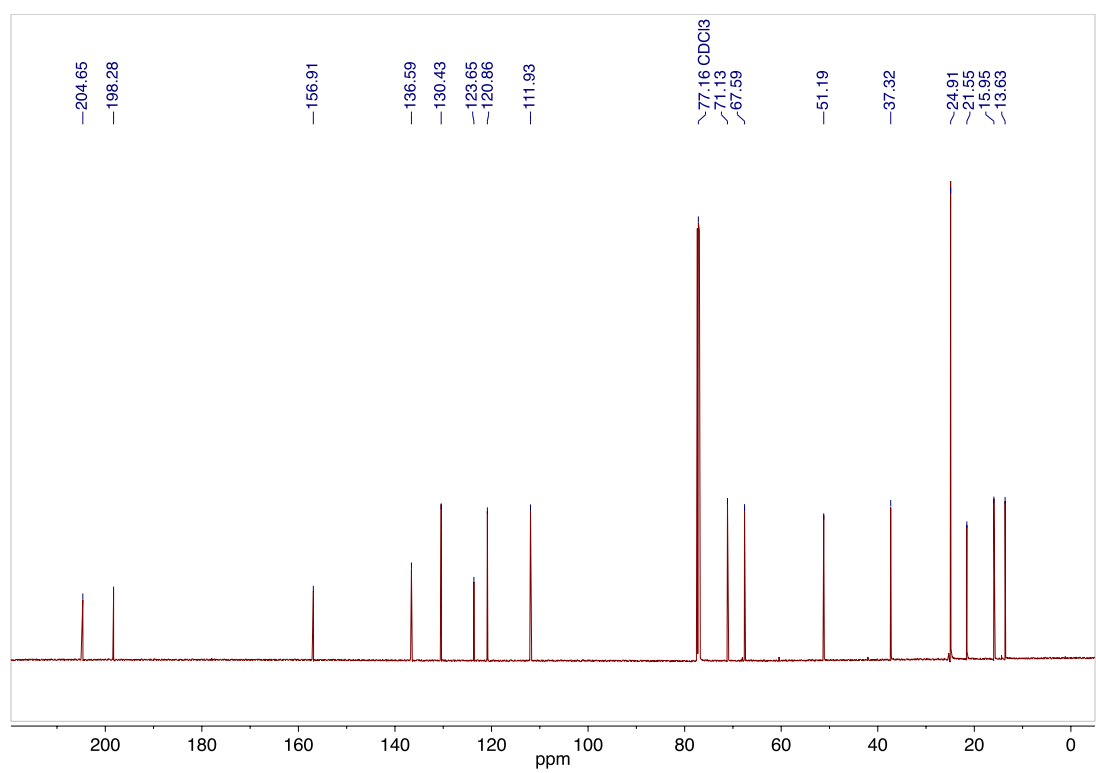
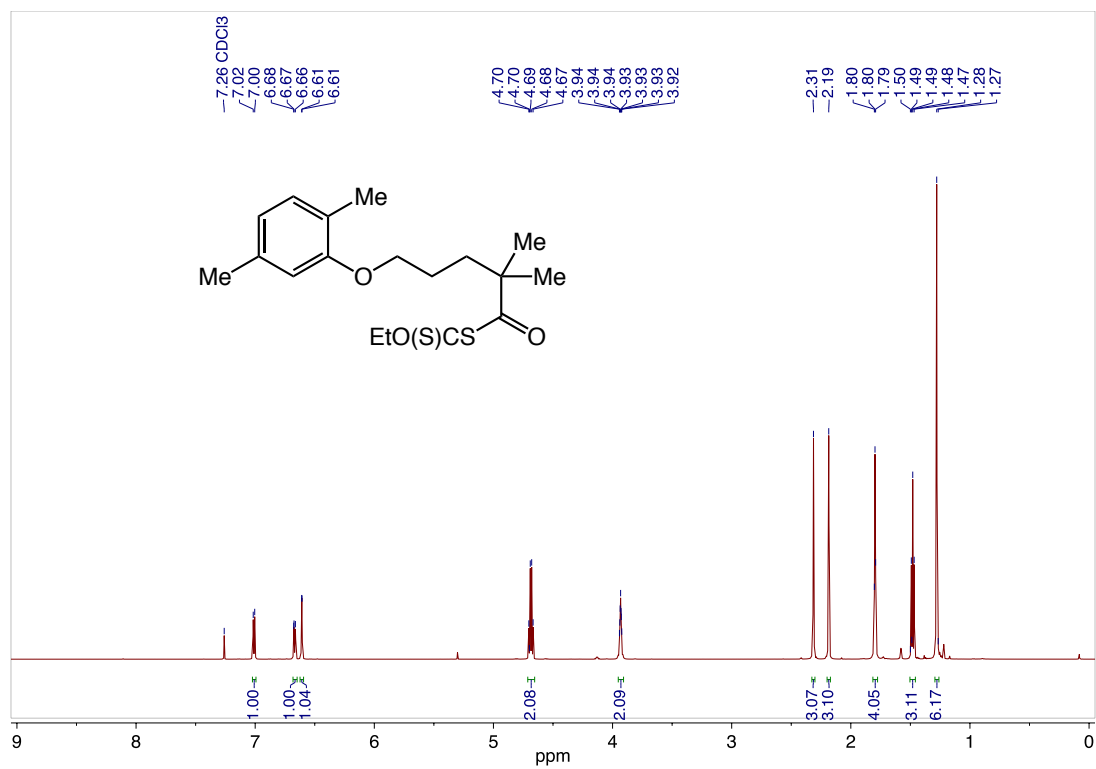


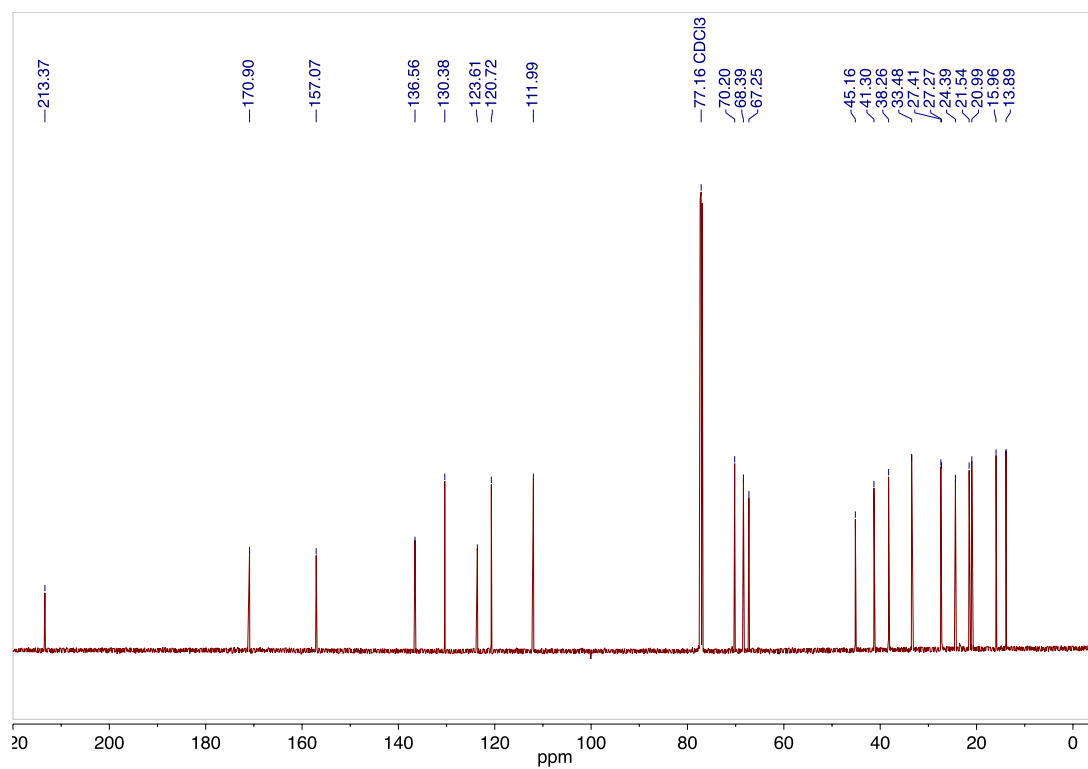
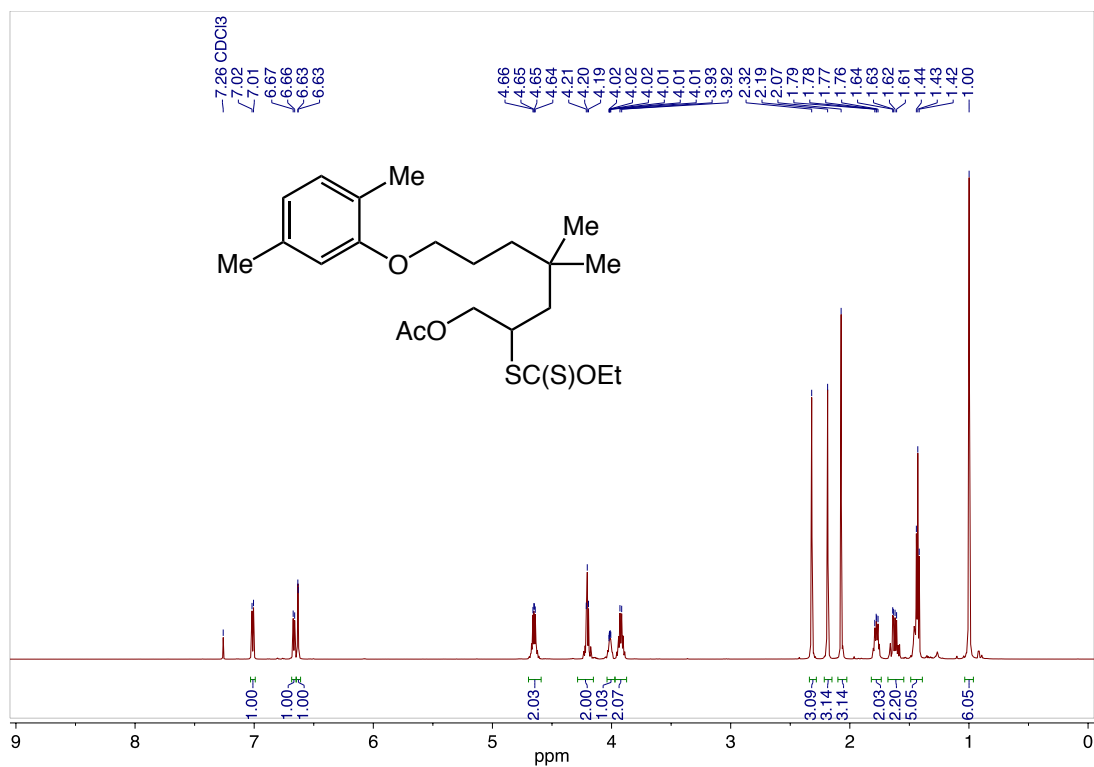
HMBC

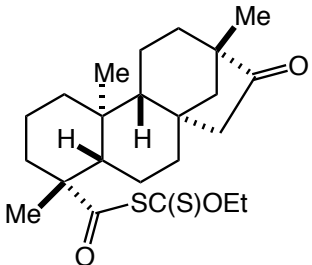


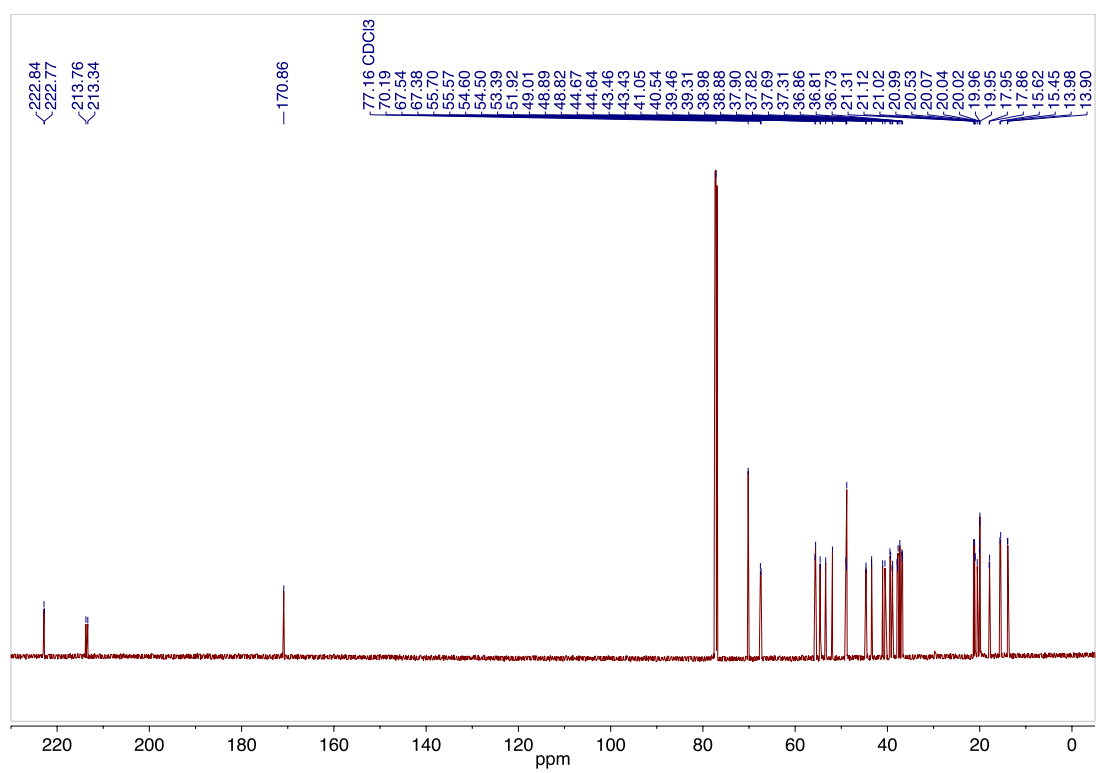
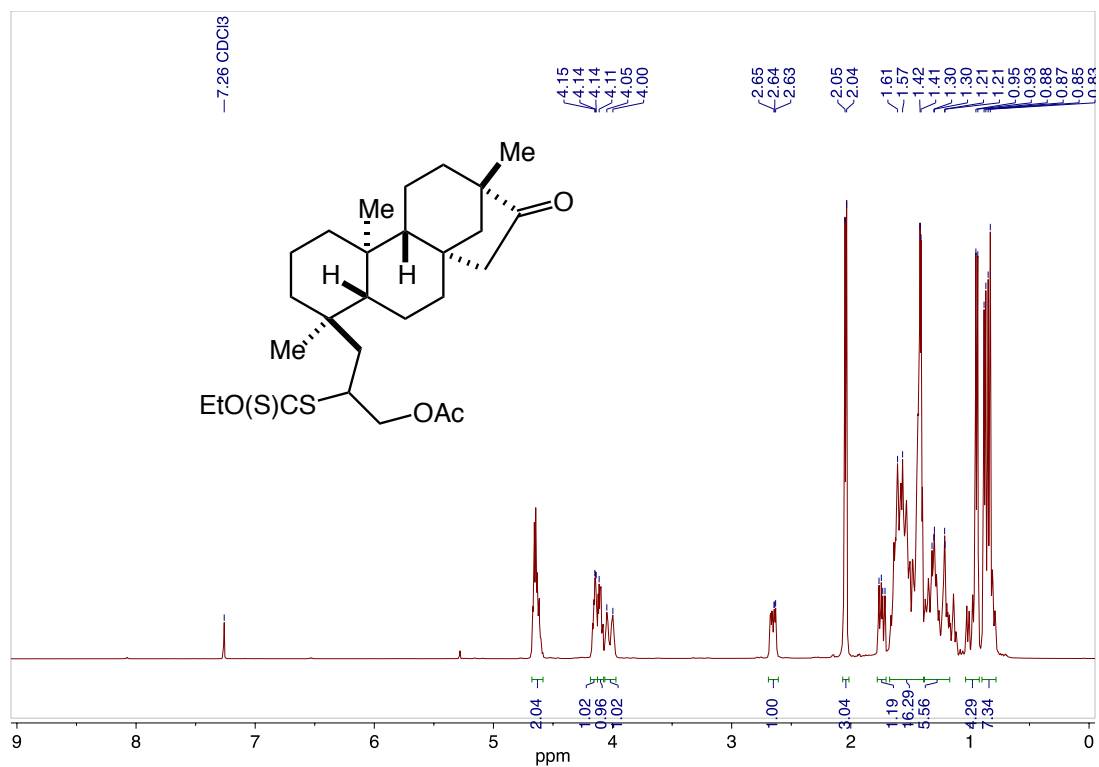
NOESY



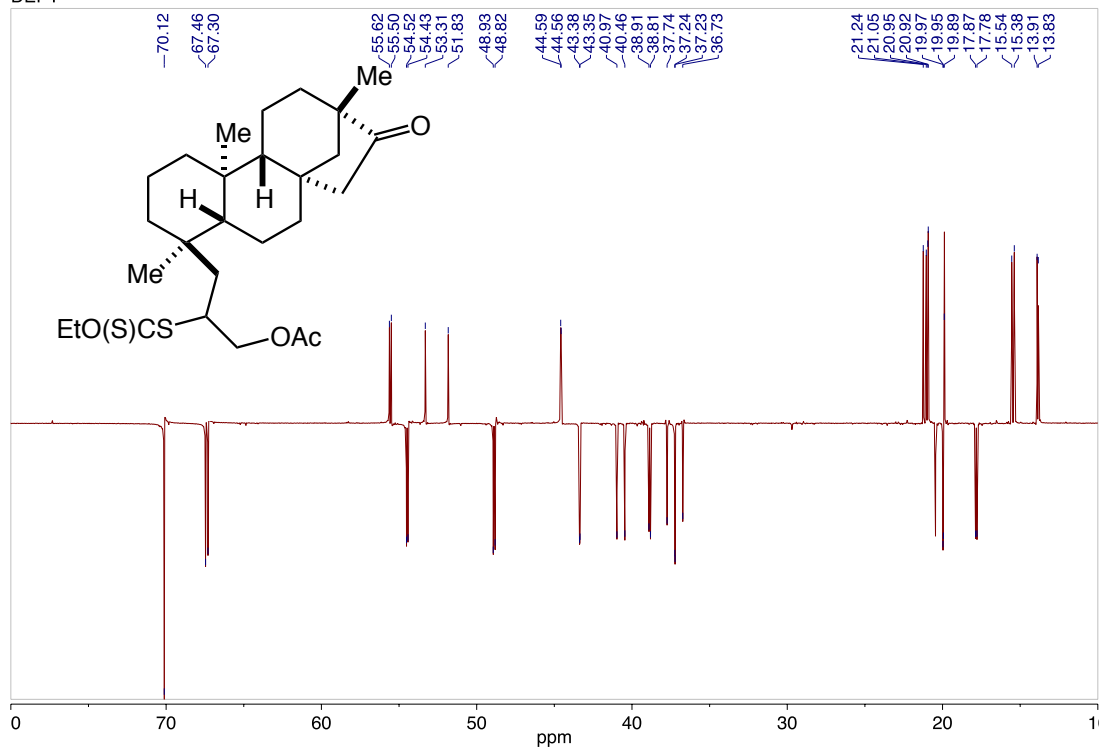




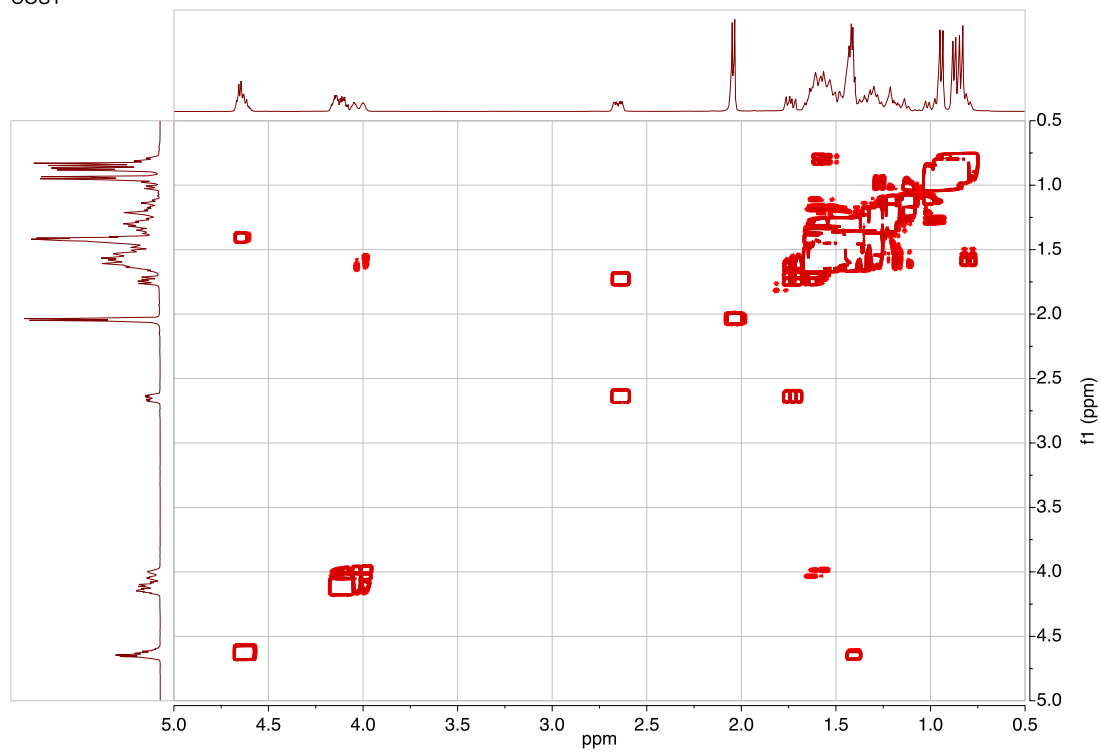




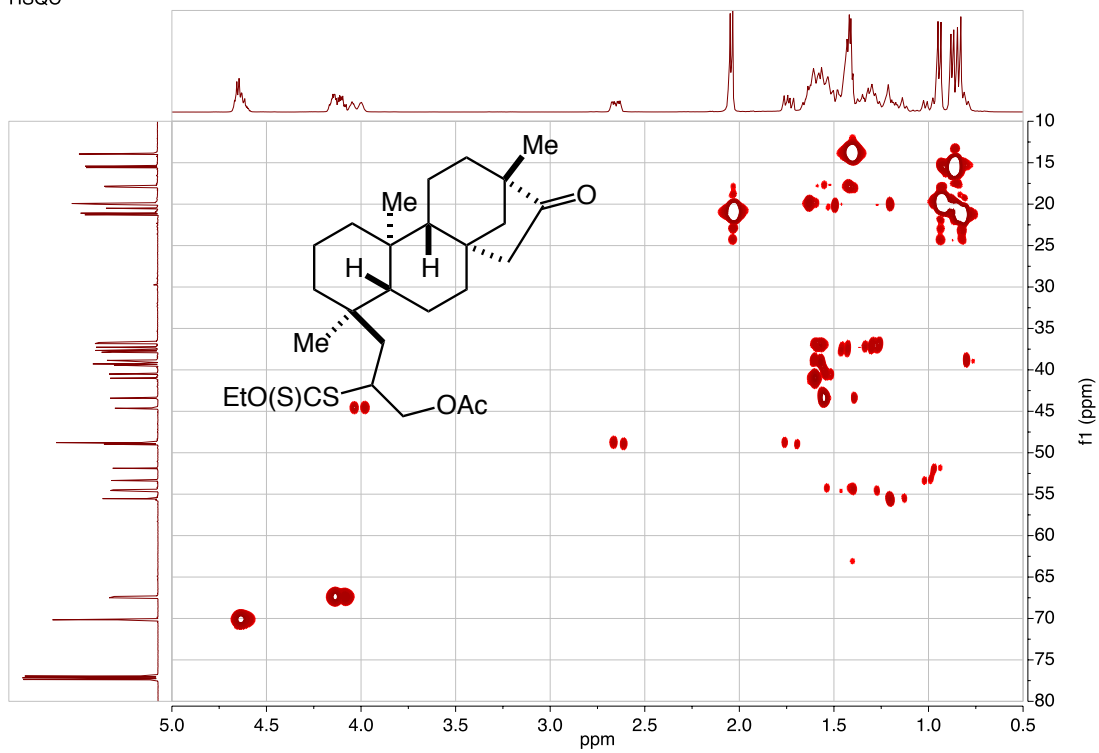
DEPT



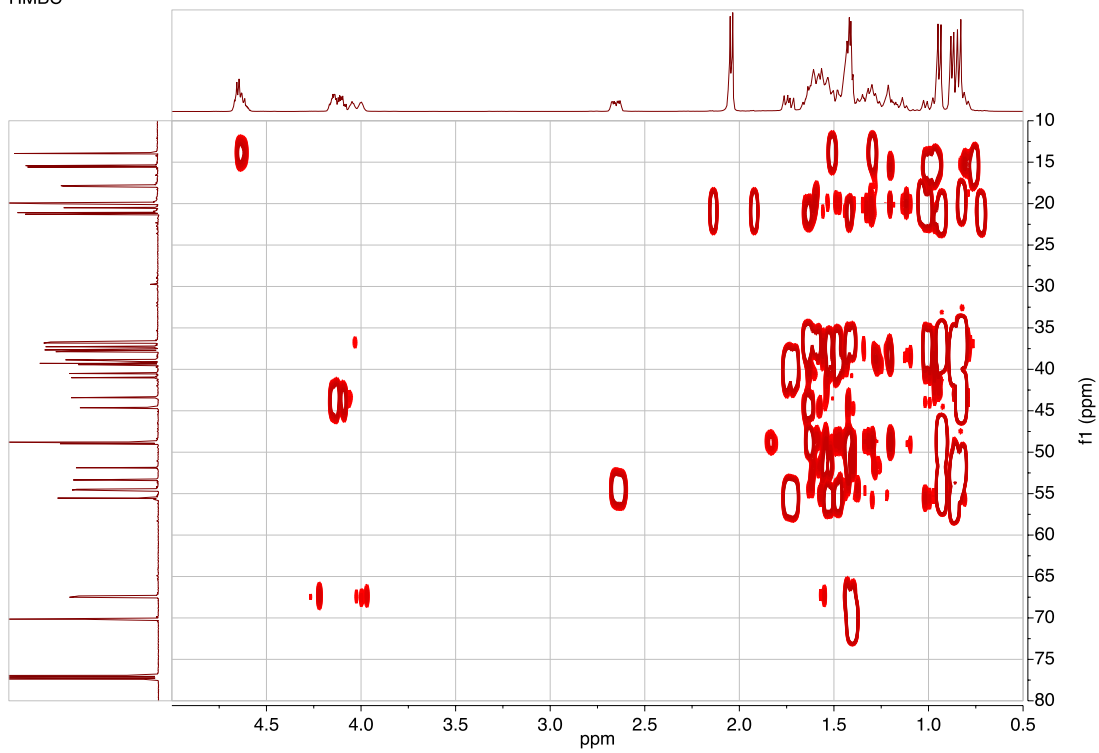
COSY



HSQC



HMBC





NOESY

